Structure-based Design and Synthesis of Inhibitors of the Mitotic Kinases Nek2 and CDK2

Honorine Lebraud

This thesis is submitted to Newcastle University

for the degree of Doctor of Philosophy

December 2014

Declaration

The work described in this thesis was carried out between October 2011 and August 2014 in the Medicinal Chemistry Laboratories, Northern Institute for Cancer Research, Bedson Building, Newcastle University, Newcastle upon Tyne, UK, NE1 7RU and in the Cancer Structural Biology Laboratories, Paul O'Gorman Building, Northern Institute for Cancer Research, Newcastle University, Newcastle upon Tyne, UK, NE2 4HH. Part of the research was conducted in collaboration with scientists at the University of Leicester, Henry Welcome Building, Lancaster Rd, Leicester, LE1 9HN and the CRUK Centre for Cancer Therapeutics, The Institute of Cancer Research, 15 Cotswold Rd, Sutton, Surrey, UK, SM2 5NG and 237 Fulham Road, London, SW3 6JB.

All of the research described in this thesis is original and does not incorporate any material or ideas previously published or presented by other authors except where due reference is given in the text.

No part of this thesis has been previously submitted for a degree, diploma or any qualification at any other university.

Acknowledgements

I would like to start by thanking my supervisors Prof. Roger Griffin and Prof. Bernard Golding who supported me and guided me through my PhD, from whom I continuously learned and with whom I had fantastic discussions. I am also grateful to Dr Céline Cano and Dr Ian Hardcastle for their helpful advice from time to time. I want to thank the Faculty of Medical Sciences and Cancer Research UK for funding my PhD and the research carried out at the Northern Institute for Cancer Research (NICR).

I am very grateful to Prof. Jane Endicott and Prof. Martin Noble for their time and support during my structural biology placement. I want to thank Dr Martyna Pastok who supervised me in the biology lab, Stephen Hallett for his time teaching me how to process crystallography data and Dr Arnaud Basle for his help with the crystal harvesting and data collection.

I would like to acknowledge all the collaborators on the Nek2 project at the Institute for Cancer Research (ICR) and the CDK2 project, especially Prof. Herbie Newell and Lan-Zhen Wang at the NICR.

I want to express my gratitude to our technical team, Dr Karen Haggerty, Carlo Bawn for his help with the kinetic studies and Amy Heptinstall who has made working in the lab much easier. I want to say a special thank you to Dr Benoit Carbain who was there whenever I needed help and Dr Duncan Miller for his advice, help and expertise in medicinal chemistry. I want to thank the rest of the group, past and present, who have made working in the lab here at Newcastle University a pleasure: Bian Zhang, Nicholas Martin, James Pickles, Santosh Adhikari, Annalisa Bertoli, Andrew Shouksmith, Judith Unterlass, Dr Sarah Cully, Dr Lauren Molyneux, Dr David Turner, Dr Chris Matheson, Dr Stephanie Myers, Dr Tim Blackburn, Dr Stephen Hobson, Dr Suzannah Harnor, Dr Claire Wilson and Dr Tom Gale.

J’aimerais remercier mes parents, Martine et Bruno Lebraud, pour avoir été présents et m’avoir soutenu tout au long de mes études, des Classes Préparatoires (deux ans qui nous aurons marqué!) à la thèse. Le parcours a été long mais la fin est là!

Pour finir, j’aimerais remercier mon compagnon, Tristan Reuillon, sans qui je ne serais jamais venue au UK pour faire ma thèse; merci d’être là pour moi (et notre Cookie!) au quotidien et de m’encourager sans cesse dans le travail.

Abstract

Cyclin-dependent kinase 2 (CDK2) and Nek2 (Never-In-Mitosis A related kinases) are cell-cycle associated serine-threonine kinases that play an important role in the regulation of cellular proliferation and mitosis. Aberrant CDK2 and Nek2 activity are strongly associated with cancer, and inhibitors of these protein kinases are of potential therapeutic use as antitumour agents.

Inhibitors of Nek2 –Previous studies identified a series of 2-aminoaryl-6-ethynylpurines (*e.g.* **42**), as potent and selective irreversible Nek2 inhibitors with good antitumour activity *in vitro* and *in vivo*. 6-Ethynylpurine **42** binds within the ATP domain of Nek2 via a triplet of hydrogen bond interactions with the hinge region, enabling a covalent reaction between Cys-22 and the 6-ethynyl substituent. However, subsequent SAR studies indicated possible off-target activity for this series, which has been investigated through the synthesis and evaluation of control compounds engineered to be inactive against Nek2. With a view to abolishing Nek2-inhibitory activity without imposing dramatic structural changes, the effect of methylation at the purine *N*-7 (**64**) and *N*-9 (**63**) positions was studied. The corresponding isosteric 6-cyanopurine derivatives (**65**, **66**, and **67**) were also synthesised, which were expected to resemble closely 6-ethynylpurines without the capacity to react covalently. Evaluation of these derivatives in cell-based assays confirmed the presence of a growth-inhibitory activity unrelated to Nek2 inhibition. Regioselective *N*-7 methylation of **65** proved challenging, and a novel approach was developed whereby initial *N*-9 protection enabled selective methylation at the purine *N*-7 position, with concomitant loss of the *N*-9 protecting group giving the target purine **67**. Kinetic studies have also been conducted with **42**, **63** and **64** to assess the impact of *N*-7/*N*-9 methylation on the chemical reactivity of the 6-ethynyl 'warhead'. A model system was developed to investigate a possible correlation between the chemical and biological reactivity of the 6-ethynyl group of the purine derivatives with thiols.

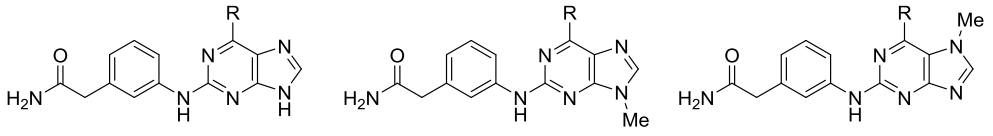

42; R = ethynyl
65; R = CN

63; R = ethynyl
66; R = CN

64; R = ethynyl
67; R = CN

Inhibitors of CDK2 –Previous studies have resulted in the identification of the purine CDK2 inhibitor **60**, found to inhibit CDK2 in a time-dependent manner (IC_{50} = 63 nM) via conjugate addition of a lysine residue (Lys89), located in the 'hinge region' of the

ATP-binding domain, to the vinyl sulfone functionality of **60**. This is thought to represent the first example of irreversible CDK2 inhibition, and prompted more detailed investigations with **60**.

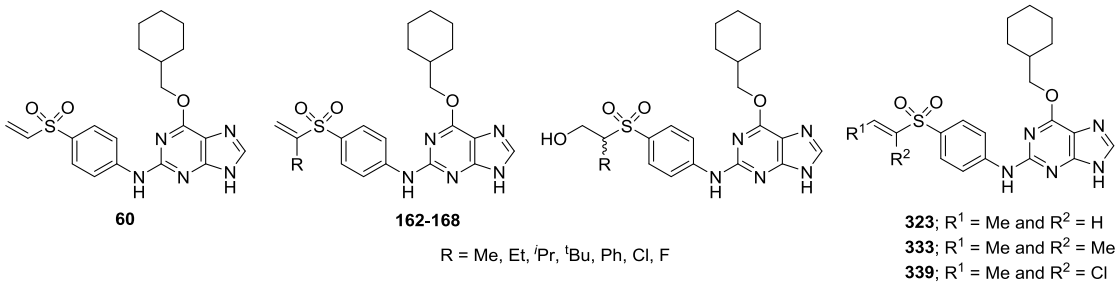

Compound **60** exhibited a short half-life in both plasma (44 min) and medium (19 min), ascribed to hydration of the vinyl sulfone. Therefore, a priority was to improve the chemical stability of **60** without compromising inhibitory potency and time-dependent inhibition. Using the crystal structure of **60** in complex with CDK2 to guide inhibitor design, a range of derivatives (**162**-**168**) have been synthesised bearing α-substituents (R) on the vinyl sulfone group. In addition, synthetic methodology was developed for the synthesis of the corresponding 2-hydroxyalkyl products which are putative ATP-competitive inhibitors. From the biological studies conducted on purine derivatives **162**-**168**, only the α-chlorovinyl sulfone compound **167** (IC_{50} (4 h) = 14 nM) has emerged as of particular interest, whereas others have shown competitive CDK2 inhibition, confirmed by *X*-ray crystallography. The β-position of the vinyl sulfone moiety has been briefly explored with purines (**323**, **333** and **339**). In this series, one inhibitor (**323**) has been shown to bind covalently to CDK2 by structural biology studies. Alternative 'warheads' to the vinyl sulfone group have been investigated and exhibited competitive CDK2 inhibitory activity in a time-dependent inhibition assay. Finally, insertion of the vinyl sulfone warhead into known CDK2 inhibitors was investigated in preliminary studies.

Abbreviations

A	ADP	Adenosine diphosphate
	ADME	Absorption, Distribution, Metabolism and Excretion
	APC	Anaphase promoting complex
	AS	Analogue-Sensitive
	ATP	Adenosine-5'-triphosphate
B	Boc	*tert*-Butyloxycarbonyl
	Brettphos	2-(Dicyclohexylphosphino)3,6-dimethoxy-2′,4′,6′-triisopropyl-1,1′-biphenyl
C	CAK	CDK-activating kinase
	CDDP	Cis-diaminedichloroplatine (II), also known as Cisplatin
	CDI	1,1'-Carbonyldiimidazole
	CDK	Cyclin-dependent kinase
	Civ1	CAK In Vivo 1
	CK	Casein kinase
	CKI	Cyclin-dependent kinase inhibitor
	CLL	Chronic lymphocytic leukaemia
	CML	Chronic myeloid leukaemia
	CYC	Cyclin
D	DABCO	1,4-diazabicyclo[2.2.2]octane
	DBU	1,8-Diazabicyclo[5.4.0]undec-7-ene
	DCC	*N*,*N*'-Dicyclohexylcarbodiimide
	DMA	Dimethylacetamide
	DMF	*N*,*N*-Dimethylformamide
	DMN	Dimethylnitrosamine
	DMP	Dess-Martin periodinane
	DMPU	N,N'-Dimethyl propylene urea
E	EDCI	*N*-(3-Dimethylaminopropyl)-*N*′-ethylcarbodiimide
	ePK	Eukaryotic protein kinase
F	FDA	Food and Drug Administration
	FGF	Fibroblast growth factor
G	GI_{50}	Concentration required to inhibit cell growth by 50%
	GIST	Gastrointestinal stromal tumour
	GPCR	G-protein coupled receptors

	GSK	Glycogen synthase kinase
	GST	Glutathione S-transferase
H	Hec	Highly expressed in cancer
	HPLC	High-performance liquid chromatography
I	IC_{50}	Concentration required for inhibition of 50% of target
	Inh-2	Inhibitor-2 protein
	IPTG	Isopropyl β-*D*-1-thiogalactopyranoside
K	KHMDS	Potassium bis(trimethylsilyl)amide
L	LC-MS	Liquid chromatography–mass spectrometry
	LDA	Lithium diisopropylamide
	LHMDS	Lithium bis(trimethylsilyl)amide
M	Mad	Mitotic arrest deficient-like
	MAPK	Mitogen-activated protein kinase
	MCL	Mantle cell lymphoma
	m-CPBA	3-Chloroperbenzoic acid
	MEF	Mouse embryonic fibroblast
	MPC	Medium pressure chromatography
	MW	Microwave
	MYCN	v-Myc avian myelocytomatosis viral oncogene neuroblastoma derived homolog
N	NIMA	Never-In-Mitosis A
	Nlp	(Nep1)-like protein
	NMP	*N*-Methyl-2-Pyrrolidone
	NNK	4-(Methylnitrosamino)-1-(3-pyridyl)-1-butanone
	NSCLC	Non-small-cell lung cancer
O	Et_3OBF_4	Triethyloxonium tetrafluoroborate
	Me_3OBF_4	Trimethyloxonium tetrafluoroborate
P	PK	Protein kinase
	PKC	Protein kinase C
	Plk	Polo-like kinase
	PMB	*para*-Methoxybenzyl
	PP1	Protein phosphatase 1
Q	qNMR	Quantitative NMR
R	Ra-Ni	Raney nickel
	Rb	Retinoblastoma

	RCC	Renal-cell carcinoma
T	TBAF	Tetra-*n*-butylammonium fluoride
	TBDMS	*tert*-Butyldimethylsilyl
	TBDPS	*tert*-Butyldiphenylsilyl
	TCI	Targeted covalent inhibitor
	TFA	Trifluoroacetic acid
	TFE	2,2,2-Trifluoroethanol
	THF	Tetrahydrofuran
	THP	Tetrahydropyran
	TIPS	Triisopropylsilyl
	TK	Tyrosine kinase
	TMS	Trimethylsilyl
	TMSOTf	Trimethylsilyl trifluoromethanesulfonate
V	VEGF	Vascular endothelial growth factor
W	Wnt	Int/Wingless family
X	Xantphos	4,5-Bis(diphenylphosphino)-9,9-dimethylxanthene

Contents

Chapter 1. Targeted Cancer Therapy and the Cell Cycle

1.1 Cancer evolution towards a targeted therapy

Cancer has always been present, throughout centuries,[1] but in former times never represented a major cause of death due to short life expectancy. In the medical archives, breast cancer was first mentioned around 3000-2500 BC in T*he Edwin Smith Surgical Papyrus*.[1] Major understanding and progress in cancer research were made during the 20th century with the introduction of chemotherapy.[1] Discovered during the First World War and known to attack bone marrow and lymphoid tissues, mustard gas was first used as a chemotherapeutic agent in 1942 for human lymphoma.[2] From this molecule, research focussed on developing other anti-cancer drugs such as topoisomerase inhibitors,[3] antimetabolite agents[3] and microtubule inhibitors.[3] The most important discovery, leading to a better understanding of cancer at a molecular level, was the human DNA structure decoded in 1953 by Francis Crick and James Watson,[4] aided by *X*-ray images of DNA provided by Rosalind Franklin. Discoveries through the centuries contributed to the understanding of cancer, a term that embraces not one but over one hundred diseases.

1.1.1 Causes of cancer

In 40% of all cases, cancer can be avoided through changes in lifestyle.[5] One of the major risk factors is tobacco smoke and tar, which contribute to carcinogenesis, owing to the presence of numerous mutagenic compounds.[6] Tobacco smoking and chewing can cause lung, oesophagus, stomach, pancreas, liver, bladder, kidney and cervical cancers,[5] all having poor diagnosis and making tobacco a major death risk.[5] Alcohol consumption is another lifestyle factor, with ethanol considered a co-carcinogen and thought to facilitate cell division and proliferation.[7] By liberating mutagenic free radicals, alcohol could also potentially be a cancer initiator.[8] In addition, oxidative metabolism of ethanol generates acetaldehyde, known to be a genotoxic compound causing mutations and chromosomal aberrations in cells, and is classified as a possible carcinogen to humans.[9] Acetaldehyde is present is tobacco, vehicle emissions but, more importantly, is found in several fruits, vegetables and cooked meats.[9] Diet represents another risk factor due to a general tendency to eat food rich in calories and animal fat and low in fiber, resulting in acceleration of the risk of developing cancer.[10] Mutagenic free radicals are generated from polyunsaturated fatty acids contained in animal fat.[11] By contrast, the anti-oxidant properties of fruits and vegetables can help in protection against free-radical damage.[5]

Obesity is a concern in cancer development even though no direct evidence has been demonstrated.[5] Carcinogens can accumulate in adipose tissue, increasing the risk of cancer.[12] Being overweight also increases the risk of diabetes and cardiovascular diseases, contributing to mortality.[5] It is worth noting that some chemotherapeutic agents elicit cardiovascular toxicity, which may cause problems when treating obese patients for cancer.[5]

The environment represents another risk. Viruses can induce cancer, with the most common being *Human Papilloma Virus* and *Hepatitis B*, responsible for cervical and liver cancer, respectively.[13, 14] Radiation arising from human nuclear activities, *X*-rays in medicine for diagnosis or treatment purposes, or UV-rays from the sun can induce skin cancer.[15] Exposure to air pollution, in which mutagens such as benzene and buta-1,3-diene are found, from vehicle exhausts and factory smoke can be responsible for inducing cancer.[5]

Cosmetics and medicines are factors to consider. Cosmetics can contain carcinogens such as paraben, suspected to be a risk factor for breast cancer.[16] Pesticides used in intensive farming are generally classified as potential carcinogens,[5] as they enter the body through ingestion, inhalation and skin contact.[17] They are found in water and in fruits and vegetables.[5] Also, contraceptives have been shown to increase slightly the risk of breast cancer.[5]All these factors constitute minor risks taken individually, but all together they can have a major impact on health.

1.1.2 Hallmarks of cancer – Towards targeted chemotherapy

Understanding the hallmarks of cancer is crucial for developing safer therapies for patients as the previous generation of chemotherapeutic agents caused too many undesired effects. In the process of tumourigenesis, tumour cells acquire properties, progressively through different mechanisms, allowing them to survive, proliferate and metastasise.[18] These capabilities are known as the hallmarks of cancer (*Figure 1*).[18] Douglas Hanahan and Robert A Weinberg have described the main hallmarks of cancer from the results and observations obtained in cancer research over the last ten years. Understanding the biology of cancer and the role of tumour environment is essential to improve cancer research.[18]

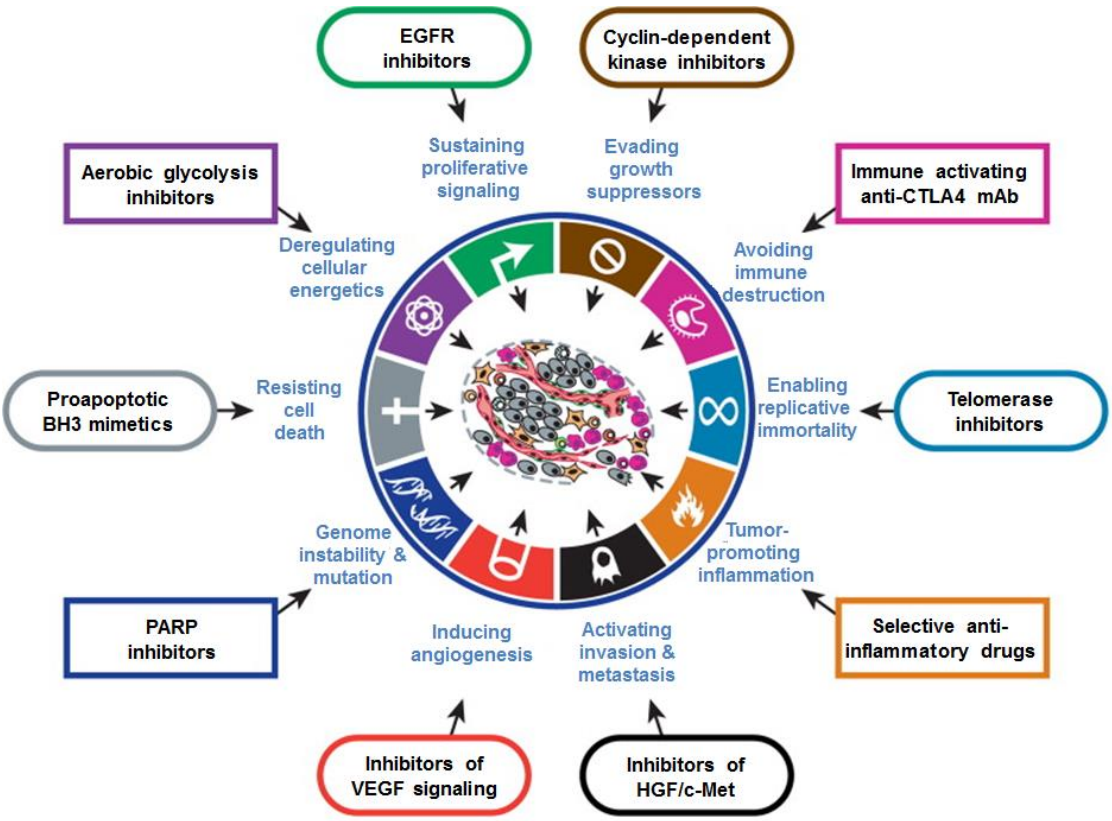

Figure 1 - The Hallmarks of cancer[18] (from D. Hanahan and R. A. Weinberg, 2011) – Description of the properties acquired by tumour cells to divide indefinitely and invade tissues, and the class of inhibitors developed for each hallmark.

One of the main properties acquired by tumour cells is indefinite division.[18] Contrary to normal cells, which control their production of growth-promoting signals to enter cell-cycle and division, tumour cells can proliferate without restraint by deregulating these growth factors.[18] By binding to receptors on the cell-surface, the growth signals send a message regulating the cell cycle and cell growth, therefore influencing cell survival and energy metabolism. However, a high level of proliferative signaling has been demonstrated in cell culture to drive the tumour cell into a non-proliferative-state, called senescence.[19] This phenomenon may constitute a limit to tumour cell proliferation, but some cancer cells can adapt and interfere with this senescence state, by evading the negative pathways, depending mostly on tumour suppressor genes that regulate cell division.[18] Defects in the retinoblastoma-associated (Rb) pathway, which regulates the growth-and-division cycle of the cell, may lead to uncontrolled cell proliferation.[20] In addition, tumour protein p53 can transiently stop the cell cycle or trigger apoptosis by responding to an excess of stress and abnormal signals from the cell. Defects in the p53 pathway may thus result in persistent cell proliferation.[18] Another factor known to stop cell proliferation is cell-to-cell contact, when a population of normal cells becomes too dense; most cancer cells have lost such contact inhibition.[18]

On their way to unlimited proliferation, tumour cells have to develop the ability to resist cell death. Apoptosis represents a natural barrier to cancer development in response to high levels of oncogene signals and DNA damage.[21] Apoptosis is controlled by pro-apoptotic proteins (e.g. Bax and Bak) and anti-apoptotic proteins (e.g. Bcl-2).[21] When the apoptotic pathway is triggered, the cell is disassembled and consumed by surrounding cells and phagocytes.[18] Apoptosis may be attenuated in tumour cells by several strategies such as the loss of p53,[22] an increase of anti-apoptotic proteins and survival signals, and a decrease in pro-apoptotic proteins.[18] In tumourigenesis, necrosis appears to be an important factor. By lysing, necrotic cells release pro-inflammatory signals causing the recruitment of immune inflammatory cells to clear the residues,[23] whereas apoptotic cells are consumed by neighbours. Necrotic cells are known to enable angiogenesis, cancer cell proliferation and invasiness.[18]

As mentioned previously, one of the main properties of tumour cells is unlimited proliferation that allows the formation of a macroscopic tumour. To acquire this capability, tumour cells must counteract the limitations of excessive growth and division imposed on healthy cells.[18] This limited number of divisions is dictated by the length of telomeric DNA present in the cell.[24] Telomeres protect the end of chromosomes and each division shortens their length. After several generations of cells, telomeres are eroded, triggering a crisis mode, causing apoptosis. To prevent this, tumour cells overexpress telomerase, an enzyme responsible for extending telomeric DNA, to allow further divisions. This overexpression creates resistance to both senescence and apoptosis, and generates immortalised cells.[18]

To proliferate, tumour cells require nutrients and oxygen, and need to release their waste products and carbon dioxide.[18] In response to their needs, tumour cells stimulate the formation of new blood vessels.[25] Existing vessels exit their quiescent state to expand the vessel network under stimulation from angiogenic inducers such as VEGF or FGF.[26, 27] Some cells from the bone marrow appear to play a role in angiogenesis by facilitating tumour growth and local invasion.[28]

Alterations in shape, cell to cell adhesion and cell to extracellular matrix adhesion are characteristics allowing tumour cells to invade surrounding tissue.[18] Local invasion and metastasis arise from a multi-step process as tumour cells will first invade local tissues, close to blood and lymphatic vessels. They will move through the latter to invade distant tissues[29] and form micrometastases, and then grow into macroscopic tumours, in a process known as colonisation.[18] In this process of growing and metastasing, tumour cells

have support from neighbouring cells.[30] Macrophages and inflammatory cells, for example, can provide matrix-degrading enzymes, which help tumour cell growth.[30] Tumourigenesis cannot be studied by considering not only the tumour cells, but also the tumour and its environment. When tumour cells colonise a tissue, they need time to adapt to their new environment.[18] They are in a dormant state, finding a way to acquire the properties required to grow into macrometastases.[31] This dormant state explains why, after having their primary tumour removed, patients can develop a secondary tumour several years following surgery.

In addition to these hallmarks, the ability of cancer cells to reprogram energy metabolism and evade immune destruction has been recognised in the last ten years. Growing and dividing requires energy from the cell.[18] Under aerobic conditions, normal cells process glucose into pyruvate by glycolysis in the cytosol and pyruvate into carbon dioxide in the mitochondria.[32] Under anaerobic conditions, the main pathway to energy is glycolysis. It has been noticed that in tumour cells, glycolysis is the main route of energy metabolism, probably due to the diversity of glycolytic intermediates arising from this process, which trigger the biosynthesis of elements needed in the recruitment of new cells.[18]

Another defence mechanism along with apoptosis would be the immune system resisting tumour formation and progression.[18] The invasive growth of a tumour would imply that somehow the tumour manages to escape this immune surveillance.[33] An observation supporting the role of the immune system is the development of tumours in patients after an organ transplant. Tumour cells in a dormant state, and tightly controlled by the donor's immune system, grew freely after a patient had been immunosuppressed.[34]

The hallmarks acquired by tumour cells arise through genomic instability and immune system defects. In contradiction, the immune system helps to resist tumour growth but some cells are involved in tumour progression.[18] These cells can supply growth factors for cell proliferation, survival factors to resist apoptosis, and pro-angiogenic signals to facilitate angiogenesis.[35] However, the acquisition of hallmarks is mainly caused by DNA alterations which lead to genome instability.[18] The inhibition of pathways involved in one or several hallmarks of cancer, by single or combined chemotherapy, represents a strategic and targeted method for cancer therapy, as shown in *Figure 1*.

1.2 Protein kinases and the cell cycle

Uncontrolled cellular proliferation represents one of the hallmarks of cancer. Targeting components of the cell cycle to induce apoptosis is thus one possible strategy to stop tumour growth.

1.2.1 The cell cycle

The cell cycle is a vital and complex process for all living organisms (*Figure 2*). Errors could cause aneuploidy or genetic instability, which may lead to cell death or abnormalities such as malignancy.[36] The mitotic cell cycle comprises four main phases (G1, S, G2, M) leading to the generation of two daughter cells having a full set of chromosomes, one centrosome and the appropriate levels of cytoplasm and organelles. For this process to occur correctly, protein kinases involved in cell cycle regulation have to be coordinated. In case of an eventual error, checkpoints are present throughout the cell cycle either to arrest the process until repair occurs or to induce apoptosis if too much damage has been caused.[36]

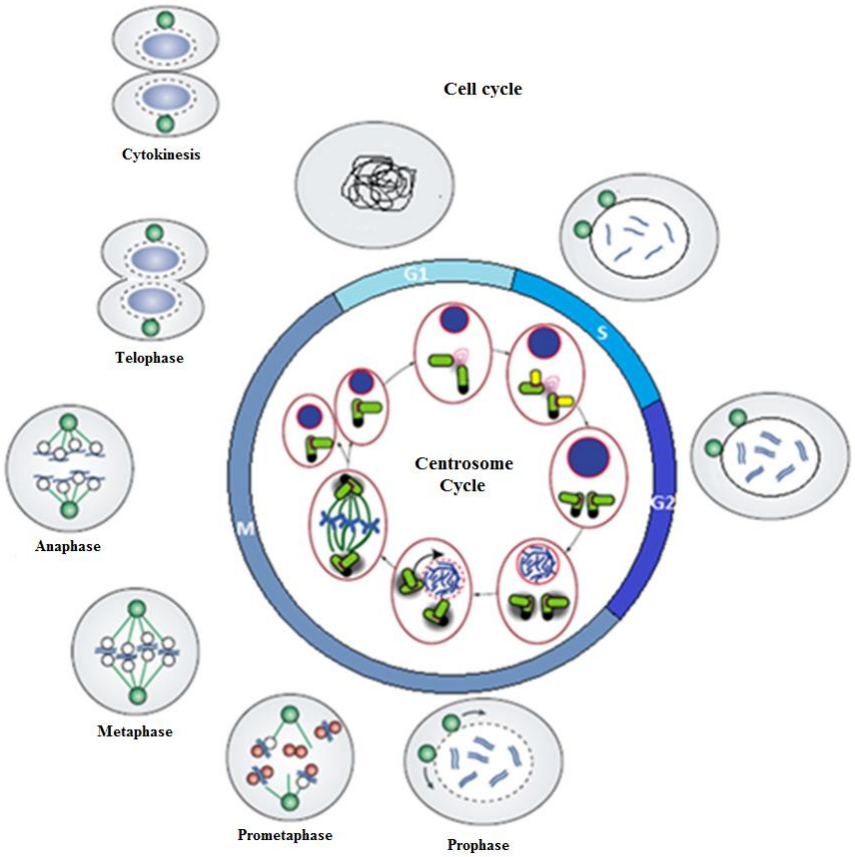

Figure 2 – The cell and centrosome cycle[37](adapted from A. R. Barr and F. Gergely, 2007) – Illustration of the different phases of the cell cycle (G1, S, G2, M) including details of mitosis, and the centrosome cycle showing the different steps in centrosome duplication and separation.

In G1 phase, chromatin condenses in the cell. Meanwhile, centrioles, components of the centrosome, undergo dissolution of their link.[37] During S phase, the link between the two centrioles is weakened which allows duplication of the centrosome. This phenomenon occurs at the same time as DNA replication. The bond between the old centriole and the new one is then reinforced to prevent further replication.[37] Before migrating apart to opposite poles, centrosomes recruit an additional pericentriolar matrix in late G2. The separation of centrosomes occurs simultaneously with the nuclear envelope breaking down. After this event, centrosomes start nucleating microtubules. Once microtubules have been generated, kinetochores of mitotic chromosomes attach to them during prometaphase, and form a bipolar spindle structure.[37] When all of the chromosomes are attached to microtubules and form an equatorial plane (metaphase), sister chromatids and centrosomes undergo segregation to opposite poles (anaphase). Once sister chromatids and centrosomes are located at each pole, the nuclear envelope is formed around them (telophase), and the chromatids disintegrate. Finally, two new cells are formed, in a process known as cytokinesis.[37]

1.2.2 The cyclin-dependent kinase (CDK) family

To date, thirteen CDKs have been identified in humans (CDK1 to CDK13).[38] They have been shown to be activated by binding to cyclin-related proteins and cyclins, which are regulated throughout the cell cycle. Proteins possessing a cyclin-binding element have also been identified in addition to the thirteen CDKs (*Figure 3*).[38] They do not have a CDK name as they have not been shown to bind to a cyclin partner, but the similarities between them and CDKs 1-13 make them members of the CDK family. CDKs can be separated into two mains groups, those involved in the cell cycle and others having a different function.

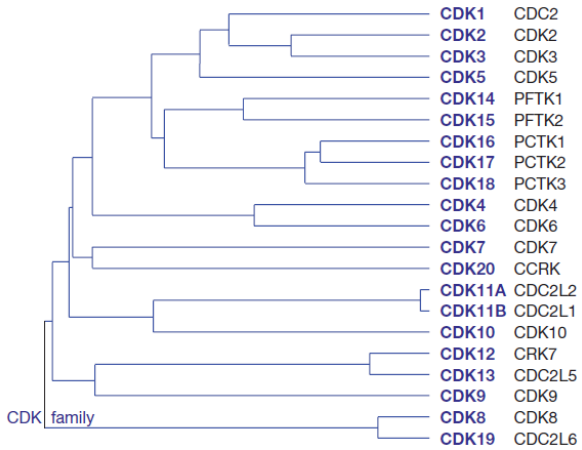

Figure 3 - Evolution of CDKs[38] (from M. Malumbres *et al*, 2009)

- *CDKs governing the cell cycle*

The best-characterised members of the CDK family are those highly involved in the cell cycle.[39] Each CDK member will have a preference for binding to a specific cyclin (CYC) partner, which will direct cell cycle progression (*Figure 4*).[39]

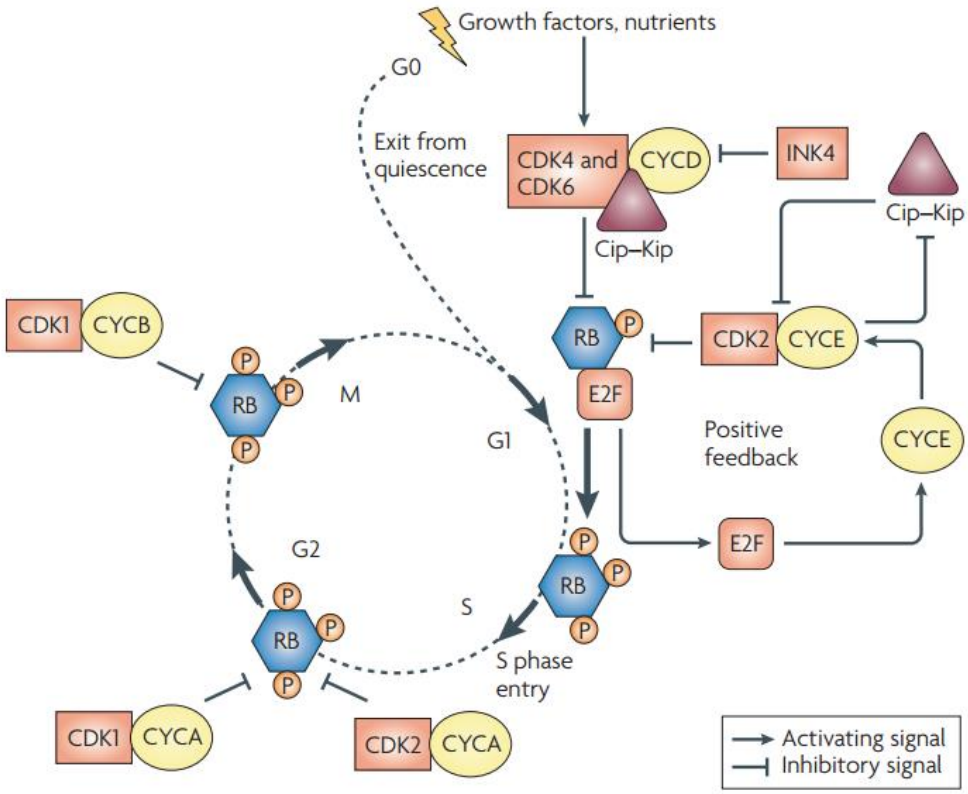

Figure 4 - Presence of CDK-cyclin (CYC) complexes during the cell cycle[40] (from S. Lapenna and A. Giordano, 2009)

Progression from G0 to G1 involves three CDKs: CDK4, 6 and 2, and their regulators. Mitogen signals stimulate the synthesis of cyclin D, while CDK4 and CDK6 are transported to the nucleus.[41] Activation of CDK4 has been studied, revealing its instability when alone. Thus, Hsp90 and p50^{Cdc37} assemble with CDK4, representing a chaperone complex essential for CDK4 stability (*Figure 5*).[41]

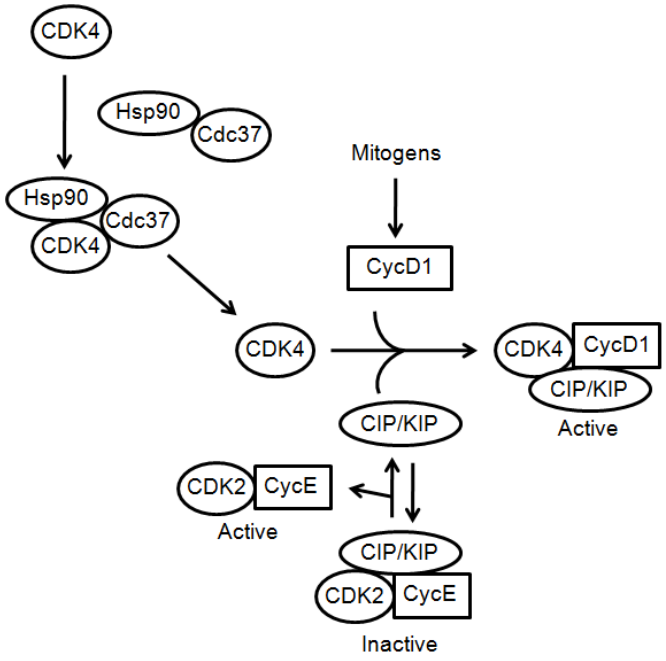

Figure 5 - CDK4 transport and activation[41] (from J. W. Harper and P.D. Adams, 2001)

CDK4 is released from its chaperone complex when in the presence of cyclin D. CIP/KIP proteins facilitate the binding, and thus the assembly, of CDK4 and cyclin D.[41] These two proteins are either freshly synthesised or released from the CDK2/cyclin E inhibition complex. Indeed, the CIP/KIP complex plays a role of inhibitor for the CDK2/cyclin E complex, but acts as an activator for the CDK4/cyclin D complex.[41] CDK4/cyclin D and CDK6/cyclin D complexes accumulate in G1 and phosphorylate members of the retinoblastoma (Rb) protein family. Phosphorylation of the Rb protein activates the synthesis of cyclin E which binds to CDK2. However, the CDK2/cyclin E complex is silenced by $p27^{KIP1}$, a cyclin-dependent kinase inhibitor (CKI).[41] In order to activate the CDK2/cyclin E complex, CDK4/cyclin D sequesters $p27^{KIP1}$ releasing activated CDK2/cyclin E. The activation of the CDK4/cyclin D/$p27^{KIP1}$ complex is a two step process where $p27^{KIP1}$ has to be phosphorylated first to allow phosphorylation of CDK4 by the CAK complex.[42] The phosphorylation of $p27^{KIP1}$ promotes the assembly and activation of the CDK4/cyclin D/$p27^{KIP1}$ complex, reducing the inhibitory effect of $p27^{KIP1}$ towards CDK2/cyclin E.[43] This last complex phosphorylates pRb inducing a positive feedback until reaching a level of activated CDK2/cyclin E complex sufficient to phosphorylate $p27^{KIP1}$, leading to its degradation by proteasomes.[41] At this point, pRb is irreversibly inactivated. The cell is now independent of mitogenic signals, and this is termed the restriction point (R) (*Figure 6*).[41]

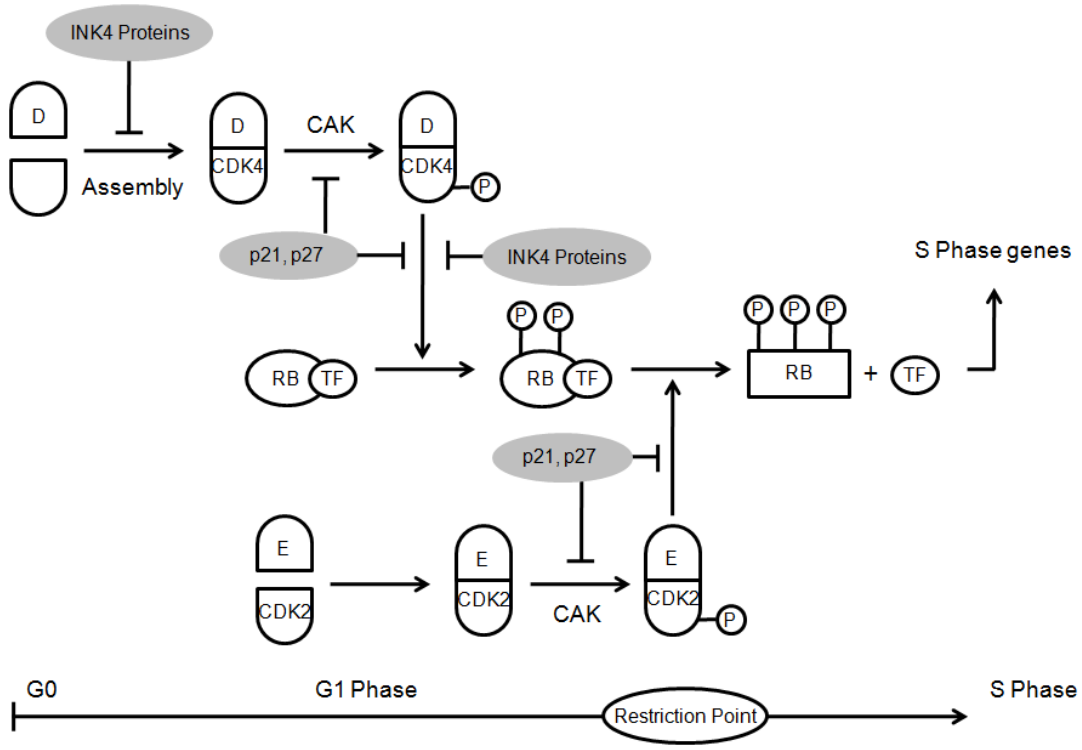

Figure 6 - Hyperphosphorylation of pRb triggering G1/S transition[44] (from G. K. Schwartz and M. A. Shah, 2005)

In parallel to pRb and $p27^{KIP1}$ inhibition for activation of S-phase kinases, pre-RC complexes, required for DNA replication in S-phase, are synthesised.[41] Thus, during G1, Anaphase Promoting Complex (APC), an E3 ubiquitin ligase, demonstrates high activity and as a consequence CDK/cyclin activity is low. At the restriction point, the activity is reversed, leading to inactivation of the APC complex (*Figure 7*).[41]

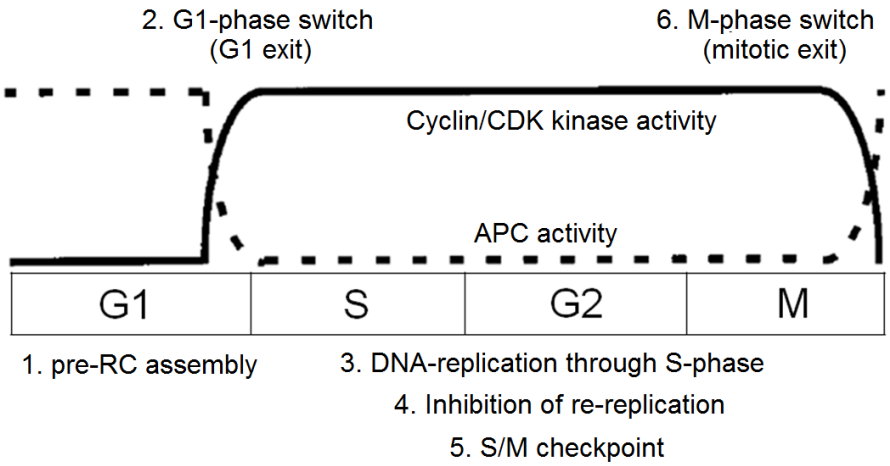

Figure 7 - APC activity versus CDK/cyclin activity throughout the cell cycle[41] (from J. W. Harper and P. D. Adams, 2001)

In S-phase, DNA replication starts as well as histone synthesis, where the CDK2/cyclin E complex is involved.[39] New DNA binds to histones and assembles into chromatin. To ensure only one replication, the CDK2/cyclin E complex is silenced by degradation of

cyclin E by Skp1/Cdc53/F-box (SCF) ubiquitin ligase.[39] Inhibition of pRb in late G1 leads to the synthesis of cyclin A and B during S phase. Once the CDK2/cyclin E complex has dissociated, CDK2 binds to the splice variants cyclin A1 and A2. The new CDK2/cyclin A complex is responsible for phosphorylation of several proteins essential for S phase exit.[39] At the end of S phase, cyclin A binds preferentially to CDK1 over CDK2 forming the CDK1/cyclin A complex. During G2, cyclin A is degraded by ubiquitin-mediated proteolysis while cyclin B is synthesised.[39] With degradation of cyclin A, CDK1 binds to cyclin B to form CDK1/cyclin B, essential for the mitosis trigger. This complex is responsible for the phosphorylation of more than 70 proteins involved in G2-M transition and through mitosis. To exit mitosis, cyclin B is degraded via ubiquitination by the APC complex.[39]

As explained by CDK orchestration of the cell cycle, CDK activity is tightly controlled by its regulators, cyclins and cyclin-dependent inhibitors (CKIs). In order to be active, the CDK/cyclin complex needs to be phosphorylated in its conserved T-loop.[39] This phosphorylation is catalysed by the CDK-Activating Kinase (CAK) complex, comprised of CDK7, cyclin H and Mat-1, which can be found mostly alone or with the core TFIIH, a multi protein complex with dual roles in transcription and DNA repair.[45] The phosphorylated CDK/cyclin complex can be inhibited by CKIs (CIP/KIP).[39] In addition, CDK can be inactivated in its monomeric form by direct binding with CKIs (INK4).[39] Eventually, when CDK binds to cyclin to form a complex not yet active, this complex can be phosphorylated by Wee1 and Myt1 kinases. This negative process is reversible thanks to the activity of Cdc25 phosphatases (*Figure 8*).[39]

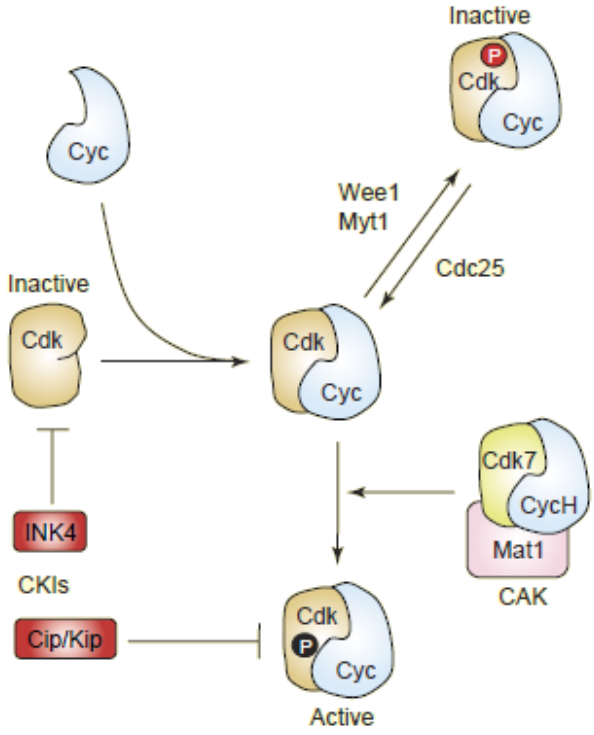

Figure 8 - Activation/inactivation of CDKs[39] (from M. Malumbres and M. Barbacid, 2005)

- *CDK activation*

CDKs are inactive in their monomeric form. For full activation, CDKs require binding to a cyclin and phosphorylation of their activation loop. However, the order of these two events differs among the CDKs, and it is likely that each CDK complex is regulated in its own way *in vivo*.[46] CDK2 comprises an N-terminal lobe (β-sheets), a C-terminal lobe (α-helix) and an ATP-binding site, that are common to other protein kinases, located at the interface of the two lobes.[47] For CDK2, the unique features are its PSTAIRE sequence (in red, *Figure 9*) and the regulatory loop (in yellow, *Figure 9*).

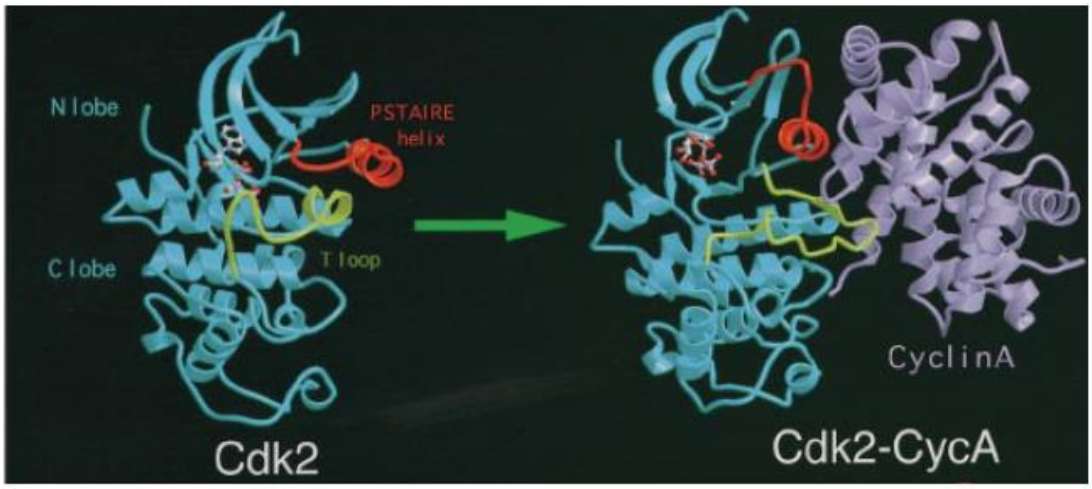

Figure 9 - Structures of CDK2 alone and in complex with cyclin A[47] (from N. P. Pavletich, 1999)

The CDK catalytic subunit is constituted of 298 amino acids in length.[47] In its inactive form, the T-loop blocks access to the substrate binding site and the conformation of the ATP pocket limits interactions with the phosphate group of ATP.[48] Binding of cyclin A to the PSTAIRE helix of CDK2 induces conformational changes including a repositioning of the PSTAIRE helix into the ATP-binding site and a realignment of the T-loop, enabling entry to the ATP-binding pocket.[47] These changes constitute the first step of the activation, and at this stage, the CDK2/cyclin complex possesses little enzymatic activity. The second activation step is phosphorylation of the T-loop by the CAK complex, accompanied by conformational changes,[47] which increase the reactivity of the complex by 1000-fold (*Figure 10*).[49] More recently, studies *in vivo* showed that CDK2 was likely to be phosphorylated in its monomeric form, and then to bind to its cyclin partner. Interestingly, these studies revealed that for CDK1, phosphorylation and cyclin-binding are mutually dependent *in vivo* and need to occur simultaneously.[46] The kinetic difference, observed *in vivo*, of CDK phosphorylation by the CAK complex and assembly with cyclin partners is likely to rule the selectivity and timing of CDK/cyclin complex formation during the cell cycle.

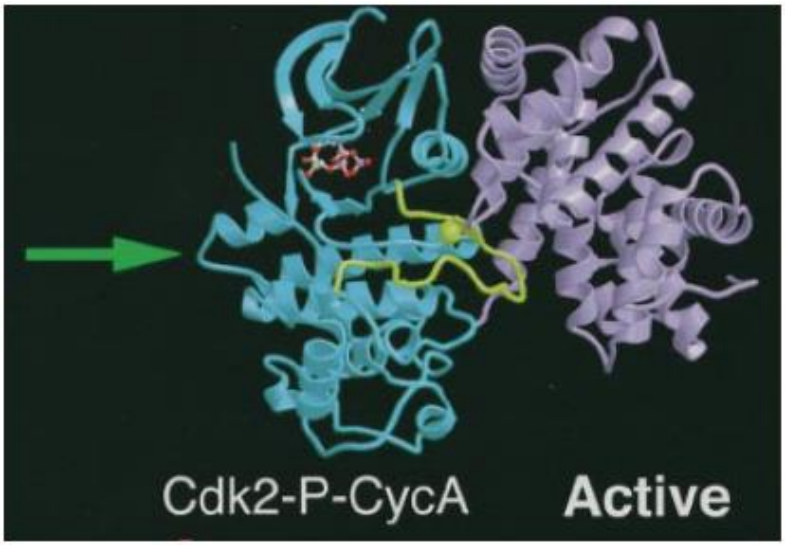

Figure 10 - Structure of the activated CDK2/cyclin A complex showing CDK2 in blue, cyclin A in purple, the activation loop in yellow and ATP binding to CDK2[47] (from N. P. Pavletich, 1999)

- *Cyclin-dependent kinase inhibitors (CKIs)*

As explained previously, CDKs can either be inactivated in their monomeric form or when in complex with a cyclin, by the binding of a CKI or by phosphorylation as reversible processes. Two types of cyclin-dependent kinase inhibitor exist: p21/27 and

INK4, which differ in structure, mechanism of inhibition and specificity.[50] Their mode of action is shown in *Figure 11*.

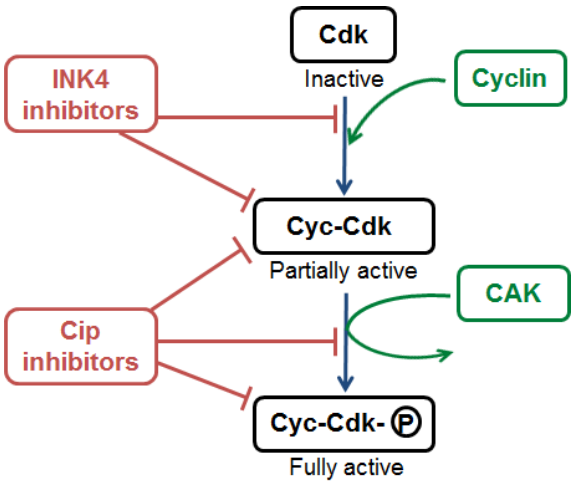

Figure 11 - CKI mode of action[47] (from N. P. Pavletich, 1999)

p21-27 family members possess a conserved amino-terminal domain of 60 residues responsible for binding and inhibition of CDKs. These inhibitors target CDKs especially at the G1/S phase.[50] The protein p21 preferentially inhibits cyclin E and D dependent kinases.[51] The level of p21 is controlled by p53. In the event of DNA damage, p53 stimulates the synthesis of p21 which will bind to and inhibit CDK/cyclin complexes, leading to cell cycle arrest during DNA repair (*Figure 12*).[51]

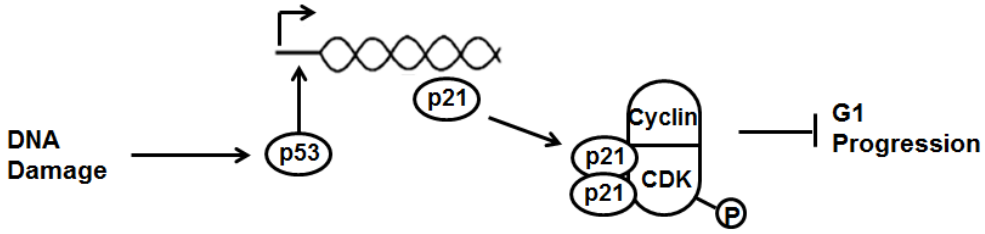

Figure 12 - Role of p21 in cell cycle arrest[51] (from C. J. Sherr and J. M. Roberts)

Protein p27 preferentially inhibits cyclin D, E, A and B dependent kinases.[51] The interaction between p27 and the CDK2/cyclin A complex has been studied.[47] Thus, p27 blocks the ATP-binding site, acting as a competitive inhibitor, by mimicking the interactions (hydrogen bonds and Van der Waals interactions) between the ATP molecule and the ATP-binding pocket of CDK2, through the insertion of an α-helix.[47] This binding invokes conformational changes preventing phosphorylation by the CAK complex (*Figure 13*).[51]

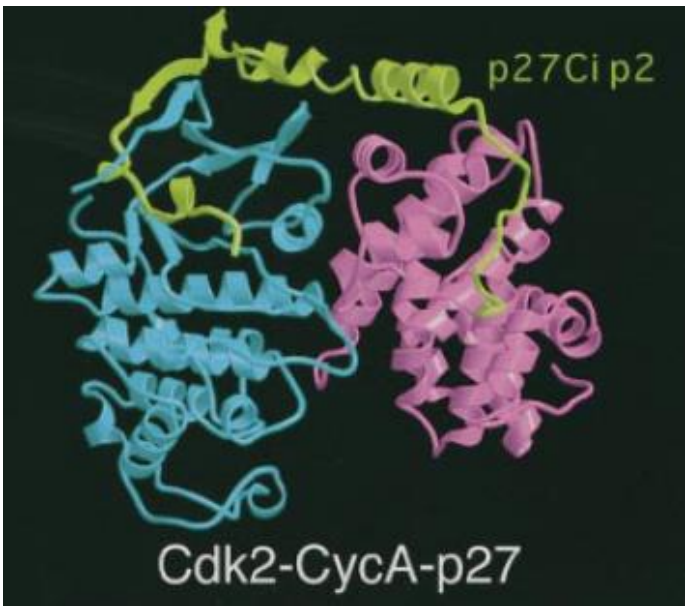

Figure 13 - p27 binding to the CDK2/cyclin A complex showing CDK2 in blue, Cyclin A in purple and p27 in yellow[47] (from N. P. Pavletich, 1999)

The INK4 family comprises p15, p16, p18 and p19, and is selective for CDK4 and 6.[50] These proteins will directly bind to CDK4 and 6 preventing assembly with cyclin D. A high level of $p16^{INK-4a}$ causes G1 arrest when CDK4/cyclin D and CDK6/cyclin D levels are too low to phosphorylate pRb.[50] After the restriction point, p16 as well as other members of this family downregulate cyclin D-dependent kinase activity.[51] The assembly of $p16^{INK-4a}$ and CDK6 has also been studied.[47] p16 interacts with both N- and C-lobes leading to allosteric changes, which further block cyclin binding. The interaction is responsible for misalignment of the N- and C-lobes, and the PSTAIRE helix (*Figure 14*),[47] causing a distortion in the ATP site reducing its ATP-binding efficiency.[47]

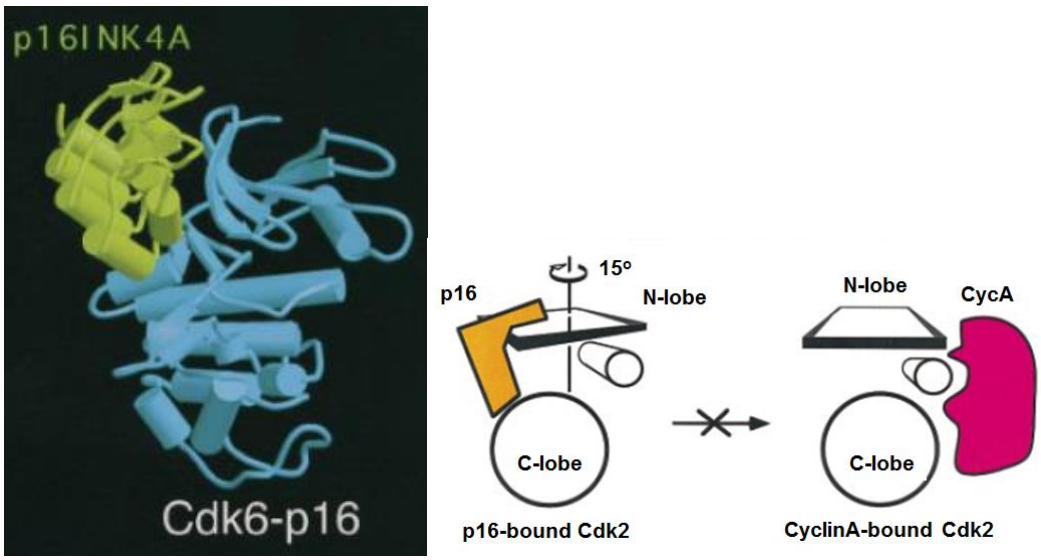

Figure 14 – Structure of p16 (in yellow) binding to CDK6 (in blue) and a schematic representation of p16 (in orange) interacting with the N- and C- lobes of CDK2 preventing the assembly with cyclin A (in pink)[47] (from N. P. Pavletich, 1999)

- *Other endogenous cyclin-dependent kinase inhibitors*

The dual-specificity kinases, Wee1 and Myt1, can phosphorylate CDK/cyclin complexes.[48] They have been shown to phosphorylate CDK1 on Thr14 (Myt1) and CDK2 on Tyr15 (Wee1),[48] and their phosphorylation affects kinase activity without blocking the ATP-binding site. CDK1/cyclin B is phosphorylated and remains inactive until the end of G2. Dephosphorylation by Cdc25 phosphatases leads to activation of the CDK1/cyclin B complex.[48]

1.2.3 Never-In-Mitosis A related kinases (Nek kinases)

Nek kinases are mammalian homologues of the Never In Mitosis A (NIMA A) protein in *Aspergillus nidulous* and Fin1 in fission yeast (*Table 1*).[52] NIMA is a serine-threonine kinase, first isolated in 1975,[53] and found to be essential for mitotic entry.[54] NIMA is implicated in the localisation of the CDK1/cyclin B complex to the nucleus to trigger chromatin condensation as well as spindle formation. Fin1 and NIMA have also been shown to play a role in cytokinesis.[55]

Table 1 - Nek2 members (*adapted from Fry, 2002*)[55]

Kinase	Species	Accession number	Percent identity to Human Nek2 in catalytic domain	Proposed functions
Nek2	Human	P51955	100	Centrosome separation Centrosome organisation
	Mouse	O35942	93	Chromatin condensation
NIMA	*Aspergillus*	P11837	44	Mitotic entry Chromatin condensation Localisation of cyclin B Replication checkpoint
Fin1p	*Schizosaccha-romyces pombe*	CAB11653	41	Mitotic spindle formation SPB organisation Mitotic entry Nuclear envelope integrity

The first members of the mammalian Nek family to be characterised were Nek1, 2 and 3 by Pawson and Nigg in the early 1990s.[56] Since then, eight other members have been identified.[57] In the early 1990s, Nurse and Hunter demonstrated that kinases related to NIMA might be mitotic regulators of the cell cycle, as they played an important role in mitosis.[58] The Nek family, with eleven members, represents 2% of the entire kinome. They share 40% of their N-terminal catalytic domain with NIMA, but differ from the C-terminal domain, which confers their own specificities.[59] From the eleven members, four have been shown to be involved in mitotic progression: Nek2, 6, 7 and 9 (*Figure 15*).[52]

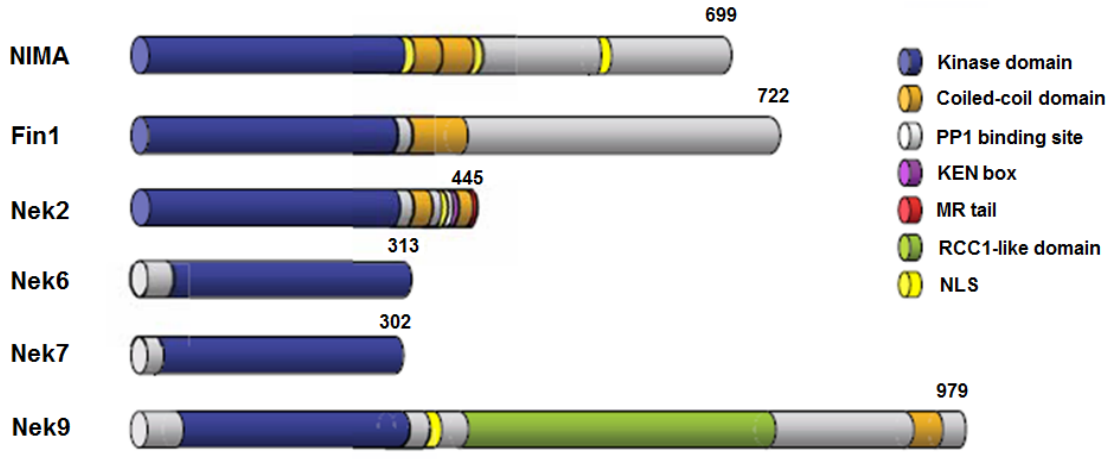

Figure 15 – Comparison of structures of Nek members[52] (from L. O'Regan *et al*, 2007)

- *Nek2*

Nek2 is the closest member to NIMA and Fin1 in terms of homology of the catalytic domain.[55] The kinase exists as three splice variants: Nek2A, 2B and 2C.[60, 61] The last of these, however, has not been widely studied or compared to Nek2A and 2B whose structures are shown in *Figure 16*. Nek2B possesses the same catalytic domain and leucine zipper (LZ) as Nek2A but differences lie in their C-terminal domain. Nek2A possesses a coiled-coil (CC) domain, a PP1c binding site and a KEN-box, not present in Nek2B.[55]

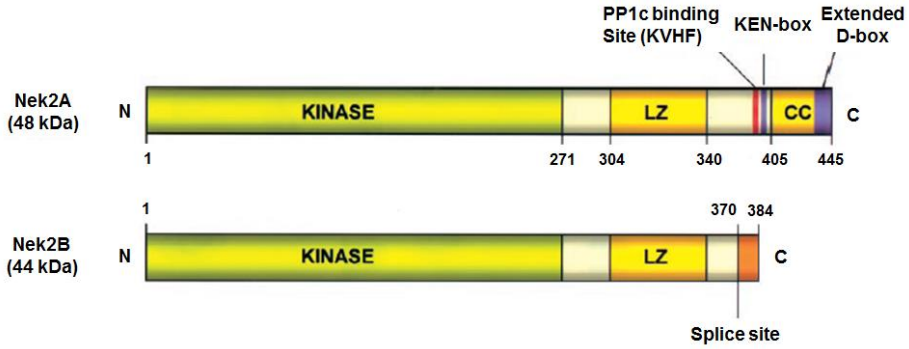

Figure 16 - Nek2A and 2B kinase domains[55] (from A. M. Fry, 2002)

Nek2 is found at the centrosomes and mitotic spindle poles throughout the cell cycle.[55] However, its concentration varies. During G1 phase, Nek2A and 2B are expressed at a low level, but at the G1/S transition, their concentrations increase until reaching a constant concentration that is maintained throughout S and G2 phases.[55] At the onset of mitosis, Nek2A disappears, being degraded by the APC/C protein complex, leaving Nek2B intact but decreasing the overall Nek2 concentration.[55]

The main role of Nek2 is to trigger centrosome separation at the G2/M transition (*Figure 17*).[52] Nek2 phosphorylates the C-Nap1/rootletin complex, two major components of the intercentriolar linkage maintaining the two centrosomes close to each other.[62, 63] This phosphorylation induces dissociation of the C-Nap1-rootletin complex and therefore breaks the link between the two centrosomes.[52] Until the onset of mitosis, Nek2 is inactivated by PP1 which binds through the KVHF motif in the C-terminal region.[64] At the G2/M transition, CDK1 stimulates binding between PP1 and Inh-2 (Inhibitor-2 protein) resulting in the activation of Nek2.[52] Nek2 can bind to and inhibit PP1, allowing auto-phosphorylation and activation.[65]

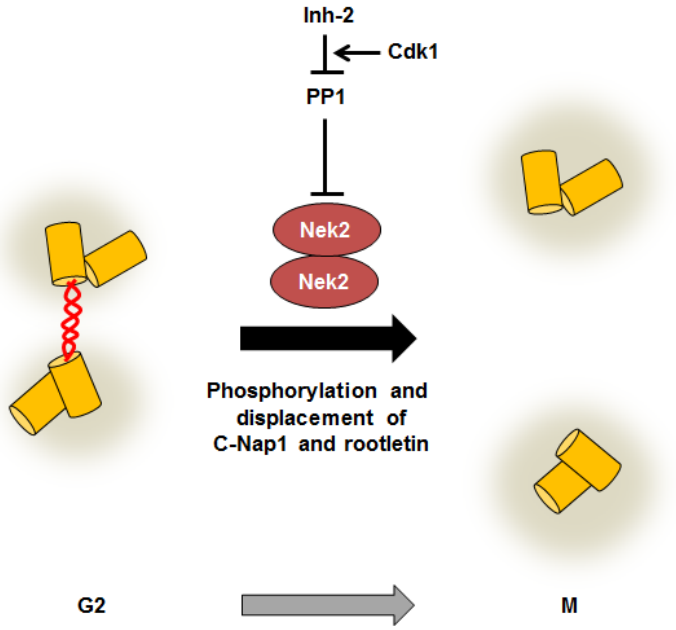

Figure 17 - Nek2 role in the G2/M phase[52] (from L. O'Regan *et al*, 2007) – CDK1 promotes the binding between Inh2 and PP1, activating Nek2. Phosphoylation of the C-Nap1/rootletin complex (in red) by Nek2 induces centrosome separation.

Nek2 has also been shown to be involved in microtubule organisation through the activation of Nlp ((Nep1)-like protein) and centrobin, both implicated in microtubule anchoring.[52] Plk1 (Polo-like kinase 1) was also suggested to be a substrate of Nek2 as Nlp is a substrate of Plk1.[52, 66] Nek2 could play an additional role in late mitosis/cytokinesis because depletion of Nek2B results in a delay in mitotic exit.[55]

Nek2 may also be directly involved in the mitotic checkpoint (*Figure 18*). Nek2 was shown to phosphorylate the Mad2/Cdc20 protein complex and also to interact with Hec1 (Highly expressed in cancer 1) and Mad1 (Mitotic arrest deficient-like 1).[67] When kinetochores are not properly attached to microtubules, Mad2 adopts a conformation allowing binding to Cdc20, leading to its inhibition.[67] Cdc20 normally activates the APC/C complex which in turn degrades securin, a protease separase inhibitor, resulting in chromosome segregation. By binding to Cdc20, Mad2 stops the segregation.[67] Therefore, by associating with the Mad2/Cdc20 complex, Nek2 might interfere with the mitotic checkpoint leading to aneuploidy and tumourigenesis.[67]

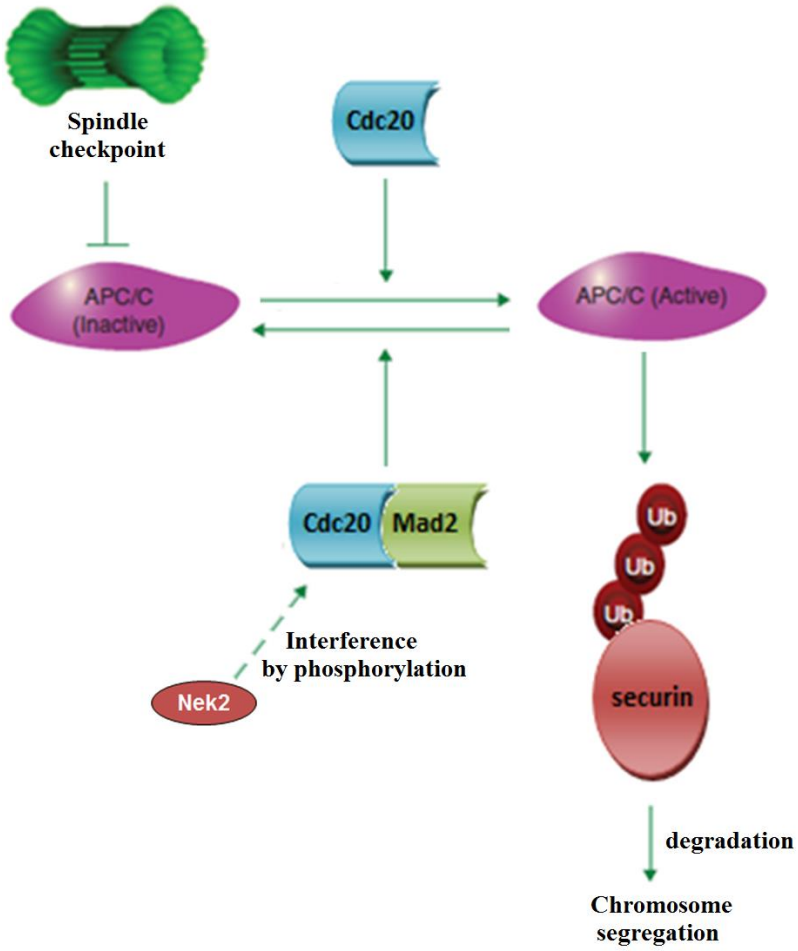

Figure 18 - Nek2 and the mitotic checkpoint – At the spindle checkpoint, the APC/C complex, activated by Cdc20, triggers the ubiquitination of securin leading to chromosome segregation. Progression to chromosome segregation can be stopped by association of Mad2 with Cdc20, a complex which can be phosphorylated by Nek2.

- *Other Nek members involved in mitosis*

Nek6 and 7 share 87% sequence identity in their kinase domains and differ only within the N-terminal domain.[59] Nek7 levels are constant during the cell cycle and are concentrated at centrosomes during interphase and mitosis, suggesting a role in recruiting γ-tubulin and homologues.[68] By contrast, Nek6 appears to be highly expressed during mitosis.[69] Both Nek6 and 7 may be substrates of Nek9 and activated through phosphorylation. To date, no substrates of Nek6 and 7 have been identified, and further investigations of these two members are needed to understand whether they have the same role.[52]

Nek9 is expressed at a constant level throughout the cell cycle but its kinase activity reaches a peak on spindle poles in mitosis.[70] Two regions of Nek9 seem important for its function: RCC1 is responsible for auto-inhibition of Nek9, permitting reasonable Nek9

concentration, and the coiled-coil domain is essential for its kinase activity, as depletion leads to a drop of activity.[52] Nek9 is involved in spindle organisation by regulating the anchoring of centrosomal microtubules by recruitment of γ-tubulin,[52] and has been shown to be essential in chromosome segregation but not for mitotic entry.[52]

1.2.4 Other cell cycle-associated kinases

Polo-like kinases (Plks) are serine-threonine kinases, with the first Plk being discovered in *Drosophila melanogaster*.[71] Four members have been identified to date: (i) Plk1 is present in late G2 and M phase and regulates mitosis,[72] (ii) Plk2, found in early G1, controls entry into S phase,[72] (iii) Plk3 is present at a constant concentration during the cell cycle and may have a function at the G2/M transition,[72] (iv) Plk4 is involved in mitotic exit.[72] Although the Plk family has several members, only Plk1 has been widely investigated, with the role of Plk2, 3 and 4 remaining unclear.

The first Aurora kinase was identified in *D. melanogaster* mutants having spindle-pole defects.[73] In mammals, three serine-threonine kinases have been identified, known as Aurora A, B and C.[74] Aurora A and B have been demonstrated to be closely involved in cell division, whereas less is known about Aurora C, which is mainly present in testis.[75]

1.3 Protein kinases as drug targets

1.3.1 Protein kinases in drug discovery

Protein kinases (PKs) catalyse the transfer of a phosphate group from adenosine-5'-triphosphate (ATP) to an amino-acid substrate, releasing adenosine diphosphate (ADP) in the process[76] (*Figure 19*). Protein phosphorylation controls a range of biological mechanisms, such as signal transduction, metabolism, transcription, cell cycle progression, cytoskeletal rearrangement, cell movement, apoptosis and differentiation.[77] Phosphorylation can be reversed by phosphatases.

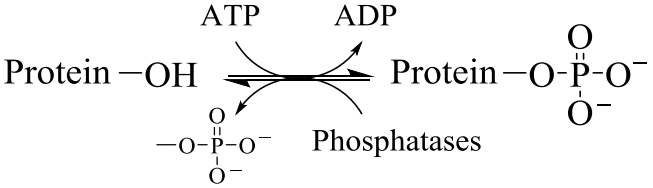

Figure 19 – Protein phosphorylation and dephosphorylation[40] (from S. Lapenna and A. Giordano, 2009)

As protein phosphorylation is essential for various biological mechanisms, disruption of this process can lead to diseases such as arthritis, diabetes, inflammation, and

immunological, neurological and metabolic disorders as well as cancer.[78, 79] In 1978, Erikson showed the oncogene potential of a protein kinase and, in 1981 Castagna demonstrated the activation of protein kinase C (PKC) by tumour promoting phorbol esters[80] (*Figure 20*). In the late 1980s, after the discovery of the activity of staurosporine against PKC, the pharmaceutical industry started to investigate protein kinase inhibitors as possible drugs.[80] But it was not until the late 1990s that the first protein kinase inhibitor, fasudil, reached the Japanese market for the treatment of cerebral vasospasm.[80] However, the myth that no potent and selective PK inhibitor was possible ended with imatinib, the most famous example of a successful PK inhibitor.[80] Selective inhibition of PKs was shown to be feasible and well tolerated by normal cells in comparison to tumour cells.[79] Since the discovery of Imatinib, PKs represent attractive targets as they are involved in every phosphotransfer cascade controlling signal transduction. Environmental and genetic alterations are the main causes of deregulation of kinase function, one of the hallmarks of many pathological conditions.[81] Approximately 180 kinases were shown to be deregulated in cancers, the immune system and infections.[81]

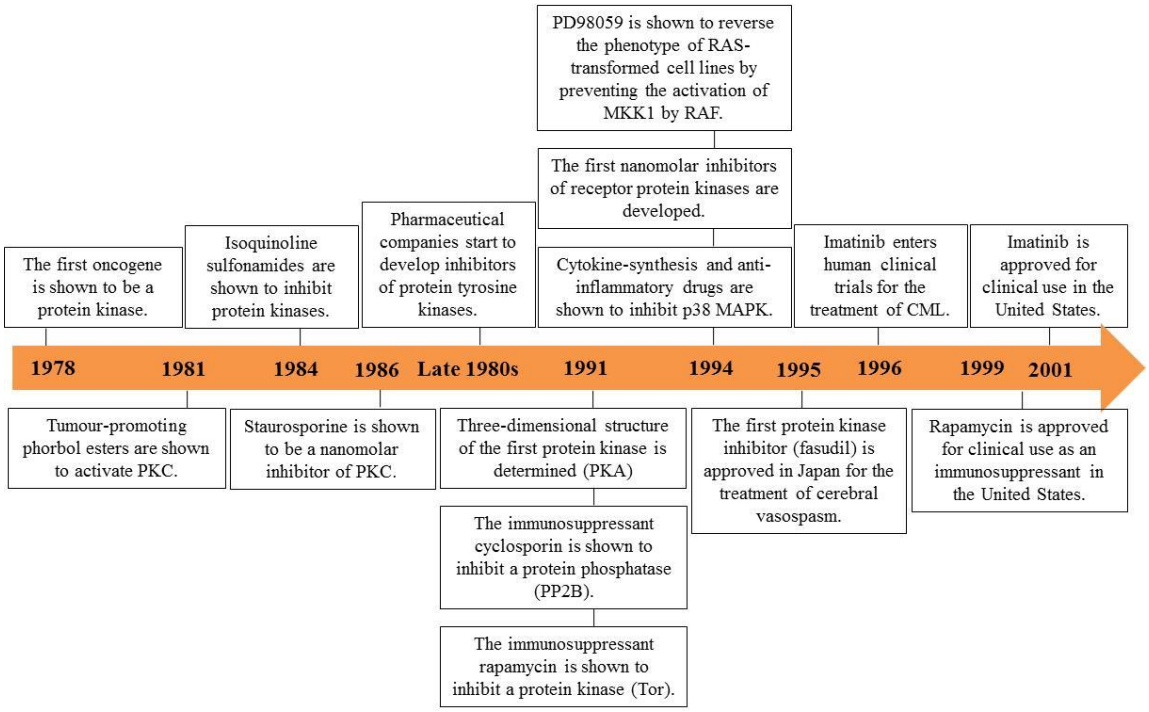

Figure 20 - Timeline of kinase inhibitor drug discovery during the 20th century[80] (from P. Cohen, 2002)

1.3.2 Protein kinase classification

The human kinome comprises 518 protein kinases, representing 1.7% of all the human genes, and 106 kinase pseudogenes that are non-functional copies of kinase genes.[77] The

human kinome is one of the largest families of genes in eukaryotes. Among the 518 kinases, 478 have been identified with a common domain called the eukaryotic protein kinase (ePK) catalytic domain.[77] The remaining 40 kinases show similar activity to the other kinases but lack the ePK domain.[77] Kinases are classified into groups, families and subfamilies according to their catalytic domain similarities, their biological functions and their similarities outside of the catalytic domain.[77] Kinases belonging to the same family have similar structure. There are seven main families, which are the AGC family named after the protein kinase A, G and C, the CAMK family with Ca^{2+}/CAM-dependent PK, the CK1 (casein kinase 1) family, the CMGC family named after the CDK, MAPK (mitogen-activated protein kinases), GSK (glycogen synthase kinases) and CDK-like kinases, the STE family, the TK (tyrosine kinase) family and the TK-like family.[82]

Another method of classification of kinases is by the amino acids that they phosphorylate.[82] Protein kinases can either transfer a phosphate group to a tyrosine residue or a serine or threonine residue, or both. They are thus separated into two main classes: tyrosine kinases and serine-threonine kinases.[82] The human kinome includes 420 serine-threonine kinases and 94 tyrosine kinases.[81]

1.3.3 Kinase structure

Protein kinases have a common general structure. They are constituted of two lobes connected by a hinge region.[78] The N-terminal lobe is formed by β sheets and one α helix, and the C-terminal lobe is mostly α helical domain with a segment called the activation loop (T-loop), a phosphorylation site to trigger kinase activity, and limited by the gatekeeper residue (*Figure 21*).

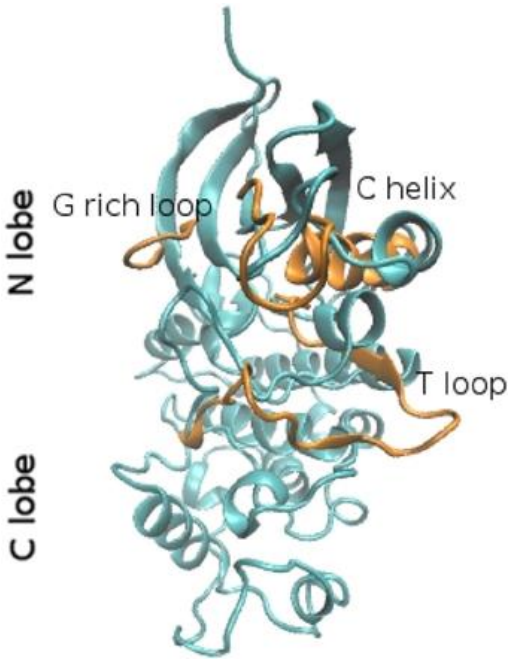

Figure 21 – Structure of CDK2 illustrating the general structure of kinases with the N-lobe containing the C-helix and the C-lobe including the T-loop – CDK2 inactive conformation in blue and CDK2 active conformation in orange[83] (from M. D'Abramo *et al*, 2014)

Understanding how ATP binds to the kinase is helpful in the design of inhibitors. The triphosphate group of ATP interacts with a group of conserved kinase residues.[76] More particularly, the triphosphate moiety and the basic side chains of these residues showed some affinity. These interactions are well conserved throughout the kinome, in contrast to the adenosine moiety binding which is less conserved.[76] *N*-1 of ATP is engaged in an interaction with hydrogen bond-donor localised within the hinge region.[76] In addition, *N*-7 of ATP interacts with hydrogen bond-acceptor carbonyl also situated in the hinge region.[76] These hydrogen bond interactions are often mimicked by small-molecule inhibitors (*Figure 22*).

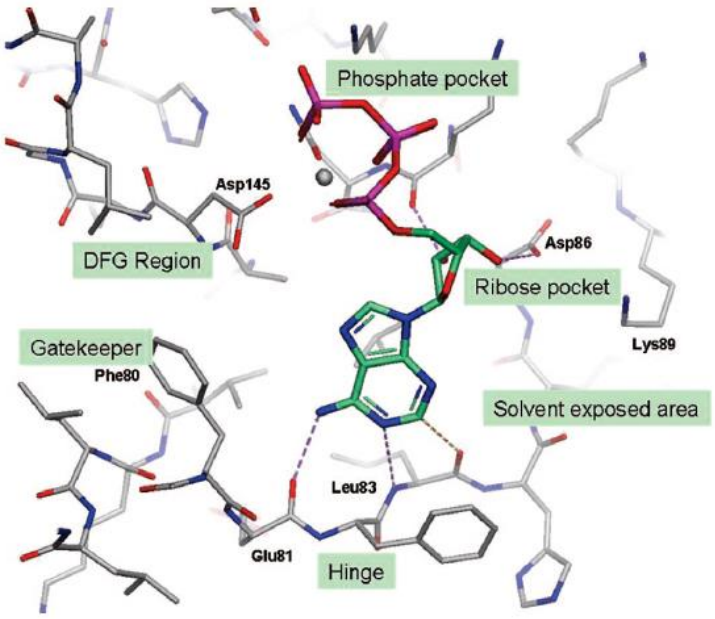

Figure 22 - ATP in complex with the CDK2 ATP-binding site[84] (from P. G. Wyatt *et al*, 2008) – the key regions are highlighted: Phosphate pocket, ribose pocket, DFG region, gatekeeper, solvent exposed area and the hinge. (Drawn from PDB code 1HCL)

In the protein phosphorylation process, the limiting step is ADP release. ATP and ADP have similar structures, so if ATP binds to the kinase, ADP is most likely to have affinity for the kinase too. However, to catalyse another phosphorylation, the kinase must release ADP to allow another ATP molecule to bind. Specific polar sites are present in the ATP binding site to facilitate ADP release by reducing the affinity of ADP for the kinase.[76] Other regions of the kinase around the ATP pocket can be exploited in the design of selective inhibitors, such as the hydrophobic pocket, adjacent to *N*-6 of adenosine, the hydrophobic channel, next to the ribose flank and the gatekeeper residues.[76] These pockets differ within the kinome and allow inhibitor selectivity.

1.3.4 Active/Inactive conformation of kinases

A kinase can be found either in its active or inactive conformation.[82] Serine/threonine and tyrosine kinases possess a conserved catalytic domain but also a conserved active conformation, rendering selective inhibition challenging.[77] For this reason, the inactive conformation appears more attractive as 'all active kinases are alike but an inactive kinase is inactive after its own fashion'.[78] The first inactive conformation to be identified was in CDK2[85] and Src[86] kinases. Since the discovery of these two inactive conformations, others have been described including those in Abl,[87] Wnk[88] and Nek2.[89] Key structural features of the active form of the kinase were found to be essential in the catalysis of phosphate transfer.[90, 91] The importance of the activation loop, in particular

the DFG-motif (Asp-Phe-Gly) in the N-terminal region, the position of the helix αC and interactions formed by the HRD motif and glycine-rich P-loop was revealed.

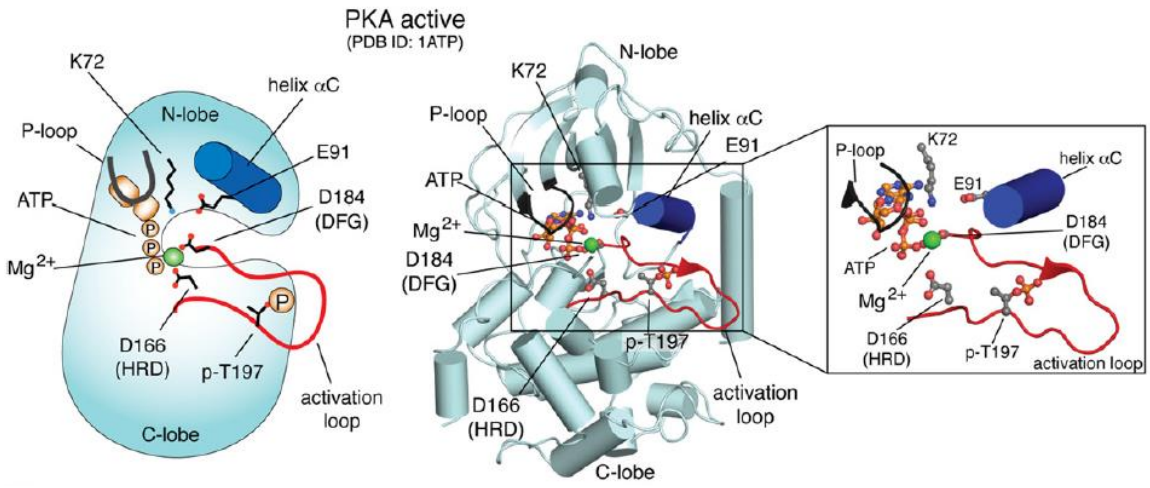

Figure 23 - Highlights of the key structural features of the active conformation of protein kinase A (PKA)[92] (from N. Jura *et al*, 2011) – activation loop, helix αC, P-loop, ATP, magnesium ion. The key catalytic residues are shown – DFG aspartate (D184), HRD aspartate (D166), catalytic lysine (K72), catalytic glutamate (E91) and the autophosphorylation site (T197).The PDB entry is 1ATP.

The side chain of the aspartate residue of the DFG-motif was shown to coordinate with Mg^{2+} and interact with the phosphate groups of ATP (*Figure 23*). In addition, the open conformation of the C-terminal region of the activation loop was highlighted, representing a platform for docking substrates.[92] A conserved glutamate residue (Glu91) in the helix α-C in the N-lobe of the kinase was demonstrated to be crucial for the active conformation as a salt bridge is formed between Glu91 and a conserved Lys72 (*Figure 23*). Both residues are important for the active conformation as mutations of Lys72 lead to the inactive conformation of the kinase.[93] The conserved HRD-motif (His-Arg-Asp) and the glycine-rich P-loop, both located in the active site, are key features of the active conformation. The glycine-rich P-loop was shown to interact with the phosphates of ATP (β and ɤ) when Asp166 of the HRD motif acts as a catalytic base with the substrate (*Figure 23*).[92]

In addition to the key structural features in the active conformation, the assembly/disassembly of hydrophobic residues forming intramolecular networks between N- and C- lobes correlates with the active/inactive conformation of the kinase[94, 95] (*Figure 24*). The first network, called the 'regulatory spine', is constituted of four residues, Leu106, Leu95 (from helix α-C), Phe185 (from the DFG-motif) and Tyr164 (from the HRD-motif) and is involved in substrate binding.[92] The assembly of the regulatory spine is dependent on the change of orientation of helix α-C and the HRD-

motif, caused by displacement of the activation loop upon activation.[94] The second network, known as the 'catalytic spine', possesses residues in the C-lobe, more specifically in helix α-F and α-D, and in the N-lobe (Ile174, Leu173, Val57, Ala70).[92, 95] Following ATP binding, the adenine ring is located in the catalytic spine and the network establishes a connection between the N- and C-lobes. Both regulatory and catalytic spines are linked by the helix α-F, which binds to the catalytic network by Met231 and Leu227, and to the regulatory network by Asp220.[92]

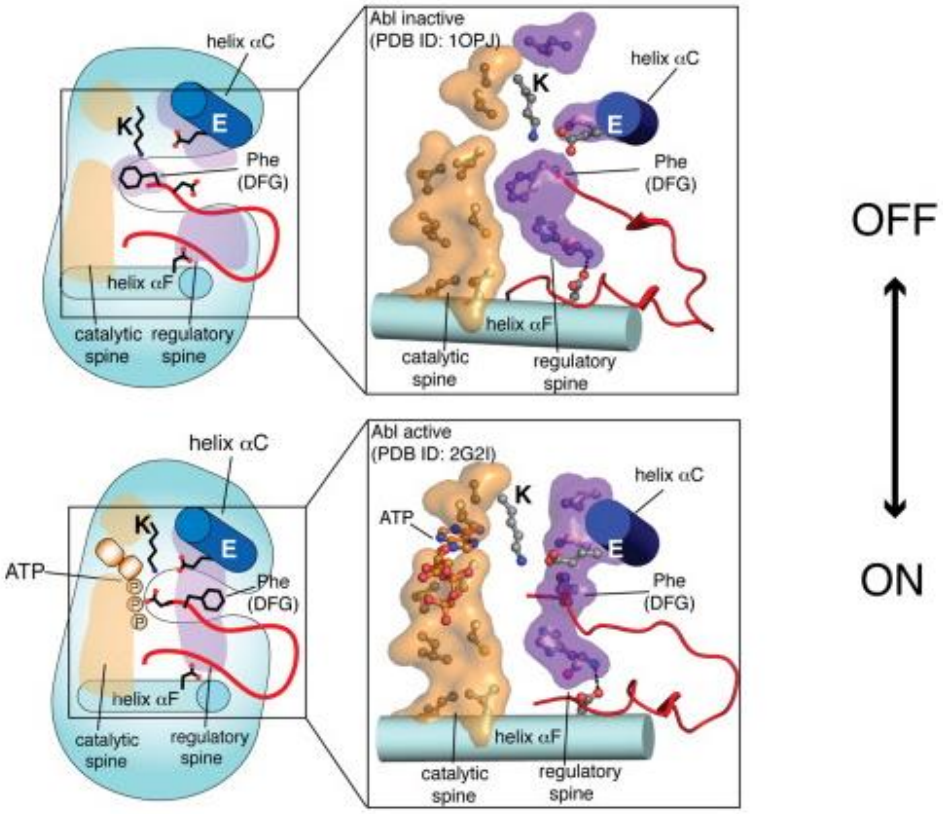

Figure 24 - Structural differences between the active and inactive conformation of a protein kinase (Abl kinase) illustrating the catalytic and regulatory spines and key residues, DFG-phenylalanine, catalytic lysine (K) and catalytic glutamate (E)[92] (from N. Jura *et al*, 2011) The PDB entries are 1OPJ and 2G2I.

Several active and inactive conformations of kinases were studied, highlighting differences with the activation loop being found to block binding of substrates.[96] This same activation segment also interfered with the ATP-binding pocket resulting in its blockade.[96] The glycine rich loop was also found to be distorted.[96] Finally, in some cases, a salt bridge exists between a Glu residue situated at the centre of the α-C helix and a Lys residue which binds to the triphosphate of ATP. This was shown to be disrupted because of the misalignment of the α-C helix in the N-terminal lobe due to the change of

conformation.[96] In all inactive conformations of kinases, at least two of the disruptions described above were found, with 60% involving the ATP-binding site blockade.[96]

1.3.5 Protein kinase inhibition by small molecules

Targeting protein kinases selectively remains challenging as they represent one of the largest gene families, and the ATP-binding site is well conserved among the kinome.[81] To date, only a small number of kinases are inhibited by kinase inhibitors approved by the FDA, while around 180 kinases have been identified as attractive targets.[81]

Table 2 - Kinase inhibitors in oncology accepted by the FDA from 2001 to 2014[97] (from T. Barf and A. Kaptein, 2012)

Generic name	Year of approval	Indication	Target kinase
Imatinib	2001	CML	Abl, c-Kit, PDGFRα/β
Gefitinib	2003	NSCLC	EGFR
Erlotinib	2004	NSCLC, pancreatic cancer	EGFR
Sorafenib	2005	Hepatocellular carcinoma, RCC	Raf, VEGFR2/3, c-Kit, PDGFRβ
Sunitinib	2006	GIST, RCC	C-Kit, VEGFR, PDGFR, FLT3
Dasatinib	2006	CML	Abl, c-Kit, PDGFR, Src
Nilotinib	2007	CML	Abl, c-Kit, PDGFR, Src, ephrin
Lapatinib	2007	Breast cancer	EGFR, ErbB2
Pazopanib	2009	RCC	VEGFR, PDGFRα/β, c-Kit
Vandetanib	2011	Thyroid cancer	VEGFR, EGFR, RET
Vemurafenib	2011	CML	Abl, c-Kit, PDGFR, Src, ephrin
Crizotinib	2011	NSCLC (ALK +ve)	ALK, MET
Ruxolitinib	2011	Myelofibrosis	JAK1/2
Axitinib	2012	RCC	VEGFR, PDGFRα/β, c-Kit
Bosutinib	2012	CML	Bcr Abl/SRC
Afatinib	2013	NSCLC	EGFR/ErbB2
Ibrutinib	2014	MCL, CLL	BTK

Drug discovery projects based on kinase inhibition represent some 30% of projects conducted by the pharmaceutical industry, making kinases the second most exploited target after G-protein coupled receptors (GPCRs).[98] Two classes of inhibitors exist:

covalent (or irreversible) inhibitors and non-covalent (or ATP-competitive) inhibitors, with the latter having received the most attention. From 2001 to 2014, of 17 approved kinase inhibitors, only two irreversible inactivators (afatinib (**6**) and ibrutinib (**8**)) have been approved by the FDA in oncology (*Table 2*).

- *Reversible inhibitors*

Most kinase inhibitors are ATP-competitive inhibitors making one to three hydrogen bonds with amino acids within the kinase hinge region, thereby mimicking interactions between the hinge region and the adenine ring of ATP.[79] Most of the inhibitors being developed do not exploit the ribose or the triphosphate bonding site.[79] Reversible inhibitors targeting the active conformation of the kinase, by binding to the ATP-pocket, are known as Type 1 inhibitors. Most of them possess a heterocycle localised in the adenine-binding region of the ATP pocket. Functional groups are added to the heterocyclic core to occupy regions not exploited by ATP, such as hydrophobic pockets, to improve selectivity and potency.[81] Vemurafenib (**1**) is a selective inhibitor of the most common mutant form of the oncogenic B-Raf tyrosine kinase, ^{V600E}B-Raf.[99] This compound exploits structural differences between the mutant and wild-type forms of B-Raf, and was shown to cause melanoma tumour growth regression in patients having the ^{V600E}B-Raf mutation by inhibiting the MAPK signalling pathway. In patients not bearing this mutation, vemurafenib seemed to enhance tumour growth.[99] Another example is vandetanib (**2**), originally investigated in clinical trials in combination therapies for patients with advanced stage NSCLC or with metastases. As no benefits were observed, this drug was withdrawn from clinical trials in 2009.[100] However, two years later, vandetanib was the first drug approved by the FDA for the treatment of metastatic medullary thyroid cancer, and was given to patients ineligible for surgery.[100]

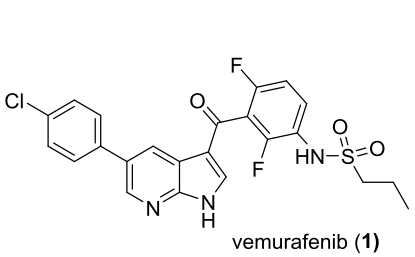

vemurafenib (**1**)

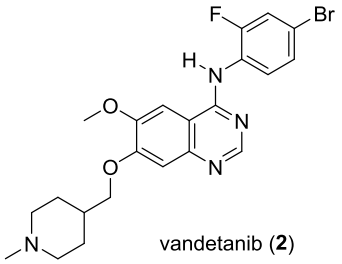

vandetanib (**2**)

Reversible inhibitors targeting the inactive conformation of a kinase are called Type 2 inhibitors. As explained previously (Chapter 1, section 1.3.4.), by moving from its active to inactive conformation, the enzyme creates a new environment for inhibitors to exploit for selectivity purposes. In the inactive conformation of Abl-1, the activation loop forms

a new hydrophobic pocket next to the ATP-binding site, which is non-existent in the active form. Imatinib exploits this new pocket (*Figure 25*).[79]

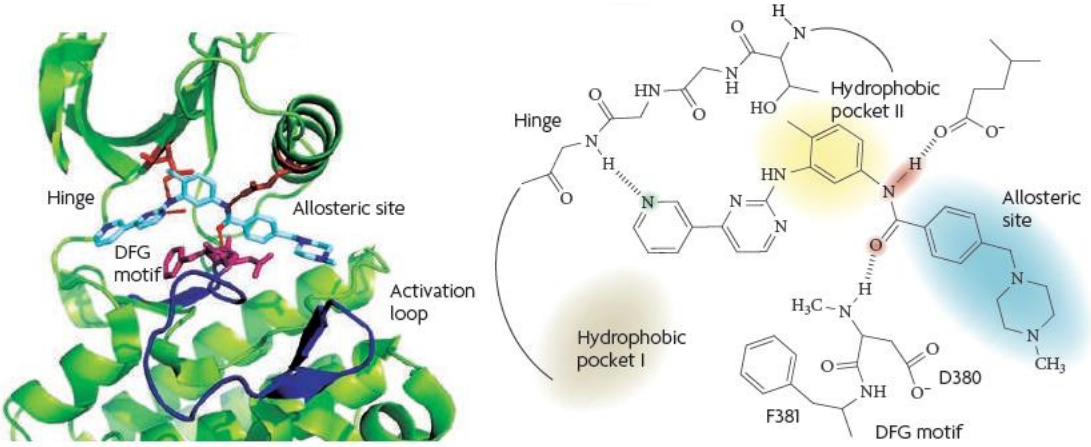

Figure 25 - Imatinib in complex with the inactive conformation of ABL1[79] (from J. Zhang *et al*, 2009) - The interactions between Imatinib and the protein are illustrated in the cartoon. The PDB entry is 1IEP.

The ATP-binding site is a well conserved site among kinases, rendering selectivity challenging. In addition, when designing ATP-competitive inhibitors, potency needs to be high for the inhibitors to compete with ATP in the cell ([ATP] = 5-15 mM).[40] Some reversible inhibitors are designed to bind to allosteric sites situated outside of the ATP pocket, and are known as allosteric inhibitors.[79] As allosteric sites are more specific to an individual kinase, these inhibitors tend to be highly selective.

- *Covalent inhibitors*

Irreversible inhibitors have been avoided in drug discovery programs because of the perceived safety and toxicity problems associated with them.[97] Compounds metabolised to highly reactive intermediates were studied in the 1970s, showing that covalent binding between these metabolites and liver proteins caused hepatotoxicity.[101] Non-selective irreversible inhibitors can bind to proteins, DNA and glutathione.[102] Drugs that are either non-selective or metabolised into active metabolites may be responsible for direct tissue damage or haptenisation of proteins, triggering an immune response (*Figure 26*).[101] In addition, with covalent inhibitors, a risk for idiosyncratic toxicity is to be considered even when no particular toxicological problems are encountered in preclinical models.[102]

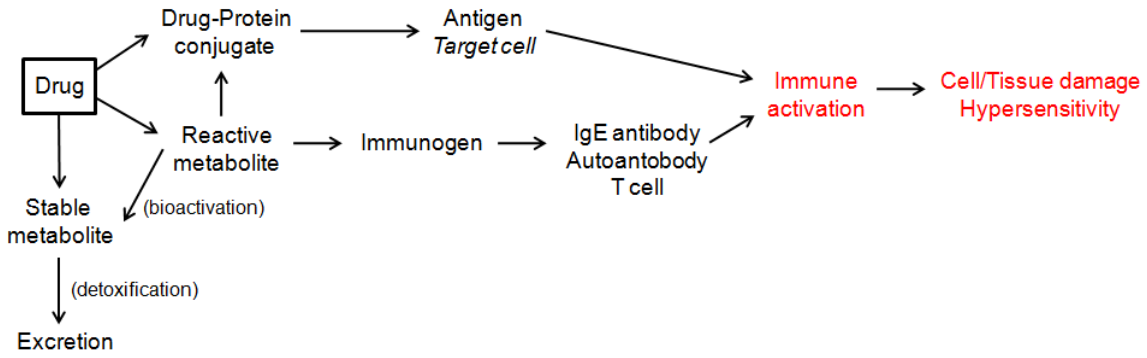

Figure 26 - Possible effects arising from covalent drugs[102] (from M. H. Potashman and M. E. Duggan, 2009)

Even though the physiological response to formation of a drug-protein complex is difficult to predict, several covalent drugs have been accepted by the FDA, with 20% in cancer therapy.[101, 102] Among these drugs, lansoprazole, clopidogrel (**5**) and esomeprazol (**9**) are examples of successful and effective marketed covalent drugs, as in 2009, they were classified as blockbusters in the top 10 selling drugs in the USA.[101]

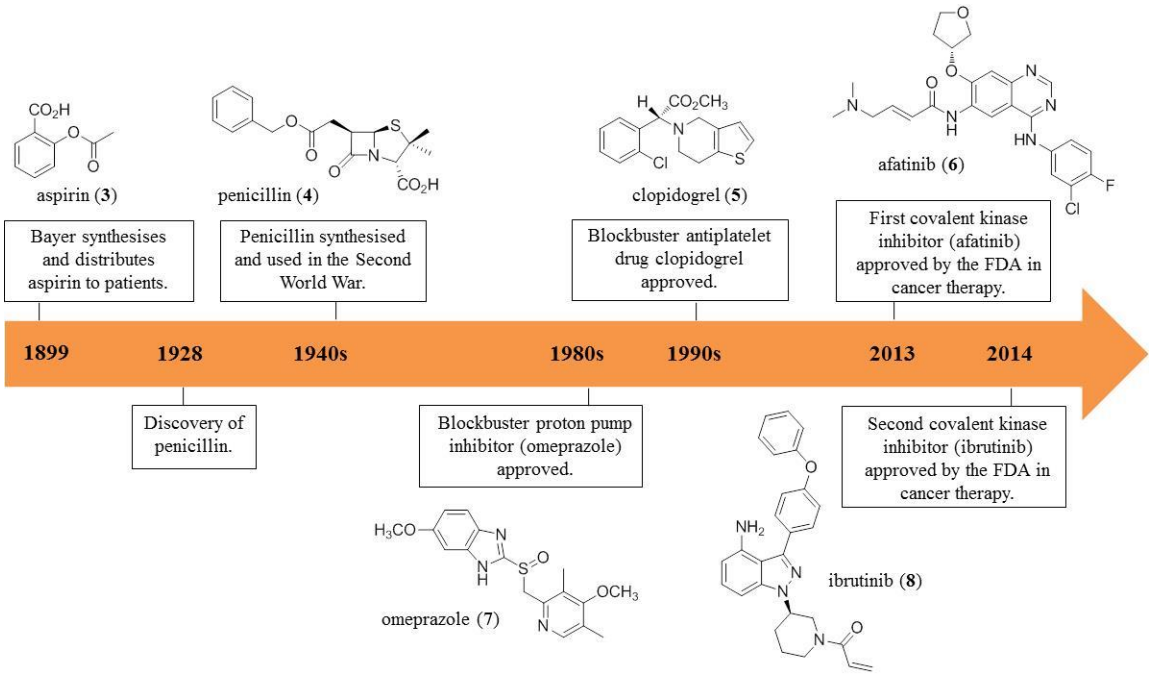

Figure 27 - Progress of covalent drugs from the 19th to the 21th century[101] (from J. Singh *et al*, 2011)

Covalent binding is not a new concept in drug discovery as the most widely consumed drug in the world is a covalent inhibitor (*Figure 27*). Thus, aspirin (**3**) is responsible for acetylation of a serine residue of cyclooxygenase 1, near the active site. Its mechanism of action was determined long after aspirin was licenced for pharmaceutical use.[103] Esomeprazole (**9**), the (*S*)-enantiomer of omeprazole (**7**) approved in the 1980s, is a proton pump inhibitor (PPI) use for gastrointestinal reflux disease. This drug is converted

into a covalent modifier of the proton pump by acid in the gastric environment (*Figure 28*).[104] Clopidogrel (**5**) is an anti-clotting agent used for treating vascular disease that was approved in the 1990s. The drug's effect is due to covalent binding to P2Y, a G-protein complex receptor.[105] Covalent drugs in oncology have been developed following a new strategy of 'targeted covalent inhibitor' (TCI), where the covalent drug targets a non-catalytic nucleophile, unique or poorly conserved among the kinome.[101] Neratinib, an irreversible pan-inhibitor of HER kinases, showed substantial activity in phase II clinical trials for the treatment of metastatic breast cancer as a monotherapy.[106] Another example is afatinib (**6**), a third generation inhibitor of EGFR which binds covalently to Cys797. This drug was approved by the FDA in 2013 for the treatment of metastatic NSCLC.[107] More recently, ibrutinib (**8**), a covalent inhibitor of BTK (Bruton's tyrosine kinase), has been approved by the FDA for the treatment of mantle cell lymphoma (MCL) and chronic lymphocytic leukaemia (CLL).[108] Ibrutinib was shown to react covalently with Cys481 through its acrylamide warhead.[109]

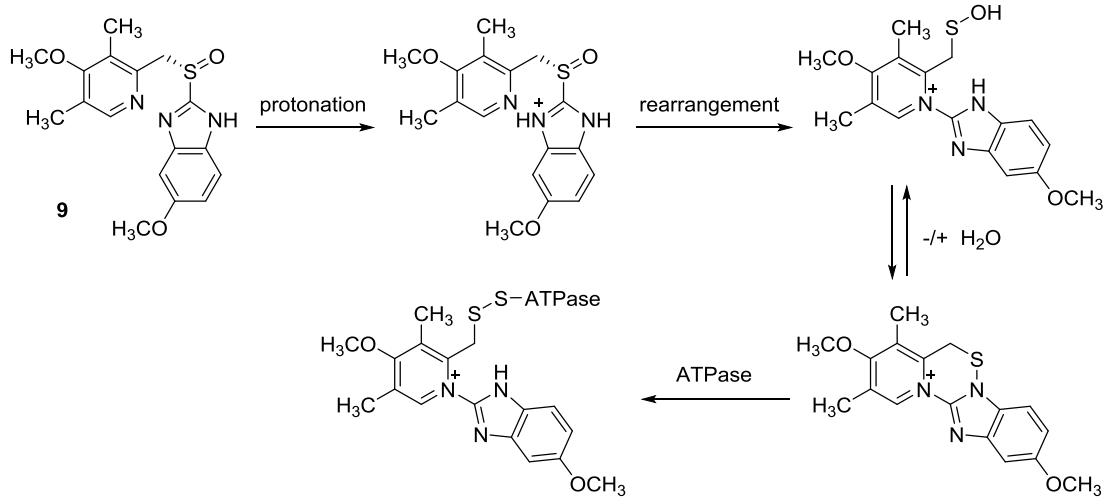

Figure 28 – Mechanism of action of esomeprazole (**9**)

In the concern of safety related to covalent drugs, the difference between highly reactive compounds and the TCI approach has to be emphasised. Highly reactive compounds are extremely electrophilic intermediates by comparison with the warheads of a TCI,[101] which are specific to one target, decreasing the risk of toxicity. However, the risk of haptenisation is still present but no current technology allows a useful risk assessment.[101] It is worth mentioning that to date, TCIs are considered for life threatening diseases where no effective therapies are available, and the benefits can therefore overcome potential immunotoxicity.[101] In the near future, more data will be available on the safety profile of TCIs thanks to current drugs in clinical trials. Until then, a compilation of toxicophores is available for medicinal chemists, listing pre-existing reactive electrophilic

functions and compounds likely to undergo metabolism. Another parameter to consider for safety purposes is the dose of drug administered to the patient. Most of the drugs withdrawn from the market were given at doses higher than 100 mg/day compared with less than 10 mg/day for drugs still on the market.[110] With covalent drugs, the dose can be lowered because target inhibition still persists after drug clearance. The enzyme's function is restored only after protein resynthesis thus differentiating pharmacokinetic from pharmacodynamic effects, therefore, giving more flexibility over the clearance of the drug.[111] This mechanism of action is a real advantage in drug resistance cases. Reversible inhibitors have to be administered more often because of their short half-life, which can lead to the development of resistance, in contrast to irreversible inhibitors that have a longer therapeutic effect.[101]

To understand better the advantages offered by covalent binding over non-covalent binding, the mechanism of action of irreversible inhibitors needs to be highlighted.[112] A covalent drug first binds in a non-covalent manner, by affinity for the protein, positioning its electrophile moiety near the specific nucleophile to be targeted (K_i). The drug then undergoes nucleophilic attack creating a covalent bond between the protein and the drug (k_2). In the case of an irreversible inhibitor, the covalent bond cannot normally be cleaved ($k_{-2} = 0$).[101] The covalent binding is dependent on the kinetics of each step (*Figure 29*). The non-covalent binding (K_i) needs to be long enough to allow nucleophilic attack (k_2) to take place. In addition, nucleophilic attack (k_2) needs to be fast enough to occur while the drug is binding non-covalently to the protein (K_i).[101]

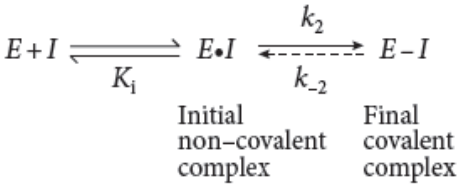

Figure 29 – Kinetics of binding of covalent drugs[101] (from J. Singh *et al*, 2011)

The formation of a covalent bond is an energetically favoured process offering high potency and good ligand efficiency.[113] Therefore, modulation and optimisation of parameters such as potency, selectivity or ADME properties are facilitated by the flexibility of structural modifications of irreversible inhibitors.[113] Possible off-target activity of covalent drugs appears to be the main concern of medicinal chemists as it is generally associated with toxicity, as explained above. Non-covalent drugs are rarely specific to only one target and are often shown to be weak inhibitors of other targets. Covalent inhibitors may offer a solution to minimise the off-target effect by giving the

opportunity to have a rapidly cleared drug after irreversible binding to the target of interest.[101] Studies have shown that the orientation of the electrophilic warhead is key for the reaction with a desired nucleophilic residue, allowing selectivity.[111] The real threat is when a protein, other than the one targeted, offers enough affinity for the drug to bind non-covalently and possesses a nucleophile allowing covalent binding.[101] Drug resistance can be limited with irreversible inhibitors as mentioned previously, and covalent binding offers a dual inhibition mechanism allowing drug resistance to be overcome. Mutations of the binding site, which dramatically affect the binding of a non-covalent drug, only affect the rate of the binding of the covalent drug.[101] Mutations of the nucleophile of interest may prevent covalent binding, but the inhibitor can still bind in a non-covalent manner.[101] Even after such mutations, irreversible inhibitors often still retain activity compared with ATP-competitive inhibitors.[114]

As the covalent drug mechanism is becoming better understood and thanks to their progress through clinical trials, then safety and efficacy information should encourage the development of this class of drugs.[101] From the mechanism of action, selectivity is a key parameter to limit off-target activity and, as a consequence, toxicity. Targeting a unique or poorly conserved nucleophile among the kinome is crucial for selectivity.[101] To date, only lysine and cysteine have been reported to react with kinase inhibitors thus creating a covalent bond,[97] and there is no report yet about nucleophilic attack from a serine or threonine residue on a kinase inhibitor. Targeting a lysine residue conserved among the kinome, such as the one located in the phosphate transfer region, would not be a good strategy for selectivity. The ideal lysine residue to target would be one located around the ATP pocket but uniquely positioned among the kinome. Reactions with lysine depend on a small equilibrium concentration of the free amino form as lysine residues are found largely in the protonated form (pK_a ~ 11). 5'-Fluorosulfonylbenzoyl adenosine (FSBA, **10**) is a compound used as an affinity label for kinases, and binds covalently to Lys56 of the non-phosphorylated and active form of p38ɣ.[97]

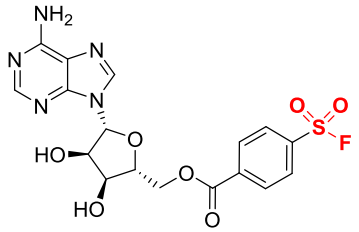

FSBA (**10**)

Cysteines are the most commonly targeted residues by covalent inhibitors. The thiol of cysteine has a pK_a of 8.5 but this value can decrease by up to 5 log units in a polar and positively charged environment.[97] Cysteine residues have been classified into four groups according to their positions in the kinase, plus another category corresponding to cysteines in the activation loop (*Figure 30*).

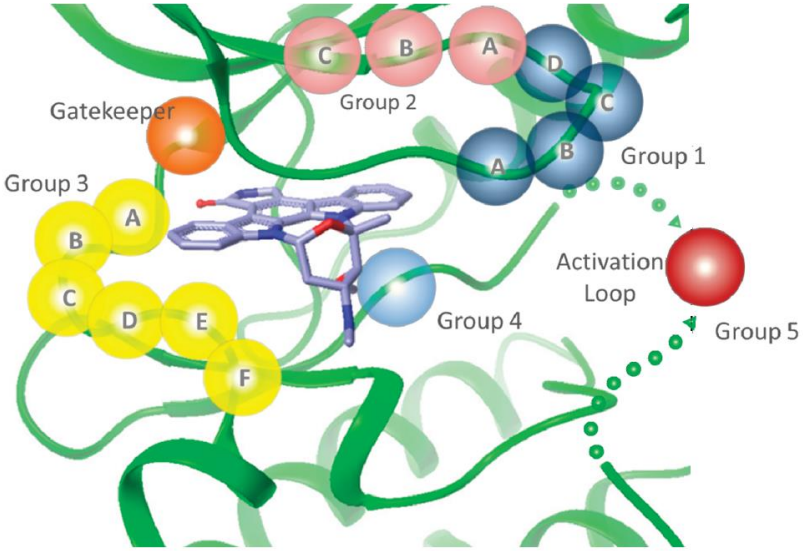

Figure 30 - Location of the cysteine residues in kinases[97] (from T. Barf and A. Kaptein, 2012) – The cysteine residues are classified into 5 groups depending on their location in the kinase. The gatekeeper residue and the activation loop are represented. The PDB entry is 1SM2.

One example of an inhibitor targeting cysteines positioned in the P-loop (Group 1) was reported. FIN-1 (**11**), a pan-inhibitor of FGFR 1, 2, 3 and 4, covalently binds to Cys486 by a Michael addition on its acrylamide moiety.[97, 115] Cysteines situated on the 'roof' of the ATP-binding site represent Group 2. Fluoromethylketone (FMK, **12**) is a small molecule covalent inhibitor of RSK1 and 2, binding by attack of Cys463 on its acyl fluoride motif.[116] Only nine other kinases have a cysteine located in subgroup 2B, offering an opportunity for selectivity. Among them are Nek2, Plk1-3, MSK1 and 2, MEKK1 and RSK3 and 4.[97] With the cysteines of Group 3 located in the hinge region and at the front of the ATP pocket, those belonging to subgroup 3F are of interest.[97] They are highly nucleophilic (low pK_a) compared with the other cysteines because of their position at the end of the αC helix. Only ten kinases are in this subgroup, offering also the possibility for selectivity.[97] PD168393 (**13**) is an inhibitor of EGFR (IC_{50} = 2 nM) and Her2 (IC_{50} = 114 nM). This compound was shown to bind covalently by reaction of Cys797 situated in the hinge region of EGFR on its acrylamide group.[117] Further development of this compound led to the synthesis of dacomitinib (**14**), currently in clinical trials for patients with advanced NSCLC.[118]

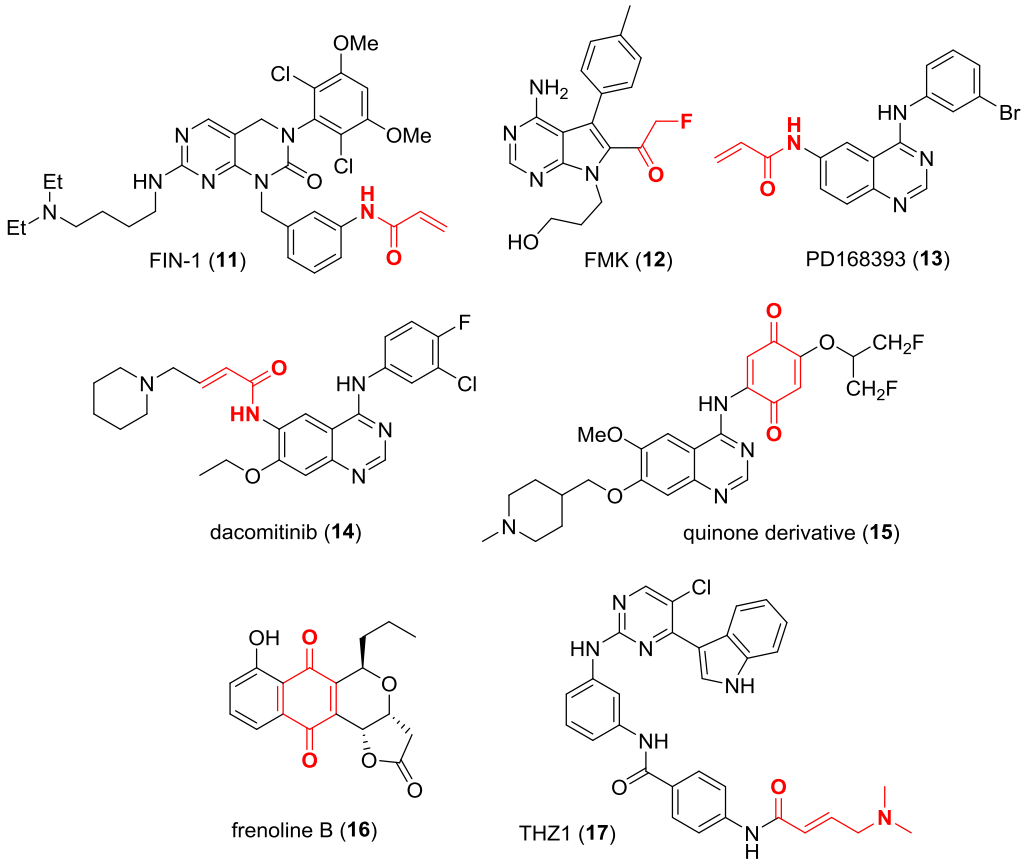

One particular cysteine residue, adjacent to the DFG-motif, is common to almost 10% of all kinases and forms Group 4.[97] A quinone derivative (**15**) was shown to bind covalently to Cys1045 of VEGFR-2 and exhibited a good selectivity profile despite the presence of the residue in other kinases.[119] The last group of cysteine residues (Group 5) is located outside of the ATP pocket within the activation loop. However, predictions as to the exact position of these cysteines are difficult because of the flexibility of the activation loop.[97] Frenoline B (**16**) is another quinonoid irreversible inhibitor of Akt-1 that binds to both Cys296 and Cys310 in the activation loop.[120] Recently, targeting a cysteine residue positioned outside the kinase domain has been achieved with the CDK7 inhibitor THZ1 (**17**).[121] This compound binds to CDK7 in a unique manner, combining interactions with the ATP-site and allosteric covalent binding to Cys312, found to be unique to CDK7 within the CDK family.

Each irreversible inhibitor possesses an electrophilic warhead allowing attack of a cysteine or lysine to form a covalent bond. Several motifs are found in these inhibitors such as Michael acceptors, epoxides or acetylenes (*Figure 31*).

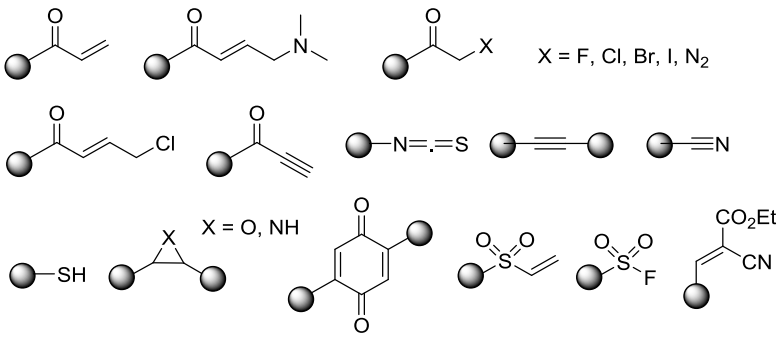

Figure 31 - Examples of electrophilic warheads[81] (from I. Shchemelinin *et al*, 2006)

Even though the kinome is composed of more than 500 kinases, only 20 of them have been targeted by irreversible inhibitors, predominantly directed at cysteine residues.[81] Until recently, only one example of an irreversible inhibitor of Nek2 has been reported (see Chapter 2, section 2.2.2.), but none for CDK2.

Chapter 2. Inhibiting the Cell Cycle Kinases, CDK2 and Nek2, in Cancer Therapy

2.1 Purines in drug discovery

Purine is the trivial name given to imidazo[4,5-*d*]pyrimidine in 1884 by Emil Fischer, who synthesised the molecule for the first time. He won the Nobel Price in 1902 for his research on sugars and purines. As shown in *Figure 32*, chemistry around the purine scaffold has been widely studied for the last 100 years, leading to the discovery of many drugs targeting numerous diseases.[122]

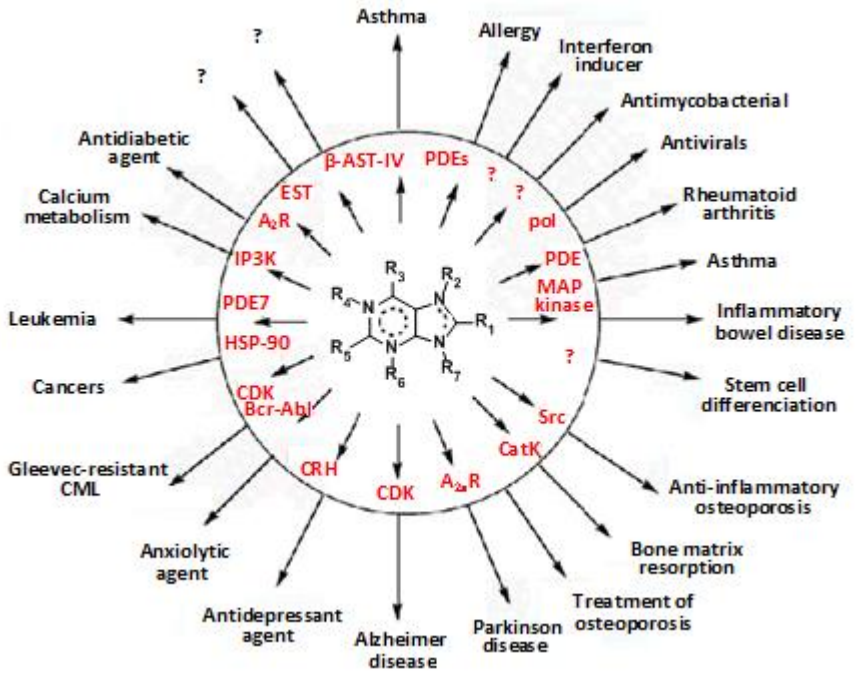

Figure 32 - Purines in drug discovery[122] (from M. Legraverend and D. S. Grierson, 2006)

Among promising drugs are 6-thio-N^9-substituted purines and agelasine (**18**) isolated from marine sponges of the *Agelas sp*. One of the components of the bone matrix is the Type I collagen whose degradation is catalysed by cathepsin K, a cysteine protease. This degradation is responsible for bone and cartilage breakdown. Targeting and inhibiting cathepsin K represents a promising strategy to treat osteoporosis. Novartis identified the interesting purine **19** *via* high-throughput screening, with the compound showing good inhibitory activity against cathepsin K (IC_{50} = 7 nM). Abnormal expression of corticotropin-releasing factor (CRF), a natural human response to stress, has been found in several neuropsychiatric diseases such as Parkinson's disease, Alzheimer's disease and depression. 2,6,9-Trisubstituted purines (*e.g.* **20**) have been identified as CRF1 antagonists and could thus be effective anxiolytic and antidepressant drugs. Another

example is the inhibition of the chaperone protein Hsp-90, a common target for all cancer types. For this reason, research has been focused on developing Hsp-90 inhibitors. An extensive SAR study on 2,8,9-trisubstituted-6-aminopurines led to the identification of compound **21**.[122]

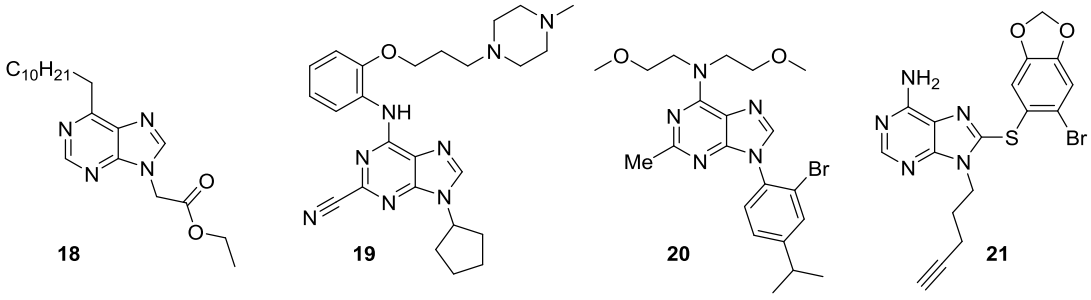

Designing potential drugs around the purine scaffold appears to be difficult, as according to the substituent pattern such compounds can target a variety of receptors and have completely different effects, as shown by the examples cited above. Selectivity towards one target over others requires studying carefully the unique features and differences of the targets. As shown in *Figure 33*, purvalanol B (**22**) and AP23137 (**23**) possess the same hydrogen bond interactions due to their purine scaffold, but thanks to their substituents they are highly selective to their kinase targets, CDK2 and Scr (proto-oncogene tyrosine-protein kinase), respectively. The isopropyl group on the 8-position of purvalanol B (**22**) interacts perfectly with a small hydrophobic pocket of CDK2. In contrast the 8-substituent on AP23137 (**23**) fits into a larger hydrophobic pocket of Scr and reaches two amino acids forming additional hydrogen bonds, which is not possible in the small hydrophobic site of CDK2.[122]

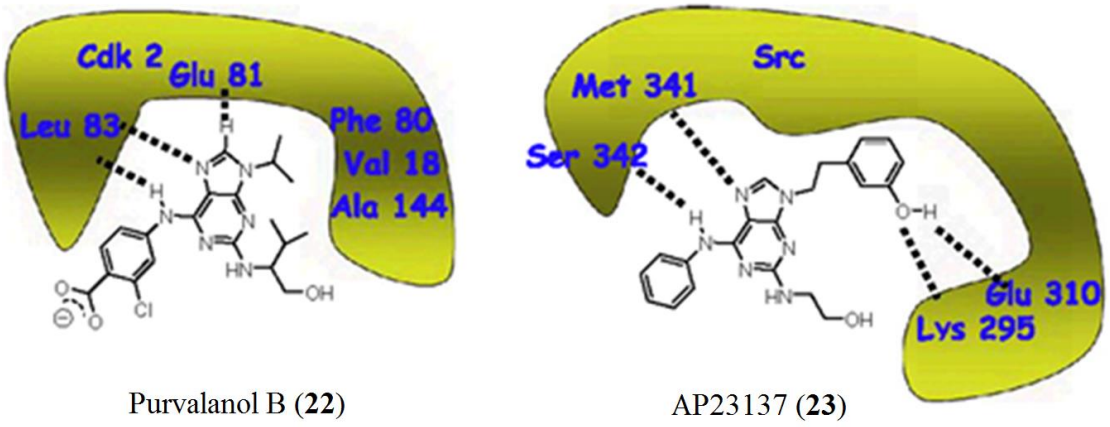

Figure 33 - Importance of substituents for selectivity[122] (from M. Legraverend and D. S. Grierson, 2006). Variations of substituents on the purine scaffold modify the binding mode of the inhibitors, creating the opportunity for selectivity.

2.2 Nek2: a valid target in cancer research

2.2.1 Nek2 and cancer

As described previously, defects in the Nek2 pathway lead commonly to aneuploidy and chromosomal instability, key features in tumourigenesis. Nek2 has been shown to be abnormally expressed (2- to 5-fold higher than in normal cells) in several human cancers especially breast, cervical and prostate cancer, and in lymphomas.[123] Overexpression of Nek2 can be explained by different mechanisms. One explanation would be the presence, more often, of the Nek2 locus 1q32.1 resulting in gene amplification.[124] Another possibility would be sequestration of p107/p130, proteins of Rb, by E7 protein from human papillomavirus (HPV).[124] Nek2 expression is regulated by the E2F4 transcription factor via p107/p130. By sequestering p107/p130, E7 protein allows the expression of Nek2.[124] Finally, any defects in Nek2 degradation or ubiquitylation by $APC/C^{Cdc20/Cdh1}$ would also lead to an overexpression of Nek2.[124]

To improve therapies available for patients, a specific molecular target, essential for the development of a particular tumour, should be identified. A research group in Japan studied the expression of Nek2 in several tumour types such as breast, cervical and colorectal cancer.[123, 125] Colorectal cancer represents the second most common cancer type in Japan with poor outcomes for late stage diseases.[125] Breast cancer is one of the most common cancers in Asia as well as worldwide.[123] Two main types of breast cancer arise: receptor positive to estrogen, progesterone and ErbB2 (ER-positive) and receptor negative (ER-negative).[123] The latter shows resistance to existing therapies, and there is a need for an effective drug.[123] Finally, cholangiocarcinoma, the most common form of liver cancer in Southeast Asia, shows poor prognosis for patients.[126] In these three types of cancer, Nek2 was shown to be overexpressed.

HUCCT1, TFK1, HuH28 and CCKS1 are cholangiocarcinoma cell lines.[126] Nek2 was found to be overexpressed in these four tumour cell lines by comparison with the normal fibroblast cell line HFF, representing the control (*Figure 34*).[126] Nek2 expression was also demonstrated to be high in both ER-positive and ER-negative breast cancer cell lines compared to HFF cells (*Figure 34*).[123] Finally, Nek2 was elevated in HCT-15, DLD-1, Colo320 and Colo205, four colorectal tumour cell lines (*Figure 34*).[125]

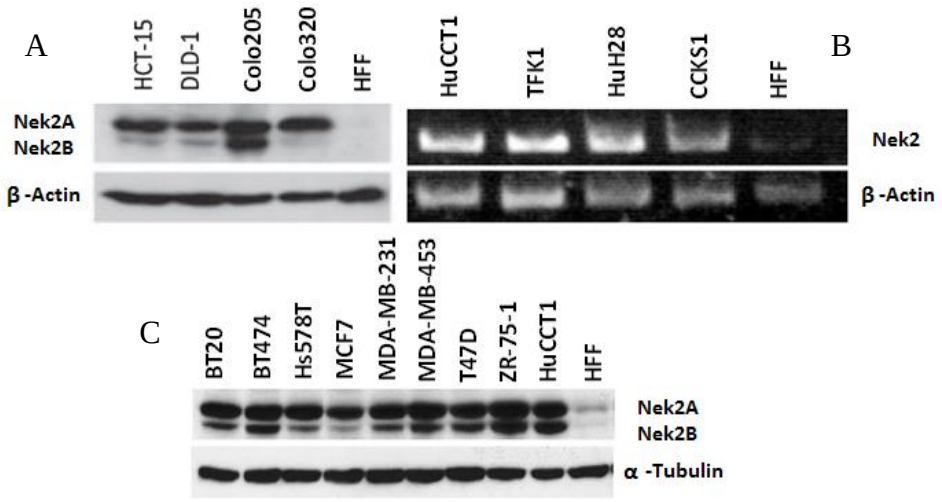

Figure 34 - Nek2 expression in colorectal, cholangiocarcinoma and breast cancer cell lines[123, 125, 126] (from N. Tsunoda *et al*, 2009, K. Suzuki *et al*, 2010 and T. Kokuryo *et al*, 2007). Western blot analyses showing the expression of Nek2 and its splice variants, Nek2A and Nek2B, in several cell lines of colorectal cancer (A), cholangiocarcinoma (B) and breast cancer (C). B-Actin and α-tubulin are used as loading controls.

The effect of Nek2 on tumour growth and survival was examined in either the HUCCT1,[1] DLD-1[2] or MCF-7[3] xenograft nude mouse model.[123, 125, 126] After a period of inoculation (variable according to the cell line), nude mice were treated either with Nek2 siRNA or control siRNA. Tumour sizes in mice treated with Nek2 siRNA were clearly reduced compared with control siRNA or control. Suppression of Nek2 using Nek2 siRNA led to arrest of tumour growth and increased survival in each tumour type (*Figure 35*).[123, 125, 126]

[1] Cholangiocarcinoma cell line
[2] Colorectal tumour cell line
[3] Breast cancer cell line

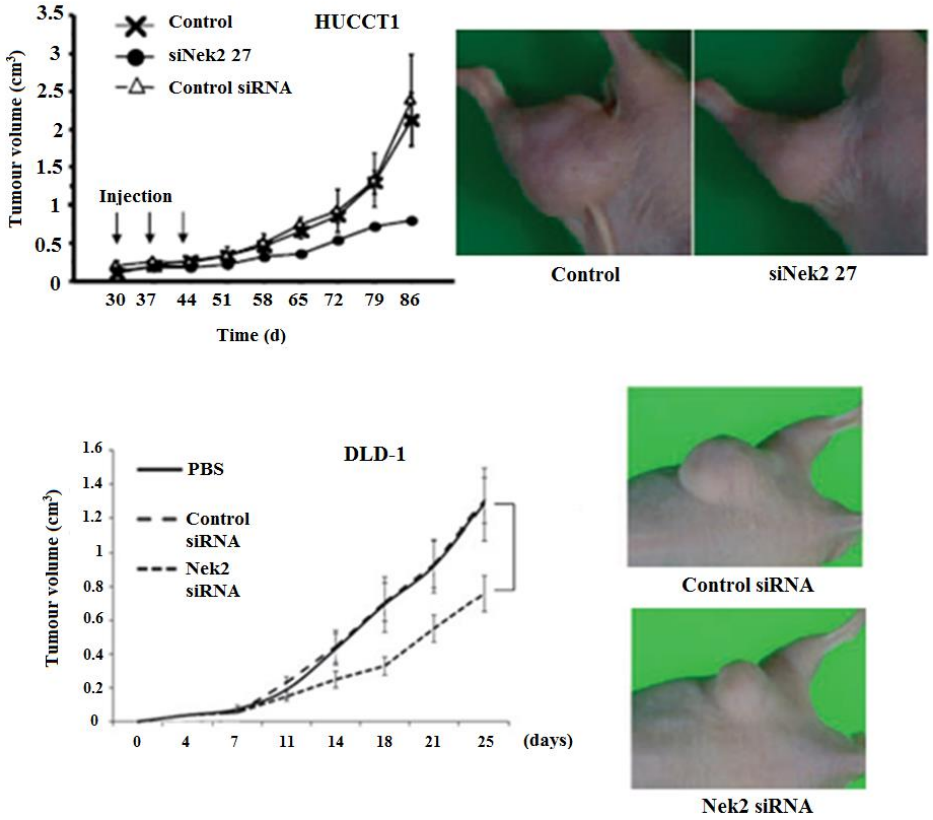

Figure 35 - Effect of Nek2 suppression on tumour growth in nude mice[123, 125, 126] (from K. Suzuki *et al*, 2010 and T. Kokuryo *et al*, 2007). In HUCCT1 and DLD-1 cell lines, Nek2 suppression by siRNA was shown to reduce the tumour size by comparison to the control experiments (control, PBS and control siRNA). The visualisation of tumour regression is imaged for both cell lines.

Following these results, DLD-1 xenograft nude mice were treated with Nek2 siRNA in combination with cisplatin (CDDP).[125] Combination treatment was shown to be more effective on tumour proliferation than Nek2 siRNA alone or control siRNA with CDDP.[125] The tumour size was also reduced significantly, using the combination treatment (*Figure 36*).[125]

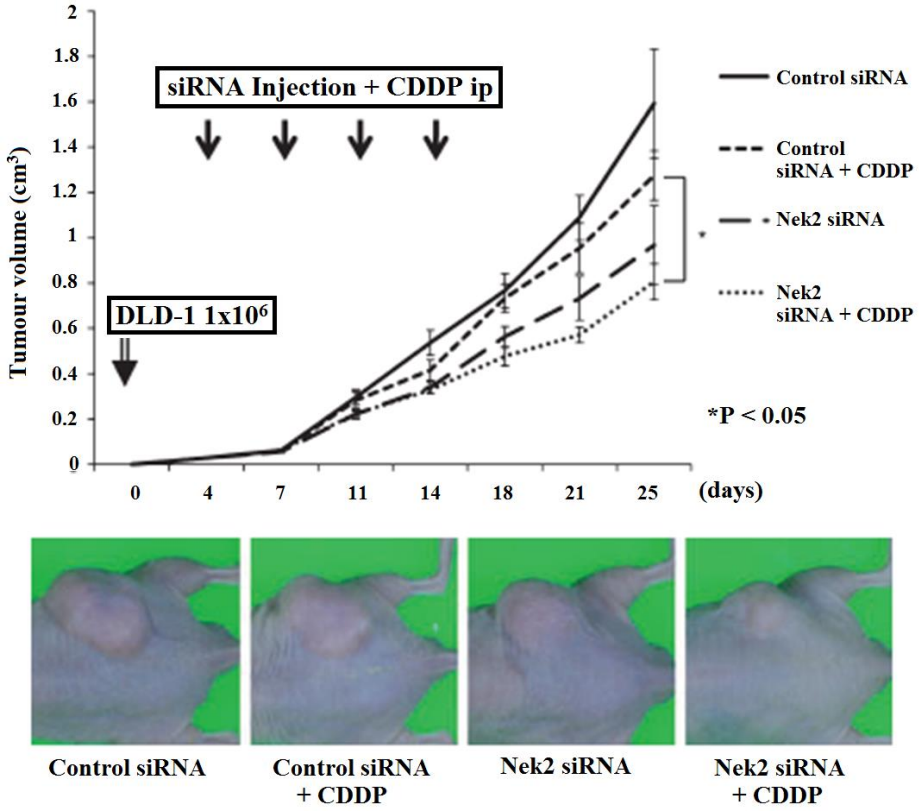

Figure 36 - Effect of Nek2 siRNA in combination with CDDP on tumour growth[125] (from K. Suzuki *et al*, 2010). Using colorectal tumour cell line (DLD-1) in nude mice, the combination of Nek2 suppression with treatment of cisplatin (Nek2 siRNA + CDDP) was shown to reduce the tumour size more efficiently than cisplatin alone (control siRNA + CDDP) and Nek2 suppression alone (Nek2 siRNA). Images illustrate the tumour size depending on the treatment.

Studies using Nek2 siRNA treatment of a breast tumour cell line showed a regression in colony formation and invasion of surrounding tissues.[123] Nek2 siRNA treatment of breast carcinoma cells reduced by 4-fold the number of cell colonies formed compared with the control experiment.[123] This study was carried out on both MCF-7 (ER-positive) and Hs578T (ER-negative) cell lines (*Figure 37*). In both cell lines, Nek2 siRNA was shown to be efficient in reducing colony formation.[123] This observation demonstrated the dependence of these cell lines on Nek2 for tumourigenic growth. Nek2 siRNA treatment was also demonstrated to be efficient in the reduction of invasiness in both MCF-7 and Hs578T cell lines (*Figure 37*).[123] This assay supported the role of Nek2 in tumour invasion.

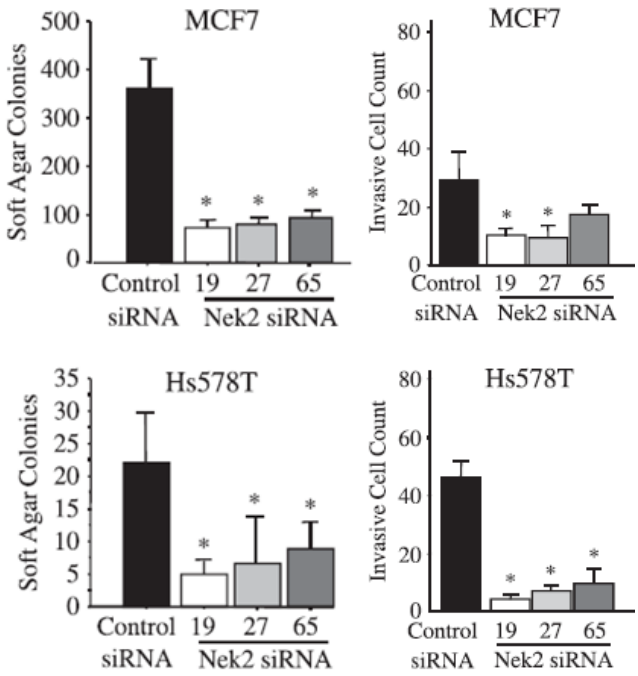

Figure 37 - Effect of Nek2 depletion on colony formation and invasiveness of breast cancer cell lines, MCF7 (ER-positive) and Hs578T (ER-negative)[123] (from N. Tsunoda *et al*, 2009) – number of colonies counted for the control and each siNek2 treatments (on the left) and number of cells that penetrated the membrane in the assay using the modified Boyden chamber method (on the right).

Others studies have been conducted to understand better the modulation of Nek2 activity. In the first example, HeLa cells[4] treated with Nek2 siRNA were studied.[127] Days after transfection (from one to six), centrosome separation, cell number and apoptotic cell number were evaluated (*Figure 38*). Depletion of Nek2 by Nek2 siRNA had a crucial impact on centrosome separation,[127] and three days after cell transfection, suppression of Nek2 decreased centrosome separation by two-fold. In addition, Nek2 siRNA stopped cell growth with obtention of a flat growth curve. Nek2 siRNA was shown to induce cell growth arrest resulting in a high level of apoptotic cells.[127]

[4] Immortal cell line derived from cervical cancer

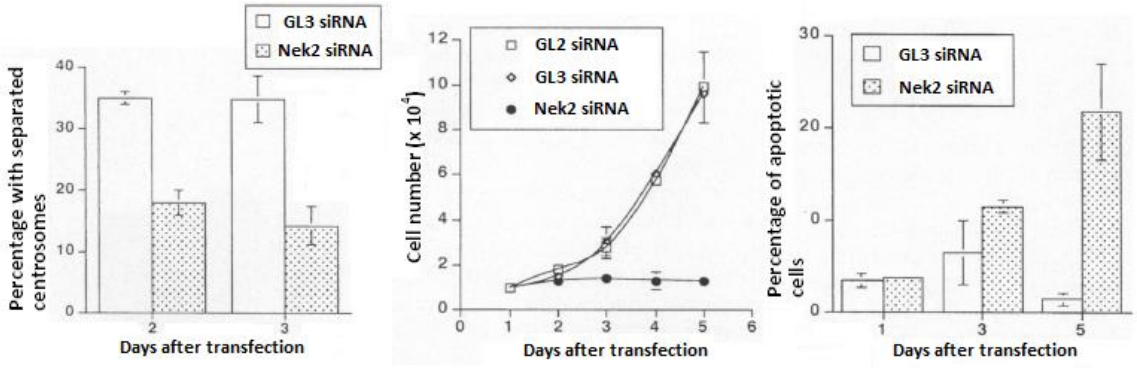

Figure 38 - Effect of Nek2 suppression on cell growth and centrosome separation[127] (from L. Fletcher *et al*, 2004). Nek2 suppression using Nek2 siRNA in HeLa cells was shown to decrease centrosome separation (by comparison with the control experiment GL3 siRNA), stop cell growth (by comparison with control experiments GL2 siRNA and GL3 siRNA) and promote apoptosis (by comparison with the control experiment GL3 siRNA).

Another experiment was conducted on mouse blastomeres to study Nek2-suppressed embryos.[128] For fragments 1 and 2 (*Figure 39*), both Nek2A and Nek2B were blocked, resulting in no embryonic development. The same observation was made when Nek2A was blocked (Fragment 3, *Figure 39*). In fragment 4 (*Figure 39*), the blockade of Nek2B did not affect embryonic development. These results underlined the critical role of Nek2A in mouse early embryogenesis.[128]

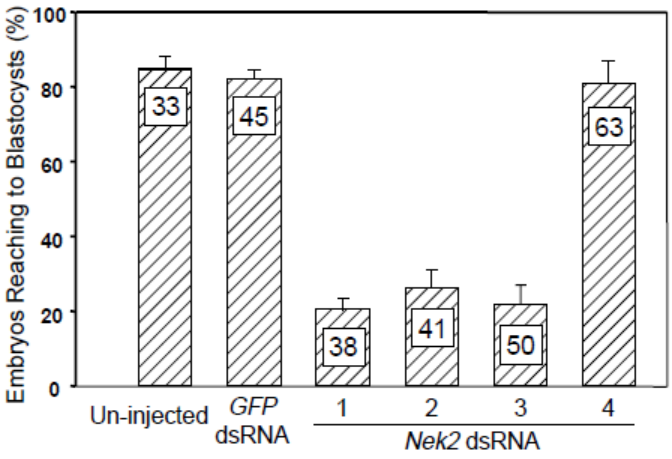

Figure 39 - Effect of Nek2 suppression in mouse embryonic development[128] (from S. Sonn *et al*, 2004). In experiments 1 and 2, both Nek2A and Nek2B were blocked using Nek2 dsRNA, causing no embryonic development. In experiment 3, only Nek2A was blocked resulting in no embryonic development. In experiment 4, only Nek2B was blocked which had no effect on the embryonic development. Control experiments were performed for comparison (un-injected and GFP siRNA).

Depletion of Nek2 in mouse blastomeres had an effect on the morphology of ova.[128] Nek2 suppression caused abnormalities such as dumbbell-like nuclei, nuclear bridges and micro-nuclei (*Figure 40*).[128] Incomplete chromosome segregation, lack of MTOC structure and abnormal spindle structures were suggested to be responsible for these

abnormalities, which would cause a delay for the progression into M phase.[128] Nek2 was shown to be critical for embryonic mitosis and chromosome segregation but was not proved essential for mitotic entry.[128]

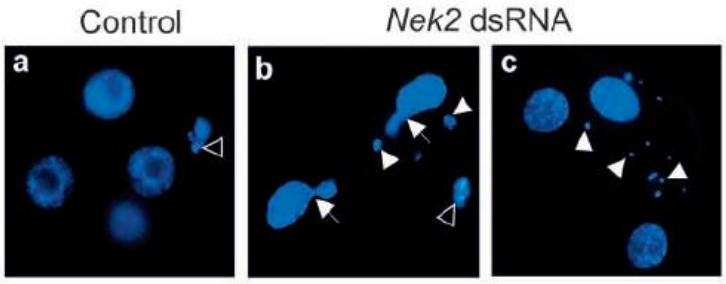

Figure 40 - Effect of Nek2 depletion on morphology of mouse embryos[128] (from S. Sonn *et al*, 2004) – formation of dumbbell-like nuclei (empty head arrows), nuclear bridges (arrows) and micro nuclei (full head arrows).

Another experiment, studying the possible interaction between Nek2A and Mitotic Arrest Deficiency (MAD) enzymes, components of the spindle checkpoint, was conducted.[129] MAD1 was shown to interact with Nek2A, with formation of a complex by co-precipitation.[129] This observation combined with the localisation of Nek2A at the kinetochores of mitotic cells, suggested that Nek2A interactions with MAD1 occurred at the kinetochores.[129] However, Nek2A was shown not to be responsible for the localisation of MAD1 at the kinetochores.[129] Nek2A interaction with MAD2 was also studied. Depletion of Nek2 provoked premature anaphase with errors during chromosome segregation.[129] Nek2A was shown to retain MAD2 at the kinetochores until the separation of all sister chromatids. This action allowed efficient chromosome segregation before the beginning of anaphase.[129]

Nek2 was found to be involved in tumourigenesis not only by promoting chromosomal instability but also by activating several tumour enabling pathways, such as the Akt pathway, known to promote growth and survival.[130] The phosphatase PP1 regulates the activation of both Nek2 and Akt by dephosphorylation. When Nek2 is overexpressed, PP1 is overcome by the level of activated Nek2 and cannot regulate the activation of Akt, the level of which becomes aberrant and leads to an up-regulation of ABC transporter family members, including the multi-drug resistance protein ABCC1 and the breast cancer resistant protein ABCG2 (*Figure 41*).[131] Nek2 was found to influence the efflux pumps and the mitotic checkpoint protein MAD2 by up-regulation, two mechanisms related to drug resistance (*Figure 41*).[131]

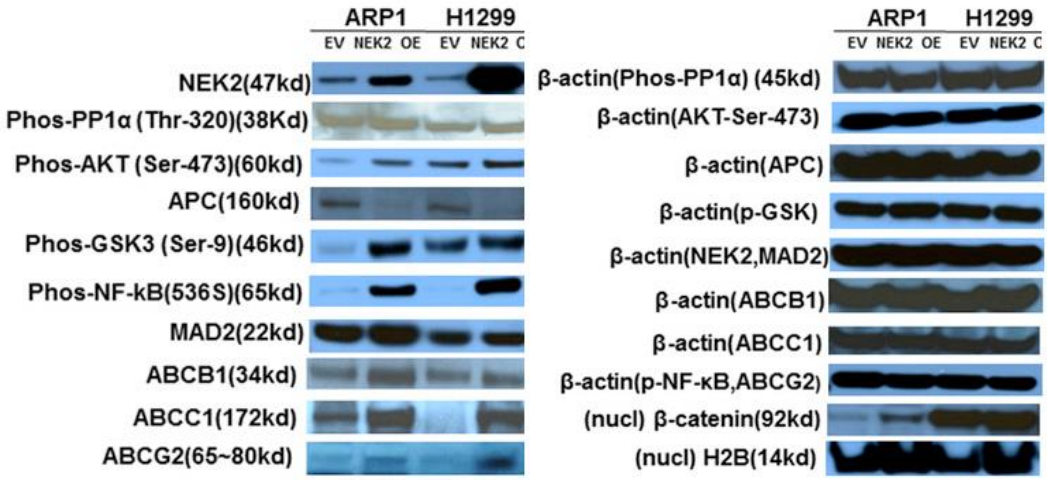

Figure 41 – Consequences of Nek2 overexpression on protein levels[131] (from W. Zhou *et al*, 2013). Western blot experiments showing the effects of Nek2 overexpression (Nek2 OE) on protein levels by comparison to the control experiment with normal Nek2 expression (EV), in two cell lines, ARP1 (multiple myeloma cell line) and H1299 (non-small cell ling carcinoma cell line).

Another crucial downstream effect of Nek2 overexpression is activation of the Wnt pathway, implicated in cancer cell survival and drug resistance. Wnt signalling depends mainly on the nuclear accumulation of β-catenin, stimulated by Nek2.[131] Nek2 was found to have a multifaceted role in tumour biology by inducing cell proliferation, chromosomal instability and drug resistance (*Figure 42*).[131]

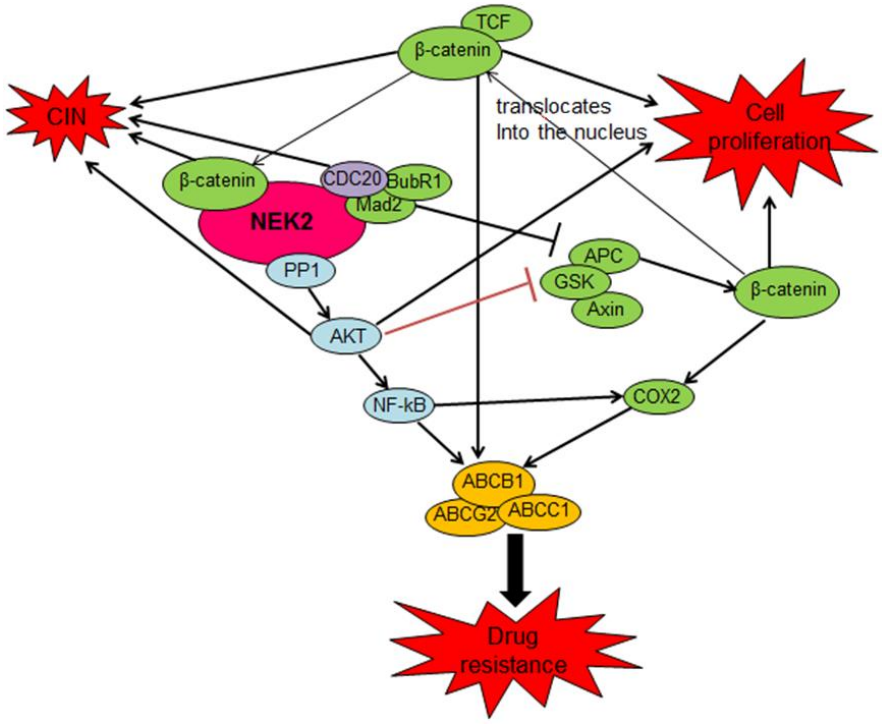

Figure 42 – Central role of Nek2 in tumour biology[131] (from W. Zhou *et al*, 2013). Interactions of Nek2 with binding partners have a crucial impact on chromosomal instability (CIN), cell proliferation and drug resistance.

2.2.2 Nek2 in drug discovery

A number of Nek2 inhibitors have been investigated, but so far none have entered clinical trials. The crystal structure of Nek2 has been solved which provides the opportunity for rational inhibitor design.[130] Nek2 possesses a characteristic ATP-binding site with the Phe147 at the base of the ATP pocket only being present in 39 human kinases (usually Leu is present at this site), and a large gate-keeper, which allows inhibitor selectivity over other kinases. However, selectivity over Plk1, which shares similarities with Nek2, appears to be more challenging. The presence of Arg136 in Plk1 does provide an opportunity for selectivity as this residue is not present in Nek2 (*Figure 43*).[130] An SAR study from a hit compound (**24**) identified by high-throughput screening led to the identification of the pyrazine derivative **25** (*Figure 44*). In parallel, a benzimidazole scaffold was developed, inspired by GSK461364A (**26**), a Plk1 inhibitor developed by GlaxoSmithKline. This study resulted in compound **27**, which demonstrated 100-fold selectivity over Plk1.[132]

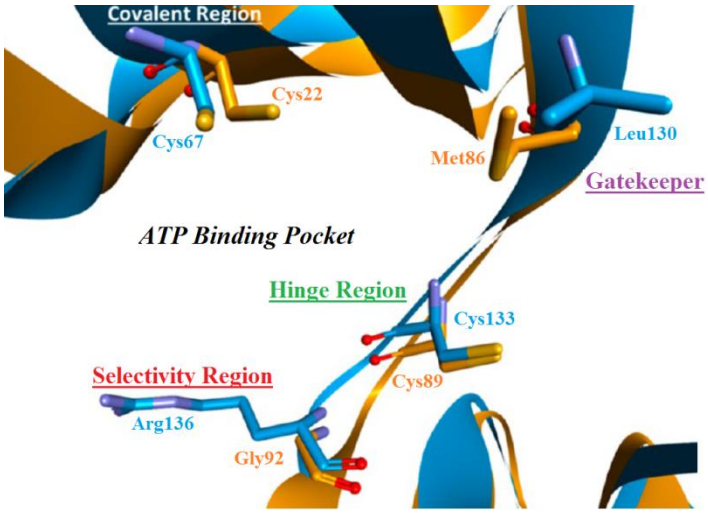

Figure 43 – Structure differences between Nek2 (orange) and Plk1 (blue)[130] (from B. Frett *et al*, 2014). Both structures show similarities in the covalent region, hinge region and the position of the gatekeeper residue with the exception of the selectivity region with the presence of Arg136 in Plk1. The PDB entries are 2XNP and 4J52.

The most promising features of the scaffolds were combined to generate a hybrid series, exemplified by compound **28** (*Figure 44*). This inhibitor exhibits good potency, selectivity and growth inhibition profile, and therefore proves to be an excellent tool compound to investigate further the role of Nek2 in tumour biology.[130]

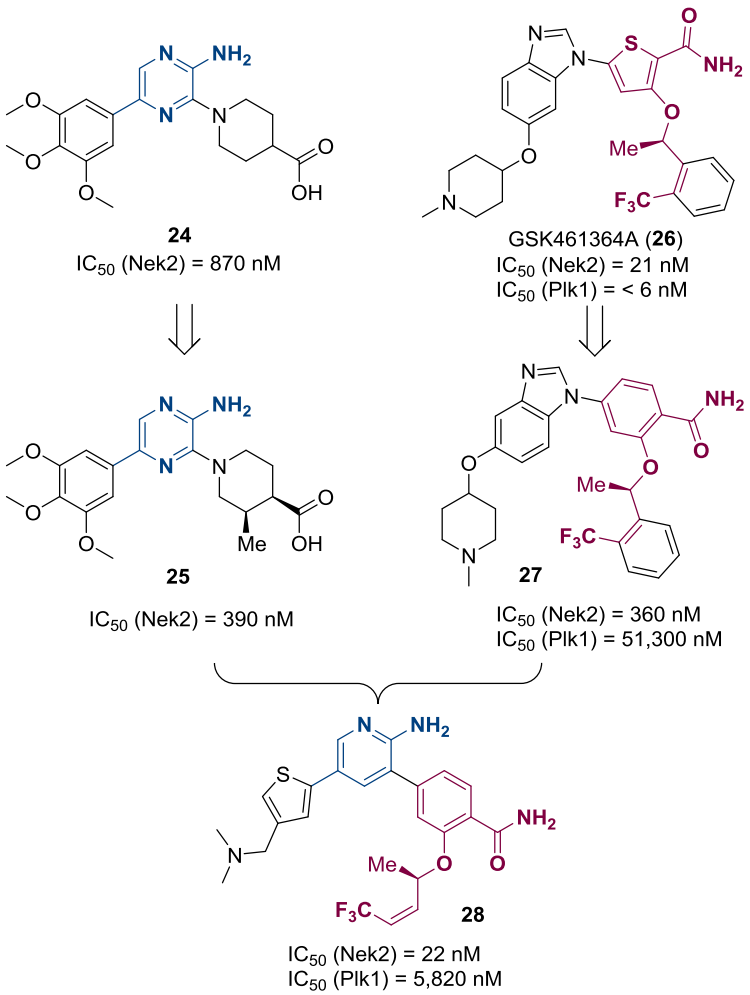

Figure 44 – Strategy used for the discovery of Nek2 inhibitors[130]

Another study was published describing the design of an irreversible inhibitor of Nek2.[133] The authors started from the crystal structure of SU11652 (**29**), an oxindole-pyrrole derivative, bound to Nek2 by forming, among other interactions, key hydrogen bonds (*Figure 45*). Inhibitors were rationally designed by changing the 5-position group where Cys22 can be reached, and also modifying the 3', 4' and 5' positions to confer more selectivity for Nek2. The most potent compounds were shown to interact with Cys22. To confirm this interaction, the most promising compounds were tested against Nek2, and a Nek2 mutant kinase where Cys22 was replaced by valine. A significant drop in activity was noticed, suggesting that these compounds act *via* alkylation of Cys22. After further modifications, propynamide compound **30** was obtained (*Figure 45*) and found to be selective over CDK1 (~30 fold), Rsk2 (5 fold) and Plk1 (>30 fold). However, compound **30** was only evaluated against a small number of kinases. Inhibition of Nek2 by **30** did not abolish mitotic entry, mitotic checkpoint, bipolar spindle assembly or chromosome segregation, suggesting that the other mitotic kinases were still fully functional.[133]

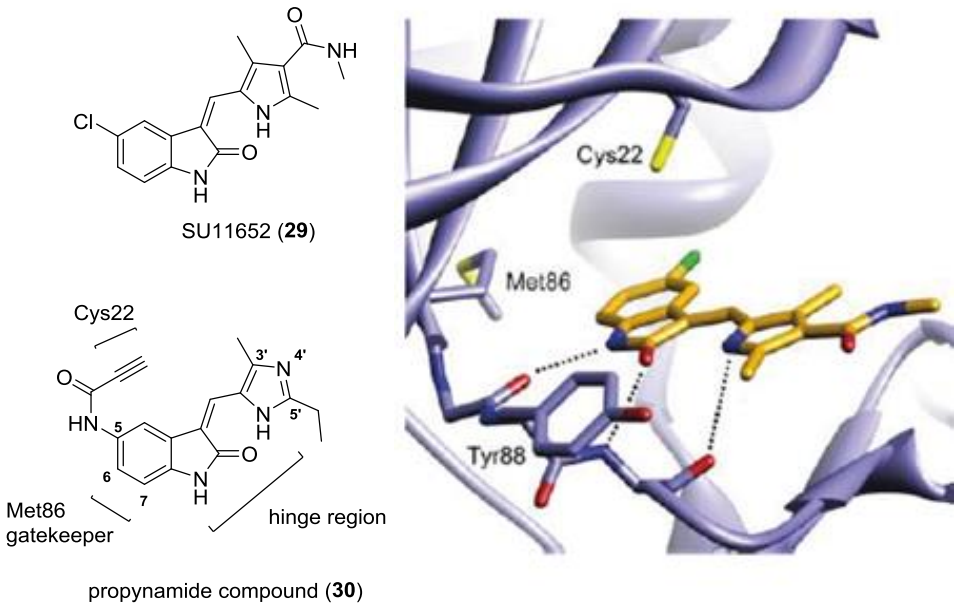

Figure 45 - Crystal structure of SU11652 (**29**) in complex with Nek2 showing a triplet of H-bonds with the hinge region and the presence of Cys22; structure of the most promising compound of the series, **30**, shown for comparison[133] (from J. C. Henise and J. Taunton, 2011) The PDB entry is 2JAV.

Another example of covalent inhibition of Nek2 was reported in the literature. The series started with the non-covalent inhibitor HCI-2388 (**31**), which demonstrated good activity against Nek2 (IC_{50} = 34 nM). Introduction of an acrylamide moiety (HCI-2389, **32**) led to a 2-fold increase in potency and time-dependent Nek2 inhibition (*Figure 46*).[134] Phosphorylation of PP1-α was studied and shown to decrease in both Nek2 overexpressing Hela cells and GFP controls after treatment with **32** (*Figure 46*). [134]

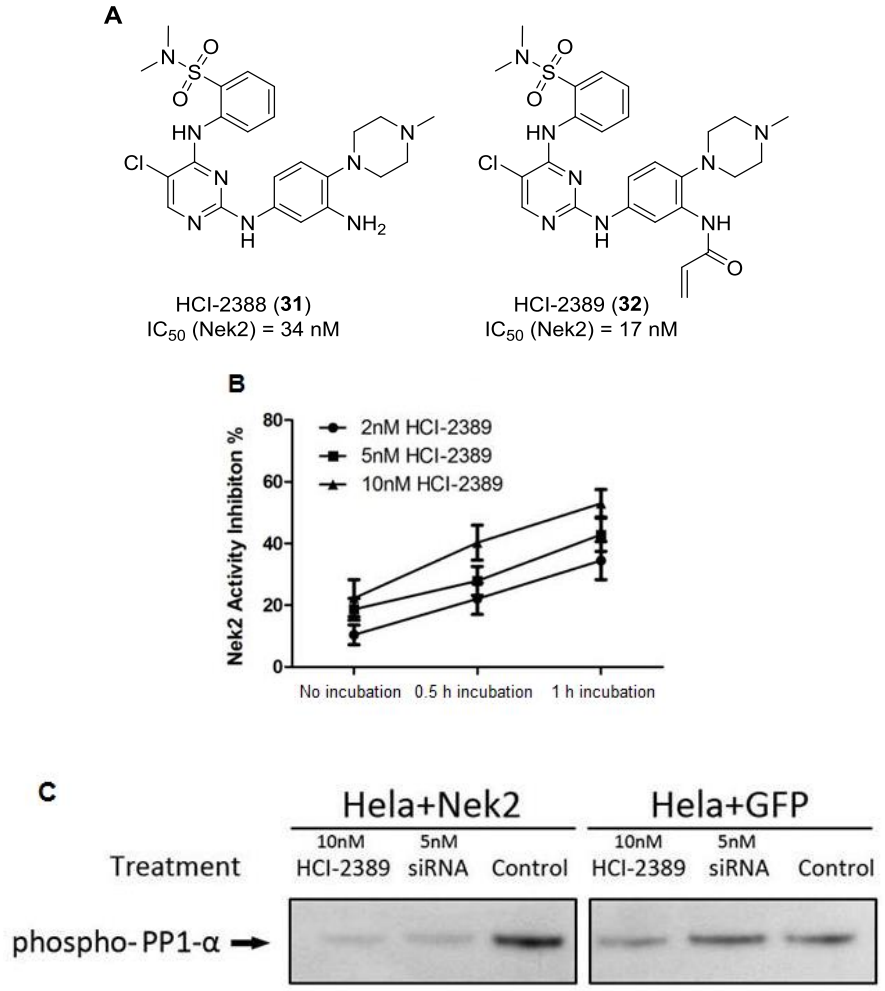

Figure 46 – A. Structures of HCI-2388 (**31**) and HCI-2389 (**32**), inhibitors of Nek2; B. Nek2 activity assay *in vitro*; C. Level of phosphorylated PP1-α in Nek2 overexpressed Hela cells (HeLa + Nek2) and GFP controls (HeLa GFP)[134] (from J. Flory *et al*, 2013).

2.2.3. Development of selective irreversible inhibitors of Nek2

From a high-throughput screen of approximately 73,000 compounds,[135] A number of 6-alkoxypurines and 4-alkoxypyrimidines, available from a previous project at Newcastle University on CDK2 inhibitors, showed modest activity against Nek2. The O^6-alkylguanine class (**33**), active against CDK2, did not express any activity against Nek2 unless substituted by an aryl group at the 2-position (**34**, **35**).

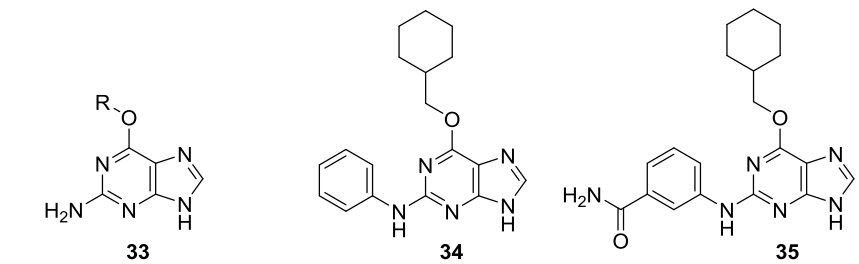

Further analogues were synthesised, guided by the crystal structure of **35** with Nek2. A triplet of donor/acceptor/donor hydrogen bonds from the purine scaffold with the hinge region of Nek2 was highlighted (*Figure 47*). This observation was rationalised from the *X*-ray crystal structure of SU11652 (**29**) in complex with Nek2, previously reported by Smerdon *et al.*[89]

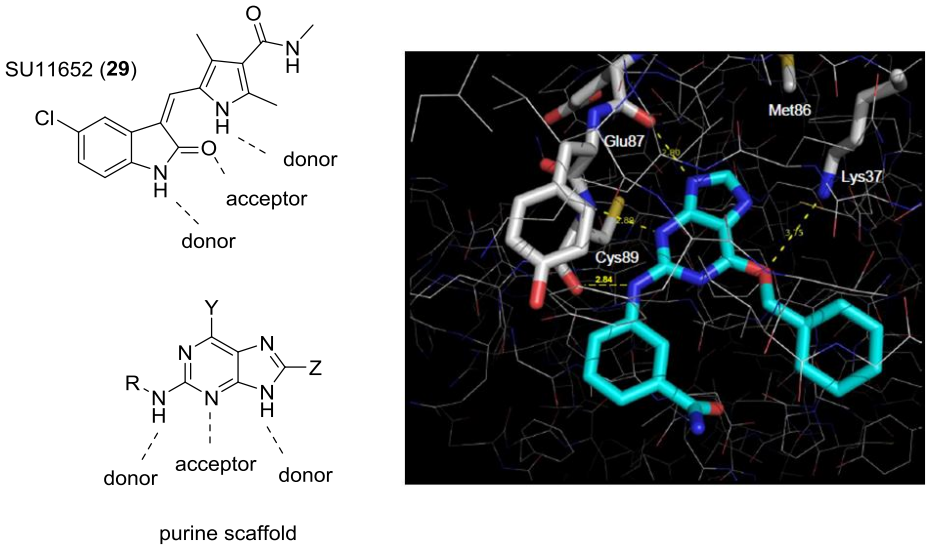

Figure 47 - Analogy of interactions between SU11652 (**29**) and purine **35** within the ATP-binding site of Nek2

The first SARs carried out suggested that the 6-cyclohexylmethoxy group, essential for CDK2 inhibition, was not a prerequisite for activity against Nek2. Substituents on the 2-arylamino group were tolerated and required a hydrogen bond donor/acceptor such as a sulfonamide (**36**), urea (**37**) or amide. 8-Substitution was tolerated, but suggested another binding mode. Knowing the essential features to inhibit Nek2, selectivity over CDK2 had to be improved.

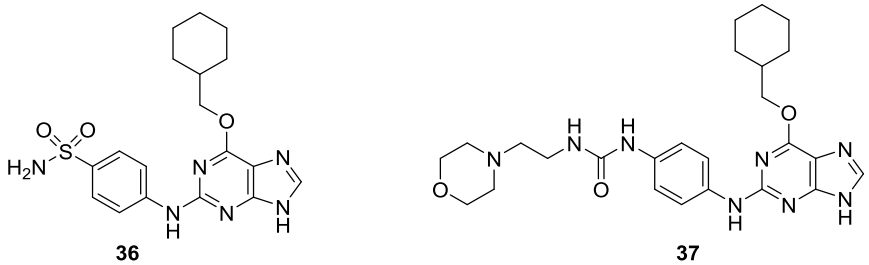

36
IC_{50} (Nek2) = 12 µM
IC_{50} (CDK2) = 5 nM

37
IC_{50} (Nek2) = 2.2 µM
IC_{50} (CDK2) = 1.1 µM

Modifications of the 6-position have been explored. Firstly, 6-unsubstituted analogues (**38**, **39**) were synthesised and showed good selectivity for Nek2 over CDK2. These examples indicated that the ribose binding pockets of Nek2 and CDK2 were different and

that these differences could be used to rationally design Nek2 selective inhibitors. Introduction of functional groups at the 6-position was investigated. The 6-ethynylpurine **40** showed a time-dependent inhibition profile against Nek2 suggesting that **40** was binding covalently to Nek2 according to the mechanism in *Figure 48*.

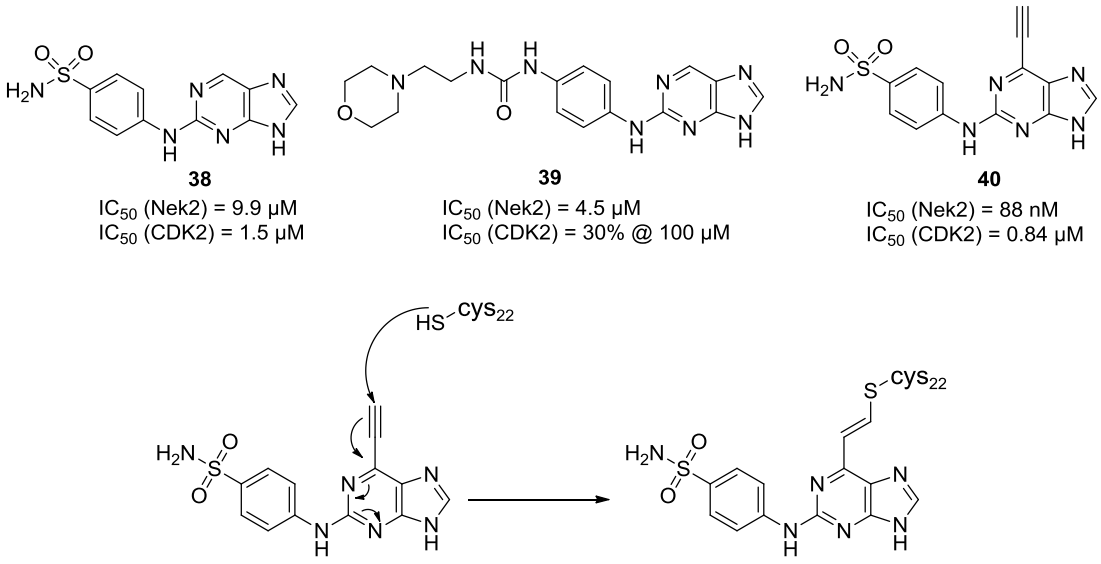

Figure 48 - Irreversible inhibition of Nek2 by compound **40**

Compound **40** was the first of the series showing high potency against Nek2 and good selectivity over CDK2, other Nek members (Nek1, 3, 6, 7 and 11) and a range of kinases. The selectivity resulted from the Cys22 residue, commonly replaced by a valine or alanine in other kinases. Only seven kinases among the kinome possess this Cys22, namely Plk 1, 2 and 3, MSK1 and 2, and MEKK1.[79]

Work on improving cell permeability and kinase selectivity led to the initial hit compound of the project (**41**). The 2-position was further explored as the 2-amino group was positioned in the specificity pocket of Nek2. This work led to the identification of the early lead compound **42**.

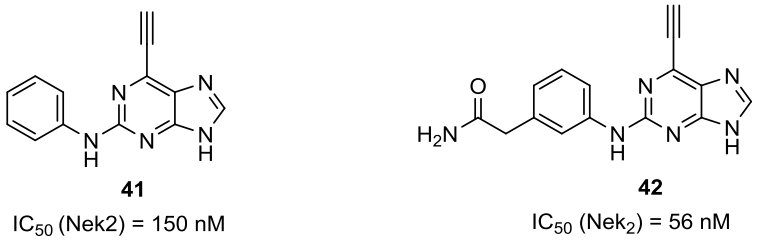

Compound **42** was more potent and selective than its analogue **41**. 6-Ethynylpurines were confirmed to be covalent inhibitors as potency was observed to increase in a time-dependent manner, one of the hallmarks of irreversible inhibitors. *X*-ray crystallography

confirmed this hypothesis, with the crystal structure of the Nek2-inhibitor complex showing a covalent bond between Cys22 and the 6-ethynyl group (*Figure 49*).

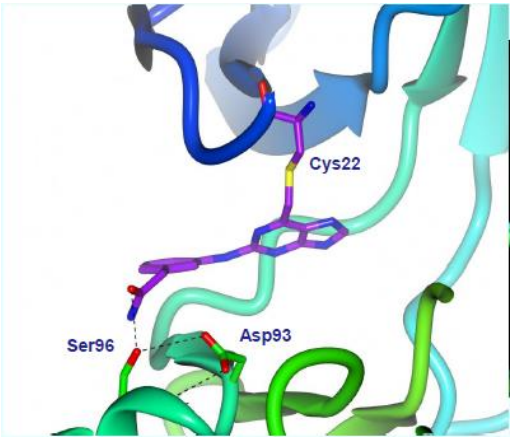

Figure 49 - Crystal structure of compound **42** in complex with Nek2 showing covalent binding between the inhibitor and Cys22[136] (from C. J. Matheson, 2012)

Compound **42** was tested against a C22A mutant kinase to confirm that covalent binding contributed to potency. After incubation for one hour, **42** was less potent against Nek2 C22A (IC_{50} = 3.5 µM) than the Nek2 wild type (IC_{50} = 0.046 µM).[131] Compound **42** was also tested in a cellular assay in different tumour cell lines and showed reasonable cellular activity (GI_{50} = 18 µM (HCT116[5]); 32 µM (HeLa[6]); 6.6 µM (MCF7[7]); 1.6 µM (REC1[8]); 5.8 µM (RIVA[9]); 2.2 µM (SKBR3[10]); 3.6 µM (T47D[11]); 3.7 µM (ZR75[12])).[131] As 6-ethynylpurines are irreversible inhibitors, compound **41** was also tested in a Comet Assay, also known as single-cell gel electrophoresis, to detect potential DNA damage. After the cells were treated with **41**, the comet tails (yellow, green and blue, *Figure 50*) were found to be similar to the comet tail of the untreated cells (red, *Figure 50*), demonstrating that **41** did not cause any DNA damage. For the control experiment, cells were exposed to ionising radiation and showed a high level of DNA breaks by comparing the comet tail to the comet head (black, *Figure 50*). This assay confirmed that **41** was not a DNA alkylating agent.

[5] Colon cancer cell line
[6] Immortal cell line derived from cervical cancer
[7] Breast cancer cell line
[8] β cell non-Hodgkin's lymphoma
[9] Diffuse large β cell lymphoma
[10] Breast adenocarcinoma cell
[11] Ductal breast epithelial cell
[12] Breast carcinoma cell

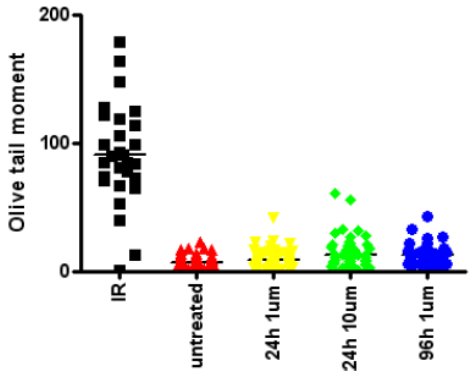

Figure 50 – Investigation of compound **41** in a Comet Assay to assess DNA damage[131] (from C. J. Matheson, 2012). Cells were treated with compound **41** at two concentrations. No DNA damage was observed after 24 h at 1 μM (yellow) and at 10 μM (green), or after 96 h at 1 μM (blue). The results obtained for the cells treated with **41** were comparable to the results observed with the untreated cells (red). As control experiments, cells expressed DNA damage after exposition to ionising irradiation (IR, black).

Compound **42** was shown to inhibit Nek2 in the enzymatic assay but studying the effect of Nek2 inhibition by **42** on downsteam substrates was also important. Therefore, U2OS cells[13] were treated with **42** at different concentrations and phosphorylation of C-Nap-1, a downstream substrate of Nek2, was measured. As predicted, C-Nap1 phosphorylation was shown to decrease with an increase of concentration of **42** (*Figure 51*).

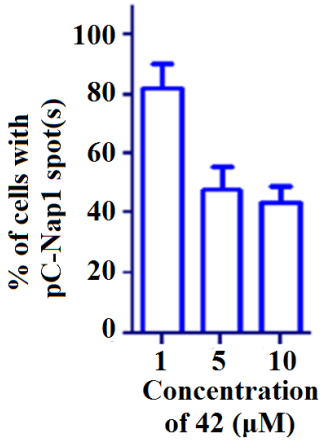

Figure 51 – Investigation of compound **42** on downstream substrates with the phospho C-Nap1 cell assay[131] (from C. J. Matheson, 2012). Phosphorylation of C-Nap1, a downstream substrate of Nek2 was shown inhibited by compound **42** at different concentrations (1, 5 and 10 μM).

A second SAR study was conducted around the lead compound **42** (*Figure 52*). The ethynyl group at the 6-position was replaced by an enamine moiety to give a competitive inhibitor, less potent than the corresponding ethynyl compound.[131] Substitution on the ethynyl group by a methyl or phenyl function reduced activity considerably, whilst a

[13] Osteosarcoma cell line

vinyl group abolished activity.[131] Modification of the imidazole ring of the purine scaffold was investigated by its replacement with a pyrrole and N^7-methylpyrazole, both changes leading to inactive compounds. However, pyrazole in place of imidazole showed poor activity by contrast to triazole which retained activity.[137] Concerning the pyrimidine ring, *N*-1 appeared to be essential for activity as its removal abolished potency.[132] Changing substituents on the 2-arylamino group was tolerated.[131] Several analogues were synthesised showing activity against Nek2, with the carboxamide moiety of **42** being the best group. All compounds prepared in this project were assessed in both enzymatic and cellular assays. Surprisingly, enzymatic (IC_{50}) and cellular (GI_{50}) results were poorly correlated, suggesting a possible off-target effect of these inhbitors.

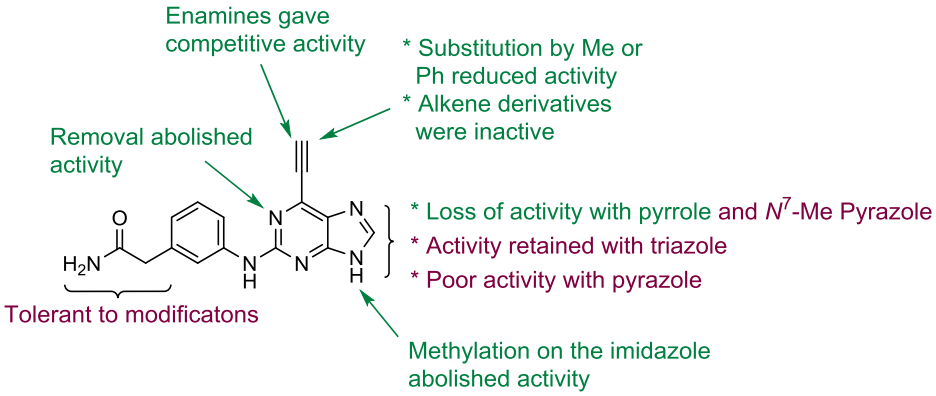

Figure 52 – SAR study in the Nek2 project based on results obtained from inhibitors **41** (green) and **42** (purple)

2.3. CDK2 as a potential drug target

2.3.1. CDK2 and cancer

CDK2 has been shown to be overexpressed in a number of tumours. Deregulation of cyclin E, one partner of CDK2, is often observed in cancer.[138] One disorder is the generation of a low-molecular-weight (LMW) isoform of cyclin E, a shorter version of the full-length cyclin E. LMW cyclin E is associated with an increase of mammary tumours and increased metastasis.[138]

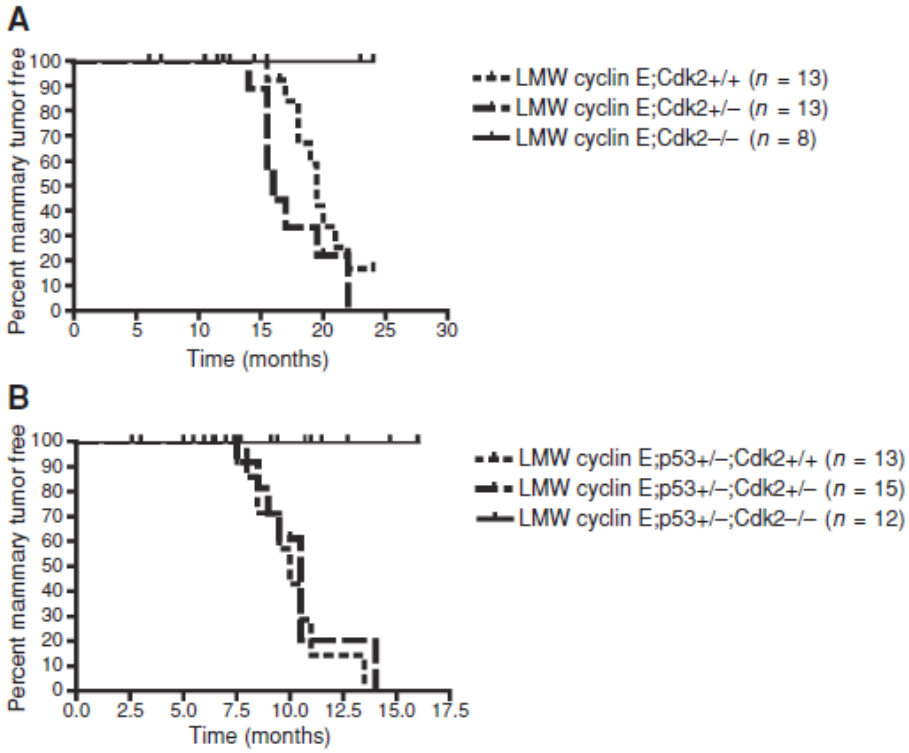

Figure 53 - Effects of CDK2 suppression on breast tumour formation in nude mice[138] (from S. Alki *et al*, 2011). A. CDK2 suppression was studied with a p53+/+ background. Partial suppression (CDK2 +/-) was shown to delay slightly the tumour formation by comparison to the control experiment when CDK2 is fully expressed (CDK2 +/+). Complete suppression (CDK2 -/-) was shown to prevent tumour formation. B. CDK2 suppression was studied with a p53-/- background. Partial suppression (CDK2 +/-) had no effect on tumour formation by comparison to the control experiment (CDK2 +/+). Complete suppression (CDK2 -/-) was shown to prevent tumour formation.

CDK2 binds to LMW cyclin E causing an augmentation of its activity. LMW cyclin E is critical in tumourigenesis, especially as cells expressing LMW-cyclin E appear to be resistant to existing therapies such as anti-oestrogens and aromatase inhibitors.[138] Studies showed that suppressing CDK2 in mice with either p53+/+ or p53+/- background prevents the formation of breast tumours induced by LMW cyclin E (*Figure 53*). This suggests the critical role, not only of LMW cyclin E, but of the complex CDK2/LMW cyclin E.[138] As a consequence, CDK2 was inhibited by meriolin (**43**) and roscovitine (**44**), two known non-selective CDK2 inhibitors. LMW cyclin E p53+/- double transgenic mice were treated twice daily for seven days. Tumour development was delayed, probably due to a decrease in proliferation and apoptosis (*Figure 54*).[138] Therefore, specific CDK2 inhibitors could be one possible efficient therapy for LMW cyclin E induced tumours.

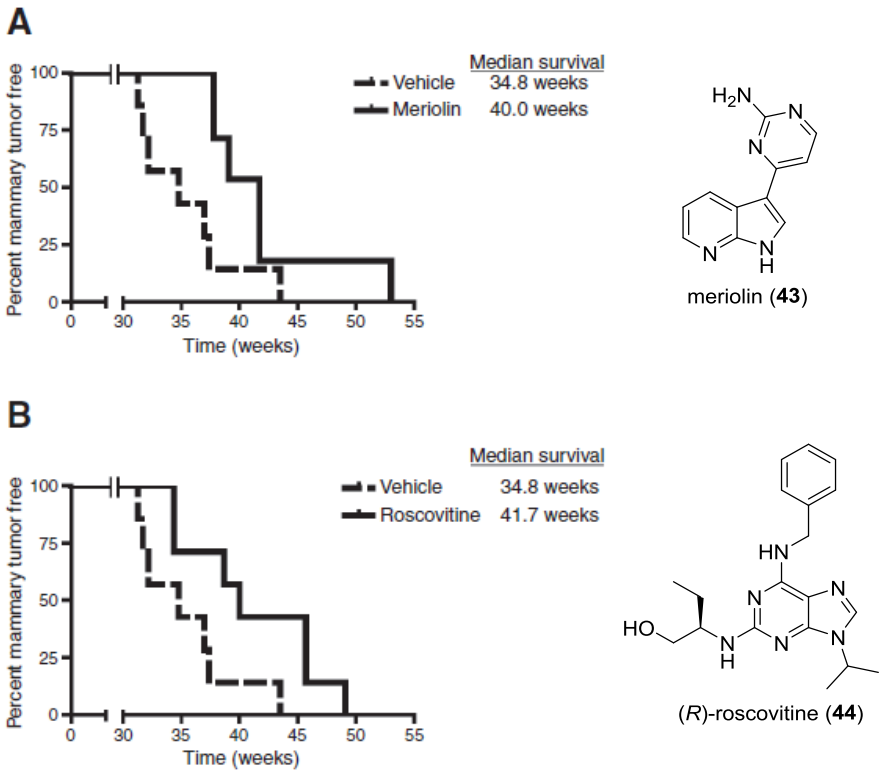

Figure 54 - Effects of CDK2 inhibitors (**43** and **44**) on tumour development in p53+/- double transgenic mice[138] (from S. Alki *et al*, 2011). Treatment with meriolin (A) and (*R*)-roscovitine (B) was shown to delay the tumour formation by comparison to the control experiment (Vehicle), thus, improving survival.

The critical role of the cyclin E/Cdk2 complex was also shown in amplified 19q12 incorporating cyclin E1 (CCNE1) cell lines. CCNE1 genomic amplification was observed in high-grade serous ovarian cancer (HGSC), the most common type of epithelial ovarian cancer, which is often associated with poor overall survival, and where primary treatment often fails.[139] CDK2 knockdown (*Figure 55* - A) or inhibition by a small molecule CDK inhibitor (dinaciclib (**45**), *Figure 55* - B) was shown to have a dramatic effect on the formation of colonies in cell lines with amplified CCNE1 compared with normal cell lines.[139] These experiments validated the therapeutic role of CDK2 inhibitors in HGSC with amplified CCNE1.

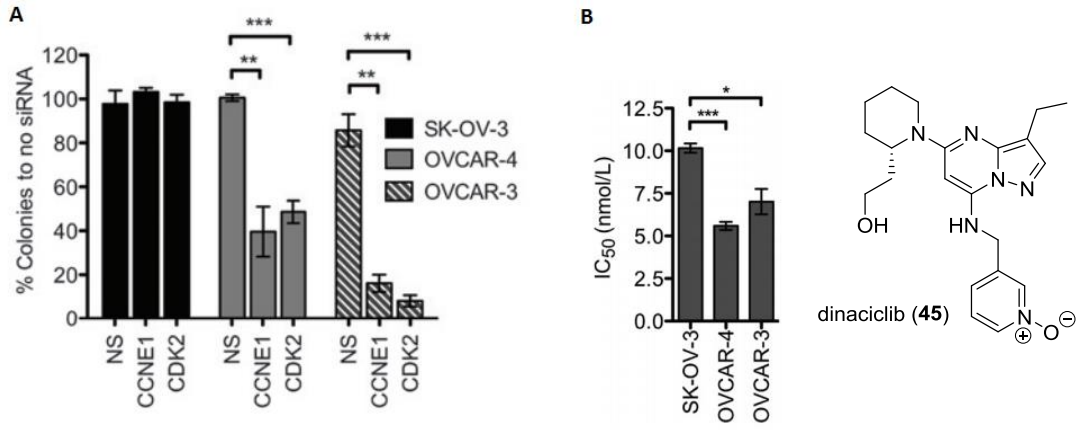

Figure 55 – Effects of CDK2 knockdown (A) or inhibition by dinaciclib (**44**) (B) on colony formation in different cell lines (SK-OV-3 (CCNE1 unamplified), OVCAR-4 (CCNE1 gained), OVCAR-3 (CCNE1 amplified))[139] (from D. Etemadmoghadam *et al*, 2013). A. CDK2 knockdown was shown to decrease colony formation in cells with amplified cyclin E1. CCNE1 knockdown also affected the colony formation in OVCAR-4 and OVCAR-3 cell lines, in the same range as CDK2 knockdown. The control experiment was conducted with normal expression of CDK2 and CCNE1 (NS). B. CDK2 inhibition by dinaciclib was shown to reduce colony formation in OVCAR-4 and OVCAR-3 cell lines.

Anti-oestrogen resistance is highly dependent on CDK activity, and so CDK inhibition would be a strategy to address this resistance.[140] The role of CDK1 and CDK2 in both anti-oestrogen resistant (LCC9) and sensitive (MCF7) cell lines was investigated. CDK2 knockdown caused a G1 accumulation of cells in both cell lines. CDK1 knockdown provoked a G2/M accumulation in all cell lines. Combined CDK1/CDK2 silencing had the most important impact, with a high G2/M accumulation of cells and diminution of colony formation with partial apoptosis (*Figure 56*).[140] A high reduction of colony formation was noticed when CDK1 was knocked down, compared to CDK2.[140] This observation might be related to the ability of CDK1 to replace CDK2 in its absence, a property that CDK2 does not possess. From these results, two dual inhibitors of CDK1 and 2, NU2058 and NU6102, were tested. These two drugs induced cell cycle arrest and apoptosis.[140]

CDK2 activity was shown to be crucial not only in breast cancer but also in colorectal carcinoma.[141] Normal and tumour tissues from patients suffering from primary colorectal cancer were investigated. CDK2 and 1 activity were found to be higher in 8/8 cancer tissues and 7/8 patients in healthy tissues.[141] In cancer tissues, CDK2 expression was found to be 40-fold higher than in adjacent tissues. These data indicated a possible role of CDK2 in colorectal carcinoma.[141]

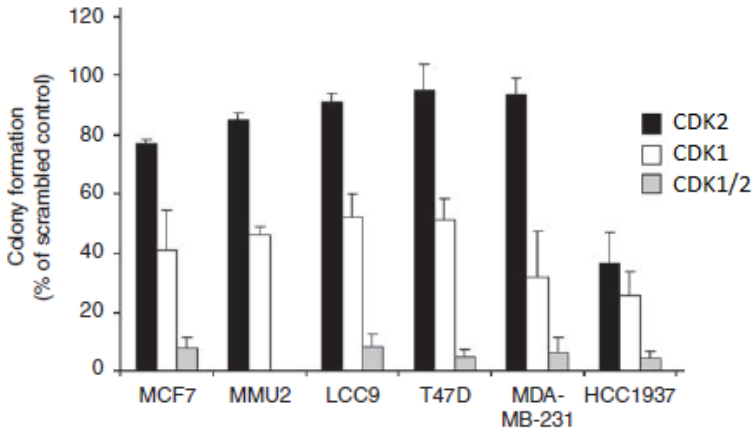

Figure 56 - Effects of CDK1/2 knockdown on colony formation in different cell lines[140] (from N. Johnson *et al*, 2009). CDK1 knockdown alone (black) was shown to prevent colony formation in all cell lines more efficiently than CDK2 knockdown alone (white). Dual CDK1 and CDK2 knockdown (grey) considerably reduced colony formation.[14]

2.3.2 CDK2, a viable cancer therapeutic target?

CDK2 activity has been studied closely in several tumour cell lines. To understand its role, CDK2 expression was suppressed (*Figure 57*).[142] CDK2 was first inhibited by $p27^{KIP1}$, released from CDK4 in UO126 cell lines. CDK2 was also inhibited by sequestration of cyclin E using ectopic dominant-negative (DN) CDK2. Eventually, CDK2 was suppressed through antisense oligonucleotides.[142] Inhibition of CDK2 by these methods did not cause growth arrest in colon cancer cells.[142] CDK2 activity was found to be dispensable for G1/S transition in colon carcinoma and no cell accumulation was noticed in G0/G1.[142] From these observations, CDK2 did not appear to be essential in cell cycle progression.

[14] MCF7 (breast cancer cell line), MMU2 and LCC9 (resistant MCF7 cell line), T47D (ductal breast epithelial cell), MDA-MB-231 (breast adenocarcinoma cell line) and HCC1937 (breast carcinoma cell line).

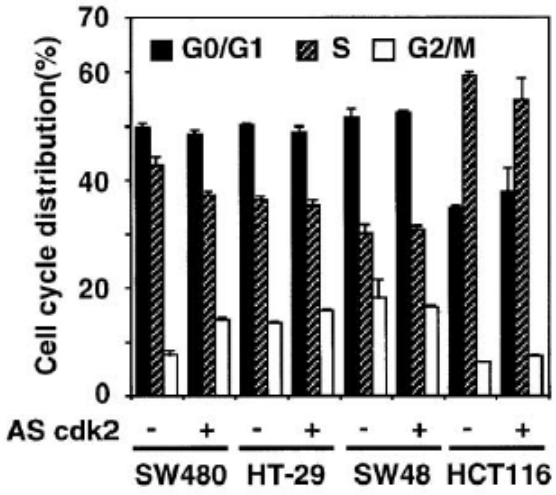

Figure 57 - CDK2 does not block cancer cell proliferation[142] (from O. Tetsu and F. McCormick, 2003). CDK2 expression was suppressed through antisense oligonucleotides in four different colon cancer cell lines. No change in the cell cycle distribution was observed when CDK2 expression was suppressed (-) by comparison to a normal CDK2 activity (+).

CDK2 inhibition was also studied using small molecules in direct comparison with CDK2 knockdown. CDK2 was genetically modified to form a CDK2 analogue-sensitive (AS) version selectively inhibited by 1-NM-PP1 (**46**). Inhibition of $CDK2^{AS}$ by **46** showed a decrease in MCF proliferation (*Figure 58* - A), whereas CDK2 knockdown by siRNA resulted in an increase of proliferation (*Figure 58* - B).[143]

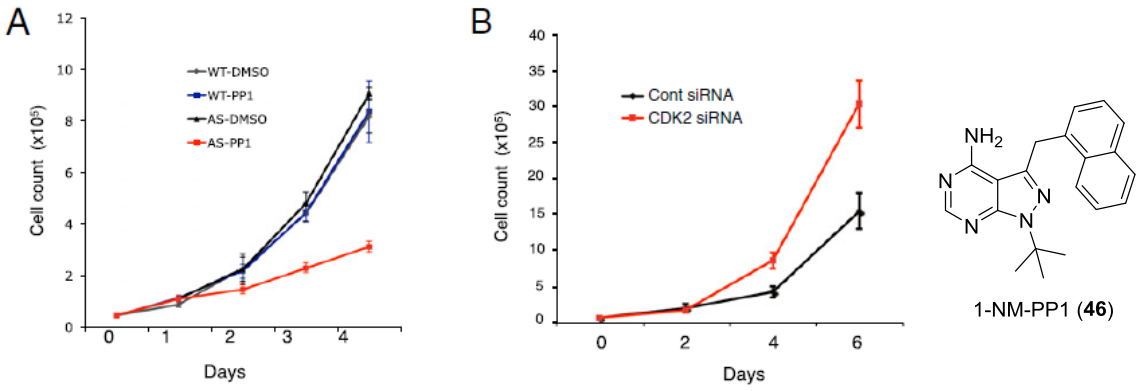

Figure 58 - Cell proliferation profile after small molecule (**46**) inhibition (A) or genetic loss (B)[143] (from D. Horiuchi *et al*, 2012). A. CDK2 inhibtion using **46** had no effect on cell proliferation in the wild-type cells (WT-PP1 versus WT-DMSO) but was shown to decrease considerably cell proliferation in the $CDK2^{AS}$ cells (AS-PP1 versus AS-DMSO). B. CDK2 knockdown (CDK2 siRNA) was shown to promote cell proliferation by comparison to the control experiment (Cont. siRNA).

With genetic loss, cyclin E binds to CDK1 as its CDK2 partner is absent. However, when CDK2 is inhibited, cyclin E does not switch partner and as a result does not bind to

CDK1.[143] Observations on MCF proliferation were also applicable to the HCT116[15] cell line where proliferation decreased when inhibition was carried out using the small molecule 1NM-PP1 (**46**).[143] CDK2 was also shown to be required for 3D-anchorage independent growth of cells overexpressing oncogenes (MYC, Ras or v-ABL) on soft agar (*Figure 59*).[143] These results emphasise the difference between genetic loss and inhibition by a small molecule inhibitor.

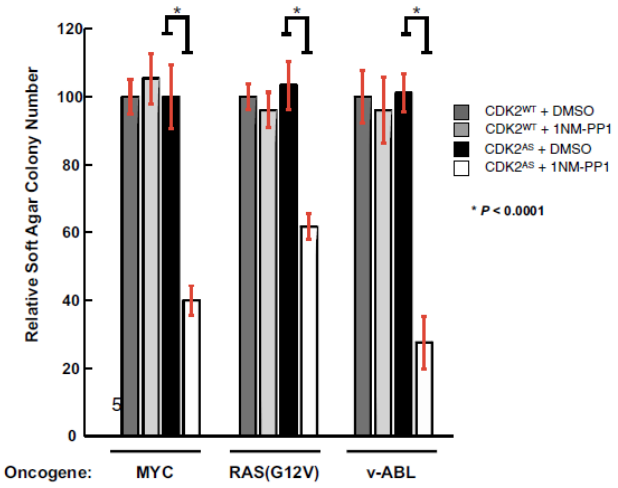

Figure 59 - Effect of small molecule inhibition on colony formation on soft agar[143] (from D. Horiuchi *et al*, 2012). CDK2 inhibition by small molecule (PP1) was shown to reduce colony formation in $CDK2^{AS}$ cells ($CDK2^{AS}$+PP1) overexpressing different oncogenes (MYC, Ras, v-ABL) by comparison to the control experiment ($CDK2^{AS}$+DMSO). In the wild-type cells, CDK2 inhibition by small molecule ($CDK2^{WT}$+PP1) had no effect on colony formation by comparison to the control experiment ($CDK2^{WT}$+DMSO).

Other studies, conducted on CDK2-/- mice, confirmed the non-central role of CDK2.[144] CDK2 knockdown in mice induced prenatal lethality but survivors did not suffer from any malformations, although they were smaller than the CDK2+/+ mice. The expression of the other crucial cell cycle regulators was monitored with no observation of any change in expression of CDK4, 6 and 1 or of cyclin E1 and A2.[144] In addition, the expression of $p27^{T187}$ was similar in both CDK2+/+ and CDK2-/- mice suggesting phosphorylation by other kinases.[144] However, loss of CDK2 in mouse embryonic fibroblasts (MEFs) revealed a delay in S-phase entry. CDK2 seems to be important in timing for entry into S-phase (*Figure 60*) but is replaceable by other kinases, such as CDK4, for p27 phosphorylation, for example.[144]

[15] Colon cancer cell line

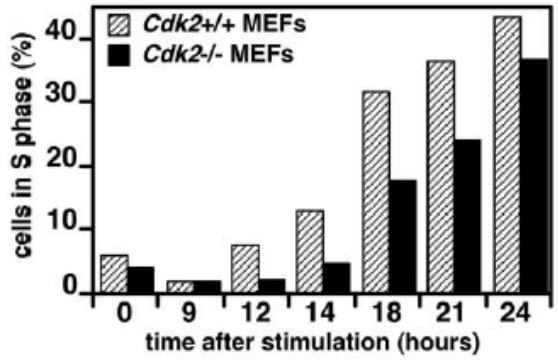

Figure 60 - CDK2 influence on S-phase entry[144] (from C. Berthet *et al*, 2003). A delay in S-phase was observed in mouse embryonic fibroblasts (MEFs) when CDK2 was knocked down(CDK2-/-, black) by comparison to normal CDK2 expression (CDK2+/+, grey).

CDK4 was suggested as a substitute for CDK2 for the phosphorylation of p27. As such, CDK4-/-, CDK2-/- mice were studied.[145] These mice were normal at birth but died after 24 h due to heart tissue problems. Expression of cell cycle regulators was monitored in these mice, revealing no change in activity compared with normal mice (*Figure 61* - A).[145] An augmentation of CDK6/cyclin D2 and CDK1/cyclin E1 was observed (*Figure 61* - B) and pRb was still present (*Figure 61* - C), suggesting phosphorylation by another CDK/cyclin complex.[145]

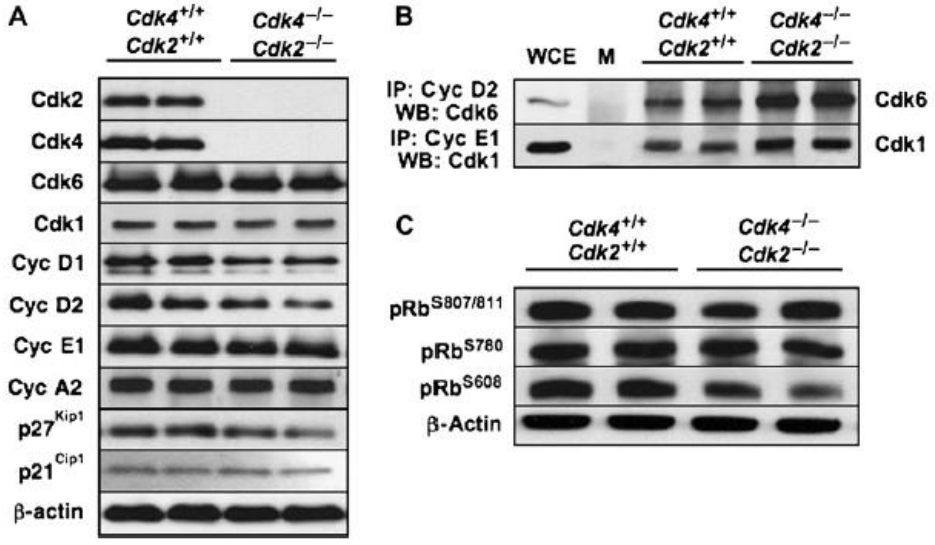

Figure 61 - Expression of cell cycle regulators in both CDK4-/-, CDK2-/- and CDK4 +/+, CDK2+/+ mice[145] (from C. Barriere *et al*, 2007). Western blot analyses show the level of expression of cell cycle regulators in CDK4+/+, CDK2+/+ and in CDK4-/-, CDK2-/- mice. β-actin is used as a loading control.

In higher eukaryotes, several CDKs are expressed, by comparison with unicellular organisms possessing a single CDK, for a more precise control of cell cycle events.[146] The loss of one or several CDKs seems to be compensated by other CDKs. The expression of cell cycle regulators in CDK4-/-, CDK2-/-, CDK6-/- mice was studied and

found to be unchanged.[146] Rb was still phosphorylated at sites thought to be CDK2 specific. When CDK1, cyclin A2 and cyclin B1 were lacking, problems of cell division appeared.[146] CDK1 was shown to interact with all the cyclins involved in the cell cycle in the absence of interphase CDKs. The cell cycle can be represented as shown in *Figure 62*, with CDK1 as the master of the cell cycle interacting with different cyclins.[146]

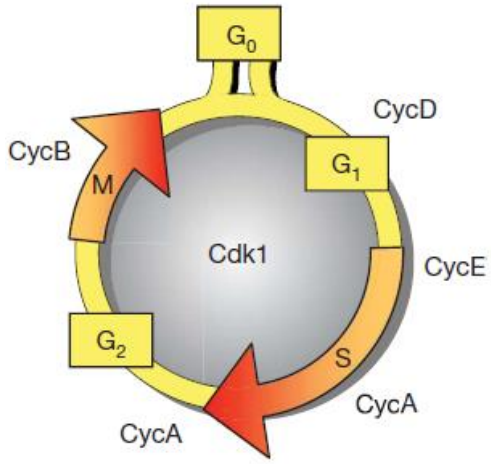

Figure 62 - CDK1 as the only essential CDK for the cell cycle[146] (from D. Santamaria *et al*, 2007).

These observations have to be interpreted carefully as genetic background was revealed to be extremely important.[147] CDK2 was found to be overexpressed in MYCN-amplified neuroblastoma, leading to poor prognosis.[147] Suppression of CDK2 by shRNA caused apoptosis. On the contrary, silencing CDK2 in MYCN single copy neuroblastoma cell lines resulted in an increase or no visible change in fibroblast growth (*Figure 63*).[147] These results differed from previously reported observations suggesting the relation between genetic background and efficiency of silencing CDK2 in cancer therapy.

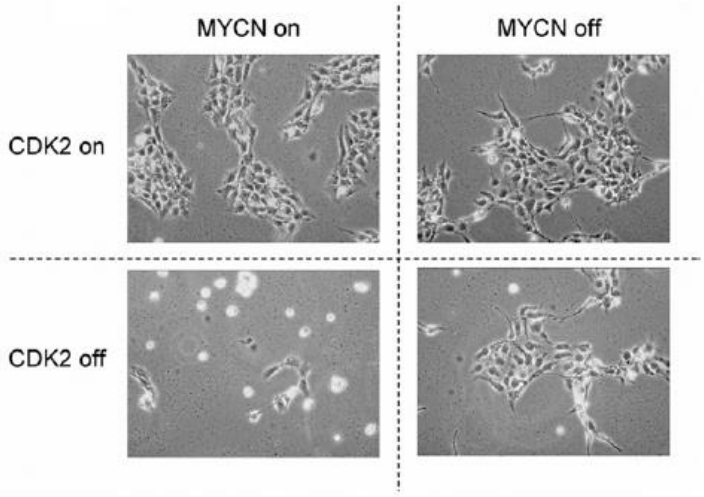

Figure 63 - Effect of CDK2 silencing on the IMR32 (neuroblastoma) cell line with MYCN amplification[147] (from J. J. Molenaar *et al*, 2009). Overexpression of CDK2 (CDK2 on) was observed in MYCN-amplified neuroblastoma (MYCN on) by comparison to MYCN single copy neuroblastoma (MYCN off). Suppression of CDK2 (CDK2 off) using CDK2 shRNA in MYCN-amplified neuroblastoma (MYCN on) caused apoptosis. Suppression of CDK2 (CDK2 off) using CDK2 shRNA in MYCN single copy neuroblastoma (MYCN off) had no effect on cell growth.

CDK2 appears to be a controversial target with results questioning its importance in cancer therapy but recent results are re-positioning CDK2 as a crucial regulator of the cell cycle. Combination therapy would represent an effective and viable strategy. Inhibition studies have been conducted on CDK1/2 and PI3K, a lipid kinase.[148] The results showed apoptosis when inhibition of the three kinases was combined. This observation was confirmed by R-roscovitine (**44**), a dual CDK1 and 2 inhibitor, combined with PIK-90, a PI3K inhibitor, on nude mice implanted with GBM43 cells.[148] The combined therapy showed promising results after 12 days of treatment, with significant tumour regression observed compared to monotherapies (*Figure 64*). Dual PI3K and CDK1/2 inhibition seems to induce synthetic lethality in $PTEN^{WT}$ glioma xenografts *in vivo*.[148] These observations supported the therapeutic viability of CDK2 inhibition alone or in combination.

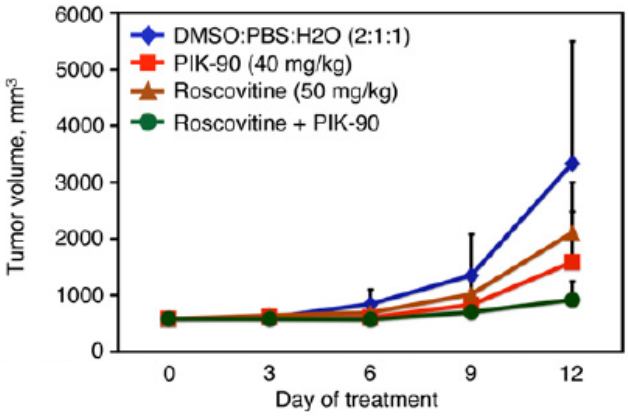

Figure 64 - Effects of roscovitine and PIK-90 on tumour size in $PTEN^{WT}$ glioma xenografts[148] (from C. K. Cheng *et al*, 2012). Inhibition of PI3K with PIK-90 (brown) or inhibition of CDK1/2 with roscovitine (red) had similar effects on the tumour size, with a delay in tumour formation by comparison to the control experiment (blue). Dual inhibition of PI3K and CDK1/2 (green) induced synthetic lethality.

2.3.3. CDK2 inhibitors

- *Purine-based inhibitors*

6-Dimethylaminopurine (**47**) was the first CDK inhibitor reported in the literature.[149] Its activity was first noticed in sea urchin oocytes where mitosis, but not protein biosynthesis, was blocked. Inhibition of CDK1 (IC_{50} = 120 µM) was shown to be responsible for this activity.[149] Further purine derivatives were examined, leading to more potent compounds such as isopentenyladenine (**48**) and olomoucine (**49**), moderately potent against CDK1 (IC_{50} = 7 µM), CDK2 (IC_{50} = 7 µM) and CDK5 (IC_{50} = 3 µM) but selective over a number of other kinases.[150] From the discovery of olomoucine, efforts were made in the synthesis of 2,6,9-trisubstituted purines leading to *R*-roscovitine (**44**), a structural analogue of **49**.[149] This compound, acting as a suppressor of gene transcription, was shown to be 10-fold more potent than **49** (IC_{50} (CDK1) = 0.45 µM, IC_{50} (CDK2) = 0.70 µM, IC_{50} (CDK5) = 0.16 µM)[149] and was found to inhibit proliferation of colon, NSCL, breast and prostate human cancer xenografts.[151] *R*-Roscovitine (**44**) underwent clinical investigation where its efficiency as single agent was demonstrated in several tumour types.[44] The compound was investigated in phase II clinical trials in leukaemias as monotherapy, and in NSCL and metastatic breast cancer in combinatorial trials.[44]

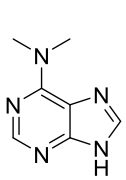

6-dimethylaminopurine (**47**)

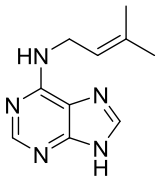

isopentenyladenine (**48**)

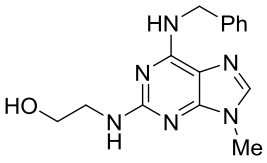

olomoucine (**49**)

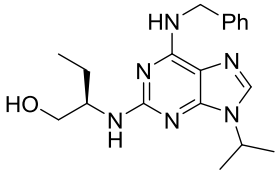

(*R*)-roscovitine (**44**)

Further analogues of **44** were synthesised such as purvalanol A (**50**) and B (**22**). Purvalanol A (**50**) was shown to be selective for CDK2, 4 and 5.[150] Studies on the mechanism of action of **50** revealed inhibition of CDK partners (*e.g.* protein Rb, cyclin A and cyclin E).[152] This molecule appeared to cause reversible G2 arrest, characteristic of CDK2 inhibition in living cells, without affecting S-phase. Cell death and inhibition of cell proliferation were also noticed on proliferating cells treated with **50**.[152] Purvalanol B (**22**) was shown to act in a similar manner but appeared to be more potent against CDK2/cyclin A complex (IC_{50} (**22**) = 6 nM versus IC_{50} (**50**) = 70 nM).[149]

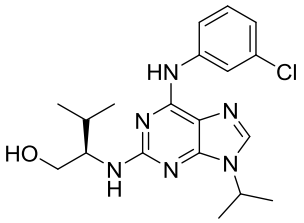

purvalanol A (**50**)

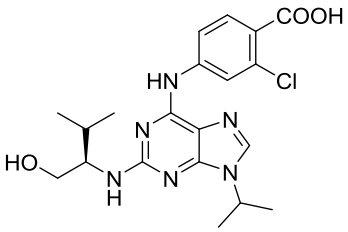

purvalanol B (**22**)

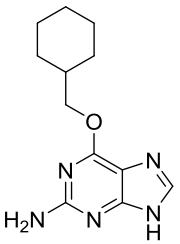

NU2058 (**51**)

R-Roscovitine (**44**), purvalanol A (**50**) and purvalanol B (**22**) are structural analogues and were shown to share the same binding mode to CDK2. Contrary to ATP, which binds to CDK2 via one H-bond each to Glu81 and Leu83, these compounds interact primarily with Leu83. The *N*-7 of the purine scaffold acts as a H-bond acceptor, instead of *N*-1 with ATP, for NH of Leu83 (red in *Figure 65*), while NH at the 6-position plays the role of the H-bond donor with the carbonyl of Leu83 (blue in *Figure 65*).

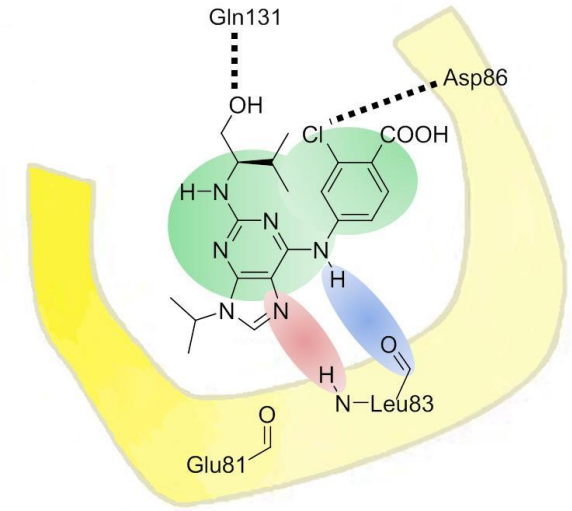

Figure 65 - Binding mode of purvalanol B (**22**) with CDK2 showing interactions with key residues[149] (from A. Huwe *et al*, 2003).

Another purine, NU2058 (**51**), was shown to be moderately potent against CDK2 (IC_{50} = 12 µM) and CDK1 (IC_{50} = 5 µM).[153] Interestingly, this compound demonstrated a different binding mode from ATP or the 2,6,9-trisubstituted purines (see *Chapter 2*, section 2.3.4.).

- *Other classes of inhibitors*

Flavopiridol (**52**) is a semisynthetic flavonoid, isolated from the leaves and stems of *Amora rohituka*, an Indian plant (*Figure 66*).[151] This drug was initially developed as an EGFR inhibitor, but was later shown to bind to CDK2, 7 and 9.[154] Flavopiridol was found to induce apoptotic cell death by activating the MAPK pathway, as well as inhibiting the production of anti-apoptotic molecules such as p21, bcl-2 or cyclin D1, and transcription, as a result of CDK9 inhibition.[44] Indeed, CDK9 plays an important role in the initiation and elongation of mRNA, essential in protein synthesis.[155] Compound **52** was shown to induce cell cycle arrest and apoptosis in squamous head and neck cell lines[44] and to have a growth inhibition effect on breast and lung cancer cell lines and prostate and head and neck tumour xenografts.[150] Even though the effects of this drug were significant, results of clinical trials using flavopiridol as a single agent on solid tumours were disappointing because of a poor response.[156-158]

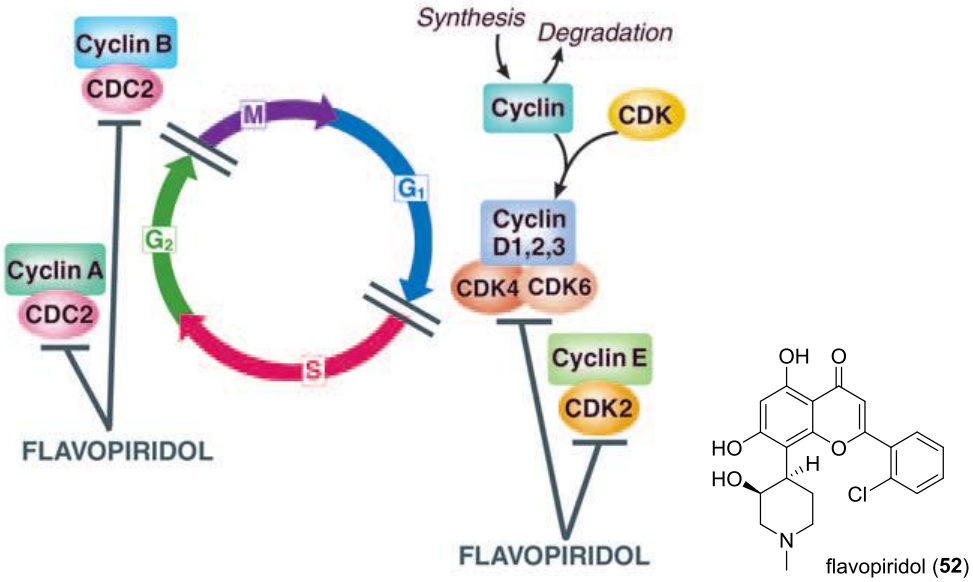

Figure 66 - Structure of flavopiridol (**52**) and effects on the cell cycle[44] (from G. K. Schwartz and M. A. Shah, 2005). Flavoripidol inhibits cdc2 (CDK1) in complex with cyclin A or with cyclin B. Flavoripidol also inhibits CDK2/cyclin E as well as CDK4 and 6.

AT7519 (**53**), developed by Astex, is a multi-CDK inhibitor active against CDK5 and 9, but with a preference for CDK2.[40] This compound showed antiproliferative activity in different human tumour cell lines and evoked tumour regression in colon cancer xenograft models.[40] Compound **53** has been investigated in phase I clinical trials.[40]

NU6027 (**54**), a pyrimidine analogue of the CDK2 purine inhibitor NU2058 (**51**), was shown to bind to CDK2.[149] This compound is an ATP-competitive inhibitor which inhibits both CDK1 and CDK2 (IC_{50} (CDK1) = 2.5 µM, IC_{50} (CDK2) = 1.3 µM).[153] Compound **54** was found to be more potent in cellular tests (10 µM) than its purine analogue **51**.[153] NU6027 (**54**) binds in a similar manner to NU2058 (**51**) with a triplet of H-bonds (*Figure 67*).[149]

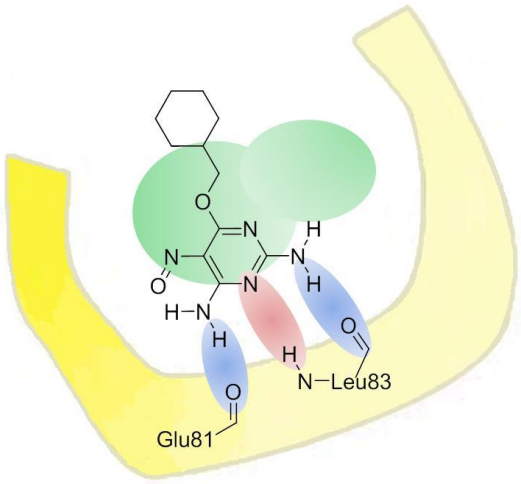

Figure 67 - Binding mode of **54** in the ATP pocket of CDK2 showing key H-bond interactions with the hinge region[149] (from A. Huwe *et al*, 2003).

BMS-387032 (**55**) (or SNS-032) is an aminothiazole analogue that selectively inhibits CDK2, 7 and 9.[44] This drug was shown to induce cell cycle arrest and apoptosis in several tumour cell lines such as ovarian carcinoma.[44] The *in vivo* activity was confirmed in animal models including ovarian and colon cancer.[154] This compound is currently being investigated in phase I clinical trials, in several refractory solid tumours and B-lymphoid malignancies.[154]

Another class of CDK inhibitor is based on the imidazopyridine pharmacophore. An example of this type is AZ703 (**56**), a selective inhibitor of CDK1/cyclin B (IC_{50} = 6 nM), CDK2/cyclin E (IC_{50} = 4 nM) and CDK2/ cyclin A (IC_{50} = 3 nM).[159] Compound **56** was shown to induce G1/S and G2/M phase arrest, and had an antiproliferative effect on several tumour cell lines *in vitro* such as breast, lung and colorectal cancer.[159] Inhibition of phosphorylation of p27 on Thr187 and pRb on Thr821 was observed after exposure to **56**.[159]

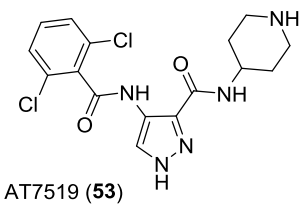

AT7519 (**53**)

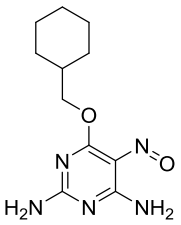

NU6027 (**54**)

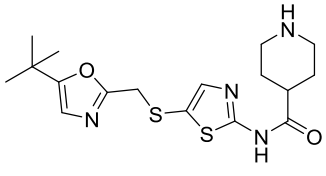

BMS-387032 (**55**)

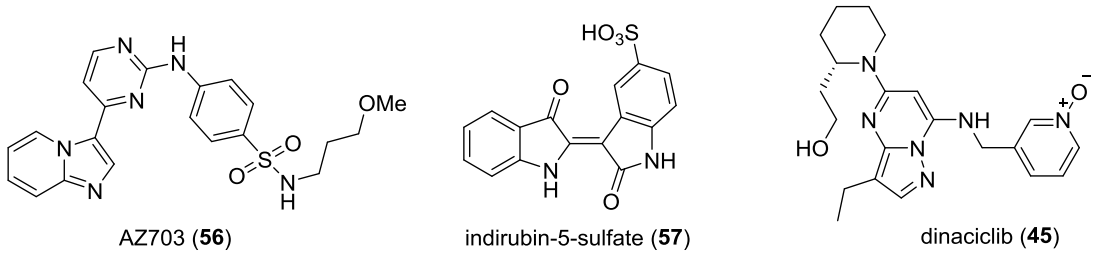

Oxindoles were also investigated and several were shown to be 10-fold more potent for CDK2 over CDK1.[160] These compounds inhibit tumour cell proliferation with an 8-fold selectivity for tumour cells over normal cells and block cell progression into S-phase.[160] An example of this series is indirubin-5-sulfate (**57**), which interacts with Glu81 and Leu83 residues of CDK2, in a similar manner to ATP (*Figure 68*).[149]

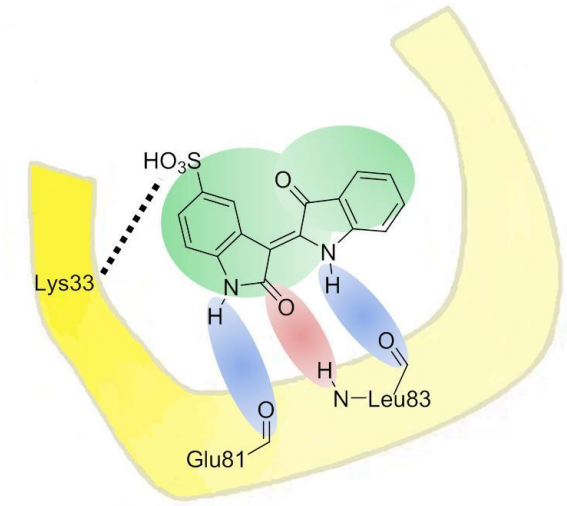

Figure 68 - Binding mode of indirubin-5-sulfate (**57**) with CDK2 highlighting interactions with key residues, mainly from the hinge region[149] (from A. Huwe *et al*, 2003).

By comparison with first generation CDK inhibitors, discontinued in clinical trials due to selectivity problems, dinaciclib (**45**) was shown to be strongly selective for the CDK family, exhibiting activity against CDK2, 5, 1 and 9 (IC_{50} = 1, 1, 3 and 4 nM, respectively).[161] After treatment of several human tumour cell lines with **45**, cell cycle arrest was observed, demonstrating antiproliferative activity regardless of the tumour type or genetic background.[161] Dinaciclib (**45**), developed by Merck, has progressed to phase III clinical trials for refractory chronic leukemia.[162] The crystal structure of **45** with CDK2 revealed binding within the ATP-binding pocket, and interesting interactions such as the hydrogen bond between Lys89 and the *N*-oxide moiety (Chapter 9, section 9.2.).[162]

2.3.4 Covalent CDK2 inhibitors

Abnormalities in genes encoding proteins involved in CDK pathways such as p16, cyclin D (direct interaction), p53 (indirect interaction) or pRb (substrate), have often been observed in human tumours.[153] These results underline the need for the identification of CDK inhibitors more specific to one particular CDK, but still retaining cellular potency.[153] This area might be wide as tumour cells express different sensitivity towards CDK inhibitors according to the tumour type studied.[40] First and second generation CDK inhibitors were invariably ATP-competitive with poor selectivity. The third generation of CDK inhibitors[163] would ideally target the cell cycle in a reversible manner for normal cells but would have a lethal effect on tumour cells.[159] Design is a key feature in the synthesis of selective inhibitors, where the crystal structure of the enzyme is essential for guidance. Several *X*-ray structures of inhibitors in complex with CDK2 have been solved, as cited previously, guiding the synthesis of further inhibitors.[159]

As mentioned above, NU2058 (**51**) is an ATP-competitive purine-based inhibitor with an IC_{50} of 5 µM for CDK1 and 12 µM for CDK2.[164] Compound **51** was shown to bind to the Thr160 phosphorylated CDK2-cyclin A complex, via a triplet of hydrogen bonds between the purine core and the residues Leu83 and Glu81 within the hinge region (blue circle, *Figure 69*). The O^6-cyclohexylmethyl moiety was shown to interact with the ribose site whereas the imidazole ring of the purine core is engaged in an aromatic-aromatic contact with Phe80. SAR studies showed that a cyclohexylmethyl group at the O^6-position was optimal for activity.[164] Compound **51** emerged as a structural lead for the design of further CDK2 inhibitors.

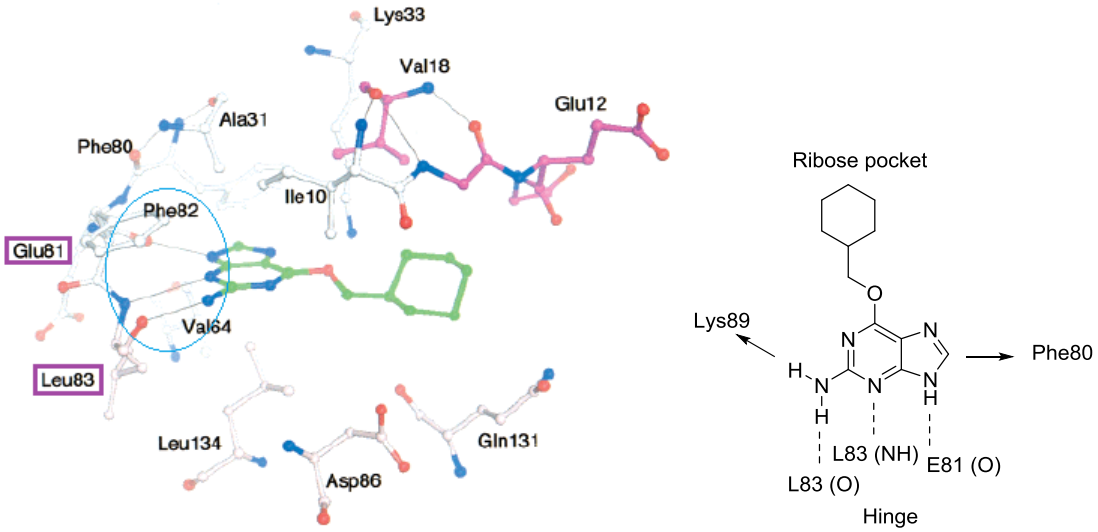

Figure 69 - Crystal structure of **51** in complex with CDK2 highlighting the triplet of H-bonds with the hinge region[153] (from C. E. Arris *et al*, 2000). The PDB entry is 1E1V.

Further optimisations employing a structure-based approach led to the synthesis of **58**, a potent CDK2 inhibitor (IC_{50} = 5.4 nM).[164] The crystal structure of **58** in complex with CDK2 showed the same interactions as for **51**. However, the introduction of a sulfonamide moiety allowed additional interactions. One oxygen of the sulfonamide moiety is involved in hydrogen-bonding with the NH of the backbone Asp86 residue (r_{NH-O} = 3.1Å) while the NH_2 of the sulfonamide moiety is involved in hydrogen-bonding with the carbonyl of the same Asp86 residue (r_{NH2-O} = 2.9Å) (*Figure 70*).[165]

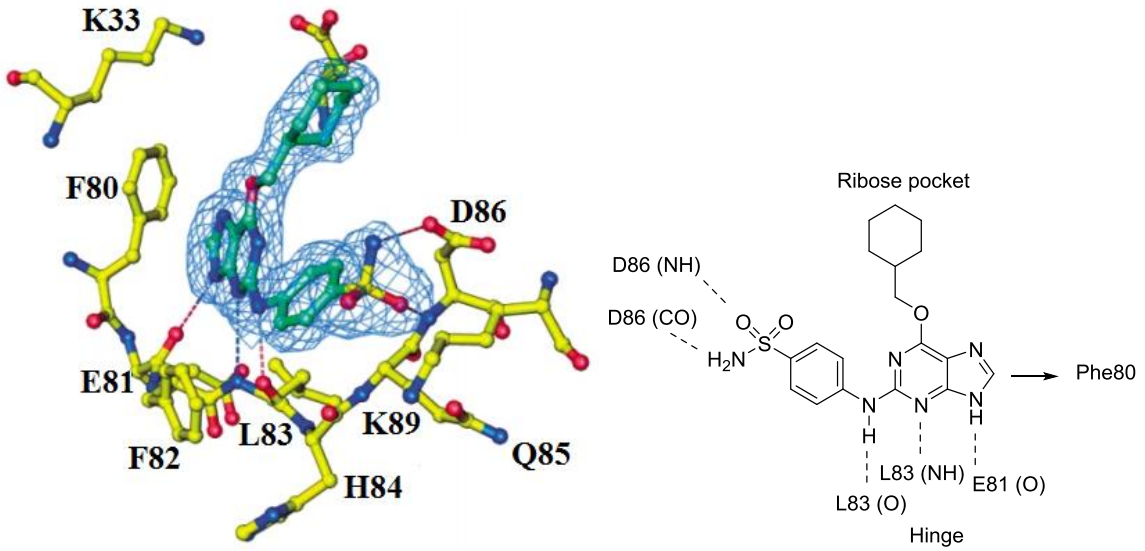

Figure 70 - Crystal structure of **58** with CDK2 showing the triplet of H-bonds of the 2-aminopurine scaffold with the hinge region and the H-bond interaction between the sulfonamide group and Asp86[164] (from T. G. Davies *et al*, 2002). The PDB entry is 1H1S.

To enhance the cellular activity of **58** found in the range 1-10 µM,[165] isosteric replacement of the sulfonamide moiety of **58** was investigated with a series of

carboxamide- and urea-based purine derivatives. This strategy was unsuccessful with the sulfonamide being the best group for CDK2 activity. The high potency of **58** was due to its interactions with Asp86, and so to maintain this crucial interaction, sulfone-based inhibitors were synthesised. [166] Despite an overall reduction of activity against CDK2 with these inhibitors, this series identified a vinyl sulfone (**60**), shown to inhibit CDK2 in a time-dependent manner. To confirm the covalent binding between **60** and CDK2, a mass spectrometric analysis was performed. Affinity labelling experiments were carried out with **60** and **59**, a control compound with an ethyl group instead of the vinyl substituent. The mass spectrometric profile of **59** was similar to the blank experiment, with no change in mass observed (*Figure 71*). However, when the experiment was conducted with **60**, an increase of 414 Da was observed, which corresponded to the molecular weight of **60** (*Figure 71*).[167] This observation suggested that **60** was covalently bound to CDK2.

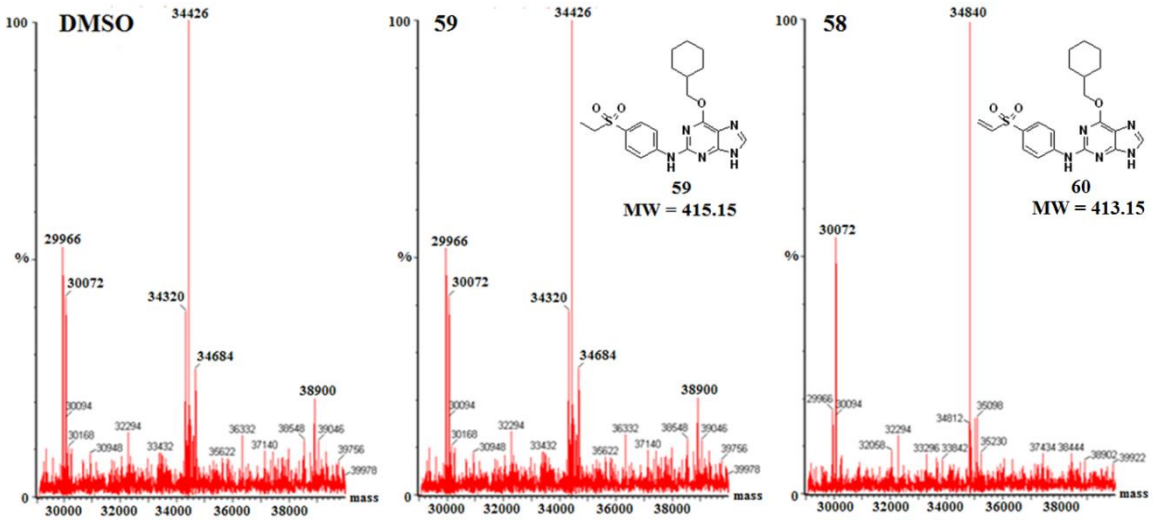

Figure 71 – Mass spectrometric analysis of **59** and **60** with CDK2/cyclin A[167] (from E. Meschini, 2011). The experiment with compound **59** showed the same mass spectrometry profile as the control experiment (DMSO). The experiment with compound **60** showed an increase of 413 by comparison to the control experiment (DMSO) which corresponds to the molecular weight of compound **60**, indicating covalent binding.

Two residues, Lys88 and Lys89, were potentially sufficiently reactive and close enough to the vinyl sulfone moiety of **60** to form a covalent bond. To confirm this hypothesis, a mass spectrometric experiment was conducted on **60** with a mutant CDK2, Lys88E/Lys89V, where Lys88 was replaced by a glutamic acid and Lys89 by a valine. No difference in mass was observed between the blank experiment and that performed with **60**, suggesting that **60** did not bind to the mutant form of CDK2 (*Figure 72*).[167] The hypothesis that either Ly88 or Lys89 reacted covalently with **60** was, therefore, confirmed.

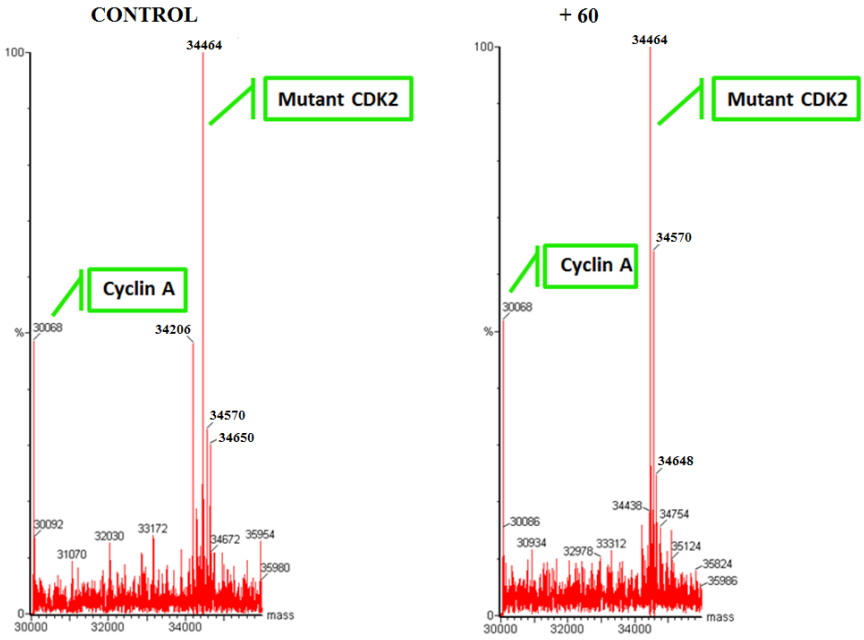

Figure 72 - Mass spectrometric analysis of **60** with mutant CDK2(Lys88E/Lys89V)/cyclin A [167] (from E. Meschini, 2011). The mass spectrometry profiles of the protein with compound **60** and the control experiement (DMSO) are identical. No covalent binding occurs.

The crystal structure of compound **60** in complex with CDK2 was solved. This inhibitor was shown to bind to the hinge region of the kinase via a triplet of hydrogen bonds, identical to **58**, and an interaction through the sulfone moiety with the backbone residue Asp86 was also present. Crucially, a covalent bond between the vinyl sulfone moiety and the backbone residue Lys89 was observed (*Figure 73*).[167] Compound **60** is the first irreversible CDK2 inhibitor described to date in the literature.[165]

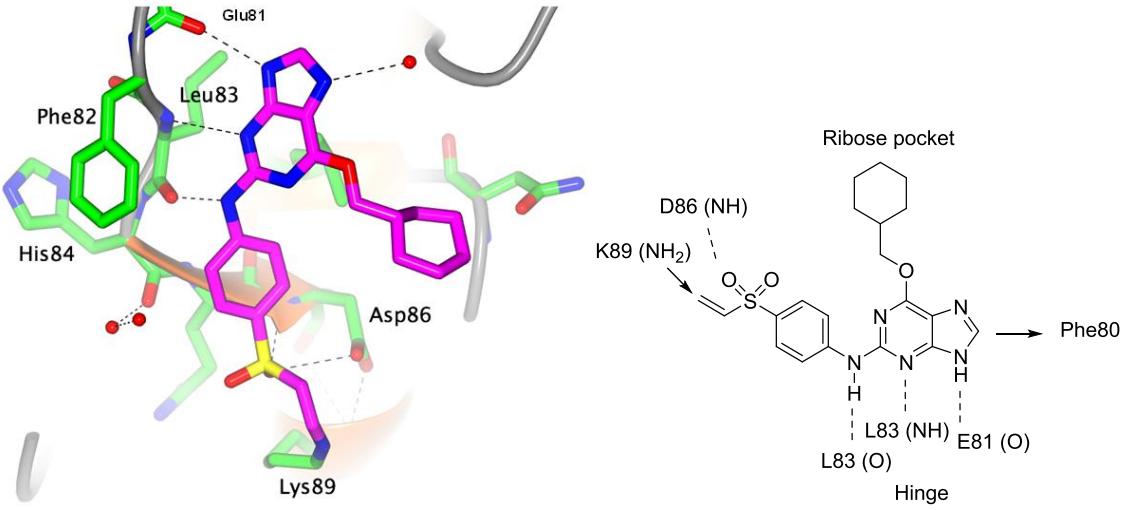

Figure 73 – Co-crystal structure of **60** with CDK2[167] showing the H-bond interactions with the hinge region, the interaction with the sulfone group and Asp86, and the covalent binding between Lys89 and the vinyl sulfone warhead (from E. Meschini, 2011).

The probable mechanism by which Lys89 reacts with the vinyl sulfone moiety of **60** is shown below (*Scheme 1*), and involves a Michael addition reaction leading to the formation of a covalent bond between Lys89 and **60**.[167] The high reactivity of **60** caused stability and selectivity issues, and the results obtained from a time-dependent assay against were probably representative of both the potency of **60** (IC_{50} = 63 nM[165]) and its decomposition.

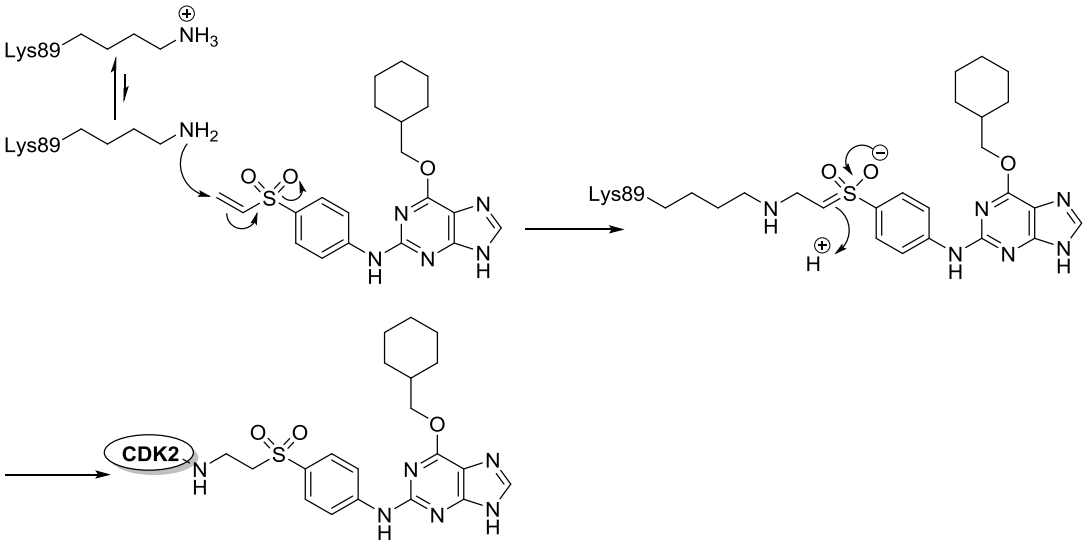

Scheme 1 – Possible mechanism for the covalent reaction of **60** with Lys89 of CDK2.

2.4. Objectives of the thesis

The thesis is divided into two parts with the work carried out within the Nek2 project described first (Chapters 3 and 4) followed by the work done within the CDK2 projects (Chapters 5, 6, 7, 8 and 9).

The objectives of the first project were the design and synthesis of control compounds to assess the potential off-target effect of the 2-aryl-6-ethynylpurine inhibitors of Nek2 by perturbing their main interactions with Nek2, the covalent binding with Cys-22 and the triplet of H-bonds with the hinge region. This work confirmed the presence of the off-target activity of the 2-aryl-6-ethynylpurine series leading to the closure of the project. N-7 methylation of purines was shown to abolish Nek2 inhibitory activity but retained the cellular potency. Based on this result, a series of N-7 methylated purines was developed with the objective to discriminate the off-target activity over Nek2 inhibition but the strategy was unsuccesful. Kinetic studies have also been conducted on selected 6-ethynylpurines to assess the impact of *N*-7/*N*-9 methylation on the chemical reactivity of the 6-ethynyl 'warhead'. A model system was developed to investigate a possible

correlation between the chemical and biological reactivity of the 6-ethynyl group of the purine derivatives with thiols.

The objective of the second project was to improve the chemical stability of a covalent inhibitor of CDK2, the first to be described in the literature, through modifications of its vinyl sulfone warhead that reacts with Lys89, while retaining the covalent binding with CDK2. Substitutions of the vinyl sulfone at the α- and β- positions were investigated as well as the replacement of the vinyl sulfone group by other electrophilic warheads. This work led to the discovery of an α-chloro derivative showing the best time-dependent inhibition profile against CDK2 so far within the project. To explore further the potential of the vinyl sulfone as a reactive warhead, this group was introduced into known CDK2 inhibitors.

Chapter 3. Assessment of Potential Off-target Biological Activity of 6-Ethynylpurine Nek2 Inhibitors

A disparity was observed between the enzyme inhibitory activity and growth inhibition of the 6-ethynylpurine Nek2 inhibitors. Therefore, control compounds were required to assess the possibility of an off-target activity from the 6-ethynylpurine series. In this chapter, the synthesis of such compounds is described as well as their Nek2 inhibitory activities and cellular potencies (section 3.1). As the off-target activity was confirmed, a series of *N*-7 methylated purines was synthesised with the aim of discriminating the off-target effect from the Nek2 inihibition. The biological results of this series are discussed (section 3.2).

Methylation at the *N*-7 and *N*-9 position of compounds **41** and **42** was expected to perturb the triplet of donor/acceptor/donor hydrogen bonds (see Chapter 2) responsible for binding to the hinge region of Nek2 (**61**-**64**).

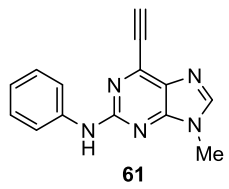

61

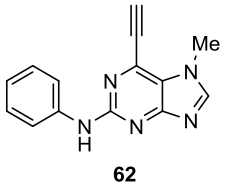

62

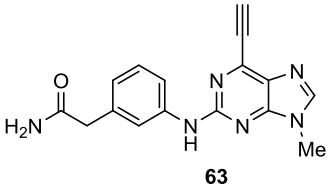

63

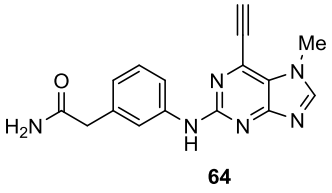

64

The introduction of a 6-cyano group, bioisosteric with 6-ethynyl, was expected to block the addition of Cys22. The 6-cyano derivative **65** was synthesised along with the 6-cyanopurines having a methyl group at the *N*-9 and *N*-7 positions (**66** and **67**, respectively), intended to abolish both covalent binding and interactions with the hinge region.

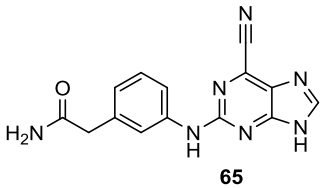

65

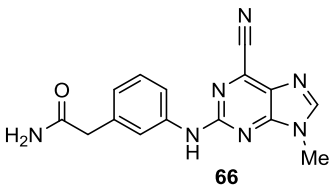

66

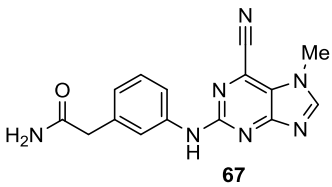

67

3.1. Synthesis of control compounds 61-64

3.1.1. Synthesis of N^9- and N^7-methyl purines

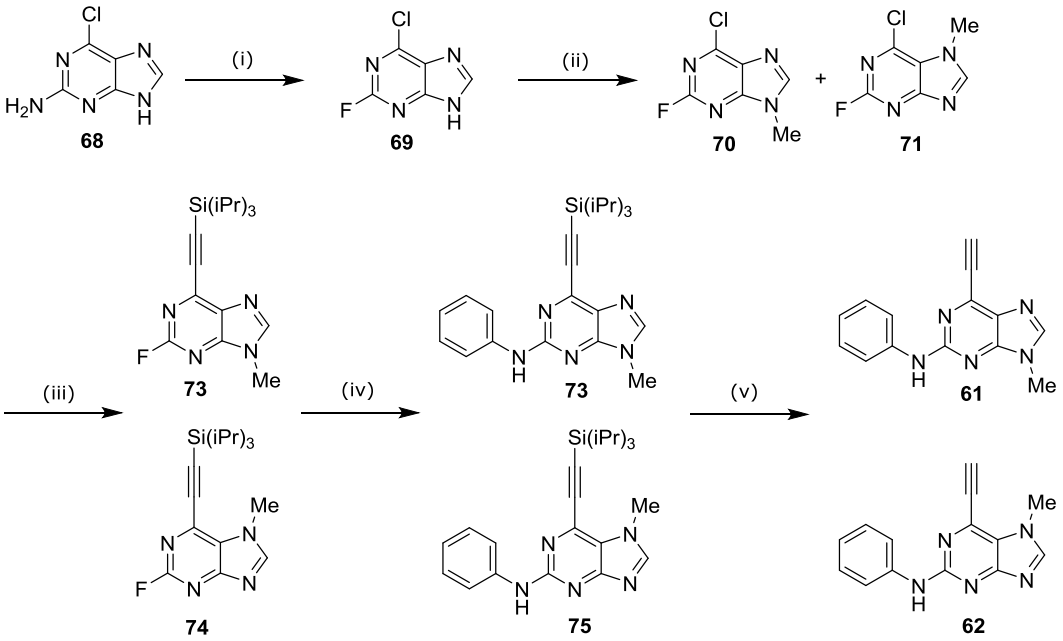

Scheme 2 - *Reagents and conditions*: (i) HBF_4, $NaNO_2$, r.t., 18 h, 50%;(ii) MeI, K_2CO_3 in DMF, r.t., 18h, 92%; (iii) triisopropylsilylacetylene, CuI, $Pd(PPh_3)_2Cl_2$, Et_3N in THF, r.t., 18 h, 49% (**72**), 22% (**74**); (iv) TFA, aniline in TFE, 140 °C, 15 min, MW, 34% (**73**), 62% (**75**); (v) TBAF in THF, r.t., 10 min, 56% (**61**), 47% (**62**).

The synthetic scheme for the synthesis of the N^9- and N^7-methylpurine derivatives (**61** and **62**, respectively) started with the commercially available 2-amino-6-chloropurine **68**, which was subjected to a Balz-Schiemann reaction[168] to insert a fluoro group at the 2-position (**69**) (*Scheme 2*). Methylation of compound **69** was performed using MeI and K_2CO_3 in DMF.[153] The isomers **70** and **71** were obtained as an inseparable mixture (ratio 7:3 of N^9- (**70**) and N^7-methylpurines (**71**), respectively). The Sonogashira reaction[169] was conducted on the mixture of isomers. At this stage, the two isomers were separable, leading to 49% of the N^9-methyl isomer **72** and 22% of the N^7-methyl compound **74**. An NMR method based on the shift of the $C_8\mathbf{H}$ of the purine was used to identify the two isomers, using the knowledge that the more deshielded $C_8\mathbf{H}$ signal corresponds to the *N*-7 isomer (*Figure 74*).[170]

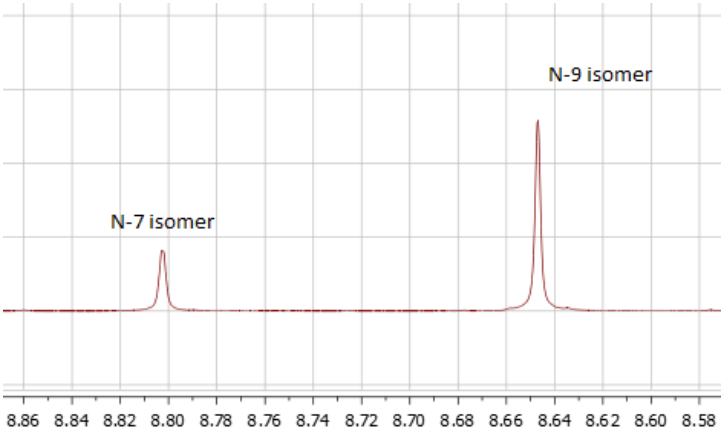

Figure 74 – Identification of N^7- (**74**) and N^9-methyl (**72**) isomers by ^{1}H NMR

Aromatic substitution under microwave heating was performed at the purine 2-position on each of the two isomers, leading to N^9-methyl isomer **73** in 34% and N^7-methyl isomer **75** in 62% yield.[171] TFA catalysed the reaction by protonation of *N*-1, which facilitated nucleophilic attack by aniline to form the Meisenheimer-Jackson intermediate.[171] Loss of fluoride from this intermediate afforded the target compounds (*Scheme 3*). Deprotection of the TIPS group using TBAF was performed using a calcium sulfonate scavenger resin to complex the tetrabutylammonium species remaining in the reaction mixture.[172] Compounds **61** and **62** were obtained in 56% and 47% yield, respectively.

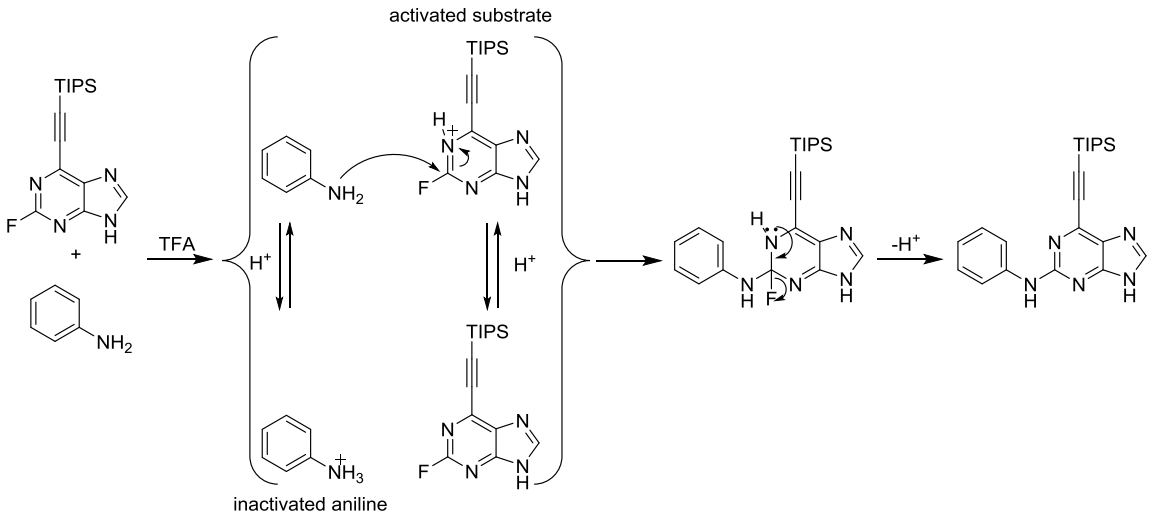

Scheme 3 - S_NAr mechanism under TFA-TFE conditions

A similar synthetic route was followed for the preparation of the control compounds **63** and **64** having the substituted 2-arylamino group at the 2-position. The diversity was introduced during the nucleophilic aromatic substitution using the TFA/TFE method (*Scheme 4*).

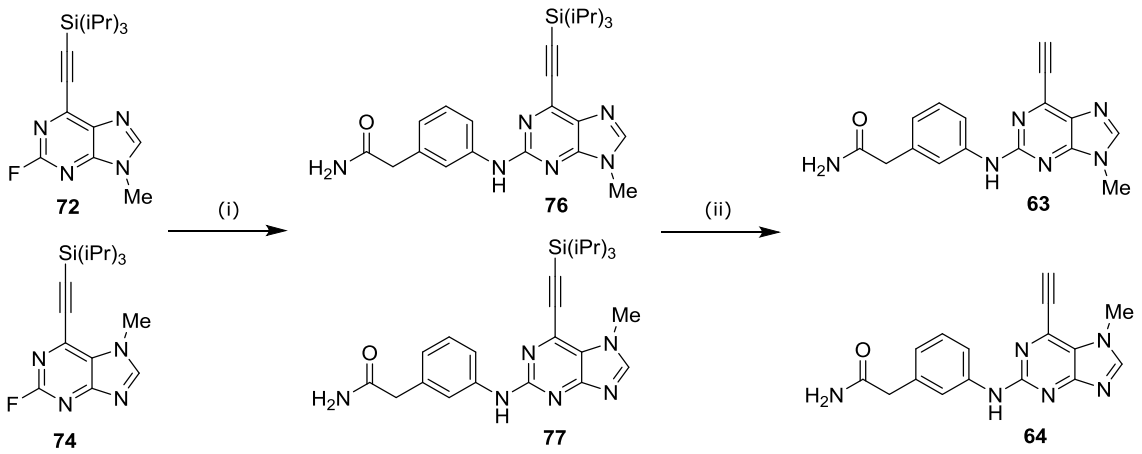

Scheme 4 - *Reagents and conditions*: (i) TFA and **79** in TFE, 140 °C, 15 min, MW, 43% (**76**), 52% (**77**); (v) TBAF in THF, r.t., 10 min then scavenger beads, r.t., 18 h, 56% (**63**), 21% (**64**).

As 2-(3-aminophenyl)acetamide **79** was not commercially available, the aniline was prepared from 3-aminophenylacetic acid **78** in two steps in a one-pot procedure.[136] Firstly the methyl ester of carboxylic acid **78** was formed, and then ammonia was used to obtain the desired carboxamide **79** (*Scheme 5*).

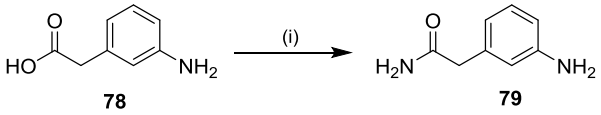

Scheme 5 - *Reagents and conditions*: (i) $SOCl_2$ in MeOH then aq. NH_3, 41%.

3.1.2. Synthesis of 6-cyanopurine control compounds

- *Synthesis of 6-cyanopurine derivative **65***

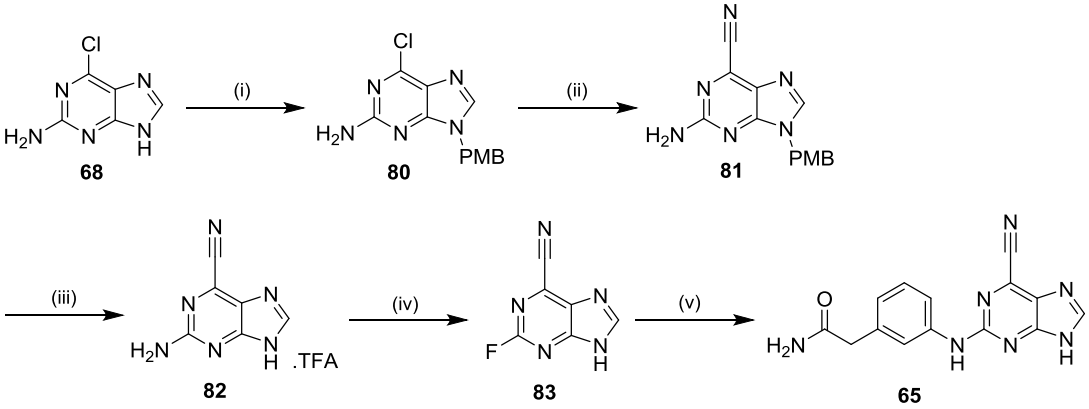

Scheme 6 - *Reagents and conditions*: (i) PMBCl, Cs_2CO_3 in DMF, 60 °C, 18 h; (ii) DABCO, Et_4NCN in MeCN, r.t., 18h; (iii) neat TFA, 70 °C, 5 h; (iv) HBF_4, $NaNO_2$, r.t., 18 h; (v) TFA, TFE, 140 °C, 30 min, MW.

The previous method used within the group (*Scheme 6*) showed some weaknesses such as a poor yield of the fluorination step as well as in the nucleophilic aromatic substitution.

To improve the overall yield of the synthesis, iodination of the protected 2-amino-6-cyano purine **81**, instead of the traditional fluorination, was considered. From the iodo derivative **84**, a Buchwald reaction was investigated (*Scheme 7*).

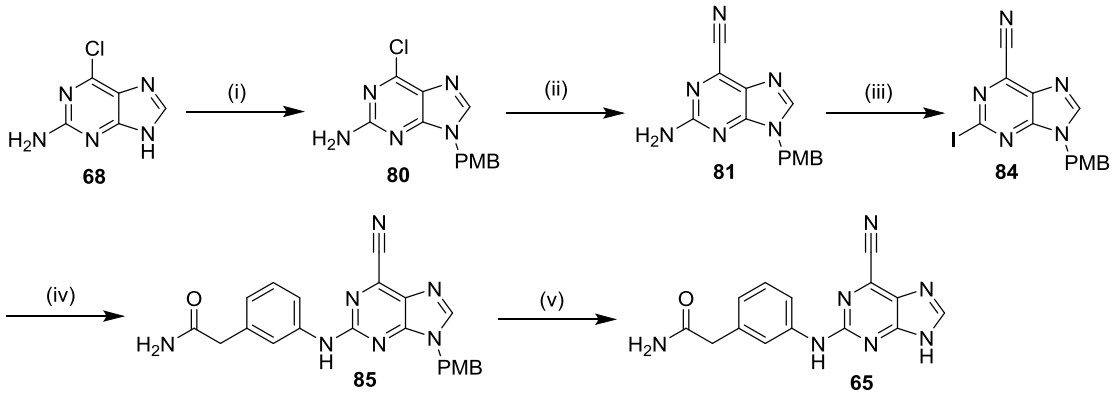

Scheme 7 - *Reagents and conditions*: (i) PMBCl, Cs_2CO_3 in DMF, 60 °C, 18 h, 60%; (ii) DABCO, Et_4NCN in MeCN, r.t., 18h, 62%; (iii) isoamyl nitrite, CH_2I_2, CuI in THF, 70 °C, 2 h, 62%; (iv) Brettphos, K_2CO_3, **79**, $Pd(OAc)_2$ in DME, 120 °C, 20 min, MW, 43%; (v) TFA, 70 °C, 5 h, 47%.

In terms of *N*-9 protecting group choice, THP was previously employed within the group but was cleaved under the cyanation conditions. Benzyl was also used previously but found to be impossible to remove. The PMB group was chosen as orthogonal to cyanation conditions. 2,4-Dimethoxybenzyl was also considered as it would have been easier to remove than PMB. However, attempts to synthesise the reagent 2,4-dimethoxybenzyl chloride were unsuccessful,[173] the compound being extremely unstable. Regioselectivity was observed for PMB protection as only the N^9-PMB compound **80** was isolated in a satisfactory yield. The cyanation step was performed using DABCO and Et_4NCN leading to compound **81** in 60% yield.[136] This reaction involves the formation of an intermediate where DABCO acts as nucleophile and displaces the chloro group to form a better leaving group. This intermediate underwent a nucleophilic attack by Et_4NCN to form the desired compound **81**. Iodination[174] was then carried out with some difficulties as the iodo derivative **84** appeared to be light-sensitive. In order to minimise degradation, the reaction mixture was protected from light and stored in the freezer under nitrogen. The yields for this reaction were approximately 50% and poorly reproducible. Buchwald reaction was tried initially on compound **84** under microwave heating using Xantphos as ligand, $Pd(OAc)_2$ as catalyst, and Cs_2CO_3 as base in dioxane. However, the yield was relatively low (34%). From these results and based on the user's guide for Buchwald reactions,[175] DMA was used as solvent, K_2CO_3 as base, $Pd(OAc)_2$ as palladium source and Brettphos as ligand. Using these conditions, the yield was improved to 43%.

PMB deprotection was performed in neat TFA under reflux.[136] Compound **65** was obtained in six steps with an overall yield of 4%.

- *Synthesis of N^9- and N^7-methyl derivatives of 6-cyanopurine (**66** and **67**)*

For this synthesis, a similar route to that described in the section above was first considered (*Scheme 8*), but with methylation replacing the PMB protection to allow for the cyanation. Methylation using methyl iodide led to a mixture of N^9- and N^7-methylpurines (**86**/**87**) in a ratio of 4:1, respectively. No purification was performed on this mixture of isomers as they were insoluble in common solvents, and the insolubility of this mixture (**86**/**87**) proved to be an important problem for the following step. The cyanation reaction was tried in different solvents such as MeCN, NMP and DMPU but no reaction occurred. When the temperature was slightly increased to 50 °C, degradation of the starting material (**86**/**87**) was noticed and no target compound (**88**/**89**) was formed.

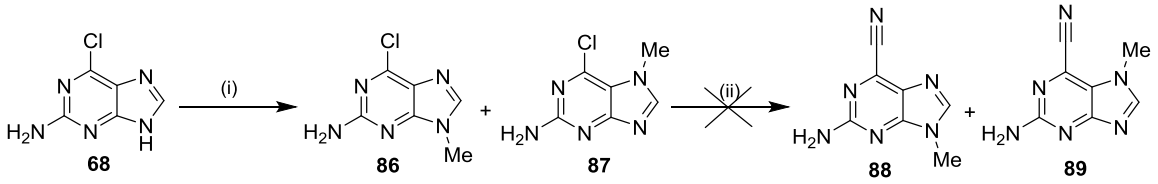

Scheme 8 - *Reagents and conditions*: (i) MeI, K_2CO_3 in DMF, r.t., 18 h, 89%; (ii) DABCO, Et_4NCN in MeCN, r.t., 18 h, 62%.

As a result, another strategy was considered (*Scheme 9*), where halogenation was performed first, followed by cyanation and coupling. The iodination performed on the mixture of **86**/**87** led to one desired intermediate, the N^9-Me isomer **90**, in 30% yield. A Buchwald reaction was carried out on compound **90** under the conditions detailed in section 3.1.2. Unfortunately, although the reaction mixture was clean, the cross-coupling took place at the unwanted 6-position (**91**) (observed by LC-MS, product not isolated). As the Buchwald reaction did not give the result expected, cyanation was attempted on compound **90** but only degradation was observed.

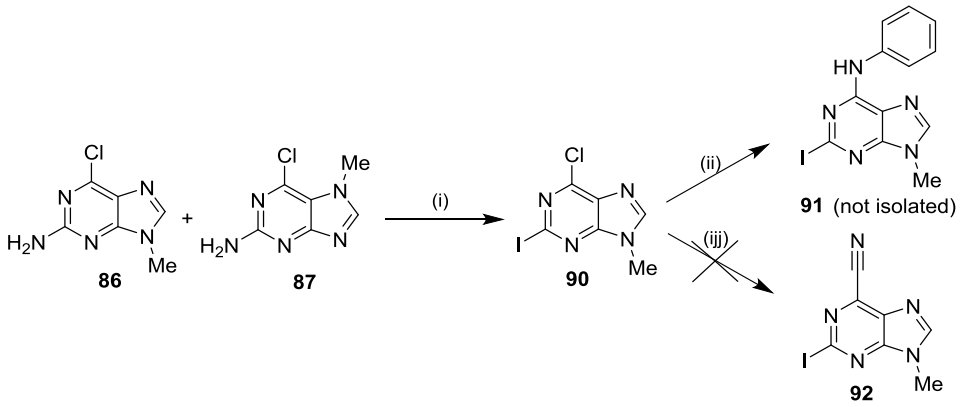

Scheme 9 - *Reagents and conditions*: (i) isoamyl nitrite, CH_2I_2, CuI in THF, 70 °C, 2 h, 30%; (ii) Brettphos, K_2CO_3, aniline, $Pd(OAc)_2$ in DME, 120 °C, 20 min, MW; (iii) DABCO, Et_4NCN in MeCN, r.t., 18 h.

As the first attempts led to no satisfactory results, fluorination of the mixture of isomers **86**/**87** was attempted (*Scheme 10*). The same observation as for the iodination was made: only the N^9-Me isomer **70** was retrieved after purification, suggesting the minor formation of N^7-methyl isomer. Cyanation and nucleophilic aromatic substitution reactions were attempted on compound **70**, but the cyanation reaction was unsuccessful with degradation again being observed. When nucleophilic aromatic substitution reaction at the 2-position was attempted, the unwanted regioisomer **94** was obtained, with substitution occurring exclusively at the 6-position, as observed by LC-MS.

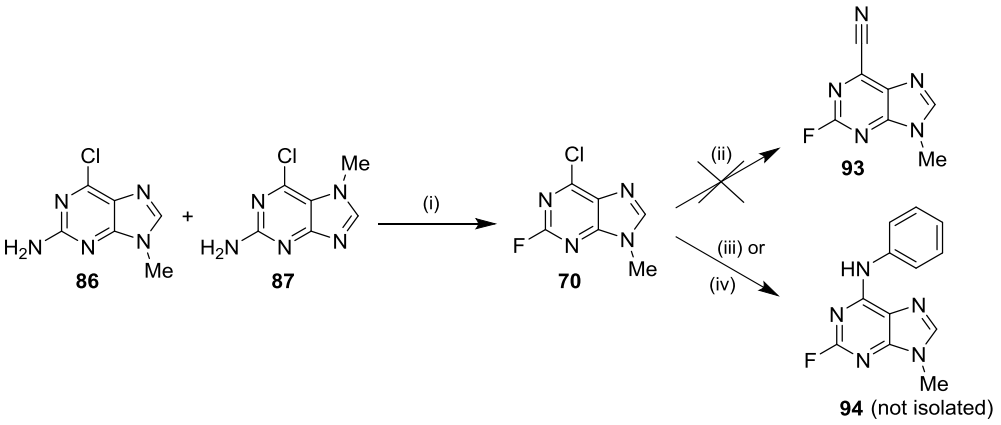

Scheme 10 - *Reagents and conditions*: (i) HBF_4, $NaNO_2$, r.t., 18 h, 50%; (ii) DABCO, Et_4NCN in MeCN, r.t., 18 h; (iii) TFA, aniline in TFE, 140 °C, 15 min, MW; (iv) aniline in TFE, 140 °C, 15 min, MW.

For both iodination and fluorination of compounds **86**/**87**, the yields were modest, probably explained by the quality of the starting material, which had not been purified. From all of these results, the useful observation made was that the 6-position of the purine scaffold was the most reactive. Indeed, in the case of the nucleophilic aromatic

substitution, although fluoro is generally a better leaving group than chloro, substitution with the 2-fluoro-6-chloropurine **70** occurred exclusively at the 6-position (*Scheme 10*).

Another strategy was considered (*Scheme 11*), which was similar to an approach previously used within the group. Thus, isolation of the unprotected purine **82**, following PMB deprotection, was achieved by recrystallisation from MeOH: NH_3 (3:1).

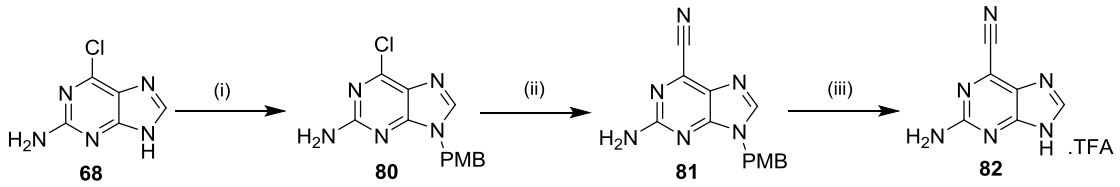

Scheme 11 - *Reagents and conditions*: (i) PMBCl, Cs_2CO_3 in DMF, 60 °C, 18 h, 60%; (ii) DABCO, Et_4NCN in MeCN, r.t., 18 h, 62%; (iii) neat TFA, 70 °C, 5 h, 74%.

From the intermediate **82**, direct methylation using MeI with either K_2CO_3 or Cs_2CO_3 was conducted. The base was changed to study any differences in reaction rate and regioselectivity between the formation of N^9- and N^7-methyl compounds, **88** and **89**, respectively. In both cases, methylation was complete after one hour and led almost exclusively to the N^9-Me isomer **88**, as the N^7-Me isomer **89** represented less than 1% (*Scheme 12*) (ratio determined by ^{1}H NMR). This result was interesting as it suggested that the 6-cyano group directed the methylation preferentially at the *N*-9 position compared with the 6-chloro group, where a mixture of N^7- and N^9-methylpurines was obtained. As the objective was to synthesise both isomers, this approach was stopped. The iodination reaction on compound **82** failed, suggesting that the N^9H of the purine should be protected (*Scheme 12*). No further investigations were conducted on this scheme as the methylation gave selectively one isomer (**88**) and the iodination reaction failed.

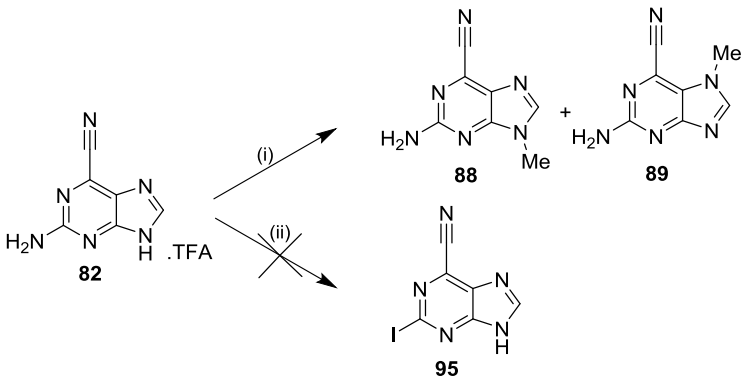

Scheme 12 - *Reagents and conditions*: (i) MeI, K_2CO_3 in DMF, r.t., 18 h, 59% (**88**), <1% (**89**); (ii) isoamyl nitrite, CH_2I_2, CuI in THF, 70 °C, 2 h.

Solubility of the compounds was a major concern. The phenylthiomethyl group was considered to confer better solubility (*Scheme 13*). This group was chosen to act as a protecting group which should cleave under hydrogenation conditions using Raney nickel to give the desired *N*-methylpurines. Phenylthiomethyl was introduced using chloromethylphenyl sulfide under the same conditions as for the PMB group.[176] Surprisingly, the two isomers, **96** and **97**, obtained were separable by recrystallisation thanks to differences in polarity. After work-up, N^7-protected isomer **97** was partially recrystallised from MeOH, whereas the N^9-protected isomer **96** was soluble. After confirmation of structure by ^{1}H NMR, compound **97** was isolated pure in 20% yield, and isomer **96** was obtained in 64% yield with residual isomer **97** (4:1 of **96**: **97**). At this stage, an attempt at deprotection was made on compound **97**, the less soluble isomer, under hydrogenation conditions using Raney nickel. No deprotection occurred at r.t., but started slowly at 40 °C, and at 100 °C, the deprotection step was complete after 20 minutes. Although the result was encouraging, the question of the cyano group stability under these rigorous conditions remained uncertain.

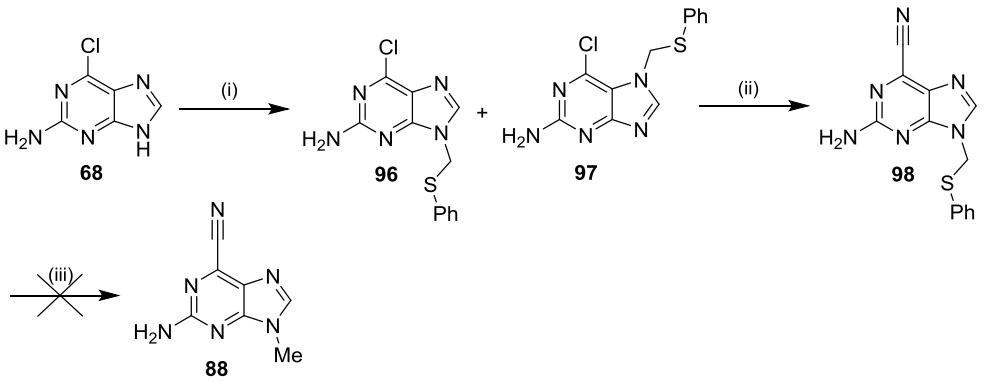

Scheme 13 - *Reagents and conditions*: (i) $PhSCH_2Cl$, Cs_2CO_3 in DMF, 60 °C, 18 h, 67% (**96**), 19% (**97**); (ii) DABCO, Et_4NCN in MeCN, r.t., 18 h, 61%; (iii) Ra-Ni, H-cube in DMF, r.t.

Cyanation was carried out on both isomers, **96** and **97**, with the reaction occurring when the methylphenyl sulfide group was at the *N*-9 position but not at the *N*-7 position. This result could be explained by steric hindrance imposed by the phenylthiomethyl group. As discussed previously, the cyanation reaction proceeded through an intermediate formed by DABCO (*Scheme 14*). This group might not be compatible with another bulky group located nearby, at the *N*-7 position, resulting in no reaction. In the case of the N^9-protected isomer **96**, cyanation was successful with a yield of 61%. Unfortunately, deprotection of compound **98** by hydrogenation with Ra-Ni, resulted in concomitant reduction of the cyano group to the corresponding amine, and this approach was abandoned.

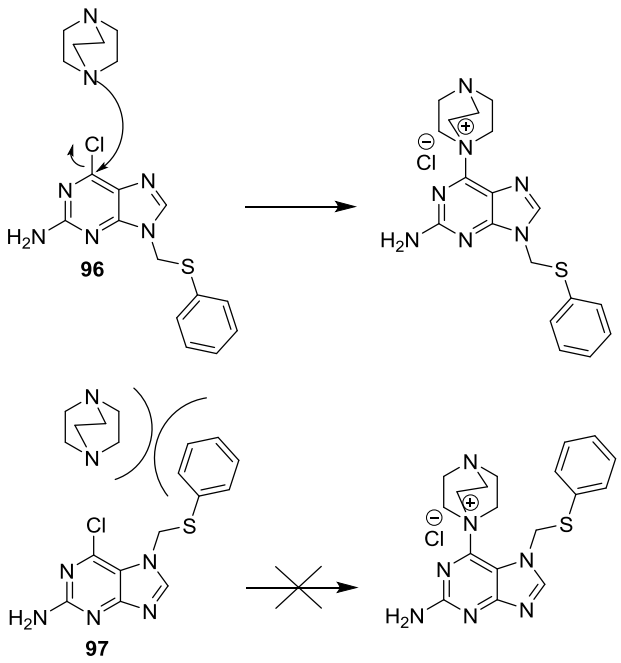

Scheme 14 – Displacement of the 6-chloro group of **96** and **97** by DABCO

Another idea to obtain the N^7-methyl intermediate **89**, the most difficult to synthesise according to the studies detailed above, was derived from knowledge of the *N*-7 methylation of guanine residues in DNA by methylating agents (see chapter 3, section 3.1.3). A new strategy for the synthesis of both *N*-methyl isomers was established (*Scheme 15*). The N^7-methyl derivative **67** was obtained from direct methylation of the PMB protected precursor **85** with a yield of 56%, using the one-pot procedure developed (see chapter 3, section 3.1.3.).[177] The N^9-methyl isomer **66** was obtained by direct methylation of compound **65** in 40% yield.

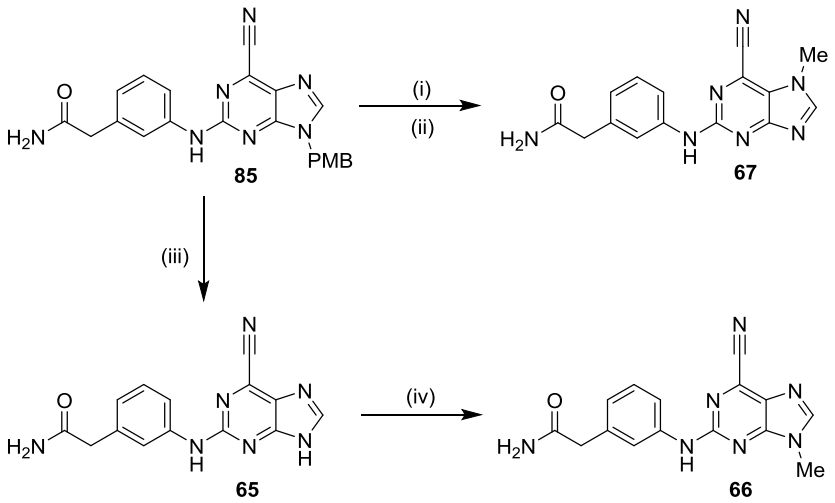

Scheme 15 - *Reagents and conditions*: (i) Me_3OBF_4 in TFE, r.t.; (ii) 100 °C, 20 min, MW, 56%, (iii) neat TFA, 70 °C, 5 h, 47%; (iv) MeI, K_2CO_3 in DMF, r.t., 18 h, 40%.

3.1.3. One-pot process for the selective N-7 methylation of purines

- *Mimicking a biological mechanism*

Commonly, methyl iodide in the presence of potassium carbonate or[153] sodium hydride[178], or diazomethane[179] are reagents used to methylate purines. The regioselectivity of these two reagents favours methylation at the *N*-9 position as the *N*-7 isomer represents only 20% of the mixture of both isomers. Only a few examples were found in the literature for the selective *N*-7 alkylation of purines. The method used by Kotek et al[180] consisted of protecting the *N*-9 position, reducing the imidazole ring of the purine, and then alkylating at *N*-7. Finally, they deprotected at *N*-9 and reoxidised the imidazole ring. Even if this method was effective with reported overall yields of between 55 and 87%, this five-step procedure showed some disadvantages such as stability problems arising from the formation of dihydropurines. This scaffold appeared unstable to electron-donating groups resulting in diversity limitations at the 2- and 6-positions. Khoda et al[181] used another approach by methylating the *N*-7 position with methyl iodide while *N*-9 was protected by a ribose. The protecting group was subsequently hydrolysed under acidic conditions. Unfortunately, only one example was given and the use of acidic conditions might be incompatible with other groups on the molecule. Dalby *et al*[182] developed another approach using methyl(aquo)cobaloxime to coordinate to purine *N*-3. A hydrogen bond was formed between the *N*-9 and the dimethylglyoximato oxyanion, preventing alkylation on *N*-9 and orientating it to *N*-7. However, this method was successful only on 6-chloropurine and 2,6-dichloropurine, and failed when attempted on 2-amino-6-chloropurine because of solubility problems.

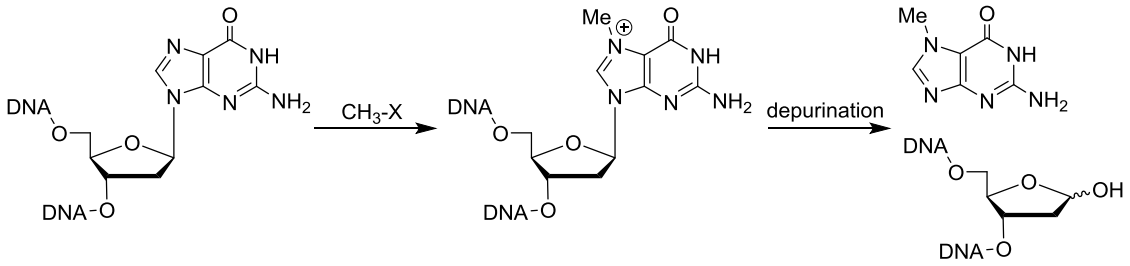

Scheme 16 - Mechanism of depurination by DNA glycosylases[183]

To date, no mild and general method exists to selectively alkylate *N*-7 over *N*-9 on purines. A new approach was designed, inspired by the *N*-7 alkylation of guanine residues in DNA, a common DNA damaging process (*Scheme 16*).[184] Alkylation of guanine residues arises from exposure to methylating agents, forming N^7-methylguanine (7-mG).[185] Nitrosamines are an example of alkylating agents, which form, *via* metabolic

activation by cytochrome P450 enzymes, highly reactive diazonium ions.[185] 4-(Methylnitrosamino)-1-(3-pyridyl)-1-butanone (NNK) is a nitrosamine found especially in tobacco and has been associated with lung cancer.[186] In the same family of compounds, dimethylnitrosamine (DMN) was studied as inducer of liver, kidney and lung tumours.[185] The damaged DNA is repaired by DNA glycosylases, enzymes responsible for the removal of alkylated purine nucleobases by depurination.[183, 187]

If DNA is not repaired, depurination occurs spontaneously because of the positive charge on *N*-7; generating mutagenic abasic sites (*Scheme 17*),[188] which are in equilibrium with the ring-opened aldehyde form. Loss of a proton at the α-position of the aldehyde moiety leads to a DNA strand break.[188] To mimic chemically the natural methylation occurring on guanine residues, dimethyl sulfate is commonly used as in the Maxam-Gilbert procedure for DNA sequencing.[189]

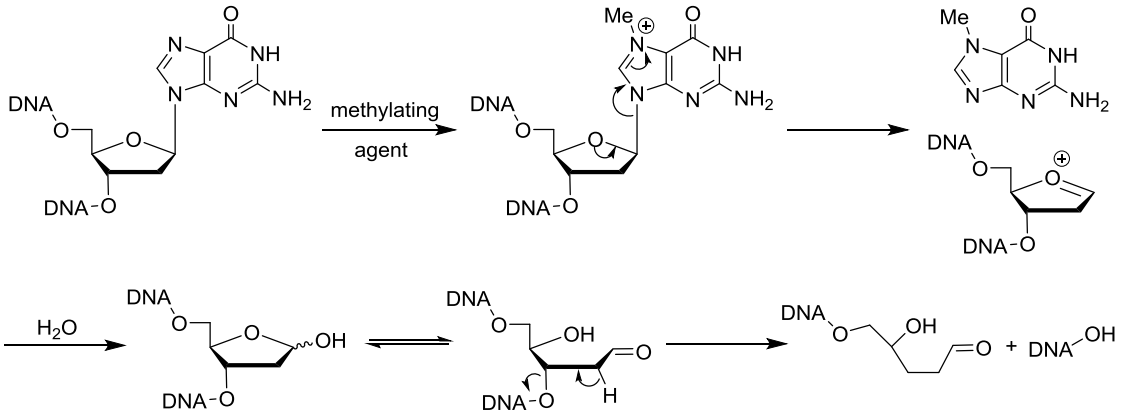

Scheme 17 - Depurination mechanism[188]

To perform the selective *N*-7 methylation on the target purines, trimethyloxonium tetrafluoroborate was preferred as methylating agent for its ease of handling compared with the traditional Me_2SO_4 or MeI. PMB was selected as protecting group and TFE[190] was chosen as reaction solvent for its good solubilisation of trimethyloxonium tetrafluoroborate and the purine, its non-nucleophilic character, and for its slightly acidic nature ($pK_a \sim 12$)[191]. Studies on the depurination of 7-mG showed that this process was accelerated under acidic conditions and by heating.[188] Accordingly, the slightly acidic character of TFE can be used to trigger PMB deprotection after the *N*-7 methylation by heating under microwave conditions.

- *Reaction optimisation*

Trimethyloxonium tetrafluoroborate was used as the methylating agent for the reaction, which was complete after 2 hours at room temperature. Different conditions were studied for the deprotection (*Table 3*) as heating overnight at 70 ^{o}C did not trigger PMB removal.

Table 3 - Conditions investigated for the PMB deprotection

% of TFA	Conditions	Results
0	70 °C overnight, heating	No deprotection
	120 °C, 5 min, MW	Deprotection (impure)
	100 °C, 20 min, MW	Deprotection (complete)
10	r.t. overnight	No deprotection
	70 °C, 4 h	Deprotection (impure)
20	r.t. overnight	No deprotection
	70 °C, 4 h	Deprotection (impure)
30	r.t. overnight	No deprotection
	70 °C, 4 h,	Deprotection (impure)
50	r.t. overnight	No deprotection
	70 °C, 2.5 h	Deprotection (complete)
100	r.t. overnight	Deprotection (complete)

From the results listed in *Table 3*, the best conditions were heating under microwave irradiation at 100 °C as this led to a complete and clean reaction in 65% yield. The weakly acidic character of TFE was enough to trigger PMB deprotection on heating (*Scheme 18*).

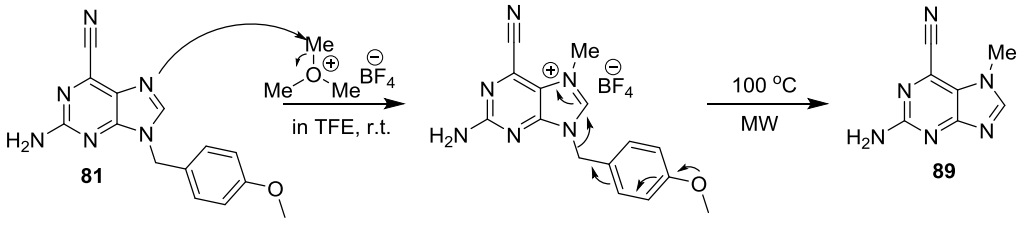

Scheme 18 - Proposed mechanism for the selective N^7-methylation of purine

- *Application of the method*

Conditions used to synthesise compound **67** were applied as a one-pot process to a range of 9-(4-methoxybenzyl)-purine substrates. The results are reported in *Table 4*.

Table 4 - Results of *N*-7 methylation on diverse 9-(4-methoxybenzyl)purine-based substrates

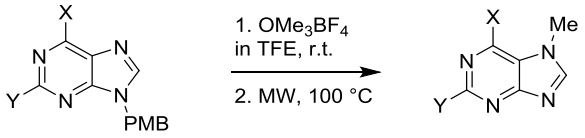

X	Y	Time for deprotection	Compound	Isolated yield (%)
CN	NH_2	20 min	**89**	65
CN	I	10 min	**99**	66
CN	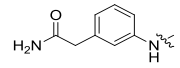	10 min[1]	**67**	56
Cl	NH_2	10 min[1]	**87**[2]	68
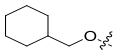	NH_2	10 min	**100**	60
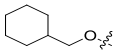	I	20 min	**101**	45
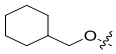	CN	20 min	**102**	70
OEt	NH_2	10 min	**103**	66
OEt	I	10 min	**104**	73
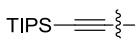	NH_2	20 min	**105**	40
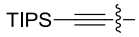	I	10 min	**106**	58
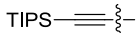	F	10 min	**74**	42

[1]TFA was added to give a final concentration of 50%; [2]TFA salt was obtained.

The method offered acceptable yields ranging from 43% to 73%. This process showed good tolerance towards steric hindrance, as the reaction proceeded in good yield with TIPS and cyclohexylmethyl groups at the 6-position (entries **105**, **106**, **74** and **100**-**102**, respectively). In addition, the reaction was tolerant to the groups at the 2-position as the yields were not affected. In the case of the reaction of 2-amino-6-cyanopurine **89**, with methyl iodide, the *N*-9 isomer was obtained almost exclusively (see section 3.1.2.). This method appeared to be a viable alternative approach to prepare selectively the *N*-7 over the *N*-9 methylpurine, and is also a method to provide the N^7-methyl isomer when only the N^9-methyl isomer was obtained by traditional methylating agents. These conditions were also applied to 9-tetrahydropyranylpurine compounds (*Table 5*). In this case, room temperature was enough to trigger the THP deprotection during the reaction, although the reaction mixtures were less clean and more difficult to purify than for the corresponding PMB protected compounds.

Table 5 - Results of *N*-7 methylation on 9-tetrahydropyranylpurine compounds

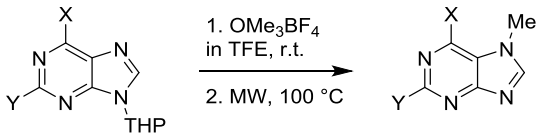

R	X	Y	Compound	Isolated yield (%)
THP	H	F	**107**	57
THP	TIPS—≡—	F	**74**	41

To confirm that methylation had occurred at the *N*-7 position, a crystal structure of compound **101** was determined. The methyl group on *N*-7 (*N*-1 on *Figure 75*) is on the same side of the molecule as the cyclohexylmethoxy group at the 6-position (C-5 on *Figure 75*) of the purine. From the crystal structure, it is evident that the methyl group is at the expected position, on the *N*-7 of the purine.

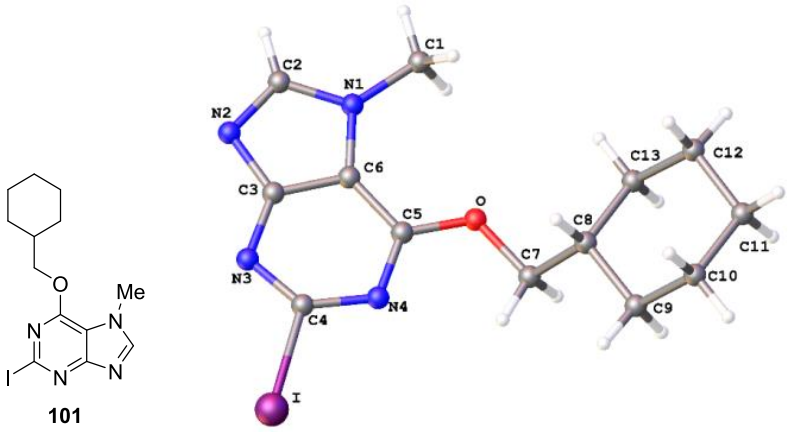

Figure 75 - Crystal structure of **101**

To investigate whether these conditions could be applied to other alkyl groups, trimethyloxonium tetrafluoroborate was replaced by triethyloxonium tetrafluoroborate. Selective *N*-7 ethylation was again observed, demonstrating that this method can indeed be extended to larger alkyl groups (*Table 6*).

Table 6 - Results of *N*-7 ethylation using the one-pot process

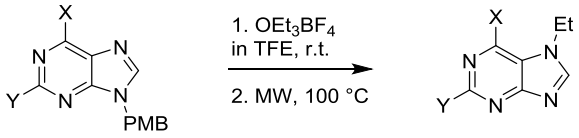

X	Y	Time for deprotection	Compound	Isolated yield (%)
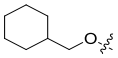	NH_2	10 min	**108**	40
OEt	NH_2	10 min	**109**	58
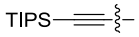	NH_2	No reaction	**110**	-
CN	NH_2	10 min	**111**	28

Selective *N*-7 ethylation offered the same satisfactory results as the corresponding methylation when carried out on 6-alkoxypurines (*Table 6*, entries **108** and **109**). By comparison with methylation, ethylation appears to be more difficult with a cyano group at the 6-position (*Table 6*, entry **111** compared with *Table 4*, entry **89**). This reaction is moderately tolerant to steric hindrance though as the 6-triisopropylsilylethynyl group appeared to be too large for ethylation to occur (*Table 6*, entry **110**).

3.1.4. Biological results for the control compounds

The four control compounds in the 6-ethynyl series (**61**-**64**) were assessed in an enzymatic (IC_{50}) and cellular assay (GI_{50}). The N^7-methyl derivatives, **62** and **64**, were essentially inactive against Nek2 in the enzymatic assay (IC_{50} = 15% @ 50 μM and 50% @ 100 μM, respectively), but the N^9-methyl isomers, **61** and **63**, retained low potency (IC_{50} = 28 μM and 4.0 μM, respectively). The N^7-methyl isomers, **62** and **64**, although inactive against Nek2, showed growth inhibition in a tumour cell line (SKBR3) (GI_{50} = 0.3 μM and 2.9 μM, respectively). Taken together, the enzymatic and cellular results suggested that the activity of these compounds was, at least in part, the result of an off-target Nek2-independent effect.

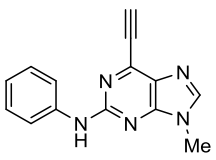

61

Nek2: IC_{50} = 28 μM
GI_{50} (SKBR3) = 0.2 μM

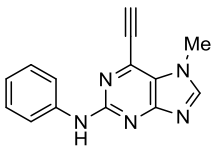

62

Nek2: IC_{50} = 15% @ 50 μM
GI_{50} (SKBR3) = 0.3 μM

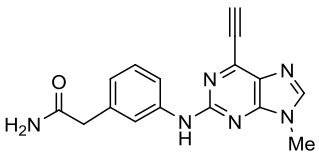

63

Nek2: IC_{50} = 4.0 μM
GI_{50} (SKBR3) = 1.1 μM

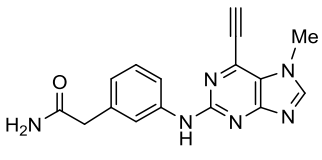

64

Nek2: IC_{50} = 50% @ 100 μM
GI_{50} (SKBR3) = 2.9 μM

A ‘Dundee’ kinase screen was also performed against 121 different kinases for each compound at 1 μM. From these results, the inhibitors seemed highly selective, as activity only against Bruton’s tyrosine kinase (BTK) and aurora kinases A (AK-A) and B (AK-B) was observed (*Table 7*). These results suggested that the off-target activity was unlikely to arise from kinase inhibition, although it is recognised that this is only a proportion of the entire kinome.

Table 7 - Kinase screening results[1]

Compound[2]		**Nek2 inhibition**	**Other kinase inhibition**
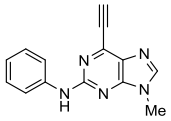	(**61**)	64%	BTK : 36%
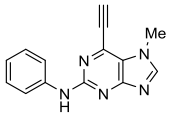	(**62**)	29%	BTK : 84% AK-A : 34%
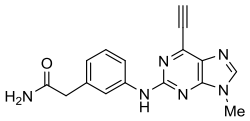	(**63**)	29%	AK-B : 51% AK-A : 4%
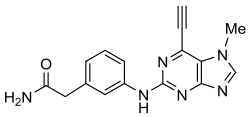	(**64**)	6%	AK-A : 37%

[1] See Appendix for the complete results of the Dundee kinase screen. [2] Evaluated at 1.0 μM.

A crystal structure of compound **63** in complex with Nek2 was determined to understand the binding mode of the molecule (*Figure 76*). Purine **63** bound in the same orientation as the other 6-ethynylpurines, and reaction with Cys22 on the ethynyl group still occurred, explaining the retention of Nek2 inhibitory activity. Perturbing the donor/acceptor/donor motif in this case was shown to modulate but not abolish the Nek2 inhibitory activity.

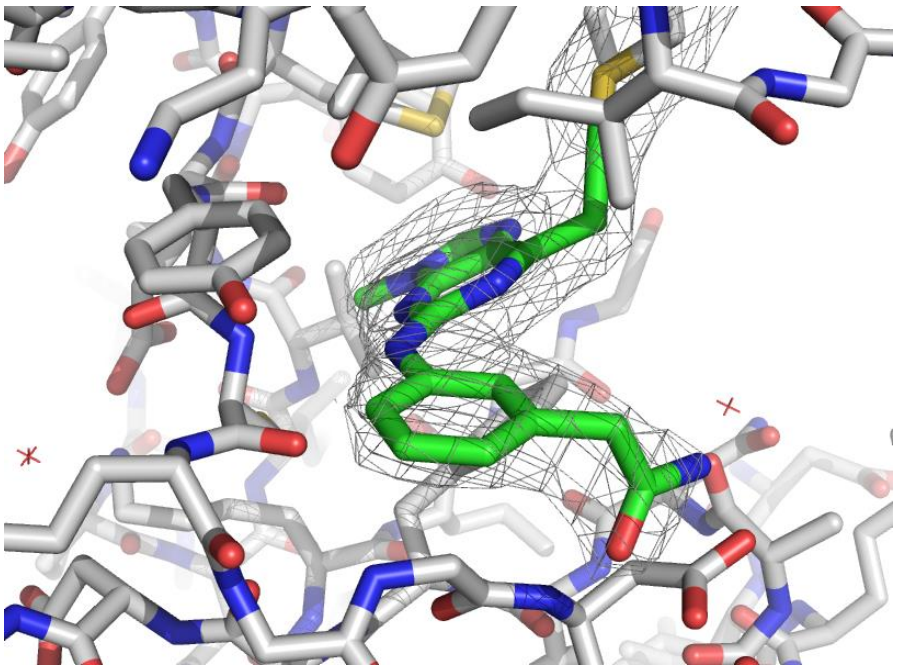

Figure 76 – Co-crystal structure of compound **63** in complex with Nek2.

The three control compounds in the 6-cyano series (**65**, **66** and **67**) were evaluated in both the enzymatic and cellular assays. As expected, these purines were less active against Nek2 than their corresponding 6-ethynyl bioisosteres (**42**, **63** and **64**, respectively). However, they still showed the same relative potency with the parent compound **65** being the most potent (IC_{50} = 2.9 μM). Having a methyl substituent at the *N*-9 position (**66**) was shown to retain potency (IC_{50} = 38 μM), whereas a methyl group at the *N*-7 position (**67**) essentially abolished activity against Nek2 and cellular potency (IC_{50} = 20% @ 100 μM; (GI_{50} = >100 μM). These compounds did not show any sign of off-target activity from their enzymatic and cellular results.

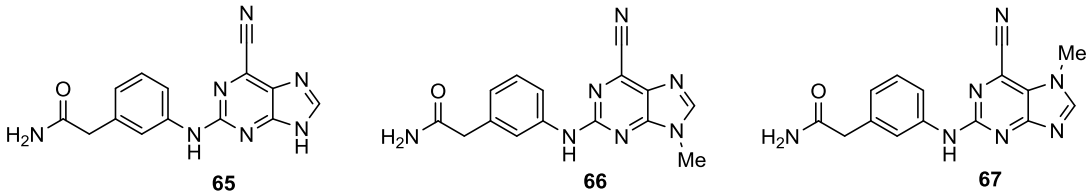

Compounds synthesised in section 3.1 of this chapter were tested for their Nek2 inhibitory activity by Kathy Boxall, Sam Burns, Yvette Newblatt and Maura Westlake under the supervision of Dr Wynne Aherne in the Analytical Screening and Technology Laboratory of the CR UK Centre for Cancer Therapeutics, The Institute of Cancer Therapeutics, Sutton, Surrey, UK, SM2 5NG.

3.2. Attempted discrimination of off-target activity from Nek2 inhibition - Synthesis of a focused library of N^7-methylpurines

Purine-based control compounds have been synthesised and as suggested from their biological activity, the cellular growth inhibition seemed to arise from an off-target effect rather than as a result of Nek2 inhibition. *N*-7 Methylation abolished activity against Nek2 (IC_{50} results) but did not affect potency in the SKBR3 tumour cell line. From these results, the proposed strategy was to separate Nek2 inhibition from off-target activity. Nek2 potency could easily be abolished by *N*-7 methylation, but nothing was known about the nature of the off-target activity, apart from that it was unlikely to be related kinase according to the Dundee screen. The work described in this section consisted in finding compounds that did not affect the off-target activity. For that purpose, compounds having different potency against Nek2, and with structurally different anilines at the 2-position, were methylated at the *N*-7 position. The strategy was to obtain a GI_{50} value related only to the off-target growth inhibition. If a compound possessed a modest or weak GI_{50}, then the off-target locus would not be affected and the parent N^9H analogue of this compound would potentially be Nek2 selective (*Figure 77*).

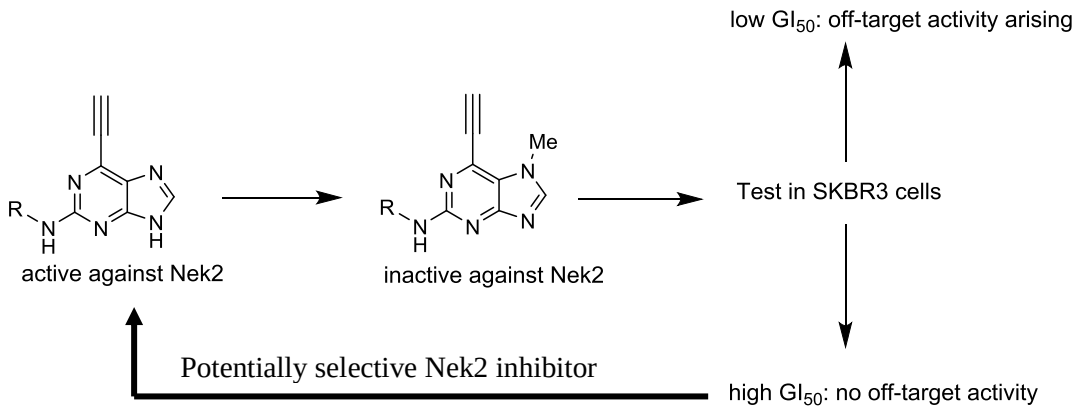

Figure 77 - Strategy to identify a selective Nek2 inhibitor

Eleven anilines were chosen (*Figure 78*) to be inserted at the 2-position of the purine for this small library of purine-based inhibitors, with only six being commercially available (**112**-**117**). The five remaining (**118**-**122**) had to be synthesised.

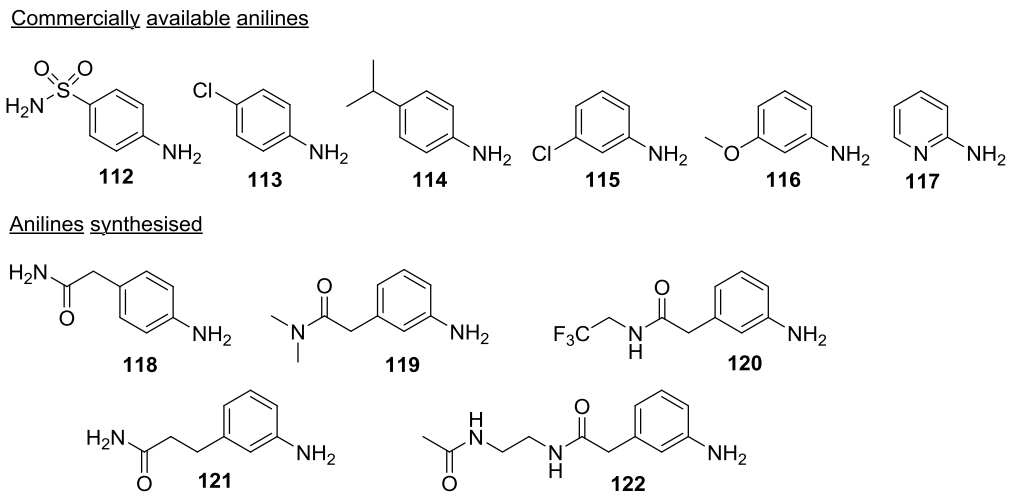

Figure 78 – Anilines used for the library of N^7-methylpurines

3.2.1. Synthesis of the inhibitors

The best route to synthesise the eleven compounds was to have a common intermediate and introduce diversity at the final step. Thus, the first purine intermediate to be synthesised was the 2-fluoro compound **74** (*Scheme 19*).

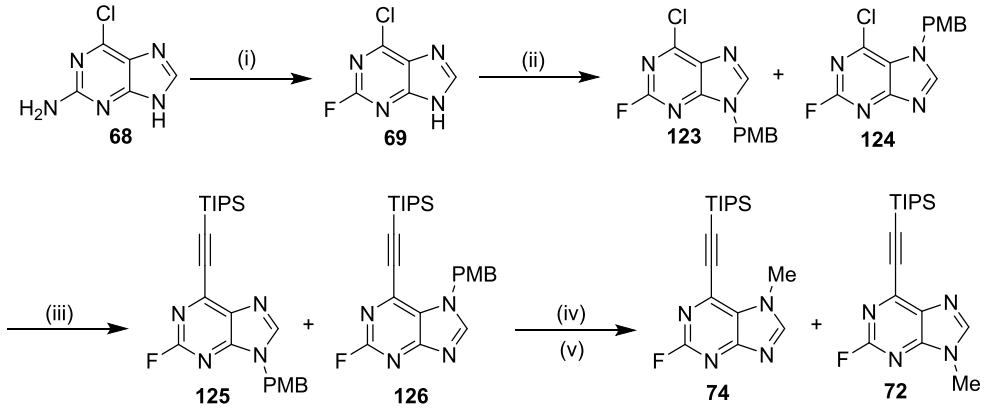

Scheme 19 - *Reagents and conditions*: (i) HBF_4, $NaNO_2$, r.t., 18 h, 50%; (ii) PMBCl, Cs_2CO_3 in DMF, 60 °C, 18 h, 38%; (iii) triisopropylsilylacetylene, CuI, $Pd(PPh_3)_2Cl_2$, Et_3N in THF, r.t., 18 h, 40% (**125**) and 21% (**126**); (iv) OMe_3BF_4 in TFE, r.t.; (v) 100 °C, 20 min, MW, 52% (**72**) and 42% (**74**).

The synthesis of the 2-fluoro intermediate **74** started with the Balz-Schiemann reaction followed by PMB protection. Unfortunately, a mixture of isomers (**123**/**124**) was obtained. A Sonogashira reaction was performed, followed by methylation using trimethyloxonium tetrafluoroborate. This route was not ideal as it offered a poor overall yield, mainly because of the mixture of isomers that required separation. From intermediate **74** only four compounds were prepared using TFA/TFE conditions for coupling, followed by TBAF deprotection (*Table 8*).

Table 8 – Summary of yields for the synthesis of the target N^7-methylpurines **131-134**.

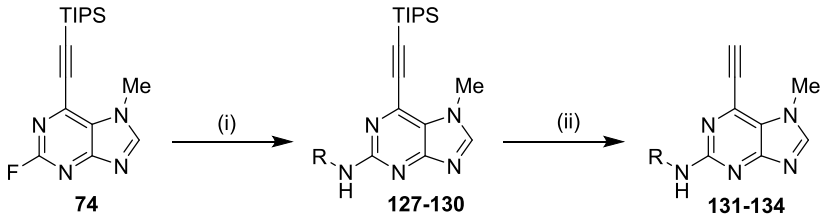

Reagents and conditions: (i) TFA in TFE, 140 °C, 30 min, MW; (ii) TBAF in THF, r.t., 5 min.

R group	Compound – yield for step (i)	Compound – yield for step (ii)
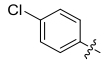	**127** – 52%	**131** – 45%
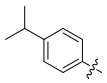	**128** – 43%	**132** – 40%
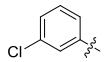	**129** – 62%	**133** – 41%
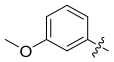	**130** – 66%	**134** – 43%

As the synthesis of the 2-fluoro intermediate **74** was not ideal, in particular working with a mixture of isomers, efforts were focused on synthesising the intermediate bearing an iodo group at the 2-position (**106**), as the synthetic scheme was better defined (*Scheme 20*).

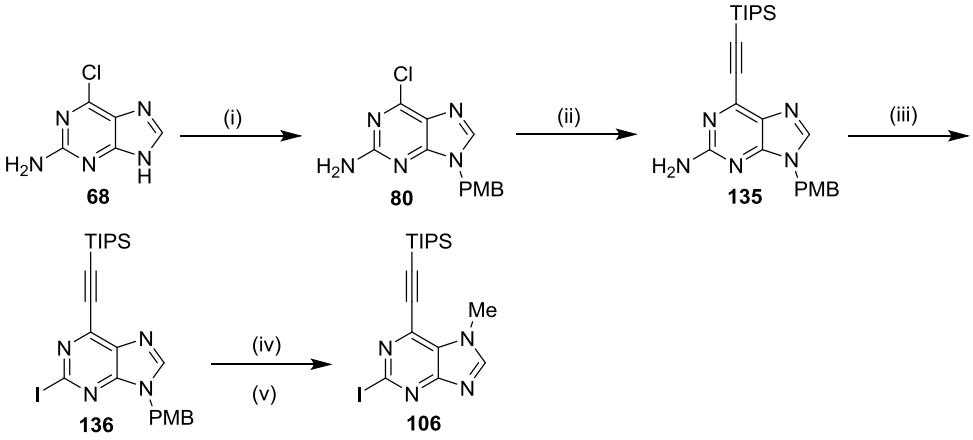

Scheme 20 - *Reagents and conditions*: (i) PMBCl, Cs_2CO_3 in DMF, 60 °C, 18 h, 60%; (ii) triisopropylsilylacetylene, CuI, $Pd(PPh_3)_2Cl_2$, Et_3N in THF, r.t., 18 h, 65%; (iii) isoamyl nitrite, CH_2I_2, CuI in THF, 70 °C, 2 h, 30%; (iv) OMe_3BF_4 in TFE, r.t.; (v) 100 °C, 20 min, MW, 58%.

The synthesis of the 2-iodo intermediate **106** started with PMB protection of the commercially available 2-amino-6-chloropurine **68**, which occurred selectively at the purine *N*-9 position. A Sonogashira reaction was performed, followed by iodination to afford compound **136** in good yield. The last step was the one pot selective N^7-

methylation using trimethyloxonium tetrafluoroborate. This route offered a four-step selective synthesis of the intermediate **106**.

Amides **118** and **121** were obtained from the corresponding carboxylic acid using thionyl chloride in methanol to form the methyl ester, which was then treated with ammonia to afford the corresponding amide in good yield (*Scheme 21*).[136]

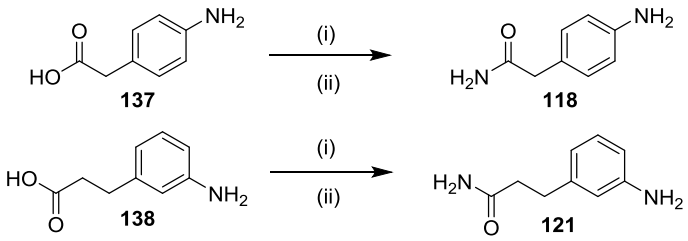

Scheme 21 - *Reagents and conditions*: (i) $SOCl_2$ in MeOH, r.t., 3 h; (ii) NH_3 aq, r.t., 18 h, 48% (**118**) and 72% (**121**) over 2 steps.

The three other aniline reagents were synthesised from 3-nitrophenylacetic acid **139**. Compound **119** was obtained by amide coupling using dimethylamine in the presence of EDCI, followed by zinc reduction. Amide **120** was synthesised using a different method from peptide coupling conditions. 3-Nitrophenylacetic acid **139** was first converted into the acyl chloride with phosphorus trichloride and reacted directly with the amine present in the mixture.[192] The isolated intermediate **141** was reduced with zinc (*Scheme 22*).

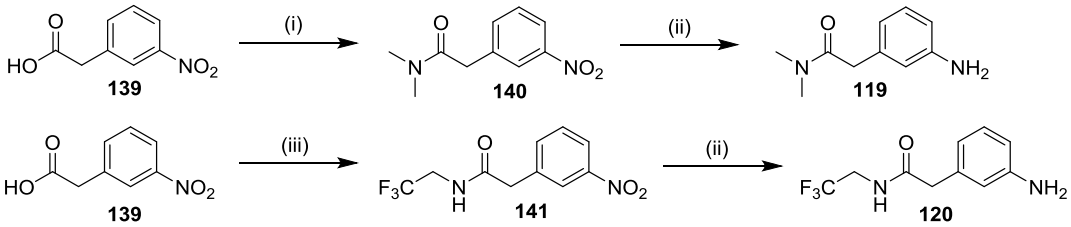

Scheme 22 - *Reagents and conditions*: (i) EDCI, HOBt, NMe_2, DIPEA in MeCN, r.t., 18 h, 82%; (ii) Zn, AcOH in MeOH, 50 °C, 2 h, 94% (**119**) and 93% (**120**); (iii) $POCl_3$, 2,2,2-trifluoro-1-ethanamine in MeCN, 140 °C, 5 min, MW, 80%.

The last aniline **122** was more difficult to synthesise as the two previous methods described above, either with phosphorus trichloride or with EDCI, failed when attempted with *N*-acetylethylenediamine. Surprisingly, when another coupling agent, CDI, was used, the desired intermediate **142** was obtained in 41% yield. The amide **142** was reduced using zinc to give compound **122** in 88% yield (*Scheme 23*).

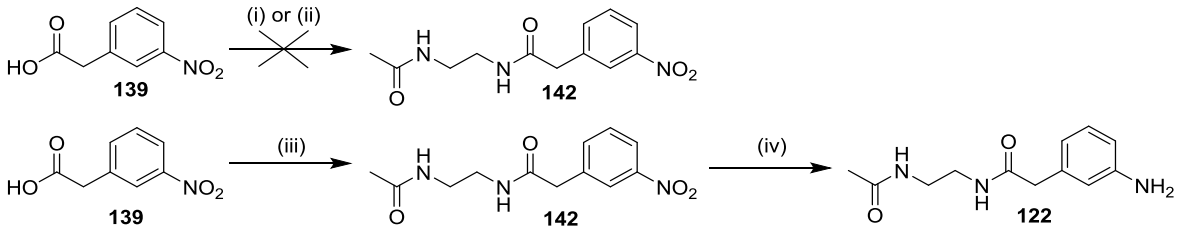

Scheme 23 - *Reagents and conditions*: (i) EDCI, HOBt, *N*-acetylethylenediamine, DIPEA in MeCN, r.t., 18 h; (ii) $POCl_3$, *N*-acetylethylenediamine in MeCN, 140 °C, 5 min, MW; (iii) CDI, DIPEA, r.t. 2 h then *N*-acetylethylenediamine, r.t., 2 h, 41%; (iv) Zn, AcOH in MeOH, 50 °C, 2 h, 88%.

Buchwald couplings were performed between the 2-iodo intermediate **106** and the seven aniline reagents, followed by TIPS deprotection using TBAF (*Table 9*).

Table 9 – Summary of yields for the synthesis of the target N^7-methylpurines **150**-**156**.

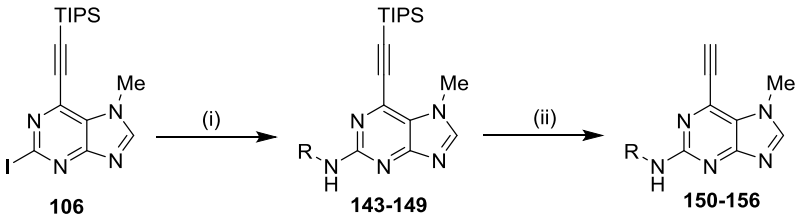

Reagents and conditions: (i) Amine, K_2CO_3, $Pd_2(dba)_3$, XPhos in THF, 80 ^oC, 18 h; (ii) TBAF in THF, r.t., 5 min.

R group	Compound – yield for step (i)	Compound – yield for step (ii)
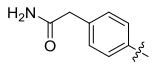	**143** – 43%	**150** – 47%
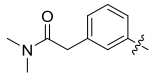	**144** – 45%	**151** – 31%
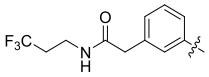	**145** – 49%	**152** – 73%
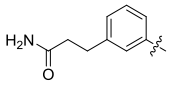	**146** – 73%	**153** – 28%
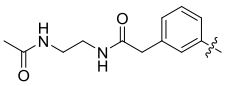	**147** – 47%	**154** – 64%
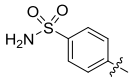	**148** – 35%	**155** – degradation
	**149** – 43%	**156** - degradation

The conventional conditions to deprotect the TIPS group using TBAF at room temperature failed with the 2-amino(benzenesulfonamide) or the 2-pyridyl group (**155** and **156**, respectively). As this reaction was usually fast at r.t., the temperature was lowered to -78 ^0C to control the reaction. This was successful for the 2-pyridyl compound

149, giving a yield of 45% compared to degradation at r.t. (*Scheme 24*). Unfortunately, with the 2-amino(benzenesulfonamide) **148**, the target product **155** was observed by LC-MS but proved impossible to isolate. Various methods were tried including reverse phase, alumina or silica chromatography and preparative TLC. Eventually, TIPS deprotection was tried using fluoride on polymer support (*Scheme 24*). These conditions offered a clean reaction with sole formation of the target compound **155**. As the compound was suspected to be unstable, no further purification was attempted, other than trituration in DCM. The desired product was obtained 97% pure by HPLC analysis.

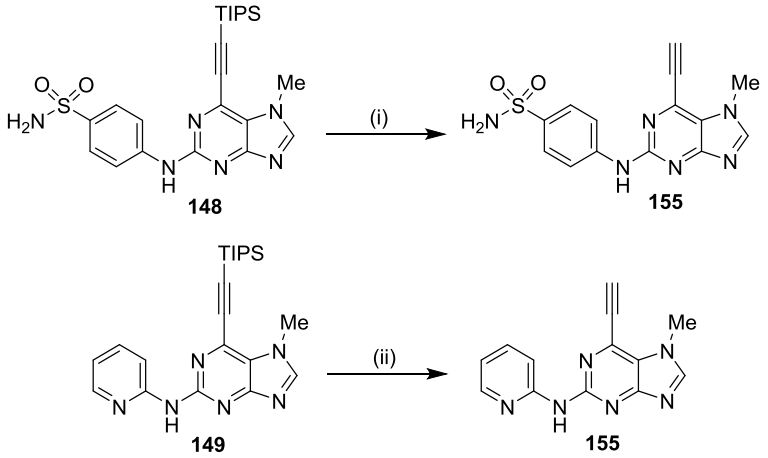

Scheme 24 - *Reagents and conditions* (i) Fluoride on polymer support in MeOH, r.t., 2 h, 37%; (ii) TBAF in THF, -78 ^{0}C, 5 min, 45%.

3.2.2. Biological results

As mentioned previously, the major problem with the Nek2 inhibitors designed to date was their off-target activity in cells. N^7-methylpurines, compared to their N^9-methyl counterparts, which retained some potency against Nek2, were completely inactive in the Nek2 assay, but as active as the corresponding parent NH purines in cells. Finding an N^7-methyl compound with modest cellular activity might lead to a selective Nek2 inhibitor, which would be the corresponding parent NH compound. The results of the designed library are shown in *Table 10*. Unfortunately, all GI_{50} values were comparable. Only compound **154** showed no potency in cells, likely because of poor cell permeability. By comparison with the 6-cyano series, all of the 6-ethynylpurines had similar GI_{50} values, suggesting that off-target activity probably arises from the 6-ethynyl moiety and not from the groups at the 2-position.

Table 10 - Biological results of N^7-methylated purines

Compound		GI_{50}[1]	ClogP (tPSA)	Nek2 inhibitory activity (IC_{50})of parent (N^9H) compound
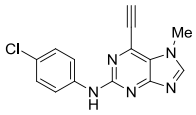	(**132**)	1.0 µM	3.40 (52.4)	160 nM
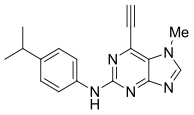	(**132**)	0.7 µM	4.11 (52.4)	400 nM
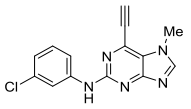	(**133**)	1.2 µM	3.40 (52.4)	210 nM
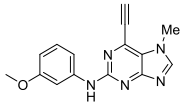	(**134**)	0.7 µM	2.60 (61.6)	94 nM
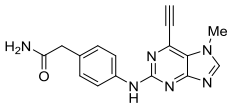	(**150**)	3.2 µM	0.99 (95.4)	93 nM
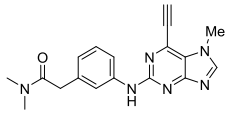	(**151**)	1.3 µM	1.50 (72.7)	90 nM
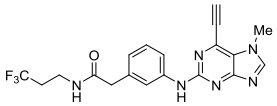	(**152**)	1.2 µM	2.00 (81.5)	78 nM
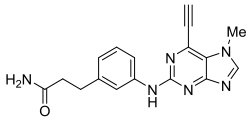	(**153**)	2.1 µM	1.52 (95.4)	79 nM
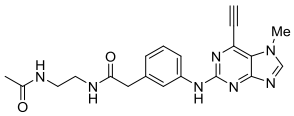	(**154**)	68.9 µM	0.81 (110.6)	190 nM
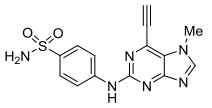	(**155**)	4.3 µM	0.85 (112.5)	140 nM
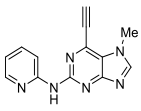	(**156**)	0.39 µM	1.24 (64.7)	2.04 µM

[1] Evaluated in SKBR3 cell line.

These biological results are in accordance with the results of the N^7-methyl-6-ethynylpurine kinetic studies (Chapter 4, section 4.7.). In these studies, compounds **62** and **64** have been shown to be far more reactive than their NH parents. Having a methyl group at the *N*-7 position increased the reactivity of the 6-ethynyl substituent towards nucleophilic attack. The compounds synthesised for this library did not represent control

compounds but highly reactive species. Finding a selective Nek2 inhibitor might be more challenging, and identification of the off-target(s) is essential if the biological results described are to be explained.

Compounds synthesised in section 3.2 of this chapter were tested for their Nek2 inhibitory activity by Kathy Boxall, Sam Burns, Yvette Newblatt and Maura Westlake under the supervision of Dr Wynne Aherne in the Analytical Screening and Technology Laboratory of the CR UK Centre for Cancer Therapeutics, The Institute of Cancer Therapeutics, Sutton, Surrey, UK, SM2 5NG.

Chapter 4. Kinetic Studies of Nek2 Inhibitors by Quantitative ^{1}H NMR

6-Ethynylpurines have been shown to bind covalently to the cysteine residue (Cys22) in the ATP binding site of the Nek2 kinase.[193] In this chapter, kinetic studies using the quantitative ^{1}H NMR (qNMR) method were conducted employing a model system previously optimised within the group,[194] in order to help quantify the reactivity of 6-ethynylpurines towards Cys22. The thiol of Cys22 reacts through a Michael-type addition at the 6-ethynyl moiety of the purine. Alkynes attached to a carbonyl, nitro or cyano group or suitable heterocycle[195-197] are known to undergo 1,4-addition reactions, especially with soft nucleophiles such as thiols.[198] 6-Ethynylpurines are thus time-dependent inhibitors of the Nek2 kinase.

4.1. Applications of qNMR

Nuclear Magnetic Resonance (NMR) is a technique most generally used for the structure determination of small molecules.[199] Its use can be extended to quantitative studies, as first reported by Jungnickel and Forbes in 1963.[200] Quantitative NMR (qNMR) is mainly accomplished with ^{1}H because of its high sensitivity and abundance in the environment compared with other nuclei such as ^{31}P and ^{13}C.[199] qNMR represents an especially useful analytical tool for pharmaceutical companies,[199] as the purity of a drug and quantification of active drug and excipients in a drug formulation can be determined.[201] In natural products research, qNMR gives valuable information on the structure of the molecule and an estimate of the purity of bioactive agents in the sample studied.[202] The technique can help in the determination of the presence of possible tautomeric forms of a molecule,[202] and is also used in metabolomics in combination with mass spectrometry.[203] In combinatorial chemistry, purification is often not required before analysis of the sample by qNMR.[199] The rate of a reaction and the rate of product formation or consumption can be determined by qNMR.[204] At the same time, indications of the structure of the product(s) can be obtained.[204]

4.2. Optimisation of qNMR parameters

From the examples given above, qNMR has been shown to be a very powerful and useful technique, widely used in diverse fields of chemistry and biochemistry.[199] However, a number of parameters need to be optimised before and after the experiment. The ^{1}H NMR experiment is composed of a relaxation time delay followed by a 90^{o} pulse, and ends with the acquisition of the signal (*Figure 79*).[205]

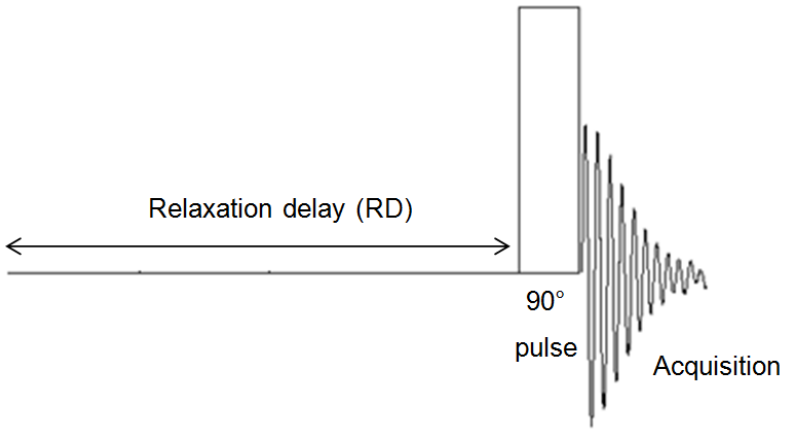

Figure 79 - ^{1}H NMR components

The repetition time (T_R) represents the time required by the NMR instrument to acquire a single-scan spectrum,[199] and depends directly on the relaxation delay (RD) and the acquisition time.[199] The optimum RD is, by convention, 5 times the longitudinal relaxation (T1).[206] When the nucleus is relaxing to return to its equilibrium state, the position of its spin can be followed in an (x,y,z) landmark, where the z component is the longitudinal relaxation T1, and the (x, y) component is the transverse relaxation T2 (*Figure 80*).[207]

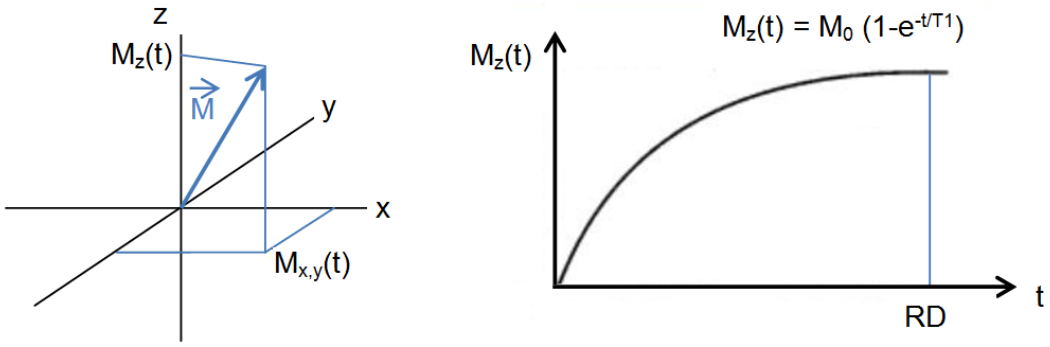

Figure 80 - Characterisation of a spin in three-dimensions

To obtain the highest signal and good accuracy of the results, the spin needs to recover fully from its 90° pulse before the next one. Just after the 90° pulse, the spin is only in the (x,y) plane. Before the next pulse, the spin needs to be re-aligned with the z axis and only possesses a longitudinal component of magnetisation. The time for the spin to acquire 99% of longitudinal magnetisation (maximum signal) is RD,[206] which is calculated through T1, and determined experimentally (see Chapter 4, section 4.3.). The other variable that T_R depends on is the acquisition time which needs to be long enough to recover FID signals fully without truncating any.[199] Signal loss will affect the quality of the spectrum.[199]

Other parameters that could affect the accuracy are the signal-to-noise ratio (S/N) and temperature.[199] Ideally, the S/N should be 250:1,[208] and if too low, the resolution of the spectrum also becomes low. The S/N can be improved by increasing the number of scans or the concentration of the sample studied.[208] In the 6-ethynylpurine studies, 4 to 8 scans per spectrum and a standard concentration of 6 mM of starting material was shown to give the optimum results. Temperature can affect the relaxation properties of the nuclei in a molecule, and it is therefore important to keep this constant during the entire experiment, which is of course also essential in kinetic studies.[205] In the 6-ethynylpurine studies described below, the temperature was maintained at 24 ± 0.01 °C.

After acquisition of the spectrum, a technique called 'windowing' is used to improve S/N. This consists of applying a filter to the data before Fourier transformation of the FID spectrum to enhance the FID signal.[199] When analysing the spectrum, phase and baseline corrections are required to minimise inaccuracies when measuring the integration of the peaks.[199] These two corrections were applied using Topspin ™.

qNMR is an accurate method when all the parameters are correctly optimised. However, to determine precisely the concentration of the molecule of interest, a reference is required.[199] The latter is introduced at a known concentration which will allow a calculation of the concentration of any known species in the studied sample. The reference must be available in a highly pure form, be soluble in the NMR solvent and be inert to the reaction environment. The signal from the reference in the ^{1}H NMR experiment must be in a region where no overlapping with other signals arises, in order to provide the most accurate signal integration, and a singlet is preferred for ease of data analysis.[199] Finally, T1 of the reference must be close to T1 of the studied molecule for the reasons explained above. As a consequence, DMF, with its aldehydic resonance at δ 7.9, was chosen for the 6-ethynylpurine qNMR studies.

4.3. Optimisation of T1

As explained previously, the relaxation time T1 needs to be optimised to afford the strongest signal possible. T1 can be measured experimentally using the inversion recovery method (*Figure 81*).[205]

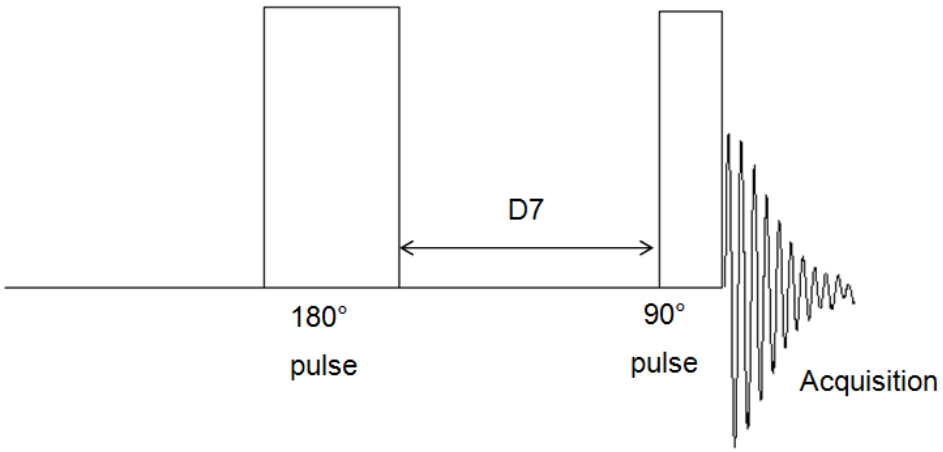

Figure 81 – The inversion recovery concept

When the sample is in the NMR instrument, the nuclei align with the magnetic field $\overrightarrow{B0}$. With this method, a pulse is applied causing a 180° rotation of the nuclei, placing them anti-parallel to $\overrightarrow{B0}$. After this pulse, the nuclei then relax to return to their initial position, parallel to $\overrightarrow{B0}$. During their relaxation, a 90° pulse is applied. If by the time this second pulse is applied, the nuclei have had time to relax, the 90° pulse propels the nuclei directly perpendicular to $\overrightarrow{B0}$ along the (x,y) axis, giving a positive signal in the ^{1}H NMR spectrum. However, if the nuclei did not have sufficient time to relax before the second pulse, the signal appears as negative in the ^{1}H NMR spectrum and the nuclei are found along the –(x,y) axis. To have a zero net signal in the ^{1}H NMR and determine D7, the nuclei need just enough time to relax until crossing the (x,y) axis (*Figure 82*).[207]

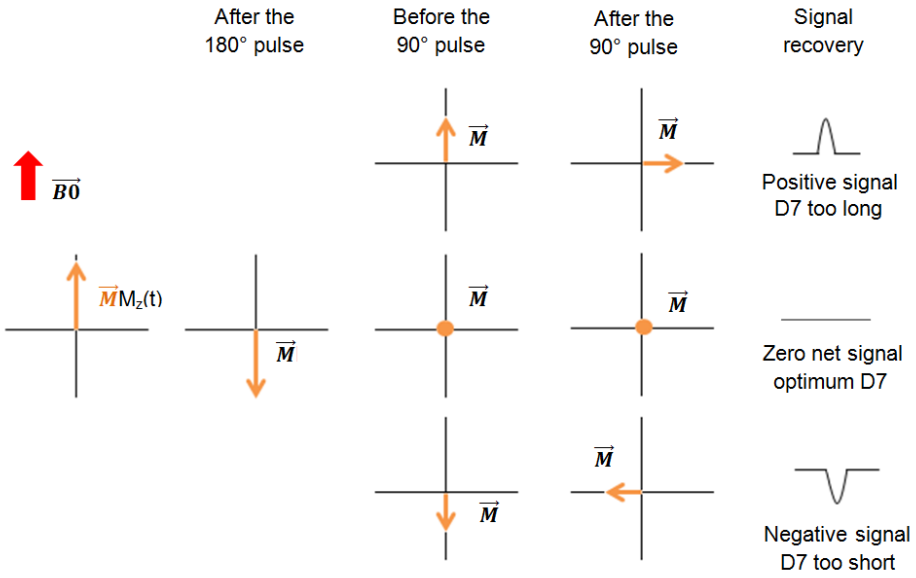

Figure 82 - Relationship between the positions of the nuclei and the signals recovered

The time given for the nuclei to relax between the two pulses is the time delay (D7) and is directly linked to T1 by the relationship D7 = ln2 x T1.[207] T1 is determined when D7 has been optimised to obtain a zero net signal. The optimum relaxation delay can be calculated from T1 (RD = 5 x T1). This optimisation was carried out on the 6-ethynylpurine **42** (*Figure 83*). The difference in relaxation between all the nuclei was observed, and the slowest proton to relax was the 6-ethynyl CH moiety. Ideally, D7 was found to be 5.0 seconds with a T1 value of 7.2 seconds. The optimum relaxation delay was therefore set as 36.0 seconds.

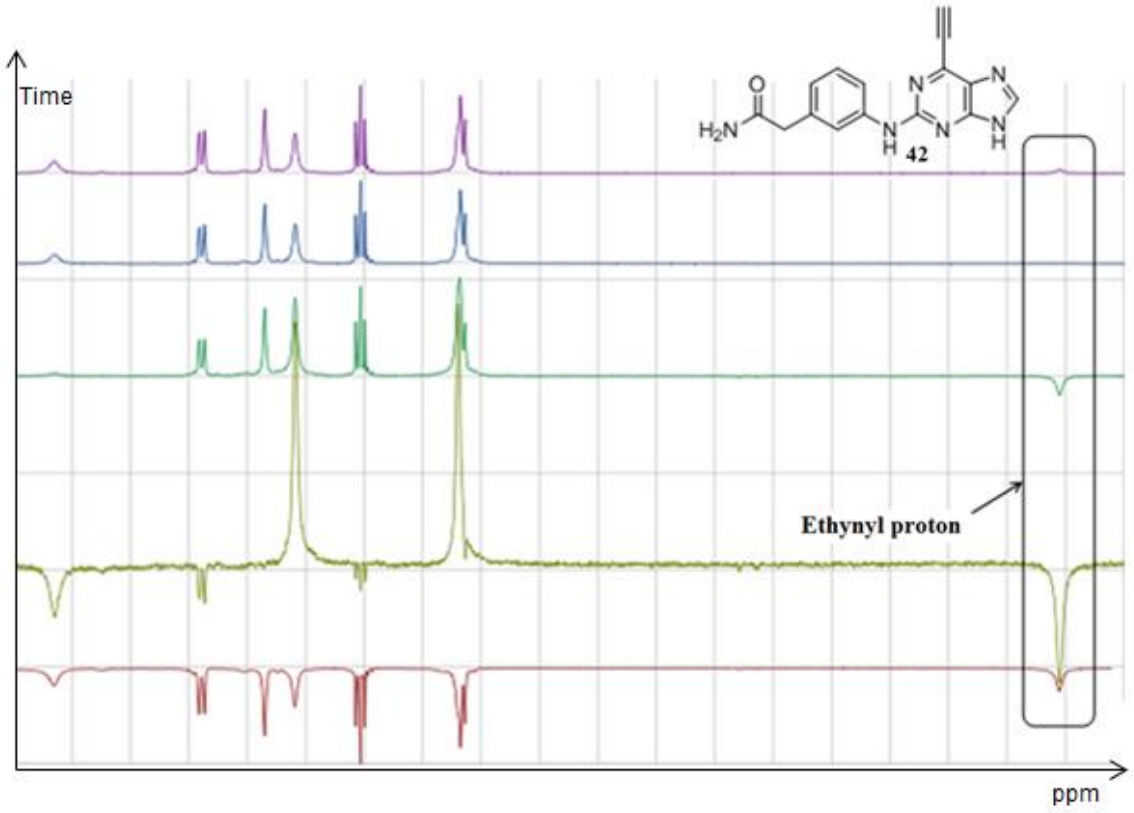

Figure 83 - Inversion recovery experiment on 6-ethynylpurine **42**

4.4. ^{1}H qNMR applied to 6-ethynylpurines

The kinetic study of the reaction between the 6-ethynylpurines and the thiol of Cys22 would assess the reactivity of the 6-ethynyl group towards Cys22. A model study was previously optimised within the group to mimic the Michael addition occurring within Nek2 kinase, using the time-resolved qNMR technique to monitor the reaction (*Scheme 25*). *N*-Acetylcysteine methyl ester **157** was used as nucleophile to mimic the Cys22 residue. However, because the reaction with this thiol was too slow, a base (DABCO) was added in catalytic quantity to generate the thiolate, which is much more reactive and

facilitates monitoring of the reaction. Ideally, the solvent for the reaction should be D_2O to mimic as closely as possible biological conditions, but for solubility reasons DMSO-d_6 was chosen.

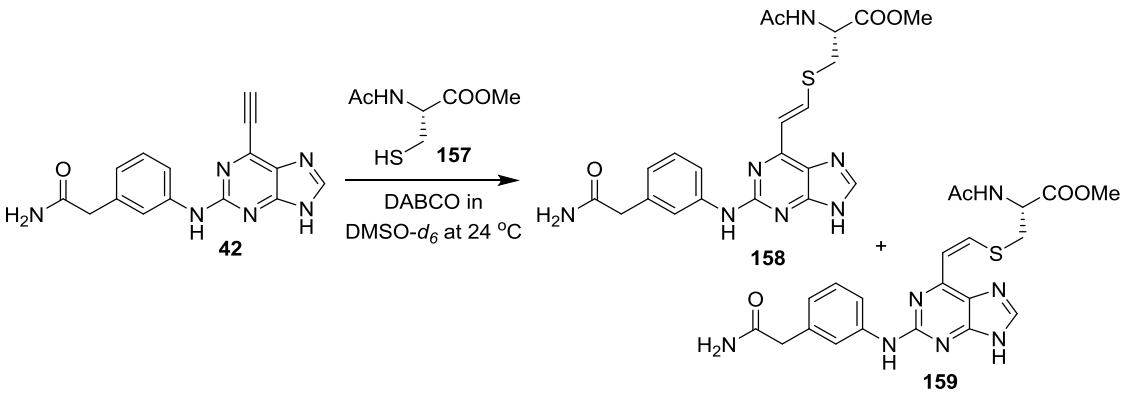

Scheme 25 - Reaction of 6-ethynylpurine **42** with reagent **157** in the presence of DABCO

The same conditions were used to study the reactivity of selected 6-ethynylpurines, and all of the reactions were carried out in a 5 mm NMR tube at a constant temperature (T = 24 ± 0.01 °C). The reactions were monitored every 10 minutes using a customised ^{1}H NMR experiment with the optimum relaxation delay determined experimentally (*see Chapter 4, section 4.3.*). The reactivity of 6-ethynylpurine **42**, a lead compound of the project, was initially studied. Methylation at the *N*-7 and *N*-9 positions of the purine has been shown to affect the reactivity of 6-ethynylpurines with Nek2 by perturbing their binding. Studies of the N^7- and N^9-methyl isomers of both compounds **41** and **42** were performed to assess the effect of the methyl group on the reactivity of the 6-ethynyl group.

4.5. Determination of *E*/*Z* isomer ratios

The Michael type addition reaction (*Scheme 25*) was carried out on a larger scale to characterise fully the two isomers formed during the kinetic studies. The conditions were adapted by changing the reaction solvent to DMF rather than DMSO for ease of isolation. The ^{1}H NMR spectrum revealed the formation of one main isomer, and to determine which isomer (*E* or *Z*) was formed, the products were isolated. The *E* isomer **158** was isolated pure but, surprisingly, the *Z* isomer **159** was obtained as an inseparable mixture with the product **160**, arising from a double addition of reagent **157**.

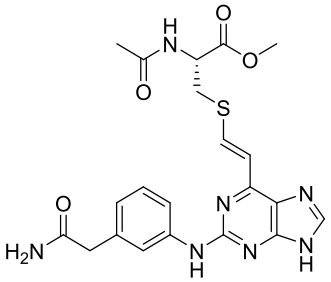

158

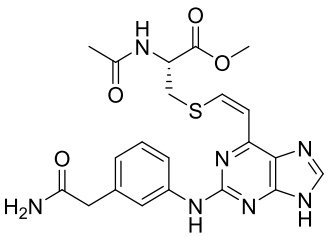

159

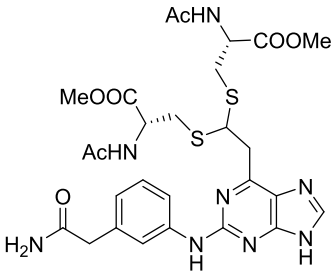

160

By comparison of the spectra of the isolated compounds, the major product (**158**) obtained was determined as the *E* isomer. The alkene resonances were not readily visible in the ^{1}H qNMR spectrum, as the signal at δ 6.88 was overlapped with one aromatic resonance, while the other alkene resonance was under the NH signal of reagent **157**. By carefully studying the ^{1}H qNMR spectrum, a small signal corresponding to the NH acetyl of compound **159** was visible at approximately δ 8.55, suggesting the formation of the *Z* isomer. The ratio between the *E* and *Z* isomers could be determined by comparison of their NH acetyl resonances, which were very well defined (*Figure 84*). The ratio of compounds **158**/**159** was found to be 9:1 (*E*: *Z* isomers). It has been reported that thiolate attack on an ethynyl-ketone affords mainly the *Z*-isomer.[209]

A comparison of the first qNMR spectrum obtained with the final one, showed the presence of unknown signals, which were present at the same concentration throughout the reaction (*Figure 85*). These signals did not arise from the starting materials, and a control experiment, repeating the kinetic experiment conditions without the purine, was conducted (*Figure 85*). The same signals were visible, indicating dimerisation of reagent **157** in low concentration (10%) with oxidation by DMSO and oxygen seeming to be the likely explanation.[210]

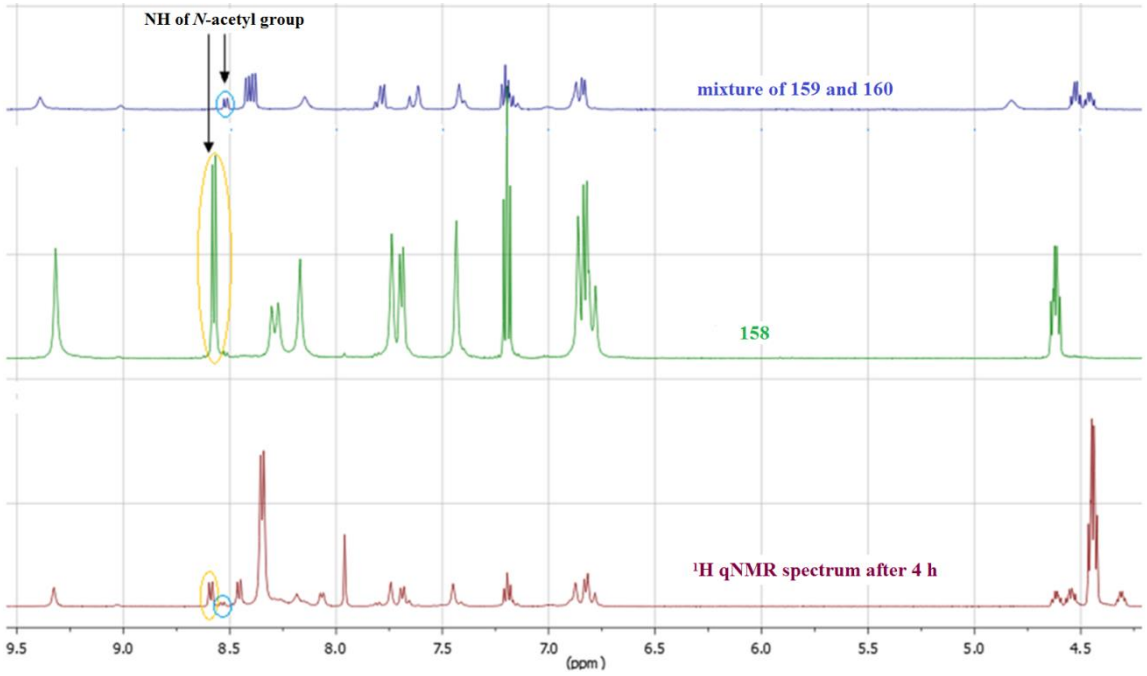

Figure 84 - ^{1}H NMR spectra illustrating the acetamido NH signals of compounds **158** and **159**

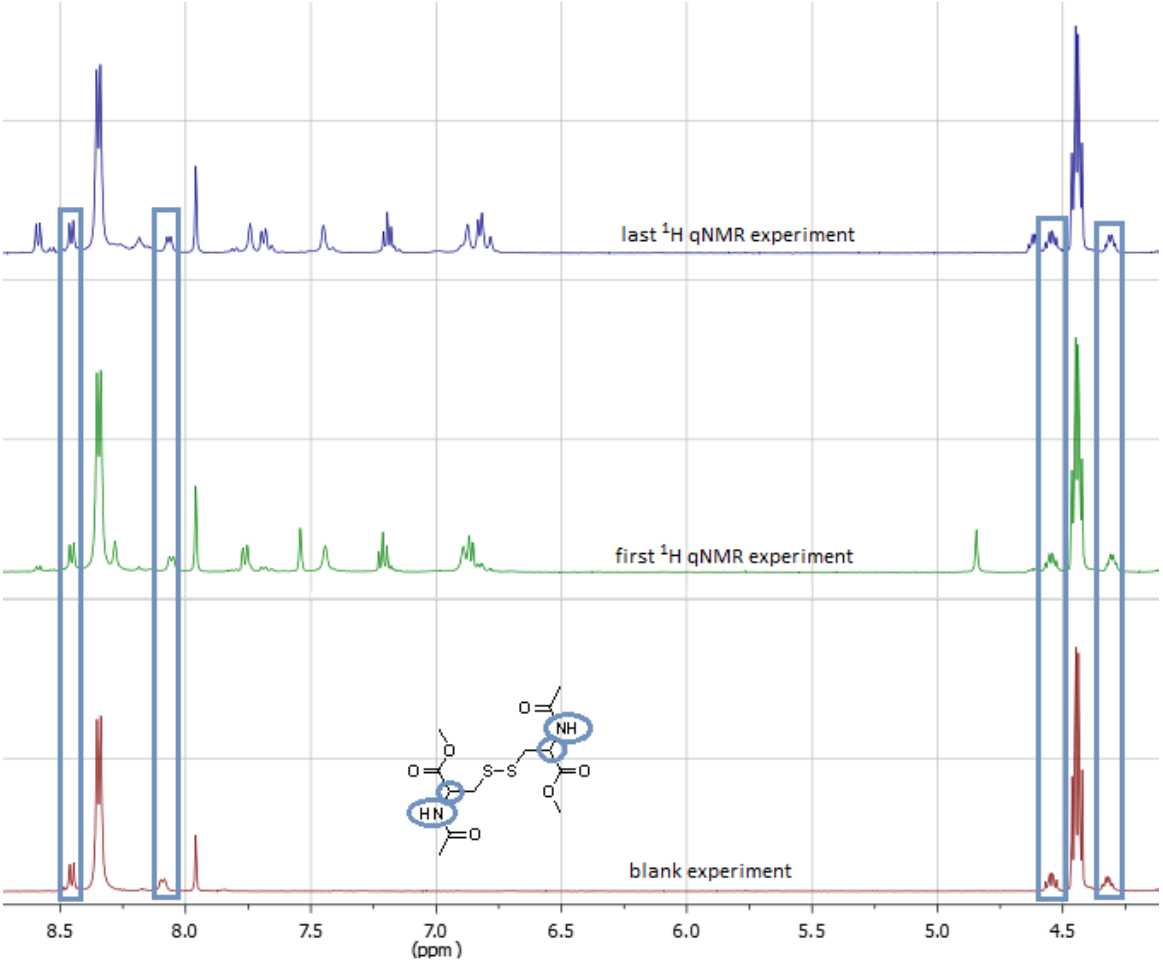

Figure 85 – ^{1}H NMR spectra indicating the signals from the dimerisation of reagent **157**

From a consideration of the reaction between compounds **42** and **157**, it may be postulated that formation of allene intermediate **161** is followed by proton transfer from protonated DABCO to give the thioethenyl product (*Scheme 26*). If the proton approaches from the opposite side of the thioether group, then the *Z*-isomer **159** will be formed. However, this reaction pathway 'pushes' the thioether group toward the purine, which may render preferable the alternative mode of protonation leading to the thermodynamically stable *E*-isomer **158**. A further possibility is that the *Z*-isomer **159** is the kinetic product, but undergoes rapid isomerisation to *E*-isomer **158** (*Scheme 27*).

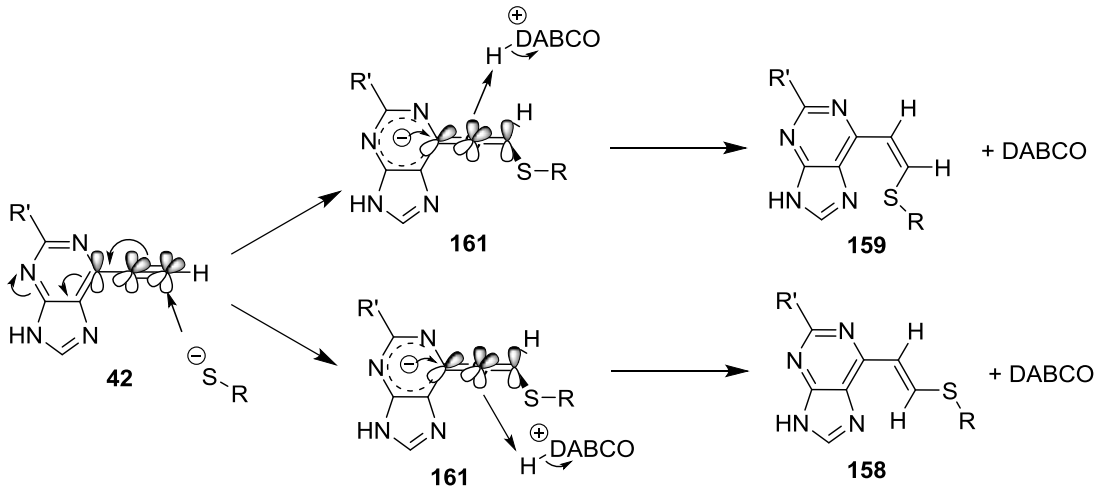

Scheme 26 – Mechanism of formation of the *E* (**158**) and *Z* (**159**) isomers from a common allene intermediate

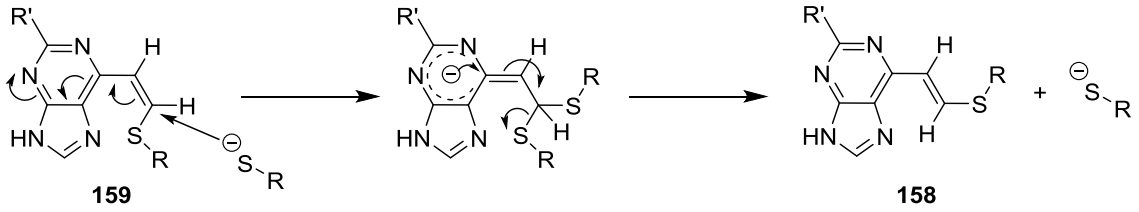

Scheme 27 - Postulated mechanism for the isomerisation of the product **159**

This stereochemical outcome differs from that observed for the irreversible inhibition of Nek2 by compound **42**. In the enzyme ATP-binding site, the stereochemistry may be determined by the positioning of Cys22 and a proton source relative to the 6-ethynyl group of compound **42**. For both the enzymatic and model systems, the direction of attack of the thiolate on the ethynyl group is presumably governed by the need to adopt a Bürgi-Dunitz approach.[211] It is widely known that a nucleophile approaches a carbonyl group at an angle of 107^{o} which maximises overlap with the π* orbital and minimises repulsion from the filled π orbital. The Bürgi-Dunitz approach can be extended to the Michael type

addition reaction observed between a 6-ethynylpurine and the Cys22 of Nek2 or *N*-acetylcysteine methyl ester **157** (*Scheme 28*).

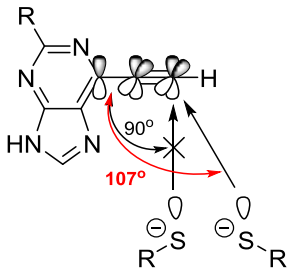

Scheme 28 – The Bürgi-Dunitz approach on 6-ethynylpurines.

4.6. Determination of the rate constant (k)

The reaction between a 6-ethynylpurine and the thiolate **157**$^-$ formed from reagent **157** and DABCO, gave a mixture of *E*/*Z* thioenol ethers (**158**/**159**). As a mixture of isomers was obtained, the rate of the reaction was more easily determined by following the consumption of the 6-ethynylpurine rather than product formation. The rate of the reaction will be dependent on the concentrations of 6-ethynylpurine, reagent **157** and DABCO. However, compound **157** was introduced in a 10-fold excess over the 6-ethynylpurine rendering its concentration essentially constant throughout the reaction,[212] while the concentration of DABCO was considered constant. The reactions involved in the kinetic experiments can thus be expressed as follows:

$$\mathbf{157} + \text{DABCO} \underset{k'}{\overset{k}{\rightleftharpoons}} \mathbf{157}^- + \text{DABCO}^+$$

$$\mathbf{157}^- + \text{substrate} \xrightarrow{k''} \text{Intermediate}$$

$$\text{Intermediate} + \text{DABCO}^+ \xrightarrow{k''} \text{Product} + \text{DABCO}$$

The reaction between thiol **157** and DABCO rapidly achieves equilibrium compared with the attack of thiolate **157**$^-$ on the 6-ethynylpurine (substrate). The equilibrium equation for the reaction between DABCO and thiolate **157**$^-$ can be written as follows:

$$K = \frac{[\mathbf{157}^-]_e[\text{DABCO}^+]_e}{[\mathbf{157}]_e[\text{DABCO}]_e} = \frac{k}{k'} \quad (1)$$

After a short time, the initial concentration of thiol **157** can be written as:

$$[\mathbf{157}]_0 = [\mathbf{157}]_e + [\mathbf{157}^-]_e \quad (2)$$

The rate of disappearance of the 6-ethynylpurine (substrate) can be expressed as:

$$-\frac{d[sm]}{dt} = k''[sm][\mathbf{157}^-]_e = k''[sm]K[\mathbf{157}]_e \frac{[DABCO]_e}{[DABCO^+]_e} \quad (3)$$

By replacing $[\mathbf{157}^-]_e$ from *Equation 1* in *Equation 2*, the following equation was obtained:

$$[\mathbf{157}]_0 = [\mathbf{157}]_e + K[\mathbf{157}]_e \frac{[DABCO]_e}{[DABCO^+]_e} \quad (4)$$

Therefore, $[\mathbf{157}]_e$ can be expressed as:

$$[\mathbf{157}]_e = \frac{[\mathbf{157}]_0}{1+K\frac{[DABCO]_e}{[DABCO^+]_e}} \quad (5)$$

By substituting $[\mathbf{157}]_e$ in *Equation 3* by its expression from *Equation 5*, the final equation is:

$$\frac{d[product]}{dt} = k''[sm]K[\mathbf{157}]_0 \frac{[DABCO]_e}{[DABCO^+]_e + K[DABCO]_e} = k_{app}[sm] \quad (6)$$

Knowing that the peak area of an NMR signal is directly related to the number of resonances contributing to the signal, the concentration of 6-ethynylpurine remaining was determined using *Equation 7*.

$$[\text{ethynylpurine}] = [DMF] \times \frac{\text{ethynyl proton peak area}}{\text{aldehydic proton peak area}} \quad (7)$$

For each reaction, the ethynyl proton CH was chosen to represent the quantity of 6-ethynylpurine remaining, as this peak did not overlap with any other signal in the spectrum. The area of the signals of the ethynyl proton and the aldehydic proton from the DMF were carefully measured using *Topspin*™. The two peaks of interest were always integrated between the same intervals for reproducibility. The data obtained from *Topspin*™ were then manipulated with *Microsoft Excel*™ to determine the apparent rate constant k_{app} of each reaction, k_{app} being the slope of the linear graph (*Equation 6*). Finally, the half-life ($t_{1/2}$) of each reaction was calculated from the pseudo first order rate constant k_{app} (*Equation 8*).

$$t_{1/2} = \frac{\ln(2)}{k_{app}} \quad (8)$$

4.7. Results of the kinetic studies

The reaction between 6-ethynylpurine **42** and thiol **157** was monitored every 10 minutes by ^{1}H qNMR, using 8 scans per spectrum, and disappearance of the 6-ethynyl proton was time-dependent (*Figure 86*). To calculate the k_{app} constant of the reaction, a logarithm function (ln) was applied to the concentration of compound **42** and plotted against time (*Figure 87*) to give a linear relationship.

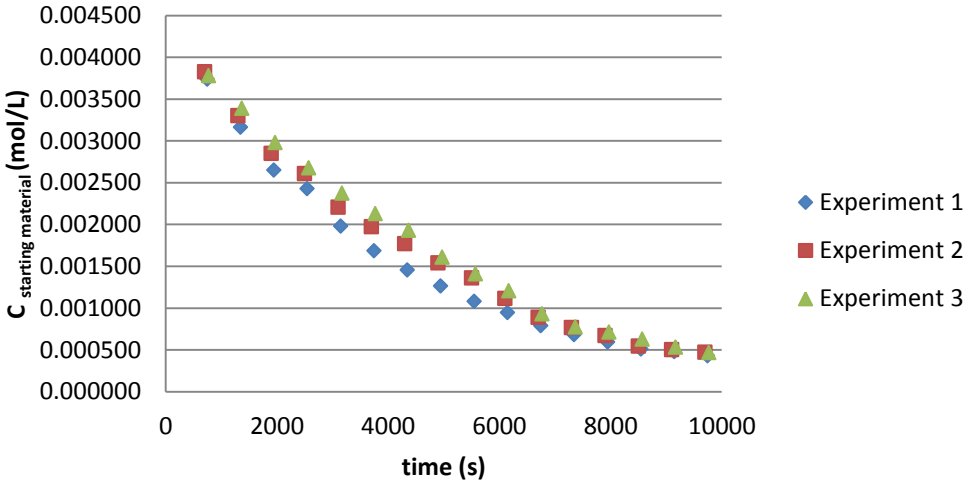

Figure 86 – Time-dependent consumption of compound **42** by thiol **157** in presence of DABCO

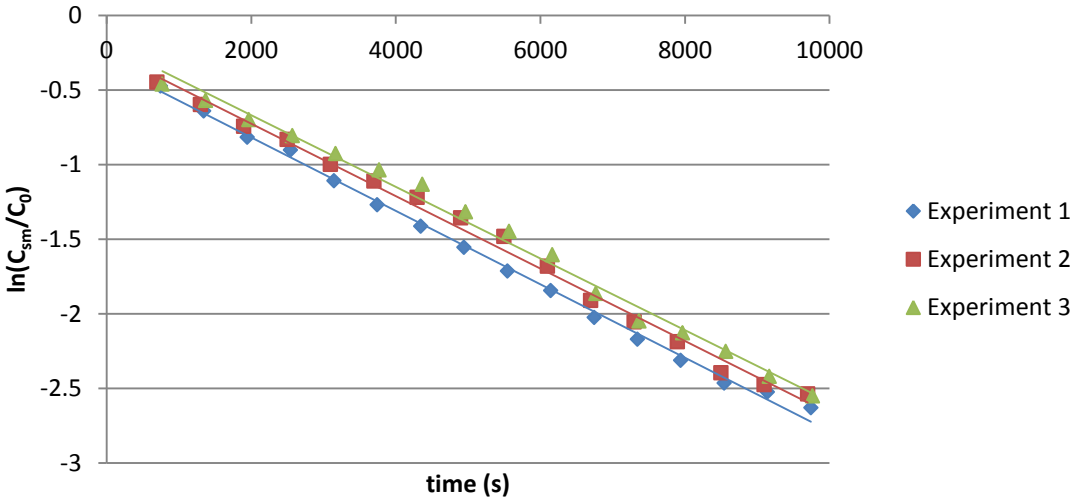

Figure 87 – Linear relationship between time of reaction and concentration of compound **42**

The same reaction was conducted in triplicate and the values obtained from each experiment were similar. The slope of the linear graph obtained from the plot ln(**42**) against time gave the *pseudo* first order rate constant of the reaction (k_{app}) (*Table 11*).

Table 11 - k_{app}, R^2, k and $t_{1/2}$ values from the kinetic experiments with compound **42**

Experiment	k_{app} (10^{-4} s^{-1})	R^2 value	$t_{1/2}$ (s)
1	2.50	1.00	2773
2	2.43	0.99	2852
3	2.40	0.99	2888

Average k_{app} = 2.44 10^{-4} s^{-1}

Average $t_{1/2}$ = 2838 s

The N^7- and N^9-methyl derivatives of compounds **42** and **41** (**61-64**) were also studied using the established ^{1}H qNMR technique. The N^7-methyl derivatives, **62** and **64**, appeared to react faster than their NH analogues, **41** and **42**, so the acquisitions were recorded every 3 minutes using only 4 scans. Data processing gave the following results (*Table 12*):

Table 12 - k_{app}, R^2, k and $t_{1/2}$ values from the kinetic experiments

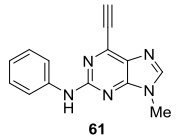

61

Experiment	k_{app} (10^{-4} s^{-1})	R^2 value	$t_{1/2}$ (s)
1	3.87	1.00	1829
2	3.86	0.99	1773
3	3.01	0.99	2303

Average k_{app} = 3.58 10^{-4} s^{-1}

Average $t_{1/2}$ = 1968 s

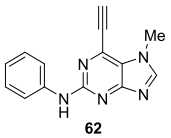

62

Experiment	k_{app} (10^{-4} s^{-1})	R^2 value	$t_{1/2}$ (s)
1	28.57	1.00	243
2	27.77	0.99	250
3	27.77	0.99	250

Average k_{app} = 28.04 10^{-4} s^{-1}

Average $t_{1/2}$ = 248 s

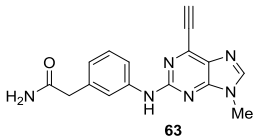

63

Experiment	k_{app} (10^{-4} s^{-1})	R^2 value	$t_{1/2}$ (s)
1	2.87	0.99	2415
2	3.11	0.99	2229
3	3.01	0.99	2303

Average k_{app} = 3.00 10^{-4} s^{-1}

Average $t_{1/2}$ = 2316 s

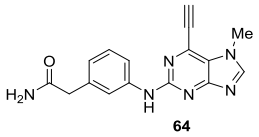

64

Experiment	k_{app} (10^{-4} s^{-1})	R^2 value	$t_{1/2}$ (s)
1	14.62	0.99	474
2	15.19	1.00	468
3	14.83	1.00	467

Average k_{app} = 14.88 10^{-4} s^{-1}

Average $t_{1/2}$ = 470 s

The experiments for each compound were repeated three times for accuracy of the results and as shown in *Table 2*, the results were consistent. The reactivity of the N^9-methyl compounds, **61** and **63**, was demonstrated to be close to the reactivity of the NH parents, **41** and **42**. However, the N^7-methyl compounds, **62** and **64**, were found to react 5 to 7 times faster than their NH or N^9-methyl analogues. Differences in reactivity were noticeable from the rate constant k_{app} values and the half-life values. The compounds bearing a simple aniline substituent at the 2-position showed a slightly higher reactivity than the ones having an amide substituent of the aniline ring (**61** vs **63** and **62** vs **64**). The amide function on the 2-aminoaryl group might be a weak electron-donor (because of the CH_2 group) which would reduce the electrophilicity of the ethynyl moiety, affecting the rate of addition.

4.8. Reactivity of N^7-methyl purine

One of the first observations about the reactivity of the N^7-methyl compounds was their instability during the TIPS deprotection, under TBAF conditions. A second observation was easily made from the first one, which was the contribution of the groups at the 2-position to the reactivity of the molecule, highly noticeable during TIPS deprotection (*see Chapter 3, section 3.2.1.*). Among the same library of compounds with only the 2-substituents varying, yields were very diverse. As well, within the group, TIPS deprotection was carried out on a bioisostere of compound **42** having a CH_2 group at the 2-position instead of the NH group. In this case, the deprotection was much slower and complete after two hours[137] compared to 5 minutes when having the NH group. These examples showed the influence of the groups at the 2-position on the stability of the ethynyl moiety. Another observation was the NMR shifts of the 6-ethynyl proton. The methyl group at the *N*-9 position had a slight effect on the ethynyl proton shift compared to the NH parent. The methyl group at the *N*-7 position, on the contrary, had a large effect on the shift of the ethynyl proton with almost 0.2 ppm of difference (*Table 13*). This observation correlated with the reactivity of the three compounds studied in kinetics. By comparison to the ethynyl proton shift, the carbon shift only changed slightly (*Table 13*). The last observation in NMR was the shifts of the methyl group. The resonance of the methyl group at the *N*-7 position was found to be downfield (δ 4.01) compared with the methyl group at the *N*-9 position (δ 3.76). As well, a significant change in ^{13}C NMR shift was noticed when the methyl substituent was at the *N*-7 (δ 32.8) or at the *N*-9 position (δ 29.3). This might be due to an interaction of the methyl group at the *N*-7 position with the ethynyl group.

Table 13 - ^{1}H NMR shifts of compounds **42**, **63** and **64.**

Compound	^{1}H NMR shift of 6-ethynyl proton	^{13}C NMR shift of 6-ethynyl proton	^{1}H NMR shift of methyl protons	^{13}C NMR shift of CH_3
42	4.82	86.9	-	-
63	4.84	87.1	3.76	29.3
64	4.99	87.5	4.01	32.8

From an assessment of these chemical observations in comparison with the biological results obtained for the N^7-methyl derivatives, it was clear that a methyl group at the purine *N*-7 position activated the 6-ethynyl substituent to conjugate addition. The main reason for such activation was postulated to be a 'buttressing' effect, shown to influence the rate of racemisation of optically active derivatives of biphenyls.[213]

The methyl group at the *N*-7 position of a purine scaffold was postulated to buttress the ethynyl group. As proposed from Adams' work, the N^7-methyl group should have a direct effect on bond angles.[214] Small-molecule crystal structures obtained for the two *N*-methyl isomers, **63** and **64**, showed a difference of 4° for the angle formed by the 6-ethynyl moiety and the purine core between the N^9-methylpurine **63** and the N^7-methylpurine **64** (*Figure 88*). This observation confirmed the 'repulsive' effect of the methyl function, when situated at the *N*-7 position, on the ethynyl group.

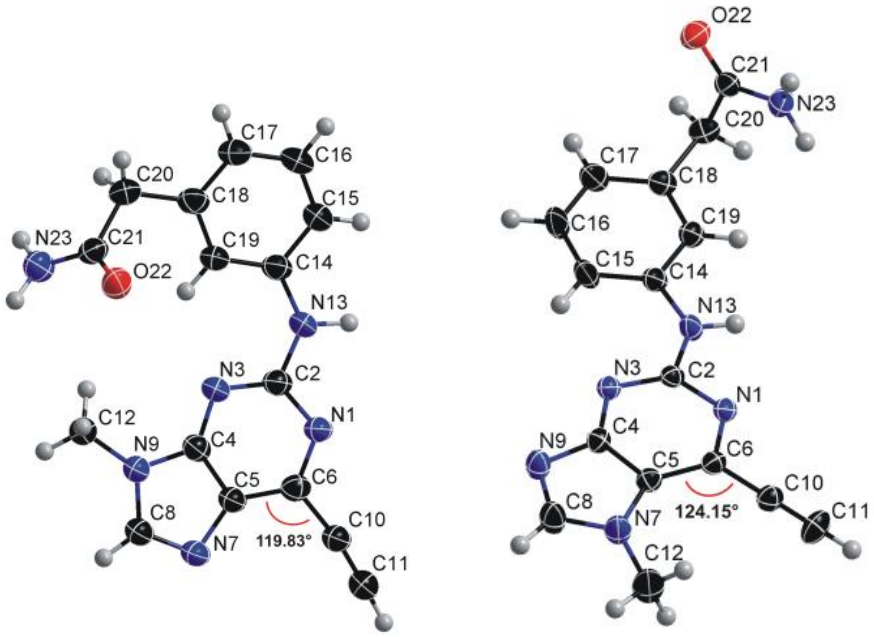

Figure 88 - *X*-Ray crystal structures of compounds **63** and **64**.

This observation supported the hypothesis of a buttressing effect between the N^7-methyl group and the 6-ethynyl moiety. This effect appeared to increase the rate of nucleophilic attack on the 6-ethynyl group during the Michael addition, and can be explained by the steric strain relief phenomenon.[215] After attack of the nucleophile, the product formed is relieved from steric strain and is, therefore, under a more favoured state. The buttressing effect of the *N*-7 methyl group on the 6-ethynyl group imposed a steric strain in the molecule which accordingly became more reactive towards nucleophilic attack to be relieved from this unfavorable state.

Chapter 5. Substitution on the Vinyl Sulfone of 6-(Cyclohexylmethoxy)-*N*-(4-(vinylsulfonyl)phenyl)-9*H*-purin-2-amine: Effects on Covalent Inhibition of CDK2

The stability of vinyl sulfone **60** was shown to be compromised in plasma and cell culture medium (*Figure 89*). The main source of degradation was found to be hydration of **60**, owing to the instability of the vinyl sulfone group in the presence of water. With the objective of improving chemical stability while retaining the biological activity of **60**, analogues were synthesised and tested against CDK2. To fully understand the biological results of this new series, the 2-hydroxyalkyl compound derived from each vinyl sulfone was also prepared.

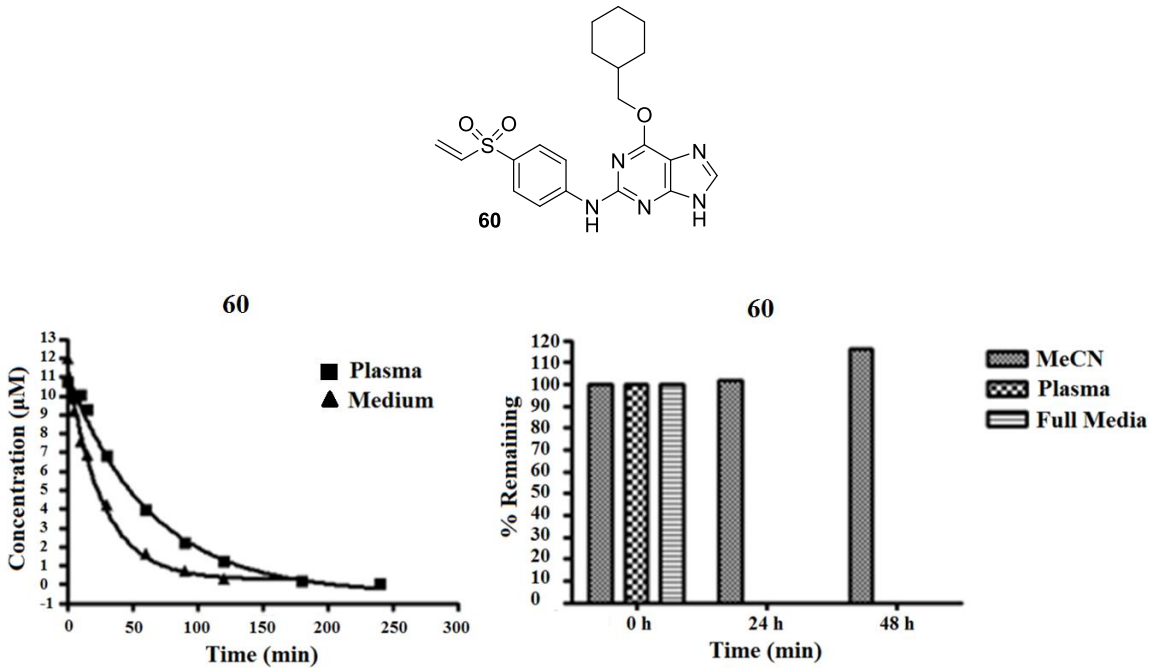

Figure 89 - Stability of **60** in plasma, cell culture medium and acetonitrile[167]

In this chapter, the synthesis of selected α- and β-substituted vinyl sulfones is described. Such compounds, especially with electron-withdrawing substituents, have been rarely described in the literature. It was necessary to develop new routes to these target compounds, for which considerable experimentation was required that was partly frustrated by their reactivity and lability.

5.1. Introduction of α-alkyl/aryl groups on the vinyl sulfone of 60

In the crystal structure of vinyl sulfone **60** bound to CDK2, the vinyl sulfone group is orientated towards the solvent region, offering possibilities for structural modifications.

The α-position was first modified to investigate the influence of alkyl, aryl and electron-withdrawing groups on the chemical reactivity of the vinyl sulfone warhead. The strategy towards the synthesis of these targets consisted of preparing an aniline derivative, which was reacted with 2-iodopurine **171** (*Scheme 29*). The aniline functional groups (FG) enabled formation of the desired vinyl sulfone moiety at the final stage of the synthesis.

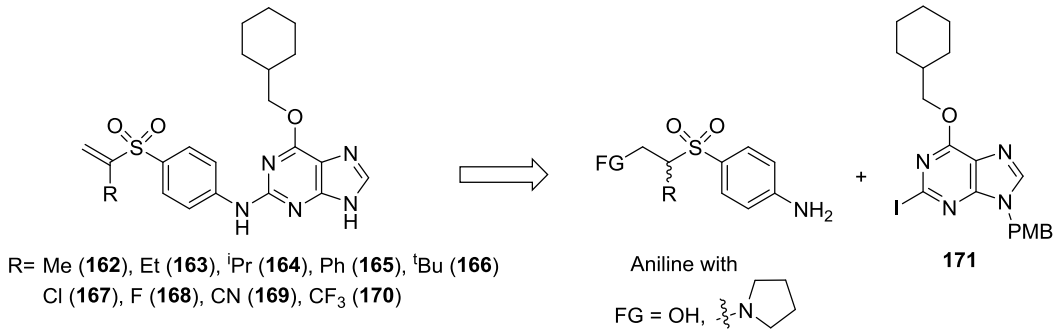

Scheme 29 – Synthetic strategy for the preparation of the α-substituted vinyl sulfones **162-170**

The common purine intermediate **171** was synthesised in three steps starting with protection of the purine *N*-9 of compound **68** with a PMB group, followed by nucleophilic aromatic substitution at the purine 6-position and, finally, iodination at the 2-position of the purine (*Scheme 30*).

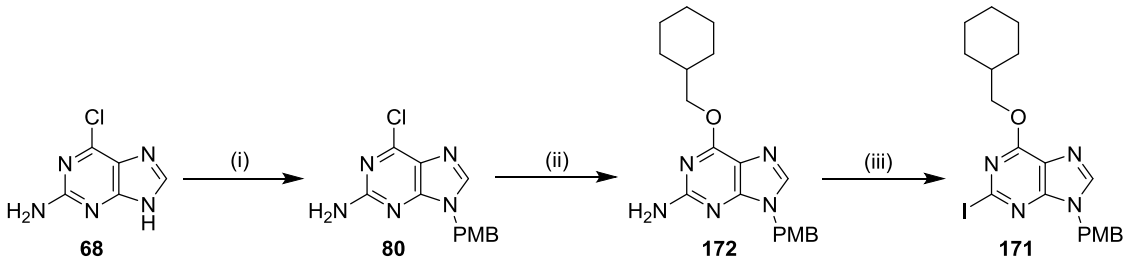

Scheme 30 - *Reagents and conditions*: (i) Cs_2CO_3, 4-methoxybenzyl chloride in DMF, 60 ^oC, 18 h, 60%; (ii) NaH, cyclohexylmethanol, r.t., 18 h, 70%; (iii) CH_2I_2, CuI, isoamyl nitrite in THF, 65 ^oC, 2 h, 67%.

5.1.1. α-Methyl analogue of vinyl sulfone 60

Alkylation of thiophenol **173** with reagent **174** was performed in quantitative yield. The aldehyde **178** was obtained by consecutive hydrolysis of ester **175**, followed by reduction of the resultant carboxylic acid **176** with borane, both steps occurring in high yields. The alcohol **177** was oxidised with the Dess-Martin periodinane to furnish aldehyde **178** in quantitative yield. Reductive amination of aldehyde **178** was carried out using sodium trimethoxyborohydride to give the tertiary amine **179**. Finally, the nitro group of

compound **179** was reduced to the aniline **180** in the presence of zinc and acetic acid in excellent yield (*Scheme 31*).

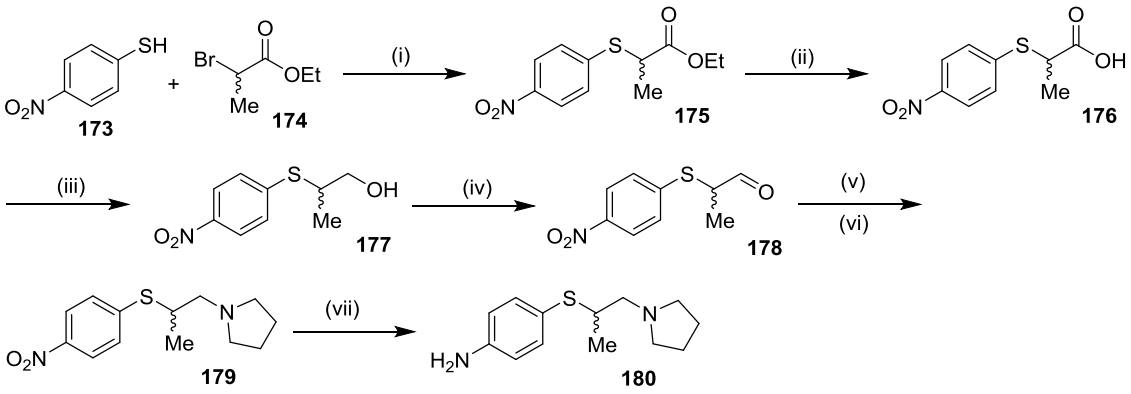

Scheme 31 - *Reagents and conditions*: (i) Et_3N in DCM, r.t., 3 h, 94%; (ii) LiOH in THF, 50 °C, 2 h, 88%; (iii) 1M borane in THF, r.t., 2 h, 76%; (iv) DMP in DCM, r.t., 3 h, 89%; (v) pyrrolidine, AcOH in toluene, r.t., 1 h; (vi) $NaBH(OMe)_3$, r.t., 2 h, 85%; (vii) Zn, AcOH in MeOH, 50 °C, 1 h, 98%.

The aniline **180** was reacted with the intermediate **171** in a Buchwald coupling, followed by PMB deprotection in TFA to afford the intermediate **181** in 52% overall yield (*Scheme 32*). The last step of the scheme was a one-pot procedure involving oxidation of sulfide **181** with *m*-CPBA followed by a Cope type-elimination.[166] For the parent compound **60**, *N*-oxidation was sufficient to trigger the Cope type-elimination with formation of the vinyl sulfone and release of *N*-hydroxypyrrolidine. However, when a methyl group was present, a base was required for elimination, as the methyl substituent may have been too bulky and prevented the intermediate *N*-oxide from deprotonating at the α-position of the sulfone group. A weakly nucleophilic base (Cs_2CO_3) was chosen to prevent any reaction with the highly reactive vinyl sulfone moiety formed.

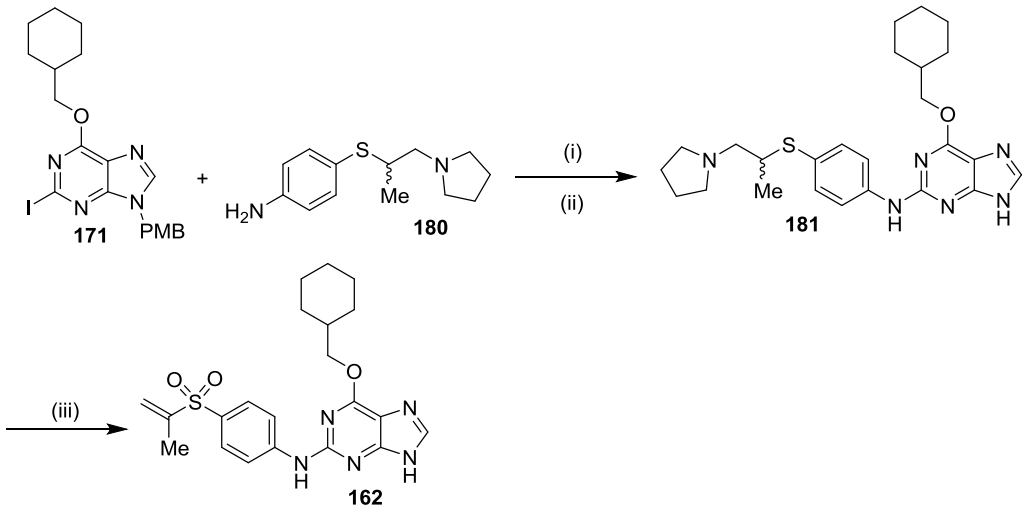

Scheme 32 - *Reagents and conditions*: (i) K_2CO_3, XPhos, $Pd(dba)_2$ in MeCN, 80 °C, 18 h; (ii) TFA, 70 °C, 2 h, 62%; (iii) *m*-CPBA, Cs_2CO_3 in DCM, 0 °C, 0.5 h, 33%.

The synthesis of the corresponding 2-hydroxyalkyl derivative of **162** started with the previously prepared aniline **177**. Sulfide **177** was oxidised to the sulfone and the nitro group of compound **182** was reduced to the corresponding aniline **183**, both steps proceeding in high yields. The aniline **183** was reacted with intermediate **171** to afford the 2-hydroxyalkyl derivative **184** after a Buchwald coupling and PMB deprotection (*Scheme 33*).

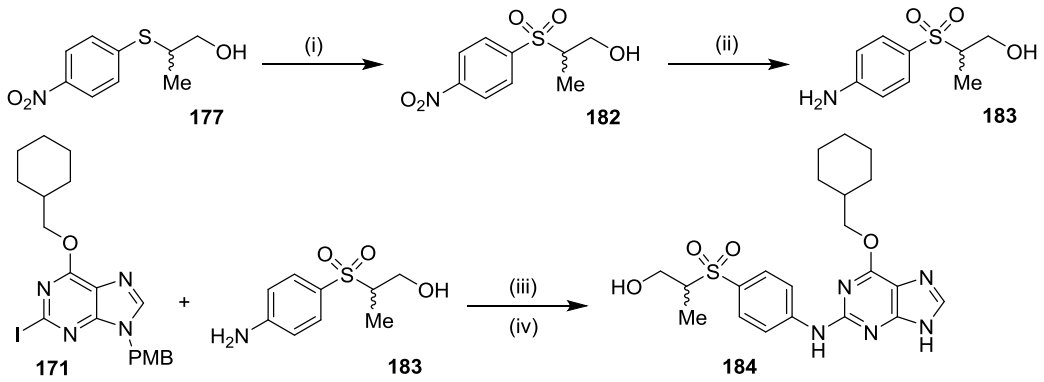

Scheme 33 - *Reagents and conditions* : (i) *m*-CPBA in DCM, 0 ^oC, 0.5 h, 72%; (ii) Zn, AcOH in MeOH, 50 °C, 1 h, 91%; (iii) K_2CO_3, XPhos, $Pd(dba)_2$ in MeCN, 80 °C, 18 h; (iv) TFA, 70 °C, 2 h, 44%.

5.1.2. α-Ethyl, isopropyl and phenyl derivatives of vinylsulfone 60

With the objective of probing the space available at the α-position of the vinyl sulfone warhead of **60**, larger groups were introduced. A common scheme was developed to introduce an ethyl, isopropyl and phenyl group, respectively. The same strategy as for the methyl derivative **162** was first considered, having a pyrrolidine moiety as precursor to the vinyl sulfone. Alkylation of thiophenol **173** with reagents **185**, **186** and **187**,

respectively, followed by hydrolysis and reduction with borane afforded the corresponding alcohols **194-196**. However, oxidation with DMP led to extensive degradation when a phenyl (**196**) or ethyl group (**194**) was present and only a 20% yield was obtained when an isopropyl group (**198**) was in place (*Table 14*).

Table 14 – Summary of yields for the synthesis of aldehydes **197-199**.

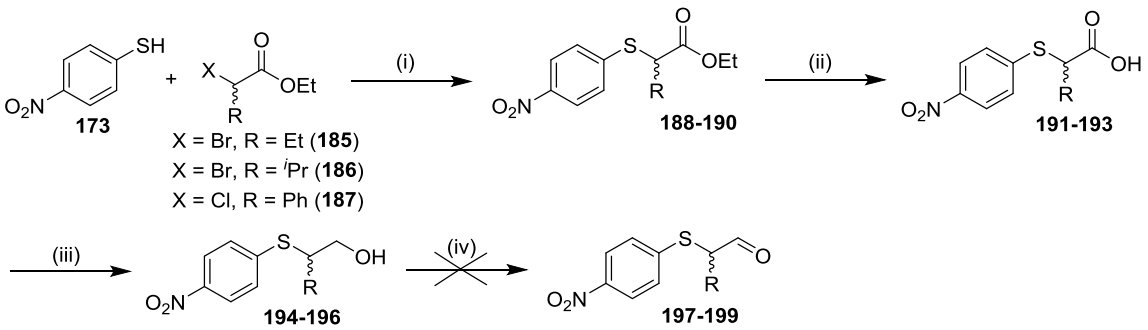

Reagents and conditions: (i) Et_3N in DCM, r.t., 3 h; (ii) LiOH in THF, 50 °C, 2 h; (iii) 1M borane in THF, r.t., 2 h; (iv) DMP in DCM, r.t., 3 h.

R group	Yield for step (i)	Yield for step (ii)	Yield for step (iii)	Yield for step (iv)
Et	**188** – 90%	**191** – 89%	**194** – 74%	**197** – degradation
^{i}Pr	**189** – 46%	**192** – 93%	**195** – 84%	**198** – 20%
Ph	**190** – 66%	**193** – 96%	**196** – 62%	**199** - degradation

Other oxidative methods were investigated including the Pfitzner-Moffatt procedure,[216] but no reaction was observed. Swern conditions were attempted but led to complete degradation when ethyl (**194**) and phenyl (**196**) groups were present, with a similar LC-MS profile to the Dess-Martin periodinane procedure being observed, suggesting reactivity problems associated with the presence of the sulfide group. With an isopropyl group, the aldehyde **198** was obtained in 66% yield (*Scheme 34*). As a general method was preferred, this approached was discontinued.

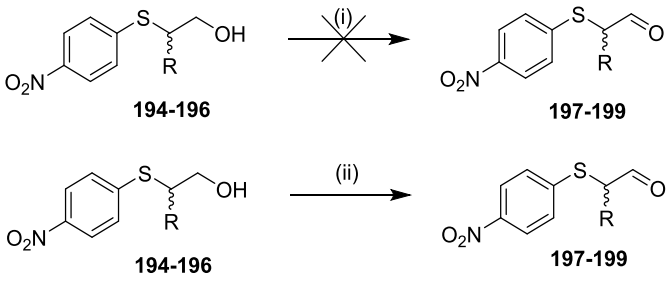

Scheme 34 - *Reagents and conditions*: (i) DCC, Et_3N, TFA in DMSO/toluene, r.t., 18 h; (ii) DMSO, oxalyl chloride, Et_3N in DCM, - 78 °C, 2 h, 0% (Et, **197**), 66% (^{i}Pr, **198**), 0% (Ph, **199**).

The strategy of utilising a leaving group to introduce the pyrrolidine moiety was then investigated. A mesyl group was first considered but attempts to mesylate the alcohol **194** led only to a mixture of chloro compounds (**200** and **201**) (*Scheme 35*). Indeed, the lone pair of the sulfur displaced the mesyl group presumably leading to the formation of an episulfonium ion. The chloride counterion can then attack on either face (red or blue), the 'red' being favoured by stabilisation of positive charge present in the transition state and the 'blue' being favoured by steric considerations (*Scheme 35*).

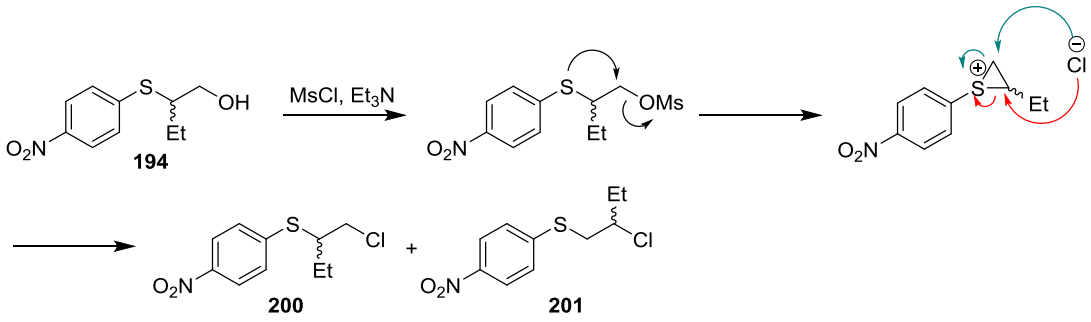

Scheme 35 – Mechanism for the mesylation reaction on alcohol **194**

The chloro compounds (**200** and **201**) were isolated as 1:1 ratio of the isomers. An excess of pyrrolidine was added to **200**/**201**, but no substitution was observed either at room temperature or by heating at reflux. Microwave heating was also tried but elimination was observed leading to an inseparable mixture of alkenes **204**-**206** (*Scheme 36*). Thus, although the chloro compounds (**200** and **201**) were stable to nucleophilic attack, under microwave heating, elimination reactions were observed and led to alkenes **204**-**206**.

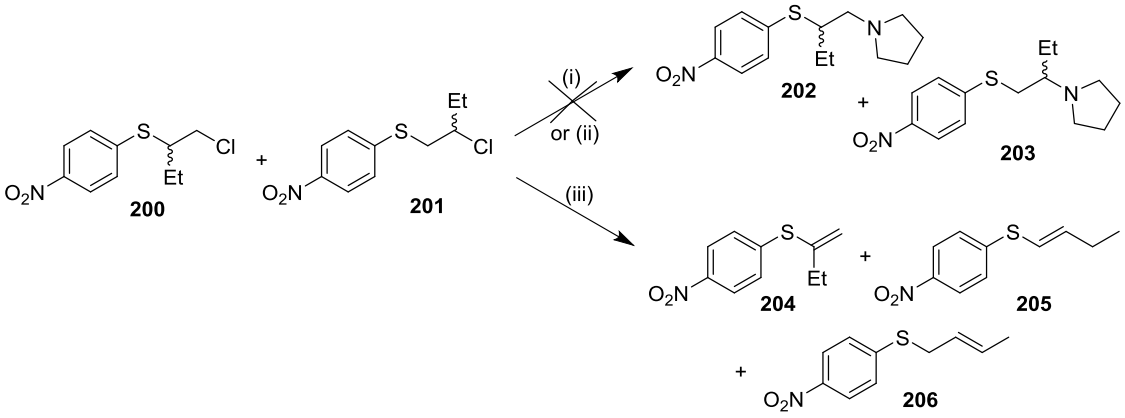

Scheme 36 - *Reagents and conditions*: (i) pyrrolidine, r.t., 18 h, no reaction; (ii) pyrrolidine in MeCN, reflux, 2 h, no reaction; (iii) pyrrolidine in MeCN, MW, 150 °C, 4 bar, 30 min.

The 2-hydroxyalkyl derivatives of vinylsulfones **163**-**165** were required and so the synthesis of these compounds was performed (*Table 15*) with the idea of using the leaving group strategy on these compounds (**213**-**215**) to obtain the desired vinyl sulfones **163**-**165**.

Table 15 – Summary of yields for the synthesis of 2-hydroxyalkyl derivatives **213**-**215**.

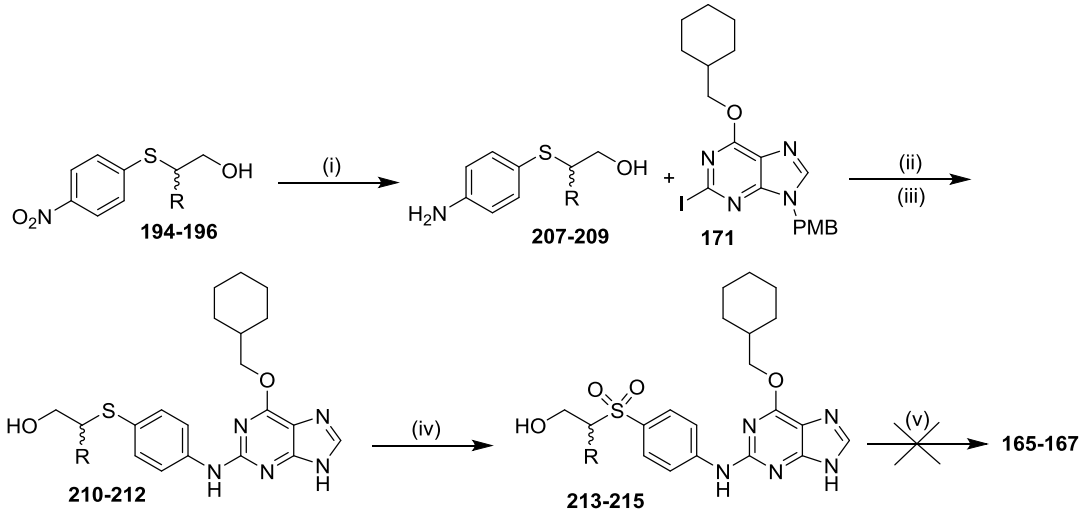

Reagents and conditions: (i) Zn, AcOH in MeOH, 70 °C, 2 h; (ii) K_2CO_3, XPhos, $Pd(dba)_2$ in MeCN, 80 °C, 18 h; (iii) TFA, 70 °C, 2 h; (iv) *m*-CPBA, Cs_2CO_3 in DCM, 0 °C, 30 min; (v) MsCl, Et_3N in DCM, r.t., 1 h then pyrrolidine.

R group	Yield for step (i)	Yield for steps (ii) and (iii)	Yield for step (iv)
Et	**207** – 77%	**210** – 63%	**213** – 28%
^{i}Pr	**208** – 79%	**211** – 28%	**214** – 36%
Ph	**209** – 85%	**212** – 26%	**215** – 56%

The nitro group of compounds **194-196** was reduced to the corresponding aniline (**207-209**). The anilines **207**-**209** were reacted with intermediate **171** in a Buchwald cross-coupling reaction, followed by PMB deprotection as a one-pot procedure, affording the purine intermediates **210-212** in moderate yields. Oxidation of sulfides **210-212** to the required sulfones was achieved with *m*-CPBA. From the 2-hydroxyalkyl derivatives **213-215**, the corresponding mesylates were formed using methanesulfonyl chloride and an excess of triethylamine, but not isolated (confirmed by LC-MS). Pyrrolidine was used in an attempt to displace the mesyl group, but only the parent alcohols **213-215** were retrieved. A possible mechanism to explain this observation is shown in *Scheme 37*, and was supported by the isolation and characterisation of the pyrrolidine by-product (**216**) formed.

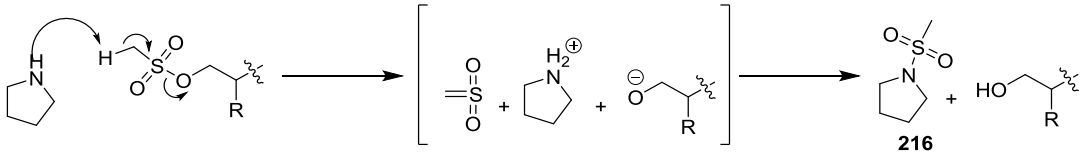

Scheme 37 – Side-reaction observed during the attempted displacement of the mesyl group by pyrrolidine leading to the formation of **216**

In the light of these results, tosylate, a larger group than mesylate, was considered. The tosylate intermediate was observed by LC-MS. Elimination was attempted by heating but no reaction was observed. Pyrrolidine was then used to displace the tosylate group but only the parent alcohol was obtained. Isolation and characterisation of the by-product formed during this reaction suggested a similar mechanism to that seen for the mesyl displacement reaction (*Scheme 37*). A last attempt was made from alcohol **213**, using a thermal rearrangement with an acetate group, as reported in the literature.[217] The acetate **217** was readily synthesised from alcohol **213** using acetic anhydride. After isolation, acetate **217** was heated under microwave irradiation at 170 °C for 1 hour but no reaction was observed. Caesium carbonate was added to trap the acetic acid that would form but instead, triggered deacetylation to give the alcohol **213**. This strategy (*Scheme 38*) was discontinued.

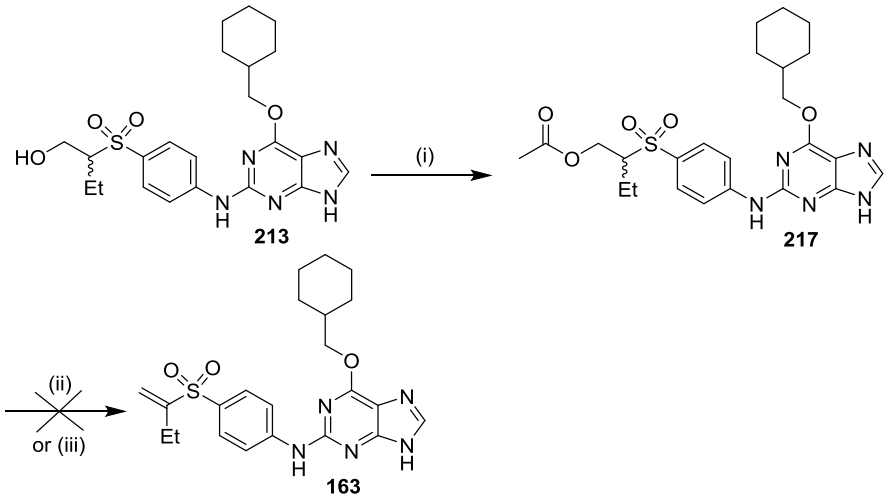

Scheme 38 - *Reagents and conditions*: (i) Ac_2O, Et_3N, DMAP in DCM, r.t., 2 h, 60%; (ii) MeCN, MW 170 °C, 1 h; (iii) Cs_2CO_3 in MeCN, MW 100 °C, 15 min.

From the attempts made previously, key information was obtained. Oxidation of the sulfides **194-196** was required, and the leaving group had to be chosen carefully to avoid regeneration of starting material as seen with mesylate and tosylate groups. After considering these results, the benzenesulfonyl group was selected (*Table 16*).

Table 16 – Summary of yields for the synthesis of the anilines **224**-**226**.

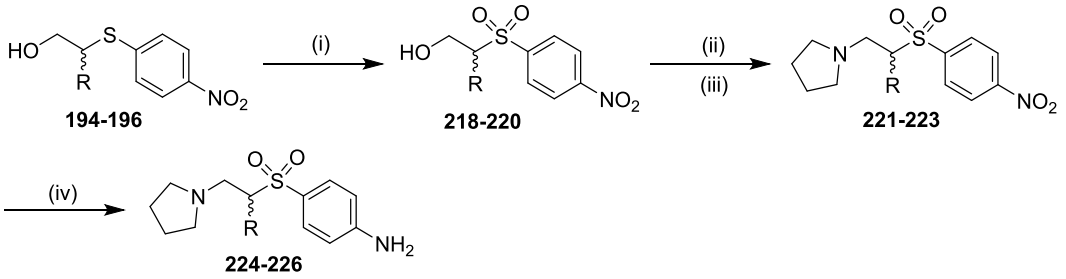

Reagents and conditions: (i) *m*-CPBA in DCM, 0 °C, 15 min; (ii) $PhSO_2Cl$, Et_3N in DCM, r.t., 18 h; (iii) pyrrolidine, r.t., 1 h; (iv) Zn, AcOH in MeOH, 50 °C, 1 h.

R group	Yield for step (i)	Yield for steps (ii) and (iii)	Yield for step (iv)
Et	**218** – 97%	**221** – 75%	**224** – 75%
^{i}Pr	**219** – 68%	**222** – 65%	**225** – 76%
Ph	**220** – 66%	**223** – 61%	**226** – 90%

Compounds **194-196** were first oxidised with *m*-CPBA to give the corresponding sulfones **218**-**220** in high yields, which were reacted with benzenesulfonyl chloride and then pyrrolidine, in a one-pot procedure, to form the target tertiary amines **221-223**. This step was further investigated to gain an understanding of the possible mechanism. Interestingly, the pyrrolidine did not directly substitute for the benzenesulfonyl group. Pyrrolidine first acted as a base to deprotonate at the α-position of the sulfone, which triggered elimination of the benzenesulfonate. The vinyl sulfone moiety thus formed reacted directly with pyrrolidine to give the tertiary amines **221**-**223** (*Scheme 39*). This step was high yielding for the three compounds studied. The last step was reduction of the nitro group to the corresponding amine to afford anilines **224-226** in good yields. This method allowed the synthesis of all three desired anilines, compared with the other approaches attempted that either failed or were only applicable to one analogue.

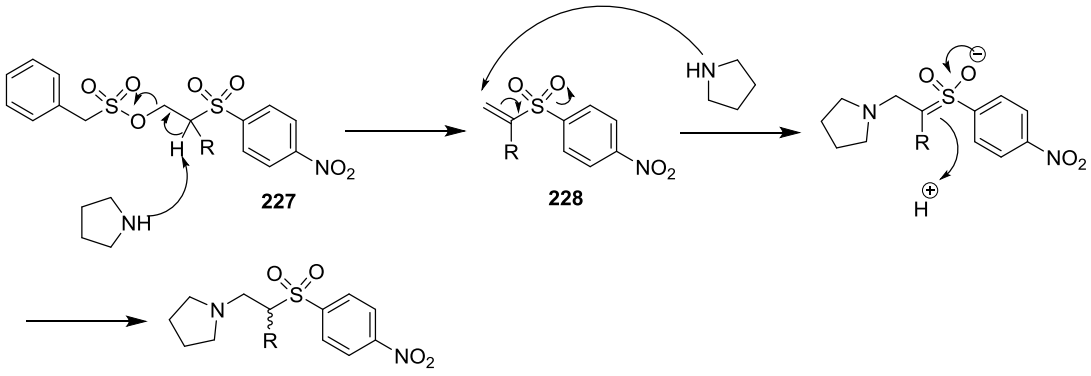

Scheme 39 – Postulated mechanism of the one-pot reaction to convert the protected alcohol **227** to the corresponding amine

When the one-pot procedure using benzenesulfonyl chloride was applied to alcohol **196**, the alkene **229** was formed. In this case, pyrrolidine acted as a base effecting an elimination (*Scheme 40*). The resulting alkene is not electron-deficient and therefore, does not undergo nucleophilic attack by pyrrolidine, in contrast to the vinyl sulfone **228** above (*Scheme 39*).

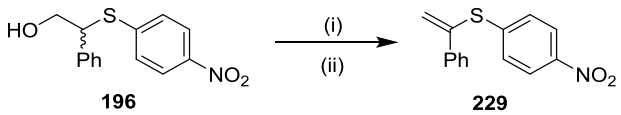

Scheme 40 - *Reagents and conditions*: (i) benzenesulfonyl chloride, Et_3N in DCM, r.t., 18 h; (ii) pyrrolidine, r.t., 1 h, 74%.

The anilines **224-226** were reacted with intermediate **171** in the Buchwald reaction, followed by PMB deprotection. The corresponding *N*-oxide derivatives of amines **230-232** were formed using *m*-CPBA and in the presence of caesium carbonate, the desired vinyl sulfone targets **163-165** were obtained. The yields were rather low, reflecting the reactivity issues with these compounds (*Table 17*).

Table 17 – Summary of yields for the synthesis of the α-substituted vinyl sulfones **163-165**.

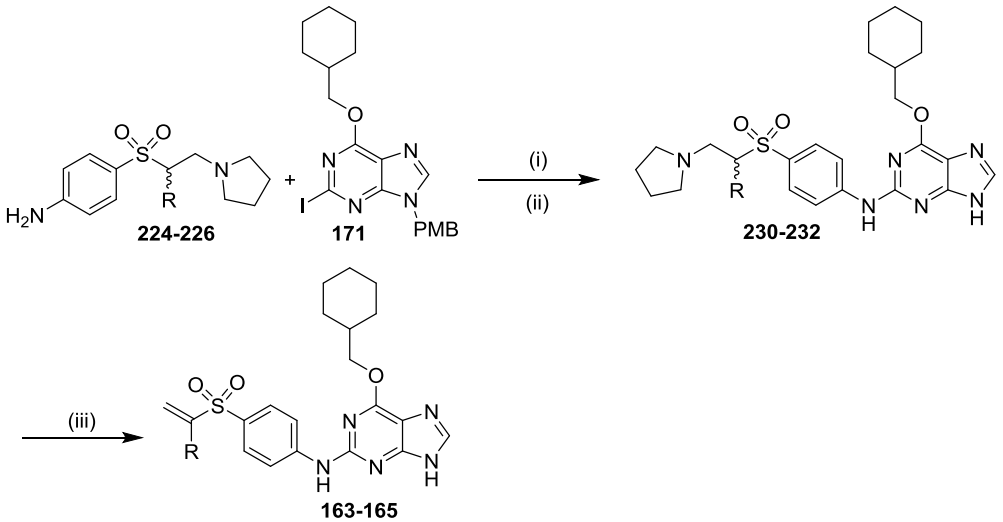

Reagents and conditions: (i) K_2CO_3, XPhos, $Pd(dba)_2$ in MeCN, 80 °C, 18 h; (ii) TFA, 70 °C, 2 h; (iii) *m*-CPBA, Cs_2CO_3 in DCM, r.t., 15 min, 23%.

R group	Yield for steps (i) and (ii)	Yield for step (iii)
Et	**230** – 35%	**163** – 23%
^{i}Pr	**231** – 18%	**164** – 23%
Ph	**232** – 47%	**165** – 29%

5.1.3. α-t-Butyl analogue of vinylsulfone 60

The last target purine in the α-alkyl series was the *t*-butyl compound **166** for which several synthetic approaches were attempted. The first strategy entailed formation of a silyl enol ether **234**, to be used subsequently in a Mukaiyama reaction (*Scheme 41*).

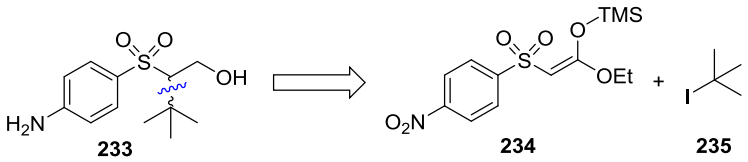

Scheme 41 – First retrosynthetic approach for the synthesis of aniline **233**.

Various conditions were used for the synthesis of the silyl enol ether **234** from the ester **237**, obtained in two steps from thiophenol **175** (*Scheme 42*). The base, solvent and TMS source were varied (*Table 18*). The use of TMSCl and LDA in THF afforded 20% conversion according to ^{1}H NMR analysis but was not reproducible. No literature precedent was found for the formation of a silyl enol ether on such a substrate (**237**), which raised the question of stability of the desired product.

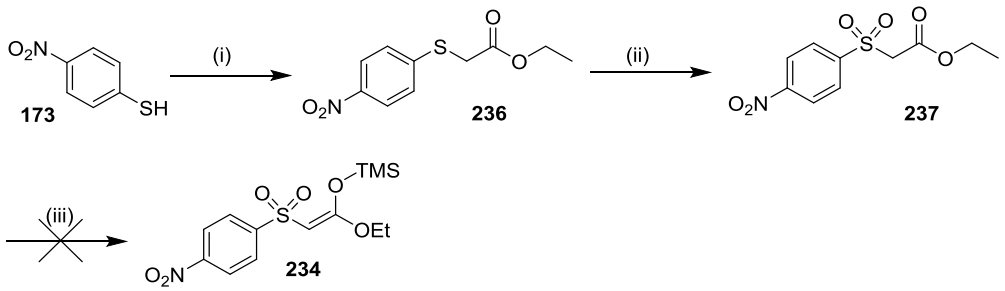

Scheme 42 - *Reagents and conditions*: (i) ethyl chloroacetate, Et_3N in DCM, r.t., 1 h, 95%; (ii) *m*-CPBA in DCM, r.t., 30 min, 86%; (iii) see *Table 18*.

Table 18– Conditions studied for the formation of silyl enol ether **234**

		TMS source	
		TMS-Cl	TMS-Tf
Base	Et_3N	No reaction in toluene	No reaction in THF
	NaH	No reaction in toluene	No reaction in THF
	LDA	20% conversion in THF – not reproducible	-

Another approach required formation of the sulfur-carbon bond of compound **238** with an electrophilic source of sulfur (*Scheme 43*). Thus, either 4-nitrobenzenesulfenyl chloride (**240**) or 4-nitrobenzenesulfonyl chloride (**242**) was reacted with ethyl 3,3-

dimethylbutyrate (**239**), previously treated with LDA (*Scheme 44*). These reactions led only to a complex mixture with no evidence of formation of the desired products, **238** and **241**.

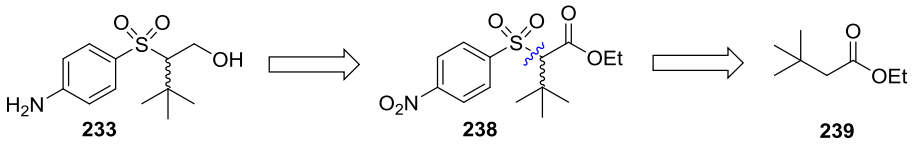

Scheme 43 – Second retrosynthetic approach to the synthesis of aniline **233**.

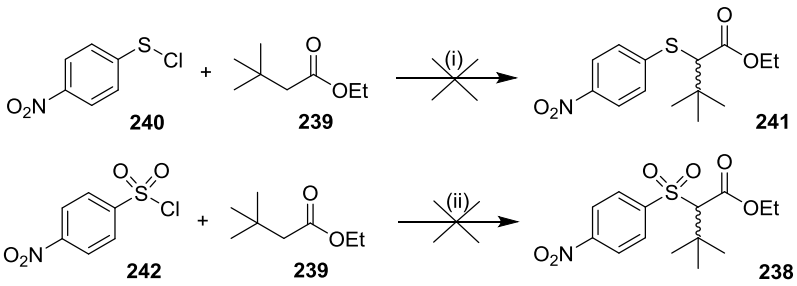

Scheme 44 - *Reagents and conditions*: (i) LDA in THF, -78 ^{o}C; (ii) LDA in THF, -78 ^{o}C.

As the previous approaches were inconclusive, the synthesis of the thiol **244**, from ketone **246**, was explored prior to reaction with 1-fluoro-4-nitrobenzene (**245**) (*Scheme 45*).

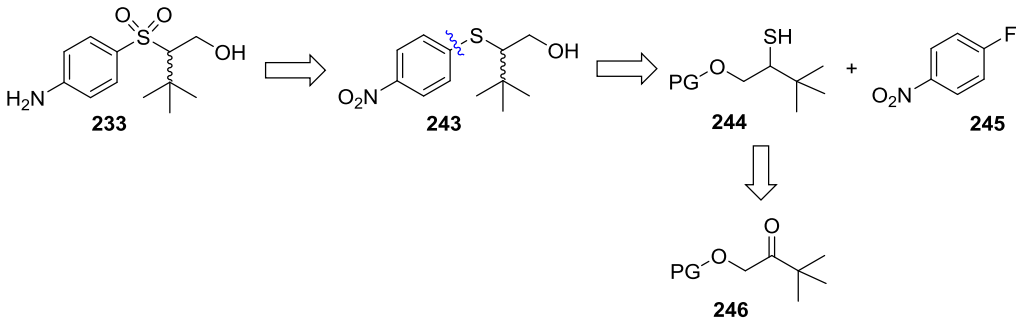

Scheme 45 – Third retrosynthetic approach for the synthesis of aniline **233**.

The first step attempted was displacement of the chloro group from 1-chloropinacolone (**247**) by an alkoxide to form compound **246** (*Scheme 46*). Several conditions were tried using NaH and benzyl alcohol, and different solvents (THF, MeCN and DMF) in the absence or presence of potassium iodide. KHMDS was also used as an alternative to sodium hydride but under all conditions, no reaction was observed.

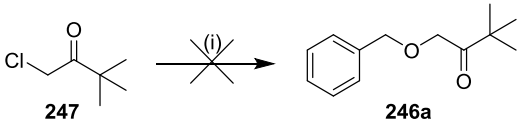

Scheme 46 - *Reagents and conditions*: (i) NaH or KHMDS in THF or MeCN or DMF.

As displacement of the chloro group by an alkoxide proved unsuccessful, this reaction was conducted with a carboxylate following conditions found in the literature,[218] and surprisingly, proceeded to give the ester **246b** in quantitative yield (*Scheme 47*). The second step was the transformation of ketone **246b** into thioketone **248**. Achieving selectivity over the ester function was uncertain but two conditions were tried, namely Lawesson's reagent and hexamethyldisilathiane with TMS-Tf, for which no reaction was observed in either case. This was probably due to the steric bulk imposed by the *t*-butyl group of compound **246b** preventing the approach of reagents onto the ketone.

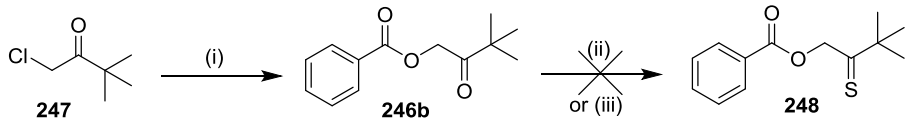

Scheme 47 - *Reagents and conditions*: (i) benzoic acid, DIPEA in DMF, r.t., 2 h, 67%; (ii) Lawesson's reagent in toluene, 110 ^{o}C, 18 h; (iii) hexamethyldisilathiane, TMSTf in MeCN, r.t., 18 h.

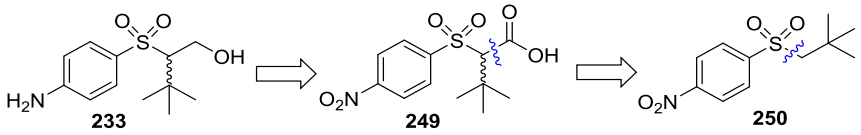

Scheme 48 – Fourth retrosynthetic approach for the synthesis of aniline **233**.

From the outset it was recognised that access to aniline **233** would be challenging. Although the retrosynthetic analysis of this last approach was obvious (*Scheme 48*), this method was tried last as concerns were raised as to an S_N2 reaction on a sterically hindered electrophile, known to be disfavoured. Encouragingly, the reaction between thiophenol **173** and 1-iodo-2,2-dimethylpropane (**251**) was achieved (*Scheme 49*). Oxidation of sulfide **252** led to intermediate **250**. Hydrocarbonylation was performed using LHMDS and solid CO_2, affording 45% conversion to carboxylic acid **249**. No higher yield was obtained but sulfone **250** was recovered and re-used. Consecutive reduction of the carboxylic acid and nitro groups gave the desired aniline **233**. The successful route (*Scheme 49*) profited from the relatively high nucleophilicity of the thiolate of **173**, which enabled S_N2 displacement on the sterically hindered reagent **251**, as well as the ability of the relatively small electrophile CO_2 to capture the anion from **250**.

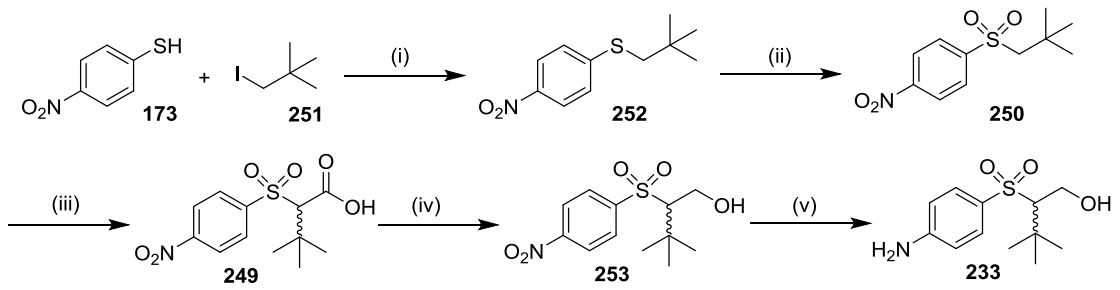

Scheme 49 - *Reagents and conditions*: (i) K_2CO_3 in DMF, r.t., 18 h, 68%; (ii) *m*-CPBA in DCM, r.t., 1 h, 86%; (iii) LHMDS in THF, -78 ^oC for 1 h then CO_2, r.t., 1 h, 49%; (iv) 1M borane in THF, 50 ^oC, 18 h, 73%; (v) Zn, AcOH in MeOH, r.t., 1 h, 84%.

Aniline **233** was reacted with intermediate **171** under Buchwald conditions followed by PMB deprotection to afford the desired 2-hydroxyalkyl derivative **254** (*Scheme 50*). The latter was converted into the corresponding target vinyl sulfone **166** by forming a mesylate which was then eliminated by DBU. From the same scheme, both 2-hydroxyalkyl derivative **254** and vinyl sulfone compound **166** were obtained.

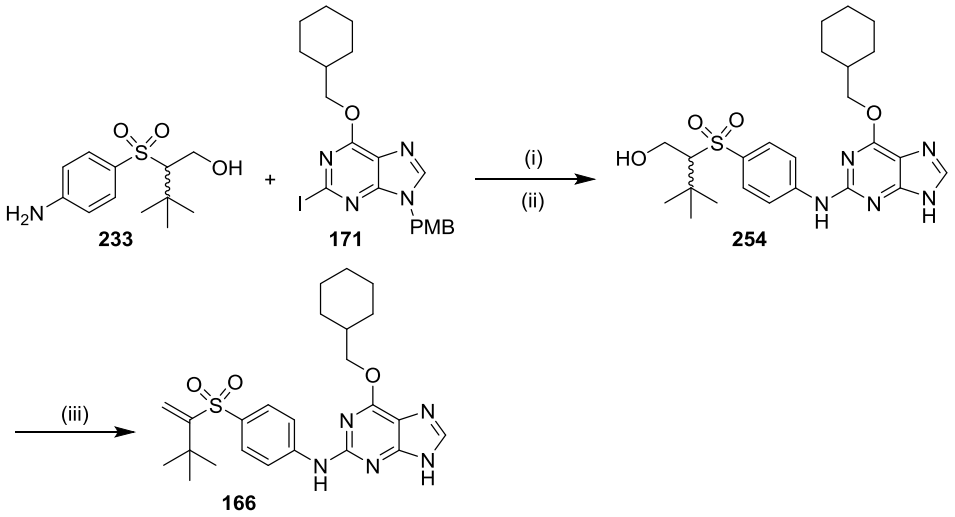

Scheme 50 - *Reagents and conditions*: (i) K_2CO_3, XPhos, $Pd(dba)_2$ in MeCN, 80 °C, 18 h; (ii) TFA, 70 °C, 2 h, 55%; (iii) MsCl, Et_3N in DCM, r.t., 1 h then DBU, r.t., 0.5 h, 69%.

5.2. Introduction of α-electron-withdrawing groups on the vinyl sulfone of 60

To explore further the α-position of the vinyl sulfone warhead of **60**, electron-withdrawing groups were introduced. Having such a group at this position has been described in the literature, endowing a reversible covalent character to the inhibitor (*Scheme 51*).[219]

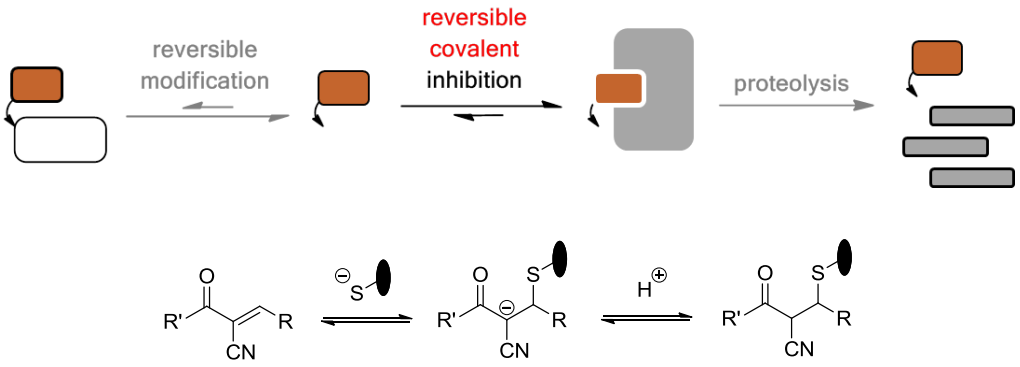

Scheme 51 – Mechanism for reversible covalent inhibition (*adapted from Lee, 2012*)[219]

Inspired by this idea, chloro, fluoro and trifluoromethyl groups, electron-withdrawing by the inductive effect, were first investigated at the α-position of the vinyl sulfone warhead of compound **60**. The cyano group, electron-withdrawing by virtue of inductive and mesomeric effects, was also considered.

5.2.1. α-Chloro analogue of vinylsulfone 60

Chlorination at a methylene group between a sulfone and ester moiety has previously been reported.[220] This type of reaction was initially attempted on substrate **257** bearing only a sulfone group (*Scheme 52*), but no target compound was obtained.

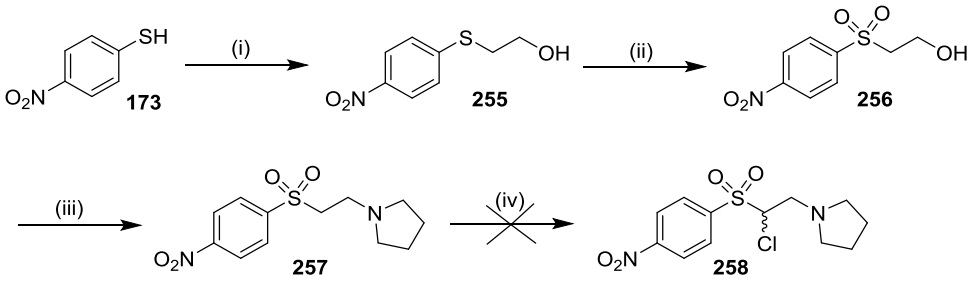

Scheme 52 - *Reagents and conditions*: (i) 2-chloroethanol, KOH in EtOH, reflux, 18 h, 96%; (ii) *m*-CPBA in DCM, 0 °C, 30 min, 84%; (iii) benzenesulfonyl chloride, Et_3N in DCM, r.t., 18 h; (iii) pyrrolidine, r.t., 1 h, 67%; (iv) NaH, NCS in THF, r.t., 18 h.

The reaction was incomplete and heating led to an intractable mixture. One main product was isolated from the reaction carried out at room temperature, for which LC-MS and ^{1}H NMR analysis indicated formation of the elimination product **259**, which could have been formed through loss of HCl from the dichlorinated product (*Scheme 53*).

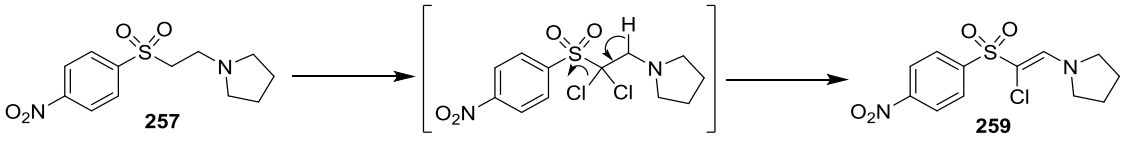

Scheme 53 - Possible mechanism for the formation of the elimination product **259**.

To repeat more closely the literature conditions, chlorination was performed on substrate **261**, which was obtained by the following route (*Scheme 54*):

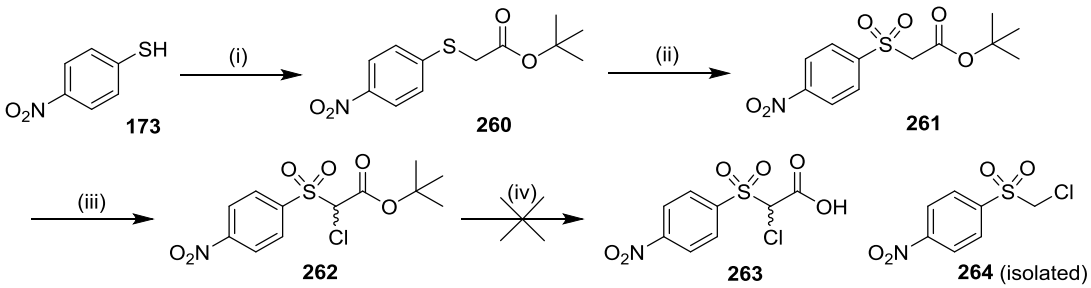

Scheme 54 - *Reagents and conditions*: (i) *tert*-butyl chloroacetate, Et_3N in DCM, r.t., 1 h, 90%; (ii) *m*-CPBA in DCM, r.t., 30 min, 95%; (iii) NaH, NCS in THF, r.t., 18 h, 78%; (iv) 10% TFA in DCM, r.t., 18 h.

Monochlorination at the methylene group between the sulfone and the *t*-butyl ester, by controlling the stoichiometry, afforded the chlorinated compound **262** in good yield. The *t*-butyl ester was chosen for its easy cleavage under acidic conditions, but in the presence of TFA, decarboxylation of ester **262** was observed leading to the β-chloromethyl sulfone **264**. Hydrolysis of ester **262** under basic conditions gave only a mixture of compounds, and to avoid the hydrolysis step, reduction of the ester was considered. As ethyl esters are preferred for reduction, the synthesis was repeated using ethyl ester **237** instead of the *t*-butyl ester **261** (*Scheme 55*). DIBAL was preferred for the reduction of ester **265** to minimise dehalogenation. However, although the desired alcohol **266** was obtained under these conditions, dehalogenation was also observed (LC-MS analysis), explaining the moderate yield of 56%.

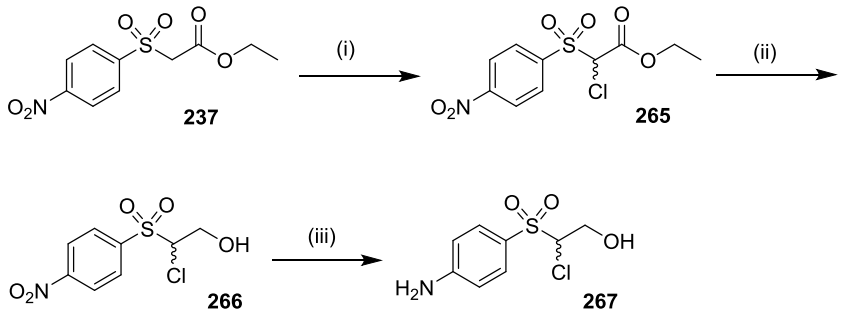

Scheme 55 - *Reagents and conditions*: (i) NaH, NCS in THF, r.t., 18 h, 66%; (ii) DIBAL in THF, 0 ^{o}C, 2 h, 66%; (iii) Zn, AcOH in MeOH, r.t., 1 h, 84%.

Reduction of the nitro group of compound **266** gave the aniline **267**, which was coupled to intermediate **171**, in the one-pot process comprising Buchwald coupling and PMB deprotection. By this route, the two target compounds, vinyl sulfone **167** and 2-

hydroxyalkyl derivative **268**, were synthesised. The vinyl sulfone **167** was obtained as described previously from alcohol **268**, via an intermediate mesylate (*Scheme 56*).

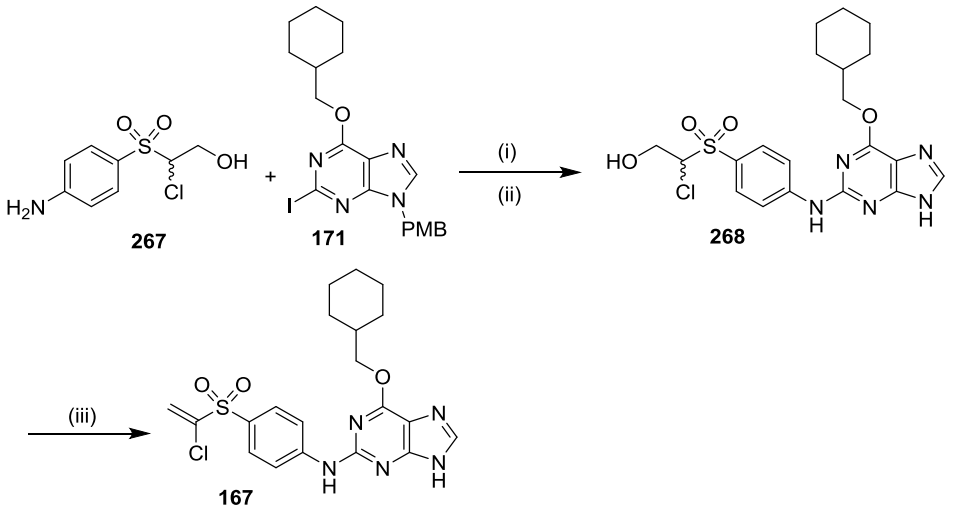

Scheme 56 - *Reagents and conditions*: (i) K_2CO_3, XPhos, $Pd(dba)_2$ in MeCN, 80 °C, 18 h; (ii) TFA, 70 °C, 2 h, 33%; (iii) MsCl, Et_3N in DCM, r.t., 22%.

5.2.2. α-Fluoro derivative of vinylsulfone 60

The fluoro compounds **168** and **272** were obtained in a similar manner to that employed for the α-chlorovinyl sulfone target **167**. The only difference in the synthetic scheme was the step utilised for introduction of the fluoro group (*Scheme 57*). This was attempted following literature conditions, using Selectfluor,[221] and led to a 64% yield of the fluorinated compound **269**.

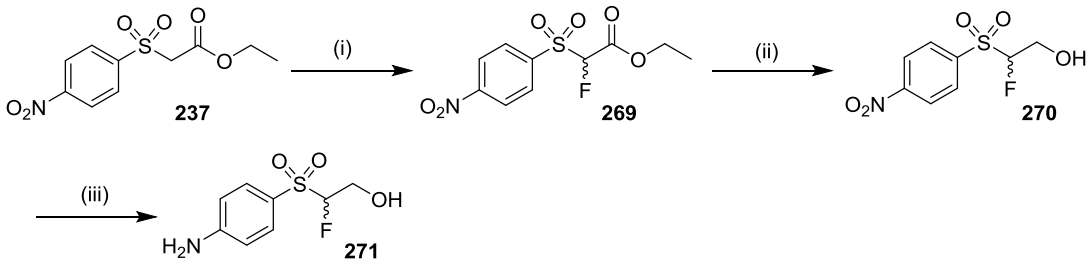

Scheme 57 - *Reagents and conditions*: (i) NaH, Selectfluor in THF, r.t., 18 h, 62%; (ii) DIBAL in THF, 0 ^{o}C, 2 h, 68%; (iii) Zn, AcOH in MeOH, r.t., 1 h, 62%.

The aniline **271** was coupled to intermediate **171** in the one-pot process described previously (*Scheme 58*). The vinyl sulfone **168** was obtained from the 2-hydroxyalkyl derivative **272** via a mesylate intermediate.

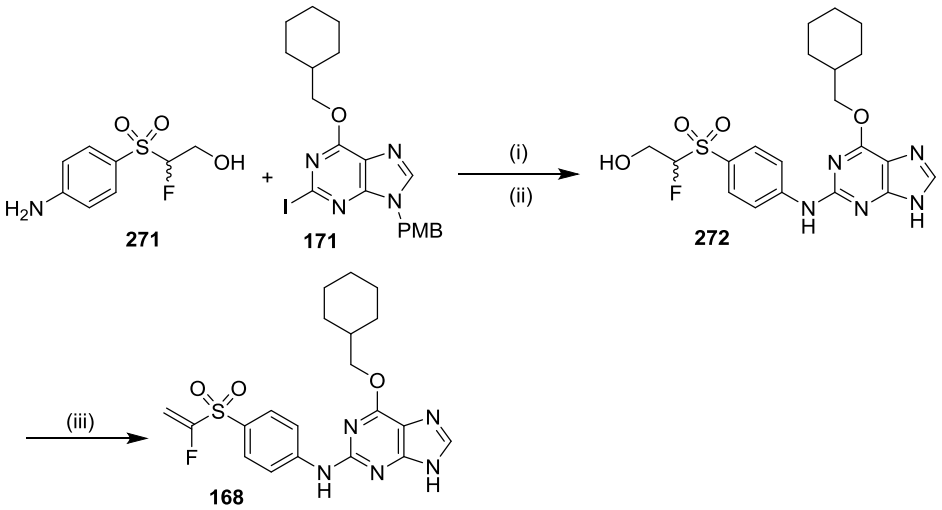

Scheme 58 - *Reagents and conditions*: (i) K_2CO_3, XPhos, $Pd(dba)_2$ in MeCN, 80 °C, 18 h; (ii) TFA, 70 °C, 2 h, 33%; (iii) MsCl, Et_3N in DCM, r.t., 10%.

5.2.3. α-Cyano analogue of vinylsulfone 60

Insertion of a cyano group at the α-position of the vinyl sulfone warhead proved to be difficult and remains to be achieved. The first approach for the synthesis of this target involved nucleophilic displacement of the chloro group from compound **274** to give the cyano derivative **273** (*Scheme 59*).

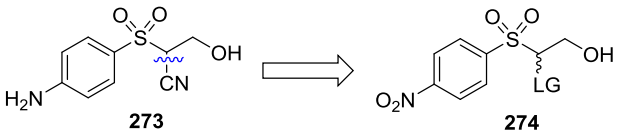

Scheme 59 – First retrosynthetic approach for the introduction of an α-cyano group

This reaction was first tried on the chloro compound **265** obtained previously, but no reaction was observed (*Scheme 60*). The same conditions were applied to substrate **276**, synthesised from alcohol **266** and protected with a TBDMS group (*Scheme 61*). However, no product (**277**) was isolated.

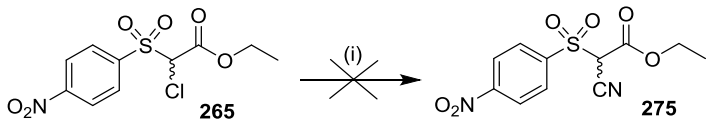

Scheme 60 - *Reagents and conditions*: (i) Et_4NCN in MeCN, 18 h.

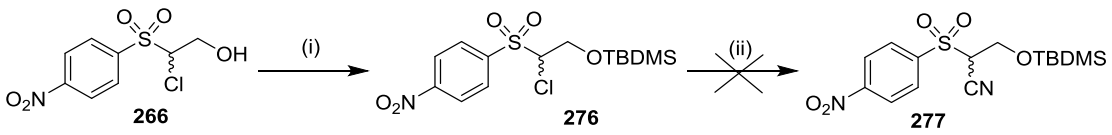

Scheme 61 - *Reagents and conditions*: (i) TBDMSCl, imidazole in DCM, 0 ^{o}C, 18 h, 85%; (ii) Et_4NCN in MeCN, 18 h.

Another strategy required formation of epoxide **278**, followed by ring opening by attack of cyanide (*Scheme 62*).

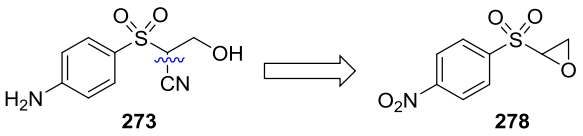

Scheme 62 – Second retrosynthetic approach for the introduction of an α-cyano group

Epoxide **278** was prepared from alcohol **266** under basic conditions but only isolated in low yield because of loss in the work-up of the reaction owing to the polarity of compound **278** (*Scheme 63*). A one-pot process was considered with epoxide formation being followed by ring opening. Different conditions were investigated to favour attack on the internal carbon of the epoxide (*Scheme 63*). Indeed, in the literature, some examples reported nucleophilic attack at the most substituted carbon via coordination of the epoxide oxygen to a metal centre.[222] This approach was attempted on epoxide **278** using both copper cyanide and zinc cyanide.

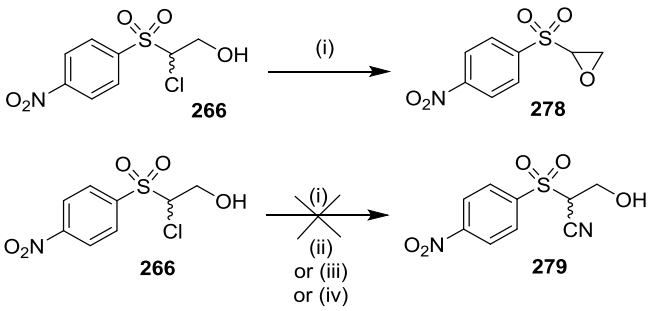

Scheme 63 - *Reagents and conditions*: (i) Cs_2CO_3 in MeCN, r.t., 25%; (ii) Et_4NCN in MeCN, r.t.; (iii) Cu(CN) in MeCN, r.t.; (iv) $Zn(CN)_2$ in MeCN, r.t.

Under the three reaction conditions attempted, the same compound (**280**) was formed, arising from nucleophilic attack at the terminal carbon of the epoxide **278**, leading to formation of the sulfinic acid **280** (LC-MS and ^{1}H NMR analysis) and presumably 2-cyanoethanal (**281**) (*Scheme 64*).

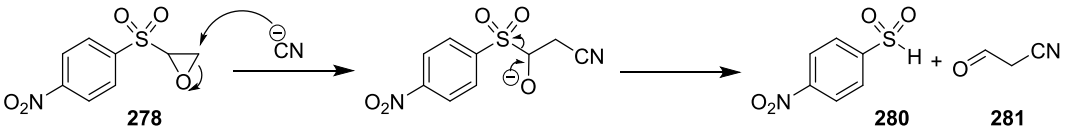

Scheme 64 - Mechanism of epoxide ring opening of compound **278**

Another strategy considered was cyanation with an electrophilic source of cyanide (*Scheme 65*).[223]

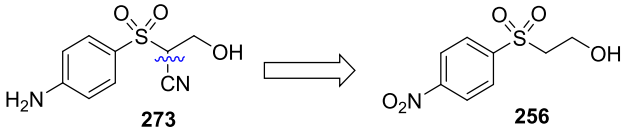

Scheme 65 – Third retrosynthetic approach for the introduction of an α-cyano group

A literature precedent was found reporting the use of tosyl cyanide.[224] This reaction was attempted on substrate **282**, obtained from ester **237** via reduction to the alcohol and protection with a benzyl group. These conditions for the cyanation were unsuccessful as no reaction to give compound **283** was observed (*Scheme 66*).

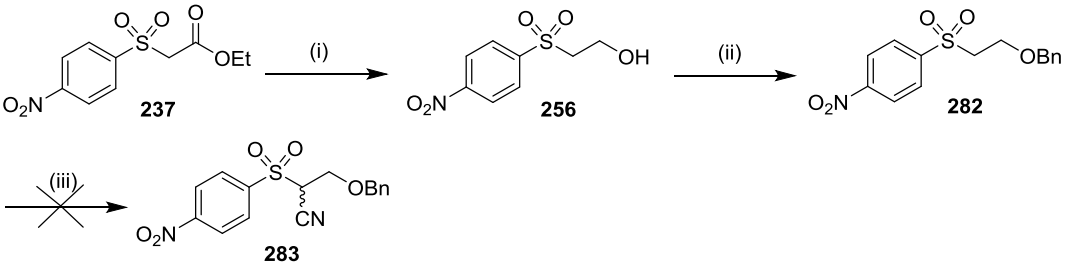

Scheme 66 - *Reagents and conditions*: (i) DIBAL in THF, 0 °C, 2 h, 62%; (ii) NaH, BnBr in DMF, r.t., 3 h, 59%; (iii) LDA, TsCN in THF, -78 °C to 0 °C.

The fourth attempt required the use of methyl cyanoacetate (**285**). Deprotonation of methyl cyanoacetate (pK_a ~ 13 in DMSO[225]) can be easily achieved using a base such as caesium carbonate (*Scheme 67*).

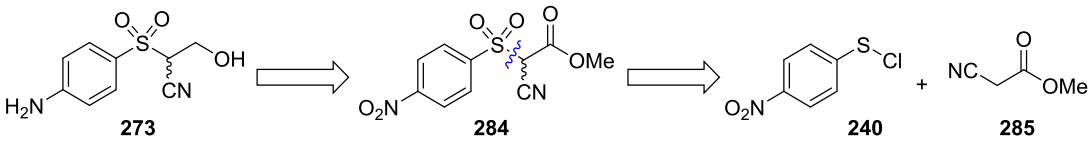

Scheme 67 – Fourth retrosynthetic approach for the introduction of an α-cyano group

Two reagents were tried as electrophiles, 4-nitrobenzenesulfenyl chloride (**240**) and 4-nitrobenzenesulfonyl chloride (**242**). Reaction with compound **240** was not conclusive (*Scheme 68*). However, the reaction with compound **242** was successful, and the use of

molecular sieves was found to be crucial to prevent formation of the sulfonic acid (*Scheme 69*).

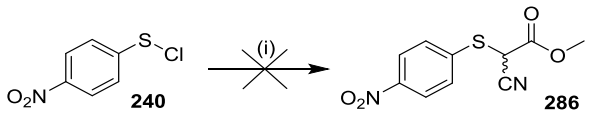

Scheme 68 - *Reagents and conditions*: (i) **285**, Cs_2CO_3 in DCM, r.t..

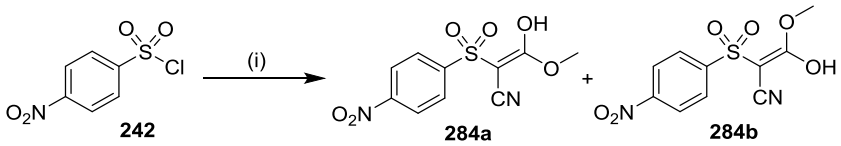

Scheme 69 - *Reagents and conditions*: (i) **285**, Cs_2CO_3, molecular sieves, in DCM, 0 ^oC, 51%.

By ^1H NMR analysis, the ester moiety of compound **284** was found to exist primarily in its enolic form, with a mixture of both *E* and *Z* isomers (**284a** and **284b**) being observed. The next step was reduction of the ester **284** into the corresponding alcohol **279**. To reduce selectively the ester moiety in the presence of the cyano group, lithium pyrrolidinoborohydride was first employed but no reaction was observed, and sodium borohydride was also unsuccessful (*Scheme 70*). As reduction of the ester group of compound **284** proved unsuccessful, hydrolysis was attempted but no reaction was observed (*Scheme 70*). Probably, the ester moiety, in its enolic form, was unreactive. As a consequence, this route was discontinued.

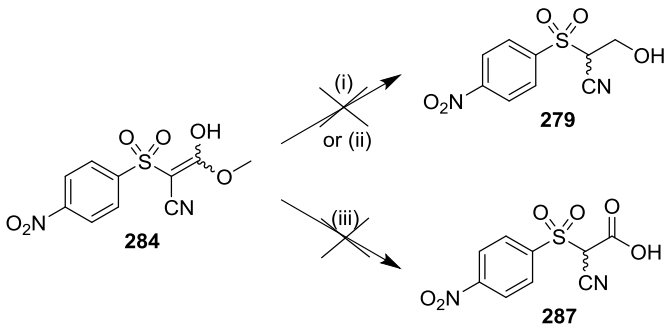

Scheme 70 - *Reagents and conditions*: (i) Lithium pyrrolidinoborohydride in THF, r.t., 18 h; (ii) $NaBH_4$ in MeOH, r.t., 2 h; (iii) 2M LiOH in THF, 50 ^oC, 5 h.

Another approach involved the formation of β-cyanomethyl sulfone **288**, prior to the introduction of an alkyl group (*Scheme 71*).

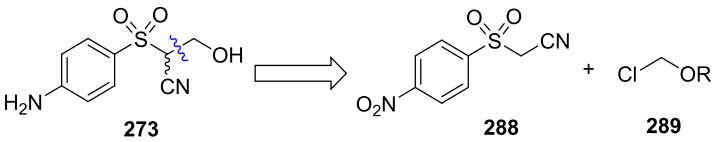

Scheme 71 – Fifth retrosynthetic approach for the introduction of an α-cyano group

Formation of intermediate **288** was achieved in high yield (*Scheme 72*). To facilitate deprotonation at the α-position of the cyano group, the sulfide **290** was converted into the corresponding sulfone **288** (pK_a ~ 21 in DMSO for the sulfide and 12 in DMSO for the sulfone[225]). Introduction of an alkyl group using a chloromethyl ether reagent (**289**) was attempted to obtain the protected hydroxyl group at the desired position. Two reagents were tried, chloromethyl methyl ether (**289**, R = Me) and benzyl chloromethyl ether (**289**, R = Bn), both commercially available at low technical grade purity. Reactions with these two reagents led to the formation of the same unidentified by-product (*Scheme 72*). This route may have been successful if the reagents would have been available at higher purity. Purification of the reagents was not attempted due to their toxicity.

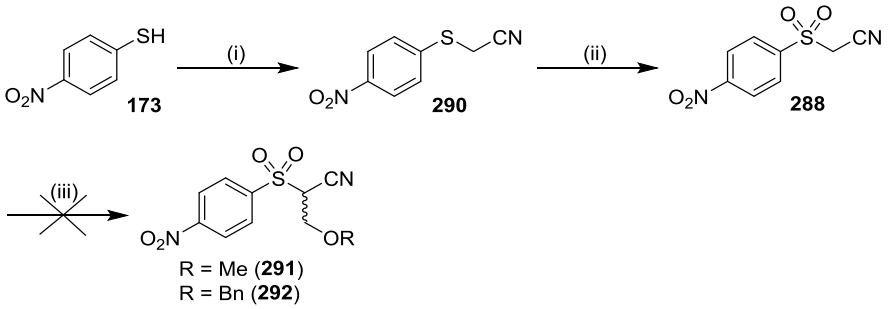

Scheme 72 - *Reagents and conditions*: (i) iodoacetonitrile, Et_3N in DCM, r.t., 1 h, 87%; (ii) *m*-CPBA in DCM, r.t., 1 h, 33%; (iii) NaH, **289** in THF, r.t.

In summary, several strategies were investigated for the synthesis of the desired aniline **273**. This unsuccessful work emphasised the challenges of introducing several polar functional groups on a small labile molecule, and further efforts on this target were discontinued for the time being.

5.2.4. α-Trifluoromethyl derivative of vinylsulfone 60

To form the desired aniline **293**, the approach considered was disconnection at the sulfur as shown in *Scheme 73*.

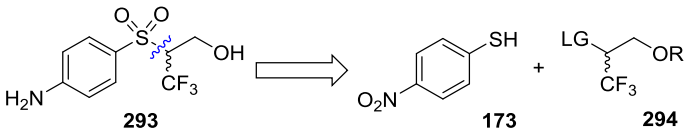

Scheme 73 – First retrosynthetic approach for the introduction of an α-trifluoromethyl group

3,3,3-Trifluoropropane-1,2-diol (**296**) was a key intermediate obtained by reduction of ester **295**.[226] The secondary alcohol was selectively protected in good yield with a TBDPS group (**297**) (*Scheme 74*).

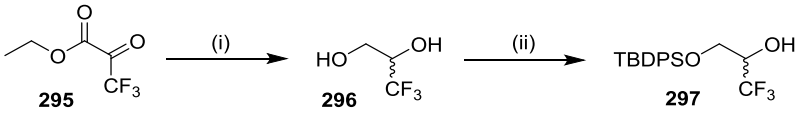

Scheme 74 - *Reagents and conditions*: (i) $LiAlH_4$ in THF, reflux, 2h, 82%;.(ii) TBDPSCl, imidazole in DCM, 0 °C, 1h, 75%.

Formation of a leaving group from the tertiary alcohol **297** was investigated. Attempted preparation of the triflate **298**, using several conditions, or the mesylate **299** failed. However, tosylate and benzenesulfonyl intermediates, **300** and **301**, respectively, were obtained, and both intermediates were reacted with thiophenol **173** (*Scheme 75*).

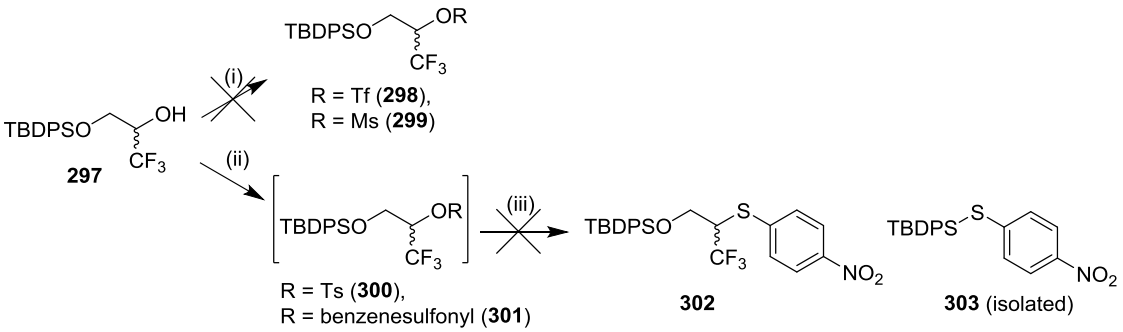

Scheme 75 - *Reagents and conditions*: (i) Tf_2O, Et_3N in DCM, 0 °C, 2 h or NaH, in THF then Tf_2O, or NaH in THF then *N*-phenyltriflimide, 2 h, or MsCl, Et_3N in DCM, 2 h; (ii) TsCl, Et_3N in DCM, r.t., 2 h, or benzenesulfonyl chloride, Et_3N in DCM, 5 h; (iii) **173**, Et_3N in DCM, r.t.

A new product slowly appeared in both reactions (after 4 days of heating), and after isolation proved to be a by-product (**303**) arising from attack of the thiolate on the silicon of the TBDPS protecting group (*Scheme 76*). Attack on a carbon at the α-position of a CF_3 group is known to be challenging.[227]

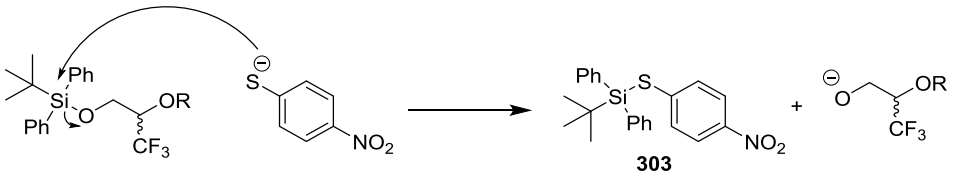

Scheme 76 – Putative mechanism for formation of by-product **303**

Another protecting group was chosen because of this side reaction. Benzylation was attempted on the diol **296** using two different conditions, but no reaction was observed (*Scheme 80*). However, the protected alcohol **304** was obtained from the reaction between epoxide **306** and alcohol **305** (*Scheme 77*).

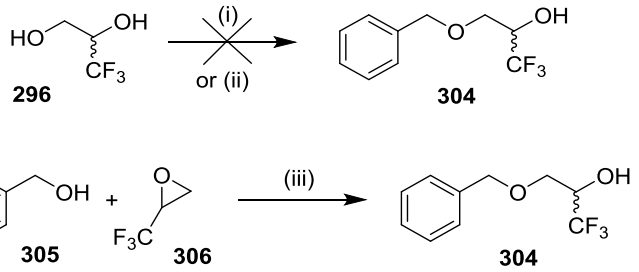

Scheme 77 - *Reagents and conditions*: (i) BnBr, DIPEA in MeCN, r.t.; (ii) BnBr, K_2CO_3, KI in MeCN, r.t.; (iii) $BF_3.Et_2O$, 40 °C, 18 h, 85%.

Formation of triflate **307** and tosylate **308** from the alcohol **304** was observed and these were treated directly with the thiolate **173**$^-$ but no reaction was observed (*Scheme 78*).

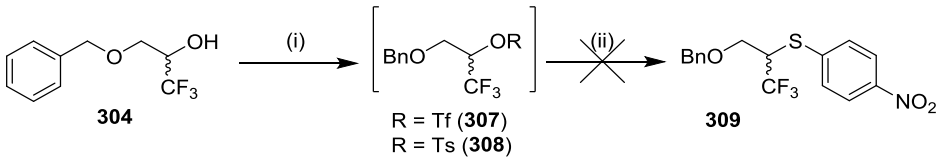

Scheme 78 - *Reagents and conditions*: (i) Tf_2O, Et_3N in DCM, 0 °C or TsCl, Et_3N in DCM, r.t.; (ii) **173**, Et_3N in DCM, r.t.

Another approach was considered for the synthesis of aniline **293** using a reagent (**310**) providing an electrophilic source of CF_3 (*Scheme 79*).[228]

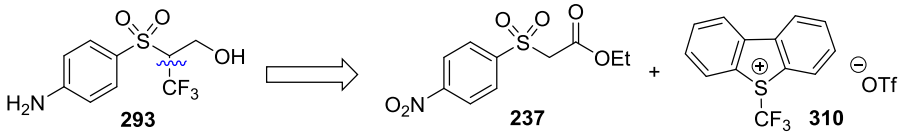

Scheme 79 – Second retrosynthetic approach for the introduction of an α-trifluoromethyl group

Several conditions were studied on two different substrates using the reagent 5-(trifluoromethyl)dibenzothiophenium trifluoromethanesulfonate (**310**). In each case, the

same LC-MS profile was obtained indicating the presence of starting material and unidentified by-products (*Scheme 80*).

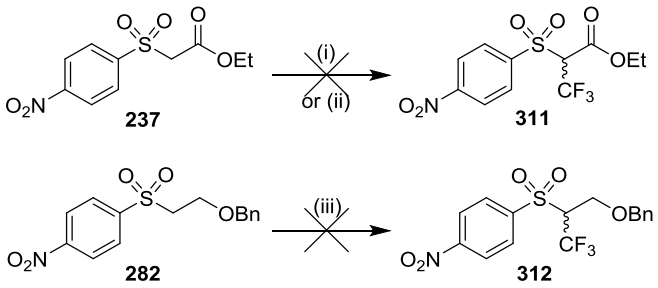

Scheme 80 - *Reagents and conditions*: (i) **310**, NaH in THF, r.t.; (ii) **310**, NaH in MeCN, MW, 110 °C, 30 min; (iii) **310**, LDA in THF, -78 °C.

As an alternative, the synthesis of a trifluoromethylalkyl derivative **313** was attempted, which would then be functionalised as an ester or carboxylic acid (*Scheme 81*).

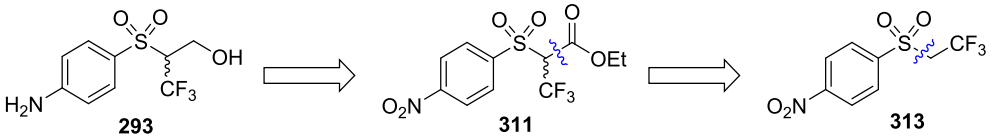

Scheme 81 – Third retrosynthetic approach for the introduction of an α-trifluoromethyl group

The first step of the synthetic route was successful, in satisfying yield, and this was followed by oxidation of sulfide **314** to sulfone **313** (*Scheme 82*). Insertion of the ethyl ester moiety at the α-position of the sulfone group of **313** was attempted (*Table 19*). Several conditions were tried, varying the base and the temperature, but no desired product (**311**) was formed.

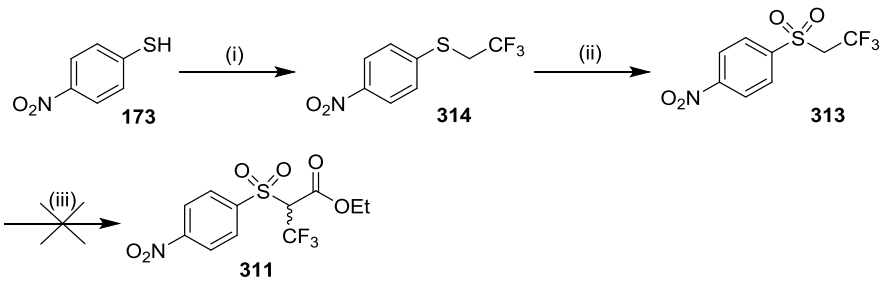

Scheme 82 - *Reagents and conditions*: (i) ICH_2CF_3, Rongalit, K_2CO_3 in DMF, r.t., 18 h, 62%; (ii) *m*-CPBA in DCM, 1 h, 63%; (iii) diethyl carbonate in THF, see *Table 19* for conditions investigated.

Table 19 – Conditions tried for the functionalisation of sulfone **313**

		Temperature	
		r.t.	70 °C
Base	LHMDS	Unknown compound isolated.	LC-MS indicated impurities
	KHMDS	LC-MS indicated impurities - After purification, no target compound obtained.	LC-MS indicated impurities
	NaH	No reaction	-

As the introduction of an ester group onto sulfone **313** was unsuccessful, the insertion of a carboxylic acid was investigated, using LHMDS and solid CO_2 (*Scheme 83*). The LC-MS of the crude mixture showed formation of both the carboxylic acid **315** and an unknown compound, with the latter being the major product. After a study of the ^1H NMR spectrum and LC-MS analysis, formation of the corresponding acyl fluoride **316** was suggested, arising from the mechanism shown in *Scheme 84*.

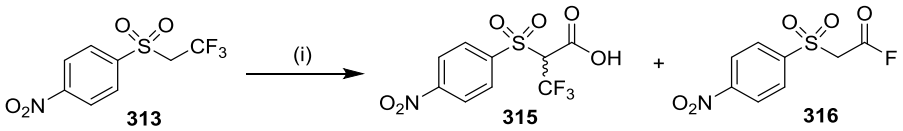

Scheme 83 - *Reagents and conditions*: (i) LHMDS, CO_2 in THF, -78 °C to r.t., 1 h.

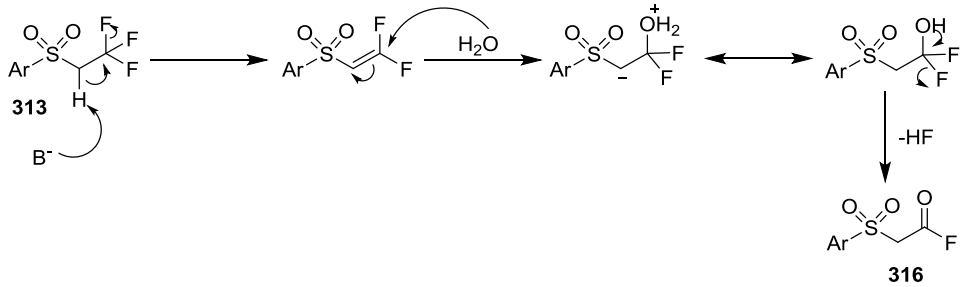

Scheme 84– Mechanism for the formation of acyl fluoride **316**

Several strategies were attempted for the synthesis of the desired aniline **293** but none were successful. Despite the results, interesting chemistry was highlighted along with the difficulties of synthesising these highly functionalised intermediates.

5.3. Introduction of a β-methyl group on the vinyl sulfone warhead of 60

In parallel with modifications at the α-position of the vinyl sulfone warhead of compound **60** (Chapter 5, sections 5.1 and 5.2), the β-position was also investigated. From examining the crystal structure of vinyl sulfone **60** bound to CDK2, space was perceived

to be available at this position to accommodate groups, as the vinyl sulfone pointed towards the solvent. However, it was recognised that substitution at the β-position could render attack from Lys89 more difficult because of steric hindrance.

5.3.1. β-methyl analogue of vinylsulfone 60

Nucleophilic attack by thiophenol **173** on the chloroketone **317** proceeded in quantitative yield to give compound **318**. Reductive amination of ketone **318** afforded amine **319**. The nitro function of intermediate **319** was reduced to give the desired aniline **320** in good overall yield (*Scheme 85*).

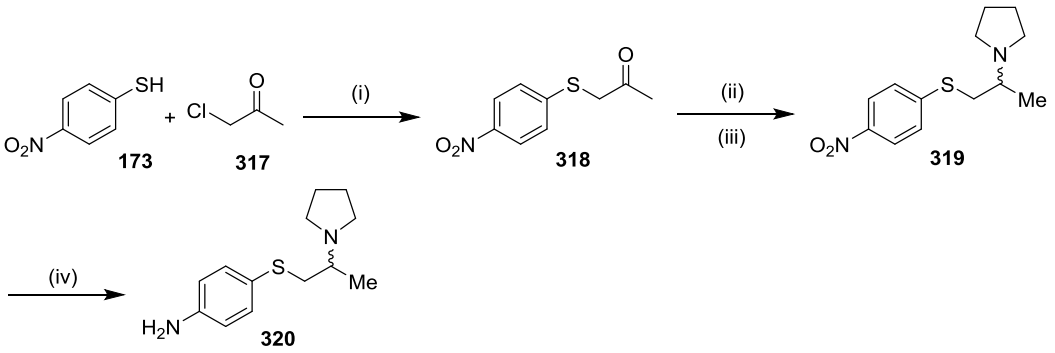

Scheme 85 - *Reagents and conditions*: (i) Et_3N in DCM, r.t., 3 h, 98%; (ii) pyrrolidine, AcOH in toluene, r.t., 1 h; (iii) $NaBH(OMe)_3$, r.t., 2 h, 57%; (iv) Zn, AcOH in MeOH, 50 °C, 1 h, 64%.

As previously described, Buchwald reaction and PMB deprotection were carried out as a one-pot procedure leading to the intermediate **321** in 50% yield. However, oxidation of sulfide **321** with *m*-CPBA, followed by addition of caesium carbonate led only to degradation. Conversion of the sulfide **321** to the sulfone **322** was performed using oxone, which enabled better control over the oxidation step.[229] The sulfone intermediate **322** underwent Cope elimination using *m*-CPBA and caesium carbonate, leading to the target compound **323**, albeit in low yield, as exclusively the *E*-isomer (determined by ^{1}H NMR analysis) (*Scheme 86*).

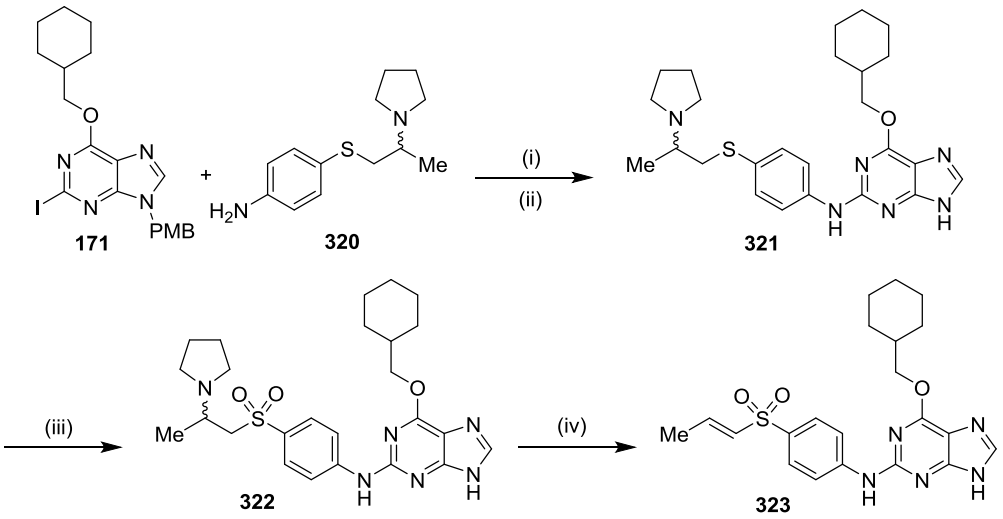

Scheme 86 - *Reagents and conditions*: (i) K_2CO_3, XPhos, $Pd(dba)_2$ in MeCN, 80 °C, 18 h; (ii) TFA, 70 °C, 2 h, 50%; (iii) oxone, H_2O in MeOH, r.t., 1 h, 38%; (iv) *m*-CPBA, Cs_2CO_3 in DCM, 0 °C, 30 min, 15%.

The 2-hydroxyalkyl derivative **327** was synthesised directly from compound **318** in four steps (*Scheme 87*). The aniline **326** was reacted with intermediate **171** as before to afford the target compound **327**.

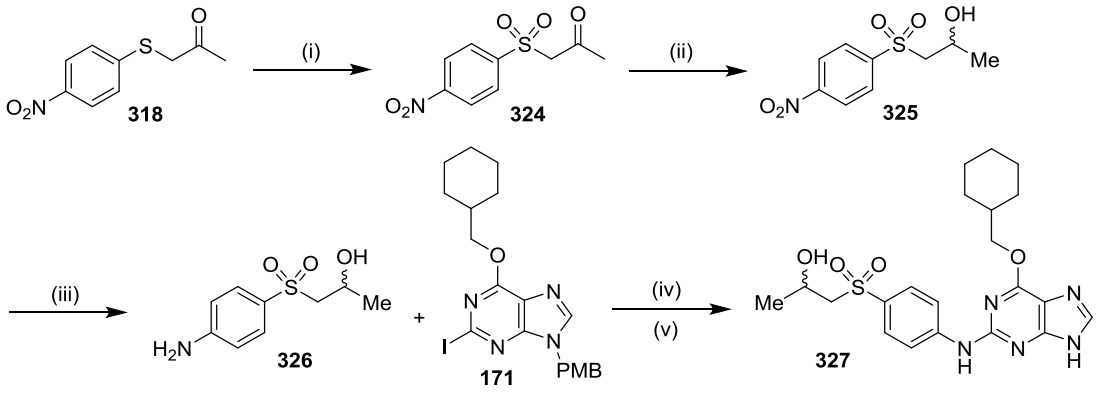

Scheme 87 - *Reagents and conditions*: (i) *m*-CPBA in DCM, 0 ^oC, 1 h, 73%; (ii) Dibal in THF, 0 ^oC, 3 h, 92%, (iii) Zn, AcOH in MeOH, 50 °C, 1 h, 84% (iv) K_2CO_3, XPhos, $Pd(dba)_2$ in MeCN, 80 °C, 18 h; (v) TFA, 70 °C, 2 h, 31%.

5.3.2. α,β-Dimethyl analogue of vinylsulfone 60

To complete the series of methyl derivatives of vinyl sulfone **60**, the α,β-dimethyl compounds, **332** and **333**, were prepared to enable evaluation of the combined effect of the two methyl groups. The synthetic scheme was similar to those discribed previously, starting from the thiophenol **173**. The desired aniline **331** was formed in four steps in good overall yield, and was obtained as a mixture of diastereoisomers (4: 1) (*Scheme 88*).

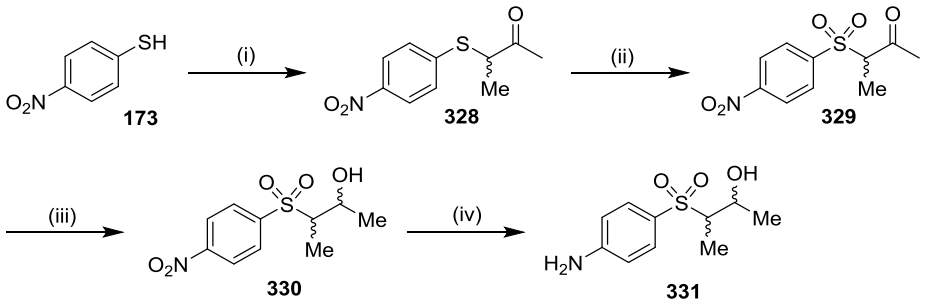

Scheme 88 - *Reagents and conditions*: (i) 3-chloro-2-butanone, Et_3N in DCM, r.t., 1 h, 89%; (ii) *m*-CPBA in DCM, 0 °C, 1 h, 92%; (iii) Dibal in THF, 0 °C, 3 h, 99%, (iv) Zn, AcOH in MeOH, 50 °C, 1 h, 78%.

A Buchwald coupling reaction between aniline **331** and the intermediate **171**, followed by PMB deprotection, afforded the 2-hydroxyalkyl derivative **332** as a mixture of diastereoisomers (9:1) (*Scheme 89*). To obtain the corresponding vinyl sulfone **333**, the mesylate was prepared from the alcohol **332** and elimination was performed using DBU. After addition of DBU, both vinyl sulfone **333** and 2-hydroxyalkyl compound **332** were visible. Competition was observed between deprotonation of the hydrogen at the α-position of the sulfone group leading to elimination of the mesylate, and deprotonation of the methyl group of the mesylate to regenerate compound **332**. This observation presumably accounted for the low yield of this last step in the synthesis of target **333**. The vinyl sulfone compound **333** was obtained as a mixture of *E* and *Z* isomers (2:1 *E*:*Z*, ratio determined by ^{1}H NMR analysis).

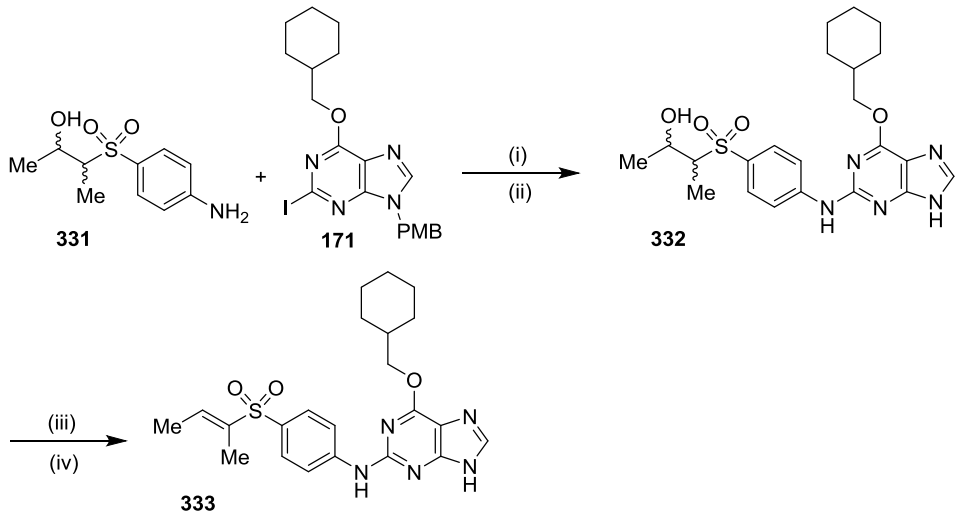

Scheme 89 - *Reagents and conditions*: (i) K_2CO_3, XPhos, $Pd(dba)_2$ in MeCN, 80 °C, 18 h; (ii) TFA, 70 °C, 2 h, 46%, (iii) MsCl, Et_3N in DCM, r.t., 1 h; (iv) DBU, 17%.

5.3.3. α-Chloro-β-methyl analogue of vinylsulfone 60

From the biological activity observed for the α-chlorovinyl sulfone **167** (see Chapter 8) and the crystal structure of the β-methylvinyl sulfone **323** in complex with CDK2, the α-chloro-β-methyl analogue of **60** was deemed to be an interesting target to assess the combined effects of the α-chloro and β-methyl groups on the vinyl sulfone. To synthesise the aniline **337**, an analogous strategy to that used for the α-chloro target **167** was followed. Chlorination of compound **324** was then attempted under the conditions established previously but dichlorination (**335**) with loss of the acetyl group was observed. Other conditions were tried such as hydrogen peroxide and potassium chloride,[230] but a similar observation was made (*Scheme 90*). The protons are relatively acidic in compounds **324-334** (pK_a of **324** ~ 12 in DMSO[225]), evidently favouring further chlorination. The chlorination was performed on the sulfide **318** (pK_a ~ 19 in DMSO[225]), but again, formation of the dichloro compound **335** was observed.

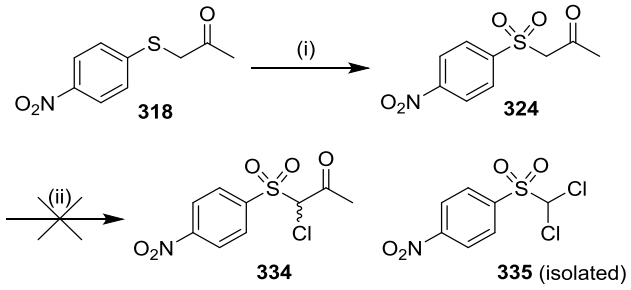

Scheme 90 - *Reagents and conditions*: (i) *m*-CPBA in DCM, 0 ^{o}C, 1 h, 73%; (ii) NaH, NCS in THF, r.t. or KCl, H_2O_2 in AcOH, r.t.

Owing to the difficulties encountered with direct chlorination, another strategy had to be considered. The new approach entailed introduction of the methyl ketone on the chloro alkyl intermediate **264**, obtained by hydrolysis with *in situ* decarboxylation of the ester **265**. Several bases and alkylating agents were investigated at -78 ^{o}C in THF to determine the best combination, which proved to be LHMDS and EtOAc (*Scheme 91*, *Table 20*).

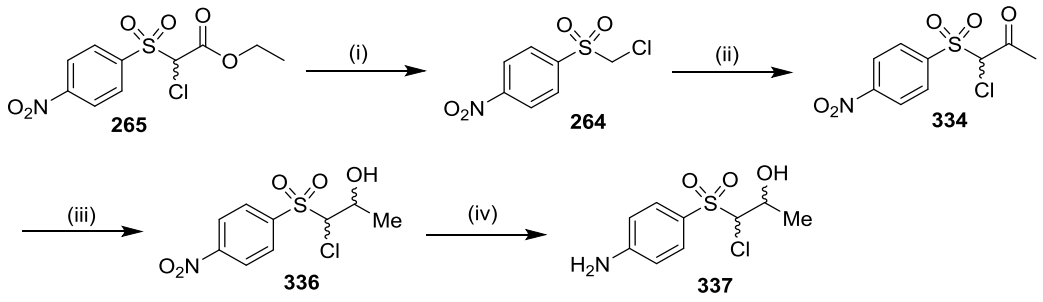

Scheme 91 - *Reagents and conditions*: (i) LiOH in THF, 70 ^{o}C, 2 h, 88 %; (ii) see Tables 4 and 5; (iii) $Zn(BH_4)_2$ in Et_2O/THF, r.t., 0.5 h, 73% over 2 steps; (iv) Zn, AcOH in MeOH, r.t., 1 h, 71%.

Table 20 – Conditions studied for the acetyl group introduction onto **264**

		Acetyl source		
		Acetaldehyde	Acetyl chloride	Ethyl Acetate
Base	n-BuLi	10% conversion[a]	No conversion[a]	No conversion[a]
	KHMDS	-	-	10% conversion[a]
	LHMDS	-	-	50% conversion[a]

[a.] Conversion estimated by LC-MS

Following this study, optimisations were carried out by varying the amount of LHMDS, EtOAc and reaction time. Varying the amount of EtOAc (*Table 21*, Exp2 and 4) or the reaction time (*Table 21*, Exp3) had little effect on the reaction outcome. However, increasing slightly the amount of LHMDS (*Table 21*, Exp5) improved the product formation up to 80%. The best conditions were found to be LHMDS (1.5 eq) and EtOAc (2.5 eq) for 1 h.

Table 21 – Effect of reaction parameters on the conversion of **264** into **334**

	Exp1	**Exp2**	**Exp3**	**Exp4**	**Exp5**
EtOAc	1.2 equiv.	2.5 equiv.	2.5 equiv.	10 equiv.	2.5 equiv.
LHMDS	1.2 equiv.	1.2 equiv.	1.2 equiv.	1.2 equiv.	1.5 equiv.
Time of reaction	30 min	30 min	1 h	1 h	1 h
Conversion[a]	50%	55%	60%	60%	80%

[a.] Conversion estimated by LC-MS

Reduction of ketone **334** was attempted with DIBAL but led to a mixture of products, none of which was the desired alcohol **336**. A milder, less basic reducing agent, $Zn(BH_4)_2$[231] was used (*Scheme 96*) and successfully gave the intermediate **336**, which was further reduced to the aniline **337**, obtained as a mixture of diastereoisomers (2:1).The 2-hydroxyalkyl derivative **338** and the vinylsulfone **339** were synthesised following the synthetic scheme previously described (*Scheme 92*). The 2-hydroxyalkyl derivative **338** was obtained as a mixture of diastereoisomers (2: 1) and the vinyl sulfone **339** as a single isomer (determined by NMR analysis).

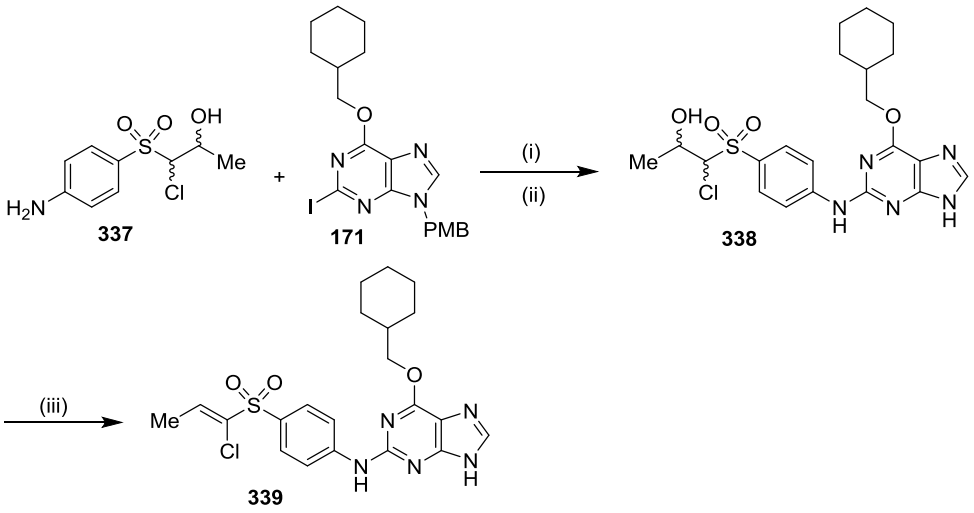

Scheme 92 - *Reagents and conditions*: (i) K_2CO_3, XPhos, $Pd(dba)_2$ in MeCN, 80 °C, 18 h; (ii) TFA, 70 °C, 2 h, 17%; (iii) MsCl, Et_3N in DCM, r.t., then DBU, r.t., 0.5 h, 50%.

5.4. Synthesis of a cyclic analogue of 60

Another interesting target was compound **349** where the vinyl function is constrained within a six-membered ring. A similar route to that used previously was first investigated (*Scheme 93*). Thiophenol **173** was reacted with cyclohexene oxide **340** to give a 1:1 mixture of enantiomers **341**. The sulfide **341** was oxidised to the corresponding sulfone **342** using *m*-CPBA. The strategy using benzenesulfonyl chloride to introduce the pyrrolidine moiety was, in this case, unsuccessful, with only starting material **342** being isolated (*Scheme 93*).

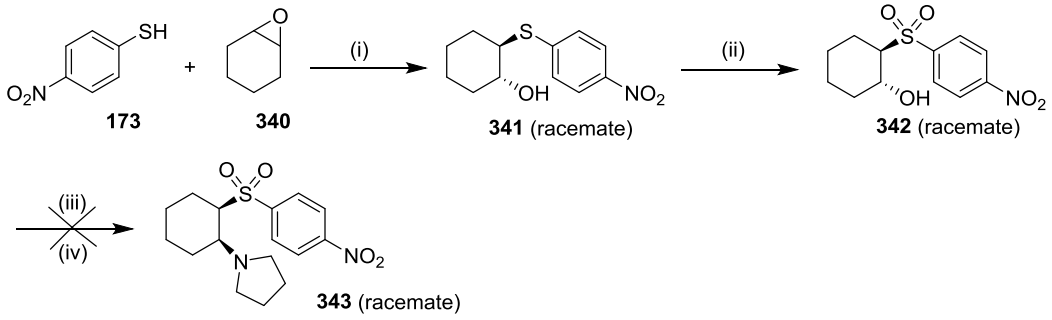

Scheme 93 - *Reagents and conditions*: (i) DIPEA in DCM, r.t., 18 h, 60%; (ii) *m*-CPBA in DCM, r.t., 1 h, 92%; (iii) benzenesulfonyl chloride, Et_3N in DCM, r.t., 18 h; (iv) pyrrolidine, r.t., 1 h.

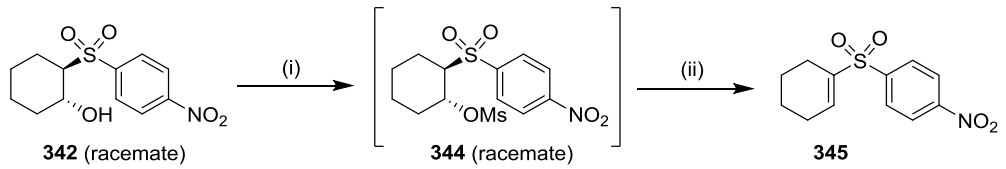

Scheme 94 - *Reagents and conditions*: (i) MsCl, Et_3N in DCM, r.t., 1 h; (ii) DBU, r.t., 1 h, 56%.

Formation of the mesylate **344** was carried out as detailed previously and DBU was added to trigger the elimination (*Scheme 94*).[232] As these conditions proved successful, they were applied to the synthesis of the target vinyl sulfone **345** (*Scheme 95*). Thus, compound **342** was reduced to the aniline **346**, which was subjected to Buchwald coupling and PMB deprotection to afford the 2-hydroxyalkyl compound **347** as a mixture of enantiomers. The purine derivative **347** was transformed into the corresponding mesylate and elimination was accomplished using DBU. However, the compound obtained (by LC-MS) was the N^9-mesyl derivative **348** rather than the required vinyl sulfone **349**. To deprotect the N^9-H of the purine, an excess of DBU was introduced leading to the target vinyl sulfone **349**.

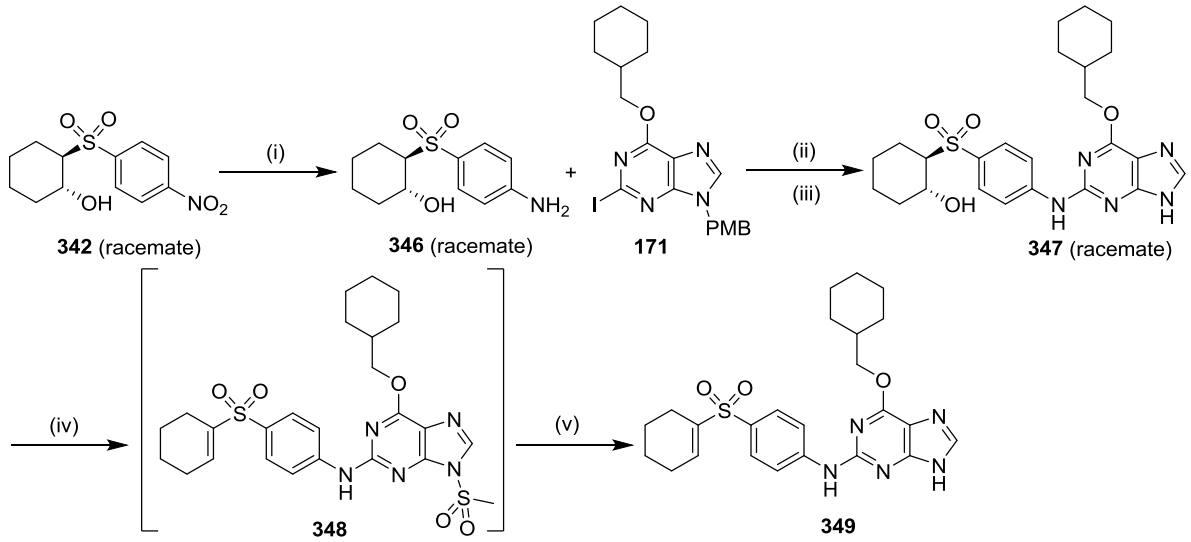

Scheme 95 - *Reagents and conditions*: (i) Zn, AcOH in MeOH, 50 °C, 1 h, 92%; (ii) K_2CO_3, XPhos, $Pd(dba)_2$ in MeCN, 80 °C, 18 h; (iii) TFA, 70 °C, 2 h, 57%; (iv) MsCl, Et_3N in DCM, r.t., 1 h; (v) DBU (excess), r.t., 1 h, 23%.

Chapter 6. Structural Biology on Selected Purine Inhibitors in Complex with CDK2/cyclin A

In the CDK2 project, central to this thesis, inhibitors were designed and synthesised using a structure-based approach employing the crystal structure of the lead compound (**60**) in complex with CDK2/cyclin A. In this chapter, the co-crystal structures of selected purine inhibitors in complex with CDK2/cyclin A are discussed, from protein expression to the interpretation of the results with the objective to understand how modifications of the vinyl sulfone warhead of compound **60** influenced the binding mode of new compounds. *X*-ray crystallography emerged as a valuable tool in drug discovery in the 1980s.[233] High throughput screening (HTS) has been used for approximately two decades to identify hits against specific targets. Once identified, a detailed analysis of a crystal structure of a protein-ligand complex is now routinely used to highlight specific interactions between the ligand and the protein at an atomic level.[234] Drug design can be guided by the structure of the protein in complex with the ligand. Another approach to hit identification is fragment-based design, which has emerged in the last decade, and where small fragments are identified as hits using high throughput *X*-ray crystallography.[235] An extensive design protocol starts to optimise interactions with the protein, with only a few compounds being synthesised.[235] *X*-ray crystallography is an essential technique in drug discovery whatever the approach chosen, and constitutes the basis for almost every contemporary drug development program today.

6.1. CDK2/cyclin A complex as a structural target

CDK2 was expressed in its full length, which corresponded to 298 amino acids (~34 kDa), whereas only a truncated version of cyclin A was expressed (between amino acids 173 and 432, ~30kDa), comprising the CDK2 binding domain and the two cyclin box folds (*Figure 90*).[49]

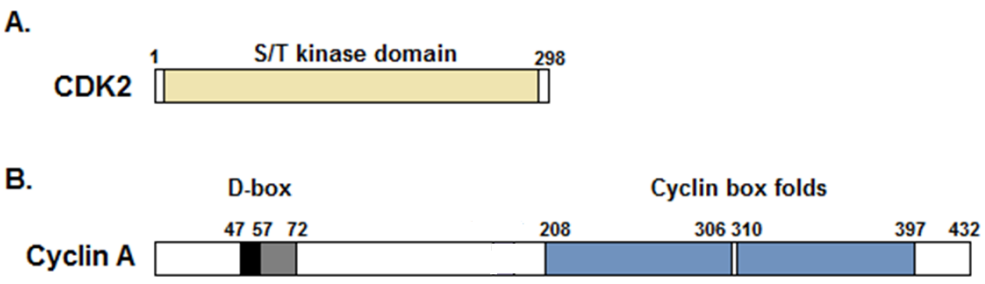

Figure 90 – A. Schematic representation of CDK2; B. Schematic representation of cyclin A (*adapted from Noble, 1997*)[49]

6.2. Expression of GST-tagged CDK2 and CIV1 constructs in *E. coli*

The protein of interest was the protein cyclin A/CDK2^{Thr160} and therefore expression of cyclin A and CDK2^{Thr160} was required. To express CDK2 in its phosphorylated form, CIV1, the equivalent of the human CAK complex, was also expressed using the modified pGEX6P-1 vector and the construct, which was transformed into the *E. coli* expression host strain BL21(DE3)pLys/S. The vector contained genes encoding for a replication origin, an antibiotic resistance (for ampicillin), a lac operon and a GST-tag with 3C- and thrombin-protease cleavage site for CDK2 and CIV1, respectively.[236] Protein expression was induced by the addition of IPTG (*Figure 91*).

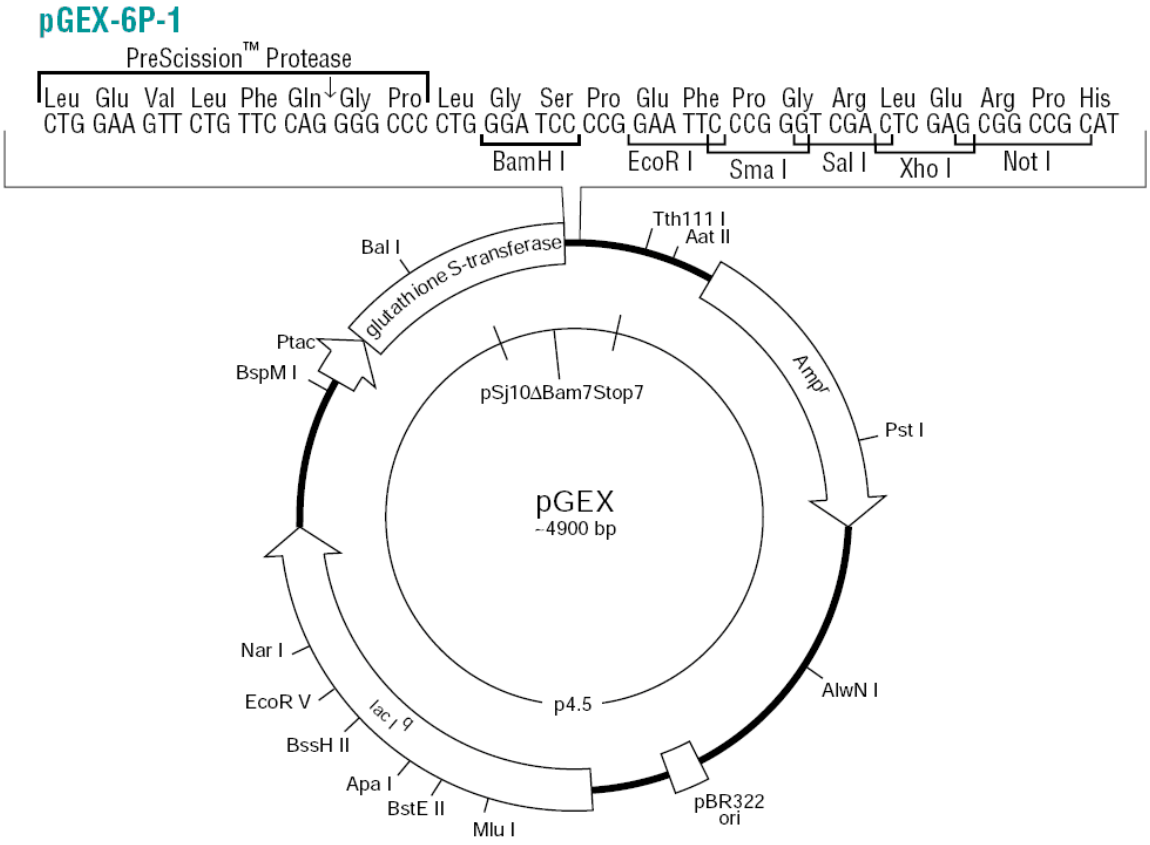

Figure 91 – pGEX6P-1 expression vector containing the lac operon (lac I), the ampicillin resistance gene (Amp) and the GST-tag with 3C-protease cleavage sequence (PreScission Protease)[236]

6.3. Expression of the cyclin A construct in *E. coli*

The pET vector, modified to express cyclin A, was transformed into BL21(DE3)pLys/S competent *E. coli* cells. The vector contained genes encoding for the lac operon, a T7 promoter specific to T7 RNA polymerase, and an ampicillin resistance gene. The pET vector, unlike the pGEX vector, offers an indirect regulation where the gene of interest is not transcribed unless T7 RNA polymerase is present.[237] Addition of IPTG activates the

lac operator on the gene encoding for T7 polymerase, which in this case triggers the expression of cyclin A (*Figure 92*).[237]

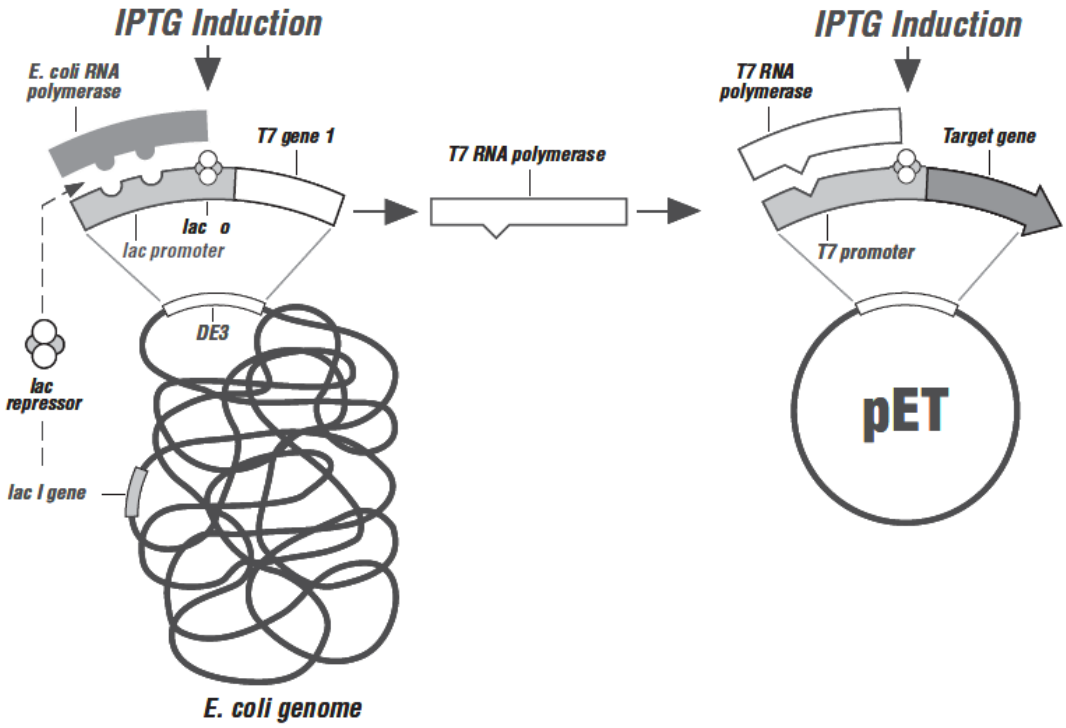

Figure 92 – The pET system with the production of T7 RNA polymerase following IPTG induction, which is key for the generation of the target gene cyclin A.[237]

6.4. Purification of the CDK2/cyclin A complex

The bacterial cells were lysed and the supernatant fluid containing GST-tagged CDK2^{Thr160} was mixed with the supernatant containing cyclin A to form the target CDK2^{Thr160}/cyclin A complex as a GST-tagged protein. This complex was purified by affinity chromatography and eluting with glutathione. The GST-tag was cleaved with 3C-protease, used as a GST fusion protein itself for purification purposes. 3C-Protease recognises the sequence LeuGluValLeuPheGln/GlyPro and cleaves between the Gln and Gly residues (*Figure 91*).[236] The resulting mixture was purified by size exclusion chromatography (*Figure 93*).

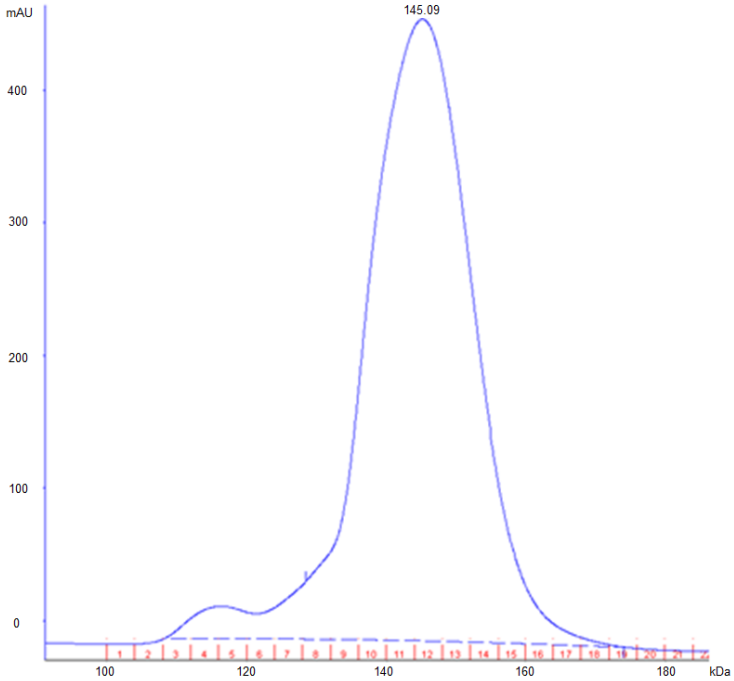

Figure 93 – Size exclusion chromatogram using a HiLoad 26/60 Superdex 75 column

After purification, the CDK2^{Thr160}/cyclin A complex (~64 kDa) was found to be contaminated with GST dimer (~52 kDa), which co-eluted during the size exclusion chromatography. The fractions containing the CDK2^{Thr160}/cyclin A complex were combined and loaded onto a fresh glutathione column to remove the GST dimer contaminant by affinity chromatography (*Figure 94*).

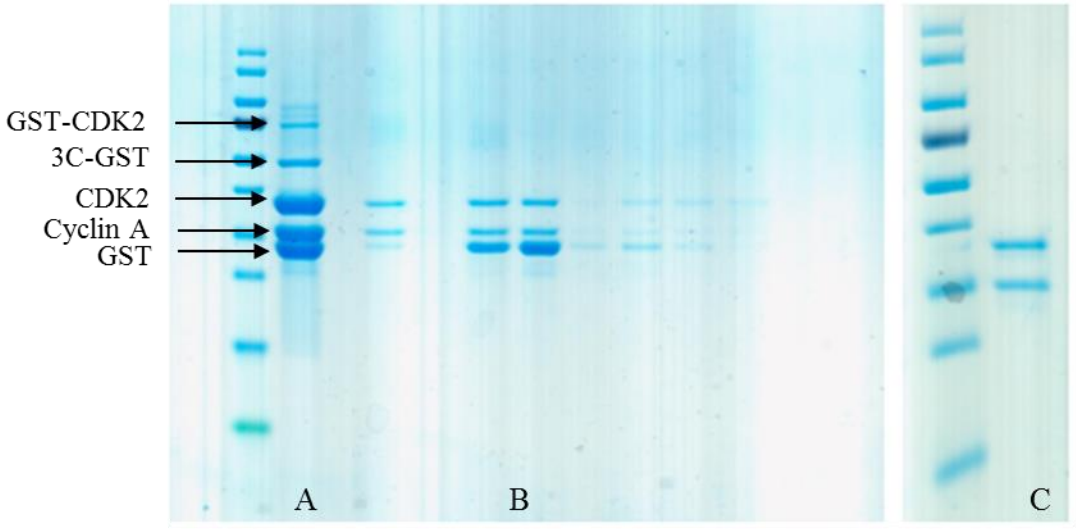

Figure 94 - Electrophoresis showing the different steps of the purification of the CDK2/cyclin A complex (A. After first glutathione column; B. After size exclusion chromatography using Superdex 75 column; C. Pure CDK2^{Thr160}/cyclin A complex obtained after the second affinity chromatography purification step).

6.5. Crystal formation and data collection

The purified CDK2^{Thr160}/cyclin A complex was obtained in good yield (~11 mg/mL) and was mixed with the appropriate inhibitors. Crystallisation conditions for CDK2 were already established (0.8 M KCl, 1.1 M ammonium sulfate, 0.1 M Hepes pH 7.0), but a small matrix screen around the known conditions was set up to further optimise the crystallisation. Usually, several parameters can be optimised such as protein concentration, pH, the precipitant, precipitant concentration, the buffer type and the temperature.[238] In this study, only the concentrations of ammonium sulfate (0.8 to 1.3 M, 0.1 increment) and salt (KCl, 0.6 to 0.95 M, 0.05 increment) were modified. Screens were performed in 2-subwell 96 well plates. The protein mixture and crystallisation solution were mixed in the subwells, in 100 nL drops, using a 'Mosquito' robot. Crystallisation trays were stored at 4 ^{o}C in a Rokagu Minstrel incubator, for up to two weeks and crystal formation was monitored through automated imaging of the drops recorded at a set time point. Crystals were grown using the sitting drop vapour diffusion method where the protein became supersaturated and was driven out of the solution in the form of crystals. Crystallisation was helped by the precipitant, which caused proteins to adhere to each other by competing for solvent (*Figure 95*).

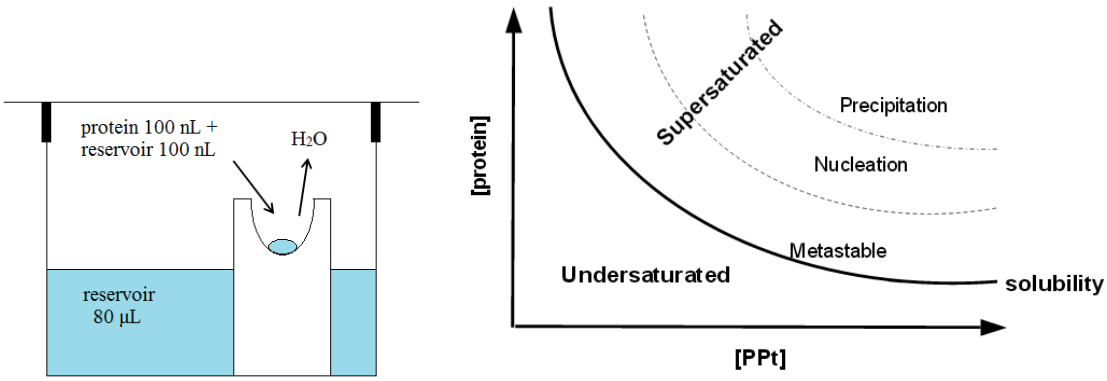

Figure 95 - Principles of the sitting drop vapour diffusion crystallisation and protein solubility phases[238]

After ten days, crystals appeared under the conditions containing 1.2 or 1.3 M ammonium sulfate and 0.75 or 0.8 M KCl (*Figure 96*). Once crystals were formed, they were harvested at 4 °C by the 'loop mount' method.[238] They were then soaked into a cryogenic solution containing 30% of saturated ammonium sulfate or sodium sulfate before being flash frozen in liquid nitrogen. The use of a cryoprotectant has the advantage of protecting the crystals from radiation damage caused by *X*-ray analysis, and avoiding the

formation of hexagonal ice, known to diffract *X*-rays, in contrast to water glass. The crystals were stored in liquid nitrogen until studied by *X*-ray crystallography.

Figure 96 – A drop containing crystals formed under the conditions of 1.3 M ammonium sulfate and 0.8 M KCl

The protein expression, purification, and crystallisation were carried out with the help of Professor Jane Endicott, Dr Martyna Pastok and Stephen Hallett. The crystal harvesting and data collection was performed with the help of Dr Arnaud Basle.

6.6. Highlights of the *X*-ray crystal structure determinations

The resolution obtained from *X*-ray analysis of the crystals was in the range of 3.1 to 2.1Å. Data analysis was performed only on one crystal per inhibitor (4 crystals were sent for each inhibitor in complex with CDK2 to the Diamond Light Source in Oxford, UK) having a resolution of 2.1 – 2.0 Å. Data were processed using XDS[239] and Aimless[240]. The molecular replacement was applied using MOLREP[241] and a CDK2/cyclin A structure. Rigid-body and restrained refinement was performed using REFMAC5.[242] Inhibitor models were positioned into the electron density in the active site using JLigand in COOT.[243] Finally, the structures were further refined by Professor Martin Noble to assess the presence of covalent binding between the inhibitors and CDK2.

For modulating the reactivity of the vinyl sulfone warhead of compound **60**, the α-position was more thoroughly investigated (see *Chapter 5*). Understanding the binding mode of inhibitors bearing α-substituents was important to interpret the biological results obtained from the time-dependent assays. The *X*-ray crystal structure of the compound bearing a methyl group at the α-position of the vinyl sulfone moiety (**162**) was obtained at 2.1 Å resolution (*Figure 97*). The inhibitor **162** was shown to bind in a similar manner

to compound **60** with the purine interacting with the hinge region, the cyclohexyl substituent positioned in the ribose pocket and the vinyl sulfone directed towards the solvent. The *X*-ray crystal structure of the ethyl analogue **163** was also determined at 2.1 Å resolution (*Figure 98*). A similar binding mode was observed as for compound **162**. No interaction with Lys89 was present in both *X*-ray crystal structures, demonstrating that α-alkyl substituents hindered the attack from Lys89 onto the vinyl sulfone.

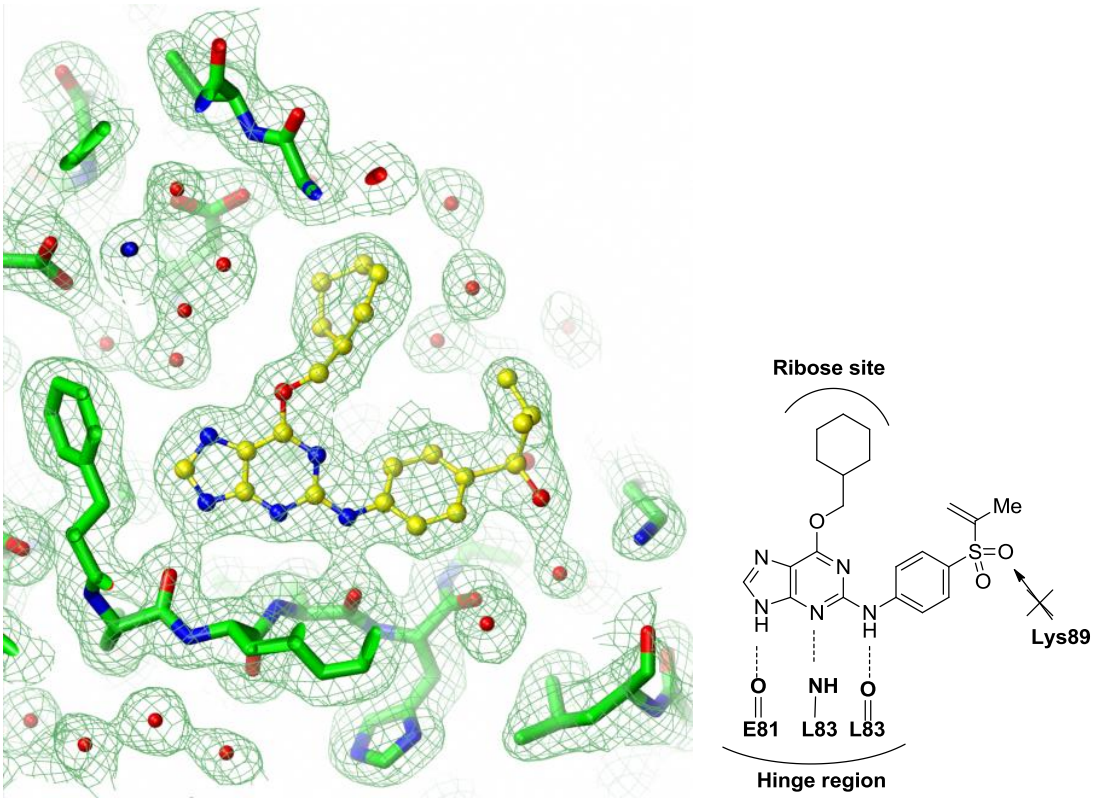

Figure 97 - Purine **162** in complex with CDK2/cyclin A. The structure was determined at 2.1 Å resolution.

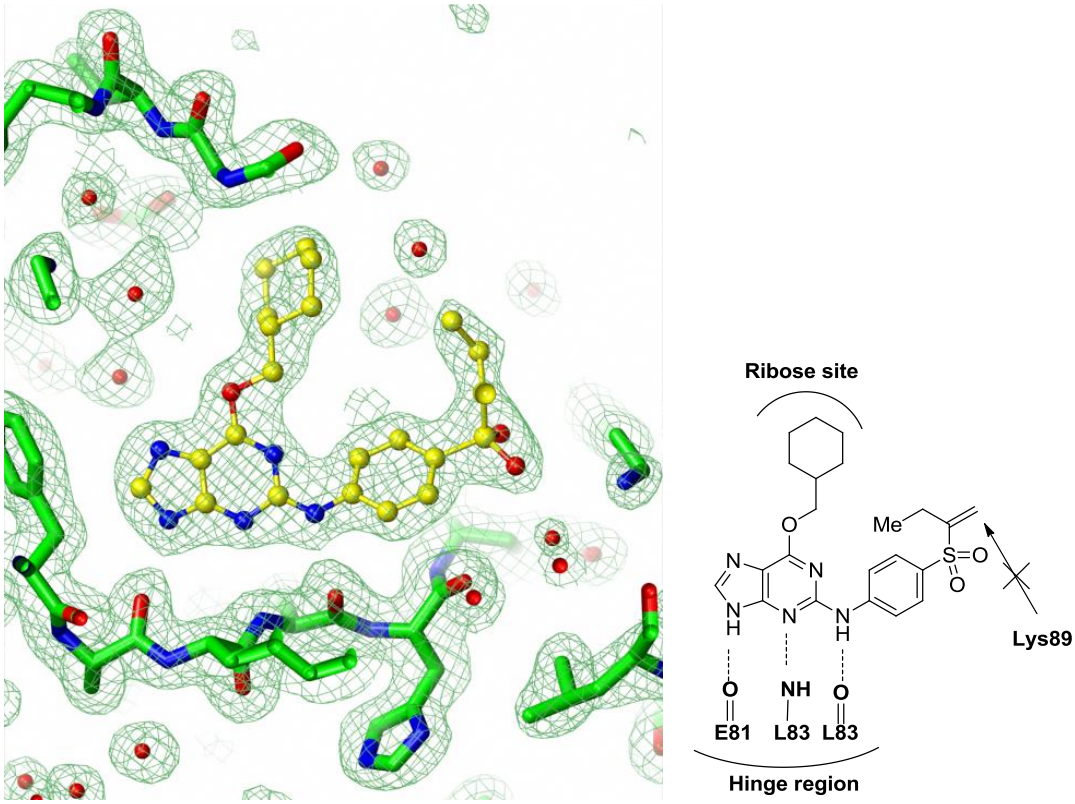

Figure 98 – Purine **163** in complex with CDK2/cyclin A. The structure was determined at 2.1 Å resolution.

Both analogues retained potency in the time-dependent assay against CDK2, which can be attributed to the binding mode of the compound, consistent throughout this series, and showing that the triplet of H-bonds with the hinge region and the interaction of the purine 6-cyclohexylmethyl group with the ribose pocket are crucial for activity.

In the biological assay to determine the activity of the inhibitors against CDK2, the 2-hydroxyalkyl compounds showed activity similar to their vinyl sulfone parents. To rationalise this observation, the *X*-ray crystal structure of the 2-hydroxyalkyl analogue **184** was obtained at 2.0 Å resolution (*Figure 99*). The hydroxyl group did not make any new interactions with the protein and the activity of this compound against CDK2 was attributed to its binding mode, with crucial interactions arising within the hinge region and the ribose pocket.

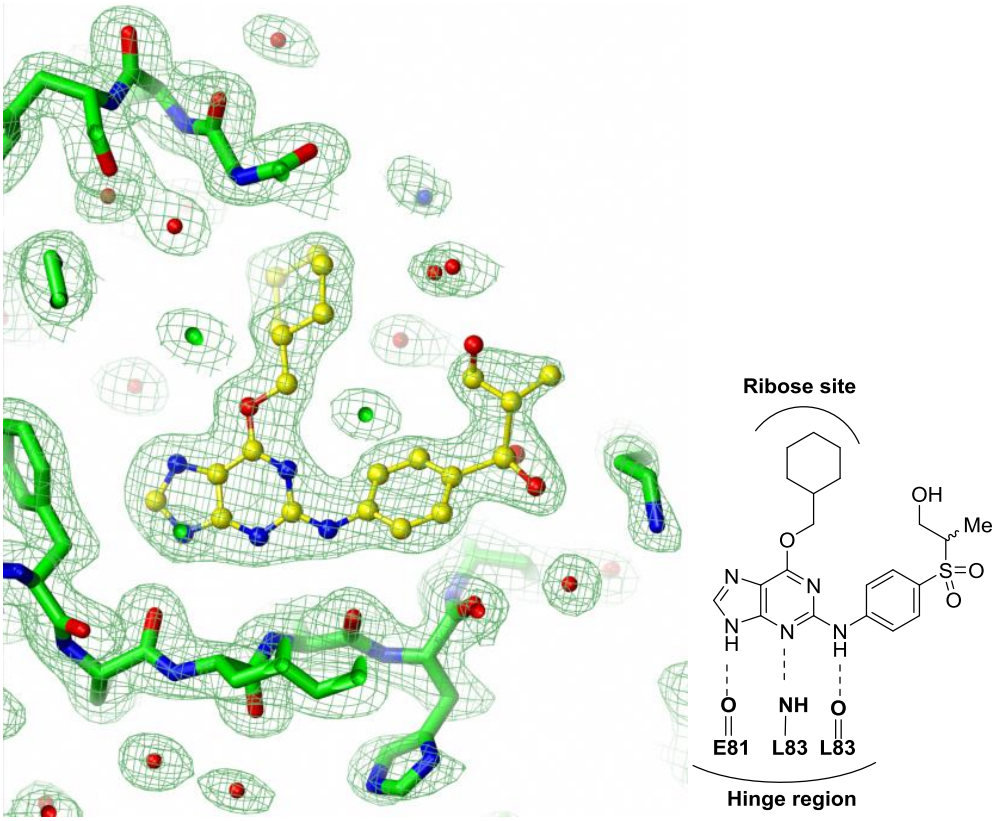

Figure 99 – Purine **184** in complex with CDK2/cyclin A. The structure was determined at 2.0 Å resolution.

The inhibitor bearing a methyl group at the β-position of the vinyl sulfone warhead (**323**) had a similar time-dependent inhibition profile to the α-methyl analogue (**162**) (see *Chapter 8*). The *X*-ray crystal structure of inhibitor **323** was obtained at 2.1 Å resolution (*Figure 100*) and showed the same interactions within the hinge region and the ribose pocket. However, with the methyl group at the β-position, Lys89 was able to attack the vinyl sulfone to make a covalent interaction. The mobility of Lys89 was noteworthy as its position in this *X*-ray crystal structure (*Figure 100*) was different from that observed for the previous crystal structures described (*Figures 97-99*).

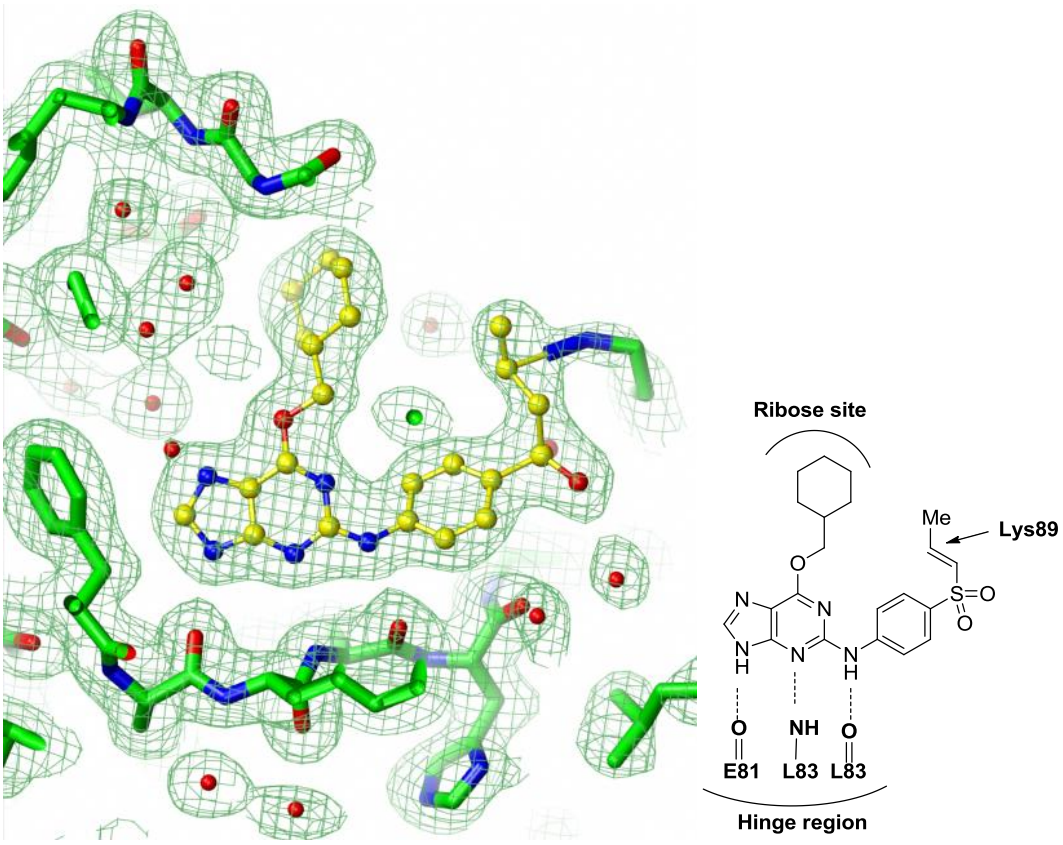

Figure 100 – Purine **323** in complex with CDK2/cyclin A. The structure was determined at 2.1 Å resolution.

The difference in reactivity between compounds **162** and **323** may be rationalised by two explanations. When a nucleophile reacts with a carbonyl group, the nucleophile approaches from an angle of 107°, termed the Bürgi-Dunitz angle (see *Chapter 4*, *section 4.5.*).[211] Assuming that this concept can be extended to Michael additions[244] and to electron-deficient double bonds, then it is important to consider this reaction in the context of the protein environment. From the crystal structures (*Figures 97 and 98*), the orientation of Lys89 appears to be sub-optimal for attack onto the vinyl sulfone group via a Bürgi-Dunitz angle. Having a group at the α-position may provoke a twist in the conformation of the vinyl sulfone warhead. In addition to the Bürgi-Dunitz angle itself, the Bürgi-Dunitz trajectory also has to be considered. If approach of the nucleophile along the preferred trajectory is impeded, e.g. by a substituent in the molecule undergoing attack, then the rate of reaction may be considerably reduced. In this respect, the β-methyl group may cause greater difficulties as such a group is more likely to interfere with the nucleophile's trajectory than a group in the α-position. However, since the structural biology results indicated a covalent interaction only with a group at the β-position, this suggests that other factors may be involved.

Another explanation for the observations made from the binding mode of these inhibitors is the stability of the intermediate formed during the Michael addition. When the nucleophile attacks the vinyl sulfone warhead, an intermediate is formed leading to a negative charge adjacent to a methyl group (**162**) or a hydrogen atom (**323**). A methyl group, being electron-donating, would destabilise the negative charge by comparison with hydrogen, rendering the intermediate less stable and therefore, product formation less favoured (*Figure 101*). This explanation rationalises the difference in reactivity observed between the inhibitors **162** and **323**, although the Bürgi-Dunitz concept is still relevant for the type of reaction discussed.

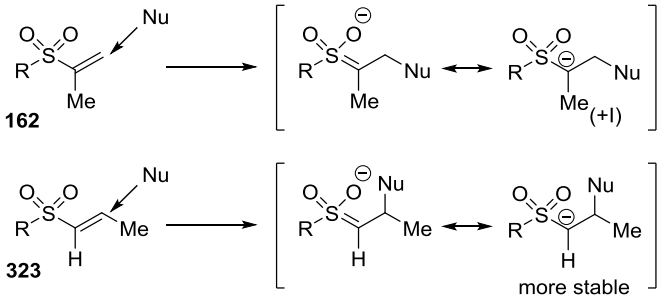

Figure 101 - A possible explanation for the difference of reactivity between inhibitors **162** and **323**.

Chapter 7. Investigation of New Electrophilic Warheads for Covalent Inhibition of CDK2

Following the discovery of the vinyl sulfone purine **60**, the first reported covalent inhibitor of CDK2, initially only analogues of the vinyl sulfone were synthesised (*Chapter 5*). In this chapter, the design and synthesis of analogues of purine **60** bearing a different electrophilic warhead are discussed with the objective of investigating the possibility of an alternative group at this position on the purine.

7.1. Acrylamide analogue of 60

The acrylamide group is a widely used electrophilic substituent for covalent binding in kinase inhibitors.[81, 106, 107, 118] To maintain the interaction between the sulfone and Asp86 of CDK2, compound **353** was designed. Buchwald coupling with purine **171** to afford the intermediate **351**, followed by reaction with acryloyl chloride, gave a di-acrylamide compound **352**, even though the stoichiometry was controlled. Compound **352** underwent PMB deprotection using TFA to give the acrylamide **353**, with adventitious loss of one acrylamide group (*Scheme 96*).

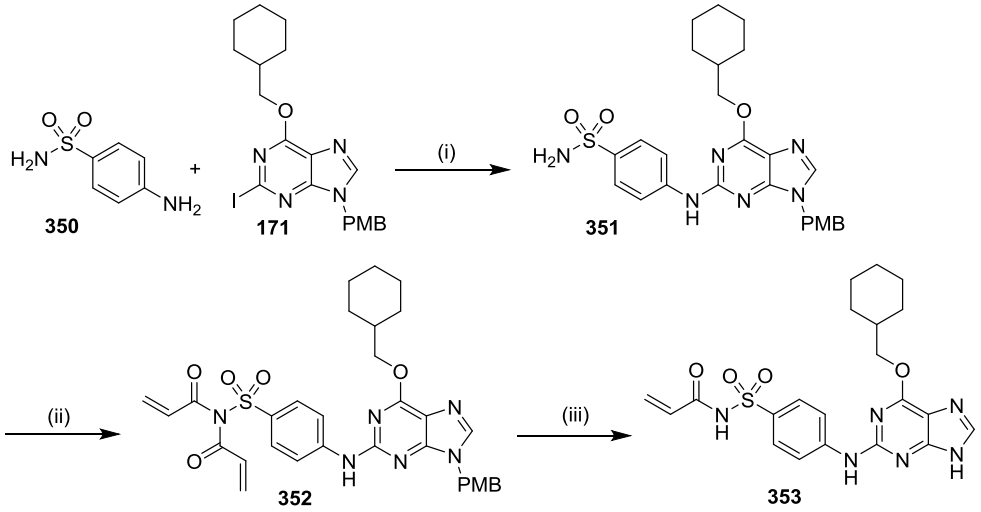

Scheme 96 - R*eagents and conditions*: (i) K_2CO_3, XPhos, Pd(dba) in MeCN, 80 °C, 18 h, 21%; (ii) acryloyl chloride, Et_3N in DCM, r.t., 2 h, 29%; (iii) TFA, 70 °C, 2 h, 53%.

7.2. Vinyl sulfonamide analogue of 60

Because acrylamide was a popular electrophilic warhead and the lead compound **60** of the CDK2 project contained a vinyl sulfone group, the vinyl sulfonamide **362** was of interest. The aniline **359** was constructed in a similar way to the previous targets. 4-Nitroaniline **354** failed to react with 2-chloroethanesulfonyl chloride, presumably because

the amino group was not sufficiently nucleophilic. *p*-Phenylenediamine **356** was mono-protected to give aniline **357**, which reacted with 2-chloroethanesulfonyl chloride to yield the sulfonamide **358**. Addition of pyrrolidine to the vinyl sulfonamide **358** afforded the aniline **359** (*Scheme 97*).

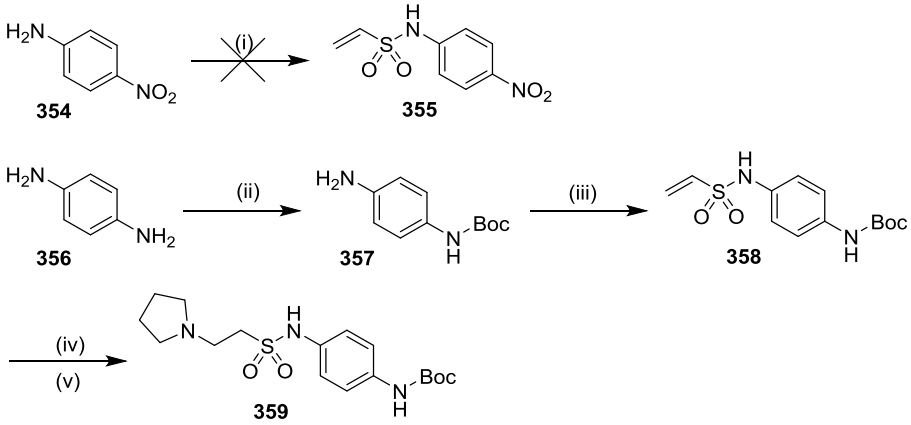

Scheme 97 - R*eagents and conditions*: (i) $Cl(CH_2)_2SO_2Cl$, DIPEA in DCM, r.t, 2 h; (ii) Et_3N, Boc_2O in DMF, r.t., 3 h, 84%; (iii) $Cl(CH_2)_2SO_2Cl$, DIPEA in DCM, r.t, 2 h, 36%; (iv) benzenesulfonyl chloride, Et_3N in DCM, r.t., o/n; (v) pyrrolidine, r. t., 60%.

An Ullmann-type reaction between the aniline **359** and intermediate **171** was performed, followed by Boc and PMB deprotection to give the intermediate **360** (*Scheme 98*). As the PMB group proved difficult to remove, microwave heating was required, which led, according to LC-MS analysis, to the trifluoroacetamide **360**. The trifluoroacetamide group was easily cleaved with sodium borohydride to afford intermediate **361**. When *m*-CPBA was used for the Cope elimination step, the compound **362** could not be directly isolated in a pure state.

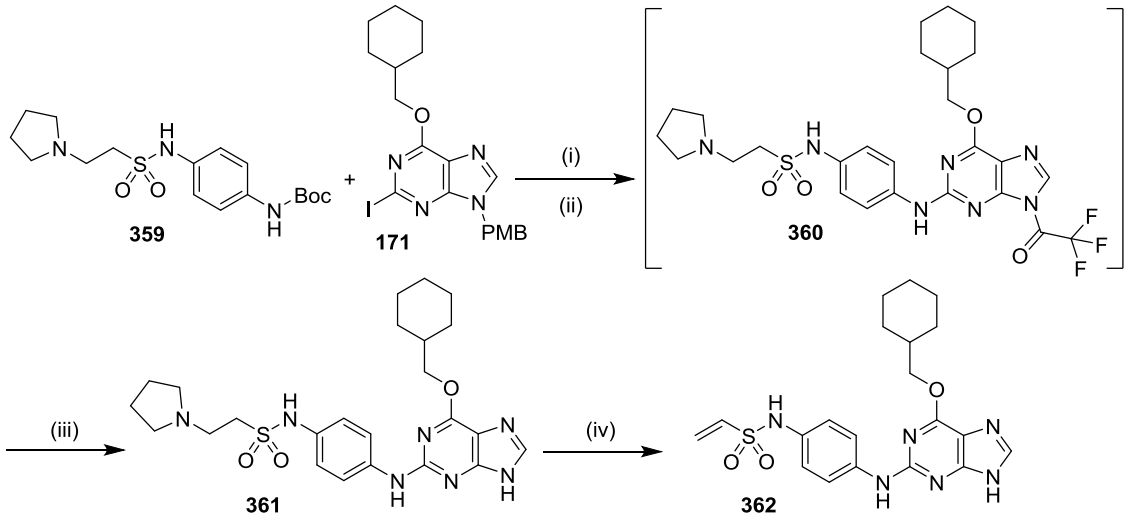

Scheme 98 - R*eagents and conditions*: (i) CuI, 2-thiophenecarboxylic acid in DMSO, 60 °C, 5 h; (ii) TFA, 110 °C, MW, 45 min; (iii) $NaBH_4$ in MeOH, r.t., 15 min, 34% (over 3 steps); (iv) *m*-CPBA in DCM, r.t., 30 min.

Another synthetic route was considered that avoided the use of *m*-CPBA (*Scheme 99*). The first step was Buchwald coupling between intermediate **171** and aniline **354**, followed by PMB deprotection to afford intermediate **363**. Reduction of the nitro group gave aniline **364**. However, after several attempts at purification, no product was obtained. Hydrogenation with Pd/C under H_2 was performed as alternative conditions for the reduction giving a clean reaction and the subsequent step was carried out on the crude compound **364**. The final step showed complete reaction with formation of the vinyl sulfonamide **362** but, purification by column chromatography, either on silica or alumina, did not provide pure enough compound. ^{1}H NMR analysis showed the presence of the desired target and minor impurities. The stability of the compound was assessed in acidic, basic and neutral aqueous environment, with no visible degradation by LC-MS. The isolation of compound **362** in a pure state was eventually achieved by semi-prep HPLC.

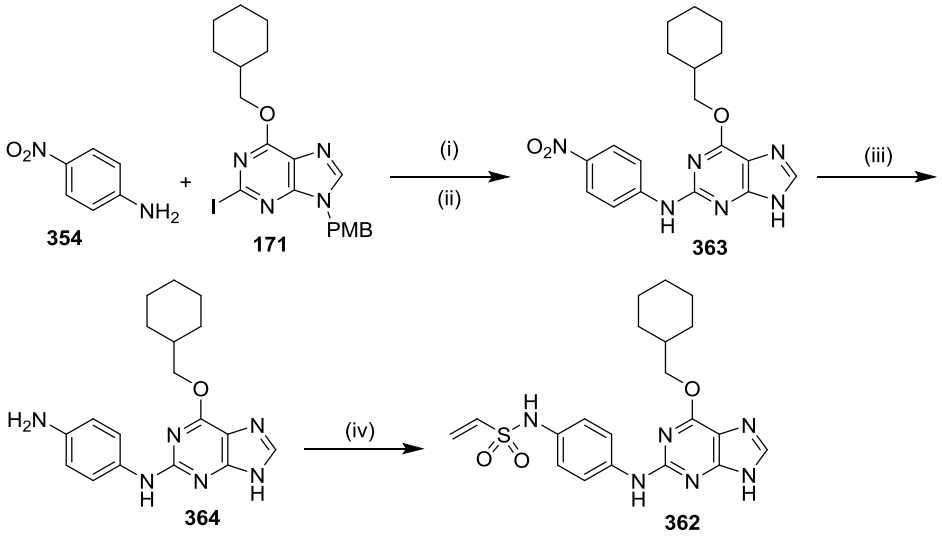

Scheme 99 - R*eagents and conditions*: (i) K_2CO_3, XPhos, $Pd(dba)_2$ in MeCN, 80 °C, 18 h; (ii) TFA, reflux, 5 h, 42%; (iii) Pd/C, H_2 in MeOH, 40 °C, 2 h, 97%; (iv) $Cl(CH_2)_2SO_2Cl$, DIPEA in DCM, r.t, 2 h, 3%.

7.3. β-Ketosulfone analogue of 60

As discussed previously, hydrolysis of the vinyl sulfone warhead of **60** was a major problem (see *Chapter 5*). An attractive inhibitor would be a compound with the potential for irreversible binding, but reacting preferentially with an amino group (from Lys89) compared with water. The β-ketosulfone could offer this selectivity via a mechanism comparable to a reductive amination. The iminium ion formed from the reaction of the ketone with Lys89 could lead to a resonance-stabilised ene-sulfonamide (*Scheme 100*).

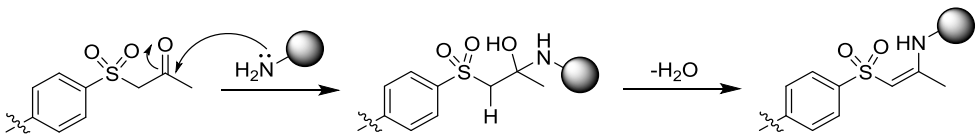

Scheme 100 - Possible reaction between Lys89 of CDK2 and the β-ketosulfone moiety

The β-ketosulfone intermediate **324**, available from one of the syntheses described previously, underwent nitro reduction to form the aniline **365**. The optimised one-pot process, Buchwald reaction followed by PMB deprotection, was then performed to provide the target compound **366** (*Scheme 101*).

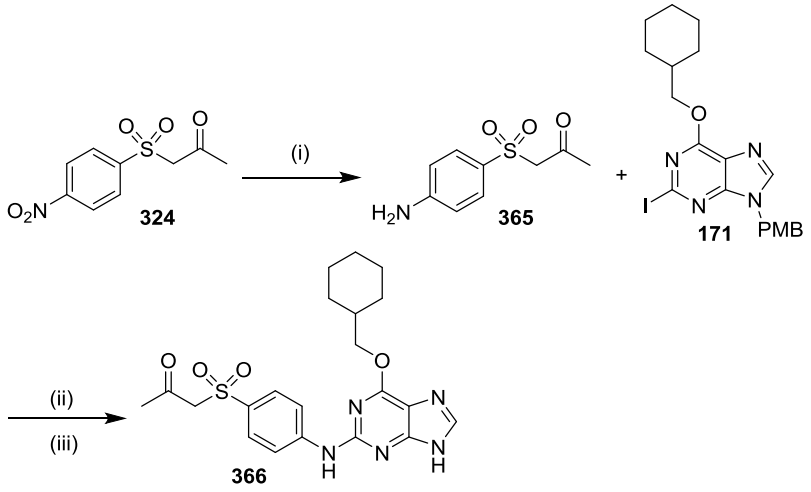

Scheme 101 - *Reagents and conditions*: (i) Zn, AcOH in MeOH, r.t., 1h, 77%; (ii) K_2CO_3, XPhos, $Pd(dba)_2$ in MeCN, 80 °C, 18 h; (iii) TFA, reflux, 5 h, 45%.

7.4. α-Halosulfone derivatives of compound 60

During the preparation of the α-chlorovinyl sulfone derivative **167**, the chloromethyl sulfone intermediate **264** was obtained. This substance was of interest because of its potential reactivity towards Lys89 of CDK2 (*Scheme 102*) by analogy with the known reactivity of α-chloroketones.

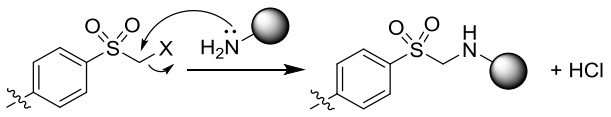

Scheme 102 - Possible reaction between Lys89 and the α-haloalkyl derivative

Intermediate **264** was reduced to the corresponding aniline **367**, which was reacted with intermediate **171** under the standard conditions, to afford the α-chloromethyl sulfone **368** (*Scheme 103*).

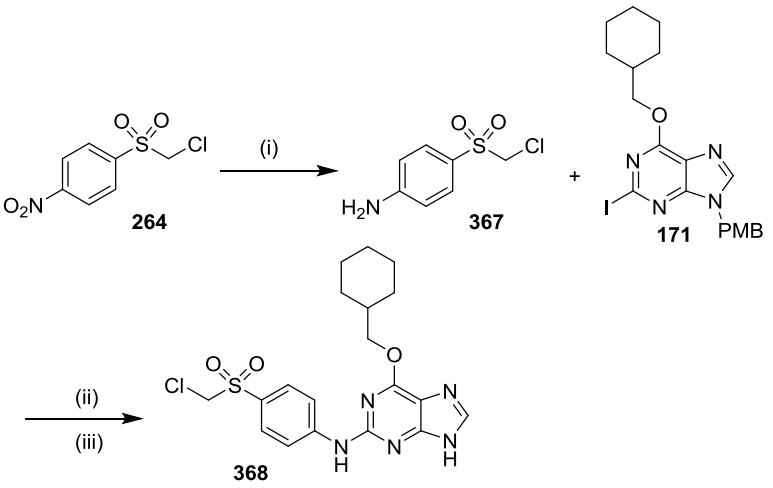

Scheme 103 - *Reagents and conditions*: (i) Zn, AcOH in MeOH, r.t., 1h, 70%; (ii) K_2CO_3, XPhos, $Pd(dba)_2$ in MeCN, MW, 100 °C, 30 min; (iii) TFA, reflux, 5 h, 47%.

Although fluoride is a poor leaving group in S_N2 reactions, the α-fluoromethyl derivative **372** was of interest because the synthesis of the α-fluoromethyl sulfone compound **370** from an ester had no literature precedent. Hydrolysis was performed on ester **269**, but decarboxylation did not occur readily by comparison with the chloro compound **265** (see *Chapter 5*, section 5.2.1.). The carboxylic acid **369** was therefore heated by microwave irradiation to trigger decarboxylation. Reduction of the nitro group afforded the aniline **371**, which was then reacted with intermediate **171** to give the target compound **372** (*Scheme 104*).

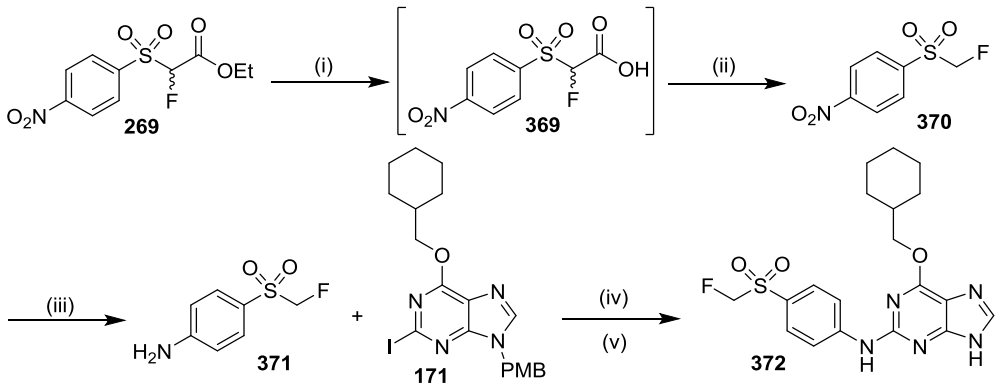

Scheme 104 - *Reagents and conditions*: (i) LiOH in THF, 50 °C, 2 h; (ii) in MeCN, MW, 180 °C, 1 h, 79% over 2 steps; (iii) Zn, AcOH in MeOH, r.t., 1 h, 78%; (iv) K_2CO_3, XPhos, $Pd(dba)_2$ in MeCN, MW, 100 °C, 30 min; (v) TFA, reflux, 5 h, 23%.

7.5. α-Trifluoromethylsulfone derivative of 60

From the results obtained previously (Chapter 5, section 5.2.4.), the α-trifluoromethyl sulfone group was interesting as it could react with Lys89 according to two mechanisms. The protons on a methylene flanked by a sulfone and a trifluoromethyl group are

relatively acidic (estimated pK_a ~ 12 in DMSO[225]). Removal of such a proton could be followed by fluoride elimination to give an extremely reactive difluorovinyl sulfone for reaction with Lys89 (*Scheme 105*, Mechanism 1). Furthermore, this species in the presence of water may lead to an acyl fluoride, which could also react with Lys89 (*Scheme 105*, Mechanism 2).

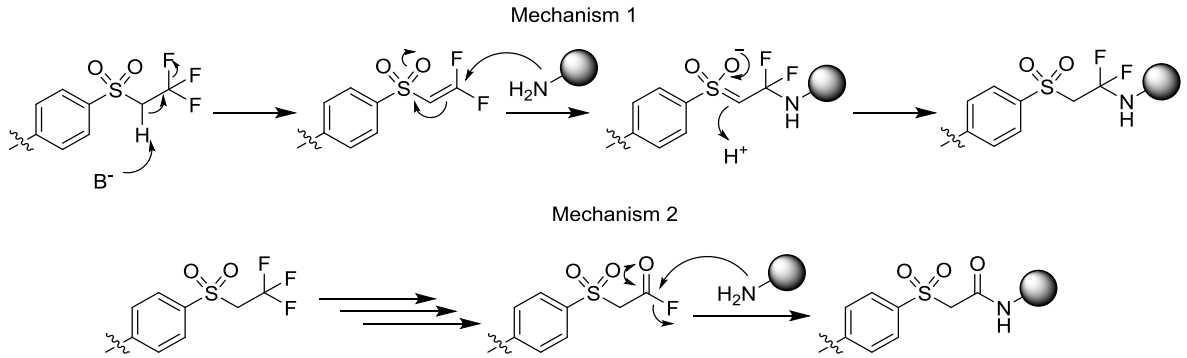

Scheme 105 - Possible reactions between Lys89 and the α-trifluoromethylsufone derivative.

The synthesis of this purine derivative (**375**) was straightforward with reduction of intermediate **314** to the aniline **373**, which was reacted with intermediate **171**. The final oxidation step provided the desired product **375** (*Scheme 106*). Oxidation was performed at the final step to avoid working with a reactive functionality throughout the synthesis, which could have led to side reactions.

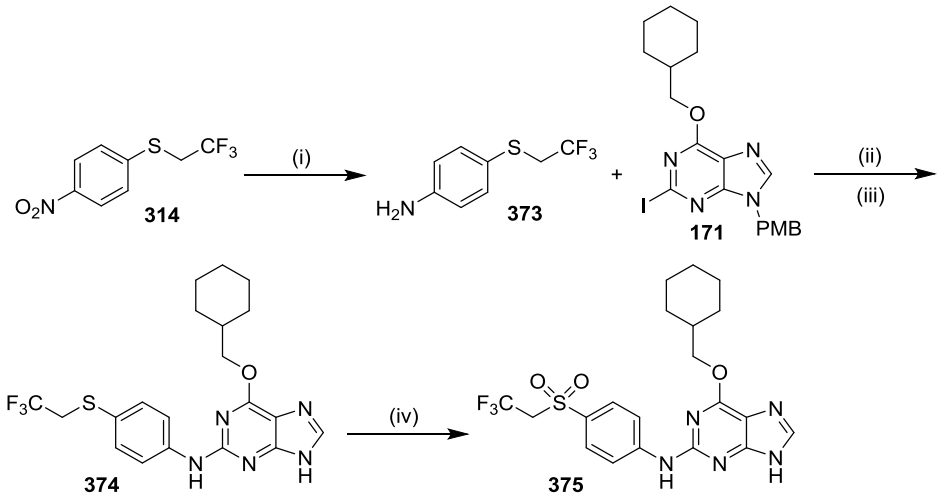

Scheme 106 - *Reagents and conditions*: (i) Zn, AcOH in MeOH, r.t., 1h, 85%; (ii) K_2CO_3, XPhos, $Pd(dba)_2$ in MeCN, MW, 100 °C, 30 min; (iii) TFA, reflux, 5 h, 43%; (iv) *m*-CPBA in DCM, r.t., 2 h, 40%.

7.6. Vinyl ketone analogue of 60

The effect of several substituents on the vinyl moiety was assessed, but the importance of the sulfone group still remained to be determined. The corresponding vinyl ketone **389** was therefore of interest. The synthesis of the appropriate aniline was attempted following two different routes. The first scheme considered (*Scheme 107*) was lengthy with reduction of both ketone and ester groups of compound **376** required to give the diol **378**, followed by selective protection of the alcohol **378** and oxidation of the alcohol **379**, with a difficult final deprotection step (*Scheme 107*). Other protecting groups than TBDPS could have been explored but a shorter route was clearly more desirable.

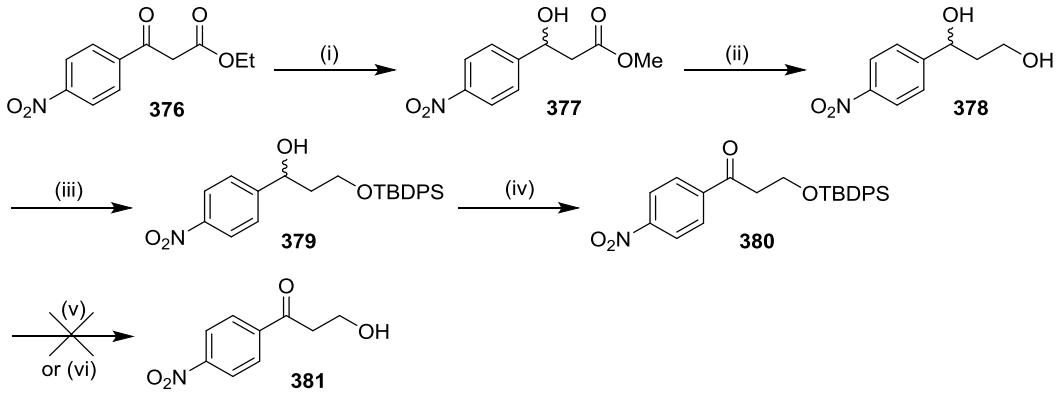

Scheme 107 - *Reagents and conditions*: (i) $NaBH_4$ in MeOH, r.t., 1 h, 64%; (ii) Dibal in THF, 0 ^oC, 1 h, 78%; (iii) imidazole, TBDPSCl in DCM, 0 ^oC, 1 h, 44%; (iv) DMP in DCM, r.t., 2 h, 85%; (v) TBAF in THF, 0 ^oC, 1 h, degradation; (v) or fluoride on polymer support in THF, r.t., 18 h, no reaction observed.

A Stille reaction on the acyl chloride **382** gave the desired vinyl ketone **383** (*Scheme 108*). Completing the synthesis with this reactive group in place would have been challenging, and hence a masking approach was necessary. Addition of pyrrolidine to the vinyl ketone led to intermediate **384**. With this group in place, Cope elimination would have enabled formation of the vinyl ketone at the final step of the synthesis. However, nitro reduction under the usual conditions led to degradation. Hydrogenation could have been attempted as an alternative but, in parallel, a more promising route was also investigated.

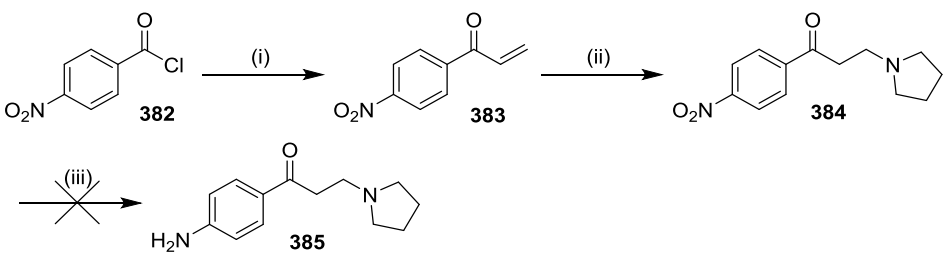

Scheme 108 - *Reagents and conditions*: (i) tributyl(vinyl)tin, $Pd(PPh_3)_4$ in THF, 65 ^oC, 1 h, 35%; (ii) pyrrolidine in DCM, r.t., 2 h, 51%; (iii) Zn, AcOH in MeOH, r.t., 1h, degradation observed.

To synthesise the majority of the previous target compounds, an aniline intermediate was first formed and then coupled with the 2-iodopurine intermediate **171**. Another strategy was considered starting with a Buchwald reaction between aniline **386** and intermediate **171** (*Scheme 109*). A Weinreb amide **388** was prepared from the corresponding ester **387** in good yield, and addition of vinylmagnesium chloride to the amide afforded the desired vinyl ketone **389**. From the Weinreb amide **388**, another target (**390**) was also synthesised by the addition of ethynylmagnesium bromide (*Scheme 110*). From this approach, from the common intermediate **388**, two new warheads were introduced onto the purine.

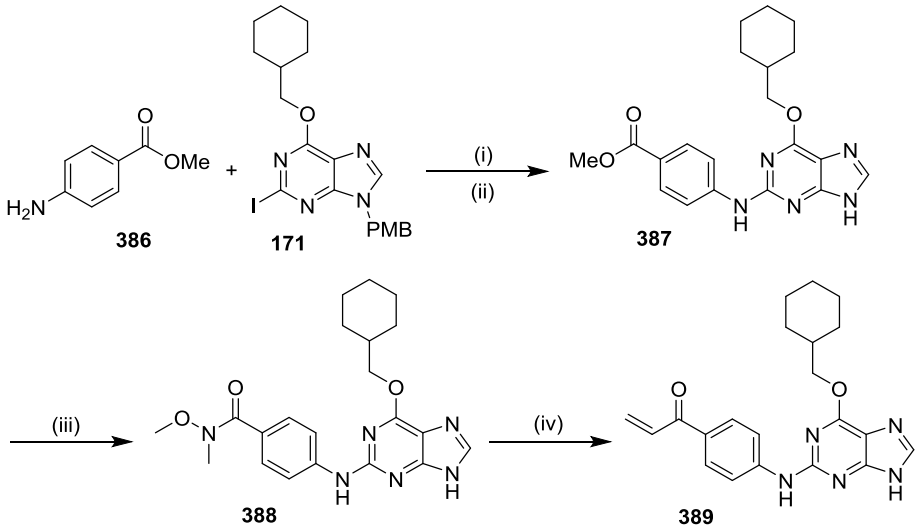

Scheme 109 - *Reagents and conditions*: (i) K_2CO_3, XPhos, $Pd(dba)_2$ in MeCN, MW, 100 °C, 30 min; (ii) TFA, reflux, 5 h, 55%; (iii) isopropylmagnesium chloride, *N*,*O*-dimethylhydroxylamine in THF, 0 °C, 2 h, 97%; (iv) vinylmagnesium chloride in THF, 0 °C, 2 h, 36%.

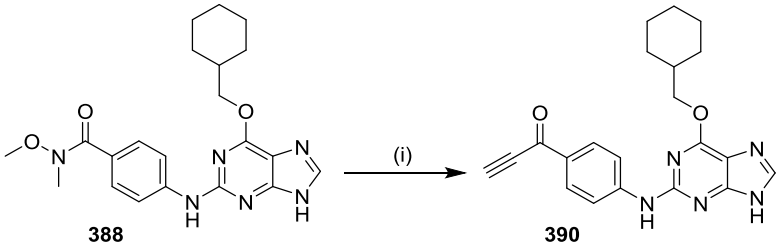

Scheme 110 - *Reagents and conditions*: (i) ethynylmagnesium bromide in THF, r.t., 18 h, 25%.

Chapter 8. Biological Evaluation of the CDK2 Inhibitors

In this chapter, the biological results of the inhibitors synthesised as described in Chapters 5 and 7 are presented and discussed. Each inhibitor was tested in an enzyme kinetic experiment which determined an inhibition profile of the studied compound over time. The kinetic assays were run up to 4 hours as results after this period were found not to be useful. Vinyl sulfones were shown to exhibit stability issues (see *Chapter 5*) and if the studied vinyl sulfone did not react with the enzyme during the 4 hours of the assay, it is possible that the inhibitor had degraded, partially or completely, into its 2-hydroxyalkyl derivative. Covalent inhibitors are known to react with the target enzyme gradually with time at a rate depending on the reactivity of the inhibitor.[101] Therefore, if the experiment illustrates an increase of activity with time, this observation can be interpreted as covalent binding occurring between the studied inhibitor and enzyme. However, as the experiments were conducted only once (n = 1), and the inhibitors were incubated with the enzyme for 30 min prior to the first measurement, covalent inhibition, if suspected by the time-dependent inhibition profile of the inhibitor, had to be confirmed by structural biology studies. Indeed, some covalent inhibitors can react so quickly with the enzyme (e.g. during the incubation time) and therefore demonstrate a profile with activities within the same range throughout the experiment. Thus, the kinetic measurements could only provide an indication of the possibility of covalent binding and always required confirmatory structural biology studies.

8.1. The α-substituted vinyl sulfone series

Each vinyl sulfone derivative was assessed in a time-dependent assay against CDK2 (n = 1). The graphs illustrating CDK2 inhibition versus the concentration of the studied inhibitor are shown below (*Figure 102*). In the alkyl/aryl series (**162**-**166**), the crucial observation was that there was no clear case of time-dependent inhibition compared to compound **60**, indicating a lack of covalent binding between the inhibitors and CDK2. In addition, a loss of potency was noticed for groups larger than methyl (IC_{50} > 500 nM for **164-166** and IC_{50} > 200 nM for **163**), but no correlation was found between the potencies and the size of the groups at the α-position.

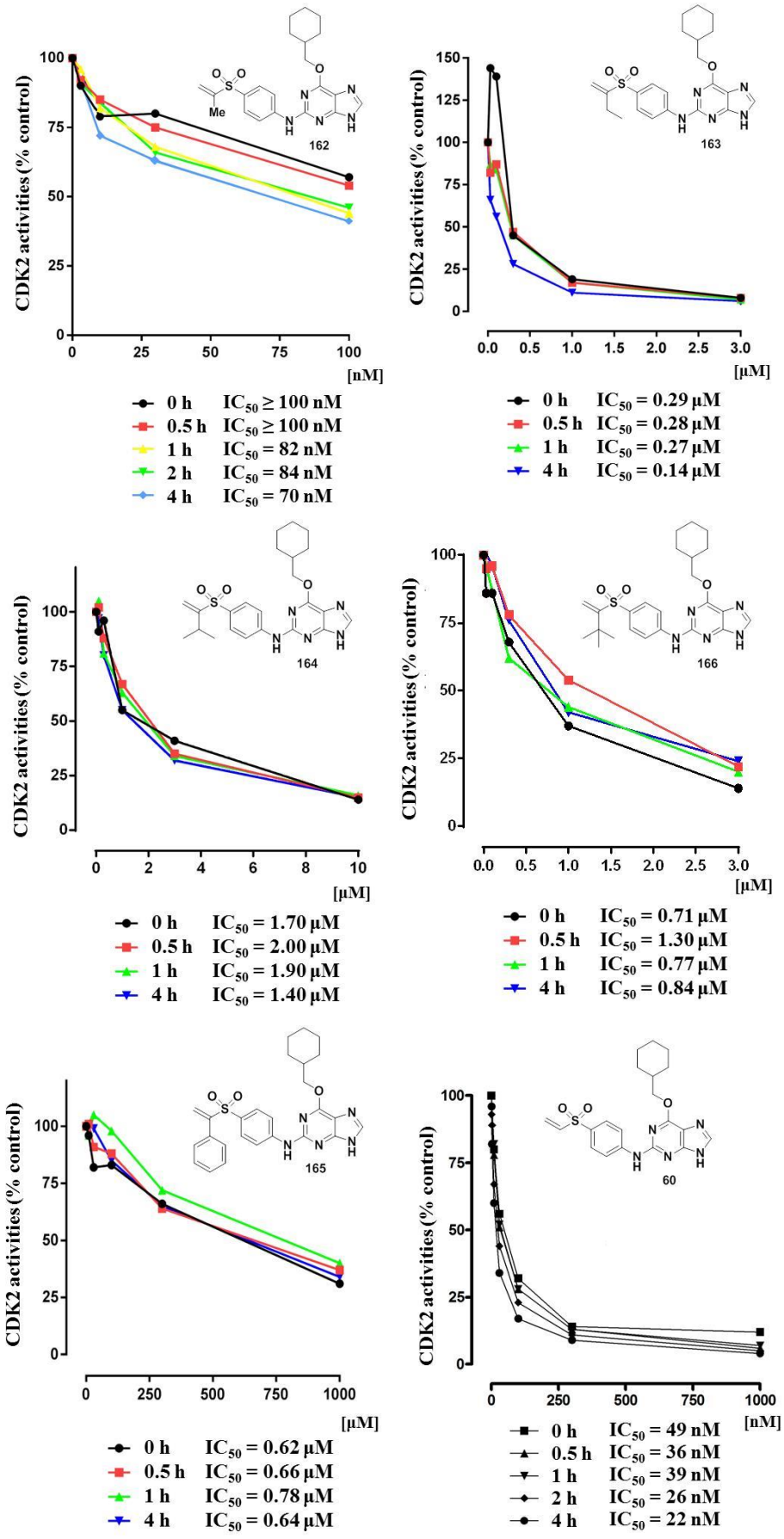

Figure 102– Biological results for compounds **162-166** and **60** in the time-dependent assay against CDK2

The 2-hydroxyalkyl derivatives corresponding to each vinyl sulfone were also evaluated against CDK2. The activities observed for these compounds were found to be within the same range exhibited for the parent vinyl sulfones (or they were less active) (*Table 22*). Moreover, the similar potencies exhibited by the pairs of inhibitors (vinyl sulfone and its corresponding 2-hydroxyalkyl analogue) needed to be investigated, and structural biology studies were carried out on selected purines (see *Chapter 7*).

Table 22 – Activity (IC_{50} values) of the 2-hydroxyalkyl compounds against CDK2 and initial activity of the corresponding vinyl sulfone inhibitors against CDK2 for comparison

	R group	Me (**184**)	Et (**213**)	^{i}Pr (**214**)	^{t}Bu (**254**)	Ph (**215**)
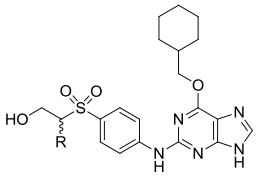	**CDK2 inhibitory activity (IC_{50} µM)**	0.08	0.13	0.37	2.20	2.00
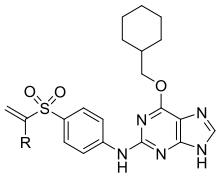	**Initial CDK2 inhibitory activity (IC_{50} µM)**	>100	0.29	1.70	0.71	0.62

For vinyl sulfones bearing electron-withdrawing groups at the α-position, the derivative bearing a chloro group (**167**) demonstrated an excellent time-dependent inhibition profile compared with **60**, with an initial potency of 361 nM that changed to 14 nM after 4 h (*Figure 103*). A crystal structure of compound **167** in complex with CDK2 would be required to confirm unambiguously the presence of a covalent interaction. The corresponding 2-hydroxyalkyl derivative **268** also exhibited evidence of a time-dependent inhibition (*Figure 103*), possibly due to conversion of the compound **268** into its vinyl sulfone parent **167**. This explanation needs validation through an investigation of the stability of compound **167** under various conditions.

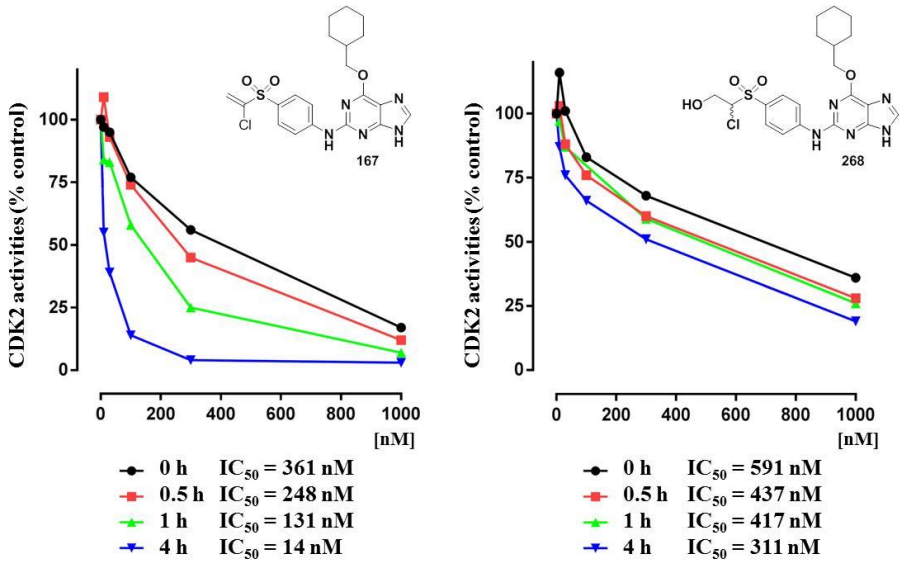

Figure 103 - Biological results for compounds **167** and **268** in the CDK2 kinetic assay

The fluoro derivative **168** did not exhibit a time-dependent inhibition profile compared with the chloro analogue **167**, but behaved as an ATP-competitive inhibitor (*Figure 104*). However, its 2-hydroxyalkyl derivative **272** proved unexpectedly potent after 30 min (IC_{50} = 67 nM), raising doubts as to its stability, and the activity observed could be arising from a by-product generated during degradation. A mechanism was postulated requiring the generation of two by-products. The potential by-product **372** was synthesised and tested against CDK2 but was found to be only moderately potent (Chapter 8, section 8.3.). Therefore, the possibility that inhibitory activity may arise from the formaldehyde generated was suggested (*Scheme 111*).

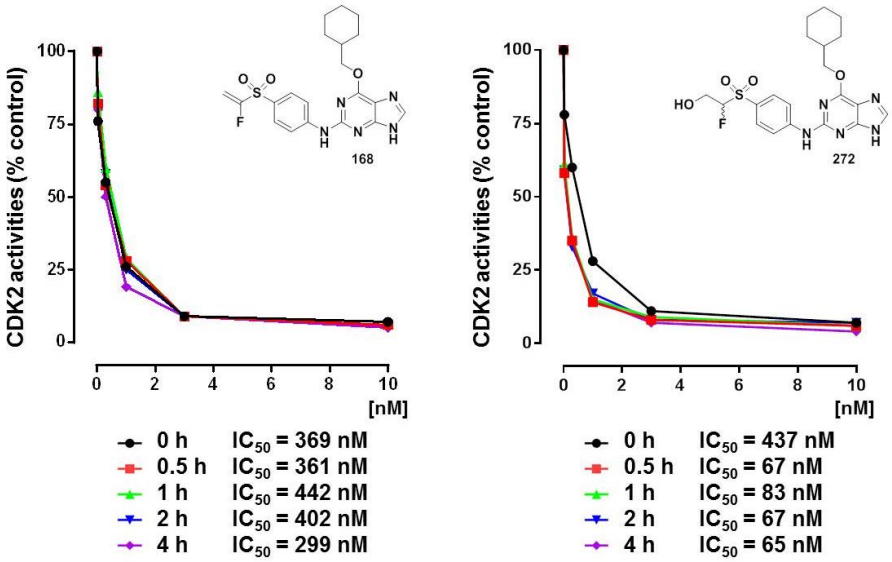

Figure 104 – CDK2-inhibitory activity of compounds **168** and **272** in the time-dependent assay against CDK2

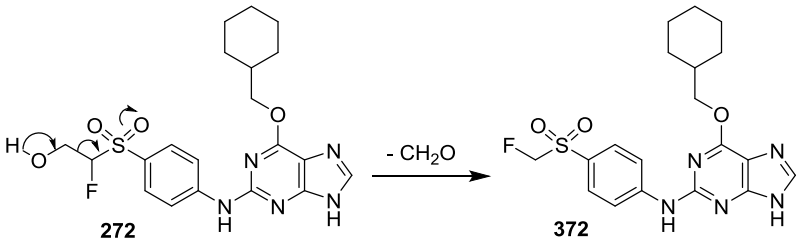

Scheme 111 – Proposed mechanism for the formation of **372** from **272**

From the biological results for this series, taken in combination with those of the structural biology (Chapter 6), the loss of covalent binding, when the vinyl sulfone warhead was functionalised with an α-alkyl, aryl or fluoro group, could be explained by the stability of the intermediate formed (Chapter 6, Section 6.6). Notably, the first explanation that a small twist of the vinyl sulfone warhead conformation, induced by a group at the α-position, did not correlate with the biological activity observed for the α-chloro derivative **167**. However, the stability of the intermediate formed during the Michael addition may explain the results observed across both the alkyl/aryl (**162**-**166**) and electron-withdrawing (**167**, **168**) series. When an alkyl group is positioned in the α-position of the carbanion, the latter is destabilised by an inductive effect (+I) imparted by those groups, which can be quantified by Hammett σ_p values (-0.17 (Me), -0.15 (Et, ^{i}Pr) and -0.20 (^{t}Bu)[245]). Inhibitors **162**-**166** exhibited ATP-competitive behaviour in the time-dependent assay against CDK2. On the contrary, the carbanion should have been stabilised by the inductive electron-withdrawing (-I) groups, F and Cl (σ_p values 0.06 and 0.23,[245] respectively), but only the chloro derivative **167** showed a time-dependent inhibition profile against CDK2. This observation may be explained by postulating that the lone pair of the carbanion interacts unfavourably with the lone pairs of the fluoro group, to a greater extent than with the lone pairs of the chloro group (*Figure 105*). This overlap is favoured by the similar sizes of F (50 pm[246]) and C (70 pm[246]) atoms and the length of the F-C bond (1.35 Å[247]) compared with the Cl-C bond (1.76 Å[248]). The lone pairs of the F atom tend to destabilise adjacent carbanion centres, and may explain therefore, the ATP-competitive behaviour of compound **168** in the time-dependent assay against CDK2. From a theoretical viewpoint, only the Cl group of compound **167** has a significant stabilising effect on the carbanion intermediate of the Michael addition, and accordingly only the vinyl sulfone purine bearing this group was shown to behave as a time-dependent CDK2 inhibitor.

Figure 105 – Lone pair effect in the destabilisation of a carbanion

8.2. The β-substituted vinyl sulfone series

Each vinyl sulfone (**323**, **333**, **339** and **349**) was evaluated in the time-dependent assay against CDK2 (n = 1). From the graphs obtained, none of the inhibitors exhibited a time-dependent inhibition profile and a loss of potency was observed compared with compound **60** (*Figure 106*). The only modification tolerated was the insertion of a methyl group at the β-position (**323**). A crystal structure of compound **323** in complex with CDK2 was determined, which confirmed covalent binding to CDK2 (Chapter 6, section 6.6.). This result was rather unexpected given the time-dependent inhibition profile of vinyl sulfone **323**, which indicated only modest irreversible inhibition. Indeed, the α-methyl (**162**) and the β-methyl (**323**) compounds exhibited a similar profile in the time-dependent assay, but only vinyl sulfone **323** was found to be a covalent inhibitor of CDK2. Moreover, the initial time zero set-point was actually recorded after 30 min incubation of the inhibitor with the protein during which covalent binding could have occurred but was not recorded. Therefore, the time-dependent assay gives a good first estimation of the behaviour of the inhibitor, but crystallographic studies are invaluable to confirm the presence of a covalent interaction with CDK2.

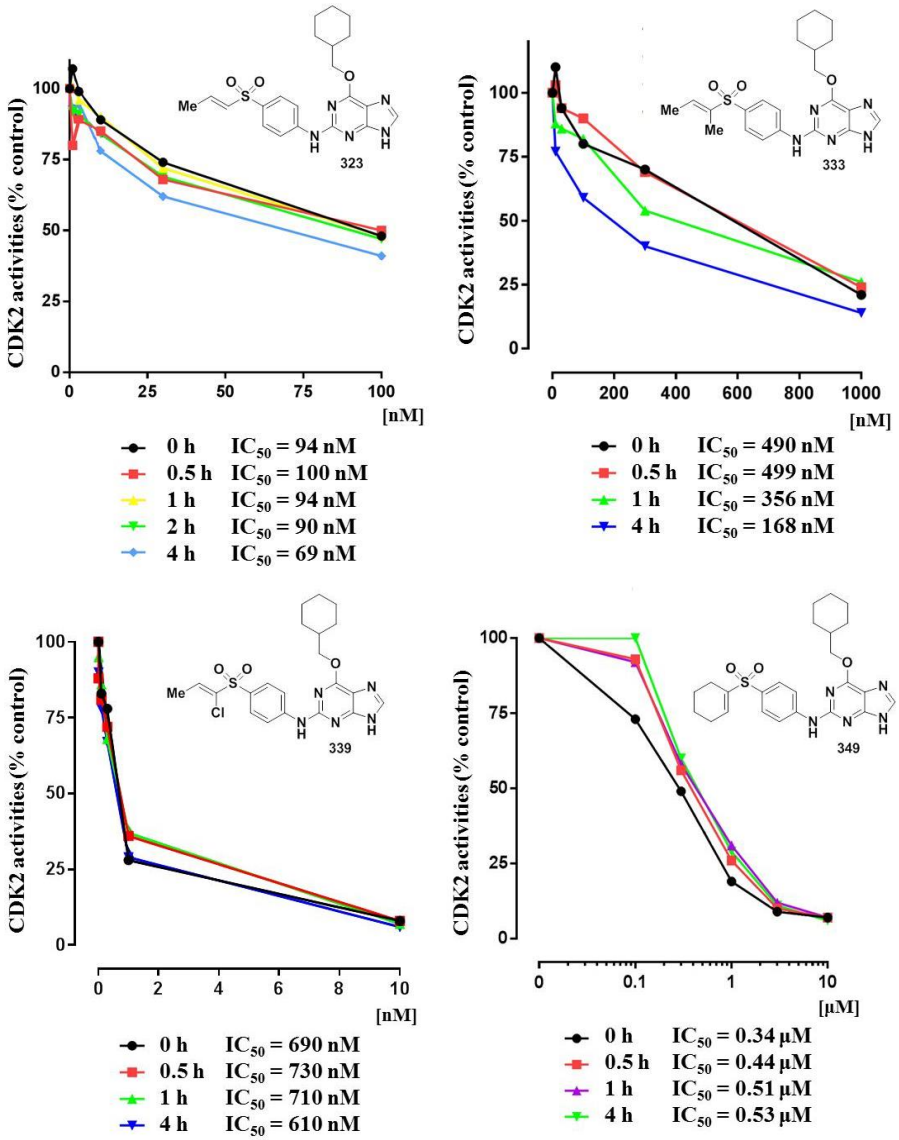

Figure 106 – Time-dependent inhibition profile of compounds **323**, **333**, **339** and **349** against CDK2

Compound **339** was designed with the idea of combining the effect of the α-chloro and β-methyl groups which gave excellent results, best time-dependent inhibition in the assay and covalent inhibition shown by structural biology, respectively. The results obtained for inhibitor **339** were rather disappointing with loss of time-dependent inhibition and loss of potency. Having an α,β-disubstituted vinyl sulfone (**333**, **339** and **349**) did not seem to be tolerated. As discussed in Chapter 6, having a group at the α-position must twist slightly the vinylsulfone group rendering the attack from Lys89 along the Burgi-Dunitz trajectory difficult. Moreover, the group positioned in β-position of the α-substituted vinyl sulfone imposes steric hindrance along the Burgi-Dunitz trajectory, perturbing attack from Lys89. These two major arguments may explain the biological results observed for these α,β-disubstituted vinyl sulfones.

The 2-hydroxyalkyl analogues (**327**, **332**, **338** and **347**) were also assessed and were found to exhibit moderate CDK2-inhibitory activity (*Table 23*). The results were consistent with these compounds acting as ATP-competitive inhibitors. Compound **338** was assessed in the enzyme kinetic assay (*Figure 107*) as the α-chloro analogue **268** showed a slight time-dependent inhibition profile. Compound **338** exhibited an ATP-competitive inhibition profile with activity within the same range of its vinyl sulfone parent **339**.

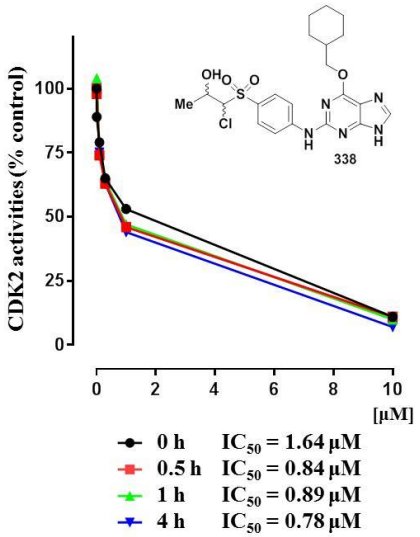

Figure 107 - Time-dependent inhibition profile of compound **338** against CDK2

Table 23 – Activity (IC_{50} values) of the 2-hydroxyalkyl compounds against CDK2

Compound		Activity against CDK2 (IC_{50} values)
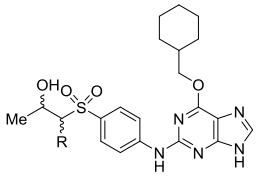	R = H (**327**)	0.16 μM
	R = Me (**332**)	0.64 μM
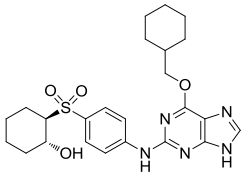	(**347**)	0.50 μM

8.3. New warheads

As a general observation from the results for this series, none of the inhibitors exhibited a time-dependent inhibition profile and activity against CDK2 was found to vary for each inhibitor (*Figure 108*). Adding an acrylamide moiety adjacent to a sulfone group (**353**) essentially abolished potency against CDK2 (IC_{50} (4 h) = 4.9 μM). This result highlighted

the importance of the size of the warhead group. In this case, the extra atoms added to the sulfone substituent increased the length of the group, presumably rendering attack from Lys89 unfavourable. The vinyl sulfonamide **362** showed a loss of potency (IC_{50} (4 h) = 0.51 μM) by comparison with compound **60**, suggesting that the interaction between the sulfone and Asp86, lost on introduction of the NH group, was crucial for activity. The β-ketosulfone derivative **366** showed interesting activity with acceptable potency against CDK2 (IC_{50} (4 h) = 117 nM). From previous results with compound **323**, which did not appear to exhibit time-dependent inhibition in the biological assay, but showed covalent binding to CDK2 in the structural biology study, the β-ketosulfone **366** would be a good candidate for further analysis to determine its binding mode. This compound would be particularly interesting as it should react specifically with amines (*e. g.* Lys89) over water and would, therefore, solve the problem of stability of the vinyl sulfone warhead towards hydration.

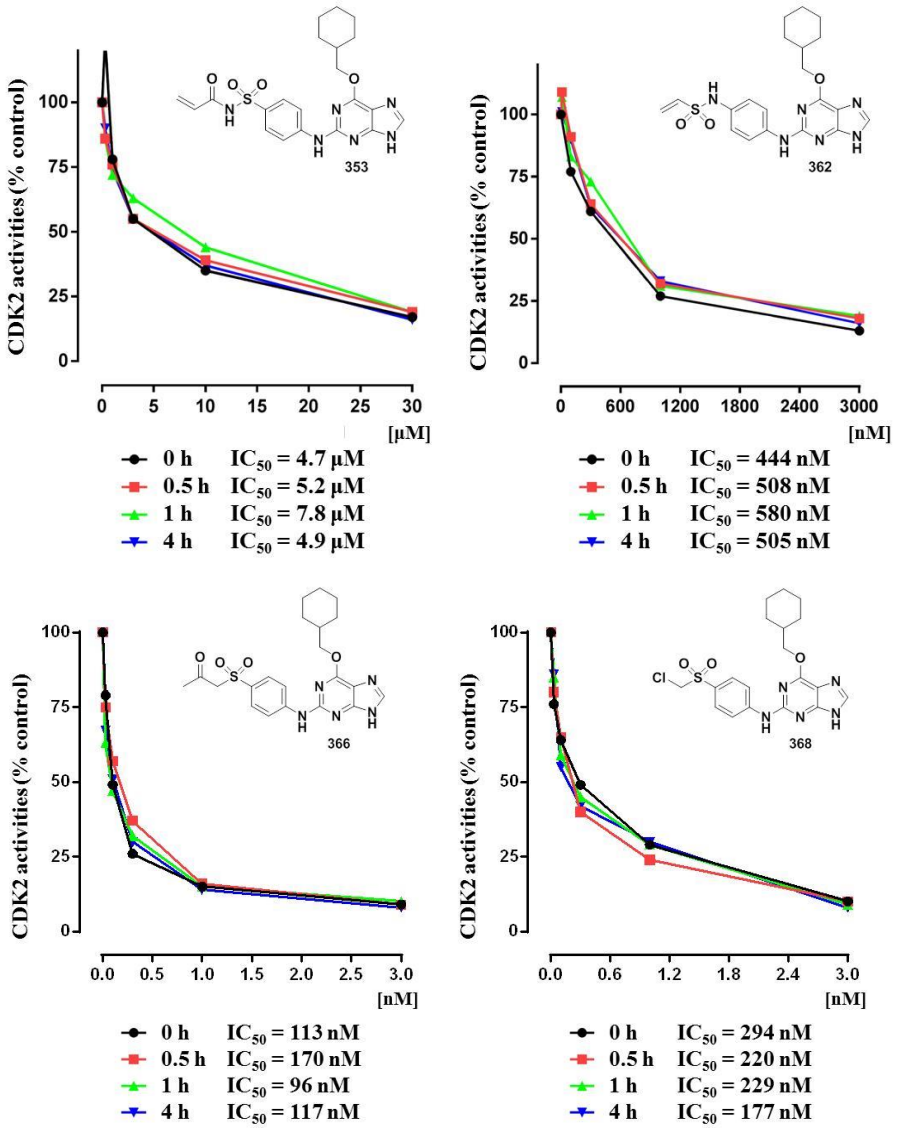

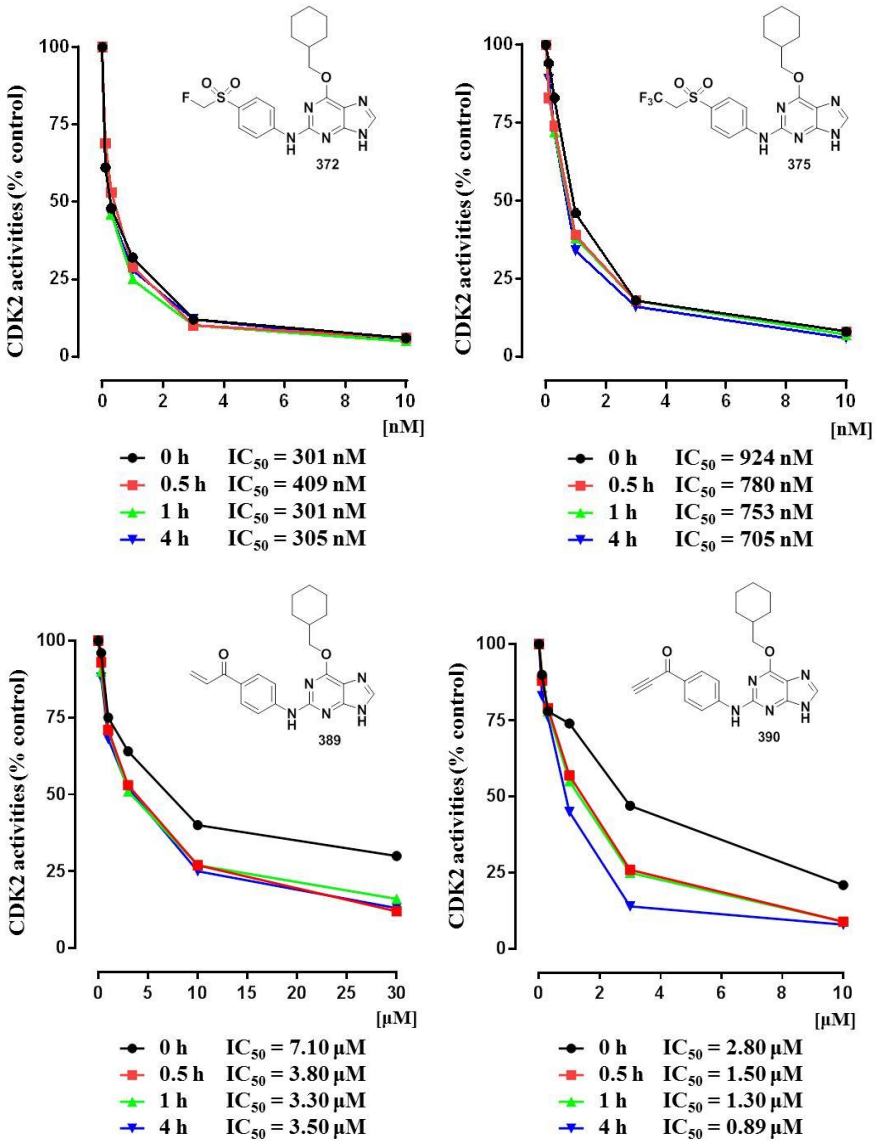

Figure 108 - Time-dependent inhibition profile of compounds **353**, **362**, **366**, **368**, **372**, **375**, **389** and **390** against CDK2

The α-halosulfone compounds, **368** and **372**, were found to be moderate inhibitors of CDK2 with an ATP-competitive inhibition profile (IC_{50} (4 h) = 177 nM and IC_{50} (4 h) = 305 nM, respectively). These compounds may not be sufficiently reactive for nucleophilic attack from Lys89, or, alternatively, Lys89 is positioned too far from the electrophile. The trifluoromethyl analogue **375** did not exhibit good CDK2-inhibitory activity (IC_{50} (4 h) = 705 nM), presumably reflecting the poor reactivity of this electrophilic group. Vinyl ketone **389** was designed to assess the importance of the sulfone group in the vinyl sulfone warhead of compound **60**. Surprisingly, compound **389** was found to be only weakly potent against CDK2 with a ~55-fold drop in potency (IC_{50} (4 h) = 3.5 µM) by comparison with compound **60**. Results obtained for vinyl ketone **389** showed the importance of the sulfone group and its interaction with Asp86. The sulfone

group can be postulated to orientate the vinyl moiety in the right position for attack from Lys89. Compound **390** was synthesised as an analogue of compound **389**. A loss of potency was observed by comparison with compound **60** (IC_{50} (4 h) = 0.89 μM), which can be attributed to the loss of interaction with Asp86 of CDK2. However, activities were shown to decrease with time with an initial potency of 2.80 μM that changed to 0.89 μM after 4 h. This observation suggests that compound **390** may have reacted covalently with CDK2, but slowly due to the reactivity of its electrophilic warhead (i.e. ethynyl ketone). This observation needs, however, to be considered carefully as the experiment was conducted only once and therefore, only structural biology studies could give further details on the binding mode of compound **390**.

Compounds synthesised in Chapters 5 and 7 were tested for their CDK2 inhibitory activity by Lan-Zhen Wang under the supervision of Professor Herbie Newell in the Biology Laboratory of the Northern Institute for Cancer Research, Newcastle upon Tyne, UK.

Chapter 9. Covalent Inhibition of CDK2: Beyond Purines

In this chapter, with the irreversible inhibition of CDK2 being at an early stage, modifications of known CDK2 inhibitors were investigated, by introducing appropriately positioned electrophilic warheads, such as a vinyl sulfone, to target Lys89. To achieve such modifications, the selected CDK2 inhibitors required a position on the molecule suitable for functionalisation, which would enable a potential interaction with Lys89. Non-covalent inhibition of CDK2 has been extensively studied over the past two decades (see *Chapter 2*, section 2.3.3.) but only one covalent inhibitor of CDK2 (**60**) has been reported to date. Modification of the electrophilic vinyl sulfone warhead of **60** has been investigated (see *Chapters 5*, *6* and *8*). The vinyl sulfone warhead was found to be common feature of protease inhibitors[249-251] but quite rare in kinase inhibitors,[252] rendering this group attractive in the design of new covalent CDK2 inhibitors.

9.1. Modification of the potent pyrazole inhibitor 391

The sulfonamide **391** is a potent CDK2 inhibitor (0.3 nM), whereas its piperidine analogue **392** demonstrated only modest activity by comparison (0.14 μM),[253,84] emphasing the importance of the sulfonamide group. Interactions between the pyrazole ring of compound **392** and the hinge region of CDK2 were highlighted in the crystal structure (*Figure 109*), with the piperidine ring pointing towards the specificity pocket where Lys89 is positioned. The difference in potency between inhibitors **391** and **392** was attributed to additional interactions between the sulfone of compound **391** and a neighbouring residue (Asp86), and to the substituents on the aromatic ring (Cl (**391**) vs F (**392**)) interacting with the ribose pocket.

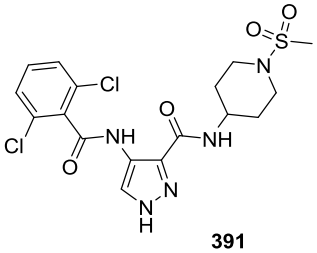

391

IC_{50} (CDK2) = 0.3 nM

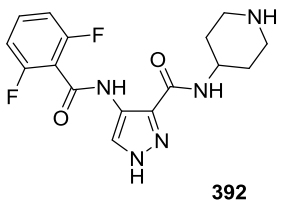

392

IC_{50} (CDK2) = 0.14 uM

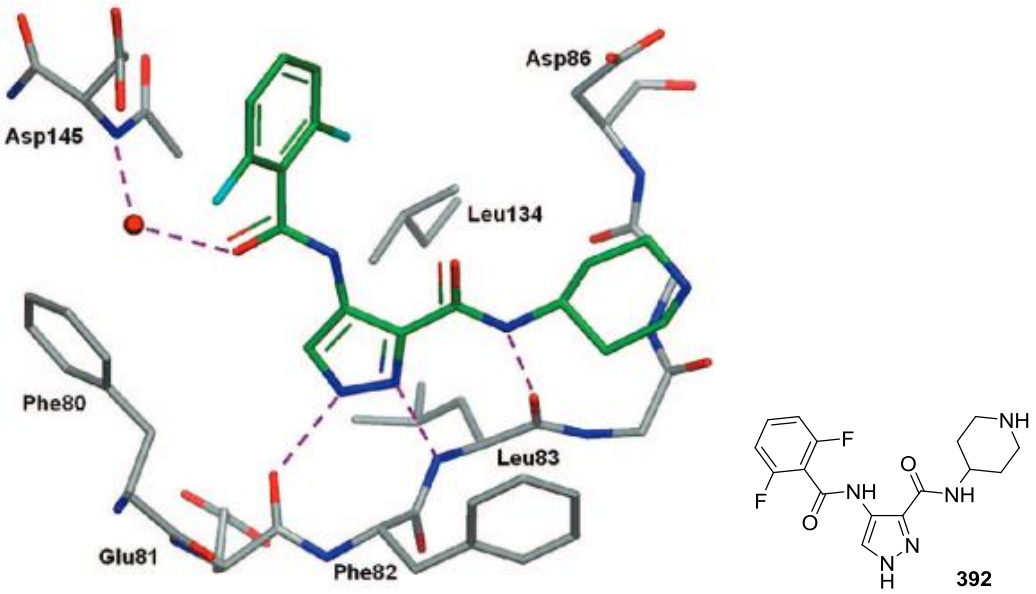

Figure 109- Co-crystal structure of inhibitor **392** within the ATP-binding pocket of CDK2.[84] The PDB entry is 2VTQ.

Insertion of a vinyl sulfone group on the *N*-piperidine of **391** was the obvious modification to generate a potential covalent inhibitor. As only the crystal structure of compound **392** in complex with CDK2 was available, two models were created with Discovery Studio Visualizer[254] (Accelrys) where the *N*-piperidine of pyrazole **392** was functionalised with either a vinyl sulfone (**393**) (*Figure 110*) or a vinyl ketone (**394**) group (*Figure 111*).

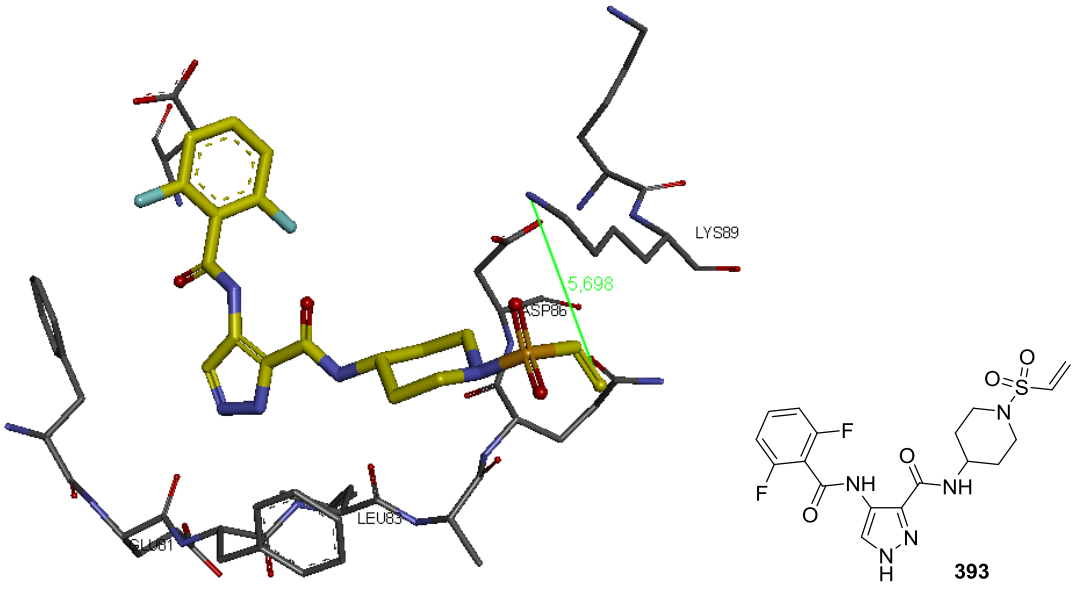

Figure 110 - Model structure of compound **393** with CDK2 created with Discovery Studio Visualizer showing the distance between Lys89 and the vinyl sulfonamide warhead

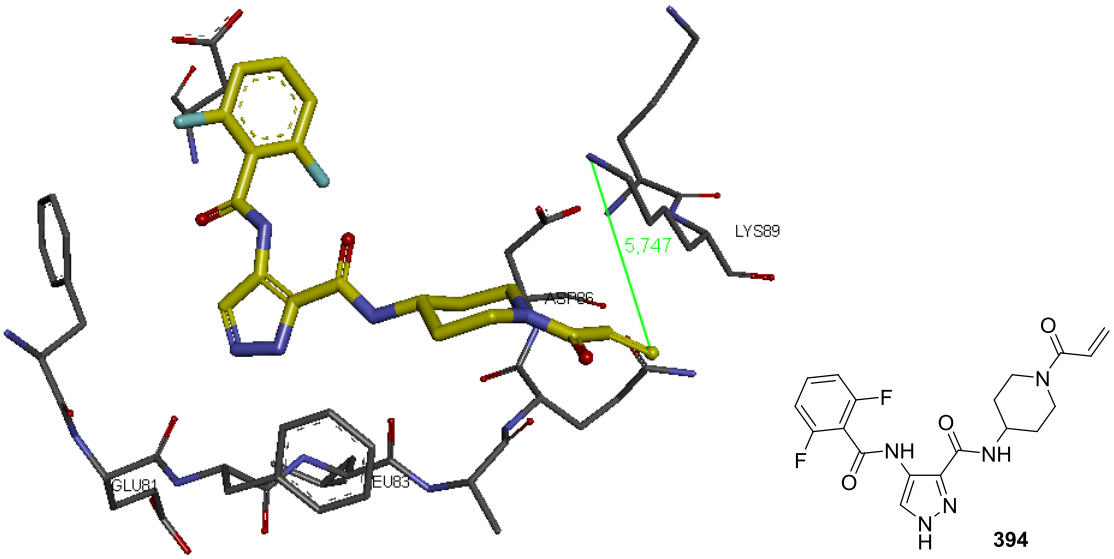

Figure 111 - Model structure of compound **394** with CDK2 created with Discovery Studio Visualizer showing the distance between Lys89 and the acrylamide warhead.

Both models suggested that the Lys89 was too far from the electrophilic site (~ 5.7 Å). However, it is important to note that the flexibility of Lys89 (highlighted in Chapter 6) may facilitate proximation of the two groups for covalent modification to occur. The models supported the potential for introducing an electrophile on the *N*-piperidino motif, and therefore, both the vinyl sulfone (**395**) and vinyl ketone (**396**) groups were added to the inhibitor **391**, which showed higher potency than compound **392** against CDK2.

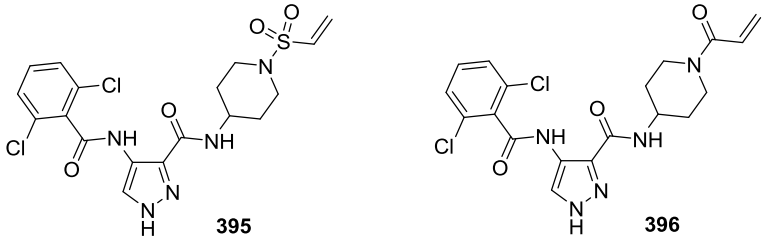

9.1.1. Covalent analogues of the pyrazole CDK2 inhibitor 391

The common intermediate **401** for the generation of **395** and **396** was synthesised in four steps following a literature procedure[84] (*Scheme 112*), including two amide couplings. Pyrazole **401** was then reacted with either 2-chloroethanesulfonyl chloride or acryloyl chloride to give the vinyl sulfonamide **395** and the acrylamide derivative **396**, respectively (*Scheme 113*).

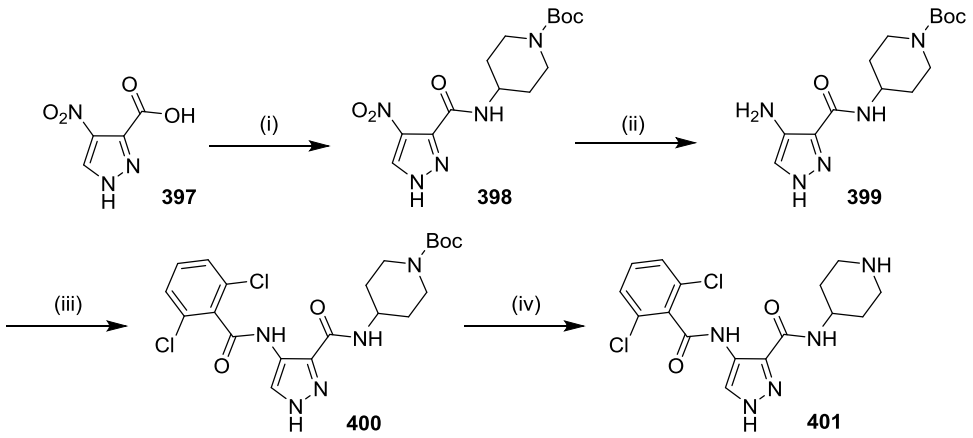

Scheme 112 - R*eagents and conditions*: (i) 4-amino-1-boc-piperidine, HOAt, EDCI.HCl in DMF, r.t., 18 h; (ii) Pd/C, H_2 in MeOH/DMF (5:1), 40 °C, 18 h, 36% (over 2 steps); (iii) 2,6-dichlorobenzoic acid, HOAt, EDCI.HCl in DMF, r.t., 18 h, 62%; (iv) in TFE, MW, 160 °C, 4 h, 61%.

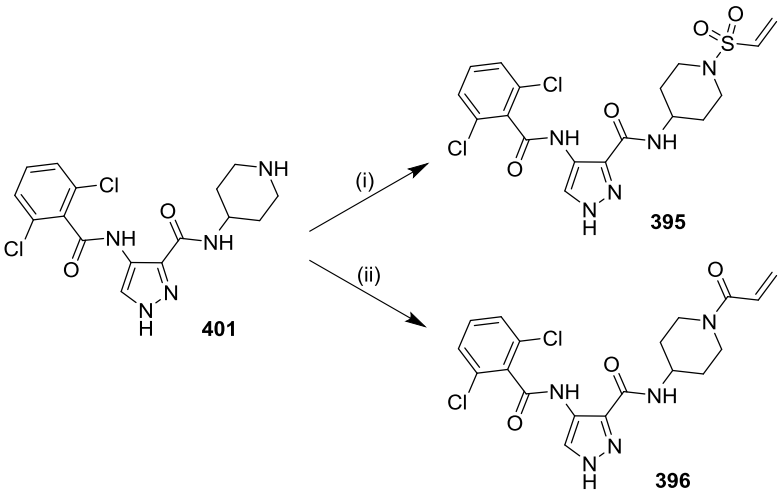

Scheme 113 - R*eagents and conditions*: (i) 2-chloroethanesulfonyl chloride, DIPEA in DCM, r.t., 15 min, 34%; (ii) acryloyl chloride, DIPEA in THF, 0 °C, 1 h, 53%.

9.1.2. Biological results of the new covalent CDK2 inhibitors, 395 and 396

Compounds **395** and **396** were designed from the highly potent CDK2 inhibitor **391**, with the objective of achieving covalent inhibition of CDK2. Both inhibitors were assessed in the kinetic assay against CDK2. The vinyl sulfonamide **395** showed extremely good activity against CDK2 and was found to be equipotent with compound **391** (*Figure 112*). Activities were found to increase with time, from 0.44 nM at 0 h to 0.20 nM at 4 h. These results suggest that compound **395** might react covalently with CDK2 but very rapidly. Further investigations, including structural biology, would be required on compound **395** as it could be a selective, potent and covalent inhibitor of CDK2.

Compound **396** exhibited an ATP-competitive behavior with good potency but with a 30-fold drop in activity compared to compound **391** (*Figure 112*). This decrease of activity could be attributed to a loss of interaction with Asp86, possible when a sulfone group is present on the molecule (*e.g.* compound **395**).

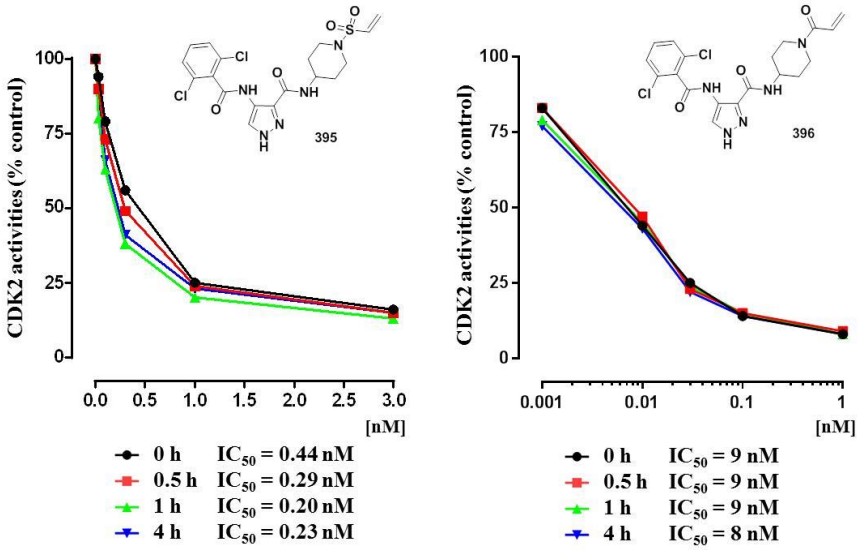

Figure 112 – Results of the kinetic assay against CDK2 for compounds **395** and **396**

Both compounds **395** and **396** were tested for their CDK2 inhibitory activity by Lan-Zhen Wang under the supervision of Professor Herbie Newell in the Biology Laboratory of the Northern Institute for Cancer Research, Newcastle upon Tyne, UK.

9.2. Modification of the CDK2 inhibitor dinaciclib (45)

Dinaciclib (**45**) is a potent inhibitor of CDKs 1, 2, 5 and 9 (IC_{50} = 3, 1, 1 and 4 nM, respectively –Chapter 2). The compound has been shown to interact with the hinge region of CDK2 *via* two H-bonds with Leu83 (*Figure 113*). The piperidine moiety occupies the ribose pocket and the pyridine *N*-oxide is orientated towards the solvent region, interacting with Lys89 in its protonated form to create a salt interaction.[162] It was interesting to note the interaction with the protonated form of Lys89, as the neutral form of the same residue reacts covalently with the vinyl sulfone purine **60**.

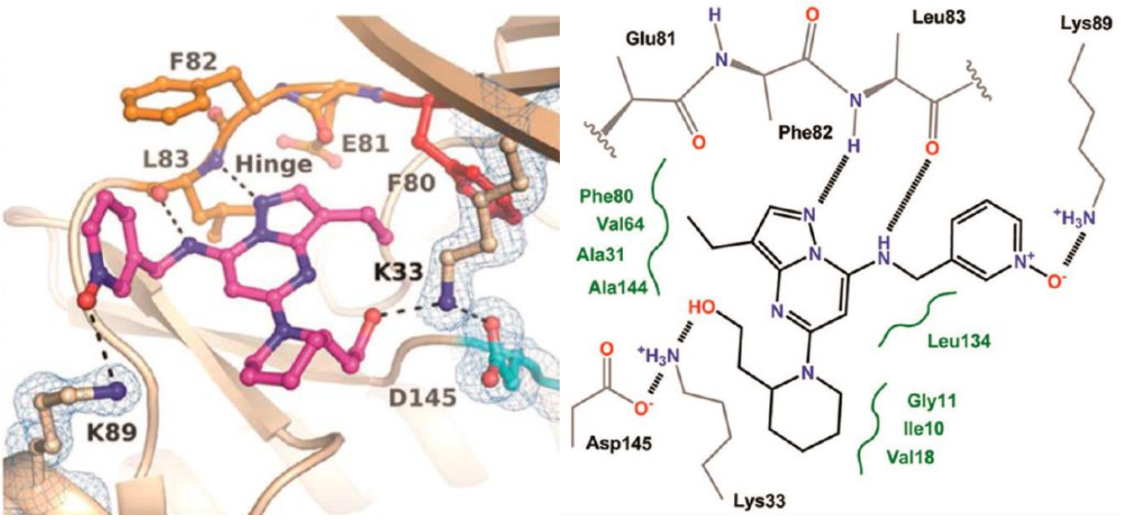

Figure 113 – Interactions between dinaclib (**45**) and the ATP-binding domain of CDK2.[162] The PDB entry is 3QXP.

The example of dinaciclib taken with the results obtained through modifications of **60**, highlighted the versatility of Lys89, a mobile residue that can interact with inhibitors as a nucleophile (Michael addition on **60**) or as a H-bond donor (dinaciclib). Lys89 was a residue offering flexibility in the design of CDK2 inhibitors and selectivity over CDK4 and 6, which have a Thr residue at this position. From the crystal structure of dinaciclib (**45**) in complex with CDK2, a vinyl sulfone was modelled at the pyridine *N*-oxide position using Discovery Studio Visualizer (Accelrys). From the model (*Figure 114*), Lys89 would be ~4.0Å from the electrophilic vinyl group of **402**, but would be closer to the sulfone group, suggesting that a H-bond interaction could be preferred over Michael addition.

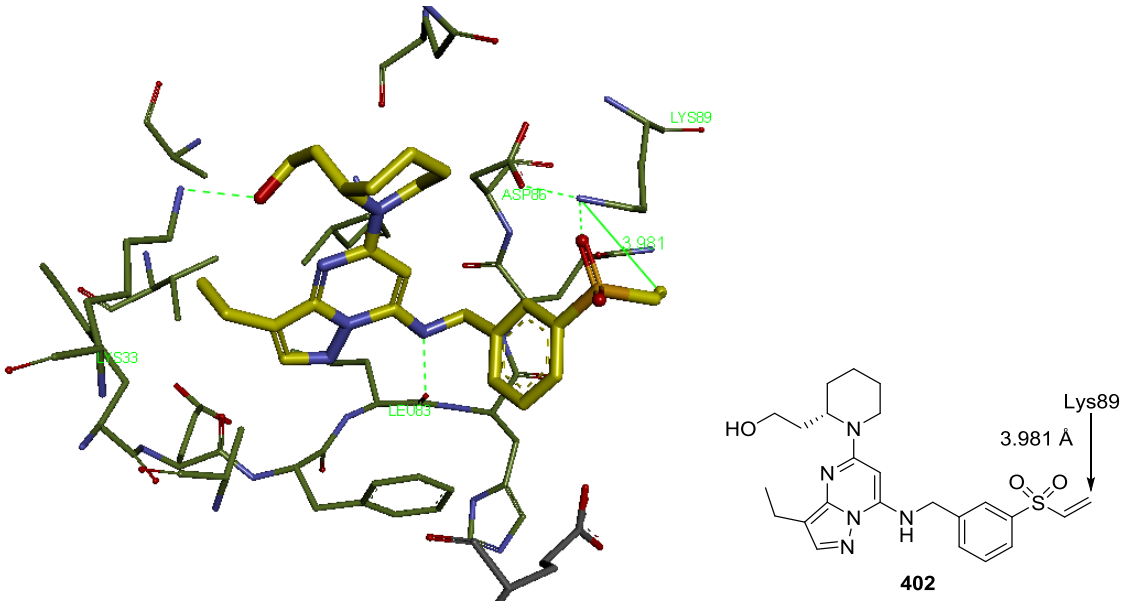

Figure 114 –Model structure of **402**, having a *meta*-vinyl sulfone group, showing possible interactions with CDK2

The vinyl sulfone warhead was also modelled at the *ortho*-position of the phenyl ring of dinaciclib (*Figure 115*). From the model, Lys89 would be situated ~0.7Å from the vinyl group and the sulfone of the warhead would interact with Asp86. Both models offered two attractive targets but in the interests of time, a synthetic route was developed only for target **403**.

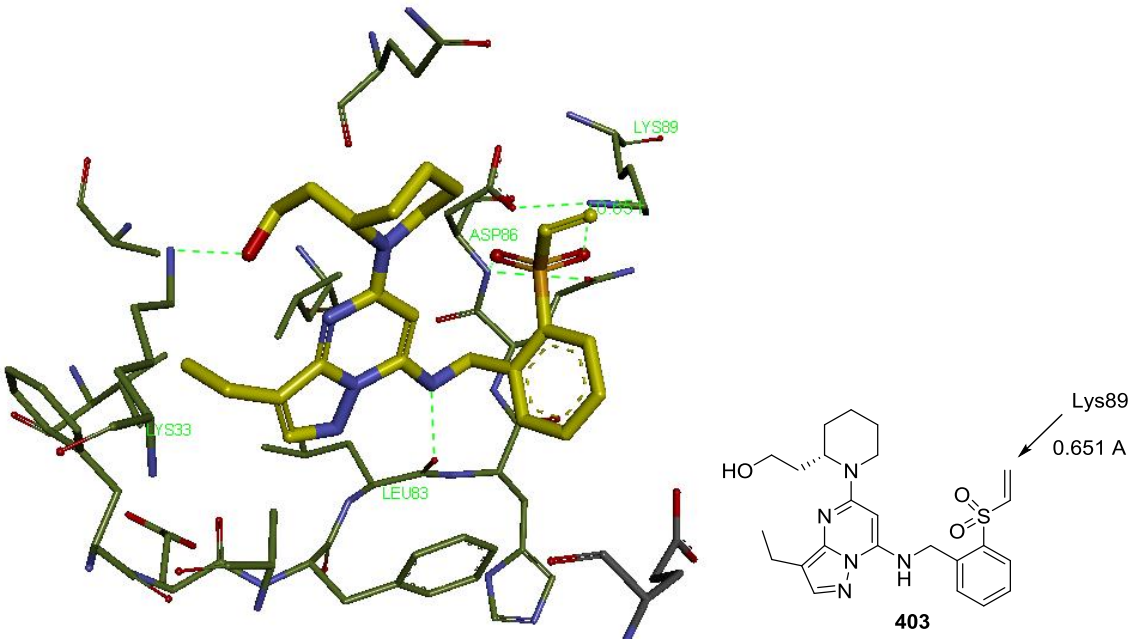

Figure 115 - Model structure of **403**, having an *ortho*-vinyl sulfone group, illustrating the possible interaction with CDK2

A similar synthetic route to dinaciclib (**45**) was considered for the synthesis of **403**, with initial preparation of the heterocyclic core **414**, which could then be functionalised by the

benzylamine **409** and the piperidine moiety. The synthesis of the benzylamine **409** started with the formation of the methyl ester **405** from the benzoic acid **404** (*Scheme 114*). The ester was converted into the corresponding amide **406**,[255] which was alkylated at the thiol group of **406**. A low yield was obtained for these two steps, probably due to the instability of intermediate **406** to oxidation. Oxidation of sulfide **407** gave compound **408**. Simultaneous reductions of the methyl ester and the amide moieties of intermediate **408** were attempted using $LiAlH_4$ but led to the isolation of an unknown compound in poor yield. The selective reduction of the ester into the alcohol should be first investigated followed by the reduction of the amide group to obtain the desired benzylamine **409**.

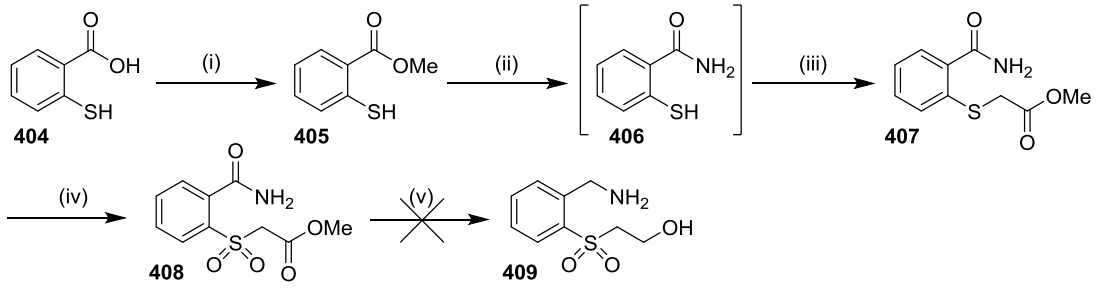

Scheme 114 - R*eagents and conditions*: (i) H_2SO_4 in MeOH, reflux, 48 h, 89%; (ii) formamide, 25% wt/wt NaOMe in MeOH in DMF, 70 ^oC then 110 ^oC, 2 h; (iii) ethyl chloroacetate, Et_3N in DCM, 13% over 2 steps; (iv) *m*-CPBA in DCM, r.t., 3 h, 73%; (v) $LiAlH_4$ in THF, r.t., 16 h.

The synthesis of the heterocyclic core started with the formation of the 3-aminopyrazole **412**. Deprotonation of butyronitrile **410** for reaction with ethyl formate was performed successfully with LiHMDS, as with potassium *t*-butoxide no reaction was observed (*Scheme 115*), to afford 3-aminopyrazole **412** in good yield. This intermediate was then reacted with dimethyl malonate to give compound **413**. The next step would be aromatisation and chlorination of compound **413** to give intermediate **414**. Consecutive nucleophilic aromatic substitutions on **414** would offer the intermediate **416**. Mesylation followed by elimination would give the target vinyl sulfone **403**. However, owing to time limitations, further work on this target was not undertaken.

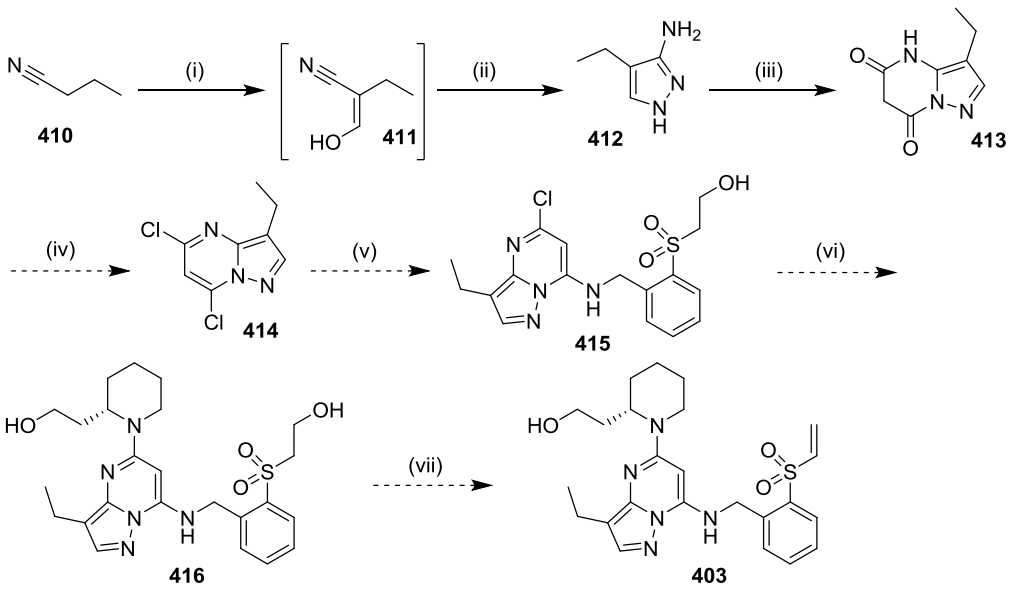

Scheme 115 - R*eagents and conditions*: (i) LiHMDS, ethyl formate in THF, -78 ^{o}C, 30 min; (ii) $N_2H_4.H_2O$, AcOH in EtOH, 80 ^{o}C, 40 h, 54%; (iii) dimethyl malonate, NaOH in MeOH, 65 ^{o}C, 16 h, 74%; (iv) $POCl_3$, *N*,*N*-dimethylaniline, reflux; (v) $K_3PO_4.H_2O$, **409** in water/MeCN, reflux; (vi) Na_2CO_3, (S)-piperidine-2-ethanol in water/NMP, 150 ^{o}C; (vii) MsCl, Et_3N in DCM, r.t. then DBU.

Chapter 10. Conclusions and Future Work

Interest in covalent inhibitors has emerged in the past few years and therefore, tool compounds are required to contribute to the understanding of the value of covalent binding in drug discovery. This thesis has been dedicated to the design and synthesis of purine-based covalent inhibitors of the mitotic kinases, Nek2 and CDK2.

In the Nek2 project, the synthesis of control compounds was described aiming to confirm the presence of an off-target activity of the 6-ethylnylpurine series by perturbing the main interactions with Nek2, namely the covalent binding between Cys-22 and the 6-ethynyl group, and the triplet of H-bonds with the hinge region. With the 6-cyanopurine **65**, the possibility of Michael addition was removed, thus diminishing activity against Nek2. Perturbing both the covalent binding and the triplet of H-bonds with **66** and **67** abolished the Nek2 inhibitory activity. To synthesise the N^7-methyl-6-cyanopurine derivative (**67**), a selective and high yielding one-pot procedure was developed which allowed for the selective *N*-7 methylation of various purines and represented an improvement to existing methods. The covalent binding of the inhibitors was shown to be essential for activity against Nek2 as illustrated by the N^9-methyl-6-ethynyl derivative **63** which retained activity. The N^7-methyl derivative **64**, while inactive against Nek2 in the enzymatic assay, was found to be potent in the cellular assay. Disconnections between the enzymatic and cellular results of the 6-ethynylpurine series were established and confirmed the presence of an off-target activity.

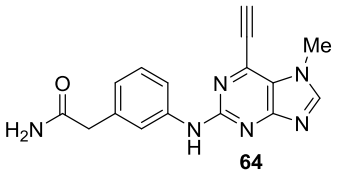

64

A small library of N^7-methyl-6-ethynylpurines was synthesised with the objective of abolishing cellular activity (*i.e.* off-target activity) by modifying the 2-aryl group. The NH parent of such compounds would potentially be selective inhibitors of Nek2. All the compounds prepared in this series demonstrated activity in cells, suggesting that the off-target activity was still present.

The reactivity of 6-ethynylpurines was further investigated by ^{1}H qNMR using a model reaction mimicking the addition of Cys-22 to the 6-ethynyl group. These studies highlighted the high reactivity of N^7-methyl-6-ethynylpurines (**62** and **64**) by comparison

with their N^9-methyl and NH analogues, which was attributed to a buttressing effect of the N^7-methyl group on the 6-ethynyl moiety and a steric strain relief phenomenon.

Efforts in the CDK2 project were focussed on modulating the chemical reactivity of the vinyl sulfone warhead without affecting the potency or the covalent binding mode of the inhibitor **60**, the first irreversible inhibitor of CDK2. Insertion of substituents on the vinyl sulfone was aimed at improving the chemical stability of compound **60** towards hydration. Several α-substituted vinyl sulfone analogues (**162**-**168**) were prepared and assessed in a time-dependent assay against CDK2. The corresponding 2-hydroxyalkyl derivatives were synthesised for screening for CDK2 inhibitory activity and as reference standards for future HPLC stability studies on the vinyl sulfone inhibitors. Compounds bearing an α-alkyl/aryl group (**162**-**166**) demonstrated ATP-competitive behaviour in the enzymatic kinetic assay. In this series, only the α-methyl group (**162**) was tolerated from the activity obtained against CDK2. α-Electron-withdrawing groups (**167**, **168**) were investigated but the chemistry in this series was challenging, highlighting the difficulties of synthesising highly functionalised molecules of this type. The compound bearing an α-fluoro group (**168**) showed ATP-competitive behaviour while the best time-dependent inhibition profile was obtained for the inhibitor bearing an α-chloro group (**167**). At the α-position of the vinyl, only a chloro group seemed to maintain the time-dependent inhibition of CDK2, suggesting potential covalent binding, while other groups have shown loss of time-dependent inhibition. The chloro derivative **167** should be co-crystallised with CDK2 to confirm the presence of the covalent bond as an α-chloro vinyl sulfone would represent a novel electrophilic warhead.

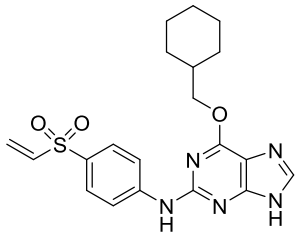

60

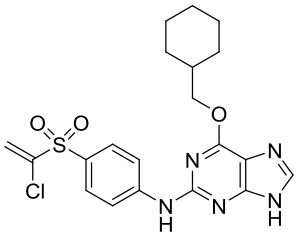

167

The β-position of the vinyl moiety was briefly explored by insertion of a methyl group alone (**323**) and in combination with other groups at the α-position (**333**, **339** and **349**). All the compounds in this series showed ATP-competitive behaviour in the kinetic assay. Interestingly, disubstitution of the vinyl function was not tolerated, as exemplified by compound **339**, bearing an α-chloro and a β-methyl group, which lost the excellent time-dependent inhibition profile and potency exhibited by the α-chloro vinyl sulfone

compound **167**. The corresponding 2-hydroxyalkyl derivatives were also assessed against CDK2 and revealed similar potency to their corresponding vinyl sulfone analogues. Structural biology studies were performed on selected vinyl sulfone inhibitors (**162**, **163** and **323**) with the objective of understanding their binding mode with CDK2. Substitution at the α-position was not tolerated for covalent binding, while insertion of a β-methyl group (**323**) was shown to be tolerated with the presence of a covalent bond between Lys89 and the modified vinyl sulfone group. Following these results, further investigation of the β-position should be carried out. These results highlighted the limits of the biological assay, which can only be used for the identification of potential covalent inhibitors for structural biology studies. Crystal structure of the 2-hydroxyalkyl derivative **184** with CDK2 revealed a similar binding mode to the corresponding vinyl sulfone analogue, explaining the similar activity observed for the pair of inhibitors.

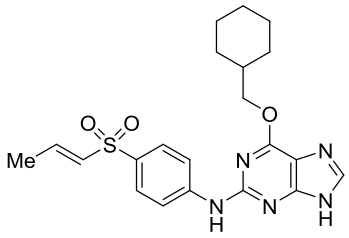

323

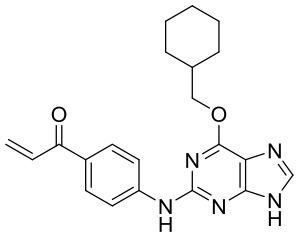

389

The vinyl sulfone group of compound **60** was replaced by other potential electrophilic warheads to assess the importance of both the vinyl and sulfone groups. All the inhibitors prepared in this series demonstrated ATP-competitive inhibitory activity in the kinetic assay with the exception of the ethynyl ketone **390**, which showed modest activity against CDK2 but with evidence for time-dependent inhibition. In addition, the β-ketosulfone **366** seemed to retain activity against CDK2. Further analyses of compounds **366** and **390** by structural biology to elucidate their binding mode would be interesting. Another interesting observation from this series of compounds was the 55-fold reduction in activity observed when the sulfone group was replaced by a ketone (compound **389**), demonstrating the crucial importance of the sulfone for activity. The sulfone presumably interacts with Asp86 placing the vinyl group in the perfect position for attack of Lys89, crucial for covalent binding. To date, the best replacement of the vinyl sulfone warhead of **60** is the α-chlorovinyl sulfone group (**167**) which showed a remarkable time-dependent inhibition profile with a potency relatively modest at time zero, suggesting improved chemical stability. However, each inhibitor has only been tested once, so biological evaluation should be repeated to confirm the observations made so far. To investigate further the potential of the vinyl sulfone group as an electrophilic warhead and

its use on other scaffolds and in other projects, chemical stability studies of the most promising compounds (**167** and **323**) would need to be assessed.

With the objective of expanding the investigation of covalent inhibition of CDK2 and the use of the vinyl sulfone warhead, a potent ATP-competitive CDK2 inhibitor (**391**), developed by Astex Pharmaceuticals, was modified with the aim of inhibiting CDK2 covalently. The vinyl sulfonamide **395** was found to be equipotent with the parent compound **391** and possibly exhibited a modest time-dependent inhibition profile. Further analysis by structural biology is required as this compound could potentially represent a selective and extremely potent covalent inhibitor of CDK2.

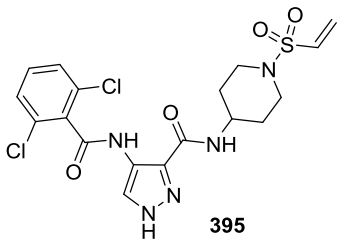

395

Chapter 11. Experimental

11.1 Synthesis

Chemicals and Solvents

All commercial reagents were purchased from Aldrich Chemical Company, Alfa Aesar, or Lancaster Synthesis Ltd. The chemicals were of the highest available purity. Unless otherwise stated, chemicals were used as supplied without any further purification. Anhydrous solvents were obtained from AcroSealTM or Aldrich (SureSealTM bottles) and were stored under nitrogen. Petrol refers to the fraction with a boiling range between 40 and 60 °C.

Chromatography

Thin layer chromatography utilised to monitor reaction progress was conducted on plates pre-coated with Si F_{254}, NH_2 F_{254s} or RP-18 F_{254s}. The eluent was as stated (where this consisted of more than one solvent, the ratio is stated as volume: volume) and visualisation was either by ultraviolet light. 'Flash' column chromatography was carried out at medium pressure using a Varian automated purification system with pre-packed silica cartridges or Biotage KP-NH cartridges. When stated, compounds were purified via semi-preparative HPLC on an Agilent 1200 Modular Preparative HPLC system using an ACE 5 Phenyl 150 x 21.2 mm column.

Analytical techniques

Melting points were determined using a VWR Stuart SMP40 apparatus and are uncorrected. ^{1}H, ^{19}F and ^{13}C nuclear magnetic resonance (NMR) spectra were obtained as either $CDCl_3$ or MeOD or DMSO-d_6 solutions and recorded at 500 MHz, 470 MHz and 125 MHz, respectively, on a Bruker Avance III 500 spectrometer. Chemical shifts are reported in parts per million (δ) referenced to the appropriate deuterated solvent employed and relative to tetramethylsilane. Multiplicities are indicated by s (singlet), d (doublet), t (triplet), q (quartet), m (multiplet), b (broad) or combinations thereof. Liquid Chromatography – Mass Spectrometry (LC-MS) was carried out on a Waters Acquity UPLC system, with a Waters SQD ESCi source using an Acquity UPLC BEH C18 1.7 μm, 2.1 x 50 mm column with a flow rate of 0.6 mL/min. The mobile phase used was 0.1% aq. formic acid in MeCN. Fourier Transform Infrared (FTIR) spectra were recorded on a Bio-Rad FTS 3000MX diamond ATR as a neat sample. Ultraviolet (UV) absorption data

were obtained using a U-2001 Hitachi Spectrophotometer with the sample dissolved in ethanol. High resolution mass spectrometry was performed by the EPSRC National Mass Spectrometry Service, University of Wales, Swansea, Singleton Park, Swansea, SA2 8PP.

Microwave Assisted Synthesis

Reactions were heated under microwave irradiation in sealed vessels using the Biotage Initiator Sixty with robotic sample bed. Reactions were irradiated at 2.45 GHz to reach temperatures up to 250 ^{o}C at a rate of 2-5 ^{o}C/sec and pressures up to 20 bars.

11.2 Biological Evaluation

Compounds subjected to biological evaluation were obtained with a purity higher than 95%, determined by HPLC, using a Waters XSELECT CSH C18 3.5um 100 x 4.6 mm column, in basic (0.1% aq. ammonia in MeCN) and acidic (0.1% aq. formic acid in MeCN) conditions.

Compounds synthesised within the Nek2 project were tested for their Nek2 inhibitory activity by Kathy Boxall, Sam Burns, Yvette Newblatt and Maura Westlake under the supervision of Dr Wynne Aherne in the Analytical Screening and Technology Laboratory of the CR UK Centre for Cancer Therapeutics, The Institute of Cancer Therapeutics, Sutton, Surrey, UK, SM2 5NG. Inhibitory potencies are reported as half maximal inhibitory concentrations (IC_{50}) or percentage of inhibition. Assays were performed in the presence of 30 μM ATP, 1 μM 'peptide 11' substrate (5-FAM-KKLNRTLSVA-COOH) and 4 nM Nek2, using a microfluidic Caliper methodology.

Compounds synthesised within the CDK2 project were tested for their CDK2 inhibitory activity by Lan-Zhen Wang under the supervision of Professor Herbie Newell in the Biology Laboratory of the Northern Institute for Cancer Research, Newcastle upon Tyne, UK. The kinase assay was started with addition of the inhibitor (3 μL of a 10 mM diluted solution from a 100 mM stock solution) to the reaction mix, prepared by mixing CDK2/cyclin A (10 μL, 1 mg/mL) and histone H1 (150 μL, 5 mg/mL solution) in buffer (500 μL containing Tris (50 mM) and $MgCl_2$ (5 mM)). After incubation for 30 min at 0 ^{o}C, ATP (5 μL from a solution containing [^{32}P] ATP and cold ATP at a final concentration of 12.5 μM) was added. The reaction mixture was spotted on an appropriate filter. After stirring in 1% phosphoric acid solution, the filtrates were washed and transferred to scintillation vials containing 5 mL of scintillation liquid. Radioactivity was measured in a scintillation counter.

11.3 Structural Biology Experimental

Protein Expression and Purification

The pre-prepared pGEX-6P-1 vector (containing GST-CDK2 and GST-CIV1 coding sequences) and pET plasmids (containing cyclin A or CDK2) were transformed into *E. coli* strain B834/Lys-S (Novagen). CDK2 and cyclin A were grown separately in BL21 star (DE3) chemically competent cells (Invitrogen), in 500 mL cultures of Luria Broth (LB) media containing 50 μg/mL ampicillin. Cells expressing CDK2/CIV1 were grown at 37 ^{o}C until an optical density at 600 nm (OD_{600}) of 0.8-0.9 was reached. The temperature of the culture was then dropped to 20 ^{o}C as rapidly as possible and the cells were left for a further 50 min to equilibrate. Expression of CDK2 and CIV1 as GST fusion proteins was induced by the addition of 0.1 mM isopropyl β-D-1-thiogalactopyranoside (IPTG) and cells were then grown for 20-24 h at 20 ^{o}C, to ensure complete phosphorylation of CDK2 by CIV1.

The culture containing bacteria for the expression of cyclin A was grown at 37 ^{o}C to an OD_{600} of 0.5-0.6. The temperature was then reduced to 25-30 ^{o}C and the cells were left for a further 30 min to equilibrate. Cyclin A was expressed following induction with 0.1 mM IPTG and grown for another 20-24 h at 20 ^{o}C.

Cells were harvested by centrifugation (4 ^{o}C, 20 min, 4000 x g, Beckman JLA8.1 rotor) and the pellet was resuspended in 20 mL of ice-cold modified HBS with one protease inhibitor tablet (Rochecor), fast frozen in dry ice and stored at – 80 ^{o}C until further use.

As soon as thawing was apparent, RNase A (200 μL of 100 mg/mL stock), lysozyme (400 μL of 25 mg/mL stock), DNAase I (200 μL of 2 mg/mL stock) and 1M $MgCl_2$ (200 μL) were added. Once the pellets started to defreeze, they were sonicated at 0 ^{o}C (30% amplitude, 15 s on, 45 s off for 3.2 min total sonication time). The suspension was centrifuged (4 ^{o}C, 1 h, 25,000 g, Beckman JA25.50 rotor) and the supernatant obtained was removed from the pellet and stored on ice. Supernatant from CDK2/CIV1 culture was gently mixed with supernatant from cyclin A culture (ratio of 0.5: 1 CDK2: cyclin A). The mixed supernatant was purified on pre-equilibrated glutathione affinity column (glutathione Sepharose 4B, bed volume 2 mL). Proteins were cleaved from GST using 3C protease (50: 1 protein: 3C by weight) overnight at 4 ^{o}C, and purified using size-exclusion chromatography (GE Healthcare HiLoad 26/60 Superdex 75 column). The collected fractions containing the fusion protein CDK2/cyclin A were analysed by SDS-PAGE, combined and loaded onto a fresh pre-equilibrated glutathione affinity column

(glutathione Sepharose 4B, bed volume 2 mL) to remove any GST dimer left. The pure fusion protein was concentrated to 11 mg/mL and fast frozen in dry ice.

Polyacrylamide Gel Electrophoresis

SDS-PAGE was used for protein identification and semi-quantitative analysis. Pre-cast 12 well, 16% acrylamide gels (RunBlue) were used with SDS run buffer (RunBlue). Samples were mixed with SDS loading buffer (RunBlue) and denatured at 100 ^{o}C for 5 min before being loaded onto the gel. PageRuler pre-stained protein ladder (170-10 kDa, Thermo Scientific) was used as molecular weight marker. Electrophoresis was run at 175 V and gels were stained with Coomassie quick stain.

Protein concentrations were determined using UV absorbance at 280 nm using Nanodrop 2000 (Thermo Scientific). Extinction coefficients were calculated based upon amino acid content using Protparam.[256]

Protein Preparation for Crystallography

Purified CDK2-cyclin A protein (11 mg/mL) was incubated with the appropriate inhibitor (1 mM in DMSO) for 1 h before crystallisation trays were set up in 2-subwell 96 well plates using the sitting drop vapour diffusion method. Protein mixture and reservoir were pipetted into the subwells in a 1:1 and 1:2 protein: reservoir ratio using a Mosquito robot (100 nL drops). Plates were sealed and stored in the Rigaku Minstrel tray hotel at 4 ^{o}C until crystal formation (up to 4 weeks). Crystals were transferred into a solution of 70% crystallant and 30% cryoprotectant (ammonium sulfate or sodium sulfate), stored in liquid nitrogen and shipped to the Diamond Light Source, Oxford, UK.

11.4. General Procedures

General procedure A: Removal of TIPS protecting group from 6-triisopropylsilyl ethynylpurines

The desired 6-((triisopropylsilyl)ethynyl)-9*H*-purin-2-amine (0.90 mmol) was dissolved in THF (10 mL) and TBAF (1M in THF, 1.10 mmol) was added. The solution was stirred at r.t. for 5 min and scavenger beads were added. The magnetic stirrer was removed and the reaction transferred into a conical flask. The reaction was then agitated with a shaker overnight. The solvent was removed *in vacuo* and the crude mixture was purified as indicated.

General procedure B: *N*-9 methylation of purines

The desired 9*H*-purine (5.80 mmol) and K_2CO_3 (11.60 mmol) were suspended in anhydrous DMF (15 mL) under N_2. Methyl iodide (7.00 mmol) was added and the resulting solution was stirred at r.t. overnight. The solvent was removed *in vacuo* and the crude product was purified as indicated.

General procedure C: Selective *N*-7 methylation of N^9-PMB protected purines

The desired 9*H*-purine-6-carbonitrile (0.16 mmol) and trimethyloxonium tetrafluoroborate (0.16 mmol) were solubilised in TFE (2 mL) under N_2. The resulting solution was stirred at r.t. for 2 h. The reaction was purged with nitrogen, sealed and heated (microwave irradiation) at 100 °C. The solvent was removed *in vacuo* and the crude product was purified as indicated.

General procedure D: Sonogashira coupling on 6-chloropurines

The desired 6-chloropurine (5.80 mmol), $Pd(PPh_3)_2Cl_2$ (0.10 mmol) and Cu(I)I (0.10 mmol) were solubilised in anhydrous THF (30 mL) under N_2. Triisopropylsilyl acetylene (6.40 mmol) and Et_3N (14.50 mmol) were added. The resulting suspension was purged with N_2 during 15 min. The reaction was stirred at r.t. overnight resulting in a colour change from yellow to dark brown. The suspension was filtered through Celite and the solvent was removed *in vacuo.* The crude product was purified as indicated.

General procedure E: Nucleophilic aromatic substitution of 2-fluoropurines using TFA in TFE

2-Fluoro-6-((triisopropylsilyl)ethynyl)-9*H*-purine (1.90 mmol) was dissolved in TFE (12 mL). The appropriate aniline (3.80 mmol) and TFA (0.7 mL) were added. The reaction was purged with N_2 and sealed. The solution was heated at 140 °C for 30 min in the microwave reactor. The solvent was removed *in vacuo*. The residue obtained was resuspended in EtOAc (10 mL) and extracted with sodium carbonate (10 mL), brine (10 mL) and water (10 mL). The organic layers were combined, dried over $MgSO_4$, and the solvent was removed *in vacuo*. The crude mixture was purified as indicated.

General procedure F: Amide formation from the corresponding carboxylic acid

Thionyl chloride (23.80 mmol) was added dropwise to a stirred solution of the desired phenylacetic acid (19.90 mmol) in anhydrous MeOH (60 mL) under N_2. The solution was stirred at r.t. for 2 h. The solvent was removed *in vacuo* and aqueous ammonia (10 mL)

was added to the residue obtained. The resulting solution was stirred at r.t. for 1 h. The reaction was quenched with 4M HCl until a neutral pH was reached. Water was removed *in vacuo* and the product was purified as indicated.

General procedure G: Iodination of 2-aminopurines

Isoamyl nitrite (12.60 mmol) was added to a suspension of the desired 2-amino-9*H*-purine-6-carbonitrile (4.00 mmol), diiodomethane (12.60 mmol) and Cu(I)I (4.00 mmol) in anhydrous THF (50mL) under N_2. The reaction was stirred at reflux for 4 h and filtered through Celite. The solvent was removed *in vacuo* and the crude product was purified as indicated.

General procedure H: Zinc reduction of nitro groups to amines

The compound (2.26 mmol) was solubilised in MeOH (10 mL) and acetic acid (10 mL). Zinc powder (22.60 mmol) was added and the reaction was stirred at 50 °C for 2 h. The mixture was filtered through Celite and the solvent was removed *in vacuo*. The crude mixture was purified as indicated.

General procedure I: Buchwald cross coupling reaction on a 2-iodopurine

The appropriate 2-iodopurine (0.45 mmol) was dissolved in anhydrous MeCN (15 mL) under N_2. The desired compound (0.68 mmol), K_2CO_3 (0.91 mmol), $Pd(dba)_2$ (0.01 mmol) and XPhos (0.01 mmol)) were added. The solution was heated at 80 °C for 18 h. The solution was filtered through Celite and the solvent was removed *in vacuo*. The crude mixture was purified as indicated.

General procedure J: S_N2 reaction with 4-nitrothiophenol

The desired electrophile (21.3 mmol) was added to a stirred solution of 4-nitrothiophenol (19.4 mmol) and Et_3N (21.3 mmol) in anhydrous DCM (50 mL) at 0 °C, under N_2. The resulting solution was stirred for 1 h. After completion, the solution was diluted with DCM (50 mL) and washed with brine (3 x 50 mL). The organic layer was dried over $MgSO_4$ and the solvent was removed *in vacuo*. The crude product was purified as indicated.

General procedure K: Hydrolysis of esters under basic conditions

LiOH (2M in THF, 26.6 mL) was added to the solution of the appropriate ester (4.82 mmol) in THF (9.5 mL). The reaction was stirred for 2 h at 70 ^oC. After completion, the

reaction mixture was quenched with 4M HCl solution until a pH of 4 was reached. The resulting mixture was extracted with EtOAc (3 x 50 mL). The organic layers were combined and dried over $MgSO_4$. The solvent was removed *in vacuo* to afford the desired acid.

General procedure L: Reduction of acids using borane

1M Borane in complex with THF (13.1 mmol) was added dropwise to a stirred solution of the appropriate acid (2.61 mmol) in dry THF (30 mL) under N_2. The reaction was heated at 50 °C overnight. A saturated aqueous solution of $NaHCO_3$ (20 mL) was added dropwise at 0 °C. The mixture was extracted with EtOAc (3 x 30 mL). The organic layers were combined and dried over $MgSO_4$. The solvent was removed *in vacuo.* The crude product was purified as indicated.

General procedure M: Oxidation of sulfides with *m*-CPBA

The appropriate sulfide (4.41 mmol) was solubilised in DCM (50 mL). *m*-CPBA (9.25 mmol) was added at 0 °C and the resulting solution was stirred at 0 °C for 1 h. A saturated aqueous solution of Na_2CO_3 (50 mL) was added and the reaction was extracted with DCM (3 x 50 mL). The organic layers were combined and dried over $MgSO_4$. The solvent was removed *in vacuo.* The crude product was purified as indicated.

General procedure N: Cope elimination

The appropriate β-pyrrolidine sulfone (0.13 mmol) was solubilised in dry DCM (10 mL) under N_2. *m*-CPBA (0.15 mmol) and Cs_2CO_3 (0.33 mmol) were added to the solution and the mixture was stirred at r.t. for 30 min. The solvent was removed *in vacuo*. The product was purified as indicated.

General procedure O: Reduction of esters and ketones using DIBAL

The appropriate ester or ketone (7.81 mmol) was solubilised in dry THF (15 mL) under N_2 and cooled to 0 °C. A solution of DIBAL (1M in hexanes, 11.7 mL) was added slowly to the solution. The mixture was stirred at 0 °C for 2 h. After completion, MeOH (5 mL) was added dropwise followed by aqueous HCl (1M solution, 20 mL). The organic phase was extracted with EtOAc (3 x 30 mL) and the combined extracts were dried over $MgSO_4$. The solvent was removed *in vacuo*. The crude product was purified as indicated.

General procedure P: Formation of a vinyl sulfone moiety using methanesulfonyl chloride

The appropriate 2-hydroxyalkyl compound (0.60 mmol) was solubilised in dry DCM (6 mL) under N_2. Et_3N (0.90 mmol) and $MeSO_2Cl$ (0.90 mmol) were added. The resulting solution was stirred at r.t. for 1 h. Brine (5 mL) was added and the organic phase was extracted with DCM (3 x 5 mL). The organic layers were combined, dried over $MgSO_4$ and the solvent was removed *in vacuo*. The product was purified as indicated.

General procedure Q: One-pot reaction for the conversion of a 2-hydroxyalkyl compound to a β-pyrrolidino sulfone

The appropriate 2-hydroxyalkyl compound (5.19 mmol) was solubilised in dry DCM (30 mL) under N_2. Et_3N (7.79 mmol) and benzenesulfonyl chloride (7.79 mmol) were added to the solution. The reaction was stirred at r.t. for 18 h. Pyrrolidine (25.97 mmol) was added and the reaction was stirred for 1 h at r.t. The resulting mixture was washed with brine (3 x 50 mL). The combined organic layers were dried over $MgSO_4$ and the solvent was removed *in vacuo.* The crude product was purified as indicated.

General procedure R: ^{1}H qNMR experiment

N-Acetylcysteine methyl ester **157** (7.48 mg, 42 µmol) was added to a solution of the desired 6-ethynylpurine in DMSO-d_6 (690 µL from a stock solution in DMSO-d_6 containing 4.2 µmol of purine). The temperature was maintained at approximatively 24 °C using a water bath. A solution of DMSO-d_6 (10 µL) containing DABCO (0.14 mg, 1.26 µmol) and DMF (0.33 µL, 4.2 µmol) was added to afford a final 6-ethynylpurine concentration of 6 mM in a total volume of 700 µL. The NMR tube was inverted quickly to mix the reagents and inserted into the spectrometer cavity which was maintained at 24.0 ± 0.1 ^{o}C. The acquisition of ^{1}H qNMR data was immediately initiated. The time between the addition of the DABCO/DMF-solution and the completion of the first ^{1}H qNMR experiment was monitored for accuracy. Subsequent time intervals between experiments were calculated based on the defined parameters.

6-Ethynyl-9-methyl-*N*-phenyl-9*H*-purin-2-amine (61)[137]

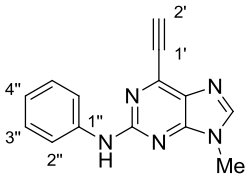

The title compound was synthesised following **general procedure A** using 9-methyl-*N*-phenyl-6-((triisopropylsilyl)ethynyl)-9*H*-purin-2-amine **73** (360 mg, 0.90 mmol) and TBAF (1M in THF, 1.10 mL, 1.10 mmol). The crude product was purified by MPC on silica (petrol: EtOAc 1: 1) to give the product **61** as a pale yellow solid (124 mg, 0.50 mmol, 56 %).

R_f 0.13 (petrol: EtOAc 1: 1); Mp = 246-248 °C; UV λ_{max} (EtOH) 261 nm; IR (cm^{-1}) 3300, 3264, 3086, 3045, 2360, 1590, 1545, 1497, 1438; ^{1}H NMR (500 MHz, DMSO-d_6) (ppm) δ 3.76 (3H, s, NCH_3), 4.85 (1H, s, H-2'), 6.96 (1H, t, *J* = 7.5 Hz, H-4''), 7.30 (2H, dd, *J* = 7.5 and 7.5 Hz, H-3''), 7.85 (2H, d, *J* = 7.5 Hz, H-2''), 8.26 (1H, s, H-8), 9.79 (1H, s, NH); ^{13}C NMR (125 MHz, DMSO-d_6) (ppm) δ 29.3 (CH_3), 78.9 (C-1'), 87.2 (C-2'), 118.3 (C-2''), 121.0 (C-4''), 128.5 (C-3''), 128.9 (C_q), 139.7 (C_q), 140.7 (C_q), 145.3 (C-8), 153.4 (C_q), 156.1 (C_q); HRMS calcd for $C_{14}H_{12}N_5$ $[M+H]^+$ 250.1087, found 250.1091.

6-Ethynyl-7-methyl-*N*-phenyl-7*H*-purin-2-amine (62)[137]

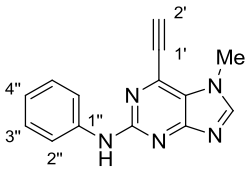

The title compound was synthesised following **general procedure A** using 7-methyl-*N*-phenyl-6-((triisopropylsilyl)ethynyl)-9*H*-purin-2-amine **75** (300 mg, 0.70 mmol) and TBAF (1M in THF, 0.90 mL, 0.90 mmol). The crude product was purified by MPC on silica (petrol: EtOAc 2: 3) to give the product **62** as a pale yellow solid (88 mg, 0.40 mmol, 47 %).

R_f 0.10 (petrol: EtOAc 1: 1); Mp = 261-263 °C; UV λ_{max} (EtOH) 271 nm; IR (cm^{-1}) 3300, 3280, 3190, 3130, 2360, 1590, 1560, 1494, 1439; ^{1}H NMR (500 MHz, DMSO-d_6) (ppm) δ 4.01 (3H, s, NCH_3), 5.00 (1H, s, H-2'), 6.92 (1H, t, *J* = 7.5 Hz, H-4''), 7.29 (2H, dd, *J* = 7.5 and 7.5 Hz, H-3''), 7.82 (2H, d, *J* = 7.5 Hz, H-2''), 8.46 (1H, s, H-8), 9.61 (1H, s, NH); ^{13}C NMR (125 MHz, DMSO-d_6) (ppm) δ 32.8 (CH_3), 78.2 (C-1'), 87.5 (C-2'),

118.0 (C-2''), 120.4 (C_q), 120.7 (C-4''), 128.4 (C-3''), 133.1 (C_q), 141.0 (C_q), 150.3 (C-8), 156.4 (C_q), 162.5 (C_q); HRMS calcd for $C_{14}H_{12}N_5$ $[M+H]^+$ 250.1087, found 250.1091.

2-(3-((6-Ethynyl-9-methyl-9*H*-purin-2-yl)amino)phenyl)acetamide (63)

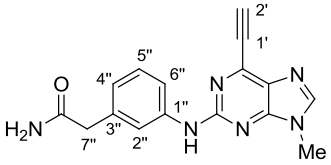

The title compound was synthesised following **general procedure A** using 2-(3-((6-ethynyl-9-methyl-9*H*-purin-2-yl)amino)phenyl)acetamide **76** (300 mg, 0.65 mmol) and TBAF (1M in THF, 0.80 mL, 0.80 mmol). The crude product was purified by MPC on silica (DCM: MeOH 19: 1) to give the product **63** as a pale yellow solid (124 mg, 0.50 mmol, 56 %).

R_f 0.63 (DCM: MeOH 9: 1); Mp = 233-235 °C; UV λ_{max} (EtOH) 271 nm; IR (cm^{-1}) 3410, 3270, 3190, 2105, 1650, 1598, 1553, 1521, 1444; ^{1}H NMR (500 MHz, DMSO-d_6) (ppm) δ 3.36 (2H, s, H-7''), 3.76 (3H, s, NCH_3), 4.84 (1H, s, H-2'), 6.85 (1H, d, *J* = 7.8 Hz, H-4''), 6.90 (1H, br s, NH_2), 7.21 (1H, dd, *J* = 7.8 and 7.8 Hz, H-5''), 7.46 (1H, br s, NH_2), 7.65 (1H, d, *J* = 7.8 Hz, H-6''), 7.82 (1H, s, H-2''), 8.25 (1H, s, H-8), 9.77 (1H, br s, NH); ^{13}C NMR (125 MHz, DMSO-d_6) (ppm) δ 29.3 (CH_3), 42.2 (C-7''), 78.9 (C-1'), 87.1 (C-2'), 116.5 (C-6''), 119.0 (C-2''), 122.0 (C-4''), 128.2 (C_q), 128.8 (C-5''), 136.7 (C_q), 139.8 (C_q), 140.6 (C_q), 145.2 (C-8), 153.3 (C_q), 156.1 (C_q), 172.2 (CO); HRMS calcd for $C_{16}H_{15}N_6O$ $[M+H]^+$ 307.1302, found 307.1308.

2-(3-((6-Ethynyl-7-methyl-7*H*-purin-2-yl)amino)phenyl)acetamide (64)

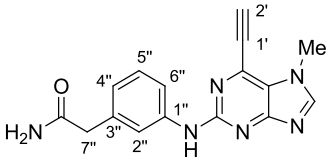

The title compound was synthesised following **general procedure A** using 2-(3-((6-ethynyl-9-methyl-9*H*-purin-2-yl)amino)phenyl)acetamide **77** (290 mg, 0.63 mmol) and TBAF (1M in THF, 0.80 mL, 0.80 mmol). The crude product was purified by MPC on silica (DCM: MeOH 19: 1) to give the product **64** as a pale yellow solid (40 mg, 0.10 mmol, 21 %).

R_f 0.65 (DCM: MeOH 9: 1); Mp = 216-218 °C; UV λ_{max} (EtOH) 273 nm; IR (cm^{-1}) 3299, 3190, 2107, 1663, 1593, 1564, 1495, 1469; ^{1}H NMR (500 MHz, DMSO-d_6) (ppm) δ 3.35 (2H, s, H-7''), 4.01 (3H, s, NCH_3), 4.99 (1H,s, H-2'), 6.85 (1H, d, *J* = 7.8 Hz, H-4''), 6.87 (1H, br s, NH_2), 7.21 (1H, dd, *J* = 7.8 and 7.8 Hz, H-5''), 7.44 (1H, br s, NH_2), 7.60 (1H, s, H-2''), 7.76 (1H, d, *J* = 7.8 Hz, H-6''),8.45 (1H, s, H-8), 9.57 (1H, br s, NH); ^{13}C NMR (125 MHz, DMSO-d_6) (ppm) δ 32.8 (CH_3), 48.6 (C-7''), 78.2 (C-1'), 87.5 (C-2'), 116.3 (C-6''), 119.0 (C-2''), 120.3 (C_q), 121.7 (C-4''), 128.2 (C-5''), 133.2 (C_q), 136.6 (C_q), 140.8 (C-8), 150.2 (C_q), 156.5 (C_q), 162.5 (C_q), 172.2 (CO); HRMS calcd for $C_{16}H_{15}N_6O$ $[M+H]^+$ 307.1302, found 307.1307.

2-(3-((6-Cyano-9*H*-purin-2-yl)amino)phenyl)acetamide (65)

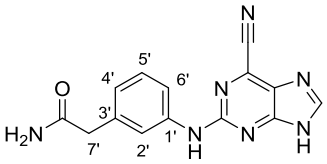

2-(3-((6-Cyano-9-(4-methoxybenzyl)-9*H*-purin-2-yl)amino)phenyl)acetamide **85** (110mg, 0.27 mmol) was solubilised in TFA (5 mL). The resulting solution was heated at 70 °C for 5 h. Then the solvent was removed *in vacuo*. The product was purified by MPC on silica (DCM: MeOH 19: 1) to give the product **65** as a yellow oil (30 mg, 0.10 mmol, 47%).

R_f 0.28 (DCM: MeOH 9: 1); UV λ_{max} (EtOH) 254 nm; IR (cm^{-1}) 3430, 3122, 2340, 1664, 1600, 1590, 1510, 1447; ^{1}H NMR (500 MHz, DMSO-d_6) (ppm) δ 3.36 (2H, s, H-7'), 6.89 (1H, br s, NH_2), 6.91 (1H, d, *J* = 7.8 Hz, H-4'), 7.24 (1H, dd, *J* = 7.8 and 7.8 Hz, H-5'), 7.45 (1H, br s, NH_2), 7.52 (1H, s, H-2'), 7.71 (1H, d, *J* = 7.8 Hz, H-6'), 8.48 (1H, s, H-8), 9.90 (1H, s, NH), 13.51 (1H, br s, N^9H); ^{13}C NMR (125 MHz, DMSO-d_6) (ppm) δ 42.4 (C-7'), 114.6 (C_q), 117.0 (C-6'), 119.8 (C-2'), 122.7 (C-4'), 126.7 (C_q),128.3 (C-5'), 136.8 (C_q), 140.0 (C-8), 150.1(C_q), 146.6 (C_q), 156.3 (CN), 172.1 (CO); HRMS calcd for $C_{14}H_{12}N_7O$ $[M+H]^+$ 294.1098, found 294.1103.

Note: One quaternary carbon was not visible on the ^{13}C NMR spectrum.

2-(3-((6-Cyano-9-methyl-9*H*-purin-2-yl)amino)phenyl)acetamide (66)

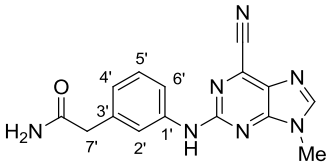

The title compound was synthesised following **general procedure B** using 2-(3-((6-cyano-9*H*-purin-2-yl)amino)phenyl)acetamide **65** (106 mg, 0.36 mmol), K_2CO_3 (60 mg, 0.43 mmol) and MeI (0.03 mL, 0.43 mmol). The crude product was purified by MPC on silica (DCM: MeOH 19: 1) to give the product **66** as a yellow solid (44 mg, 0.14 mmol, 40%).

R_f 0.55 (DCM: MeOH 9: 1); UV λ_{max} (EtOH) 266 nm; Mp = 207-209 °C; IR (cm^{-1}) 3430, 3122, 2340, 1664, 1600, 1590, 1510, 1447; ^{1}H NMR (500 MHz, DMSO-d_6) (ppm) δ 3.37 (2H, s, H-7'), 3.79 (3H, s, NCH_3), 6.90 (1H, br s, NH_2), 6.91 (1H, d, *J* = 7.8 Hz, H-4'), 7.25 (1H, dd, *J* = 7.8 and 7.8 Hz, H-5'), 7.47 (1H, br s, NH_2), 7.62 (1H, d, *J* = 7.8 Hz, H-6'), 7.78 (1H, s, H-2'), 8.48 (1H, s, H-8), 10.07 (1H, s, NH); ^{13}C NMR (125 MHz, DMSO-d_6) (ppm) δ 29.6 (NCH_3), 42.5 (C-7'), 114.3 (C_q), 117.0 (C-6'), 119.4 (C-2'), 122.8 (C-4'), 128.3 (C_q), 129.1 (C-5'), 136.9 (C_q), 139.9 (C_q), 148.2 (C_q), 154.8 (C_q), 156.2 (CN), 164.5 (C_q), 172.1 (CO); HRMS calcd for $C_{15}H_{14}N_7O$ $[M+H]^+$ 308.1254, found 308.1260.

2-(3-((6-Cyano-7-methyl-7*H*-purin-2-yl)amino)phenyl)acetamide (67)

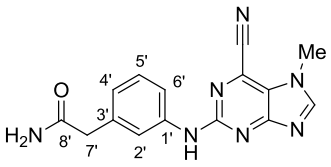

The title compound was synthesised following **general procedure C** using 2-(3-((6-cyano-9-(4-methoxybenzyl)-9*H*-purin-2-yl)amino)phenyl)acetamide **85** (67 mg, 0.16 mmol) and OMe_3BF_4 (24 mg, 0.16 mmol). The reaction was heated for 20 min at 100 °C. The crude product was purified by MPC on silica (DCM: MeOH 19: 1) to give the product **67** as a yellow solid (28 mg, 0.09 mmol, 56%).

R_f 0.55 (DCM: MeOH 9: 1); UV λ_{max} (EtOH) 254 nm; Mp = 259-261 °C; IR (cm^{-1}) 3390, 3190, 2364, 1669, 1611, 1560, 1493, 1390; ^{1}H NMR (500 MHz, DMSO-d_6) (ppm) δ 3.36 (2H, s, H-7'), 4.01 (3H, s, NCH_3), 6.89 (1H, br s, NH_2), 6.90 (1H, d, *J* = 7.8 Hz, H-4'), 7.24 (1H, dd, *J* = 7.8 and 7.8 Hz, H-5'), 7.46 (1H, br s, NH_2), 7.57 (1H, s, H-2'), 7.71 (1H,

d, J = 7.8 Hz, H-6'), 8.66 (1H, s, H-8), 9.86 (1H, s, NH); ^{13}C NMR (125 MHz, DMSO-d_6) (ppm) δ 32.3 (NCH_3), 42.4 (C-7'), 116.5 (C-6'), 119.2 (C-2'), 120.8 (C_q), 121.7 (C_q), 122.2 (C-4'), 123.1 (C_q), 128.1 (C-5'), 136.6 (C_q), 140.0 (C-8), 152.4 (C_q), 156.4 (CN), 163.9 (C_q), 171.9 (CO); HRMS calcd for $C_{15}H_{14}N_7O$ $[M+H]^+$ 308.1254, found 308.1259.

6-Chloro-2-fluoro-9*H*-purine (69)[257]

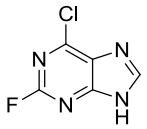

An aqueous solution of $NaNO_2$ (7.00 g, 107.2 mmol) was added dropwise over 20 min to a stirred solution of 2-amino-6-chloropurine **68** (9.00 g, 52.9 mmol) in tetrafluoroboric acid (140 mL) at 0 °C. The resulting mixture was allowed to warn to r.t. and was stirred overnight. The reaction was then cooled to 0 °C and neutralised with a saturated aqueous solution of Na_2CO_3 until reaching a pH of 7-8. The resulting mixture was extracted with EtOAc (4 x 250 mL). The solvent was removed *in vacuo* and the crude solid was purified by MPC on silica (DCM: MeOH 9: 1) to give the product **69** as an off white solid (4.60 g, 26.70 mmol, 50 %).

R_f 0.55 (DCM: MeOH 9: 1); Mp = 169-171 °C (lit.,[257] Mp = 161-162 °C); UV λ_{max} (EtOH) 271 nm; IR (cm^{-1}) 2900, 2780, 1580, 1480, 1250; ^{1}H NMR (500 MHz, DMSO-d_6) (ppm) δ 8.71 (1H, s, H-8), 14.10 (1H, s, N^9H); ^{13}C NMR (125 MHz, DMSO-d_6) (ppm) δ 128.1 (C_q), 147.5 (C-8), 148.6 (C_q), 156.0 (d, J = 212.1 Hz, C-2), 162.3 (C_q); ^{19}F NMR (470 MHz, DMSO-d_6) (ppm) δ -52.8; HRMS calcd for $C_5H_3ClFN_4$ $[M^{35}Cl+H]^+$ 173.0025, found 173.0024, $[M^{37}Cl+H]^+$ 175.0181, found 174.9994.

Mixture of 6-chloro-2-fluoro-9-methyl-9*H*-purine (70) and 6-chloro-2-fluoro-7-methyl-7*H*-purine (71)[137]

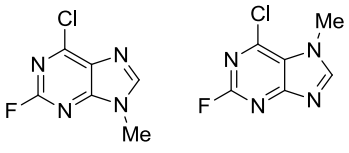

The title compounds were synthesised following **general procedure B** using 2-fluoro-6-chloropurine **69** (1.00 g, 5.80 mmol), K_2CO_3 (1.50 g, 11.6 mmol) and MeI (0.40 mL, 7.00 mmol). The crude product was purified by MPC on amine silica (DCM: MeOH 49: 1) to give the products **70** and **71** as an off white solid (1.00 g, 5.40 mmol, 92 %).

R_f 0.80 (DCM: MeOH 9: 1); IR (cm^{-1}) 3080, 1550, 1390, 1260; ^{19}F NMR (470 MHz, DMSO-*d*$_6$) (ppm) δ -52.9, -52.4;

6-Chloro-2-fluoro-9-methyl-9*H*-purine (**70**)

^1H NMR (500 MHz, DMSO-*d*$_6$) (ppm) δ 3.81 (3H, s, NCH_3), 8.64 (1H, s, H-8); LRMS calcd for $C_6H_5ClFN_4$ $[M^{35}Cl+H]^+$ 187.0, found 187.1, $[M^{37}Cl+H]^+$ 189.0, found 189.1.

6-Chloro-2-fluoro-7-methyl-7*H*-purine (**71**)

^1H NMR (500 MHz, DMSO-*d*$_6$) (ppm) δ 4.07 (3H, s, NCH_3), 8.79 (1H, s, H-8); LRMS calcd for $C_6H_5ClFN_4$ $[M^{35}Cl+H]^+$ 187.0, found 187.1, $[M^{37}Cl+H]^+$ 189.0, found 189.1.

Note: Not fully characterised as not pure.

6-Chloro-2-fluoro-9-methyl-9*H*-purine (70)

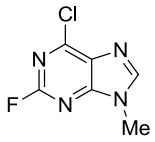

A mixture of 6-chloro-9-methyl-9*H*-purin-2-amine and 6-chloro-7-methyl-7*H*-purin-2-amine (**86**/**87**) (400 mg, 2.20 mmol) was solubilised in tetrafluoroboric acid (5 mL). The solution was cooled to 0 °C. $NaNO_2$ (300 mg, 4.36 mmol) in solution in water (2 mL) was added dropwise. The solution was then allowed to reach r.t. and was stirred for 1 h. After completion, the reaction mixture was cooled to 0°C and basified until reaching a neutral pH with a saturated aqueous solution of Na_2CO_3. The solution was extracted with EtOAc (3 x 10 mL). The organic layers were combined, dried over $MgSO_4$ and the solvent was removed *in vacuo*. The product was purified by MPC on silica (DCM: MeOH 19: 1) to give the product **70** as a colourless oil (200 mg, 1.10 mmol, 50%).

R_f 0.75 (DCM: MeOH 9: 1); UV λ_{max} (EtOH) 250 nm; IR (cm^{-1}) 3080, 1550, 1390, 1260; ^1H NMR (500 MHz, DMSO-*d*$_6$) (ppm) δ 3.82 (3H, s, NCH_3), 8.66 (1H, s, H-8); ^{13}C NMR (125 MHz, DMSO-*d*$_6$) (ppm) δ 30.2 (CH_3), 140.0 (d, *J* = 3.1 Hz, C_q), 150.0 (d, *J* = 18.2 Hz, C_q), 153.3 (C-8), 154 (d, *J* = 18.2 Hz, C_q), 156.0 (d, *J* = 213.7 Hz, C-2); ^{19}F NMR (470 MHz, DMSO-*d*$_6$) (ppm) δ -52.4; HRMS calcd for $C_6H_5ClFN_4$ $[M^{35}Cl+H]^+$ 187.0181, found 187.0181, $[M^{37}Cl+H]^+$ 189.0337, found 189.0339.

2-Fluoro-9-methyl-6-((triisopropylsilyl)ethynyl)-9*H*-purine (72)[137]

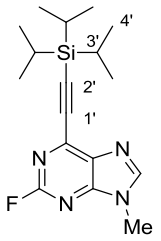

The title compound was synthesised following **general procedure D** using a mixture of 6-chloro-2-fluoro-9-methyl-9*H*-purine **70** and 6-chloro-2-fluoro-7-methyl-7*H*-purine **71** (1.00 g, 5.40 mmol), $Pd(PPh_3)_2Cl_2$ (75 mg, 0.10 mmol), Cu(I)I (21 mg, 0.10 mmol), triisopropylsilyl acetylene (1.33 mL, 5.90 mmol) and Et_3N (1.88 mL, 13.5 mmol). The crude product was purified by MPC on on silica (petrol: EtOAc 3: 2) to give the product **72** as a yellow solid (880 mg, 2.70 mmol, 49 %).

R_f 0.48 (petrol: EtOAc 3: 2); Mp = 114-116 °C; UV λ_{max} (EtOH) 255 nm; IR (cm^{-1}) 2940, 2870, 1580, 1460, 1420, 1260; ^{1}H NMR (500 MHz, DMSO-d_6) (ppm) δ 1.13-1.18 (21H, m, H-3' and H-4'), 3.80 (3H, s, NCH_3), 8.61 (1H, s, H-8); ^{13}C NMR (125 MHz, DMSO-d_6) (ppm) δ 10.5 (C-3'), 18.3 (C-4'), 29.8 (CH_3), 100.4 (C-1'), 102.2 (C-2'), 133.7 (d, J = 4.2 Hz, C_q), 140.2 (d, J = 18.1 Hz, C_q), 149.3 (C-8), 154.8 (d, J = 18.1 Hz, C_q), 157.0 (d, J = 210.6 Hz, C-2); ^{19}F NMR (470 MHz, DMSO-d_6) (ppm) δ 52.4; HRMS calcd for $C_{17}H_{26}FN_4Si$ $[M+H]^+$ 333.1905, found 333.1910.

9-Methyl-*N*-phenyl-6-((triisopropylsilyl)ethynyl)-9*H*-purin-2-amine (73)

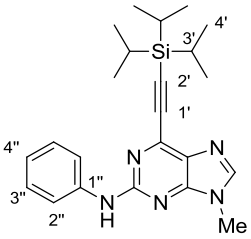

The title compound was synthesised following **general procedure E** using 2-fluoro-9-methyl-6-((triisopropylsilyl)ethynyl)-9*H*-purine **72** (880 mg, 2.60 mmol), aniline (0.70 mL, 5.30 mmol) and TFA (1.0 mL). The crude product was purified by MPC on amine silica (petrol: EtOAc 7: 3) to give the product **73** as a yellow oil (360 mg, 0.90 mmol, 34%).

R_f 0.41 (DCM: MeOH 19: 1); UV λ_{max} (EtOH) 275 nm; IR (cm^{-1}) 3240, 2940, 2860, 1590, 1580, 1540, 1440, 1390; ^{1}H NMR (500 MHz, $CDCl_3$) (ppm) δ 1.09-1.13 (21H, m, H-3'

and H-4'), 3.80 (3H, s, NCH_3), 7.03 (1H, t, *J* = 7.9 Hz, H-4''), 7.34 (2H, dd, *J* = 7.9 and 7.9 Hz, H-3''), 7.71 (1H, br s, NH), 7.72 (2H, d, *J* = 7.9 Hz, H-2''), 7.83 (1H, s, H-8); ^{13}C NMR (125 MHz, $CDCl_3$) (ppm) δ 11.2 (C-3'), 18.7 (C-4'), 29.6 (CH_3), 99.8 (C-1'), 100.5 (C-2'), 118.6 (C-2''), 122.2 (C-4''), 128.9 (C-3''), 129.3 (C_q), 139.8 (C_q), 143.6 (C-8), 153.6 (C_q), 156.2 (C_q); HRMS calcd for $C_{23}H_{32}N_5Si$ $[M+H]^+$ 406.2421, found 406.2420.

Note: One quaternary carbon was not visible on the ^{13}C NMR spectrum.

2-Fluoro-7-methyl-6-((triisopropylsilyl)ethynyl)-7*H*-purine (74)[137]

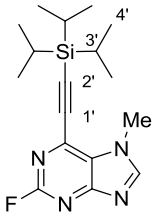

The title compound was synthesised following **general procedure D** using a mixture of 6-chloro-2-fluoro-9-methyl-9*H*-purine **70** and 6-chloro-2-fluoro-7-methyl-7*H*-purine **71** (1.00 g, 5.40 mmol), $Pd(PPh_3)_2Cl_2$ (75 mg, 0.10 mmol), Cu(I)I (21 mg, 0.10 mmol), triisopropylsilyl acetylene (1.33 mL, 5.90 mmol) and Et_3N (1.88 mL, 13.50 mmol). The crude product was purified by MPC on on silica (petrol: EtOAc 3: 2) to give the product **74** as a yellow solid (390 mg, 1.20 mmol, 22 %).

OR

The title compound was synthesised following **general procedure C** using 2-fluoro-9-(tetrahydro-2*H*-pyran-2-yl)-6-((triisopropylsilyl)ethynyl)-9*H*-purine (150 mg, 0.37 mmol) and OMe_3BF_4 (66 mg, 0.45 mmol). The crude product was purified by MPC on silica (petrol: EtOAc 3: 2) to give the product **74** as a yellow solid (51 mg, 0.15 mmol, 41%).

OR

The title compound was synthesised following **general procedure C** using 2-fluoro-9-(4-methoxybenzyl)-6-((triisopropylsilyl)ethynyl)-9*H*-purine **125** (110 mg, 0.25 mmol) and OMe_3BF_4 (45 mg, 0.30 mmol). The crude product was purified by MPC on silica (petrol: EtOAc 3: 2) to give the product **74** as a yellow solid (35 mg, 0.10 mmol, 42 %).

R_f 0.18 (petrol: EtOAc 3: 2); Mp = 97-99 °C; UV λ_{max} (EtOH) 310 nm; IR (cm^{-1}) 2940, 2870, 1560, 1460, 1430, 1295; ^1H NMR (500 MHz, DMSO-d_6) (ppm) δ 1.13-1.18 (21H, m, H-3' and H-4'), 4.11 (3H, s, NCH_3), 8.79 (1H, s, H-8); ^{13}C NMR (125 MHz, DMSO-

d$_6$) (ppm) δ 10.6 (C-3'), 18.3 (C-4'), 33.2 (CH_3), 99.9 (C-1'), 102.4 (C-2'), 124.7 (d, *J* = 4.4 Hz, C_q), 133.8 (d, *J* = 18.1 Hz, C_q), 153.4 (C-8), 157.0 (d, *J* = 207.5 Hz, C-2), 164.0 (d, *J* = 18.1 Hz, C_q); ^{19}F NMR (470 MHz, DMSO-*d*$_6$) (ppm) δ -52.58; HRMS calcd for $C_{17}H_{26}FN_4Si$ $[M+H]^+$ 333.1905, found 333.1911.

7-Methyl-*N*-phenyl-6-((triisopropylsilyl)ethynyl)-7*H*-purin-2-amine (75)[137]

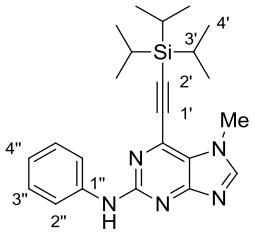

The title compound was synthesised following **general procedure E** using 2-fluoro-7-methyl-6-((triisopropylsilyl)ethynyl)-7*H*-purine **74** (390 mg, 1.20 mmol), aniline (0.30 mL, 2.40 mmol) and TFA (0.50 mL). The crude product was purified by prep-TLC (DCM: MeOH 19: 1) to give the product **75** as a yellow oil (300 mg, 0.70 mmol, 62%).

R_f 0.46 (DCM: MeOH 19: 1); UV λ_{max} (EtOH) 273 nm; IR (cm^{-1}) 3050, 2945, 2870, 1590, 1560, 1500, 1463, 1437; ^{1}H NMR (500 MHz, $CDCl_3$) (ppm) δ 1.10-1.14 (21H, m, H-3' and H-4'), 4.02 (3H, s, NCH_3), 6.93 (1H, t, *J* = 7.3 Hz, H-4''), 7.18 (1H, s, NH), 7.25 (2H, dd, *J* = 7.9 and 7.3 Hz, H-3''), 7.70 (2H, d, *J* = 7.9 Hz, H-2''), 7.89 (1H, s, H-8); ^{13}C NMR (125 MHz, $CDCl_3$) (ppm) δ 11.3 (C-3'), 18.6 (C-4'), 33.3 (CH_3), 100.6 (C-1'), 101.0 (C-2'), 118.4 (C-2''), 121.8 (C-4''), 128.9 (C-3''), 140.1 (C-8), 156.9 (C_q); HRMS calcd for $C_{23}H_{32}N_5Si$ $[M+H]^+$ 406.2421, found 406.2422.

Note: Four quaternary carbons were not visible on the ^{13}C NMR spectrum.

2-(3-((9-Methyl-6-((triisopropylsilyl)ethynyl)-9*H*-purin-2-yl)amino)phenyl) acetamide (76)

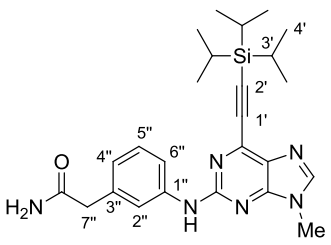

The title compound was synthesised following **general procedure E** using 2-fluoro-9-methyl-6-((triisopropylsilyl)ethynyl)-9*H*-purine **72** (330 mg, 1.00 mmol), 2-(3-aminophenyl)acetamide **79** (350 mg, 1.90 mmol) and TFA (0.40 mL). The crude product

was purified by prep-TLC (DCM: MeOH 19: 1) to give the product **76** as a yellow solid (200 mg, 0.40 mmol, 43%).

R_f 0.17 (DCM: MeOH 19: 1); Mp = 175-177 °C; UV λ_{max} (EtOH) 276 nm; IR (cm^{-1}) 3300, 3180, 2944, 2865, 1660, 1595, 1553, 1516, 1442, 1393; ^{1}H NMR (500 MHz, DMSO-d_6) (ppm) δ 1.14-1.19 (21H, m, H-3' and H-4'), 3.36 (2H, s, H-7''), 3.77 (3H, s, NCH_3), 6.85 (1H, d, *J* = 7.8 Hz, H-4''), 6.90 (1H, br s, NH_2), 7.20 (1H, dd, *J* = 7.8 and 7.8 Hz, H-5''), 7.45 (1H, br s, NH_2), 7.62 (1H, d, *J* = 7.8 Hz, H-6''), 7.91 (1H, s, H-2''), 8.24 (1H, s, H-8), 9.79 (1H, br s, NH); ^{13}C NMR (125 MHz, DMSO-d_6) (ppm) δ 10.6 (C-3'), 18.4 (C-4'), 29.3 (CH_3), 42.6 (C-7''), 98.1 (C-1'), 101.6 (C-2'), 116.5 (C-6''), 118.9 (C-2''), 121.9 (C-4''), 128.2 (C_q), 128.7 (C-5''), 136.7 (C_q), 140.0 (C_q), 140.6 (C_q), 145.1 (C-8), 153.3 (C_q), 156.0 (C_q), 172.2 (CO); HRMS calcd for $C_{25}H_{35}N_6OSi$ $[M+H]^+$ 463.2636, found 463.2634.

2-(3-((7-Methyl-6-((triisopropylsilyl)ethynyl)-7*H*-purin-2-yl)amino)phenyl) acetamide (77)

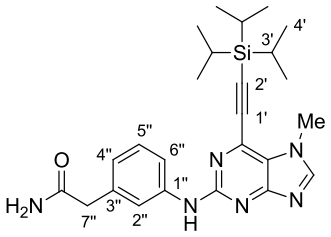

The title compound was synthesised following **general procedure E** using 2-fluoro-7-methyl-6-((triisopropylsilyl)ethynyl)-7*H*-purine **74** (330 mg, 1.00 mmol), 2-(3-aminophenyl)acetamide **79** (350 mg, 1.90 mmol) and TFA (0.40 mL). The crude product was purified by prep-TLC (DCM: MeOH 19: 1) to give the product **77** as a yellow oil (240 mg, 0.51 mmol, 52%).

R_f 0.76 (DCM: MeOH 9: 1); UV λ_{max} (EtOH) 276 nm; IR (cm^{-1}) 3300, 3180, 2944, 2940, 1672, 1605, 1567, 1497, 1464, 1389; ^{1}H NMR (500 MHz, DMSO-d_6) (ppm) δ 1.14-1.19 (21H, m, H-3' and H-4'), 3.38 (2H, s, H-7''), 4.03 (3H, s, NCH_3), 6.84 (1H, d, *J* = 7.8 Hz, H-4''), 6.87 (1H, br s, NH_2), 7.19 (1H, dd, *J* = 7.8 and 7.8 Hz, H-5''), 7.43 (1H, br s, NH_2), 7.68 (1H, s, H-2''), 7.74 (1H, d, *J* = 7.8 Hz, H-6''), 8.44 (1H, s, H-8), 9.61 (1H, br s, NH); ^{13}C NMR (125 MHz, DMSO-d_6) (ppm) δ 10.7 (C-3'), 18.4 (C-4'), 32.8 (CH_3), 42.1 (C-7''), 98.6 (C-1'), 101.0 (C-2'), 116.2 (C-6''), 119.0 (C-2''), 120.0 (C_q), 121.6 (C-4''), 128.1 (C-5''), 133.2 (C_q), 136.6 (C_q), 140.9 (C_q), 148.5 (C_q), 150.2 (C-8), 156.5 (C_q), 172.2 (CO); HRMS calcd for $C_{25}H_{35}N_6OSi$ $[M+H]^+$ 463.2636, found 463.2633.

2-(3-Aminophenyl)acetamide (79)[258]

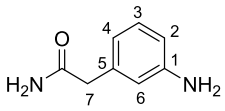

The title compound was synthesised following **general procedure F** using 3-aminophenylacetic acid **78** (3.00 g, 19.9 mmol) and $SOCl_2$ (1.70 mL, 23.8 mmol). The crude product was purified by MPC on silica (DCM: MeOH 19: 1) to give the product **79** as a pale yellow solid (1.23 g, 8.20 mmol, 41 %).

R_f 0.48 (DCM: MeOH 9: 1); Mp = 156-158 °C; UV λ_{max} (EtOH) 238 nm; IR (cm^{-1}) 3410, 3300, 3175, 1666, 1607, 1492, 1463, 1396; ^{1}H NMR (500 MHz, DMSO-d_6) (ppm) δ 3.19 (2H, s, H-7), 5.00 (2H, br s, NH_2), 6.40-6.42 (2H, m, H-2 and H-4), 6.47 (1H, s, H-6), 6.81 (1H, br s, NH_2), 6.92 (1H, dd, *J* = 7.7 and 7.7 Hz, H-3), 7.34 (1H, br s, NH_2); ^{13}C NMR (125 MHz, DMSO-d_6) (ppm) δ 42.6 (C-7), 112.0 (C-2), 114.6 (C-6), 116.6 (C-4), 128.6 (C-3), 136.9 (C_q), 148.4 (C_q), 172.4 (CO); HRMS calcd for $C_8H_{11}N_2O$ $[M+H]^+$ 151.0866, found 151.0863.

6-Chloro-9-(4-methoxybenzyl)-9*H*-purin-2-amine (80)[259]

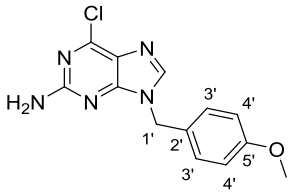

2-Amino-6-chloropurine **68** (6.00 g, 35.5 mmol) and Cs_2CO_3 (13.80 g, 42.6 mmol) were dissolved in anhydrous DMF (80 mL) under N_2. 4-Methoxybenzylchloride (6.00 mL, 42.6 mmol) was then added and the reaction was stirred at 60 °C overnight. The solvent was removed *in vacuo*. The residue obtained was resuspended in EtOAc (50 mL) and washed with brine (50 mL) and water (50 mL). The organic layer was dried over $MgSO_4$ and the solvent was removed *in vacuo*. The product was purified by MPC on silica (DCM: MeOH 19: 1) to give **80** the product as an off-white solid (6.10 g, 21.00 mmol, 60%).

R_f 0.64 (DCM: MeOH 9: 1); Mp = 176-178 °C; UV λ_{max} (EtOH) 310 nm; IR (cm^{-1}) 3440, 3208, 2830, 1614, 1560, 1514, 1244; ^{1}H NMR (500 MHz, DMSO-d_6) (ppm) δ 3.73 (3H, s, OCH_3), 5.21 (2H, s, H-1'), 6.91 (2H, d, *J* = 8.7 Hz, H-3'), 6.94 (2H, s, NH_2), 7.26 (2H, d, *J* = 8.7 Hz, H-4'), 8.21 (1H, s, H-8); ^{13}C NMR (125 MHz, DMSO-d_6) (ppm) δ 45.5 (C-1'), 54.9 (CH_3), 114.1 (C-3'), 123.3 (C_q), 128.5 (C_q), 128.8 (C-4'), 143.0 (C-8), 149.4

(C_q), 153.9 (C_q), 158.9 (C_q), 159.9 (C_q); HRMS calcd for $C_{13}H_{13}ClN_5O$ $[M^{35}Cl+H]^+$ 290.0803, found 290.0808, $[M^{37}Cl+H]^+$ 292.0960, found 292.0778.

2-Amino-9-(4-methoxybenzyl)-9*H*-purine-6-carbonitrile (81)[136]

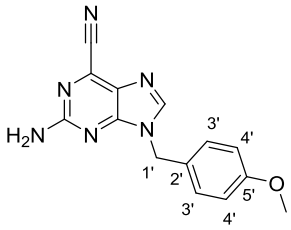

6-Chloro-9-(4-methoxybenzyl)-9*H*-purin-2-amine **80** (2.00 g, 6.90 mmol) and Et_4NCN (2.20 g, 13.8 mmol) were dissolved in dry MeCN (80 mL) under N_2. DBU (1.50 mL, 13.8 mmol) was then added and the reaction mixture was stirred at r.t. for 4 h. Aqueous ammonium hydroxide (50 mL) was added to the reaction and it was stirred for a further 1 h. DCM (50 mL) was added and the organic layer was extracted, washed with brine (50 mL) and water (50 mL). The organic layer was then dried over $MgSO_4$ and the solvent was removed *in vacuo*. The product was purified by MPC on silica (DCM: MeOH 19: 1) to give the product **81** as pale yellow solid (1.20 g, 4.30 mmol, 62%).

R_f 0.34 (petrol: EtOAc 1: 1); Mp = 172-174 °C; UV λ_{max} (EtOH) 353 nm; IR (cm^{-1}) 3471, 3099, 2160, 1611, 1584, 1511, 1405, 1245; ^{1}H NMR (500 MHz, DMSO-d_6) (ppm) δ 3.73 (3H, s, OCH_3), 5.24 (2H, s, H-1'), 6.91 (2H, d, J = 8.7 Hz, H-3'), 7.12 (2H, s, NH_2), 7.27 (2H, d, J = 8.7 Hz, H-4'), 8.44 (1H, s, H-8); ^{13}C NMR (125 MHz, DMSO-d_6) (ppm) δ 45.5 (C-1'), 55.1 (CH_3), 114.1 (C_q), 114.5 (C-3'), 128.2 (C_q), 129.0 (C_q), 129.7 (C-4'), 146.3 (C-8), 154.9 (C_q), 157.1 (C_q), 158.9 (C_q), 160.5 (CN); HRMS calcd for $C_{14}H_{13}N_6O$ $[M+H]^+$ 281.1145, found 281.1150.

TFA salt of 2-amino-9*H*-purine-6-carbonitrile (82)

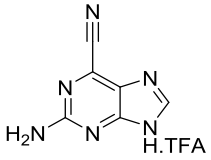

2-Amino-9-(4-methoxybenzyl)-9*H*-purine-6-carbonitrile **81** (1.00 g, 3.60 mmol) was dissolved in TFA (50 mL) and heated at 70 °C for 4 h. TFA was removed *in vacuo*. The residue was suspended in MeOH and the resulting precipitate was filtrated to give the product **82** as a yellow solid (680 mg, 2.60 mmol, 74%).

R_f 0.38 (DCM: MeOH 9: 1); Mp = 239-241 °C; UV λ_{max} (EtOH) 335 nm; IR (cm^{-1}) 3448, 3321, 2160, 1640, 1579, 1472, 1367; ^{1}H NMR (500 MHz, DMSO-d_6) (ppm) δ 6.95 (2H, s, NH_2), 8.34 (1H, s, H-8), 13.14 (1H, s, N^9H); ^{13}C NMR (125 MHz, DMSO-d_6) (ppm) δ 117.0 (q, J = 299.8 Hz, CF_3), 144.8 (C_q), 152.0 (C-8), 158.0 (q, J = 30.2 Hz, CO), 158.5 (C_q), 160.5 (C_q); ^{19}F NMR (470 MHz, DMSO-d_6) (ppm) δ -73.5; HRMS calcd for $C_6H_5N_6$ $[M+H]^+$ 161.0570, found 161.0569.

Note: One quaternary carbon was not visible on the ^{13}C NMR spectrum.

2-Iodo-9-(4-methoxybenzyl)-9*H*-purine-6-carbonitrile (84)

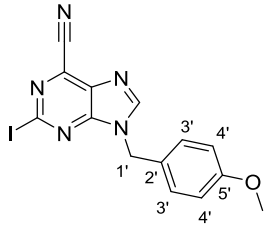

The title compound was synthesised following **general procedure G** using 2-amino-9-(4-methoxybenzyl)-9*H*-purine-6-carbonitrile **81** (1.12 g, 4.00 mmol), CH_2I_2 (1.70 mL, 12.6 mmol), Cu(I)I (762 mg, 4.00 mmol) and isoamyl nitrite (1.70 mL, 12.6 mmol). The crude product was purified by MPC on silica (DCM: MeOH 9: 1) to give the product **84** as pale yellow oil (1.20 g, 4.30 mmol, 62%).

R_f 0.43 (petrol: EtOAc 1: 1); UV λ_{max} (EtOH) 291 nm; IR (cm^{-1}) 3115, 2160, 1590, 1564, 1512, 1328, 1251; ^{1}H NMR (500 MHz, DMSO-d_6) (ppm) δ 3.73 (3H, s, OCH_3), 5.44 (2H, s, H-1'), 6.93 (2H, d, J = 8.4 Hz, H-3'), 7.34 (2H, d, J = 8.4 Hz, H-4'), 8.94 (1H, s, H-8); ^{13}C NMR (125 MHz, DMSO-d_6) (ppm) δ 46.5 (C-1'), 55.1 (CH_3), 113.4 (C_q), 114.2 (C-3'), 119.2 (C_q), 127.3 (C_q), 129.4 (C-4'), 135.0 (C_q), 150.5 (C-8), 153.9 (C_q), 159.2 (CN), 170.3 (C_q); HRMS calcd for $C_{14}H_{11}IN_5O$ $[M+H]^+$ 392.0003, found 392.0006.

2-(3-((6-Cyano-9-(4-methoxybenzyl)-9*H*-purin-2-yl)amino)phenyl)acetamide (85)

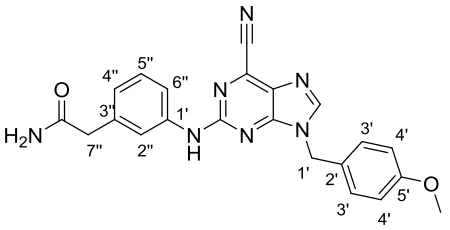

2-Iodo-9-(4-methoxybenzyl)-9*H*-purine-6-carbonitrile **84** (400 mg, 1.02 mmol), 2-(3-aminophenyl)acetamide **79** (307 mg, 2.05 mmol), K_2CO_3 (282 mg, 2.05 mmol),

diacetoxypalladium (5 mg, 0.02 mmol) and Brettphos (11 mg, 0.02 mmol) were suspended in anhydrous DME (4 mL) under N_2. The reaction was purged with N_2, sealed and heated under microwaves for 20 min at 120 °C. The solution was filtered through Celite and the solvent was removed *in vacuo*. The product was purified by MPC on silica (DCM: MeOH 19: 1) to give the product **85** as a yellow solid (180 mg, 0.44 mmol, 43%).

R_f 0.41 (DCM: MeOH 19: 1); Mp = 236-238 °C; UV λ_{max} (EtOH) 253 nm; IR (cm^{-1}) 3446, 3250, 2160, 1683, 1615, 1521, 1458, 1405, 1245; ^{1}H NMR (500 MHz, DMSO-d_6) (ppm) δ 3.39 (2H, s, H-7''), 3.72 (3H, s, OCH_3), 5.37 (2H, s, H-1'), 6.90 (1H, br s, NH_2), 6.94 (3H, m, H-4'' and H-3'), 7.26 (1H, dd, *J* = 7.8 and 7.8 Hz, H-5''), 7.41 (2H, d, *J* = 7.8 Hz, H-4'), 7.46 (1H, br s, NH_2), 7.61 (1H, d, *J* = 7.8 Hz, H-6''), 7.73 (1H, s, H-2''), 8.65 (1H, s, H-8), 10.09 (1H, s, NH); ^{13}C NMR (125 MHz, DMSO-d_6) (ppm) δ 42.4 (C-7''), 46.1 (C-1'), 55.1 (OCH_3), 114.1 (C-3'), 114.2 (C_q), 117.0 (C-6''), 119.6 (C-2''), 122.9 (C-4''), 128.0 (C_q), 128.3 (C_q), 129.1 (C-5''), 129.5 (C-4'), 129.7 (C_q), 136.8 (C_q), 139.8 (C_q), 147.2 (C-8), 154.0 (C_q), 156.1 (C_q), 159.0 (CN), 172.1 (CO); HRMS calcd for $C_{22}H_{20}N_7O_2$ $[M+H]^+$ 414.1673, found 414.1675.

Mixture of 6-chloro-9-methyl-9*H*-purin-2-amine (86) [260] and 6-chloro-7-methyl-7*H*-purin-2-amine (87)

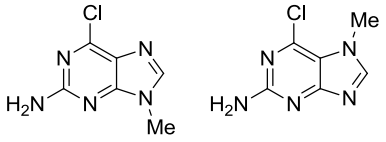

The title compounds were synthesised following **general procedure B** using 2-amino-6-chloropurine **68** (6.00 g, 35.5 mmol), K_2CO_3 (4.90 g, 35.50 mmol) and MeI (2.20 mL, 35.50 mmol). The residue obtained was resuspended in MeOH and a precipitate appeared which was collected by filtration to give the products **86** and **87** as a pale yellow solid (5.80 g, 31.70 mmol, 89 %).

R_f 0.33 (DCM: MeOH 9: 1); IR (cm^{-1}) 3403, 3123, 1611, 1532, 1474;

6-Chloro-9-methyl-9*H*-purin-2-amine (**86**)

^{1}H NMR (500 MHz, DMSO-d_6) (ppm) δ 3.64 (3H, s, CH_3), 6.91 (2H, s, NH_2), 8.08 (1H, s, H-8); MS $[M^{35}Cl+H]^+$ 184.1, $[M^{37}Cl+H]^+$ 186.1.

6-Chloro-7-methyl-7*H*-purin-2-amine (**87**)

^{1}H NMR (500 MHz, DMSO-d_6) (ppm) δ 3.91 (3H, s, CH_3), 6.60 (2H, s, NH_2), 8.30 (1H, s, H-8); MS $[M^{35}Cl+H]^+$ 184.1, $[M^{37}Cl+H]^+$ 186.1.

Note: Not fully characterised as not pure

TFA salt of 6-chloro-7-methyl-7*H*-purin-2-amine (87)

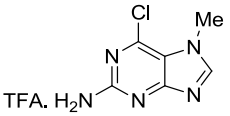

The title compound was synthesised following **general procedure C** using 2-amino-9-(4-methoxybenzyl)-9*H*-purine-6-carbonitrile **80** (100 mg, 0.34 mmol) and OMe_3BF_4 (61 mg, 0.41 mmol). TFA (3 mL) was added after completion of the methylation to have a 50% TFA solution. The reaction was heated for 10 min at 100 °C. The crude product was recrystallised using petrol and DCM to afford the product **87** as a beige solid (70 mg, 0.24 mmol, 68%).

R_f 0.42 (DCM: MeOH 9: 1); Mp = 168-171 °C; UV λ_{max} (EtOH) 302 nm; IR (cm^{-1}) 2380, 1630, 1583, 1391, 1030; ^{1}H NMR (500 MHz, DMSO-d_6) (ppm) δ 4.00 (3H, s, NCH_3), 8.90 (1H, s, H-8); ^{13}C NMR (125 MHz, DMSO-d_6) (ppm) δ 34.6 (CH_3), 107.6 (C_q), 114.2(CF_3), 130.0 (C_q), 138.8 (C_q), 149.6 (C-8), 153.3 (C_q), 154.8 (CO); ^{19}F NMR (470 MHz, DMSO-d_6) (ppm) δ -75.2; HRMS calcd for $C_6H_7ClN_5$ $[M^{35}Cl+H]^+$ 184.0384, found 184.0384, $[M^{37}Cl+H]^+$ 186.0541, found 186.0353.

2-Amino-9-methyl-9*H*-purine-6-carbonitrile (88)

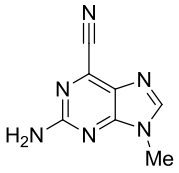

The title compound was synthesised following **general procedure B** using 2-amino-9*H*-purine-6-carbonitrile **82** (150 mg, 0.58 mmol), K_2CO_3 (257 mg, 1.87 mmol) and MeI (0.06 mL, 0.93 mmol). The crude product was purified by MPC on silica (petrol: EtOAc 1: 1) to give the product **88** as a yellow solid (60 mg, 0.34 mmol, 59%).

R_f 0.14 (petrol: EtOAc 2: 3); Mp = 259-262 °C; UV λ_{max} (EtOH) 335 nm; IR (cm^{-1}) 3464, 2361, 1634, 1608, 1579, 1468; ^{1}H NMR (500 MHz, DMSO-d_6) (ppm) δ 3.66 (3H, s,

CH_3), 7.09 (1H, br s, NH_2), 8.31 (1H, s, H-8); ^{13}C NMR (125 MHz, DMSO-d_6) (ppm) δ 29.3 (CH_3), 114.6 (C_q), 128.2 (C_q), 129.3 (C_q), 147.1 (C-8), 154.4 (C_q), 160.4 (CN); HRMS calcd for $C_7H_7N_6$ $[M+H]^+$ 175.0727, found 175.0726.

2-Amino-7-methyl-7*H*-purine-6-carbonitrile (89)

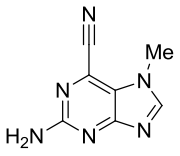

The title compound was synthesised following **general procedure C** using 2-amino-9-(4-methoxybenzyl)-9*H*-purine-6-carbonitrile **81** (100 mg, 0.36 mmol) and OMe_3BF_4 (54 mg, 0.36 mmol). TFA (2 mL) was added and the reaction was heated for 20 min at 100 °C. The crude product was purified by MPC on silica (DCM: MeOH 19: 1) to give the product **89** as a beige solid (40 mg, 0.23 mmol, 65%).

R_f 0.30 (DCM: MeOH 9: 1); Mp = 273-275 °C; UV λ_{max} (EtOH) 254 nm; IR (cm^{-1}) 3412, 3185, 2360, 1610, 1501; ^{1}H NMR (500 MHz, DMSO-d_6) (ppm) δ 3.94 (3H, s, NCH_3), 6.79 (2H, s, NH_2), 8.51 (1H, s, H-8); ^{13}C NMR (125 MHz, DMSO-d_6) (ppm) δ 32.2 (CH_3), 114.5 (C_q), 120.1 (C_q), 122.9 (C_q), 151.9 (C-8), 160.5 (C_q), 164.6 (CN); HRMS calcd for $C_7H_7N_6$ $[M+H]^+$ 175.0727, found 175.0726.

6-Chloro-2-iodo-9-methyl-9*H*-purine (90)

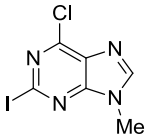

The title compound was synthesised following **general procedure G** using a mixture of 6-chloro-9-methyl-9*H*-purin-2-amine **86** and 6-chloro-7-methyl-7*H*-purin-2-amine **87** (50 mg, 0.27 mmol), CH_2I_2 (0.11 mL, 1.35 mmol), Cu(I)I (52 mg, 0.81 mmol) and isoamyl nitrite (0.11 mL, 0.81 mmol). The crude product was purified by MPC on silica (DCM: MeOH 19: 1) to give the product **90** as pale yellow oil (24 mg, 0.08 mmol, 30%).

R_f 0.59 (DCM: MeOH 9: 1); UV λ_{max} (EtOH) 261 nm; IR (cm^{-1}) 1586, 1328; ^{1}H NMR (500 MHz, DMSO-d_6) (ppm) δ 3.82 (3H, s, CH_3), 8.56 (1H, s, H-8); ^{13}C NMR (125 MHz, DMSO-d_6) (ppm) δ 30.2 (CH_3), 117.5 (C_q), 130.7 (C_q), 148.2 (C-8), 153.3 (C_q); HRMS calcd for $C_6H_5ClIN_4$ $[M^{35}Cl+H]^+$ 294.9242, found 294.9247, $[M^{37}Cl+H]^+$ 296.9398, found 296.9401.

Note: One quaternary carbon was not visible on the ^{13}C NMR spectrum.

6-Chloro-9-((phenylthio)methyl)-9*H*-purin-2-amine (96)

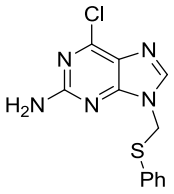

2-Amino-6-chloropurine **68** (1.00 g, 5.92 mmol) and Cs_2CO_3 (2.30 g, 7.10 mmol) were suspended in anhydrous DMF (50 mL) under N_2. Chloromethyl phenyl sulfide (0.95 mL, 7.10 mmol) was added slowly. The reaction was then heated at 40 °C for 24 h. The reaction mixture was filtered and the solvent was removed *in vacuo*. The residue was suspended in MeOH and the resulting precipitate was filtered. The filtrate was purified by MPC on silica (DCM: MeOH 19: 1) to give **96** as a yellow oil (1.16 g, 3.97 mmol, 67%).

R_f 0.32 (DCM: MeOH 9: 1); ^1H NMR (500 MHz, DMSO-d_6) (ppm) δ 5.56 (2H, s, CH_2), 7.03 (2H, br s, NH_2), 7.32-7.39 (5H, m, H-ar), 7.83 (1H, s, H-8); LRMS calcd for $C_{12}H_{11}ClN_5S$ $[M^{35}Cl+H]^+$ 291.0, found 292.2, $[M^{37}Cl+H]^+$ 292.0, found 294.3.

Note: Not fully characterised as contaminated with compound **97**.

6-Chloro-7-((phenylthio)methyl)-7*H*-purin-2-amine (97)

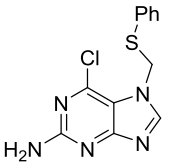

2-Amino-6-chloropurine **68** (1.00 g, 5.92 mmol) and Cs_2CO_3 (2.30 g, 7.10 mmol) were suspended in anhydrous DMF (50 mL) under N_2. Chloromethyl phenyl sulphide (0.95 mL, 7.10 mmol) was added slowly. The reaction was then heated at 40 °C for 24 h. The reaction mixture was filtered and the solvent was removed *in vacuo*. The residue was suspended in MeOH and the resulting precipitate was filtered to give **97** as a pale yellow solid (327 mg, 1.12 mmol, 19%).

R_f 0.20 (DCM: MeOH 9: 1); Mp = 168-170 °C; UV λ_{max} (EtOH) 304 nm; IR (cm^{-1}) 3412, 3174, 3070, 1629, 1545, 1496, 1299; ^1H NMR (500 MHz, DMSO-d_6) (ppm) δ 5.75 (2H, s, CH_2), 6.74 (2H, br s, NH_2), 7.30-7.36 (5H, m, H-ar), 7.96 (1H, s, H-8); ^{13}C NMR (125 MHz, DMSO-d_6) (ppm) δ 50.2 (CH_2), 113.8 (C_q), 128.6 (C-ar), 129.4 (2 x C-ar), 131.0 (C_q), 132.9 (2 x C-ar), 142.9 (C_q), 148.9(C-8), 160.3 (C_q), 164.6 (C_q); HRMS calcd for

$C_{12}H_{11}ClN_5S$ $[M^{35}Cl+H]^+$ 292.0418, found 292.0423, $[M^{37}Cl+H]^+$ 294.0575, found 294.0393.

2-Amino-9-((phenylthio)methyl)-9*H*-purine-6-carbonitrile (98)

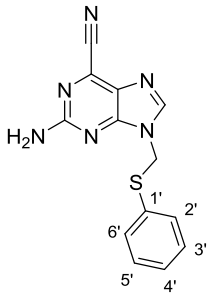

6-Chloro-9-((phenylthio)methyl)-9*H*-purin-2-amine **96** (1.1 g, 3.78 mmol) and Et_4NCN (710 mg, 4.54 mmol) were dissolved in anhydrous MeCN (30 mL) under N_2. DBU (0.80 mL, 7.56 mmol) was then added and the reaction mixture was stirred at r.t. for 4 h. Aqueous ammonium hydroxide (30 mL) was added to the reaction and it was stirred for a further 1 h. DCM (30 mL) was added and the organic layer was extracted, washed with brine (30 mL) and water (30 mL). The organic layer was then dried over $MgSO_4$ and the solvent was removed *in vacuo*. The product was purified by MPC on silica (petrol: EtOAc 2: 3) to give the product **98** as pale yellow solid (650 mg, 2.31 mmol, 61%).

R_f 0.23 (petrol: EtOAc 3: 2); Mp = 185-187 °C; UV λ_{max} (EtOH) 337 nm; IR (cm^{-1}) 3465, 3277, 3169, 2360, 1612, 1578, 1469, 1282; ^{1}H NMR (500 MHz, DMSO-d_6) (ppm) δ 5.65 (2H, s, CH_2), 7.24 (2H, br s, NH_2), 7.38-7.46 (5H, m, H-ar), 8.11 (1H, s, H-8); ^{13}C NMR (125 MHz, DMSO-d_6) (ppm) δ 46.0 (CH_2), 114.3 (C_q), 127.2 (C_q), 128.2 (C-4'), 129.4 (2 x C-ar), 129.9 (C_q), 131.6 (C_q), 131.9 (2 x C-ar), 145.4 (C-8), 154.5 (C_q), 160.4 (CN); HRMS calcd for $C_{13}H_{11}N_6S$ $[M+H]^+$ 283.0760, found 283.0765.

2-Iodo-7-methyl-7*H*-purine-6-carbonitrile (99)

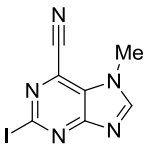

The title compound was synthesised following **general procedure C** using 2-iodo-9-(4-methoxybenzyl)-9*H*-purine-6-carbonitrile **84** (110 mg, 0.28 mmol) and OMe_3BF_4 (42 mg, 0.28 mmol). The reaction was heated for 10 min at 100 °C. The crude product was purified by MPC on silica (petrol: EtOAc 2: 3) to give the product **99** as a colourless oil (53 mg, 0.19 mmol, 66%).

R_f 0.63 (DCM: MeOH 9: 1); UV λ_{max} (EtOH) 302 nm; IR (cm^{-1}) 2360, 1604, 1345; ^1H NMR (500 MHz, DMSO-d_6) (ppm) δ 4.07 (3H, s, NCH_3), 8.91 (1H, s, H-8); ^{13}C NMR (125 MHz, DMSO-d_6) (ppm) δ 32.7 (CH_3), 113.4 (C_q), 118.4 (C_q), 123.7 (C_q), 126.4 (C_q), 153.9 (C-8), 163.4 (CN); HRMS calcd for $C_7H_5IN_5$ $[M+H]^+$ 285.9584, found 285.9589.

6-(Cyclohexylmethoxy)-7-methyl-7*H*-purin-2-amine (100)

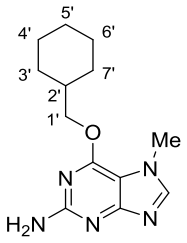

The title compound was synthesised following **general procedure C** using 6-(cyclohexylmethoxy)-9-(4-methoxybenzyl)-9*H*-purin-2-amine **172** (100 mg, 0.27 mmol) and OMe_3BF_4 (45 mg, 0.30 mmol). The reaction was heated for 10 min at 100 °C. The crude product was purified by MPC on silica (DCM: MeOH 9: 1) to give the product **100** as a white solid (43 mg, 0.11 mmol, 60%).

R_f 0.46 (DCM: MeOH 9: 1); Mp = 167-169 °C; UV λ_{max} (EtOH) 274 nm; IR (cm^{-1}) 3162, 2926, 2852, 1575, 1390, 1324, 1159; ^1H NMR (500 MHz, DMSO-d_6) (ppm) δ 1.05-1.12 (2H, m, H-3' and H-7'), 1.17-1.30 (3H, m, H-5', H-4' and H-6'), 1.65-1.68 (1H, m, H-5'), 1.72-1.75 (2H, m, H-4' and H-6'), 1.79-1.82 (3H, m, H-2', H-3' and H-7'), 3.84 (3H, s, NCH_3), 4.21 (2H, d, J = 6.2 Hz, H-1'), 6.07 (2H, s, NH_2), 7.99 (1H, s, H-8); ^{13}C NMR (125 MHz, DMSO-d_6) (ppm) δ 25.3 (C-4' and C-6'), 26.0 (C-5'), 29.2 (C-3' and C-7'), 33.4 (NCH_3), 36.7 (C-2'), 70. (C-1'), 106.5 (C_q), 145.5 (C-8), 157.2 (C_q), 159.6 (C_q), 163.6 (C_q); HRMS calcd for $C_{13}H_{20}N_5O$ $[M+H]^+$ 262.1662, found 262.1667.

6-(Cyclohexylmethoxy)-2-iodo-7-methyl-7*H*-purine (101)

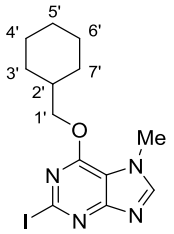

The title compound was synthesised following **general procedure C** using 6-(cyclohexylmethoxy)-2-iodo-9-(4-methoxybenzyl)-9*H*-purine **171** (100 mg, 0.21 mmol) and OMe_3BF_4 (38 mg, 0.25 mmol). The reaction was heated for 20 min at 100 °C. The crude product was purified by MPC on silica (DCM: MeOH 9: 1) to give the product **101** as a yellow solid (33 mg, 0.09 mmol, 45%).

R_f 0.30 (DCM: MeOH 9: 1); Mp = 187-189 °C; UV λ_{max} (EtOH) 248 nm; IR(cm^{-1}) 2927, 2851, 1536, 1415, 1332, 1123; ^{1}H NMR (500 MHz, DMSO-d_6) (ppm) δ 1.10-1.15 (2H, m, H-3' and H-7'), 1.17-1.31 (3H, m, H-5', H-4' and H-6'), 1.65-1.68 (1H, m, H-5'), 1.72-1.74 (2H, m, H-4' and H-6'), 1.81-1.83 (3H, m, H-2', H-3' and H-7'), 3.96 (3H, s, NCH_3), 4.28 (2H, d, *J* = 6.2 Hz, H-1'), 8.38 (1H, s, H-8); ^{13}C NMR (125 MHz, DMSO-d_6) (ppm) δ 25.2 (C-4' and C-6'), 25.9 (C-5'), 29.0 (C-3' and C-7'), 33.9 (NCH_3), 36.6 (C-2'), 72.2 (C-1'), 113.2 (C_q), 117.4 (C_q), 147.7 (C-8), 156.0 (C_q), 162.3 (C_q); HRMS calcd for $C_{13}H_{18}IN_4O$ $[M+H]^+$ 373.0520, found 373.0524.

6-(Cyclohexylmethoxy)-7-methyl-7*H*-purine-2-carbonitrile (102)

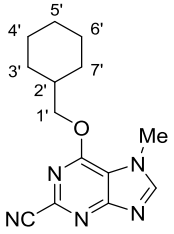

The title compound was synthesised following **general procedure C** using 6-(cyclohexylmethoxy)-9-(4-methoxybenzyl)-9*H*-purine-2-carbonitrile (33 mg, 0.09 mmol) and OMe_3BF_4 (16 mg, 0.11 mmol). The reaction was heated for 20 min at 100 °C. The crude product was purified by MPC on silica (DCM: MeOH 19: 1) to give the product **102** as a beige solid (17 mg, 0.06 mmol, 70%).

R_f 0.65 (DCM: MeOH 9: 1); Mp = 168-170 °C; UV λ_{max} (EtOH) 250 nm; IR (cm^{-1}) 2927, 2853, 2190, 1546, 1442, 1341, 1140; ^{1}H NMR (500 MHz, DMSO-d_6) (ppm) δ 1.05-1.12

(2H, m, H-3’ and H-7’), 1.14-1.30 (3H, m, H-5’, H-4’ and H-6’), 1.64-1.66 (1H, m, H-5’), 1.70-1.74 (2H, m, H-4’ and H-6’), 1.80-1.85 (3H, m, H-2’, H-3’ and H-7’), 4.03 (3H, s, NCH_3), 4.38 (2H, d, *J* = 6.2 Hz, H-1’’), 8.67 (1H, s, H-8); ^{13}C NMR (125 MHz, DMSO-d_6) (ppm) δ 25.2 (C-4’ and C-6’), 25.9 (C-5’), 29.0 (C-3’ and C-7’), 34.1 (NCH_3), 36.6 (C-2’), 72.6 (C-1’), 115.3 (C_q), 116.6 (C_q), 134.9 (C_q), 149.7 (C-8), 157.2 (C_q), 160.4 (CN); HRMS calcd for $C_{14}H_{18}N_5O$ $[M+H]^+$ 272.1506, found 272.1511.

6-Ethoxy-7-methyl-7*H*-purin-2-amine (103)

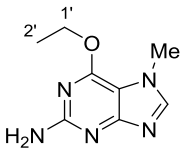

The title compound was synthesised following **general procedure C** using 6-ethoxy-9-(4-methoxybenzyl)-9*H*-purin-2-amine (100 mg, 0.28 mmol) and OMe_3BF_4 (50 mg, 0.33 mmol). The reaction was heated for 10 min at 100 °C. The crude product was purified by MPC on silica (DCM: MeOH 19: 1) to give the product **103** as a colourless oil (35 mg, 0.18 mmol, 66%).

R_f 0.60 (DCM: MeOH 9: 1); UV λ_{max} (EtOH) 275 nm; IR (cm^{-1}) 3347, 3081, 2895, 1568, 1385, 1290; ^1H NMR (500 MHz, DMSO-d_6) (ppm) δ 1.38 (3H, t, *J* = 7.1 Hz, H-2’), 3.84 (3H, s, NCH_3), 4.45 (2H, q, *J* = 7.1 and 14.2 Hz, H-1’), 6.09 (2H, s, NH_2), 8.00 (1H, s, H-8); ^{13}C NMR (125 MHz, DMSO-d_6) (ppm) δ 14.3 (C-2’), 33.3 (NCH_3), 61.5 (C-1’), 114.3 (C_q), 130.0 (C_q), 145.6 (C-8), 157.0 (C_q), 159.5 (C_q); HRMS calcd for $C_8H_{12}N_5O$ $[M+H]^+$ 194.1036, found 194.1037.

6-Ethoxy-2-iodo-7-methyl-7*H*-purine (104)

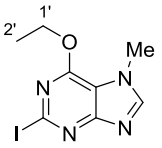

The title compound was synthesised following **general procedure C** using 6-ethoxy-2-iodo-9-(4-methoxybenzyl)-9*H*-purine (100 mg, 0.24 mmol) and OMe_3BF_4 (43 mg, 0.29 mmol). The reaction was heated for 10 min at 100 °C. The crude product was purified by MPC on silica (DCM: MeOH 49: 1) to give the product **104** as a pale beige solid (55 mg, 0.19 mmol, 73%).

R_f 0.84 (DCM: MeOH 9: 1); Mp = 122-124 °C; UV λ_{max} (EtOH) 266 nm; IR (cm^{-1}) 2980, 1610, 1484, 1331, 1128; ^{1}H NMR (500 MHz, DMSO-d_6) (ppm) δ 1.41 (3H, t, J = 7.1 Hz, H-2'), 3.95 (3H, s, NCH_3), 4.53 (2H, q, J = 7.1 and 14.2 Hz, H-1'), 8.38 (1H, s, H-8); ^{13}C NMR (125 MHz, DMSO-d_6) (ppm) δ 14.1 (C-2'), 33.8 (NCH_3), 63.5 (C-1'), 117.4 (C_q), 147.8 (C-8), 155.8 (C_q), 162.3 (C_q); HRMS calcd for $C_8H_{10}IN_4O$ $[M+H]^+$ 304.9894, found 304.9899.

7-Methyl-6-((triisopropylsilyl)ethynyl)-7*H*-purin-2-amine (105)

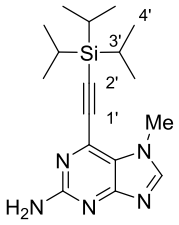

The title compound was synthesised following **general procedure C** using 9-(4-methoxybenzyl)-6-((triisopropylsilyl)ethynyl)-9*H*-purin-2-amine **135** (100 mg, 0.23 mmol) and OMe_3BF_4 (41 mg, 0.28 mmol). The reaction was heated for 20 min at 100 °C. The crude product was purified by MPC on silica (DCM: MeOH 9: 1) to give the product **105** as a yellow oil (30 mg, 0.09 mmol, 40%).

R_f 0.40 (DCM: MeOH 9: 1); UV λ_{max} (EtOH) 337 nm; IR (cm^{-1}) 3311, 2943, 2865, 1562, 1295; ^{1}H NMR (500 MHz, DMSO-d_6) (ppm) δ 1.12-1.15 (21H, m, H-3' and H-4'), 3.96 (3H, s, NCH_3), 6.41 (2H, s, NH_2), 8.30 (1H, s, H-8); ^{13}C NMR (125 MHz, DMSO-d_6) (ppm) δ 10.6 (C-3'), 18.4 (C-4'), 32.8 (CH_3), 97.5 (C-1'), 101.6 (C-2'), 133.2 (C_q), 139.8 (C_q), 141.7 (C_q), 150.0 (C-8), 160.3 (C_q); HRMS calcd for $C_{17}H_{28}N_5Si$ $[M+H]^+$ 330.2108, found 330.2114.

2-Iodo-7-methyl-6-((triisopropylsilyl)ethynyl)-7*H*-purine (106)

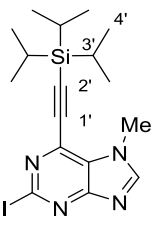

The title compound was synthesised following **general procedure C** using 2-iodo-9-(4-methoxybenzyl)-6-((triisopropylsilyl)ethynyl)-9*H*-purine **136** (65 mg, 0.12 mmol) and OMe_3BF_4 (22 mg, 0.14 mmol). The reaction was heated for 10 min at 100 °C. The crude

product was purified by MPC on silica (DCM: MeOH 49: 1) to give the product **106** as a colourless oil (30 mg, 0.07 mmol, 58%).

R_f 0.63 (DCM: MeOH 9: 1); UV λ_{max} (EtOH) 294 nm; IR (cm^{-1}) 2943, 2864, 1590, 1470, 1388, 1350; ^{1}H NMR (500 MHz, DMSO-d_6) (ppm) δ 1.15-1.17 (21H, m, H-3' and H-4'), 4.08 (3H, s, NCH_3), 8.68 (1H, s, H-8); ^{13}C NMR (125 MHz, DMSO-d_6) (ppm) δ 10.5 (C-3'), 18.4 (C-4'), 33.1 (NCH_3), 99.8 (C-1'), 102.0 (C-2'), 119.2 (C_q), 125.7 (C_q), 133.6 (C_q), 151.9 (C-8), 162.3 (C_q); HRMS calcd for $C_{17}H_{26}IN_4Si$ $[M+H]^+$ 441.0966, found 441.0966.

2-Fluoro-7-methyl-7*H*-purine (107)

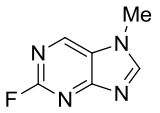

The title compound was synthesised following **general procedure C** using 2-fluoro-9-(tetrahydro-2*H*-pyran-2-yl)-9*H*-purine (100 mg, 0.45 mmol) and OMe_3BF_4 (80 mg, 0.54 mmol). The crude product was purified by MPC on silica (DCM: MeOH 49: 1) to give the product **107** as a colourless oil (39 mg, 0.26 mmol, 57%).

R_f 0.41 (DCM: MeOH 9: 1); UV λ_{max} (EtOH) 267 nm; IR (cm^{-1}) 3091, 2945, 1606, 1399; ^{1}H NMR (500 MHz, DMSO-d_6) (ppm) δ 3.81 (3H, s, NCH_3), 8.59 (1H, s, H-8), 9.05 (1H, s, H-6); ^{13}C NMR (125 MHz, DMSO-d_6) (ppm) δ 33.2 (NCH_3), 143.5 (d, J = 16 Hz, C-6), 148.7 (d, J = 3 Hz, C-5), 150.0 (d, J = 16 Hz, C-4), 152.1 (C-8), 158.0 (d, J = 206 Hz, C-2); ^{19}F NMR (470 MHz, DMSO-d_6) (ppm) δ -53.1; HRMS calcd for $C_6H_6FN_4$ $[M+H]^+$ 153.0571, found 153.0568.

6-(Cyclohexylmethoxy)-7-ethyl-7*H*-purin-2-amine (108)

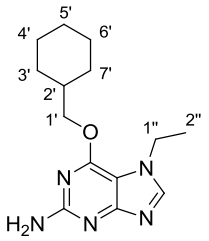

6-(Cyclohexylmethoxy)-9-(4-methoxybenzyl)-9*H*-purin-2-amine **172** (150 mg, 0.41 mmol) and OEt_3BF_4 (93 mg, 0.49 mmol) were solubilised in TFE (5 mL) under N_2. The resulting solution was stirred at r.t. for 2 h. The reaction was purged with nitrogen, sealed and heated under microwaves at 100 °C. The solvent was removed *in vacuo* and the crude

product was purified by MPC on silica (DCM: MeOH 9: 1) to give the product **108** as a colourless oil (45 mg, 0.16 mmol, 40%).

R_f 0.45 (DCM: MeOH 9: 1); Mp = 73-76 °C; UV λ_{max} (EtOH) 258 nm; IR (cm^{-1}) 3101, 2925, 2863, 1577, 1358, 1017; ^{1}H NMR (500 MHz, DMSO-d_6) (ppm) δ 1.03-1.11 (2H, m, H-3' and H-7'), 1.16-1.31 (3H, m, H-5', H-4' and H-6'), 1.38 (3H, t, *J* = 7.2 Hz, H-2''), 1.66-1.68 (1H, m, H-5'), 1.72-1.75 (2H, m, H-4' and H-6'), 1.80-1.82 (3H, m, H-2', H-3' and H-7'), 4.20-4.24 (4H, m, H-1' and H-1''), 6.13 (2H, s, NH_2), 8.09 (1H, s, H-8); ^{13}C NMR (125 MHz, DMSO-d_6) (ppm) δ 16.6 (C-2''), 25.3 (C-4' and C-6'), 26.0 (C-5'), 29.2 (C-3' and C-7'), 36.8 (C-2'), 41.8 (C-1''), 70.7 (C-1'), 105.2 (C_q), 144.7 (C-8), 156.8 (C_q), 159.5 (C_q), 163.5 (C_q); HRMS calcd for $C_{14}H_{22}N_5O$ $[M+H]^+$ 276.1819, found 276.1820.

6-Ethoxy-7-ethyl-7*H*-purin-2-amine (109)

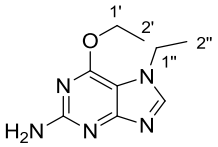

6-Ethoxy-9-(4-methoxybenzyl)-9*H*-purin-2-amine (90 mg, 0.30 mmol) and OEt_3BF_4 (69 mg, 0.36 mmol) were solubilised in TFE (3.8 mL) under N_2. The resulting solution was stirred at r.t. for 2 h. The reaction was purged with nitrogen, sealed and heated under microwaves at 100 °C. The solvent was removed *in vacuo* and the crude product was purified by MPC on silica (DCM: MeOH 9: 1) to give the product **109** as a colourless oil (36 mg, 0.17 mmol, 58%).

R_f 0.43 (DCM: MeOH 9: 1); Mp = 158-161 °C; UV λ_{max} (EtOH) 258 nm; IR (cm^{-1}) 3451, 3178, 2828, 1569, 1382, 1255; ^{1}H NMR (500 MHz, DMSO-d_6) (ppm) δ 1.36-1.39 (6H, m, H-2'' and H-2'), 4.20 (2H, q, *J* = 7.2 Hz, H-1''), 4.46 (2H, q, *J* = 7.1 Hz, H-1'), 6.18 (2H, s, NH_2), 8.11 (1H, s, C_8H); ^{13}C NMR (125 MHz, DMSO-d_6) (ppm) δ 14.4 (C-2'), 16.4 (C-2''), 41.7 (C-1''), 61.7 (C-1'), 105.6 (C_q), 144.7 (C_q), 156.7 (C-8), 159.4 (C_q), 163.2(C_q); HRMS calcd for $C_9H_{14}N_5O$ $[M+H]^+$ 208.1193, found 208.1191.

2-Amino-7-ethyl-7*H*-purine-6-carbonitrile (111)

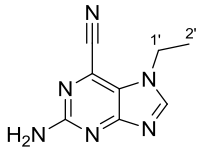

2-Amino-9-(4-methoxybenzyl)-9*H*-purine-6-carbonitrile **81** (220 mg, 0.79 mmol) and OEt_3BF_4 (180 mg, 0.94 mmol) were solubilised in TFE (10 mL) under N_2. The resulting solution was stirred at r.t. for 2 h. The reaction was purged with nitrogen, sealed and heated under microwaves at 100 °C. The solvent was removed *in vacuo* and the crude product was purified by MPC on silica (DCM: MeOH 19: 1) to give the product **111** as a pale yellow solid (41 mg, 0.22 mmol, 28%).

R_f 0.43 (DCM: MeOH 9: 1); Mp = 270-273 °C; UV λ_{max} (EtOH) 370 nm; IR (cm^{-1}) 3416, 3190, 2360, 1640, 1567, 1502, 1302; ^{1}H NMR (500 MHz, DMSO-d_6) (ppm) δ 1.47 (3H, t, *J* = 7.3 Hz, C-2'), 4.34 (2H, q, *J* = 7.3 Hz, C-1'), 6.80 (2H, s, NH_2), 8.59 (1H, s, H-8); ^{13}C NMR (125 MHz, DMSO-d_6) (ppm) δ 15.7 (C-2'), 40.7 (C-1'), 114.5 (C_q), 119.0 (C_q), 122.7 (C_q), 151.0 (C-8), 160.5 (C_q), 164.9 (CN); HRMS calcd for $C_8H_9N_6$ $[M+H]^+$ 189.0883, found 189.0880.

2-(4-Aminophenyl)acetamide (118)[136]

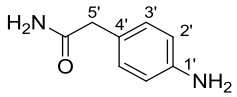

The title compound was synthesised following **general procedure F** using 4-aminophenylacetic acid **137** (500 mg, 3.31 mmol) and $SOCl_2$ (0.30 mL, 3.97 mmol). The crude product was purified by MPC on silica (DCM: MeOH 9: 1) to give the product **118** as a beige solid (240 mg, 1.60 mmol, 48%).

R_f 0.45 (DCM: MeOH 9: 1); Mp = 151-153 °C; UV λ_{max} (EtOH) 290 nm; IR (cm^{-1}) 3345, 3152, 1630, 1516, 1409; ^{1}H NMR (500 MHz, DMSO-d_6) (ppm) δ 3.15 (2H, s, H-5'), 4.89 (2H, br s, NH_2), 6.49 (2H, d, *J* = 8.3 Hz, H-2'), 6.74 (1H, br s, $CONH_2$), 6.90 (2H, d, *J* = 8.3 Hz, H-3'), 7.25 (1H, br s, $CONH_2$); ^{13}C NMR (125 MHz, DMSO-d_6) (ppm) δ 41.5 (C-5'), 113.5 (C-2'), 123.4 (C-4'), 129.4 (C-3'), 147.1 (C-1'), 172.9 (CO); HRMS calcd for $C_8H_{11}N_2O$ $[M+H]^+$ 151.0866, found 151.0864.

2-(3-Aminophenyl)-*N*,*N*-dimethylacetamide (119)[136]

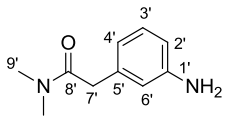

The title compound was synthesised following **general procedure H** using *N*,*N*-dimethyl-2-(3-nitrophenyl)acetamide **140** (470 mg, 2.26 mmol) and zinc powder (1.50 g, 22.6 mmol). The crude product was purified by MPC on silica (DCM: MeOH 9: 1) to give the product **119** as an off-white solid (380 mg, 2.13 mmol, 94%).

R_f 0.53 (DCM: MeOH 9: 1); Mp = 50-53 °C; UV λ_{max} (EtOH) 240 nm; IR (cm^{-1}) 3425, 3352, 3244, 1597, 1490, 1460, 1132; ^{1}H NMR (500 MHz, DMSO-d_6) (ppm) δ 2.82 (3H, s, H-9'), 2.95 (3H, s, H-9'), 3.50 (2H, s, H-7'), 5.01 (2H, br s, NH_2), 6.35 (1H, d, *J* = 7.7 Hz, H-4'), 6.41 (1H, d, *J* = 7.7 Hz, H-2'), 6.43 (1H, s, H-6'), 6.93 (1H, dd, *J* = 7.7 and 7.7 Hz, H-3'); ^{13}C NMR (125 MHz, DMSO-d_6) (ppm) δ 34.9 (C-9'), 37.2 (C-9'), 40.3 (C-7'), 112.0 (C-4'), 114.0 (C-2'), 116.2 (C-6'), 128.8 (C-3'), 136.1 (C-5'), 148.7 (C-1'), 170.3 (CO); HRMS calcd for $C_{10}H_{15}N_2O$ $[M+H]^+$ 179.1179, found 179.1179.

2-(3-Aminophenyl)-*N*-(2,2,2-trifluoroethyl)acetamide (120)[136]

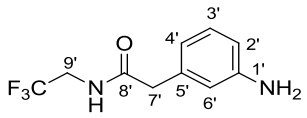

The title compound was synthesised following **general procedure H** using 2-(3-nitrophenyl)-*N*-(2,2,2-trifluoroethyl)acetamide **141** (280 mg, 1.07 mmol) and zinc powder (695 mg, 10.7 mmol). The crude product was purified by MPC on silica (DCM: MeOH 9: 1) to give the product **120** as a pale yellow oil (230 mg, 0.99 mmol, 93%).

R_f 0.45 (DCM: MeOH 9: 1); UV λ_{max} (EtOH) 239 nm; IR (cm^{-1}) 3302, 3205, 3066, 1652, 1560, 1396, 1148; ^{1}H NMR (500 MHz, DMSO-d_6) (ppm) δ 3.33 (2H, s, H-7'), 3.86-3.93 (2H, m, H-9'), 5.01 (2H, br s, NH_2), 6.39 (1H, d, *J* = 7.6 Hz, H-4'), 6.41-6.43 (1H, m, H-2'), 6.45 (1H, m, H-6'), 6.92 (1H, dd, *J* = 7.6 and 7.6 Hz, H-3'), 8.64 (1H, t, *J* = 6.2 Hz, NH); ^{13}C NMR (125 MHz, DMSO-d_6) (ppm) δ 39.8 (q, *J* = 20.7 Hz, C-9'), 42.1 (C-7'), 112.2 (C-2'), 114.5 (C-6'), 116.4 (C-4'), 124.0 (q, *J* = 279.2 Hz, CF_3), 128.7 (C-3'), 136.1 (C-5'), 148.5 (C-1'), 171.1 (CO); ^{19}F NMR (470 MHz, DMSO-d_6) (ppm) δ -70.7; HRMS calcd for $C_{10}H_{12}F_3N_2O$ $[M+H]^+$ 233.0896, found 233.0898.

3-(3-Aminophenyl)propanamide (121)[261]

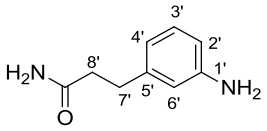

The title compound was synthesised following **general procedure F** using 3-(3-aminophenyl)propionic acid **138** (500 mg, 3.00 mmol) and $SOCl_2$ (0.27 mL, 3.64 mmol). The crude product was purified by MPC on silica (DCM: MeOH 9: 1) to give the product **121** as a white solid (360 mg, 2.20 mmol, 72%).

R_f 0.43 (DCM: MeOH 9: 1); Mp = 78-80 °C; UV λ_{max} (EtOH) 288 nm; IR (cm^{-1}) 3335, 3162, 1659, 1624, 1408; ^{1}H NMR (500 MHz, DMSO-d_6) (ppm) δ 2.28 (2H, t, *J* = 7.6 Hz, H-7'), 2.63 (2H, t, *J* = 7.6 Hz, H-8'), 4.93 (2H, br s, NH_2), 6.34-6.39 (3H, m, H-2', H-6' and H-4'), 6.74 (1H, br s, $CONH_2$), 6.90 (1H, dd, *J* = 8.1 and 8.1 Hz, H-3'), 7.27 (1H, br s, $CONH_2$); ^{13}C NMR (125 MHz, DMSO-d_6) (ppm) δ 31.2 (C-7'), 36.8 (C-8'), 111.6 (C-ar), 113.8 (C-ar), 115.7 (C-ar), 128.7 (C-3'), 142.0 (C-5'), 148.5 (C-1'), 173.4 (CO); HRMS calcd for $C_9H_{13}N_2O$ $[M+H]^+$ 165.1022, found 165.1020.

***N*-(2-Acetamidoethyl)-2-(3-aminophenyl)acetamide (122)**[136]

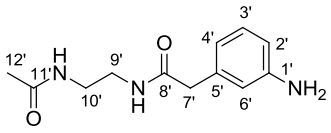

The title compound was synthesised following **general procedure H** using *N*-(2-acetamidoethyl)-2-(3-nitrophenyl)acetamide **142** (180 mg, 0.68 mmol) and zinc powder (440 mg, 6.80 mmol). The crude product was purified by MPC on silica (DCM: MeOH 9: 1) to give the product **122** as a colourless oil (140 mg, 0.60 mmol, 88%).

R_f 0.37 (DCM: MeOH 9: 1); UV λ_{max} (EtOH) 239 nm; IR (cm^{-1}) 3421, 3296, 1679, 1636, 1549, 1493, 1438; ^{1}H NMR (500 MHz, DMSO-d_6) (ppm) δ 1.79 (3H, s, H-12'), 3.07-3.09 (4H, m, H-9' and H-10'), 3.22 (2H, s, H-7'), 4.98 (2H, br s, NH_2), 6.38-6.42 (2H, m, H-2' and H-4'), 6.45 (1H, s, H-6'), 6.91 (1H, dd, *J* = 7.7 and 7.7 Hz, H-3'), 7.87 (1H, br s, NH), 7.98 (1H, br s, NH); ^{13}C NMR (125 MHz, DMSO-d_6) (ppm) δ 22.6 (C-12'), 38.3 (C-9'), 38.4 (C-10'), 42.7 (C-7'), 112.0 (C-2'), 114.5 (C-6'), 116.5 (C-4'), 128.6 (C-3'), 136.7 (C-5'), 148.5 (C-1'), 169.3 (CO), 170.5 (CO); HRMS calcd for $C_{12}H_{18}N_3O_2$ $[M+H]^+$ 236.1394, found 236.1396.

Mixture of 6-chloro-2-fluoro-9-(4-methoxybenzyl)-9*H*-purine (123) and 6-chloro-2-fluoro-7-(4-methoxybenzyl)-7*H*-purine (124)

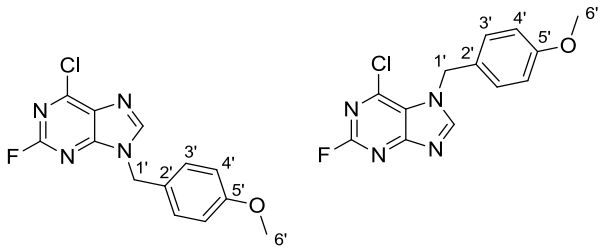

2-Fluoro-6-chloropurine **69** (4.10 g, 23.80 mmol) and Cs_2CO_3 (11.6 g, 35.8 mmol) were dissolved in anhydrous DMF (80 mL) under N_2. 4-Methoxybenzylchloride (3.90 mL, 28.6 mmol) was then added and the reaction was stirred at 60 °C overnight. The solvent was removed in vacuo. The residue obtained was resuspended in EtOAc (50 mL) and washed with brine (50 mL) and water (50 mL). The organic layer was dried over $MgSO_4$ and the solvent was removed *in vacuo*. The product was purified by MPC on silica (DCM: MeOH 19: 1) to give the products **123**/**124** as a yellow oil (2.64 g, 9.05 mmol, 38%).

R_f 0.80 (DCM: MeOH 9: 1); IR (cm^{-1}) 2942, 2865, 1596, 1559, 1252, 1016; ^{19}F NMR (470 MHz, DMSO-d_6) (ppm) δ -52.9, -52.4.

6-Chloro-2-fluoro-9-(4-methoxybenzyl)-9*H*-purine (**123**)

^1H NMR (500 MHz, DMSO-d_6) (ppm) δ 3.72 (3H, s, H-6'), 5.39 (2H, s, H-1'), 6.91 (2H, d, *J* = 8.7 Hz, H-4'), 7.35 (2H, d, *J* = 8.7 Hz, H-3'), 8.81 (1H, s, H-8); LRMS calcd for $C_{13}H_{11}ClFN_4O$ $[M^{35}Cl+H]^+$ 293.1, found 293.2, $[M^{37}Cl+H]^+$ 295.1, found 295.1.

6-Chloro-2-fluoro-7-(4-methoxybenzyl)-7*H*-purine (**124**)

^1H NMR (500 MHz, DMSO-d_6) (ppm) δ 3.73 (3H, s, H-6'), 5.66 (2H, s, H-1'), 6.88 (2H, d, *J* = 8.7 Hz, H-4'), 7.22 (2H, d, *J* = 8.7 Hz, H-3'), 9.03 (1H, s, H-8); LRMS calcd for $C_{13}H_{11}ClFN_4O$ $[M^{35}Cl+H]^+$ 293.1, found 293.4, $[M^{37}Cl+H]^+$ 295.1, found 295.5.

Note: Not fully characterised as not pure.

2-Fluoro-9-(4-methoxybenzyl)-6-((triisopropylsilyl)ethynyl)-9*H*-purine (125)

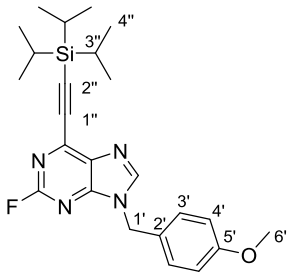

The title compound was synthesised following **general procedure D** using a mixture of 6-chloro-9-(4-methoxybenzyl)-9*H*-purin-2-amine **123** and 6-chloro-7-(4-methoxybenzyl) -7*H*-purin-2-amine **124** (2.64 g, 9.00 mmol), $Pd(PPh_3)_2Cl_2$ (127 mg, 0.18 mmol), Cu(I)I (34 mg, 0.18 mmol), triisopropylsilyl acetylene (2.23 mL, 9.90 mmol) and Et_3N (3.15 mL, 22.6 mmol). The crude product was purified by MPC on silica (petrol: EtOAc 1: 1) to give **125** was isolated as a brown solid (1.60 mg, 3.70 mmol, 40%)

R_f 0.28 (petrol: EtOAc 9: 1); Mp = 107-110 °C; UV λ_{max} (EtOH) 302 nm; IR (cm^{-1}) 2947, 2867, 1558, 1512, 1317, 1230; ^{1}H NMR (500 MHz, DMSO-d_6) (ppm) δ 1.13-1.18 (21H, m, H-3'' and H-4''), 3.72 (3H, s, H-6'), 5.27 (2H, s, H-1'), 6.80 (2H, d, *J* = 8.7 Hz, H-4'), 7.21 (2H, d, *J* = 8.7 Hz, H-3'), 8.77 (1H, s, H-8); ^{13}C NMR (125 MHz, DMSO-d_6) (ppm) δ 10.5 (C-3''), 18.4 (C-4''), 46.3 (C-1'), 55.1 (C-6'), 100.3 (C-1''), 102.5 (C-2''), 114.3 (C-4'), 127.3 (C_q), 129.3 (C-3'), 133.8 (d, *J* = 4.1 Hz, C_q), 140.5 (d, *J* = 18.2 Hz, C_q), 149.0 (C-8), 154.2 (d, *J* = 18.2 Hz, C_q), 157.0 (d, *J* = 210.5 Hz, C-2), 159.0 (C_q); ^{19}F NMR (470 MHz, DMSO-d_6) (ppm) δ -51.9; HRMS calcd for $C_{24}H_{32}FN_4OSi$ $[M+H]^+$ 439.2324, found 439.2323.

2-Fluoro-7-(4-methoxybenzyl)-6-((triisopropylsilyl)ethynyl)-7*H*-purine (126)

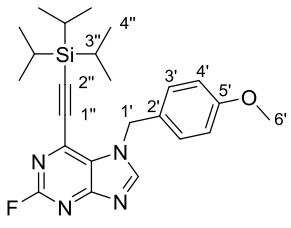

The title compound was synthesised following **general procedure D** using a mixture of 6-chloro-9-(4-methoxybenzyl)-9*H*-purin-2-amine **123** and 6-chloro-7-(4-methoxybenzyl) -7*H*-purin-2-amine **124** (2.64 g, 9.00 mmol), $Pd(PPh_3)_2Cl_2$ (127 mg, 0.18 mmol), Cu(I)I (34 mg, 0.18 mmol), triisopropylsilyl acetylene (2.23 mL, 9.90 mmol) and Et_3N (3.15 mL, 22.6 mmol). The crude product was purified by MPC on silica (petrol: EtOAc 1: 1) to give **126** was isolated as a brown solid (0.85 mg, 1.90 mmol, 21%)

R_f 0.28 (petrol: EtOAc 7: 3); Mp = 106-108 °C; UV λ_{max} (EtOH) 274 nm; IR (cm^{-1}) 2940, 2870, 1580, 1460, 1420, 1260; ^{1}H NMR (500 MHz, DMSO-d_6) (ppm) δ 1.04-1.09 (21H, m, H-3'' and H-4''), 3.72 (3H, s, H-6'), 5.75 (2H, s, H-1'), 6.90 (2H, d, *J* = 8.7 Hz, H-4'), 7.19 (2H, d, *J* = 8.7 Hz, H-3'), 8.90 (1H, s, H-8); ^{13}C NMR (125 MHz, DMSO-d_6) (ppm) δ 10.6 (C-3''), 18.2 (C-4''), 48.1 (C-1'), 55.1 (C-6'), 99.8 (C-1''), 103.5 (C-2''), 114.2 (C-4'), 123.8 (d, *J* = 4.1 Hz, C_q), 128.0 (C_q), 128.1 (C-3'), 133.8 (d, *J* = 18.3 Hz, C_q), 152.8 (C-8), 157.0 (d, *J* = 210.6 Hz, C-2), 159.0 (C_q), 164.1 (d, *J* = 18.3 Hz, C_q); ^{19}F NMR (470 MHz, DMSO-d_6) (ppm) δ -52.4; HRMS calcd for $C_{24}H_{32}FN_4OSi$ $[M+H]^+$ 439.2324, found 439.2324.

_N_-(4-Chlorophenyl)-7-methyl-6-((triisopropylsilyl)ethynyl)-7_H_-purin-2-amine (127)

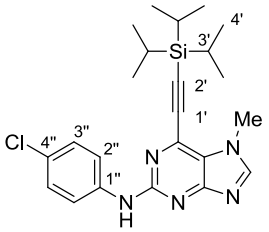

The title compound was synthesised following **general procedure E** using 2-fluoro-7-methyl-6-((triisopropylsilyl)ethynyl)-7*H*-purine **74** (190 mg, 0.57 mmol), 4-chloroaniline **113** (145 mg, 1.14 mmol) and TFA (0.22 mL). The crude product was purified by MPC on amine silica (petrol: EtOAc 1: 9) to give the product **127** as a yellow solid (130 mg, 0.30 mmol, 52%).

R_f 0.67 (DCM: MeOH 9: 1); Mp = 196-198 °C; UV λ_{max} (EtOH) 278 nm; IR (cm^{-1}) 3179, 2941, 2864, 1563, 1462, 1321; ^{1}H NMR (500 MHz, DMSO-d_6) (ppm) δ 1.14-1.21 (21H, m, H-3' and H-4'), 4.04 (3H, s, NCH_3), 7.32 (2H, d, *J* = 8.8 Hz, H-3''), 7.89 (2H, d, *J* = 8.8 Hz, H-2''), 8.47 (1H, s, H-8), 9.83 (1H, s, NH); ^{13}C NMR (125 MHz, DMSO-d_6) (ppm) δ 10.6 (C-3'), 18.4 (C-4'), 32.9 (CH_3), 98.9 (C-1'), 100.8 (C-2'), 119.3 (C-3''), 120.2 (C_q), 124.0 (C_q), 128.2 (C-2''), 133.3 (C_q), 140.0 (C_q), 150.3 (C-8), 156.2 (C_q), 162.4 (C_q); HRMS calcd for $C_{23}H_{31}ClN_5Si$ $[M^{35}Cl+H]^+$ 440.2032, found 440.2032, $[M^{37}Cl+H]^+$ 442.2003, found 442.2004.

***N*-(4-Isopropylphenyl)-7-methyl-6-((triisopropylsilyl)ethynyl)-7*H*-purin-2-amine (128)**

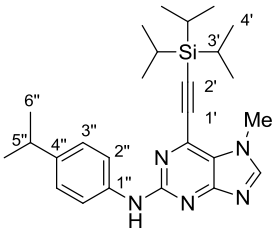

The title compound was synthesised following **general procedure E** using 2-fluoro-7-methyl-6-((triisopropylsilyl)ethynyl)-7*H*-purine **74** (190 mg, 0.57 mmol), 4-isopropylamine **114** (0.16 mL, 1.14 mmol) and TFA (0.22 mL). The crude product was purified by MPC on amine silica (petrol: EtOAc 1: 9) to give the product **128** as a yellow oil (110 mg, 0.25 mmol, 43%).

R_f 0.83 (DCM: MeOH 9: 1); UV λ_{max} (EtOH) 277 nm; IR (cm^{-1}) 2951 , 2866, 1562, 1433, 1390; ^{1}H NMR (500 MHz, DMSO-d_6) (ppm) δ 1.14-1.17 (21H, m, H-3' and H-4'), 1.19 (6H, d, *J* = 7.0 Hz, H-6''), 2.81-2.88 (1H, m, H-5''), 4.03 (3H, s, NCH_3), 7.17 (2H, d, *J* = 8.6 Hz, H-3''), 7.73 (2H, d, *J* = 8.6 Hz, H-2''), 8.43 (1H, s, H-8), 9.53 (1H, s, NH); ^{13}C NMR (125 MHz, DMSO-d_6) (ppm) δ 10.7 (C-3'), 18.4 (C-4'), 24.1 (2 x C-6''), 32.8 (CH_3), 32.9 (C-5''), 98.5 (C-1'), 101.0 (C-2'), 118.3 (C-3''), 120.2 (C_q), 126.1 (C-2''), 127.3 (C_q), 133.3 (C_q), 138.8 (C_q), 140.8 (C-8), 153.3 (C_q), 156.7 (C_q); HRMS calcd for $C_{26}H_{38}N_5Si$ $[M+H]^+$ 448.2891, found 448.2883.

***N*-(3-Chlorophenyl)-7-methyl-6-((triisopropylsilyl)ethynyl)-7*H*-purin-2-amine (129)**

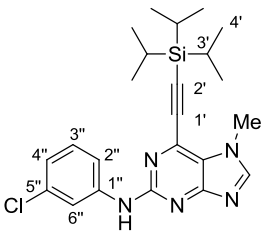

The title compound was synthesised following **general procedure E** using 2-fluoro-7-methyl-6-((triisopropylsilyl)ethynyl)-7*H*-purine **74** (220 mg, 0.65 mmol), 3-chloroaniline **115** (0.14 mL, 1.30 mmol) and TFA (0.25 mL). The crude product was purified by MPC on amine silica (petrol: EtOAc 1: 9) to give the product **129** as a yellow solid (180 mg, 0.41 mmol, 62%).

R_f 0.45 (DCM: MeOH 9: 1); Mp = 196-200 °C; UV λ_{max} (EtOH) 275 nm; IR (cm^{-1}) 3322, 2947, 2866, 1590, 1556, 1463; ^{1}H NMR (500 MHz, DMSO-d_6) (ppm) δ 1.14-1.21 (21H,

m, H-3’ and H-4’), 4.04 (3H, s, NCH_3), 6.94 (1H, d, *J* = 8.2 Hz, H-4’’), 7.29 (1H, dd, *J* = 8.2 and 8.2 Hz, H-3’’), 7.66 (1H, d, *J* = 8.2 Hz, H-2’’), 8.17 (1H, s, H-6’’), 8.49 (1H, s, H-8), 9.90 (1H, s, NH); ^{13}C NMR (125 MHz, DMSO-d_6) (ppm) δ 10.6 (C-3’), 18.4 (C-4’), 32.9 (CH_3), 99.0 (C-1’), 100.9 (C-2’), 116.7 (C-2’’), 116.9 (C-6’’), 120.1 (C_q), 120.4 (C-4’’), 130.0 (C-3’’), 133.0 (C_q), 133.1 (C_q), 142.6 (C_q), 150.5 (C-8), 156.0 (C_q), 162.4 (C_q); HRMS calcd for $C_{23}H_{31}ClN_5Si$ $[M^{35}Cl+H]^+$ 440.2032, found 440.2030, $[M^{37}Cl+H]^+$ 442.2003, found 442.2001.

_N_-(3-Methoxyphenyl)-7-methyl-6-((triisopropylsilyl)ethynyl)-7_H_-purin-2-amine (130)

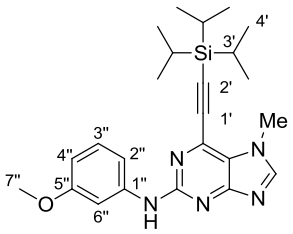

The title compound was synthesised following **general procedure E** using 2-fluoro-7-methyl-6-((triisopropylsilyl)ethynyl)-7*H*-purine **74** (220 mg, 0.65 mmol), *m*-anisidine **116** (0.15 mL, 1.30 mmol) and TFA (0.25 mL). The crude product was purified by MPC on silica (petrol: EtOAc 1: 9) to give the product **130** as a yellow oil (190 mg, 0.44 mmol, 66%).

R_f 0.49 (DCM: MeOH 9: 1); UV λ_{max} (EtOH) 223 nm; IR (cm^{-1}) 3260, 2943, 2864, 1599, 1542, 1494, 1387; ^{1}H NMR (500 MHz, DMSO-d_6) (ppm) δ 1.14-1.21 (21H, m, H-3’ and H-4’), 3.74 (3H, s, H-7’’), 4.04 (3H, s, NCH_3), 6.50 (1H, d, *J* = 8.2 Hz, H-4’’), 7.16 (1H, dd, *J* = 8.2 and 8.2 Hz, H-3’’), 7.36 (1H, d, *J* = 8.2 Hz, H-2’’), 7.66 (1H, s, H-6’’), 8.46 (1H, s, H-8), 9.63 (1H, s, NH); ^{13}C NMR (125 MHz, DMSO-d_6) (ppm) δ 10.5 (C-3’), 18.4 (C-4’), 32.9 (CH_3), 54.6 (C-7’’), 98.7 (C-1’), 100.9 (C-2’), 104.1 (C-6’’), 105.7 (C-4’’), 110.5 (C-2’’), 120.0 (C_q), 129.1 (C-3’’), 133.1 (C_q), 142.3 (C_q), 150.3 (C-8), 156.2 (C_q), 159.7 (C_q), 162.4 (C_q); HRMS calcd for $C_{24}H_{34}N_5OSi$ $[M+H]^+$ 436.2527, found 436.2522.

***N*-(4-Chlorophenyl)-6-ethynyl-7-methyl-7*H*-purin-2-amine (131)**

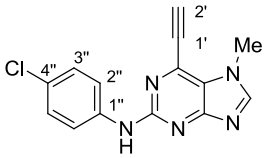

The title compound was synthesised following **general procedure A** using *N*-(4-chlorophenyl)-7-methyl-6-((triisopropylsilyl)ethynyl)-7*H*-purin-2-amine **127** (130 mg, 0.30 mmol) and TBAF (1M in THF, 0.30 mL, 0.30 mmol). The crude product was purified by MPC on silica (DCM: MeOH 19: 1) to give the product **131** as yellow oil (38 mg, 0.13 mmol, 45%).

R_f 0.31 (DCM: MeOH 9: 1); UV λ_{max} (EtOH) 275 nm; IR (cm^{-1}) 3276, 3124, 2116, 1596, 1540, 1489; ^{1}H NMR (500 MHz, DMSO-d_6) (ppm) δ 4.01 (3H, s, NCH_3), 5.02 (1H, s, H-2'), 7.34 (2H, d, *J* = 8.9 Hz, H-3''), 7.86 (2H, d, *J* = 8.9 Hz, H-2''), 8.48 (1H, s, H-8), 9.80 (1H, s, NH); ^{13}C NMR (125 MHz, DMSO-d_6) (ppm) δ 32.8 (CH_3), 78.3 (C-1'), 87.7 (C-2'), 119.4 (C-2''), 120.5 (C_q), 124.0 (C_q), 128.3 (C-3''), 133.1 (C_q), 140.1 (C_q), 150.6 (C-8), 156.0 (C_q), 162.4 (C_q); HRMS calcd for $C_{14}H_{11}ClN_5$ $[M^{35}Cl+H]^+$ 284.0697, found 284.0703, $[M^{37}Cl+H]^+$ 286.0668, found 286.0672.

6-Ethynyl-*N*-(4-isopropylphenyl)-7-methyl-7*H*-purin-2-amine (132)

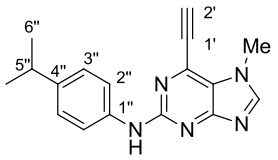

The title compound was synthesised following **general procedure A** using *N*-(4-isopropylphenyl)-7-methyl-6-((triisopropylsilyl)ethynyl)-7*H*-purin-2-amine **128** (110 mg, 0.25 mmol) and TBAF (1M in THF, 0.25 mL, 0.25 mmol). The crude product was purified by MPC on silica (DCM: MeOH 19: 1) to give the product **132** as yellow solid (29 mg, 0.10 mmol, 40%).

R_f 0.36 (DCM: MeOH 9: 1); Mp = no melt, degradation; UV λ_{max} (EtOH) 274 nm; IR (cm^{-1}) 3290, 2963, 2116, 1594, 1470, 1383; ^{1}H NMR (500 MHz, DMSO-d_6) (ppm) δ 1.20 (6H, d, *J* = 6.9 Hz, H-6'), 2.81-2.88 (1H, m, H-5'), 4.00 (3H, s, NCH_3), 4.98 (1H, s, H-2'), 7.16 (2H, d, *J* = 8.5 Hz, H-3''), 7.70 (2H, d, *J* = 8.5 Hz, H-2''), 8.43 (1H, s, H-8), 9.48 (1H, s, NH); ^{13}C NMR (125 MHz, DMSO-d_6) (ppm) δ 24.1 (2 x C-6'), 32.8 (CH_3), 32.9 (C-5'), 78.2 (C-1'), 87.4 (C-2'), 118.4 (C-2''), 120.1 (C_q), 126.1 (C-3''), 133.2 (C_q),

138.7 (C_q), 140.9 (C_q), 150.2 (C-8), 156.6 (C_q), 162.5 (C_q); HRMS calcd for $C_{17}H_{18}N_5$ $[M+H]^+$ 292.1557, found 292.1559.

_N_-(3-Chlorophenyl)-6-ethynyl-7-methyl-7_H_-purin-2-amine (133)

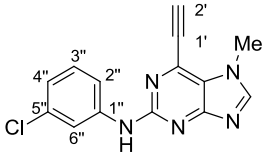

The title compound was synthesised following **general procedure A** using *N*-(3-chlorophenyl)-7-methyl-6-((triisopropylsilyl)ethynyl)-7*H*-purin-2-amine **129** (180 mg, 0.41 mmol) and TBAF (1M in THF, 0.41 mL, 0.41 mmol). The crude product was purified by MPC on silica (DCM: MeOH 19: 1) to give the product **133** as yellow oil (48 mg, 0.17 mmol, 41%).

R_f 0.40 (DCM: MeOH 9: 1); UV λ_{max} (EtOH) 273 nm; IR (cm^{-1}) 3306, 3069, 2116, 1591, 1540, 1498, 1472; ^{1}H NMR (500 MHz, DMSO-d_6) (ppm) δ 4.02 (3H, s, NCH_3), 5.04 (1H, s, H-2'), 6.96 (1H, d, *J* = 8.1 Hz, H-4''), 7.31 (1H, dd, *J* = 8.1 and 8.1 Hz, H-3''), 7.70 (1H, d, *J* = 8.1 Hz, H-2''), 8.07 (1H, s, H-6''), 8.50 (1H, s, H-8), 9.88 (1H, s, NH); ^{13}C NMR (125 MHz, DMSO-d_6) (ppm) δ 32.9 (CH_3), 78.1 (C-1'), 87.9 (C-2'), 116.3 (C-2''), 116.9 (C-6''), 120.2 (C-4''), 120.7 (C_q), 130.1 (C-3''), 133.0 (C_q), 133.2 (C_q), 142.6 (C_q), 150.6 (C-8), 155.9 (C_q), 162.4 (C_q); HRMS calcd for $C_{14}H_{11}ClN_5$ $[M^{35}Cl+H]^+$ 284.0697, found 284.0703, $[M^{37}Cl+H]^+$ 286.0668, found 286.0672.

6-Ethynyl-_N_-(3-methoxyphenyl)-7-methyl-7_H_-purin-2-amine (134)

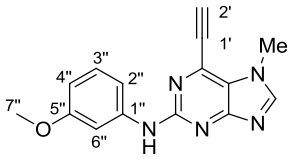

The title compound was synthesised following **general procedure A** using *N*-(3-methoxyphenyl)-7-methyl-6-((triisopropylsilyl)ethynyl)-7*H*-purin-2-amine **130** (190 mg, 0.44 mmol) and TBAF (1M in THF, 0.44 mL, 0.44 mmol). The crude product was purified by MPC on silica (DCM: MeOH 19: 1) to give the product **134** as yellow solid (52 mg, 0.18 mmol, 43%).

R_f 0.47 (DCM: MeOH 9: 1); Mp = no melt, degradation; UV λ_{max} (EtOH) 270 nm; IR (cm^{-1}) 3090, 2937, 2117, 1598, 1497, 1461, 1281, 1164; ^{1}H NMR (500 MHz, DMSO-d_6) (ppm) δ 3.75 (3H, s, H-7''), 4.01 (3H, s, NCH_3), 5.00 (1H, s, H-2'), 6.51 (1H, d, *J* = 8.1

Hz, H-4''), 7.18 (1H, dd, *J* = 8.1 and 8.1 Hz, H-3''), 7.36 (1H, d, *J* = 8.1 Hz, H-2''), 7.58 (1H, s, H-6''), 8.46 (1H, s, H-8), 9.60 (1H, s, NH); ^{13}C NMR (125 MHz, DMSO-d_6) (ppm) δ 32.8 (CH_3), 54.9 (C-7''), 78.2 (C-1'), 87.5 (C-2'), 104.2 (C-6''), 105.7 (C-4''), 110.7 (C-2''), 120.4 (C_q), 129.1 (C-3''), 133.1 (C_q), 142.1 (C-8), 150.3 (C_q), 156.3 (C_q), 159.5 (C_q), 162.4 (C_q); HRMS calcd for $C_{15}H_{14}N_5O$ $[M+H]^+$ 280.1193, found 280.1197.

9-(4-Methoxybenzyl)-6-((triisopropylsilyl)ethynyl)-9*H*-purin-2-amine (135)[136]

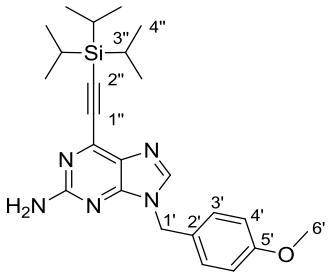

The title compound was synthesised following **general procedure D** using (6-chloro-9-(4-methoxybenzyl)-9*H*-purin-2-amine **80** (1.00 g, 3.45 mmol), $Pd(PPh_3)_2Cl_2$ (48 mg, 0.07 mmol), Cu(I)I (13 mg, 0.07 mmol), triisopropylsilyl acetylene (0.85 mL, 3.80 mmol) and Et_3N (1.18 mL, 8.61 mmol). The crude product was purified by MPC on silica (petrol: EtOAc 1: 1) to give the product **135** as a yellow oil (975 mg, 2.24 mmol, 65%).

R_f 0.33 (petrol: EtOAc 7: 3); UV λ_{max} (EtOH) 330 nm; IR (cm^{-1}) 3297, 3179, 2867, 1594, 1512, 1456, 1403, 1243; ^{1}H NMR (500 MHz, DMSO-d_6) (ppm) δ 1.11-1.14 (21H, m, H-3'' and H-4''), 3.72 (3H, s, H-6'), 5.21 (2H, s, H-1'), 6.68 (2H, s, NH_2), 6.90 (2H, d, *J* = 8.7 Hz, H-4'), 7.23 (2H, d, *J* = 8.7 Hz, H-3'), 8.19 (1H, s, H-8); ^{13}C NMR (125 MHz, DMSO-d_6) (ppm) δ 10.5 (C-3''), 18.5 (C-4''), 45.2 (C-1'), 55.0 (C-6'), 97.2 (C-1''), 101.9 (C-2''), 114.0 (C-4'), 128.7 (C-3'), 128.8 (C_q), 135.7 (C_q), 140.8 (C_q), 143.5 (C-8), 153.7 (C_q), 158.7 (C_q), 160.4 (C_q); HRMS calcd for $C_{24}H_{34}N_5OSi$ $[M+H]^+$ 436.2527, found 436.2527.

2-Iodo-9-(4-methoxybenzyl)-6-((triisopropylsilyl)ethynyl)-9*H*-purine (136)[136]

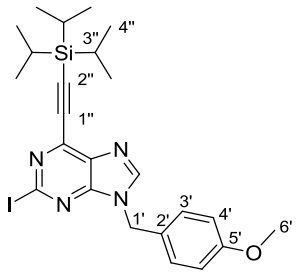

The title compound was synthesised following **general procedure G** using 9-(4-methoxybenzyl)-6-((triisopropylsilyl)ethynyl)-9*H*-purin-2-amine **135** (200 mg, 0.46 mmol), CH_2I_2 (0.19 mL, 2.28 mmol), Cu(I)I (132 mg, 0.69 mmol) and isoamyl nitrite (0.19 mL, 1.38 mmol). The crude product was purified by MPC on silica (petrol: EtOAc 4: 1) to give the product **136** as colourless oil (76 mg, 0.14 mmol, 30%).

R_f 0.79 (DCM: MeOH 9: 1); UV λ_{max} (EtOH) 311 nm; IR (cm^{-1}) 2947, 2867, 1558, 1512, 1317, 1230; ^{1}H NMR (500 MHz, DMSO-d_6) (ppm) δ 1.12-1.15 (21H, m, H-3'' and H-4''), 3.73 (3H, s, H-6'), 5.38 (2H, s, H-1'), 6.92 (2H, d, *J* = 8.7 Hz, H-4'), 7.30 (2H, d, *J* = 8.7 Hz, H-3'), 8.67 (1H, s, H-8); ^{13}C NMR (125 MHz, DMSO-d_6) (ppm) δ 10.5 (C-3''), 18.4 (C-4''), 46.2 (C-1'), 55.1 (C-6'), 100.2 (C-1''), 102.2 (C-2''), 114.1 (C-4'), 119.5 (C_q), 127.8 (C_q), 129.1 (C-3'), 134.6 (C_q), 140.2 (C_q), 147.8 (C-8), 152.7 (C_q), 159.0 (C_q); HRMS calcd for $C_{24}H_{32}IN_4OSi$ $[M+H]^+$ 547.1385, found 547.1374.

***N*,*N*-Dimethyl-2-(3-nitrophenyl)acetamide (140)**[136]

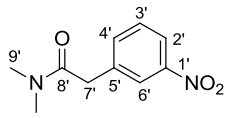

3-Nitrophenylacetic acid **139** (500 mg, 2.76 mmol), *N*-(3-dimethylaminopropyl)-*N*′-ethylcarbodiimide hydrochloride (800 mg, 4.14 mmol), 1-hydroxybenzotriazole hydrate (485 mg, 3.59 mmol) and dimethylamine hydrochloride (270 mg, 3.31 mmol) were solubilised in anhydrous MeCN (12 mL) under N_2. Then diisopropylethylamine (0.60 mL, 3.31 mmol) was added and the reaction was stirred at r.t. overnight under N_2. The solvent was removed in *vacuo*. The residue was resuspended in EtOAc (15 mL) and washed with $NaHCO_3$. The organic layer was dried over $MgSO_4$ and the solvent was removed *in vacuo*. The crude mixture was purified by MPC on silica (DCM: MeOH 19: 1) to give the product **140** as a pale yellow solid (470 mg, 2.26 mmol, 82%).

R_f 0.63 (DCM: MeOH 9: 1); Mp = 47-50 °C; UV λ_{max} (EtOH) 263 nm; IR (cm^{-1}) 1635, 1522, 1342; ^{1}H NMR (500 MHz, DMSO-d_6) (ppm) δ 2.86 (3H, s, H-9'), 3.06 (3H, s, H-9'), 3.89 (2H, s, H-7'), 7.60 (1H, dd, *J* = 7.7 and 7.7 Hz, H-3'), 7.68 (1H, d, *J* = 7.7 Hz, H-4'), 8.10 (1H, d, *J* = 7.7 Hz, H-2'), 8.11 (1H, s, H-6'); ^{13}C NMR (125 MHz, DMSO-d_6) (ppm) δ 35.1 (C-9'), 36.9 (C-9'), 38.5 (C-7'), 121.3 (C-2'), 124.2 (C-6'), 129.4 (C-3'), 136.5 (C-4'), 138.5 (C_q), 147.5 (C_q), 169.5 (CO); HRMS calcd for $C_{10}H_{13}N_2O_3$ $[M+H]^+$ 209.0921, found 209.0921.

2-(3-Nitrophenyl)-*N*-(2,2,2-trifluoroethyl)acetamide (141)[136]

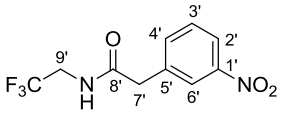

3-Nitrophenylacetic acid **139** (250 mg, 1.38 mmol) and 2,2,2-trifluoro-1-ethanamine hydrochloride (467 mg, 3.45 mmol) were solubilised in anhydrous MeCN (8 mL) under N_2. Phosphorus trichloride (0.14 mL, 1.52 mmol) was added. The reaction was purged with N_2, sealed and heated at 150 °C for 5 min under microwave heating. The solvent was removed *in vacuo*. The residue was resuspended in EtOAc (15 mL) and washed with $NaHCO_3$. The organic layer was dried over $MgSO_4$ and the solvent was removed *in vacuo*. The crude mixture was purified by MPC on silica (DCM: MeOH 19: 1) to give the product **141** as a white solid (291 mg, 1.11 mmol, 80%).

R_f 0.67 (DCM: MeOH 9: 1); Mp= 130-132 ^{0}C; UV λ_{max} (EtOH) 262 nm; IR (cm^{-1}) 3287, 1662, 1559, 1532, 1344, 1146; ^{1}H NMR (500 MHz, DMSO-d_6) (ppm) δ 3.72 (2H, s, H-7'), 3.91-3.98 (2H, m, H-9'), 7.63 (1H, dd, *J* = 7.9 and 7.9 Hz, H-3'), 7.71-7.73 (1H, m, H-4'), 8.13 (1H, ddd, *J* = 7.9, 2.3 and 1.0 Hz, H-2'), 8.17-8.18 (1H, m, H-6'), 8.88 (1H, t, *J* = 6.1 Hz, NH); ^{13}C NMR (125 MHz, DMSO-d_6) (ppm) δ 39.8 (q, *J* = 21.5 Hz, C-9'), 40.9 (C-7'), 121.6 (C-2'), 123.7 (C-6'), 124.0 (q, *J* = 279.0 Hz, CF_3), 129.7 (C-3'), 136.0 (C-4'), 137.9 (C-5'), 147.6 (C-1'), 170.2 (CO); ^{19}F NMR (470 MHz, DMSO-d_6) (ppm) δ -70.8; HRMS calcd for $C_{10}H_{10}F_3N_2O_3$ $[M+H]^+$ 263.0638, found 263.0643.

***N*-(2-Acetamidoethyl)-2-(3-nitrophenyl)acetamide (142)**[136]

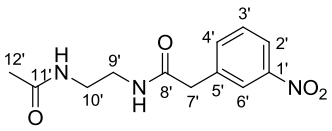

3-Nitrophenylacetic acid **139** (300 mg, 1.66 mmol) and CDI (270 mg, 1.65 mmol) were solubilised in anhydrous MeCN (15 mL) under N_2. DIPEA (0.58 mL, 3.31 mmol) was

added and the reaction was stirred at r.t. for 2 h. *N*-Acetylethylenediamine (500 mg, 4.97 mmol) was added and the solution was stirred at r.t. for 2 h. The solvent was removed *in vacuo*. The crude mixture was purified by MPC on silica (DCM: MeOH 9: 1) to give the product **142** as a white solid (180 mg, 0.68 mmol, 41%).

R_f 0.75 (DCM: MeOH 9: 1); Mp = 108-110 °C; UV λ_{max} (EtOH) 262 nm; IR (cm^{-1}) 3263, 3087, 1634, 1526 , 1346, 1446; ^{1}H NMR (500 MHz, DMSO-d_6) (ppm) δ 1.78 (3H, s, H-12'), 3.08-3.11 (4H, m, H-9' and H-10'), 3.59 (2H, s, H-7'), 7.01 (1H, dd, *J* = 7.9 and 7.9 Hz, H-3'), 7.21 (1H, d, *J* = 7.9 Hz, H-4'), 7.88 (1H, t, *J* = 4.6 Hz, NH), 8.11 (1H, d, *J* = 7.9 Hz, H-2'), 8.16 (1H, s, H-6'), 8.20 (1H, t, *J* = 4.6 Hz, NH); ^{13}C NMR (125 MHz, DMSO-d_6) (ppm) δ 22.6 (C-12'), 38.2 (C-10'), 38.5 (C-9'), 41.4 (C-7'), 121.4 (C-2'), 123.8 (C-6'), 129.6 (C-3'), 136.0 (C-4'), 138.5 (C-5'), 147.6 (C-1'), 169.3 (CO), 169.4 (CO); HRMS calcd for $C_{12}H_{16}N_3O_4$ $[M+H]^+$ 266.1135, found 266.1140.

2-(4-((7-Methyl-6-((triisopropylsilyl)ethynyl)-7*H*-purin-2-yl)amino)phenyl) acetamide (143)

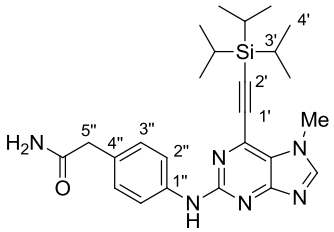

The title compound was synthesised following **general procedure I** using 2-iodo-7-methyl-6-((triisopropylsilyl)ethynyl)-7*H*-purine **106** (200 mg, 0.45 mmol), 2-(4-aminophenyl)acetamide **118** (75 mg, 0.50 mmol), K_2CO_3 (125 mg, 0.91 mmol), $Pd(dba)_2$ (10 mg, 0.01 mmol) and XPhos (5 mg, 0.01 mmol). The crude product was purified by MPC on silica (DCM: MeOH 19: 1) to give the product **143** as a yellow oil (90 mg, 0.19 mmol, 43%).

R_f 0.55 (DCM: MeOH 9: 1); UV λ_{max} (EtOH) 278 nm; IR (cm^{-1}) 3256, 3193, 2943, 2865, 1645, 1563, 1496, 1302; ^{1}H NMR (500 MHz, DMSO-d_6) (ppm) δ 1.14-1.20 (21H, m, H-3' and H-4'), 3.30 (2H, s, H-5''), 4.03 (3H, s, NCH_3), 6.82 (1H, br s, $CONH_2$), 7.16 (2H, d, *J* = 8.6 Hz, H-3''), 7.37 (1H, br s, $CONH_2$), 7.75 (2H, d, *J* = 8.6 Hz, H-2''), 8.43 (1H, s, H-8), 9.58 (1H, s, NH); ^{13}C NMR (125 MHz, DMSO-d_6) (ppm) δ 10.5 (C-3'), 18.4 (C-4'), 32.8 (CH_3), 41.7 (C-5''), 98.5 (C-1'), 101.0 (C-2'), 117.9 (C-3''), 119.8 (C_q), 128.7 (C_q), 129.0 (C-2''), 133.2 (C_q), 140.0 (C_q), 150.1 (C-8), 156.5 (C_q), 162.6 (C_q), 172.6 (CO); HRMS calcd for $C_{25}H_{35}N_6OSi$ $[M+H]^+$ 463.2636, found 463.2632.

_N_,_N_-dimethyl-2-(3-((7-methyl-6-((triisopropylsilyl)ethynyl)-7_H_-purin-2-yl) amino)phenyl)acetamide (144)

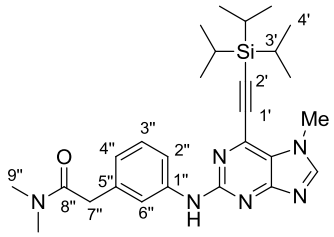

The title compound was synthesised following **general procedure I** using 2-iodo-7-methyl-6-((triisopropylsilyl)ethynyl)-7*H*-purine **106** (200 mg, 0.45 mmol), 2-(3-aminophenyl)-*N*,*N*-dimethylacetamide **119** (90 mg, 0.50 mmol), K_2CO_3 (125 mg, 0.91 mmol), $Pd(dba)_2$ (10 mg, 0.01 mmol) and XPhos (5 mg, 0.01 mmol). The crude product was purified by MPC on silica (EtOAc: MeOH 17: 3) to give the product **144** as a yellow oil (100 mg, 0.20 mmol, 45%).

R_f 0.48 (DCM: MeOH 9: 1); UV λ_{max} (EtOH) 276 nm; IR (cm^{-1}) 3314, 3178, 1679, 1616, 1496, 1306; ^{1}H NMR (500 MHz, DMSO-d_6) (ppm) δ 1.14-1.20 (21H, m, H-3' and H-4'), 2.86 (3H, s, H-9''), 3.04 (3H, s, H-9''), 3.65 (2H, s, H-7''), 4.03 (3H, s, NCH_3), 6.76 (1H, d, *J* = 7.6 Hz, H-4''), 7.20 (1H, dd, *J* = 7.6 and 7.6 Hz, H-3''), 7.70 (1H, s, H-6''), 7.71 (1H, d, *J* = 7.6 Hz, H-2''), 8.44 (1H, s, H-8), 9.61 (1H, s, NH); ^{13}C NMR (125 MHz, DMSO-d_6) (ppm) δ 10.7 (C-3'), 18.4 (C-4'), 32.8 (CH_3), 35.0 (C-9''), 37.3 (C-9''), 40.2 (C-7''), 98.6 (C-1'), 101.0 (C-2'), 116.2 (C-2''), 118.6 (C-6''), 120.0 (C_q), 121.4 (C-4''), 128.2 (C-3''), 133.2 (C_q), 136.0 (C_q), 141.1 (C_q), 150.2 (C-8), 156.5 (C_q), 162.6 (C_q), 170.1 (CO); HRMS calcd for $C_{27}H_{39}N_6OSi$ $[M+H]^+$ 491.2949, found 491.2939.

2-(3-((7-Methyl-6-((triisopropylsilyl)ethynyl)-7_H_-purin-2-yl)amino)phenyl)-_N_-(2,2,2-trifluoroethyl)acetamide (145)

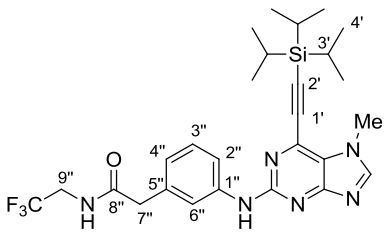

The title compound was synthesised following **general procedure I** using 2-iodo-7-methyl-6-((triisopropylsilyl)ethynyl)-7*H*-purine **106** (250 mg, 0.57 mmol), 2-(3-aminophenyl)-*N*-(2,2,2-trifluoroethyl)acetamide **120** (145 mg, 0.63 mmol), K_2CO_3 (157 mg, 1.14 mmol), $Pd(dba)_2$ (10 mg, 0.01 mmol) and XPhos (6 mg, 0.01 mmol). The crude

product was purified by MPC on silica (DCM: MeOH 19: 1) to give the product **145** as a yellow oil (150 mg, 0.28 mmol, 49%).

R_f 0.30 (DCM: MeOH 9: 1); UV λ_{max} (EtOH) 276 nm; IR (cm^{-1}) 3277, 2942, 2864, 1646, 1537, 1494, 1296; ^{1}H NMR (500 MHz, DMSO-d_6) (ppm) δ 1.14-1.21 (21H, m, H-3' and H-4'), 3.48 (2H, s, H-7''), 3.89-3.96 (2H, m, H-9''), 4.03 (3H, s, NCH_3), 6.82 (1H, d, *J* = 7.8 Hz, H-4''), 7.20 (1H, dd, *J* = 7.8 Hz, H-3''), 7.71 (1H, s, H-6''), 7.73 (1H, d, *J* = 7.8 Hz, H-2''), 8.44 (1H, s, H-8), 8.74 (1H, t, *J* = 6.1 Hz, NH), 9.63 (1H, s, NH); ^{13}C NMR (125 MHz, DMSO-d_6) (ppm) δ 10.6 (C-3'), 18.4 (C-4'), 32.8 (NCH_3), 40.0 (q, *J* = 23.0 Hz, C-9''), 42.1 (C-7''), 98.7 (C-1'), 101.0 (C-2'), 116.4 (C-2''), 118.9 (C-6''), 120.0 (C_q), 121.3 (C-4''), 126.0 (q, *J* = 279.2 Hz, CF_3), 128.2 (C-3''), 133.2 (C_q), 135.8 (C_q), 141.0 (C_q), 150.2 (C-8), 156.5 (C_q), 162.5 (C_q), 170.9 (CO); ^{19}F NMR (470 MHz, DMSO-d_6) (ppm) δ -63.9; HRMS calcd for $C_{27}H_{36}F_3N_6OSi$ $[M+H]^+$ 546.2666, found 545.2647.

3-(3-((7-Methyl-6-((triisopropylsilyl)ethynyl)-7*H*-purin-2-yl)amino)phenyl) propanamide (146)

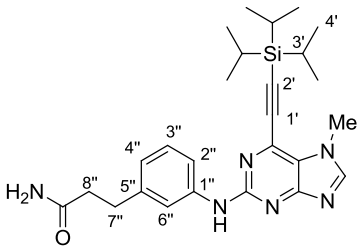

The title compound was synthesised following **general procedure I** using 2-iodo-7-methyl-6-((triisopropylsilyl)ethynyl)-7*H*-purine **106** (200 mg, 0.45 mmol), 3-(3-aminophenyl)propanamide **121** (112 mg, 0.68 mmol), K_2CO_3 (125 mg, 0.91 mmol), $Pd(dba)_2$ (10 mg, 0.01 mmol) and XPhos (5 mg, 0.01 mmol). The crude product was purified by MPC on silica (DCM: MeOH 9: 1) to give the product **146** as a yellow oil (157 mg, 0.33 mmol, 73%).

R_f 0.32 (DCM: MeOH 9: 1); UV λ_{max} (EtOH) 276 nm; IR (cm^{-1}) 3331, 3201, 2943, 2864, 1661, 1602, 1496, 1298; ^{1}H NMR (500 MHz, DMSO-d_6) (ppm) δ 1.15-1.20 (21H, m, H-3' and H-4'), 2.36 (2H, t, *J* = 8.0 Hz, H-7''), 2.77 (2H, t, *J* = 8.0 Hz, H-8''), 4.03 (3H, s, NCH_3), 6.75 (1H, br s, NH_2), 6.77 (1H, d, *J* = 7.9 Hz, H-4''), 7.17 (1H, dd, *J* = 7.9 and 7.9 Hz, H-3''), 7.26 (1H, br s, NH_2), 7.66 (1H, d, *J* = 7.9 Hz, H-2''), 7.69 (1H, s, H-6''), 8.44 (1H, s, H-8), 9.55 (1H, s, NH); ^{13}C NMR (125 MHz, DMSO-d_6) (ppm) δ 10.5 (C-3'), 18.4 (C-4'), 31.4 (C-8''), 32.8 (CH_3), 36.9 (C-7''), 98.6 (C-1'), 101.0 (C-2'), 115.8 (C-

2’’), 117.9 (C-6’’), 120.0 (C_q), 120.6 (C-4’’), 128.3 (C-3’’), 133.1 (C_q), 141.0 (C_q), 141.6 (C_q), 150.3 (C-8), 156.5 (C_q), 162.6 (C_q), 173.4 (CO); HRMS calcd for $C_{26}H_{37}N_6OSi$ $[M+H]^+$ 477.2793, found 477.2789.

_N_-(2-Acetamidoethyl)-2-(3-((7-methyl-6-((triisopropylsilyl)ethynyl)-7_H_-purin-2-yl)amino)phenyl)acetamide (147)

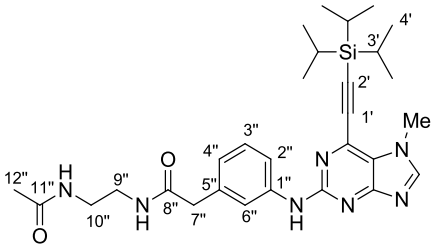

The title compound was synthesised following **general procedure I** using 2-iodo-7-methyl-6-((triisopropylsilyl)ethynyl)-7*H*-purine **106** (170 mg, 0.39 mmol), *N*-(2-acetamidoethyl)-2-(3-aminophenyl)acetamide **122** (100 mg, 0.43 mmol), K_2CO_3 (106 mg, 0.91 mmol), $Pd(dba)_2$ (8 mg, 0.01 mmol) and XPhos (4 mg, 0.01 mmol). The crude product was purified by MPC on silica (DCM: MeOH 9: 1) to give the product **147** as a yellow oil (100 mg, 0.18 mmol, 47%).

R_f 0.31 (DCM: MeOH 9: 1); UV λ_{max} (EtOH) 276 nm; IR (cm^{-1}) 3271, 3075, 2944, 2865, 1657, 1564, 1541, 1297; ^{1}H NMR (500 MHz, DMSO-d_6) (ppm) δ 1.15-1.21 (21H, m, H-3’ and H-4’), 1.79 (3H, s, H-12’’), 3.10 (4H, m, H-9’’ and H-10’’), 3.33 (2H, s, H-7’’), 4.03 (3H, s, NCH_3), 6.82 (1H, d, *J* = 7.8 Hz, H-4’’), 7.19 (1H, dd, *J* = 7.8 and 7.8 Hz, H-3’’), 7.67 (1H, s, H-6’’), 7.74 (1H, d, *J* = 7.8 Hz, H-2’’), 7.89 (1H, br s, NH), 8.08 (1H, br s, NH), 8.44 (1H, s, H-8), 9.61 (1H, s, NH); ^{13}C NMR (125 MHz, DMSO-d_6) (ppm) δ 10.7 (C-3’), 18.4 (C-4’), 22.6 (C-12’’), 32.8 (NCH_3), 38.4 (C-9’’), 38.5 (C-10’’), 42.7 (C-7’’), 98.6 (C-1’), 101.0 (C-2’), 116.3 (C-2’’), 118.8 (C-6’’), 120.0 (C_q), 121.5 (C-4’’), 128.2 (C-3’’), 133.2 (C_q), 136.4 (C_q), 140.9 (C_q), 150.2 (C-8), 156.5 (C_q), 162.5 (C_q), 169.3 (CO), 170.3 (CO); HRMS calcd for $C_{29}H_{42}N_7O_2Si$ $[M+H]^+$ 548.3164, found 548.3156.

4-((7-Methyl-6-((triisopropylsilyl)ethynyl)-7*H*-purin-2-yl)amino)benzene sulfonamide (148)

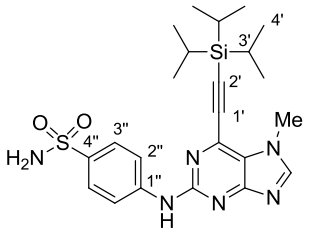

The title compound was synthesised following **general procedure I** using 2-iodo-7-methyl-6-((triisopropylsilyl)ethynyl)-7*H*-purine **106** (500 mg, 1.17 mmol), 4-aminobenzenesulfonamide **112** (215 mg, 1.25 mmol), K_2CO_3 (314 mg, 2.27 mmol), $Pd(dba)_2$ (20 mg, 0.02 mmol) and XPhos (11 mg, 0.02 mmol). The crude product was purified by MPC on silica (DCM: MeOH 19: 1) to give the product **148** as a yellow oil (195 mg, 0.40 mmol, 35%).

R_f 0.30 (DCM: MeOH 9: 1); UV λ_{max} (EtOH) 276 nm; IR (cm^{-1}) 3314, 3192, 2942, 2863, 1600, 1544, 1465, 1306, 1155; ^{1}H NMR (500 MHz, DMSO-d_6) (ppm) δ 1.14-1.24 (21H, m, H-3' and H-4'), 4.05 (3H, s, NCH_3), 7.16 (2H, s, NH_2), 7.73 (2H, d, *J* = 8.9 Hz, H-2''), 8.00 (2H, d, *J* = 8.9 Hz, H-3''), 8.51 (1H, s, H-8), 10.11 (1H, s, NH); ^{13}C NMR (125 MHz, DMSO-d_6) (ppm) δ 10.5 (C-3'), 18.6 (C-4'), 32.8 (NCH_3), 99.2 (C-1'), 100.9 (C-2'), 116.7 (C-2''), 120.5 (C_q), 126.4 (C-3''), 133.4 (C_q), 135.3 (C_q), 144.1 (C_q), 150.6 (C-8), 156.0 (C_q), 162.4 (C_q); HRMS calcd for $C_{23}H_{33}N_6O_2SSi$ $[M+H]^+$ 485.2149, found 485.2136.

7-Methyl-*N*-(pyridin-2-yl)-6-((triisopropylsilyl)ethynyl)-7*H*-purin-2-amine (149)

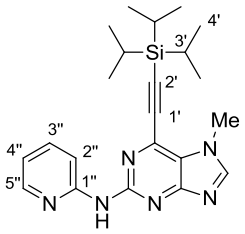

The title compound was synthesised following **general procedure I** using 2-iodo-7-methyl-6-((triisopropylsilyl)ethynyl)-7*H*-purine **106** (500 mg, 1.17 mmol), 2-aminopyridine **117** (118 mg, 1.25 mmol), K_2CO_3 (314 mg, 2.27 mmol), $Pd(dba)_2$ (20 mg, 0.02 mmol) and XPhos (11 mg, 0.02 mmol). The crude product was purified by MPC on silica (DCM: MeOH 19: 1) to give the product **149** as a yellow oil (200 mg, 0.49 mmol, 43%).

R_f 0.30 (DCM: MeOH 9: 1); UV λ_{max} (EtOH) 276 nm; IR (cm^{-1}) 3376, 3246, 1680, 1497, 1305, 1193; ^1H NMR (500 MHz, DMSO-d_6) (ppm) δ 1.15-1.22 (21H, m, H-3' and H-4'), 4.05 (3H, s, NCH_3), 6.96 (1H, ddd, *J* = 7.3, 4.9 and 1.0 Hz, H-3''), 7.75 (1H, ddd, *J* = 8.6, 7.3 and 1.9 Hz, H-4''), 8.26 (1H, m, H-2''), 8.36 (1H, d, *J* = 8.6 Hz, H-5''), 8.51 (1H, s, H-8), 9.71 (1H, s, NH); ^{13}C NMR (125 MHz, DMSO-d_6) (ppm) δ 10.6 (C-3'), 18.4 (C-4'), 32.8 (CH_3), 98.7 (C-1'), 101.0 (C-2'), 107.9 (C-2''), 111.7 (C-5''), 111.9 (C_q), 136.9 (C-4''), 137.6 (C-3''), 147.7 (C_q), 147.9 (C_q), 150.7 (C_q), 153.3 (C_8), 159.7 (C_q); HRMS calcd for $C_{22}H_{31}N_6Si$ $[M+H]^+$ 407.2374, found 407.2365.

2-(4-((6-Ethynyl-7-methyl-7*H*-purin-2-yl)amino)phenyl)acetamide (150)

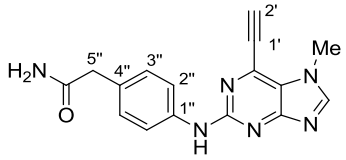

The title compound was synthesised following **general procedure A** using 2-(4-((7-methyl-6-((triisopropylsilyl)ethynyl)-7*H*-purin-2-yl)amino)phenyl)acetamide **143** (90 mg, 0.19 mmol) and TBAF (1M in THF, 0.19 mL, 0.19 mmol). The crude product was purified by MPC on silica (DCM: MeOH 9: 1) to give the product **150** as a yellow solid (28 mg, 0.09 mmol, 47%).

R_f 0.40 (DCM: MeOH 9: 1); Mp = no melt, degradation; UV λ_{max} (EtOH) 275 nm; IR (cm^{-1}) 3341, 3231, 3128, 2110, 1677, 1598, 1556, 1495, 1387, 1302; ^1H NMR (500 MHz, DMSO-d_6) (ppm) δ 3.31 (2H, s, H-5''), 4.00 (3H, s, NCH_3), 4.99 (1H, s, H-2'), 6.83 (1H, br s, NH_2), 7.17 (2H, d, *J* = 8.5 Hz, H-3''), 7.38 (1H, br s, NH_2), 7.72 (2H, d, *J* = 8.5 Hz, H-2''), 8.45 (1H, s, H-8), 9.55 (1H, s, NH); ^{13}C NMR (125 MHz, DMSO-d_6) (ppm) δ 32.8 (NCH_3), 41.7 (C-5''), 78.2 (C-1'), 87.5 (C-2'), 118.0 (C-3''), 120.3 (C_q), 128.8 (C_q), 129.0 (C-2''), 133.3 (C_q), 139.3 (C_q), 150.2 (C-8), 156.5 (C_q), 162.4 (C_q), 172.6 (CO); HRMS calcd for $C_{16}H_{15}N_6O$ $[M+H]^+$ 307.1302, found 307.1307.

2-(3-((6-Ethynyl-7-methyl-7*H*-purin-2-yl)amino)phenyl)-*N*,*N*-dimethyl acetamide (151)

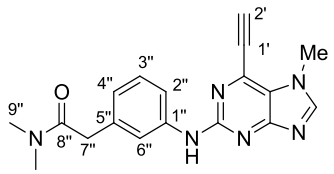

The title compound was synthesised following **general procedure A** using *N*,*N*-dimethyl-2-(3-((7-methyl-6-((triisopropylsilyl)ethynyl)-7*H*-purin-2-yl)amino)phenyl) acetamide **144** (100 mg, 0.20 mmol) and TBAF (1M in THF, 0.20 mL, 0.20 mmol). The crude product was purified by MPC on silica (DCM: MeOH 19: 1) to give the product **151** as a yellow solid (21 mg, 0.06 mmol, 31%).

R_f 0.38 (DCM: MeOH 9: 1); Mp = no melt, degradation; UV λ_{max} (EtOH) 272 nm; IR (cm^{-1}) 3200, 3094, 2108 2110, 1640, 1565, 1493, 1467, 1385; ^{1}H NMR (500 MHz, DMSO-d_6) (ppm) δ 2.86 (3H, s, H-9''), 3.05 (3H, s, H-9''), 3.66 (2H, s, C-7''), 4.01 (3H, s, NCH_3), 5.00 (1H, s, H-2'), 6.77 (1H, d, *J* = 7.9 Hz, H-4''), 7.21 (1H, dd, *J* = 7.9 and 7.9 Hz, H-3''), 7.63 (1H, s, H-6''), 7.71 (1H, d, *J* = 7.9 Hz, H-2''), 8.45 (1H, s, H-8); ^{13}C NMR (125 MHz, DMSO-d_6) (ppm) δ 32.8 (CH_3), 35.0 (C-9''), 37.2 (C-9''), 40.1 (C-7''), 78.2 (C-1'), 87.5 (C-2'), 116.2 (C-2''), 118.6 (C-6''), 120.4 (C_q), 121.5 (C-4''), 128.3 (C-3''), 133.1 (C_q), 136.0 (C_q), 141.0 (C_q), 150.3 (C-8), 156.5 (C_q), 162.6 (C_q), 170.2 (CO); HRMS calcd for $C_{18}H_{19}N_6O$ $[M+H]^+$ 335.1615, found 335.1618.

2-(3-((6-Ethynyl-7-methyl-7*H*-purin-2-yl)amino)phenyl)-*N*-(2,2,2-trifluoro ethyl)acetamide (152)

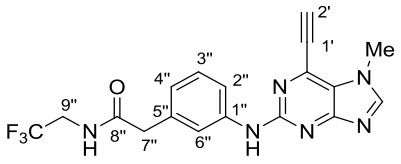

The title compound was synthesised following **general procedure A** using 2-(3-((7-methyl-6-((triisopropylsilyl)ethynyl)-7*H*-purin-2-yl)amino)phenyl)-*N*-(2,2,2-trifluoro ethyl)acetamide **145** (150 mg, 0.28 mmol) and TBAF (1M in THF, 0.29 mL, 0.29 mmol). The crude product was purified by MPC on silica (DCM: MeOH 19: 1) to give the product **152** as a yellow solid (78 mg, 0.20 mmol, 73%).

R_f 0.23 (DCM: MeOH 9: 1); Mp = no melt, degradation; UV λ_{max} (EtOH) 273 nm; IR (cm^{-1}) 3313, 3214, 3066, 2112, 1685, 1598, 1496, 1469, 1386, 1305; ^{1}H NMR (500 MHz,

DMSO-d_6) (ppm) δ 3.49 (2H, s, H-7''), 3.89-3.96 (2H, m, H-9''), 4.01 (3H, s, NCH_3), 5.00 (1H, s, H-2'), 6.83 (1H, d, *J* = 7.9 Hz, H-4''), 7.22 (1H, dd, *J* = 7.9 and 7.9 Hz, H-3''), 7.63 (1H, s, H-6''), 7.75 (1H, d, *J* = 7.9 Hz, H-2''), 8.45 (1H, s, H-8), 8.76 (1H, t, *J* = 6.3 Hz, NH), 9.59 (1H, s, NH); ^{13}C NMR (125 MHz, DMSO-d_6) (ppm) δ 32.8 (NCH_3), 39.9 (q, *J* = 20.7 Hz, C-9''), 42.1 (C-7''), 78.2 (C-1'), 87.5 (C-2'), 116.4 (C-2''), 118.9 (C-6''), 120.3 (C_q), 121.5 (C-4''), 124.0 (q, *J* = 280.3 Hz, CF_3), 128.3 (C-3''), 133.2 (C_q), 135.9 (C_q), 140.9 (C_q), 150.2 (C-8), 156.4 (C_q), 162.4 (C_q), 170.9 (CO); ^{19}F NMR (470 MHz, DMSO-d_6) (ppm) δ -70.7; HRMS calcd for $C_{18}H_{16}F_3N_6O$ $[M+H]^+$ 389.1332, found 389.1326.

3-(3-((6-Ethynyl-7-methyl-7*H*-purin-2-yl)amino)phenyl)propanamide (153)

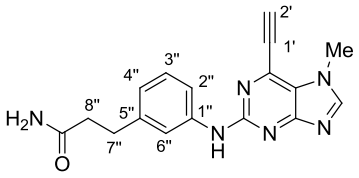

The title compound was synthesised following **general procedure A** using 3-(3-((7-methyl-6-((triisopropylsilyl)ethynyl)-7*H*-purin-2-yl)amino)phenyl)propanamide **146** (160 mg, 0.34 mmol) and TBAF (1M in THF, 0.34 mL, 0.34 mmol). The crude product was purified by MPC on silica (DCM: MeOH 9: 1) to give the product **153** as a yellow solid (30 mg, 0.10 mmol, 28%).

R_f 0.25 (DCM: MeOH 9: 1); Mp = 147-150 °C; UV λ_{max} (EtOH) 272 nm; IR (cm^{-1}) 3301, 3194, 3074, 2110, 1660, 1595, 1556, 1482, 1390, 1288; ^{1}H NMR (500 MHz, DMSO-d_6) (ppm) δ 2.34-2.37 (2H, m, H-7''), 2.76-2.79 (2H, m, H-8''), 4.01 (3H, s, NCH_3), 5.00 (1H, s, H-2'), 6.78 (1H, d, *J* = 7.8 Hz, H-4''), 6.79 (1H, br s, NH_2), 7.19 (1H, dd, *J* = 7.9 and 7.9 Hz, H-3''), 7.32 (1H, br s, NH_2), 7.58 (1H, s, H-6''), 7.72 (1H, d, *J* = 7.8 Hz, H-2''), 8.45 (1H, s, H-8), 9.54 (1H, s, NH); ^{13}C NMR (125 MHz, DMSO-d_6) (ppm) δ 31.3 (C-8''), 32.8 (CH_3), 36.8 (C-7''), 78.2 (C-1'), 87.5 (C-2'), 115.8 (C-2''), 118.0 (C-6''), 120.3 (C_q), 120.7 (C-4''), 128.3 (C-3''), 133.1 (C_q), 141.0 (C_q), 141.6 (C_q), 150.2 (C-8), 156.5 (C_q), 162.5 (C_q), 173.4 (CO); HRMS calcd for $C_{17}H_{17}N_6O$ $[M+H]^+$ 321.1458, found 321.1763.

_N_-(2-acetamidoethyl)-2-(3-((6-ethynyl-7-methyl-7_H_-purin-2-yl)amino)phenyl) acetamide (154)

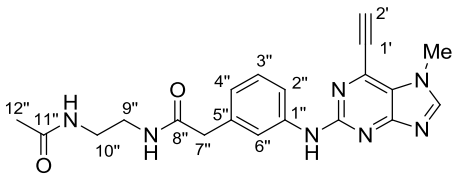

The title compound was synthesised following **general procedure A** using *N*-(2-acetamidoethyl)-2-(3-((7-methyl-6-((triisopropylsilyl)ethynyl)-7*H*-purin-2-yl) amino) phenyl)acetamide **147** (100 mg, 0.19 mmol) and TBAF (1M in THF, 0.19 mL, 0.19 mmol). The crude product was purified by MPC on silica (DCM: MeOH 9: 1) to give the product **154** as a yellow solid (46 mg, 0.12 mmol, 64%).

R_f 0.29 (DCM: MeOH 9: 1); Mp = no melt, degradation; UV λ_{max} (EtOH) 273 nm; IR (cm^{-1}) 3293, 3246, 3068, 2113, 1639, 1568, 1542, 1475, 1303, 1276; ^{1}H NMR (500 MHz, DMSO-d_6) (ppm) δ 1.79 (3H, s, H-12’’), 3.11 (4H, m, H-9’’ and H-10’’), 3.38 (2H, s, H-7’’), 4.01 (3H, s, NCH_3), 5.00 (1H, s, H-2’), 6.83 (1H, d, *J* = 7.8 Hz, H-4’’), 7.21 (1H, dd, *J* = 7.8 and 7.8 Hz, H-3’’), 7.61 (1H, s, H-6’’), 7.75 (1H, d, *J* = 7.8 Hz, H-2’’), 7.89 (1H, br s, NH), 8.09 (1H, br s, NH), 8.45 (1H, s, H-8), 9.57 (1H, s, NH); ^{13}C NMR (125 MHz, DMSO-d_6) (ppm) δ 22.6 (C-12’’’), 32.8 (CH_3), 38.4 (C-10’’), 38.5 (C-9’’), 42.7 (C-7’’), 78.2 (C-1’), 87.5 (C-2’), 116.3 (C-2’’), 118.8 (C-6’’), 120.3 (C_q), 121.6 (C-4’’), 128.2 (C-3’’), 133.2 (C_q), 136.5 (C_q), 140.9 (C_q), 150.2 (C-8), 156.5 (C_q), 162.4 (C_q), 169.3 (CO), 170.3 (CO); HRMS calcd for $C_{20}H_{22}N_7O_2$ $[M+H]^+$ 392.1829, found 392.1829.

4-((6-Ethynyl-7-methyl-7*H*-purin-2-yl)amino)benzenesulfonamide (155)

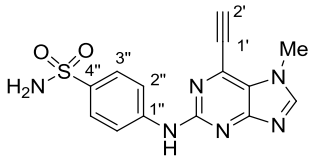

4-((7-Methyl-6-((triisopropylsilyl)ethynyl)-7*H*-purin-2-yl)amino)benzene sulfonamide **148** (80 mg, 0.17 mmol) was solubilised in 5 mL of anhydrous MeOH. Fluoride on polymer support (100 mg) was added and the reaction was agitated with a shaker for 2 h. Beads were removed and the solvent was removed *in vacuo* to give the product **155** as an orange solid (20 mg, 0.06 mmol, 37%).

R_f 0.19 (DCM: MeOH 9: 1); Mp = no melt, degradation; UV λ_{max} (EtOH) 281 nm; IR (cm^{-1}) 3253, 3080, 2953, 2113, 1596, 1561, 1493, 1466, 1309, 1149; ^{1}H NMR (500 MHz,

DMSO-d_6) (ppm) δ 4.03 (3H, s, NCH_3), 5.07 (1H, s, H-2'), 7.17 (2H, s, NH_2), 7.74 (2H, d, *J* = 8.9 Hz, H-2''), 7.97 (2H, d, *J* = 8.9 Hz, H-3''), 8.53 (1H, s, H-8), 10.10 (1H, s, NH); ^{13}C NMR (125 MHz, DMSO-d_6) (ppm) δ 32.9 (NCH_3), 78.0 (C-1'), 88.0 (C-2'), 116.9 (C-3''), 120.9 (C_q), 126.5 (C-2''), 133.3 (C_q), 135.5 (C_q), 144.1 (C_q), 150.7 (C-8), 155.7 (C_q), 162.3 (C_q); HRMS calcd for $C_{14}H_{13}N_6O_2S$ $[M+H]^+$ 329.0815, found 329.082.

6-Ethynyl-7-methyl-*N*-(pyridin-2-yl)-7*H*-purin-2-amine (156)

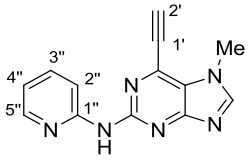

7-Methyl-*N*-(pyridin-2-yl)-6-((triisopropylsilyl)ethynyl)-7*H*-purin-2-amine **149** (200 mg, 0.49 mmol) was solubilised in dry THF (10 mL). The solution was stirred for 10 min at -78 ^{0}C and TBAF (1M in THF, 0.54 mL, 0.54 mmol) was slowly added. The reaction was stirred for 5 min at -78 ^{0}C, until completion. The crude product was purified by MPC on silica (DCM: MeOH 19: 1) to give the product **156** as an orange solid (55 mg, 0.22 mmol, 45%).

R_f 0.23 (DCM: MeOH 9: 1); Mp = no melt, degradation; UV λ_{max} (EtOH) 273 nm; IR (cm^{-1}) 3344, 3178, 3021, 2103, 1601, 1579, 1423, 1390; ^{1}H NMR (500 MHz, DMSO-d_6) (ppm) δ 4.03 (3H, s, NCH_3), 5.05 (1H, s, H-2'), 6.97 (1H, ddd, *J* = 7.3, 4.9 and 1.0 Hz, H-3''), 7.78 (1H, ddd, *J* = 8.6, 7.3 and 1.9 Hz, H-4''), 8.26 (1H, ddd, *J* = 4.9, 1.9 and 1.0 Hz, H-2''), 8.35 (1H, d, *J* = 8.6 Hz, H-5''), 8.52 (1H, s, H-8), 9.68 (1H, s, NH); ^{13}C NMR (125 MHz, DMSO-d_6) (ppm) δ 32.9 (NCH_3), 78.2 (C-1'), 88.1 (C-2'), 111.9 (C-5''), 117.0 (C-3''), 121.0 (C_q), 128.3 (C_q), 133.1 (C_q), 137.6 (C-4''), 147.9 (C-2''), 150.6 (C-8), 153.3 (C_q), 155.2 (C_q); HRMS calcd for $C_{13}H_{11}N_6$ $[M+H]^+$ 251.1040, found 251.1043.

(*E*)-methyl 2-acetamido-3-((2-(2-((3-(2-amino-2-oxoethyl)phenyl)amino)-9*H*-purin-6-yl)vinyl)thio)propanoate (158)

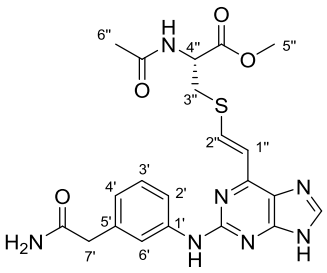

2-(3-((6-Ethynyl-9*H*-purin-2-yl)amino)phenyl)acetamide **42** (50 mg, 0.17 mmol), *N*-acetylcysteine methyl ester **157** (151 mg, 0.85 mmol) and DABCO (10 mg, 0.09 mmol) were solubilised in anhydrous DMF (8 mL). The resulting solution was stirred at r.t. for 16 h. The solvent was then removed *in vacuo*. The crude product was purified by MPC on silica (EtOAc: MeOH 9: 1) to give the product **158** as a yellow solid (41 mg, 0.09 mmol, 51 %).

R_f 0.55 (EtOAc: MeOH 9: 1); Mp = 269-272 ^{o}C; UV λ_{max} (EtOH) 273 nm; ^{1}H NMR (500 MHz, DMSO-d_6) (ppm) δ 1.88 (3H, s, H-‘’), 3.27 (1H, dd, *J* = 13.5 and 7.8 Hz, H-3’’), 3.35 (2H, s, H-7’), 3.42 (1H, dd, *J* = 13.5 and 7.8 Hz, H-3’’), 3.68 (3H, s, H-5’’), 4.60 - 4.64 (1H, m, H-4’’), 6.79 (1H, d, *J* = 15.5 Hz, H-1’’), 6.83 (1H, d, *J* = 7.8 Hz, H-4’), 6.86 (1H, br s, NH_2), 7.20 (1H, dd, *J* = 7.8 Hz, H-3’), 7.43 (1H, br s, NH_2), 7.69 (1H, d, *J* = 7.8 Hz, H-2’), 7.74 (1H, s, H-6’), 8.17 (1H, s, H-8), 8.29 (1H, d, *J* = 15.5 Hz, H-2’’), 8.57 (1H, d, *J* = 7.8 Hz, NH), 9.32 (1H, s, NH), 12.89 (1H, br s, N^9H); ^{13}C NMR (125 MHz, DMSO-d_6) (ppm) δ 22.3 (C-6’’), 33.0 (C-3’’), 42.6 (C-7’), 51.6 (C-4’’), 52.3 (C-5’’), 116.5 (C-2’), 119.1 (C-6’), 120.2 (C-1’’), 121.4 (C-4’), 123.8 (C_q), 128.1 (C-3’), 136.5 (C_q), 138.8 (C-2’’), 141.1 (C_q), 141.4 (C-8), 151.4 (C_q), 153.8 (C_q), 156.1 (C_q), 169.6 (CO), 170.7 (CO), 172.3 (CO); HRMS calcd for $C_{21}H_{24}N_7O_4S$ $[M+H]^+$ 470.1605, found 470.1602.

6-(Cyclohexylmethoxy)-*N*-(4-(prop-1-en-2-ylsulfonyl)phenyl)-9*H*-purin-2-amine (162)

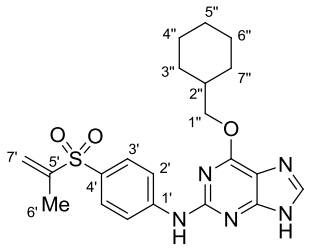

6-(Cyclohexylmethoxy)-*N*-(4-((1-(pyrrolidin-1-yl)propan-2-yl)thio)phenyl)-9*H*-purin-2-amine **181** (65 mg, 0.14 mmol) was solubilised in dry DCM (5 mL). *m*-CPBA (84 mg, 0.49 mmol) was then added to the solution and the reaction was stirred at reflux for 3 h. The solvent was removed *in vacuo*. The product was purified by prep-TLC (DCM: MeOH 9: 1) to give the product **162** as a pale orange oil (20 mg, 0.05 mmol, 33%).

R_f 0.19 (DCM: MeOH 9: 1); UV λ_{max} (EtOH) 314 nm; IR (cm^{-1}) 2931, 2842, 1572, 1421, 1025; ^{1}H NMR (500 MHz, DMSO-d_6) (ppm) δ 1.06-1.12 (2H, m, H-cyclo), 1.18-1.20 (1H, m, H-cyclo), 1.23-1.32 (2H, m, H-cyclo), 1.66 (1H, m, H-cyclo), 1.72-1.75 (2H, m, H-cyclo), 1.84-1.87 (3H, m, H-cyclo, H-2’’), 1.91 (3H, s, H-6’), 4.33 (2H, d, *J* = 6.3 Hz, H-1’’), 5.82 (1H, d, *J* = 1.6 Hz, H-7’), 6.06 (2H, d, *J* = 1.6 Hz, H-7’), 7.66 (2H, d, *J* = 8.8 Hz, H-2’), 7.68 (1H, s, NH), 7.79 (1H, s, H-8), 8.10 (2H, d, *J* = 8.8 Hz, H-3’), 9.56 (1H, s, N^9H); ^{13}C NMR (125 MHz, DMSO-d_6) (ppm) δ 15.6 (C-6’), 25.2 (2 x C-cyclo), 26.0 (C-cyclo), 29.2 (2 x C-cyclo), 36.9 (C-2’’), 71.1 (C-1’’), 117.1 (C-3’), 123.3 (C-7’), 125.9 (C_q), 127.2 (C_q), 129.0 (C-2’), 134.5 (C_q), 146.4 (C-8), 146.6 (C_q), 153.2 (C_q), 159.1 (C_q); HRMS calcd for $C_{21}H_{26}N_5O_3S$ $[M+H]^+$ 428.1751, found 428.1751.

***N*-(4-(But-1-en-2-ylsulfonyl)phenyl)-6-(cyclohexylmethoxy)-9*H*-purin-2-amine (163)**

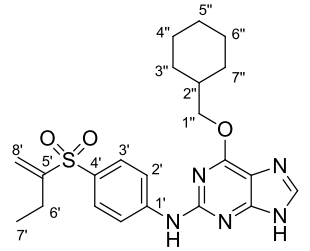

The title compound was synthesised following **general procedure N** using 6-(cyclohexylmethoxy)-*N*-(4-((1-(pyrrolidin-1-yl)butan-2-yl)sulfonyl)phenyl)-9*H*-purin-2-amine **230** (180 mg, 0.35 mmol), *m*-CPBA (90 mg, 0.39 mmol) and Cs_2CO_3 (280 mg,

0.88 mmol). The product was purified by MPC (DCM: MeOH 19: 1) to give the product **163** as a yellow oil (36 mg, 0.08 mmol, 23%).

R_f 0.48 (DCM: MeOH 19: 1); UV λ_{max} (EtOH) 317 nm; IR (cm^{-1}) 2924, 2851, 1594, 1451, 1384, 1295, 1128; ^{1}H NMR (500 MHz, DMSO-d_6) (ppm) δ 1.00 (3H, t, *J* = 7.2 Hz, H-7'), 1.06-1.14 (2H, m, H-cyclo), 1.18-1.21 (1H, m, H-cyclo), 1.24-1.31 (2H, m, H-cyclo), 1.66-1.68 (1H, m, H-cyclo), 1.72-1.75 (2H, m, H-cyclo), 1.84-1.86 (5H, m, H-cyclo, H-2''), 22.21 (2H, q, *J* = 7.2 Hz, H-7'), 4.37 (2H, d, *J* = 6.3 Hz, H-1''), 5.84 (1H, s, H-8'), 6.19 (1H, s, H-8'), 7.72 (2H, d, *J* = 8.7 Hz, H-2'), 8.05-8.07 (3H, m, H-8 and H-3'), 9.97 (1H, br s, NH), 12.97 (1H, br s, N^9H); ^{13}C NMR (125 MHz, DMSO-d_6) (ppm) δ 12.0 (C-7'), 22.0 (C-6'), 25.2 (2 x C-cyclo), 26.0 (C-cyclo), 29.2 (2 x C-cyclo), 36.8 (C-2''), 71.4 (C-1''), 115.5 (C_q), 117.6 (C-3'), 121.6 (C-8'), 128.6 (C_q), 129.0 (C-2'), 139.7 (C-8), 146.1 (C_q), 152.1 (C_q), 153.8 (C_q), 154.4 (C_q), 160.2 (C_q); HRMS calcd for $C_{22}H_{27}N_5O_3S$ $[M+H]^+$ 442.1907, found 442.1904.

6-(Cyclohexylmethoxy)-*N*-(4-((3-methylbut-1-en-2-yl)sulfonyl)phenyl)-9*H*-purin-2-amine (164)

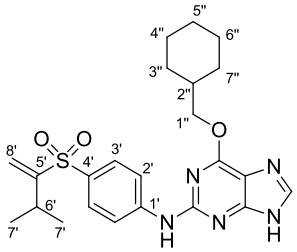

The title compound was synthesised following **general procedure N** using 6-(cyclohexylmethoxy)-*N*-(4-((3-methyl-1-(pyrrolidin-1-yl)butan-2-yl)sulfonyl)phenyl)-9*H*-purin-2-amine **231** (70 mg, 0.13 mmol), *m*-CPBA (34 mg, 0.15 mmol) and Cs_2CO_3 (108 mg, 0.33 mmol). The product was purified by MPC (DCM: MeOH 19: 1) to give the product **164** as a yellow oil (36 mg, 0.08 mmol, 23%).

R_f 0.34 (DCM: MeOH 19: 1); UV λ_{max} (EtOH) 317 nm; IR (cm^{-1}) 3348, 2926, 2852, 1593, 1532, 1450, 1389, 1291, 1123; ^{1}H NMR (500 MHz, $CDCl_3$) (ppm) δ 1.07-1.09 (6H, d, *J* = 6.8 Hz, H-7'), 1.11-1.16 (2H, m, H-cyclo), 1.21-1.24 (1H, m, H-cyclo), 1.26-1.31 (2H, m, H-cyclo), 1.70-1.73 (1H, m, H-cyclo), 1.77-1.79 (2H, m, H-cyclo), 1.91-1.93 (3H, m, H-cyclo, H-2''), 2.67-2.72 (1H, m, H-6'), 4.37 (2H, d, *J* = 5.7 Hz, H-1''), 5.78 (1H, s, H-8'), 6.36 (1H, s, H-8'), 7.81 (2H, d, *J* = 8.1 Hz, H-2'), 7.88-7.95 (3H, m, H-3' and H-8). ^{13}C NMR (125 MHz, $CDCl_3$) (ppm) δ 12.0 (C-7'), 22.0 (C-6'), 25.2 (2 x C-cyclo), 26.0 (C-cyclo), 29.2 (2 x C-cyclo), 36.8 (C-2''), 71.4 (C-1''), 115.5 (C_q), 117.6 (C-3'), 121.6

(C-8'), 128.6 (C_q), 129.0 (C-2'), 139.7 (C-8), 146.1 (C_q), 152.1 (C_q), 153.8 (C_q), 154.4 (C_q), 160.2 (C_q); HRMS calcd for $C_{23}H_{30}N_5O_3S$ $[M+H]^+$ 456.2064, found 456.2069.

6-(Cyclohexylmethoxy)-*N*-(4-((1-phenylvinyl)sulfonyl)phenyl)-9*H*-purin-2-amine (165)

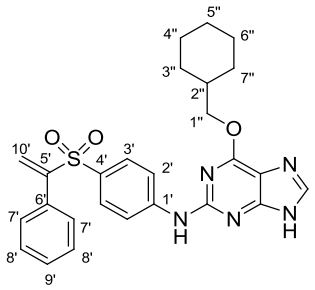

The title compound was synthesised following **general procedure N** using 6-(cyclohexylmethoxy)-*N*-(4-((1-phenyl-2-(pyrrolidin-1-yl)ethyl)sulfonyl)phenyl)-9*H*-purin-2-amine **232** (180 mg, 0.32 mmol), *m*-CPBA (82 mg, 0.35 mmol) and Cs_2CO_3 (261 mg, 0.80 mmol). The product was purified by MPC (DCM: MeOH 19: 1) to give the product **165** as an orange oil (45 mg, 0.09 mmol, 29%).

R_f 0.51 (DCM: MeOH 19: 1); UV λ_{max} (EtOH) 320 nm; IR (cm^{-1}) 2923, 2850, 1593, 1495, 1450, 1384, 1298, 1138; ^{1}H NMR (500 MHz, DMSO-d_6) (ppm) δ 1.05-1.12 (2H, m, H-cyclo), 1.18-1.20 (1H, m, H-cyclo), 1.23-1.31 (2H, m, H-cyclo), 1.66-1.68 (1H, m, H-cyclo), 1.72-1.74 (2H, m, H-cyclo), 1.81-1.87 (3H, m, H-cyclo, H-2''), 4.35 (2H, d, *J* = 6.3 Hz, H-1''), 6.18 (1H, s, H-10'), 6.47 (1H, s, H-10'), 7.34-7.38 (5H, m, H-ar), 7.56 (2H, d, *J* = 8.9 Hz, H-2'), 7.95 (2H, d, *J* = 8.9 Hz, H-3'), 8.06 (1H, s, H-8), 9.93 (1H, s, NH), 12.95 (1H, s, N^9H); ^{13}C NMR (125 MHz, DMSO-d_6) (ppm) δ 25.2 (2 x C-cyclo), 26.0 (C-cyclo), 29.2 (2 x C-cyclo), 36.8 (C-2''), 71.4 (C-1''), 115.5 (C_q), 117.0 (C_q), 117.3 (C-3'), 125.6 (C-10'), 128.3 (2 x C-ar), 128.5 (2 x C-ar), 129.0 (C-2'), 129.2 (C-ar), 139.7 (C-8), 146.1 (C_q), 150.3 (C_q), 153.7 (C_q), 154.4 (C_q), 160.1 (C_q); HRMS calcd for $C_{26}H_{28}N_5O_3S$ $[M+H]^+$ 490.1907, found 490.1910.

6-(Cyclohexylmethoxy)-*N*-(4-((3,3-dimethylbut-1-en-2-yl)sulfonyl)phenyl)-9*H*-purin-2-amine (166)

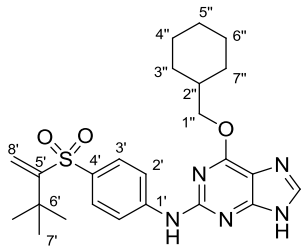

The title compound was synthesised following **general procedure P** using 2-((4-((6-(cyclohexylmethoxy)-9*H*-purin-2-yl)amino)phenyl)sulfonyl)-3,3-dimethylbutan-1-ol **254** (27 mg, 0.06 mmol), Et_3N (6.0 μL, 0.07 mmol) and MsCl (5.0 μL, 0.07 mmol). After 1 h, DBU (0.10 mL, 0.69 mmol) was added and the reaction was stirred at r.t. for 1 h. The solvent was removed *in vacuo*. The product was purified by MPC (EtOAc: MeOH 19: 1) to give the product **166** as a pale yellow oil (18 mg, 0.04 mmol, 69%).

R_f 0.19 (100 EtOAc); UV λ_{max} (EtOH) 317 nm; IR (cm^{-1}) 3260, 2925, 2852, 1592, 1450, 1317, 1114; ^{1}H NMR (500 MHz, MeOD) (ppm) δ 1.10-1.17 (2H, m, H-cyclo), 1.22-1.25 (10H, m, H-cyclo and H-7'), 1.28-1.36 (2H, m, H-cyclo), 1.70-1.72 (1H, m, H-cyclo), 1.77-1.79 (2H, m, H-cyclo), 1.90-1.92 (3H, m, H-cyclo and H-2''), 4.35 (2H, d, *J* = 6.1 Hz, H-1''), 6.00 (1H, d, *J* = 1.5 Hz, H-8'), 6.19 (1H, d, *J* = 1.5 Hz, H-8'), 7.72 (2H, d, *J* = 8.9 Hz, H-3'), 8.01-8.04 (3H, m, H-2' and H-8); ^{13}C NMR (125 MHz, MeOD) (ppm) δ 24.7 (2 x C-cyclo), 25.4 (C-cyclo), 28.6 (2 x C-cyclo), 28.7 (C-7'), 35.3 (C-6'), 36.4 (C-2''), 71.1 (C-1''), 116.6 (C-2'), 127.8 (C-8'), 131.0 (C-3'), 138.9 (C-8), 145.1 (C_q), 154.2 (C_q), 154.4 (C_q), 159.3 (C_q); HRMS calcd for $C_{24}H_{32}N_5O_3S$ $[M+H]^+$ 470.2220, found 470.2210.

Note: Three quaternary carbons were not visible on ^{13}C NMR spectrum

_N_-(4-((1-Chlorovinyl)sulfonyl)phenyl)-6-(cyclohexylmethoxy)-9_H_-purin-2-amine (167)

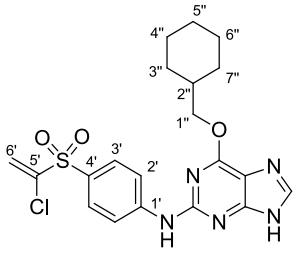

The title compound was synthesised following **general procedure P** using 2-chloro-2-((4-((6-(cyclohexylmethoxy)-9*H*-purin-2-yl)amino)phenyl)sulfonyl)ethanol **268** (90.0 mg, 0.19 mmol), Et_3N (0.03 mL, 0.20 mmol) and MsCl (16.0 μL, 0.20 mmol). The crude product was purified by MPC on silica (petrol: EtOAc 4: 1) to give the product **167** as a colourless oil (19 mg, 0.04 mmol, 22%).

R_f 0.35 (EtOAc 100); UV λ_{max} (EtOH) 322 nm; IR (cm^{-1}) 2922, 2850, 1591, 1449, 1309, 1150; ^{1}H NMR (500 MHz, MeOD) (ppm) δ 1.16-1.22 (2H, m, H-cyclo), 1.26-1.29 (1H, m, H-cyclo), 1.32-1.40 (2H, m, H-cyclo), 1.73-1.75 (2H, m, H-cyclo), 1.73-1.75 (1H, m, H-cyclo), 180-1.82 (2H, m, H-cyclo), 1.94-1.96 (3H, m, H-cyclo and H-2’’), 4.40 (2H, d, *J* = 6.2 Hz, H-1’’), 6.17 (1H, d, *J* = 3.1 Hz, H-6’), 6.67 (1H, d, *J* = 3.1 Hz, H-6’), 7.83 (2H, d, *J* = 9.0 Hz, H-3’), 8.04 (1H, br s, H-8), 8.11 (2H, d, *J* = 9.0 Hz, H-2’); ^{13}C NMR (125 MHz, MeOD) (ppm) δ 26.9 (2 x C-cyclo), 27.5 (C-cyclo), 30.8 (2 x C-cyclo), 38.7 (C-2’’), 73.3 (C-1’’), 118.9 (C-2’), 124.1 (C-6’), 127.8 (C_q), 131.4 (C-3’), 140.5 (C-8), 142.4 (C_q), 148.6 (C_q), 156.6 (C_q); HRMS calcd for $C_{20}H_{23}ClN_5O_3S$ $[M+H]^+$ 448.1205, found 448.1202.

Note: Three quaternary carbons were not visible on the ^{13}C NMR spectrum

6-(Cyclohexylmethoxy)-_N_-(4-((1-fluorovinyl)sulfonyl)phenyl)-9_H_-purin-2-amine (168)

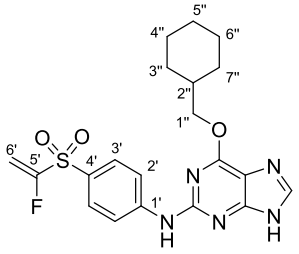

The title compound was synthesised following **general procedure P** using 2-((4-((6-(cyclohexylmethoxy)-9*H*-purin-2-yl)amino)phenyl)sulfonyl)-2-fluoroethanol **272** (155

mg, 0.35 mmol), Et_3N (0.05 mL, 0.38 mmol) and MsCl (30.0 μL, 0.38 mmol). The crude product was purified by MPC on silica (petrol: EtOAc 2: 3) to give the product **168** as a colourless oil (26 mg, 0.06 mmol, 10%).

R_f 0.17 (petrol: EtOAc 1: 1); UV λ_{max} (EtOH) 321 nm; IR (cm^{-1}) 3134, 2927, 2853, 1595, 1509, 1453, 1331, 1145; ^{1}H NMR (500 MHz, MeOD) (ppm) δ 1.14-1.21 (2H, m, H-cyclo), 1.25-1.27 (1H, m, H-cyclo), 1.29-1.40 (2H, m, H-cyclo), 1.73-1.75 (1H, m, H-cyclo), 1.80-1.83 (2H, m, H-cyclo), 1.94-1.98 (3H, m, H-cyclo and H-2''), 4.40 (2H, d, *J* = 6.1 Hz, H-1''), 5.54 (1H, dd, *J* = 4.7 and 13.3 Hz, H-6'), 5.85 (1H, dd, *J* = 4.7 and 43.3 Hz, H-6'), 7.83 (2H, d, *J* = 8.8 Hz, H-3'), 8.03 (1H, s, H-8), 8.12 (2H, d, *J* = 8.8Hz, H-2'); ^{13}C NMR (125 MHz, MeOD) (ppm) δ 26.9 (2 x C-cyclo), 27.6 (C-cyclo), 30.8 (2 x C-cyclo), 38.7 (C-2''), 73.3 (C-1''), 100.3 (d, *J* = 9.9 Hz, C-6'), 119.1 (C-2'), 128.1 (C_q), 131.0 (C-3'), 148.8 (C-8), 156.6 (C_q), 161.7 (C_q), 164.0 (C_q); ^{19}F NMR (470 MHz, MeOD) (ppm) δ -117.7; HRMS calcd for $C_{20}H_{23}FN_5O_3S$ $[M+H]^+$ 432.1500, found 432.1494.

Note: Three quaternary carbons were not visible on the ^{13}C NMR spectrum

6-(Cyclohexylmethoxy)-2-iodo-9-(4-methoxybenzyl)-9*H*-purine (171)

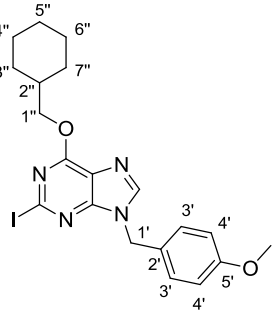

The title compound was synthesised following **general procedure G** using 6-(cyclohexylmethoxy)-9-(4-methoxybenzyl)-9*H*-purin-2-amine **172** (344 mg, 0.94 mmol), CH_2I_2 (0.38 mL, 4.70 mmol), Cu(I)I (269 mg, 1.40 mmol) and isoamyl nitrite (0.38 mL, 2.80 mmol). The crude product was purified by medium pressure chromatography on silica (petrol: EtOAc 2: 3) to give the product **171** as yellow oil (300 mg, 0.63 mmol, 67%).

R_f 0.63 (petrol: EtOAc 1: 1); UV λ_{max} (EtOH) 245 nm; IR (cm^{-1}) 2926, 2853, 1585, 1514, 1414, 1358, 1252; ^{1}H NMR (500 MHz, DMSO-d_6) (ppm) δ 1.00-1.08 (2H, m, H-3'' and H-7''), 1.16-1.30 (3H, m, H-5'', H-4'' and H-6''), 1.65-1.67 (1H, m, H-5''), 1.70-1.73 (2H, m, H-4'' and H-6''), 1.79-1.81 (3H, m, H-2'', H-3'' and H-7''), 3.73 (3H, s, OCH_3),

4.31 (2H, d, *J* = 6.2 Hz, H-1’’), 5.34 (2H, s, H-1’), 6.92 (2H, d, *J* = 8.7 Hz, H-3’), 7.27 (2H, d, *J* = 8.7 Hz, H-4’), 8.39 (1H, s, H-8); ^{13}C NMR (125 MHz, DMSO-*d*$_6$) (ppm) δ 25.1 (C-4’’ and C-6’’), 25.8 (C-5’’), 28.9 (C-3’’ and C-7’’), 36.7 (C-2’’), 46.2 (C-1’), 55.0 (OCH_3), 72.2 (C-1’’), 114.1 (C-3’), 118.3 (C_q), 120.4 (C_q), 128.2 (C_q), 129.0 (C-4’), 143.5 (C-8), 152.8 (C_q), 159.0 (C_q), 159.8 (C_q); HRMS calcd for $C_{20}H_{24}IN_4O_2$ $[M+H]^+$ 479.0938, found 479.0929.

6-(Cyclohexylmethoxy)-9-(4-methoxybenzyl)-9*H*-purin-2-amine (172)

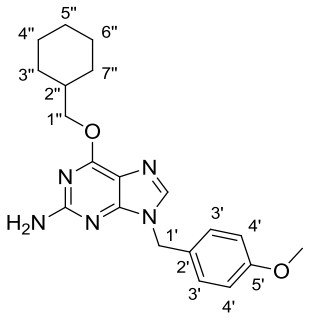

NaH (62 mg, 2.59 mmol) was added to a stirred solution of cyclohexylmethanol (0.32 mL, 2.59 mmol) in anhydrous THF (10 mL) under N_2. The resulting suspension was stirred for 1 h at r.t. then 6-chloro-9-(4-methoxybenzyl)-9*H*-purin-2-amine **80** (500 mg, 1.72 mmol) was added, and the reaction was stirred at r.t. for 16 h. Water was added (20 mL) and the organic phase was extacted with EtOAc (3 x 30 mL). The organic phases were combined, dried over $MgSO_4$ and the solvent was removed *in vacuo*. The crude product was purified by MPC on silica (petrol: EtOAc 2: 3) to give the product **172** as a white solid (445 mg, 1.21 mmol, 70%).

R_f 0.56 (petrol: EtOAc 2: 3); Mp = 147-149 °C; UV λ_{max} (EtOH) 263 nm; IR (cm $^{-1}$) 3355, 2925, 2853, 1606, 1580, 1514, 1445, 1410, 1260; ^{1}H NMR (500 MHz, DMSO-*d*$_6$) (ppm) δ 1.00-1.08 (2H, m, H-3’’ and H-7’’), 1.16-1.30 (3H, m, H-5’’, H-4’’ and H-6’’), 1.65-1.67 (1H, m, H-5’’), 1.70-1.73 (2H, m, H-4’’ and H-6’’), 1.79-1.81 (3H, m, H-2’’, H-3’’ and H-7’’), 3.72 (3H, s, OCH_3), 4.22 (2H, d, *J* = 6.2 Hz, H-1’’), 5.16 (2H, s, H-1’), 6.39 (2H, s, NH_2), 6.90 (2H, d, *J* = 8.7 Hz, H-3’), 7.22 (2H, d, *J* = 8.7 Hz, H-4’), 7.91 (1H, s, H-8); ^{13}C NMR (125 MHz, DMSO-*d*$_6$) (ppm) δ 25.2 (C-4’’ and C-6’’), 26.0 (C-5’’), 29.2 (C-3’’ and C-7’’), 36.8 (C-2’’), 45.2 (C-1’), 55.1 (OCH_3), 70.6 (C-1’’), 113.6 (C_q), 114.0 (C-3’), 128.6 (C-4’), 129.2 (C_q), 139.5 (C-8), 154.1 (C_q), 158.7 (C_q), 159.9 (C_q), 160.6 (C_q); HRMS calcd for $C_{20}H_{26}N_5O_2$ $[M+H]^+$ 368.2081, found 368.2085.

Ethyl 2-((4-nitrophenyl)thio)propanoate (175)[262]

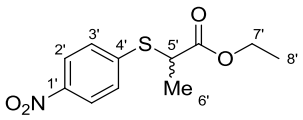

The title compound was synthesised following **general procedure J** using methyl 2-bromopropionate **174** (0.80 mL, 7.10 mmol), 4-nitrothiophenol **173** (1.00 g, 6.46 mmol) and Et_3N (1.00 mL, 7.10 mmol). The crude product was purified by MPC on silica (petrol: EtOAc 9: 1) to give the products **175** as a yellow oil (1.56 g, 6.14 mmol, 94%).

R_f 0.35 (petrol: EtOAc 4: 1); UV λ_{max} (EtOH) 331 nm; IR (cm^{-1}) 2983, 2937, 1728, 1512, 1337, 1157; ^{1}H NMR (500 MHz, DMSO-d_6) (ppm) δ 1.12 (3H, t, *J* = 7.1 Hz, H-8'), 1.49 (3H, t, *J* = 7.1 Hz, H-6'), 4.04-4.14 (2H, m, H-7'), 4.44 (1H, q, *J* = 7.1 Hz, H-5'), 7.62 (2H, d, *J* = 8.9 Hz, H-3'), 8.18 (2H, d, *J* = 8.9 Hz, H-2'); ^{13}C NMR (125 MHz, DMSO-d_6) (ppm) δ 13.8 (C-8'), 17.0 (C-6'), 42.4 (C-5'), 61.2 (C-7'), 123.9 (C-2'), 128.6 (C-3'), 144.5 (C-4'), 145.4 (C-1'), 171.3 (CO); HRMS calcd for $C_{11}H_{14}NO_4S$ $[M+H]^+$ 256.0638, found 256.0639.

2-((4-Nitrophenyl)thio)propanoic acid (176)

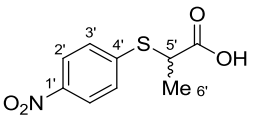

The title compound was synthesised following **general procedure K** using ethyl 2-((4-nitrophenyl)thio)propanoate **175** (1.23 g, 4.82 mmol) and LiOH (2M in THF, 26.6 mL). The product **176** was obtained without further purification as a yellow oil (962 mg, 4.24 mmol, 88%).

R_f 0.19 (petrol: EtOAc 4: 1); UV λ_{max} (EtOH) 332 nm; IR (cm^{-1}) 3120, 2932, 2828, 1704, 1577, 1503, 1338, 1197; ^{1}H NMR (500 MHz, DMSO-d_6) (ppm) δ 1.48 (3H, t, *J* = 7.1 Hz, H-6'), 4.33 (1H, q, *J* = 7.1 Hz, H-5'), 7.60 (2H, d, *J* = 8.9 Hz, H-3'), 8.18 (2H, d, *J* = 8.9 Hz, H-2'), 13.08 (1H, br s, OH); ^{13}C NMR (125 MHz, DMSO-d_6) (ppm) δ 17.2 (C-6'), 42.5 (C-5'), 123.9 (C-2'), 127.8 (C-3'), 145.0 (C-4'), 145.5 (C-1'), 172.8 (CO); HRMS calcd for $C_9H_8NO_4S$ $[M-H]^-$ 226.0180, found 226.0174.

2-((4-Nitrophenyl)thio)propan-1-ol (177)

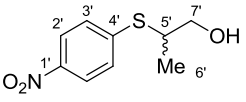

The title compound was synthesised following **general procedure L** using 2-((4-nitrophenyl)thio)propanoic acid **176** (880 mg, 3.88 mmol) and 1M Borane in complex with THF (19.4 mL, 19.40 mmol). The crude product was purified by MPC on silica (petrol: EtOAc 3: 2) to give the products **177** as a yellow oil (640 mg, 2.95 mmol, 76%).

R_f 0.35 (petrol: EtOAc 4: 1); UV λ_{max} (EtOH) 339 nm; IR (cm^{-1}) 3375, 2927, 2870, 1576, 1505, 1332, 1027; ^{1}H NMR (500 MHz, DMSO-d_6) (ppm) δ 1.32 (3H, d, *J* = 6.8 Hz, H-6'), 3.44-3.49 (1H, m, H-7'), 3.55-3.59 (1H, m, H-7'), 3.63-3.69 (1H, m, H-5'), 5.16 (1H, t, *J* = 5.6 Hz, OH), 7.54 (2H, d, *J* = 8.9 Hz, H-3'), 8.14 (2H, d, *J* = 8.9 Hz, H-2'); ^{13}C NMR (125 MHz, DMSO-d_6) (ppm) δ 17.3 (C-6'), 42.7 (C-5'), 64.7 (C-7'), 123.9 (C-2'), 127.2 (C-3'), 144.4 (C-4'), 147.1 (C-1'); HRMS calcd for $C_9H_{12}NO_3S$ $[M+H]^+$ 214.0532, found 214.0535.

2-((4-Nitrophenyl)thio)propanal (178)

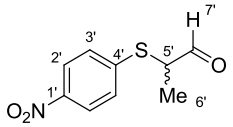

2-((4-Nitrophenyl)thio)propan-1-ol **177** (600 mg, 2.82 mmol) was solubilised in dry DCM (30 mL) under N_2. 0.3M Dess-Martin periodinane solution in DCM (10.4 mL, 3.10mmol) was added dropwise to the solution. The resulting reaction was stirred at r.t. for 2 h. Sodium thiosulfate was then added dropwise at 0 ^{o}C to quench the reaction until reaching pH 7. The mixture was then extracted with DCM (3 x 50 mL). The organic layer was dried over $MgSO_4$ and the solvent was removed *in vacuo.* The crude product was purified by MPC on silica (petrol: EtOAc 4: 1) to give the product **178** as a yellow oil (530 mg, 2.51 mmol, 89%).

R_f 0.47 (petrol: EtOAc 4: 1); UV λ_{max} (EtOH) 332 nm; IR (cm^{-1}) 2924, 2827, 1724, 1696, 1596, 1512, 1339; ^{1}H NMR (500 MHz, DMSO-d_6) (ppm) δ 1.42 (3H, d, *J* = 7.1 Hz, H-6'), 4.38-4.43 (1H, m, H-5'), 7.61 (2H, d, *J* = 8.8 Hz, H-3'), 8.18 (2H, d, *J* = 8.8 Hz, H-2'), 9.46 (1H, d, *J* = 2.5 Hz, H-7'); ^{13}C NMR (125 MHz, DMSO-d_6) (ppm) δ 13.2 (C-6'), 48.5 (C-5'), 124.0 (C-2'), 128.8 (C-3'), 143.3 (C-4'), 145.5 (C-1'), 196.2 (CO); HRMS calcd for $C_9H_{10}NO_3S$ $[M+H]^+$ 212.0378, found 212.0376.

1-(2-((4-Nitrophenyl)thio)propyl)pyrrolidine (179)

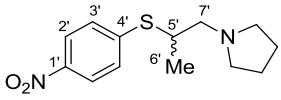

2-((4-Nitrophenyl)thio)propanal **178** (530 mg, 2.51 mmol) was dissolved in anhydrous toluene (15 mL) under N_2. Acetic acid (0.80 mL, 14.01 mmol) and $MgSO_4$ (1,04 g, 8.73 mmol) were added to the reaction. Then pyrrolidine (0.84 mL, 10.09 mmol) was added and the reaction was stirred at r.t. for 2 h. Sodium triacetoxyborohydride (240 mg, 6.16 mmol) was added and the reaction was stirred at r.t. for 16 h. The reaction mixture was quenched with aqueous $NaHCO_3$ until reaching pH 7. The solution was then extracted with EtOAc (3 x 30 mL). The organic layer was dried over $MgSO_4$ and the solvent was removed *in vacuo*. The crude product was purified by MPC on silica (DCM: MeOH 9: 1) to give the products **179** as an orange oil (568 mg, 3.13 mmol, 85%).

R_f 0.47 (DCM: MeOH 9: 1); UV λ_{max} (EtOH) 339 nm; IR (cm^{-1}) 2970, 2792, 1509, 1337; ^{1}H NMR (500 MHz, DMSO-d_6) (ppm) δ 1.32 (3H, d, *J* = 6.6 Hz, H-6'), 1.68-1.70 (4H, m, H-pyr), 2.50-2.52 (4H, m, H-pyr), 2.60 (2H, dd, *J* = 3.5 and 6.6 Hz, H-7'), 3.80 (1H, h, *J* = 6.6 Hz, H-5'), 7.56 (2H, d, *J* = 9.0 Hz, H-3'), 8.14 (2H, d, *J* = 9.0 Hz, H-2'); ^{13}C NMR (125 MHz, DMSO-d_6) (ppm) δ 19.0 (C-6'), 23.2 (2 x C-pyr), 39.9 (C-5'), 50.0 (2 x C-pyr), 60.9 (C-7'), 123.7 (C-2'), 127.7 (C-3'), 144.4 (C-4'), 146.8 (C-1').

Note: LRMS and HRMS were not available because the compound did not ionise.

4-((1-(Pyrrolidin-1-yl)propan-2-yl)thio)aniline (180)

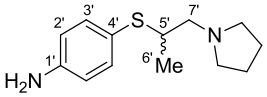

The title compound was synthesised following **general procedure H** using 1-(2-((4-nitrophenyl)thio)propyl)pyrrolidine **179** (690 mg, 2.59 mmol) and zinc powder (1.68 g, 25.94 mmol). The crude product was purified by MPC on silica (DCM: MeOH 9: 1) to give the product **180** as a yellow oil (600 mg, 2.54 mmol, 98%).

R_f 0.22 (DCM: MeOH 9: 1); UV λ_{max} (EtOH) 254 nm; IR (cm^{-1}) 3342, 2968, 2837, 1595, 1496, 1396, 1277; ^{1}H NMR (500 MHz, DMSO-d_6) (ppm) δ 1.12 (3H, d, *J* = 7.1 Hz, H-6'), 1.64-1.67 (4H, m, H-pyr), 2.36-2.35 (2H, m, H-pyr), 2.40 (2H, d, *J* = 7.1 Hz, H-7'), 2.42-2.44 (2H, m, H-pyr), 2.98 (1H, m, H-5'), 5.28 (2H, br s, NH_2), 6.52 (2H, d, *J* = 8.5 Hz, H-2'), 7.10 (2H, d, *J* = 8.5 Hz, H-3'); ^{13}C NMR (125 MHz, DMSO-d_6) (ppm) δ 19.3 (H-

6'), 23.1 (2 x C-pyr), 42.6 (C-5'), 55.6 (2 x C-pyr), 61.7 (H-7'), 114.1 (C-3'), 116.8 (C-4'), 135.8 (C-2'), 148.8 (C-1'); HRMS calcd for $C_{13}H_{21}N_2S$ $[M+H]^+$ 237.1420, found 237.1423.

6-(Cyclohexylmethoxy)-*N*-(4-((1-(pyrrolidin-1-yl)propan-2-yl)thio)phenyl)-9*H*-purin-2-amine (181)

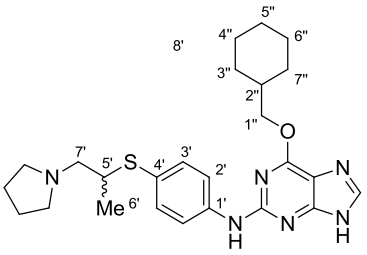

The title compound was synthesised following **general procedure I** using 6-(cyclohexylmethoxy)-2-iodo-9-(4-methoxybenzyl)-9*H*-purine **171** (460 mg, 0.96 mmol), 4-((1-(pyrrolidin-1-yl)propan-2-yl)thio)aniline **180** (250 mg, 1.06 mmol), K_2CO_3 (267 mg, 1.92 mmol), $Pd(dba)_2$ (18 mg, 0.02 mmol) and XPhos (18 mg, 0.02 mmol). The crude mixture was then filtered through Celite and the solvent was removed *in vacuo*. The crude mixture was then solubilised in TFA (15 mL). The resulting solution was heated at 70 °C for 5 h. Then the solvent was removed *in vacuo*. The product was purified by MPC on alumina (DCM: MeOH 19: 1) to give the product **181** as a pale orange oil (280 mg, 0.60 mmol, 62%).

R_f 0.22 (DCM: MeOH 9: 1); UV λ_{max} (EtOH) 300 nm; IR (cm^{-1}) 3383, 2926, 2851, 1672, 1594, 1495, 1394, 1179, 1127; ^{1}H NMR (500 MHz, DMSO-d_6) (ppm) δ 1.06-1.12 (2H, m, H-cyclo), 1.18-1.20 (1H, m, H-cyclo), 1.24-1.31 (2H, m, H-cyclo), 1.26 (3H, d, *J* = 6.7 Hz, H-6'), 1.67 (1H, d, J = 11.7 Hz, H-cyclo), 1.73 (2H, d, J = 12.8 Hz, H-cyclo), 1.85 (2H, m, H-cyclo), 1.87-1.93 (3H, m, H-pyr and H-2''), 1.97-2.02 (2H, m, H-pyr), 2.96-3.02 (1H, m, H-pyr), 3.08-3.12 (1H, m, H-pyr), 3.18-3.21 (1H, m, H-7'), 3.27-3.32 (1H, m, H-7'), 3.40-3.45 (1H, m, H-5'), 3.60-3.64 (2H, m, H-pyr), 4.35 (2H, d, *J* = 6.3 Hz, H-1''), 7.45 (2H, d, *J* = 8.8 Hz, H-2'), 7.90 (2H, d, *J* = 8.8 Hz, H-3'), 8.10 (1H, s, H-8), 9.56 (1H, s, NH); ^{13}C NMR (125 MHz, DMSO-d_6) (ppm) δ 18.3 (C-6'), 22.4 (C-pyr), 22.5 (C-pyr), 25.2 (2 x C-cyclo), 26.0 (C-cyclo), 29.2 (2 x C-cyclo), 36.8 (C-5'), 40.0 (C-2''), 53.9 (C-pyr), 54.0 (C-pyr), 58.7 (C-7'), 71.2 (C-1''), 118.6 (C-3'), 120.7 (C_q), 135.1 (C-2'), 140.1 (C-8), 141.9 (C_q), 155.0 (C_q), 157.9 (C_q), 158.1 (C_q), 159.5 (C_q); HRMS calcd for $C_{25}H_{35}N_6OS$ $[M+H]^+$ 467.2587, found 467.2582.

2-((4-Nitrophenyl)sulfonyl)propan-1-ol (182)

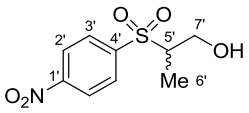

The title compound was synthesised following **general procedure M** using 2-((4-nitrophenyl)thio)propan-1-ol **177** (1.12 g, 5.26 mmol) and *m*-CPBA (2.68 g, 11.6 mmol). The crude product was purified by MPC on silica (petrol: EtOAc 1: 1) to give the product **182** as a yellow solid (930 mg, 3.80 mmol, 72%).

R_f 0.22 (petrol: EtOAc 7: 3); Mp = 95-97 ^oC; UV λ_{max} (EtOH) 251 nm; IR (cm^{-1}) 3554, 2981, 2893, 1535, 1350, 1292, 1137; ^1H NMR (500 MHz, DMSO-d_6) (ppm) δ 1.23 (3H, d, *J* = 6.7 Hz, H-6'), 3.53-3.60 (2H, m, H-5' and H-7'), 3.67-3.72 (1H, m, H-7'), 5.01 (1H, t, *J* = 5.4 Hz, OH), 8.15 (2H, d, *J* = 8.7 Hz, H-3'), 8.45 (2H, d, *J* = 8.7 Hz, H-2'); ^{13}C NMR (125 MHz, DMSO-d_6) (ppm) δ 10.4 (C-6'), 59.7 (C-7'), 61.0 (C-5'), 124.3 (C-2'), 130.3 (C-3'), 143.9 (C-4'), 150.5 (C-1'); HRMS calcd for $C_9H_{12}NO_5S$ $[M+H]^+$ 246.0431, found 246.0431.

2-((4-Aminophenyl)sulfonyl)propan-1-ol (183)

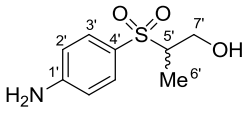

The title compound was synthesised following **general procedure H** using 2-((4-nitrophenyl)sulfonyl)propan-1-ol **182** (300 mg, 1.22 mmol) and zinc powder (796 mg, 12.2 mmol). The crude product was purified by MPC on silica (DCM: MeOH 19: 1) to give the product **183** as a pale orange oil (240 mg, 1.12 mmol, 91 %).

R_f 0.67 (DCM: MeOH 19: 1); UV λ_{max} (EtOH) 270 nm; IR (cm^{-1}) 3464, 3370, 2973, 2893, 1596, 1263, 1126; ^1H NMR (500 MHz, DMSO-d_6) (ppm) δ 1.16 (3H, d, *J* = 6.9 Hz, H-6'), 3.07-3.10 (1H, m, H-5'), 3.27-3.32 (1H, m, H-7'), 3.70-3.74 (1H, m, H-7'), 4.87 (1H, t, *J* = 5.8 Hz, OH), 6.15 (2H, br s, NH_2), 6.65 (2H, d, *J* = 8.7 Hz, H-3'), 7.42 (2H, d, *J* = 8.7 Hz, H-2'); ^{13}C NMR (125 MHz, DMSO-d_6) (ppm) δ 11.1 (C-6'), 59.9 (C-7'), 61.2 (C-5'), 112.6 (C-3'), 121.9 (C-4'), 130.3 (C-2'), 153.6 (C-1'); HRMS calcd for $C_9H_{14}NO_3S$ $[M+H]^+$ 216.0689, found 216.0687.

2-((4-((6-(Cyclohexylmethoxy)-9*H*-purin-2-yl)amino)phenyl)sulfonyl)propan-1-ol (184)

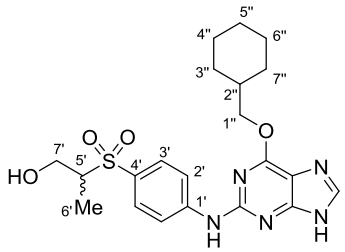

The title compound was synthesised following **general procedure I** using 6-(cyclohexylmethoxy)-2-iodo-9-(4-methoxybenzyl)-9*H*-purine **171** (171 mg, 0.36 mmol), 2-((4-aminophenyl)sulfonyl)propan-1-ol **183** (120 mg, 0.56 mmol), K_2CO_3 (100 mg, 0.72 mmol), $Pd(dba)_2$ (7 mg, 0.01 mmol) and XPhos (3 mg, 0.01 mmol). The crude mixture was then filtered through Celite and the solvent was removed *in vacuo*. The crude mixture was then solubilised in TFA (10 mL). The resulting solution was heated at 70 °C for 2 h and the solvent was removed *in vacuo*. The product was purified by medium pressure chromatography (EtOAc: MeOH 95: 5) to give the product **184** as a pale orange oil (70 mg, 0.16 mmol, 44%).

R_f 0.36 (EtOAc: MeOH 95: 5); UV λ_{max} (EtOH) 313 nm; IR (cm^{-1}) 3117, 2926, 2852, 1596, 1535, 1392, 1205, 1132; ^{1}H NMR (500 MHz, DMSO-d_6) (ppm) δ 1.08-1.14 (2H, m, H-cyclo), 1.16-1.20 (1H, m, H-cyclo), 1.21-1.22 (3H, d, *J* = 6.9 Hz, H-6'), 1.23-1.31 (2H, m, H-cyclo), 1.66-1.69 (1H, m, H-cyclo), 1.73-1.75 (2H, m, H-cyclo), 1.85-1.87 (3H, m, H-cyclo and H-2''), 3.22-3.27 (1H, m, H-5'), 3.37-3.40 (1H, m, H-7'), 3.73-3.75 (1H, m, H-7'), 4.37 (2H, d, *J* = 6.3 Hz, H-1''), 4.94 (1H, br s, OH), 7.72 (2H, d, *J* = 8.8 Hz, H-3'), 8.07 (2H, d, *J* = 8.8 Hz, H-2'), 8.10 (1H, br s, H-8), 9.94 (1H, s, NH), 13.00 (1H, s, NH); ^{13}C NMR (125 MHz, DMSO-d_6) (ppm) δ 10.9 (C-6'), 25.2 (2 x C-cyclo), 26.0 (C-cyclo), 29.2 (2 x C-cyclo), 36.8 (C-2''), 59.9 (C-7'), 61.1 (C-5'), 71.4 (C-1''), 117.2 (C-2'), 128.1 (C_q), 129.5 (C-3'), 130.3 (C_q), 146.0 (C-8), 154.5 (C_q); HRMS calcd for $C_{21}H_{28}N_5O_4S$ $[M+H]^+$ 446.1857, found 446.1848.

Note: 3 quaternary carbons were not visible on the ^{13}C NMR spectrum.

Ethyl 2-((4-nitrophenyl)thio)butanoate (188)

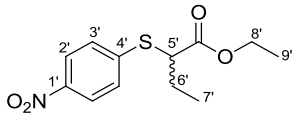

The title compound was synthesised following **general procedure J** using ethyl 2-bromobutyrate **185** (1.04 mL, 7.10 mmol), 4-nitrothiophenol **173** (1.00 g, 6.46 mmol) and Et_3N (1.00 mL, 7.10 mmol). The crude product was purified by MPC on silica (petrol: EtOAc 9: 1) to give the product **188** as a yellow oil (1.57 g, 5.83 mmol, 90%).

R_f 0.42 (petrol: EtOAc 4: 1); UV λ_{max} (EtOH) 330 nm; IR (cm^{-1}) 2972, 2880, 1729, 1577, 1337, 1261, 1155; ^1H NMR (500 MHz, DMSO-d_6) (ppm) δ 1.00 (3H, t, *J* = 7.3 Hz, H-7'), 1.13 (3H, t, *J* = 7.1 Hz, H-9'), 1.77-1.85 (1H, m, H-6'), 1.86-1.93 (1H, m, H-6'), 4.08-4.15 (2H, m, H-8'), 4.26 (1H, t, *J* = 6.8 Hz, H-5'), 7.62 (2H, d, *J* = 9.0 Hz, H-3'), 8.17 (2H, d, *J* = 9.0 Hz, H-2'); ^{13}C NMR (125 MHz, DMSO-d_6) (ppm) δ 11.1 (C-7'), 14.1 (C-9'), 24.6 (C-6'), 49.0 (C-5'), 61.4 (C-8'), 124.0 (C-2'), 128.3 (C-3'), 144.4 (C-4'), 145.5 (C-1'), 171.0 (CO); HRMS calcd for $C_{12}H_{16}NO_4S$ $[M+H]^+$ 270.0795, found 270.0794.

Ethyl 3-methyl-2-((4-nitrophenyl)thio)butanoate (189)

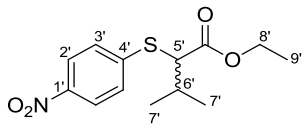

The title compound was synthesised following **general procedure J** using ethyl 2-bromoisovalurate **186** (1.16 mL, 7.10 mmol), 4-nitrothiophenol **173** (1.00 g, 6.46 mmol) and Et_3N (1.00 mL, 7.10 mmol). The crude product was purified by MPC on silica (petrol: EtOAc 4: 1) to give the product **189** as a yellow oil (920 mg, 3.25 mmol, 46%).

R_f 0.39 (petrol: EtOAc 4: 1); UV λ_{max} (EtOH) 328 nm; IR (cm^{-1}) 2967, 1727, 1577, 1512, 1336, 1148; ^1H NMR (500 MHz, DMSO-d_6) (ppm) δ 1.04 (3H, t, *J* = 6.6 Hz, H-7'), 1.09 (3H, t, *J* = 6.6 Hz, H-7'), 1.14 (3H, t, *J* = 7.1 Hz, H-9'), 2.12-2.19 (1H, m, H-6'), 4.10-4.14 (3H, m, H-5' and H-8'), 7.62 (2H, d, *J* = 9.0 Hz, H-3'), 8.17 (2H, d, *J* = 9.0 Hz, H-2'); ^{13}C NMR (125 MHz, DMSO-d_6) (ppm) δ 13.9 (C-9'), 19.7 (C-7'), 19.9 (C-7'), 30.3 (C-6'), 54.9 (C-5'), 61.0 (C-8'), 123.9 (C-2'), 128.3 (C-3'), 145.1 (C-4'), 145.3 (C-1'), 170.6 (CO); HRMS calcd for $C_{13}H_{16}NO_4S$ $[M-H]^-$ 282.0806, found 282.0796.

Ethyl 2-((4-nitrophenyl)thio)-2-phenylacetate (190)

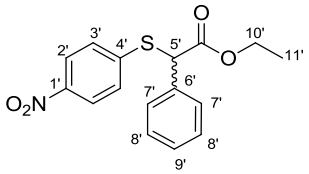

The title compound was synthesised following **general procedure J** using ethyl α-chlorophenylacetate **187** (1.22 mL, 7.10 mmol), 4-nitrothiophenol **173** (1.00 g, 6.46 mmol) and Et_3N (1.00 mL, 7.10 mmol). The crude product was purified by MPC on silica (petrol: EtOAc 9: 1) to give the product **190** as a yellow oil (1.35 g, 4.26 mmol, 66%).

R_f 0.51 (petrol: EtOAc 4: 1); UV λ_{max} (EtOH) 334 nm; IR (cm^{-1}) 2967, 2853, 1707, 1578, 1506, 1333, 1233; ^{1}H NMR (500 MHz, DMSO-d_6) (ppm) δ 1.11 (3H, t, *J* = 7.1 Hz, H-11'), 4.08-4.19 (2H, m, H-10'), 5.82 (1H, s, H-5'), 7.34-7.37 (1H, m, H-9'), 7.40 (2H, dd, *J* = 7.2 Hz, H-8'), 7.54 (2H, d, *J* = 7.2 Hz, H-7'), 7.59 (2H, d, *J* = 9.0 Hz, H-3'), 8.15 (2H, d, *J* = 9.0 Hz, H-2'); ^{13}C NMR (125 MHz, DMSO-d_6) (ppm) δ 13.7 (C-11'), 52.2 (C-10'), 61.9 (C-5'), 123.9 (C-2'), 128.1 (C-3'), 128.4 (C-7'), 128.6 (C-9'), 128.9 (C-8'), 134.7 (C-6'), 144.6 (C-4'), 145.3 (C-1'), 169.3 (CO); HRMS calcd for $C_{16}H_{14}NO_4S$ $[M-H]^-$ 316.0649, found 316.0638.

2-((4-Nitrophenyl)thio)butanoic acid (191)

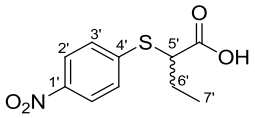

The title compound was synthesised following **general procedure K** using ethyl 2-((4-nitrophenyl)thio)butanoate **188** (790 mg, 2.94 mmol) and LiOH (2M in THF, 16.2 mL). The product **191** was obtained without further purification as a yellow oil (630 mg, 2.61 mmol, 89%).

R_f 0.25 (petrol: EtOAc 4: 1); UV λ_{max} (EtOH) 333 nm; IR (cm^{-1}) 3096, 2985, 2871, 1704, 1578, 1506, 1336, 1274; ^{1}H NMR (500 MHz, DMSO-d_6) (ppm) δ 1.01 (3H, t, *J* = 7.3 Hz, H-7'), 1.78-1.84 (1H, m, H-6'), 1.85-1.93 (1H, m, H-6'), 4.15 (1H, t, *J* = 6.9 Hz, H-5'), 7.62 (2H, d, *J* = 8.9 Hz, H-3'), 8.16 (2H, d, *J* = 8.9 Hz, H-2'), 13.1 (1H, br s, OH); ^{13}C NMR (125 MHz, DMSO-d_6) (ppm) δ 11.1 (C-7'), 24.5 (C-6'), 49.2 (C-5'), 124.0 (C-2'), 128.0 (C-3'), 145.0 (C-4'), 145.5 (C-1'), 172.4 (CO); HRMS calcd for C10H10NO4S $[M-H]^-$ 240.0336, found 240.0328.

3-Methyl-2-((4-nitrophenyl)thio)butanoic acid (192)

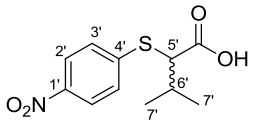

The title compound was synthesised following **general procedure K** using ethyl 3-methyl-2-((4-nitrophenyl)thio)butanoate **189** (725 mg, 2.56 mmol) and LiOH (2M in THF, 12.8 mL). The product **192** was obtained without further purification as a yellow oil (610 mg, 2.39 mmol, 93%).

R_f 0.19 (petrol: EtOAc 4: 1); UV λ_{max} (EtOH) 330 nm; IR (cm^{-1}) 2963, 2847, 1703, 1579, 1511, 1336, 1294; ^{1}H NMR (500 MHz, DMSO-d_6) (ppm) δ 1.06 (3H, t, *J* = 6.7 Hz, H-7'), 1.09 (3H, t, *J* = 6.7 Hz, H-7'), 2.12-2.18 (1H, m, H-6'), 3.99 (1H, d, *J* = 7.6 Hz, H-5'), 7.61 (2H, d, *J* = 9.0 Hz, H-3'), 8.16 (2H, d, *J* = 9.0 Hz, H-2'); ^{13}C NMR (125 MHz, DMSO-d_6) (ppm) δ 19.7 (C-7'), 20.0 (C-7'), 30.1 (C-6'), 55.3 (C-5'), 123.9 (C-2'), 127.8 (C-3'), 145.0 (C-4'), 145.9 (C-1'), 172.1 (CO); HRMS calcd for $C_{11}H_{12}NO_4S$ $[M-H]^-$ 254.0493, found 254.0485.

2-((4-Nitrophenyl)thio)-2-phenylacetic acid (193)

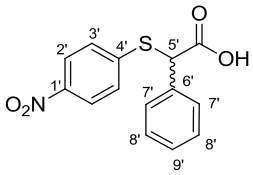

The title compound was synthesised following **general procedure K** using ethyl 2-((4-nitrophenyl)thio)-2-phenylacetate **190** (1.35 g, 4.26 mmol) and LiOH (2M in THF, 21.3 mL). The product **193** was obtained without further purification as a yellow oil (1.19 g, 4.12 mmol, 96%).

R_f 0.43 (petrol: EtOAc 3: 2); UV λ_{max} (EtOH) 332 nm; IR (cm^{-1}) 2832, 1700, 1574, 1509, 1452, 1334; ^{1}H NMR (500 MHz, DMSO-d_6) (ppm) δ 5.67 (1H, s, H-5'), 7.32-7.35 (1H, m, H-9'), 7.39 (2H, dd, *J* = 7.1 Hz, H-8'), 7.55-7.57 (4H, m, H-7' and H-3'), 8.13 (2H, d, *J* = 9.0 Hz, H-2'); ^{13}C NMR (125 MHz, DMSO-d_6) (ppm) δ 52.7 (C-5'), 123.9 (C-2'), 127.7 (C-3'), 128.4 (C-7'), 128.5 (C-9'), 128.8 (C-8'), 135.4 (C-6'), 145.1 (C-4'), 145.3 (C-1'), 170.7 (CO); LRMS calcd for $C_{14}H_{10}NO_4S$ $[M-H]^-$ 288.0, found 288.2.

2-((4-Nitrophenyl)thio)butan-1-ol (194)

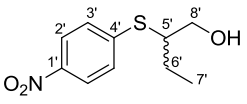

The title compound was synthesised following **general procedure L** using 2-((4-nitrophenyl)thio)butanoic acid **191** (630 mg, 2.61 mmol) and 1M Borane in complex with THF (13.1 mL, 13.1 mmol). The crude product was purified by MPC on silica (petrol: EtOAc 3: 2) to give the product **194** as a yellow oil (438 mg, 1.93 mmol, 74%).

R_f 0.37 (petrol: EtOAc 4: 1); UV λ_{max} (EtOH) 339 nm; IR (cm^{-1}) 3377, 2964, 2929, 1578, 1507, 1334; ^{1}H NMR (500 MHz, DMSO-d_6) (ppm) δ 1.01 (3H, t, *J* = 7.3 Hz, H-7'), 1.51-1.59 (1H, m, H-6'), 1.86-1.92 (1H, m, H-6'), 3.46-3.50 (1H, m, H-5'), 3.51-3.55 (1H, m, H-8'), 3.59-3.63 (1H, m, H-8'), 5.10 (1H, t, *J* = 5.7 Hz, OH), 7.55 (2H, d, *J* = 9.0 Hz, H-3'), 8.13 (2H, d, *J* = 9.0 Hz, H-2'); ^{13}C NMR (125 MHz, DMSO-d_6) (ppm) δ 11.2 (C-7'), 23.6 (C-6'), 50.0 (C-5'), 62.8 (C-8'), 123.9 (C-2'), 127.2 (C-3'), 144.3 (C-4'), 147.7 (C-1'); HRMS calcd for $C_{10}H_{14}NO_3S$ $[M+H]^+$ 228.0689, found 228.0692.

3-Methyl-2-((4-nitrophenyl)thio)butan-1-ol (195)

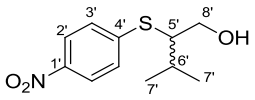

The title compound was synthesised following **general procedure L** using 3-methyl-2-((4-nitrophenyl)thio)butanoic acid **192** (610 mg, 2.39 mmol) and 1M Borane in complex with THF (12.0 mL, 12.0 mmol). The crude product was purified by MPC on silica (petrol: EtOAc 3: 2) to give the product **195** as a yellow oil (485 mg, 2.01 mmol, 84%).

R_f 0.41 (petrol: EtOAc 4: 1); UV λ_{max} (EtOH) 338 nm; IR (cm^{-1}) 3384, 2960, 2873, 1576, 1506, 1336, 1085; ^{1}H NMR (500 MHz, DMSO-d_6) (ppm) δ 0.96 (3H, t, *J* = 6.8 Hz, H-7'), 1.05 (3H, t, *J* = 6.8 Hz, H-7'), 2.22-2.28 (1H, m, H-6'), 3.45-3.49 (1H, m, H-5'), 3.55-3.65 (2H, m, H-8'), 5.08 (1H, t, *J* = 5.5 Hz, OH), 7.58 (2H, d, *J* = 9.0 Hz, H-3'), 8.13 (2H, d, *J* = 9.0 Hz, H-2'); ^{13}C NMR (125 MHz, DMSO-d_6) (ppm) δ 17.9 (C-7'), 20.4 (C-7'), 27.9 (C-6'), 55.2 (C-5'), 61.8 (C-8'), 123.9 (C-2'), 127.4 (C-3'), 144.4 (C-4'), 147.8 (C-1'); HRMS calcd for $C_{11}H_{16}NO_3S$ $[M+H]^+$ 242.0845, found 242.0850.

2-((4-Nitrophenyl)thio)-2-phenylethanol (196)[263]

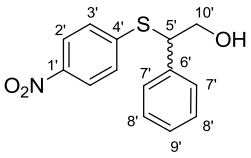

The title compound was synthesised following **general procedure L** using 2-((4-nitrophenyl)thio)-2-phenylacetic acid **193** (1.23 g, 4.26 mmol) and 1M Borane in complex with THF (12.8 mL, 12.8 mmol). The crude product was purified by MPC on silica (petrol: EtOAc 7: 3) to give the product **196** as a yellow oil (720 mg, 2.62 mmol, 62%).

R_f 0.39 (petrol: EtOAc 4: 1); UV λ_{max} (EtOH) 337 nm; IR (cm^{-1}) 3374, 2926, 2870, 1576, 1506, 1333, 1088, 852; ^{1}H NMR (500 MHz, DMSO-d_6) (ppm) δ 3.76-3.81 (1H, m, H-10'), 3.84-3.89 (1H, m, H-10'), 4.81 (1H, t, *J* = 6.5 Hz, H-5'), 5.31 (1H, t, *J* = 5.6 Hz, OH), 7.26 (1H, t, *J* = 7.8 Hz, H-9'), 7.34 (2H, dd, *J* = 7.8 Hz, H-8'), 7.49 (2H, d, *J* = 7.8 Hz, H-7'), 7.54 (2H, d, *J* = 9.0 Hz, H-3'), 8.08 (2H, d, *J* = 9.0 Hz, H-2'); ^{13}C NMR (125 MHz, DMSO-d_6) (ppm) δ 52.2 (C-5'), 64.8 (C-10'), 123.8 (C-2'), 127.4 (C-3'), 127.5 (C-7'), 128.2 (C-9'), 128.8 (C-8'), 139.0 (C-6'), 144.6 (C-4'), 146.6 (C-1'); HRMS calcd for $C_{14}H_{14}NO_3S$ $[M+H]^+$ 276.0689, found 276.0694.

3-Methyl-2-((4-nitrophenyl)thio)butanal (198)

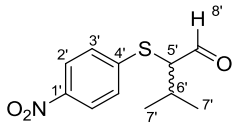

Dry DMSO (0.45 mL, 6.28 mmol) was added to a solution of oxalyl chloride (0.41 mL, 4.79 mmol) in dry DCM (35 mL) at -78 ^{o}C, under N_2. The solution was stirred at -78 °C for 30 min. 3-Methyl-2-((4-nitrophenyl)thio)butan-1-ol **195** (550 mg, 2.28 mmol) in solution in dry DCM (35 mL) was added dropwise to the reaction at -78 ^{o}C. The reaction was stirred at -78 °C for a further 1 h. Et_3N (1.93 mL, 13.69 mmol) was then added and the reaction was allowed to warm to r.t. The solution was stirred for a additional 30 min at r.t. Brine (50 mL) was added and the solution was extracted with DCM (3 x 50 mL). The organic layer was dried over $MgSO_4$ and the solvent was removed *in vacuo*. The crude product was purified by MPC on silica (petrol: EtOAc 9: 1) to give the product **198** as a yellow oil (360 mg, 1.51 mmol, 66%).

R_f 0.62 (petrol: EtOAc 4: 1); UV λ_{max} (EtOH) 326 nm; IR (cm^{-1}) 2964, 2839, 1714, 1577, 1510, 1336, 1089; ^{1}H NMR (500 MHz, DMSO-d_6) (ppm) δ 1.06 (3H, t, *J* = 6.8 Hz, H-7'), 1.09 (3H, t, *J* = 6.8 Hz, H-7'), 2.23-2.30 (1H, m, H-6'), 4.11 (1H, dd, *J* = 4.3 and 7.5 Hz, H-5'), 7.60 (2H, d, *J* = 8.9 Hz, H-3'), 8.15 (2H, d, *J* = 8.9 Hz, H-2'), 9.41 (1H, d, *J* = 4.3 Hz, H-8'); ^{13}C NMR (125 MHz, DMSO-d_6) (ppm) δ 19.3 (C-7'), 20.2 (C-7'), 27.3 (C-6'), 60.5 (C-5'), 123.9 (C-2'), 128.4 (C-3'), 143.9 (C-4'), 145.3 (C-1'), 196.0 (CO); HRMS calcd for $C_{11}H_{14}NO_3S$ $[M+H]^+$ 240.0689, found 240.0686.

2-((4-Aminophenyl)thio)butan-1-ol (207)

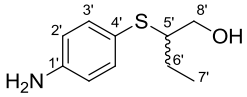

The title compound was synthesised following **general procedure H** using 2-((4-nitrophenyl)thio)butan-1-ol **194** (569 mg, 2.51 mmol) and zinc powder (1.6 g, 25.1 mmol). The crude product was purified by MPC on silica (DCM: MeOH 19: 1) to give the product **207** as a colourless oil (380 mg, 1.93 mmol, 77%).

R_f 0.35 (DCM: MeOH 19: 1); UV λ_{max} (EtOH) 263 nm; IR (cm^{-1}) 3345, 3230, 2961, 2930, 1596, 1494, 1278, 1049; ^{1}H NMR (500 MHz, DMSO-d_6) (ppm) δ 0.99 (3H, t, *J* = 7.3 Hz, H-7'), 1.24-1.33 (1H, m, H-6'), 1.68-1.75 (1H, m, H-6'), 2.61-2.66 (1H, m, H-5'), 3.24-3.28 (1H, m, H-8'), 3.47-3.50 (1H, m, H-8'), 4.69 (1H, br s, OH), 5.27 (2H, br s, NH_2), 6.51 (2H, d, *J* = 8.2 Hz, H-2'), 7.10 (2H, d, *J* = 8.2 Hz, H-3'); ^{13}C NMR (125 MHz, DMSO-d_6) (ppm) δ 11.2 (C-7'), 23.2 (C-6'), 53.6 (C-5'), 63.2 (C-8'), 114.2 (C-2'), 117.0 (C-4'), 135.7 (C-3'), 148.8 (C-1'); HRMS calcd for $C_{10}H_{14}NOS$ $[M-H]^-$ 196.0802, found 196.0801.

2-((4-Aminophenyl)thio)-3-methylbutan-1-ol (208)

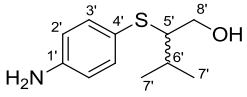

The title compound was synthesised following **general procedure H** using 3-methyl-2-((4-nitrophenyl)thio)butan-1-ol **194** (537 mg, 2.23 mmol) and zinc powder (1.45 g, 22.3 mmol). The crude product was purified by MPC on silica (DCM: MeOH 19: 1) to give the product **208** as a colourless solid (572 mg, 2.71 mmol, 79%).

R_f 0.58 (DCM: MeOH 9: 1); UV λ_{max} (EtOH) 338 nm; IR (cm^{-1}) 3351, 3229, 2958, 2872, 1597, 1494, 1176; ^{1}H NMR (500 MHz, DMSO-d_6) (ppm) δ 0.88 (3H, t, *J* = 6.8 Hz, H-7'),

1.06 (3H, t, *J* = 6.8 Hz, H-7'), 2.09-2.15 (1H, m, H-6'), 2.67-2.70 (1H, m, H-5'), 3.42-3.50 (2H, m, H-8'), 4.68 (1H, br s, OH), 5.26 (2H, br s, NH_2), 6.51 (2H, d, *J* = 8.5 Hz, H-2'), 7.11 (2H, d, *J* = 8.5 Hz, H-3'); ^{13}C NMR (125 MHz, DMSO-d_6) (ppm) δ 17.5 (C-7'), 21.0 (C-7'), 27.2 (C-6'), 60.2 (C-5'), 61.7 (C-8'), 114.3 (C-2'), 118.8 (C-4'), 135.0 (C-3'), 148.5 (C-1'); HRMS calcd for $C_{11}H_{18}NOS$ $[M+H]^+$ 212.1104, found 212.1103.

2-((4-Aminophenyl)thio)-2-phenylethanol (209)

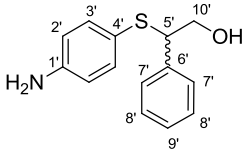

The title compound was synthesised following **general procedure H** using 2-((4-nitrophenyl)thio)-2-phenylethanol **196** (565 mg, 2.05 mmol) and zinc powder (1.3 g, 20.6 mmol). The crude product was purified by MPC on silica (DCM: MeOH 19: 1) to give the product **209** as a colourless oil (430 mg, 1.76 mmol, 85%).

R_f 0.62 (DCM: MeOH 9: 1); UV λ_{max} (EtOH) 265 nm; IR (cm^{-1}) 3379, 3308, 2940, 2896, 1595, 1491, 1263; ^{1}H NMR (500 MHz, DMSO-d_6) (ppm) δ 3.72-3.74 (2H, m, H-10'), 3.98-4.01 (1H, m, H-5'), 4.84 (1H, br s, OH), 5.29 (2H, br s, NH_2), 6.46 (2H, d, *J* = 8.4 Hz, H-2'), 7.03 (2H, d, *J* = 8.4 Hz, H-3'), 7.21-7.29 (5H, m, H-ar); ^{13}C NMR (125 MHz, DMSO-d_6) (ppm) δ 55.9 (C-5'), 63.9 (C-10'), 114.1 (C-2'), 117.3 (C_q), 126.8 (2 x C-ar), 128.0 (C_q), 128.2 (2 x C-ar), 135.5 (C-3'), 140.5 (C_q), 140.9 (C_q); HRMS calcd for $C_{14}H_{16}NOS$ $[M+H]^+$ 246.0947, found 246.0952.

2-((4-((6-(Cyclohexylmethoxy)-9-(4-methoxybenzyl)-9*H*-purin-2-yl)amino)phenyl) thio)butan-1-ol (210)

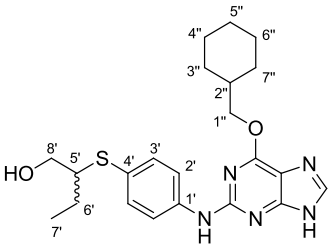

The title compound was synthesised following **general procedure I** using 6-(cyclohexylmethoxy)-2-iodo-9-(4-methoxybenzyl)-9*H*-purine **171** (500 mg, 1.05 mmol), 2-((4-aminophenyl)thio)butan-1-ol **207** (247 mg, 1.26 mmol), K_2CO_3 (289 mg, 2.09 mmol), $Pd(dba)_2$ (19 mg, 0.02 mmol) and XPhos (10 mg, 0.02 mmol). The crude mixture was then filtered through Celite and the solvent was removed *in vacuo*. The crude

mixture was then solubilised in TFA (15 mL). The resulting solution was heated at 70 °C for 2 h. Then the solvent was removed *in vacuo*. The product was purified by MPC (EtOAc: MeOH 19: 1) to give the product **210** as an orange oil (283 mg, 0.66 mmol, 63%).

R_f 0.27 (EtOAc: MeOH 19: 1); UV λ_{max} (EtOH) 278 nm; IR (cm^{-1}) 3285, 2926, 2852, 1636, 1540, 1429, 1202, 1336; ^{1}H NMR (500 MHz, DMSO-d_6) (ppm) δ 0.82 (3H, t, *J* = 7.3 Hz, H-7'), 1.06-1.12 (2H, m, H-cyclo), 1.18-1.21 (1H, m, H-cyclo), 1.24-1.29 (2H, m, H-cyclo), 1.33-1.41 (1H, m, H-6'), 1.59-1.63 (1H, m, H-6'), 1.66-1.68 (1H, m, H-cyclo), 1.72-1.75 (2H, m, H-cyclo), 1.84-1.86 (3H, m, H-cyclo and H-2''), 2.89 (2H, dd, *J* = 5.8 and 2.9 Hz, H-8'), 3.44-3.50 (1H, m, H-5'), 4.35 (2H, d, *J* = 6.3 Hz, H-1''), 4.80 (1H, d, *J* = 5.8 Hz, OH), 7.32 (2H, d, *J* = 8.8 Hz, H-2'), 7.78 (2H, d, *J* = 8.8 Hz, H-3'), 7.98 (1H, s, H-8), 9.37 (1H, s, NH), 12.80 (1H, s, N^9H); ^{13}C NMR (125 MHz, DMSO-d_6) (ppm) δ 10.3 (C-7'), 25.2 (2 x C-cyclo), 25.9 (C-cyclo), 26.0 (C-6'), 29.1 (2 x C-cyclo), 36.8 (C-2''), 41.3 (C-8'), 70.2 (C-5'), 71.2 (C-1''), 114.8 (C_q), 119.0 (C-3'), 126.9 (C_q), 130.3 (C-2'), 138.9 (C_q), 139.6 (C-8), 154.1 (C_q), 155.2 (C_q), 160.1 (C_q); HRMS calcd for $C_{22}H_{30}N_5O_2S$ $[M+H]^+$ 428.2115, found 428.2107.

2-((4-((6-(Cyclohexylmethoxy)-9*H*-purin-2-yl)amino)phenyl)thio)-3-methylbutan-1-ol (211)

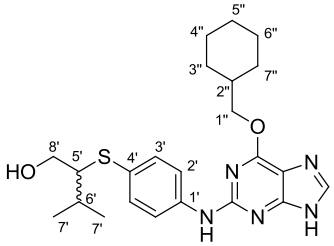

The title compound was synthesised following **general procedure I** using 6-(cyclohexylmethoxy)-2-iodo-9-(4-methoxybenzyl)-9*H*-purine **171** (500 mg, 1.05 mmol), 2-((4-aminophenyl)thio)-3-methylbutan-1-ol **208** (265 mg, 1.26 mmol), K_2CO_3 (289 mg, 2.09 mmol), $Pd(dba)_2$ (19 mg, 0.02 mmol) and XPhos (10 mg, 0.02 mmol). The crude mixture was then filtered through Celite and the solvent was removed *in vacuo*. The crude mixture was then solubilised in TFA (15 mL). The resulting solution was heated at 70 °C for 2 h. Then the solvent was removed *in vacuo*. The product was purified by MPC (EtOAc 100) to give the product **211** as a pale orange oil (127 mg, 0.29 mmol, 28%).

R_f 0.36 (EtOAc 100); UV λ_{max} (EtOH) 316 nm; IR (cm^{-1}) 3353, 3107, 2927, 2849, 1597, 1494, 1394, 1306, 1119; ^{1}H NMR (500 MHz, DMSO-d_6) (ppm) δ 0.83 (3H, t, *J* = 6.8 Hz,

H-7'), 0.86 (3H, t, *J* = 6.8 Hz, H-7'), 1.05-1.12 (2H, m, H-cyclo), 1.16-1.21 (1H, m, H-cyclo), 1.24-1.31 (2H, m, H-cyclo), 1.66-1.68 (1H, m, H-cyclo), 1.72-1.76 (3H, m, H-cyclo and H-6'), 1.83-1.85 (2H, m, H-cyclo), 1.90-1.91 (1H, m, H-2''), 2.85 (1H, dd, *J* = 7.5 and 13.1 Hz, H-8'), 2.95 (1H, dd, *J* = 4.8 and 13.1 Hz, H-8'), 3.36 (1H, m, H-5'), 4.34 (2H, d, *J* = 6.2 Hz, H-1''), 4.75 (1H, s, OH), 7.30 (2H, d, *J* = 8.7 Hz, H-2'), 7.77 (2H, d, *J* = 8.7 Hz, H-3'), 7.98 (1H, s, H-8), 9.37 (1H, s, NH), 12.80 (1H, s, N^{9}H); ^{13}C NMR (125 MHz, DMSO-d_6) (ppm) δ 16.6 (C-7'), 19.2 (C-7'), 25.2 (2 x C-cyclo), 26.0 (C-cyclo), 29.2 (2 x C-cyclo), 32.0 (C-6'), 36.8 (C-2''), 40.0 (C-8'), 71.0 (C-1''), 73.3 (C-5'), 118.9 (C-3'), 127.1 (C_q), 130.3 (C-2'), 138.9 (C_q), 139.6 (C_q), 141.9 (C_q), 154.1 (C_q), 155.2 (C_q), 160.1 (C_q); HRMS calcd for $C_{23}H_{32}N_5O_2S$ $[M+H]^+$ 442.2271, found 442.2266.

2-((4-((6-(Cyclohexylmethoxy)-9*H*-purin-2-yl)amino)phenyl)thio)-2-phenylethanol (212)

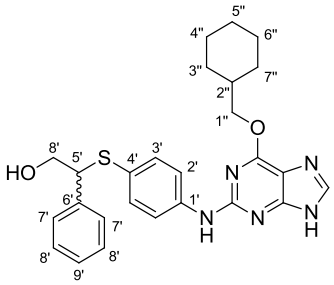

The title compound was synthesised following **general procedure I** using 6-(cyclohexylmethoxy)-2-iodo-9-(4-methoxybenzyl)-9*H*-purine **171** (500 mg, 1.05 mmol), 2-((4-aminophenyl)thio)-2-phenylethanol **209** (308 mg, 1.26 mmol), K_2CO_3 (289 mg, 2.09 mmol), $Pd(dba)_2$ (19 mg, 0.02 mmol) and XPhos (10 mg, 0.02 mmol). The crude mixture was then filtered through Celite and the solvent was removed *in vacuo*. The crude mixture was then solubilised in TFA (15 mL). The resulting solution was heated at 70 °C for 2 h. Then the solvent was removed *in vacuo*. The product was purified by MPC (EtOAc: MeOH 19: 1) to give the product **212** as an orange oil (130 mg, 0.27 mmol, 26%).

R_f 0.31 (EtOAc: MeOH 19: 1); UV λ_{max} (EtOH) 281 nm; IR (cm^{-1}) 3279, 2926, 2852, 1598, 1529, 1494, 1394, 1306; ^{1}H NMR (500 MHz, DMSO-d_6) (ppm) δ 1.05-1.13 (2H, m, H-cyclo), 1.17-1.19 (1H, m, H-cyclo), 1.24-1.32 (2H, m, H-cyclo), 1.65-1.68 (1H, m, H-cyclo), 1.72-1.75 (2H, m, H-cyclo), 1.84-1.86 (3H, m, H-cyclo and H-2''), 3.16 (2H, d, *J* = 7.4 Hz, H-8'), 3.46 (1H, br s, OH), 4.35 (2H, d, *J* = 6.3 Hz, H-1''), 4.86-4.91 (1H, m, H-5'), 7.24-7.29 (3H, m, H-ar), 7.31-7.34 (4H, m, H-ar and H-2'), 7.81 (2H, d, *J* = 8.7 Hz, H-3'), 8.08 (1H, s, H-8), 8.44 (1H, s, NH), 9.43 (1H, s, *N*^{9}H) ; ^{13}C NMR (125 MHz,

DMSO-d_6) (ppm) δ 25.4 (2 x C-cyclo), 26.1 (C-cyclo), 29.1 (2 x C-cyclo), 36.9 (C-2''), 40.6 (C-8'), 51.7 (C-5'), 71.3 (C-1''), 118.9 (C-3'), 121.5 (C_q), 125.6 (C_q), 126.7 (2 x C-ar), 127.1 (C-ar), 128.3 (2 x C-ar), 129.6 (C_q), 131.1 (C-2'), 140.2 (C_q), 142.0 (C-8), 153.3 (C_q), 157.3 (C_q), 162.7 (C_q); HRMS calcd for $C_{26}H_{33}N_6O_2S$ $[M+H+MeCN]^+$ 517.2380, found 517.2383.

2-((4-((6-(Cyclohexylmethoxy)-9*H*-purin-2-yl)amino)phenyl)sulfonyl)butan-1-ol (213)

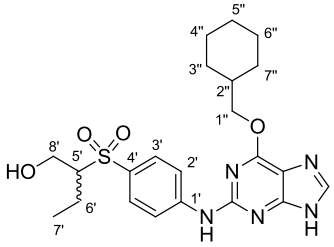

The title compound was synthesised following **general procedure M** using 2-((4-((6-(cyclohexylmethoxy)-9-(4-methoxybenzyl)-9*H*-purin-2-yl)amino)phenyl)thio) butan-1-ol **210** (280 mg, 0.66 mmol) and *m*-CPBA (305 mg, 1.31 mmol). The crude product was purified by MPC on silica (EtOAc: MeOH 9: 1) to give the product **213** as a yellow oil (85 mg, 0.18 mmol, 28%).

R_f 0.33 (EtOAc: MeOH 19: 1); UV λ_{max} (EtOH) 311 nm; IR (cm^{-1}) 3285, 2926, 2855, 1596, 1361, 1224, 1138; ^{1}H NMR (500 MHz, DMSO-d_6) (ppm) δ 0.75 (3H, t, *J* = 7.3 Hz, H-7'), 1.07-1.14 (2H, m, H-cyclo), 1.19-1.21 (1H, m, H-cyclo), 1.25-1.30 (2H, m, H-cyclo), 1.35-1.40 (1H, m, H-6'), 1.50-1.56 (1H, m, H-6'), 1.66-1.69 (1H, m, H-cyclo), 1.74-1.76 (2H, m, H-cyclo), 1.84-1.87 (3H, m, H-cyclo and H-2''), 3.28 (2H, dd, *J* = 5.8 and 3.0 Hz, H-8'), 3.75-3.81 (1H, m, H-5'), 4.38 (2H, d, *J* = 6.3 Hz, H-1''), 4.81 (1H, d, *J* = 5.8 Hz, OH), 7.76 (2H, d, *J* = 8.9 Hz, H-3'), 8.05 (2H, d, *J* = 8.9 Hz, H-2'), 8.07 (1H, s, H-8), 9.92 (1H, br s, NH), 12.97 (1H, br s, N^9H); ^{13}C NMR (125 MHz, DMSO-d_6) (ppm) δ 9.4 (C-7'), 25.2 (2 x C-cyclo), 26.0 (C-cyclo), 29.2 (2 x C-cyclo), 29.6 (C-6'), 36.8 (C-2''), 62.0 (C-8'), 66.5 (C-5'), 71.3 (C-1''), 115.5 (C_q), 117.2 (C-2'), 128.7 (C-3'), 130.9 (C_q), 139.6 (C-8), 145.7 (C_q), 153.9 (C_q), 154.6 (C_q), 160.2 (C_q); HRMS calcd for $C_{22}H_{30}N_5O_4S$ $[M+H]^+$ 460.2013, found 460.2004.

2-((4-((6-(Cyclohexylmethoxy)-9*H*-purin-2-yl)amino)phenyl)sulfonyl)-3-methyl butan-1-ol (214)

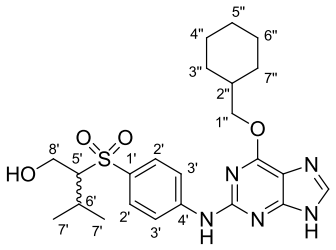

The title compound was synthesised following **general procedure M** using 2-((4-((6-(cyclohexylmethoxy)-9*H*-purin-2-yl)amino)phenyl)thio)-3-methylbutan-1-ol **211** (127 mg, 0.29 mmol) and *m*-CPBA (141 mg, 0.61 mmol). The crude product was purified by MPC on silica (DCM: MeOH 19: 1) to give the product **214** as a colourless oil (50.0 mg, 0.11 mmol, 36%).

R_f 0.37 (DCM: MeOH 9: 1); UV λ_{max} (EtOH) 318 nm; IR (cm^{-1}) 3261, 3101, 2925, 2851, 1595, 1535, 1386, 1135; ^{1}H NMR (500 MHz, DMSO-d_6) (ppm) δ 0.76 (3H, d, *J* = 6.8 Hz, H-7'), 0.80 (3H, d, *J* = 6.8 Hz, H-7'), 1.07-1.14 (2H, m, H-cyclo), 1.18-1.21 (1H, m, H-cyclo), 1.24-1.32 (2H, m, H-cyclo), 1.59-1.64 (1H, m, H-6'), 1.66-1.69 (1H, m, H-cyclo), 1.73-1.76 (2H, m, H-cyclo), 1.85-1.91 (3H, m, H-cyclo, H-2''), 3.21 (1H, dd, *J* = 3.0 and 14.6 Hz, H-8'), 3.29 (1H, dd, *J* = 8.1 and 14.6 Hz, H-8'), 3.69-3.74 (1H, m, H-5'), 4.37 (2H, d, *J* = 6.3 Hz, H-1''), 4.76 (1H, d, *J* = 5.8 Hz, OH), 7.77 (2H, d, *J* = 8.9 Hz, H-3'), 8.04 (2H, d, *J* = 8.9 Hz, H-2'), 8.07 (1H, s, H-8), 9.91 (1H, s, NH), 12.96 (1H, s, N^9H); ^{13}C NMR (125 MHz, DMSO-d_6) (ppm) δ 16.4 (C-7'), 18.4 (C-7'), 25.2 (2 x C-cyclo), 26.0 (C-cyclo), 29.2 (2 x C-cyclo), 33.2 (C-6'), 36.8 (C-2''), 60.2 (C-8'), 69.5 (C-5'), 71.3 (C-1''), 115.4 (C_q), 117.2 (C-2'), 128.7 (C-3'), 131.0 (C_q), 139.6 (C-8), 145.7 (C_q), 153.9 (C_q), 154.5 (C_q), 160.2 (C_q); HRMS calcd for C23H32N5O4S $[M+H]^+$ 474.2170, found 474.2161.

2-((4-((6-(Cyclohexylmethoxy)-9*H*-purin-2-yl)amino)phenyl)sulfonyl)-2-phenyl ethanol (215)

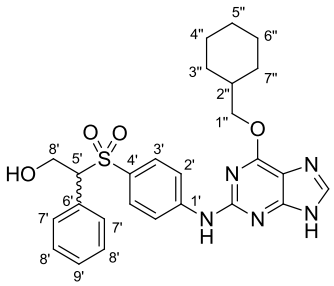

The title compound was synthesised following **general procedure M** using 2-((4-((6-(cyclohexylmethoxy)-9*H*-purin-2-yl)amino)phenyl)thio)-2-phenylethanol **212** (130 mg, 0.27 mmol) and *m*-CPBA (127 mg, 0.55 mmol). The crude product was purified by MPC on silica (EtOAc: MeOH 9: 1) to give the product **215** as a yellow oil (78 mg, 0.15 mmol, 56%).

R_f 0.40 (EtOAc: MeOH 19: 1); UV λ_{max} (EtOH) 313 nm; IR (cm^{-1}) 3296, 2926, 2850, 1596, 1534, 1453, 1395, 1298, 1138; ^{1}H NMR (500 MHz, DMSO-d_6) (ppm) δ 1.08-1.14 (2H, m, H-cyclo), 1.19-1.22 (1H, m, H-cyclo), 1.25-1.33 (2H, m, H-cyclo), 1.66-1.69 (1H, m, H-cyclo), 1.73-1.76 (2H, m, H-cyclo), 1.85-1.88 (3H, m, H-cyclo and H-2’’), 3.18 (2H, d, *J* = 5.0 Hz, H-8’), 4.11 (1H, m, OH), 4.38 (2H, d, *J* = 6.3 Hz, H-1’’), 5.20 (1H, m, H-5’), 7.21-7.24 (3H, m, H-ar), 7.28-7.31 (2H, m, H-ar), 7.72 (2H, d, *J* = 8.8 Hz, H-3’), 8.05 (2H, d, *J* = 8.8 Hz, H-2’), 8.07 (1H, s, H-8), 9.95 (1H, br s, NH), 12.98 (1H, br s, N^9H); ^{13}C NMR (125 MHz, DMSO-d_6) (ppm) δ 25.1 (2 x C-cyclo), 26.1 (C-cyclo), 29.2 (2 x C-cyclo), 36.8 (C-2’’), 51.5 (C-5’), 51.8 (C-8’), 71.1 (C-1’’), 118.9 (C-2’), 125.6 (C_q), 126.7 (2 x C-ar), 127.1 (C_q), 128.3 (2 x C-ar), 129.4 (C_q), 131.1 (C-3’), 140.1 (C_q), 142.0 (C-8), 155.3 (C_q), 157.3 (C_q), 162.7 (C_q), 168.5 (C_q); HRMS calcd for $C_{28}H_{33}N_6O_4S$ $[M+MeCN+H]^+$ 549.2279, found 549.2273.

2-((4-((6-(Cyclohexylmethoxy)-9*H*-purin-2-yl)amino)phenyl)sulfonyl)butyl acetate (217)

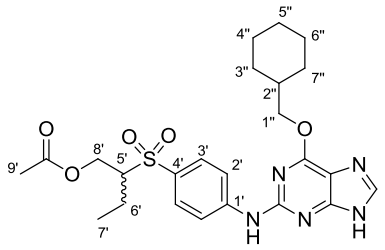

2-((4-((6-(Cyclohexylmethoxy)-9*H*-purin-2-yl)amino)phenyl)sulfonyl)butan-1-ol **213** (58 mg, 0.13 mmol) was solubilised in dry DCM (3 mL) under N_2. Et_3N (0.02 mL, 0.14 mmol), DMAP (1.5 mg, 0.01 mmol) and acetic anhydride (0.01 mL, 0.14 mmol) were added and the resukting solution was stirred at r.t. for 2 h. Na_2CO_3 was added and the reaction was extracted with DCM (3 x 10 mL). The organic layer was dried over $MgSO_4$ and the solvent was removed *in vacuo.* The crude product was purified by MPC on silica (DCM: MeOH 9: 1) to give the product **217** as a yellow oil (38 mg, 0.08 mmol, 60%).

R_f 0.18 (DCM: MeOH 19: 1); UV λ_{max} (EtOH) 313 nm; IR (cm^{-1}) 2928, 2873, 1717, 1575, 1347, 1216, 1137; ^{1}H NMR (500 MHz, MeOD) (ppm) δ 0.88 (3H, t, *J* = 7.4 Hz, H-7'), 1.15-1.21 (2H, m, H-cyclo), 1.25-1.29 (1H, m, H-cyclo), 1.32-1.40 (2H, m, H-cyclo), 1.48-1.56 (1H, m, H-6'), 1.60-1.67 (1H, m, H-6'), 1.73-1.76 (1H, m, H-cyclo), 1.81-1.83 (2H, m, H-cyclo), 1.95-1.97 (3H, m, H-cyclo and H-2''), 2.11 (3H, s, H-9'), 3.34-3.35 (1H, m, H-8'), 3.39-3.44 (1H, m, H-8'), 4.17-4.22 (1H, m, H-5'), 4.40 (2H, d, *J* = 6.1 Hz, H-1''), 7.79 (2H, d, *J* = 8.9 Hz, H-3'), 8.05 (1H, s, H-8), 8.08 (2H, d, *J* = 8.9 Hz, H-2'); ^{13}C NMR (125 MHz, MeOD) (ppm) δ 10.3 (C-7'), 26.9 (2 x C-cyclo), 27.6 (C-cyclo), 29.1 (C-6'), 30.9 (2 x C-cyclo), 38.8 (C-2''), 48.0 (C-5'), 49.9 (C-9'), 60.1 (C-8'); 73.3 (C-1''), 118.8 (C-2'), 129.4 (C_q), 130.2 (C_q), 130.3 (C-3'), 130.9 (C_q), 131.4 (C_q), 139.2 (C_q), 147.7 (C-8), 156.8 (C_q), 172.7 (CO); HRMS calcd for $C_{24}H_{30}N_5O_5S$ $[M-H]^-$ 499.1884, found 499.2122.

2-((4-Aminophenyl)sulfonyl)butan-1-ol (218)

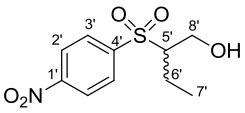

The title compound was synthesised following **general procedure M** using 2-((4-aminophenyl)thio)butan-1-ol **194** (1.00 g, 4.41 mmol) and *m*-CPBA (2.15 g, 9.25 mmol).

The crude product was purified by MPC on silica (petrol: EtOAc 3: 2) to give the product **218** as a yellow oil (1.11 g, 4.28 mmol, 97%).

R_f 0.33 (petrol: EtOAc 3: 2); UV λ_{max} (EtOH) 251 nm; IR (cm^{-1}) 3575, 2978, 2891, 1531, 1347, 1297, 1134; ^{1}H NMR (500 MHz, DMSO-d_6) (ppm) δ 0.99 (3H, t, *J* = 7.5 Hz, H-7'), 1.61-1.70 (1H, m, H-6'), 1.78-1.86 (1H, m, H-6'), 3.33-3.37 (1H, m, H-5'), 3.69-3.73 (1H, m, H-8'), 3.76-3.80 (1H, m, H-8'), 4.92 (1H, t, *J* = 5.3 Hz, OH), 8.15 (2H, d, *J* = 9.0 Hz, H-3'), 8.43 (2H, d, *J* = 9.0 Hz, H-2'); ^{13}C NMR (125 MHz, DMSO-d_6) (ppm) δ 11.0 (C-7'), 17.8 (C-6'), 57.3 (C-8'), 67.0 (C-5'), 124.2 (C-2'), 130.3 (C-3'), 144.7 (C-4'), 150.3 (C-1').

Note: LRMS and HRMS were not available because the compound did not ionise.

3-Methyl-2-((4-nitrophenyl)sulfonyl)butan-1-ol (219)

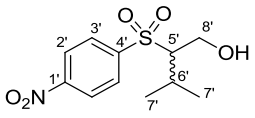

The title compound was synthesised following **general procedure M** using 3-methyl-2-((4-nitrophenyl)thio)butan-1-ol **195** (373 mg, 1.55 mmol) and *m*-CPBA (755 mg, 3.25 mmol). The crude product was purified by MPC on silica (petrol: EtOAc 3: 2) to give the product **219** as a yellow oil (287 mg, 1.05 mmol, 68%).

R_f 0.49 (petrol: EtOAc 1: 1); UV λ_{max} (EtOH) 253 nm; IR (cm^{-1}) 3512, 2968, 2879, 1528, 1349, 1297, 1145; ^{1}H NMR (500 MHz, DMSO-d_6) (ppm) δ 1.04 (3H, t, *J* = 7.0 Hz, H-7'), 1.10 (3H, t, *J* = 7.0 Hz, H-7'), 2.47-2.50 (1H, m, H-6'), 3.39-3.42 (1H, m, H-5'), 3.75-3.83 (2H, m, H-8'), 4.81 (1H, t, *J* = 5.0 Hz, OH), 8.17 (2H, d, *J* = 8.8 Hz, H-3'), 8.42 (2H, d, *J* = 8.8 Hz, H-2'); ^{13}C NMR (125 MHz, DMSO-d_6) (ppm) δ 18.0 (C-7'), 21.3 (C-7'), 25.3 (C-6'), 56.3 (C-8'), 70.3 (C-5'), 124.1 (C-2'), 129.8 (C-3'), 146.3 (C-4'), 150.2 (C-1'); HRMS calcd for $C_{11}H_{16}NO_5S$ $[M+H]^+$ 274.0744, found 274.0741.

2-((4-Nitrophenyl)sulfonyl)-2-phenylethanol (220)

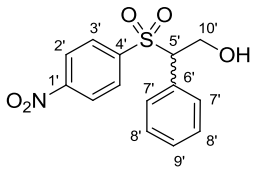

The title compound was synthesised following **general procedure M** using 2-((4-nitrophenyl)thio)-2-phenylethanol **196** (1.52 g, 4.79 mmol) and *m*-CPBA (2.34 g, 10.1 mmol). The crude product was purified by MPC on silica (petrol: EtOAc 1: 1) to give the product **220** as a yellow oil (1.11 g, 3.18 mmol, 66%).

R_f 0.58 (petrol: EtOAc 1: 1); UV λ_{max} (EtOH) 253 nm; IR (cm^{-1}) 3508, 2924, 2878, 1529, 1346, 1277, 1142, 1064; ^{1}H NMR (500 MHz, DMSO-d_6) (ppm) δ 4.01-4.06 (1H, m, H-10'), 4.16-4.21 (1H, m, H-10'), 4.85 (1H, t, *J* = 5.9 Hz, H-5'), 5.17 (1H, t, *J* = 5.4 Hz, OH), 7.34 (5H, s, H-ar), 7.99 (2H, d, *J* = 8.8 Hz, H-3'), 8.37 (2H, d, *J* = 8.8 Hz, H-2'); ^{13}C NMR (125 MHz, DMSO-d_6) (ppm) δ 59.3 (C-10'), 70.8 (C-5'), 124.1 (C-2'), 128.3 (2 x C-ar), 128.8 (C-6'), 130.2 (2 x C-ar), 130.3 (C-3'), 130.8 (C-ar), 144.3 (C-4'), 150.3 (C-1'); HRMS calcd for $C_{14}H_{12}NO_5S$ $[M-H]^-$ 306.0442, found 306.0437.

1-(2-((4-Nitrophenyl)sulfonyl)butyl)pyrrolidine (221)

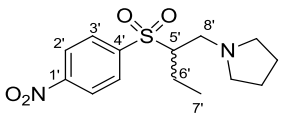

The title compound was synthesised following **general procedure Q** using 2-((4-aminophenyl)sulfonyl)butan-1-ol **218** (1.00 g, 3.86 mmol), Et_3N (1.07 mL, 7.72 mmol), benzenesulfonyl chloride (0.98 mL, 7.72 mmol) and pyrrolidine (1.61 mL, 19.3 mmol). The crude product was purified by MPC on silica (petrol: EtOAc 7: 3) to give the product **221** as a yellow oil (900 mg, 2.88 mmol, 75%).

R_f 0.20 (petrol: EtOAc 3: 2); UV λ_{max} (EtOH) 249 nm; IR (cm^{-1}) 2965, 2877, 1529, 1349, 1297, 1144; ^{1}H NMR (500 MHz, DMSO-d_6) (ppm) δ 1.05 (3H, t, *J* = 7.5 Hz, H-7'), 1.25-1.31 (2H, m, H-pyr), 1.34-1.41 (2H, m, H-pyr), 1.65-1.72 (1H, m, H-6'), 1.92-2.00 (1H, m, H-6'), 2.16-2.20 (4H, m, H-pyr), 2.56 (1H, dd, *J* = 13.0 and 5.5 Hz, H-8'), 2.80 (1H, dd, *J* = 13.0 and 8.3 Hz, H-8'), 3.59-3.64 (1H, m, H-5'), 8.16 (2H, d, *J* = 8.9 Hz, H-3'), 8.40 (2H, d, *J* = 8.9 Hz, H-2'); ^{13}C NMR (125 MHz, DMSO-d_6) (ppm) δ 11.0 (C-7'), 19.1 (C-6'), 22.9 (2 x C-pyr), 52.8 (2 x C-pyr), 53.4 (C-8'), 62.8 (C-5'), 123.8 (C-2'),

129.5 (C-3'), 146.1 (C-4'), 150.0 (C-1'); HRMS calcd for $C_{14}H_{21}N_2O_4S$ $[M+H]^+$ 312.1217, found 312.1214.

1-(3-Methyl-2-((4-nitrophenyl)sulfonyl)butyl)pyrrolidine (222)

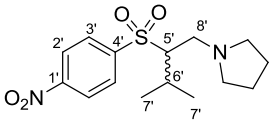

The title compound was synthesised following **general procedure Q** using 3-methyl-2-((4-nitrophenyl)sulfonyl)butan-1-ol **219** (287 mg, 1.05 mmol), Et_3N (0.22 mL, 1.58 mmol), benzenesulfonyl chloride (0.20 mL, 1.58 mmol) and pyrrolidine (0.44 mL, 5.26 mmol). The crude product was purified by MPC on silica (petrol: EtOAc 3: 2) to give the product **222** as a yellow oil (223 mg, 0.68 mmol, 65%).

R_f 0.52 (petrol: EtOAc 3: 2); UV λ_{max} (EtOH) 228 nm; IR (cm^{-1}) 2965, 2875, 1528, 1345, 1305; ^{1}H NMR (500 MHz, DMSO-d_6) (ppm) δ 1.04 (3H, t, *J* = 7.0 Hz, H-7'), 1.10 (3H, t, *J* = 7.0 Hz, H-7'), 1.13-1.17 (2H, m, H-pyr), 1.26-1.32 (2H, m, H-pyr), 2.10-2.12 (4H, m, H-pyr), 2.53-2.55 (1H, m, H-8'), 2.65-2.70 (1H, m, H-6'), 3.01 (1H, dd, *J* = 13.3 and 10.2 Hz, H-8'), 3.61-3.63 (1H, m, H-5'), 8.15 (2H, d, *J* = 8.9 Hz, H-3'), 8.37 (2H, d, *J* = 8.9 Hz, H-2'); ^{13}C NMR (125 MHz, DMSO-d_6) (ppm) δ 17.3 (C-7'), 21.1 (C-7'), 22.8 (2 x C-pyr), 25.2 (C-6'), 49.8 (C-8'), 52.3 (2 x C-pyr), 65.8 (C-5'), 123.8 (C-2'), 129.1 (C-3'), 147.7 (C-4'), 149.7 (C-1'); HRMS calcd for $C_{15}H_{23}N_2O_4S$ $[M+H]^+$ 327.1373, found 327.1367.

1-(2-((4-Nitrophenyl)sulfonyl)-2-phenylethyl)pyrrolidine (223)

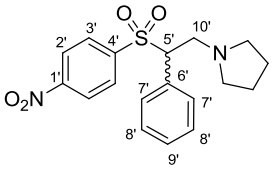

The title compound was synthesised following **general procedure Q** using 2-((4-nitrophenyl)sulfonyl)-2-phenylethanol **220** (1.11 g, 3.18 mmol), Et_3N (0.66 mL, 4.77 mmol), benzenesulfonyl chloride (0.61 mL, 4.77 mmol) and pyrrolidine (1.33 mL, 15.9 mmol). The crude product was purified by MPC on silica (petrol: EtOAc 3: 2) to give the product **223** as a yellow oil (780 mg, 1.94 mmol, 61%).

R_f 0.27 (petrol: EtOAc 3: 2); UV λ_{max} (EtOH) 251 nm; IR (cm^{-1}) 2939, 2793, 1524, 1348, 1295, 1138; ^{1}H NMR (500 MHz, DMSO-d_6) (ppm) δ 1.34-1.43 (4H, m, H-pyr), 2.23-2.32

(4H, m, H-pyr), 3.03 (1H, dd, *J* = 12.7 and 7.4 Hz, H-10'), 3.31 (1H, dd, *J* = 12.7 and 7.4 Hz, H-10'), 5.02 (1H, t, *J* = 7.4 Hz, H-5'),7.34-7.35 (3H, m, H-ar), 7.39-7.41 (2H, m, H-ar), 8.05 (2H, d, *J* = 8.8 Hz, H-3'), 8.37 (2H, d, *J* = 8.8 Hz, H-2'); ^{13}C NMR (125 MHz, DMSO-d_6) (ppm) δ 22.9 (C-pyr), 53.5 (C-pyr), 54.0 (C-10'), 67.5 (C-5'), 123.8 (C-2'), 128.3 (2 x C-ar), 128.8 (C-6'), 129.8 (2 x C-ar), 130.2 (C-3'), 131.4 (C-ar), 145.0 (C-4'), 150.1 (C-1'); HRMS calcd for $C_{18}H_{21}N_2O_4S$ $[M+H]^+$ 361.1217, found 361.1209.

4-((1-(Pyrrolidin-1-yl)butan-2-yl)sulfonyl)aniline (224)

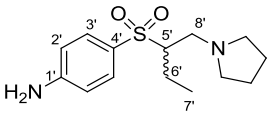

The title compound was synthesised following **general procedure H** using 1-(2-((4-nitrophenyl)sulfonyl)butyl)pyrrolidine **221** (900 mg, 2.88 mmol) and zinc powder (1.87 g, 28.9 mmol). The crude product was purified by MPC on silica (DCM: MeOH 9: 1) to give the product **224** as a colourless oil (606 mg, 2.15 mmol, 75%).

R_f 0.17 (DCM: MeOH 9: 1); UV λ_{max} (EtOH) 269 nm; IR (cm^{-1}) 3466, 3375, 2964, 2935, 1638, 1594, 1326, 1280, 1127; ^{1}H NMR (500 MHz, DMSO-d_6) (ppm) δ 0.97 (3H, t, *J* = 7.5 Hz, H-7'), 1.58-1.59 (4H, m, H-pyr), 1.64-1.70 (1H, m, H-6'), 1.73-1.79 (1H, m, H-6'), 2.22-2.25 (2H, m, H-pyr), 2.37-2.39 (2H, m, H-pyr), 2.52 (1H, dd, *J* = 12.4 and 4.5 Hz, H-8'), 2.60 (1H, dd, *J* = 12.4 and 9.0 Hz, H-8'), 3.02-3.07 (1H, m, H-5'), 6.11 (2H, s, NH_2), 6.64 (2H, d, *J* = 8.7 Hz, H-3'), 7.44 (2H, d, *J* = 8.7 Hz, H-2'); ^{13}C NMR (125 MHz, DMSO-d_6) (ppm) δ 11.3 (C-7'), 20.2 (C-6'), 23.1 (2 x C-pyr), 53.5 (2 x C-pyr), 53.8 (C-8'), 63.6 (C-5'), 112.5 (C-3'), 122.9 (C-4'), 130.2 (C-2'), 153.5 (C-1'); HRMS calcd for $C_{14}H_{23}N_2O_2S$ $[M+H]^+$ 283.1475, found 283.1472.

4-((3-Methyl-1-(pyrrolidin-1-yl)butan-2-yl)sulfonyl)aniline (225)

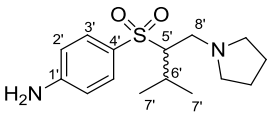

The title compound was synthesised following **general procedure H** using 1-(3-methyl-2-((4-nitrophenyl)sulfonyl)butyl)pyrrolidine **222** (220 mg, 0.67 mmol) and zinc powder (439 mg, 6.75 mmol). The crude product was purified by MPC on silica (DCM: MeOH 9: 1) to give the product **225** as a colourless oil (150 mg, 0.51 mmol, 76%).

R_f 0.33 (DCM: MeOH 9: 1); UV λ_{max} (EtOH) 270 nm; IR (cm^{-1}) 3432, 1491, 1291; ^1H NMR (500 MHz, DMSO d_6) (ppm) δ 0.98 (3H, t, *J* = 7.0 Hz, H-7'), 1.05 (3H, t, *J* = 7.0 Hz, H-7'), 1.52-1.54 (4H, m, H-pyr), 2.14-2.16 (2H, m, H-pyr), 2.27-2.29 (2H, m, H-pyr), 2.44-2.48 (1H, m, H-6'), 2.61 (1H, dd, *J* = 13.0 and5.6 Hz, H-8'), 2.71 (1H, dd, *J* = 13.0 and 8.4 Hz, H-8'), 3.08-3.10 (1H, m, H-5'), 6.06 (2H, s, NH_2), 6.61 (2H, d, *J* = 8.7 Hz, H-3'), 7.45 (2H, d, *J* = 8.7 Hz, H-2'); ^{13}C NMR (125 MHz, DMSO-d_6) (ppm) δ 17.5 (C-7'), 21.2 (C-7'), 23.0 (2 x C-pyr), 26.2 (C-6'), 50.7 (C-8'), 53.1 (2 x C-pyr), 66.4 (C-5'), 112.3 (C-3'), 124.5 (C-4'), 128.3 (C-1'), 130.0 (C-2'); HRMS calcd for $C_{15}H_{25}N_2O_2S$ $[M+H]^+$ 297.1631, found 297.1626.

4-((1-Phenyl-2-(pyrrolidin-1-yl)ethyl)sulfonyl)aniline (226)

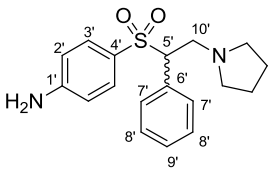

The title compound was synthesised following **general procedure H** using 1-(2-((4-nitrophenyl)sulfonyl)-2-phenylethyl)pyrrolidine **223** (780 mg, 1.94 mmol) and zinc powder (1.26 g, 19.4 mmol). The crude product was purified by MPC on silica (DCM: MeOH 9: 1) to give the product **226** as a pale orange oil (650 mg, 1.75 mmol, 90%).

R_f 0.36 (DCM: MeOH 9: 1); UV λ_{max} (EtOH) 274 nm; IR (cm^{-1}) 3379, 2967, 2853, 1593, 1282, 1137; ^1H NMR (500 MHz, DMSO-d_6) (ppm) δ 1.50-1.52 (4H, m, H-pyr), 2.20-2.24 (2H, m, H-pyr), 2.34-2.37 (2H, m, H-pyr), 3.00 (1H, dd, *J* = 12.3 and 3.8 Hz, H-10'), 3.20 (1H, dd, *J* = 12.3 and 1.7 Hz, H-10'), 4.44 (1H, dd, *J* = 10.4 and 3.8 Hz, H-5'), 6.09 (2H, s, NH_2), 6.51 (2H, d, *J* = 8.7 Hz, H-3'), 7.20 (2H, d, *J* = 8.7 Hz, H-2'); ^{13}C NMR (125 MHz, DMSO-d_6) (ppm) δ 22.9 (2 x C-pyr), 53.5 (2 x C-pyr), 54.0 (C-10'), 68.9 (C-5'), 112.3 (C-3'), 122.2 (C-6'), 127.8 (C-2'), 128.0 (C-ar), 129.9 (2 x C-ar), 130.4 (2 x C-ar), 133.2 (C-4'), 153.5 (C-1'); HRMS calcd for $C_{18}H_{23}N_2O_2S$ $[M+H]^+$ 331.1475, found 331.1466.

(4-Nitrophenyl)(1-phenylvinyl)sulfane (229)

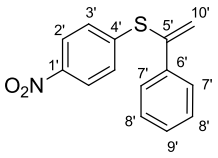

2-((4-Nitrophenyl)thio)-2-phenylethanol **196** (100 mg, 0.32 mmol) was solubilised in dry DCM (5 mL) under N_2. Et_3N (0.05 mL, 0.35 mmol) and benzenesulfonyl chloride (0.05 mL, 0.35 mmol) were added to the solution. The reaction was stirred at r.t. for 2 h. Pyrrolidine (0.13 mL, 1.58 mmol) was then added and the reaction was stirred for 30 min at r.t. The resulting mixture was washed with Brine (3 x 30 mL). The organic layer was dried over $MgSO_4$ and the solvent was removed *in vacuo*. The crude product was purified by MPC on silica (petrol: EtOAc 9: 1) to give the product **229** as a yellow oil (70 mg, 0.22 mmol, 74%).

R_f 0.55 (petrol: EtOAc 9: 1); UV λ_{max} (EtOH) 380 nm; IR (cm^{-1}) 1675, 1577, 1506, 1334, 1090; ^{1}H NMR (500 MHz, DMSO-d_6) (ppm) δ 5.99 (1H, s, H-10'), 6.28 (1H, s, H-10'), 7.33-7.38 (3H, m, H-ar), 7.42 (2H, d, *J* = 9.0 Hz, H-3'), 7.68 (2H, d, *J* = 6.6 Hz, H-ar), 8.09 (2H, d, *J* = 9.0 Hz, H-2'); ^{13}C NMR (125 MHz, DMSO-d_6) (ppm) δ 124.1 (C-2'), 125.3 (C-10'), 126.9 (2 x C-ar), 128.1 (C-3'), 128.7 (2 x C-ar), 129.0 (C-ar), 136.9 (C_q), 138.7 (C_q), 144.9 (C_q), 145.3 (C_q); HRMS calcd for $C_{14}H_{12}NO_2S$ $[M+H]^+$ 258.0583, found 258.0583.

6-(Cyclohexylmethoxy)-*N*-(4-((1-(pyrrolidin-1-yl)butan-2-yl)sulfonyl)phenyl)-9*H*-purin-2-amine (230)

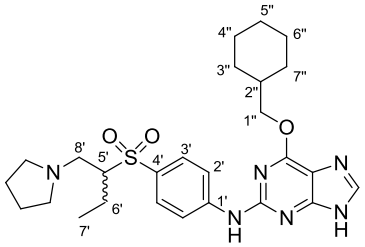

The title compound was synthesised following **general procedure I** using 6-(cyclohexylmethoxy)-2-iodo-9-(4-methoxybenzyl)-9*H*-purine **171** (406 mg, 1.28 mmol), 4-((1-(pyrrolidin-1-yl)butan-2-yl)sulfonyl)aniline **224** (200 mg, 1.06 mmol), K_2CO_3 (195 mg, 2.13 mmol), $Pd(dba)_2$ (13 mg, 0.02 mmol) and XPhos (7 mg, 0.02 mmol). The crude mixture was then filtered through Celite and the solvent was removed *in vacuo*. The crude mixture was then solubilised in TFA (15 mL). The resulting solution was heated at

70 °C for 2 h. Then the solvent was removed *in vacuo*. The product was purified by MPC (DCM: MeOH 9: 1) to give the product **230** as a yellow oil (190 mg, 0.37 mmol, 35%).

R_f 0.54 (DCM: MeOH 9: 1); UV λ_{max} (EtOH) 315 nm; IR (cm^{-1}) 2926, 2852, 1673, 1593, 1450, 1386, 1128; ^{1}H NMR (500 MHz, DMSO-d_6) (ppm) δ 0.96 (3H, t, *J* = 7.5 Hz, H-7'), 1.07-1.15 (2H, m, H-cyclo), 1.19-1.21 (1H, m, H-cyclo), 1.24-1.32 (2H, m, H-cyclo), 1.53-1.60 (1H, m, H-6'), 1.67-1.76 (4H, m, H-cyclo and H-6'), 1.85-1.91 (5H, m, H-cyclo, H-pyr, H-2''), 1.98-2.05 (2H, m, H-pyr), 2.97-3.03 (1H, m, H-pyr), 3.13-3.18 (1H, m, H-pyr), 3.48-3.52 (1H, m, H-8'), 3.58-3.61 (1H, m, H-8'), 3.68-3.74 (3H, m, H-pyr and H-5'), 4.38 (2H, d, *J* = 6.4 Hz, H-1''), 7.83 (2H, d, *J* = 9.0 Hz, H-3'), 8.14 (2H, d, *J* = 9.0 Hz, H-2'), 8.10 (1H, s, H-8), 9.48 (1H, br s, NH), 10.05 (1H, br s, N^9H); ^{13}C NMR (125 MHz, DMSO-d_6) (ppm) δ 10.3 (C-7'), 21.0 (C-6'), 22.4 (2 x C-pyr), 25.2 (2 x C-cyclo), 22.5 (C-pyr), 26.0 (C-cyclo), 29.2 (2 x C-cyclo), 36.8 (C-2''), 51.5 (C-8'), 54.5 (C-pyr), 54.6 (C-pyr), 60.9 (C-5'), 71.7 (C-1''), 117.3 (C-2'), 126.1 (C_q), 129.9 (C-3'), 146.8 (C_q), 154.3 (C_q); HRMS calcd for $C_{26}H_{37}N_6O_3S$ $[M+H]^+$ 513.2642, found 513.2630.

Note: Four quaternary carbons were not visible on the ^{13}C NMR spectrum.

6-(Cyclohexylmethoxy)-*N*-(4-((3-methyl-1-(pyrrolidin-1-yl)butan-2-yl)sulfonyl) phenyl)-9*H*-purin-2-amine (231)

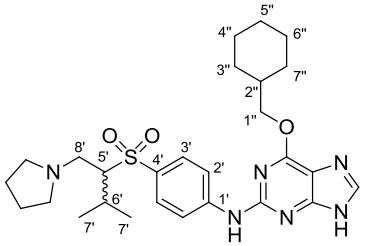

The title compound was synthesised following **general procedure I** using 6-(cyclohexylmethoxy)-2-iodo-9-(4-methoxybenzyl)-9*H*-purine **171** (385 mg, 0.81 mmol), 4-((3-methyl-1-(pyrrolidin-1-yl)butan-2-yl)sulfonyl)aniline **225** (200 mg, 0.68 mmol), K_2CO_3 (185 mg, 1.34 mmol), $Pd(dba)_2$ (13 mg, 0.02 mmol) and XPhos (7 mg, 0.02 mmol). The crude mixture was then filtered through Celite and the solvent was removed *in vacuo*. The crude mixture was then solubilised in TFA (15 mL). The resulting solution was heated at 70 °C for 2 h. Then the solvent was removed *in vacuo*. The product was purified by MPC (DCM: MeOH 9: 1) to give the product **231** as a brown oil (75 mg, 0.14 mmol, 18%).

R_f 0.49 (DCM: MeOH 9: 1); UV λ_{max} (EtOH) 316 nm; IR (cm^{-1}) 3378, 2967, 2885, 1596, 1495, 1248, 1124; ^{1}H NMR (500 MHz, MeOD) (ppm) δ 0.00 (3H, t, *J* = 7.0 Hz, H-7'), 0.05 (3H, t, *J* = 7.0 Hz, H-7'), 0.18-0.25 (2H, m, H-cyclo), 0.30-0.33 (1H, m, H-cyclo), 0.35-0.42 (2H, m, H-cyclo), 0.75-0.78 (1H, m, H-cyclo), 0.83-0.85 (2H, m, H-cyclo), 0.97-0.99 (3H, m, H-cyclo and H-2''), 1.04-1.09 (1H, m, H-6'), 1.14-1.19 (2H, m, H-pyr), 1.22-1.29 (2H, m, H-pyr), 2.17-2.21 (1H, m, H-pyr), 2.27-2.31 (1H, m, H-pyr), 2.58-2.59 (1H, m, H-8'), 2.66-2.67 (1H, m, H-8'), 2.87-2.93 (1H, m, H-pyr), 2.97-3.05 (2H, m, H-pyr and H-5'), 3.45 (2H, d, *J* = 6.1 Hz, H-1''), 6.92 (2H, d, *J* = 9.0 Hz, H-3'), 7.18-7.21 (3H, m, H-2' and H-8); ^{13}C NMR (125 MHz, MeOD) (ppm) δ 13.4 (C-7'), 18.4 (C-7'), 21.2 (2 x C-pyr), 24.2 (2 x C-cyclo), 24.8 (C-cyclo), 26.0 (C-6'), 28.0 (2 x C-cyclo), 36.0 (C-2''), 48.6 (2 x C-pyr), 63.5 (C-8'), 65.1 (C-5'), 70.7 (C-1''), 116.3 (C-2'), 125.2 (C_q), 128.6 (C-3'), 134.6 (C_q), 135.4 (C_q), 136.4 (C_q), 145.9 (C_q), 154.0 (C_q), 158.6 (C_q); HRMS calcd for $C_{27}H_{39}N_6O_3S$ $[M+H]^+$ 527.2799, found 527.2800.

6-(Cyclohexylmethoxy)-*N*-(4-((1-phenyl-2-(pyrrolidin-1-yl)ethyl)sulfonyl) phenyl)-9*H*-purin-2-amine (232)

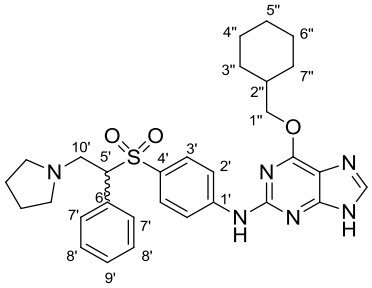

The title compound was synthesised following **general procedure I** using 6-(cyclohexylmethoxy)-2-iodo-9-(4-methoxybenzyl)-9*H*-purine **171** (385 mg, 0.81 mmol), 4-((1-phenyl-2-(pyrrolidin-1-yl)ethyl)sulfonyl)aniline **226** (250 mg, 0.67 mmol), K_2CO_3 (185 mg, 1.34 mmol), $Pd(dba)_2$ (13 mg, 0.02 mmol) and XPhos (7 mg, 0.02 mmol). The crude mixture was then filtered through Celite and the solvent was removed *in vacuo*. The crude mixture was then solubilised in TFA (15 mL). The resulting solution was heated at 70 °C for 2 h. Then the solvent was removed *in vacuo*. The product was purified by MPC (DCM: MeOH 9: 1) to give the product **232** as a brown oil (180 mg, 0.32 mmol, 47%).

R_f 0.60 (DCM: MeOH 9: 1); UV λ_{max} (EtOH) 318 nm; IR (cm^{-1}) 2926, 2851, 1671, 1594, 1449, 1389, 1199; ^{1}H NMR (500 MHz, DMSO-d_6) (ppm) δ 1.06-1.14 (2H, m, H-cyclo), 1.18-1.22 (1H, m, H-cyclo), 1.24-1.33 (2H, m, H-cyclo), 1.67-1.70 (1H, m, H-cyclo),

1.73-1.79 (4H, m, H-cyclo and H-pyr), 1.83-1.89 (3H, m, H-cyclo and H-2’’), 1.94-2.01 (2H, m, H-pyr), 3.00-3.04 (1H, m, H-pyr), 3.08-3.13 (1H, m, H-pyr), 3.36-3.41 (1H, m, H-pyr), 3.54-3.59 (1H, m, H-pyr), 4.02-4.06 (1H, m, H-10’), 4.13-4.18 (1H, m, H-10’), 4.35 (2H, d, *J* = 6.3 Hz, H-1’’), 5.01-5.04 (1H, m, H-5’), 7.30 (2H, d, *J* = 7.1 Hz, H-ar), 7.34-7.41 (5H, m, H-ar and H-3’), 7.95 (2H, d, *J* = 8.9 Hz, H-2’), 8.15 (1H, s, H-8), 9.47 (1H, br s, NH), 9.98 (1H, br s, N^9H); ^{13}C NMR (125 MHz, DMSO-d_6) (ppm) δ 22.2 (C-pyr), 22.5 (C-pyr), 25.2 (2 x C-cyclo), 26.0 (C-cyclo), 29.2 (2 x C-cyclo), 36.8 (C-2’’), 51.6 (C-10’), 52.5 (C-pyr), 54.0 (C-pyr), 65.9 (C-5’), 71.4 (C-1’’), 116.7 (C-2’), 125.6 (C_q), 128.5 (C-3’), 128.8 (C_q), 129.4 (C-ar), 129.9 (2 x C-ar), 130.2 (2 x C-ar), 137.5 (C-8), 141.1 (C_q), 145.2 (C_q), 146.3 (C_q), 153.2 (C_q), 154.9 (C_q); HRMS calcd for $C_{30}H_{37}N_6O_3S$ $[M+H]^+$ 561.2642, found 561.2645.

2-((4-Aminophenyl)sulfonyl)-3,3-dimethylbutan-1-ol (233)

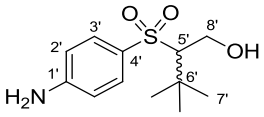

The title compound was synthesised following **general procedure H** using 3,3-dimethyl-2-((4-nitrophenyl)sulfonyl)butan-1-ol **253** (130 mg, 0.45 mmol) and zinc powder (2.35, 3.62 mmol). The crude product was purified by MPC on silica (petrol: EtOAC 3: 2) to give the product **233** as an orange oil (98 mg, 0.38 mmol, 84%).

R_f 0.49 (petrol: EtOAc 1: 1); UV λ_{max} (EtOH) 268 nm; IR (cm^{-1}) 3494, 3450, 3353, 2966, 2912, 1599, 1476, 1273, 1131; ^{1}H NMR (500 MHz, DMSO-d_6) (ppm) δ 1.16 (9H, s, H-7’), 2.87 (1H, dd, *J* = 4.5 and 4.5 Hz, H-5’), 3.65 (1H, ddd, *J* = 4.5, 4.5 and 7.9 Hz, H-8’), 3.72 (1H, ddd, *J* = 4.5, 4.5 and 7.9 Hz, H-8’), 4.52 (1H, dd, *J* = 4.5 and 4.5 Hz, OH), 6.10 (2H, s, NH_2), 6.63 (2H, d, *J* = 8.6 Hz, H-3’), 7.45 (2H, d, *J* = 8.6 Hz, H-2’); ^{13}C NMR (125 MHz, DMSO-d_6) (ppm) δ 29.4 (C-7’), 34.8 (C-6’), 58.3 (C-8’), 75.0 (C-5’), 113.1 (C-3’), 126.3 (C-4’), 130.4 (C-2’), 153.7 (C-1’); HRMS calcd for $C_{12}H_{18}NO_3S$ $[M-H]^-$ 256.1013, found 256.1003.

Ethyl 2-((4-nitrophenyl)thio)acetate (236)[264]

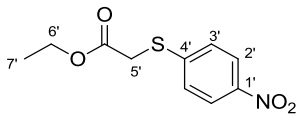

The title compound was synthesised following **general procedure J** using ethyl chloroacetate (1.51 mL, 14.2 mmol), 4-nitrothiophenol **173** (2.00 g, 12.9 mmol) and Et_3N (1.97 mL, 14.2 mmol). The crude product was purified by MPC on silica (petrol: EtOAc 4: 1) to give the product **236** as a yellow solid (2.95 g, 12.3 mmol, 95%).

R_f 0.46 (petrol: EtOAc 4: 1); Mp = 48-50 °C (lit.,[265] Mp = 46-47 °C); UV λ_{max} (EtOH) 340 nm; IR (cm^{-1}) 1722, 1502, 1330, 1165; ^{1}H NMR (500 MHz, DMSO-d_6) (ppm) δ 1.18 (3H, t, *J* = 7.1 Hz, H-7'), 4.13 (2H, q, *J* = 7.1 Hz, H-6'), 4.16 (2H, s, H-5'), 7.53 (2H, d, *J* = 9.0 Hz, H-3'), 8.14 (2H, d, *J* = 9.0 Hz, H-2'); ^{13}C NMR (125 MHz, DMSO-d_6) (ppm) δ 13.9 (C-7'), 33.3 (C-5'), 61.3 (C-6'), 123.9 (C-2'), 126.4 (C-3'), 144.8 (C-4'), 146.1 (C-1'), 168.6 (CO); HRMS calcd for $C_{10}H_{10}NO_4S$ $[M-H]^-$ 240.0336, found 240.0336.

Ethyl 2-((4-nitrophenyl)sulfonyl)acetate (237)[266]

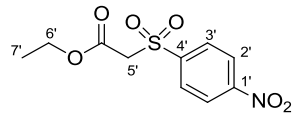

The title compound was synthesised following **general procedure M** using ethyl 2-((4-nitrophenyl)thio)acetate **236** (2.90 g, 12.1 mmol) and *m*-CPBA (5.62 g, 24.2 mmol). The crude product was purified by MPC on silica (petrol: EtOAc 4: 1) to give the product **237** as a pale yellow oil (2.84 g, 10.4 mmol, 86%).

R_f 0.40 (petrol: EtOAc 4: 1); UV λ_{max} (EtOH) 250 nm; IR (cm^{-1}) 2910, 1738, 1534, 1300, 1201, 1134; ^{1}H NMR (500 MHz, DMSO-d_6) (ppm) δ 1.08 (3H, t, *J* = 7.1 Hz, H-7'), 4.06 (2H, q, *J* = 7.1 Hz, H-6'), 4.88 (2H, s, H-5'), 8.22 (2H, d, *J* = 8.7 Hz, H-3'), 8.48 (2H, d, *J* = 8.7 Hz, H-2'); ^{13}C NMR (125 MHz, DMSO-d_6) (ppm) δ 13.7 (C-7'), 59.1 (C-5'), 61.7 (C-6'), 124.4 (C-2'), 130.0 (C-3'), 144.2 (C-4'), 150.6 (C-1'), 162.4 (CO); HRMS calcd for $C_{10}H_{10}NO_6S$ $[M-H]^-$ 272.0234, found 272.0232.

3,3-Dimethyl-2-oxobutyl benzoate (246b)

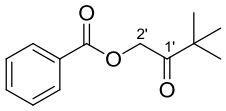

To a solution of benzoic acid (1.00 g, 8.20 mmol) in dry DMF (50 mL), under N_2, was added 1-chloropinacolone **247** (2.14 mL, 16.4 mmol) and diisopropylamine (7.12 mL, 41.0 mmol). The reaction was stirred at r.t. for 2 h. Brine (100 mL) was added and the reaction mixture was extracted with EtOAc (3 x 100 mL). The organic layers were combined and dried over $MgSO_4$. The solvent was removed *in vacuo* and the product was purified by MPC (petrol: EtOAc 9: 1) to give the product **246b** as a white solid (1.20 g, 5.45 mmol, 67%).

R_f 0.63 (petrol: EtOAc 4: 1); Mp = 74-75 ^oC; UV λ_{max} (EtOH) 273 nm; IR (cm^{-1}) 2967, 2846, 1714, 1598, 1256, 1062; ^1H NMR (500 MHz, DMSO-d_6) (ppm) δ 1.18 (9H, s, ^{t}Bu), 5.29 (2H, s, H-2'), 7.57 (2H, dd, *J* = 7.8 and 8.2 Hz, H-ar), 7.70 (1H, dd, *J* = 8.2 and 8.2 Hz, H-ar), 8.00 (2H, d, *J* = 7.8 Hz, H-ar); ^{13}C NMR (125 MHz, DMSO-d_6) (ppm) δ 25.7 (^{t}Bu), 42.2 (C), 65.5 (C-2'), 128.8 (2 x C-ar), 129.2 (2 x C-ar), 133.5 (C-ar), 165.1 (CO), 208.0 (C-1'); HRMS calcd for $C_{13}H_{17}O_3$ $[M+H]^+$ 221.1172, found 221.1169.

Note: One quaternary carbon was not visible on the ^{13}C NMR spectrum.

3,3-Dimethyl-2-((4-nitrophenyl)sulfonyl)butanoic acid (249)

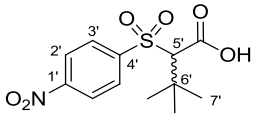

LHMDS (1M in THF, 2.33 mL, 2.33 mmol) was added to a stirred solution of 1-(neopentylsulfonyl)-4-nitrobenzene **250** (500 mg, 1.95 mmol) in dry THF (10 mL) at -78 °C, under N_2. The solution was stirred at -78 °C for 1 h then dry ice was added. The solution was allowed to warm up to r.t. and the reaction was stirred for 30 min at r.t. Water (15 mL) and EtOAc (15 mL) were added and the organic phase was washed with water (3 x 20 mL). The aqueous phase was acidified to pH 1 with 2M HCl solution and the organic phase was extracted with EtOAc (3 x 40 mL). The organic layers were combined and dried over $MgSO_4$ and the solvent was removed *in vacuo* to afford the product **249** as a pale yellow oil (290 mg, 0.10 mmol, 49%). No purification was performed.

R_f 0.45 (petrol: EtOAc 1: 4); UV λ_{max} (EtOH) 252 nm; IR (cm^{-1}) 3109, 2967, 2871, 1720, 1530, 1334, 1148; ^1H NMR (500 MHz, DMSO-d_6) (ppm) δ 1.21 (9H, s, H-7'), 4.42 (2H, s, H-5'), 8.17 (2H, d, *J* = 8.8 Hz, H-3'), 8.44 (2H, d, *J* = 8.8 Hz, H-2'), 13.30 (1 H, br s, OH); ^{13}C NMR (125 MHz, DMSO-d_6) (ppm) δ 28.4 (C-7'), 33.6 (C-6'), 77.3 (C-5'), 124.4 (C-2'), 130.2 (C-3'), 145.2 (C-4'), 150.5 (C-1'), 165.5 (CO); HRMS calcd for $C_{12}H_{16}NO_6S$ $[M+H]^+$ 302.0693, found 302.0692.

1-(Neopentylsulfonyl)-4-nitrobenzene (250)

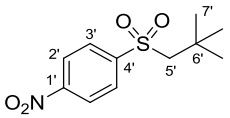

The title compound was synthesised following **general procedure M** using neopentyl(4-nitrophenyl)sulfane **252** (1.14 g, 5.07 mmol) and *m*-CPBA (2.26 g, 10.13 mmol). The crude product was purified by MPC on silica (petrol: EtOAc 4: 1) to give the product **250** as a white solid (1.12 g, 4.36 mmol, 86%).

R_f 0.55 (petrol: EtOAc 7: 3); Mp = 124-126 ^oC; UV λ_{max} (EtOH) 251 nm; IR (cm^{-1}) 2964, 2871, 1529, 1346, 1294; ^1H NMR (500 MHz, DMSO-d_6) (ppm) δ 1.11 (9H, s, H-7'), 3.43 (2H, s, H-5'), 8.21 (2H, d, *J* = 8.6 Hz, H-3'), 8.46 (2H, d, *J* = 8.6 Hz, H-2'); ^{13}C NMR (125 MHz, DMSO-d_6) (ppm) δ 29.4 (C-7'), 32.2 (C-6'), 64.9 (C-5'), 124.6 (C-2'), 129.0 (C-3'), 146.8 (C-4'), 150.3 (C-1'); HRMS calcd for $C_{11}H_{14}NO_4S$ $[M-H]^-$ 256.0638, found 256.0636.

Neopentyl(4-nitrophenyl)sulfane (252)

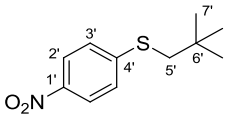

1-Iodo-2,2-dimethylpropane **251** (1.28 mL, 9.68 mmol) was added to a stirred solution of 4-nitrothiophenol **173** (1.00 g, 6.45 mmol) and K_2CO_3 (1.34 g, 9.68 mmol) in anhydrous DMF (7 mL) under N_2. The resulting solution was stirred at r.t. for 18 h. After completion, brine (20 mL) was added and the organic phase was extracted with EtOAc (3 x 20 mL). The organic layers were combined and dried over $MgSO_4$. The solvent was removed *in vacuo* and the crude product was purified by MPC on silica (petrol: EtOAc 19: 1) to give the product **252** as a yellow oil (0.99 g, 4.40 mmol, 68%).

R_f 0.70 (petrol: EtOAc 9: 1); UV λ_{max} (EtOH) 342 nm; IR (cm^{-1}) 2958, 1573, 1503, 1330; ^{1}H NMR (500 MHz, DMSO-d_6) (ppm) δ 1.04 (9H, s, H-7'), 3.08 (2H, s, H-5'), 7.55 (2H, d, *J* = 9.0 Hz, H-3'), 8.12 (2H, d, *J* = 9.0 Hz, H-2'); ^{13}C NMR (125 MHz, DMSO-d_6) (ppm) δ 28.6 (C-7'), 31.8 (C-6'), 44.7 (C-5'), 123.8 (C-2'), 126.4 (C-3'), 144.1 (C-4'), 148.5 (C-1'); HRMS calcd for $C_{11}H_{16}NO_2S$ $[M+H]^+$ 226.0896, found 226.0892.

3,3-Dimethyl-2-((4-nitrophenyl)sulfonyl)butan-1-ol (253)

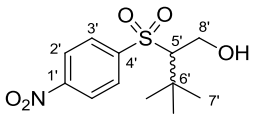

The title compound was synthesised following **general procedure L** using 3,3-dimethyl-2-((4-nitrophenyl)sulfonyl)butanoic acid **249** (400 mg, 1.33 mmol) and 1M Borane in complex with THF (6.00 mL, 5.98 mmol). The crude product was purified by MPC on silica (petrol: EtOAc 7: 3) to give the product **253** as a yellow oil (525 mg, 1.83 mmol, 73%).

R_f 0.73 (petrol: EtOAc 1: 1); UV λ_{max} (EtOH) 254 nm; IR (cm^{-1}) 3513, 2966, 2880, 1532, 1345, 1290, 1132; ^{1}H NMR (500 MHz, DMSO-d_6) (ppm) δ 1.22 (9H, s, H-7'), 3.33-3.35 (2H, m, H-5'), 3.70 (1H, ddd, *J* = 4.2, 4.2 and 8.1 Hz, H-8'), 3.76 (1H, ddd, *J* = 4.2, 4.2 and 8.1 Hz, H-8'), 4.68 (1H, dd, *J* = 4.2 and 4.2 Hz, OH), 8.15 (2H, d, *J* = 8.7 Hz, H-3'), 8.43 (2H, d, *J* = 8.7 Hz, H-2'); ^{13}C NMR (125 MHz, DMSO-d_6) (ppm) δ 29.3 (C-7'), 35.3 (C-6'), 58.1 (C-8'), 74.8 (C-5'), 124.6 (C-2'), 130.2 (C-3'), 147.7 (C-4'), 150.5 (C-1'); HRMS calcd for $C_{12}H_{16}NO_5S$ $[M-H]^-$ 286.0744, found 286.0742.

2-((4-((6-(Cyclohexylmethoxy)-9*H*-purin-2-yl)amino)phenyl)sulfonyl)-3,3-dimethylbutan-1-ol (254)

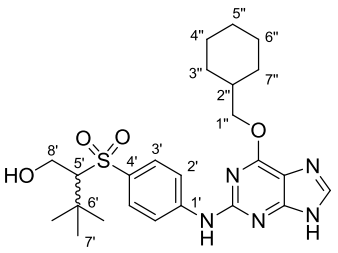

The title compound was synthesised following **general procedure I** using 6-(cyclohexylmethoxy)-2-iodo-9-(4-methoxybenzyl)-9*H*-purine **171** (112 mg, 0.23 mmol), 2-((4-aminophenyl)sulfonyl)-3,3-dimethylbutan-1-ol **233** (90 mg, 0.35 mmol), K_2CO_3 (65 mg, 0.47 mmol), $Pd(dba)_2$ (21 mg, 0.02 mmol) and XPhos (12 mg, 0.02 mmol). The

crude mixture was then filtered through Celite and the solvent was removed *in vacuo*. The crude mixture was then solubilised in TFA (7 mL). The resulting solution was heated at 70 °C for 2 h and the solvent was removed *in vacuo*. The product was purified by MPC (petrol: EtOAc 1: 9) to give the product **254** as a pale yellow oil (63 mg, 0.13 mmol, 55%).

R_f 0.20 (EtOAc 100); UV λ_{max} (EtOH) 314 nm; IR (cm^{-1}) 3309, 3169, 2925, 2852, 1575, 1501, 1334, 1270, 1120; ^{1}H NMR (500 MHz, MeOD) (ppm) δ 1.14-1.21 (2H, m, H-cyclo), 1.24-1.30 (10H, m, H-cyclo and H-7'), 1.32-1.39 (2H, m, H-cyclo), 1.73-1.75 (1H, m, H-cyclo), 1.80-1.83 (2H, m, H-cyclo), 1.94-1.96 (3H, m, H-cyclo and H-2''), 3.09 (1H, dd, *J* = 4.0 and 4.0 Hz, H-5'), 3.89 (1H, dd, *J* = 4.0 and 12.9 Hz, H-8'), 3.99 (1H, dd, *J* = 4.0 and 12.9 Hz, H-8'), 4.40 (2H, d, *J* = 6.0 Hz, H-1''), 7.81 (2H, d, *J* = 8.6 Hz, H-3'), 8.03-8.08 (3H, m, H-2' and H-8); ^{13}C NMR (125 MHz, MeOD) (ppm) δ 25.5 (2 x C-cyclo), 26.2 (C-cyclo), 28.2 (C-7'), 29.4 (2 x C-cyclo), 34.5 (C-6'), 37.3 (C-2''), 58.3 (C-8'), 71.8 (C-1''), 75.2 (C-5'), 117.2 (C-2'), 129.0 (C-3'), 131.9 (C_q), 139.9 (C-8), 146.0 (C_q), 155.4 (C_q), 160.0 (C_q); HRMS calcd for $C_{24}H_{34}N_5O_4S$ $[M+H]^+$ 488.2326, found 488.2312.

Note: Two quaternary carbons were not visible on the ^{13}C NMR spectrum.

2-((4-Nitrophenyl)thio)ethanol (255)[267]

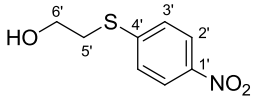

KOH (400 mg, 7.14 mmol) in water (2.6 mL) and 2-chloroethanol (1.00 mL, 15.0 mmol) were added to a stirred solution of 4-nitrothiophenol **173** (1.00 g, 6.45 mmol) in EtOH (2 mL). The reaction was heated at reflux for 18 h. Brine (10 mL) was added and the organic phase was extracted with EtOAc (3 x 10 mL). The organic layers were combined and dried over $MgSO_4$. The solvent was removed in vacuo. The product was purified by MPC (petrol: EtOAc 3: 2) to give the product **255** as a yellow solid (1.23 mg, 6.18 mmol, 96%).

R_f 0.40 (petrol: EtOAc 4: 1); Mp = 59-60 °C (lit.,[267] Mp = 57 °C); UV λ_{max} (EtOH) 377 nm; IR (cm^{-1}) 3541, 2914, 1575, 1505, 1325, 1056; ^{1}H NMR (500 MHz, DMSO-d_6) (ppm) δ 3.21 (2H, t, *J* = 6.5 Hz, H-5'), 3.65 (2H, td, *J* = 5.5 and 6.5 Hz, H-6'), 5.08 (1H, t, *J* = 5.2 Hz, OH), 7.53 (2H, d, *J* = 9.0 Hz, H-3'), 8.13 (2H, d, *J* = 9.0 Hz, H-2'); ^{13}C NMR

(125 MHz, DMSO-d_6) (ppm) δ 33.8 (C-5'), 59.3 (C-6'), 126.2 (C-3'), 128.9 (C-2'), 144.3 (C-4'), 147.8 (C-1'); HRMS calcd for $C_8H_{10}NO_3S$ $[M+H]^+$ 199.0376, found 199.1690.

2-((4-Nitrophenyl)sulfonyl)ethanol (256)

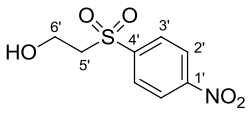

The title compound was synthesised following **general procedure M** using 2-((4-nitrophenyl)thio)ethanol **255** (1.23 g, 6.18 mmol) and *m*-CPBA (3.12 g, 13.60 mmol). The crude product was purified by MPC on silica (petrol: EtOAc 1: 1) to give the product **256** as a white crystalline solid (1.20 g, 5.19 mmol, 84%).

R_f 0.19 (petrol: EtOAc 4: 1); Mp = 123-125 °C (lit.,[268] Mp = 128 °C); UV λ_{max} (EtOH) 251 nm; IR (cm^{-1}) 3526, 3111, 2926, 1532, 1347, 1283, 1135; ^{1}H NMR (500 MHz, DMSO-d_6) (ppm) δ 3.61 (2H, t, *J* = 5.9 Hz, H-5'), 3.73 (2H, td, *J* = 5.2 and 5.9 Hz, H-6'), 4.91 (1H, t, *J* = 5.2 Hz, OH), 8.18 (2H, d, *J* = 8.9 Hz, H-3'), 8.44 (2H, d, *J* = 8.9 Hz, H-2'); ^{13}C NMR (125 MHz, DMSO-d_6) (ppm) δ 55.0 (C-6'), 57.4 (C-5'), 124.4 (C-2'), 129.5 (C-3'), 145.6 (C-4'), 150.3 (C-1'); HRMS calcd for $C_8H_{10}NO_5S$ $[M+H]^+$ 232.0274, found 232.0275.

1-(2-((4-Nitrophenyl)sulfonyl)ethyl)pyrrolidine (257)

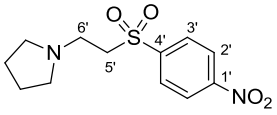

The title compound was synthesised following **general procedure Q** using 2-((4-nitrophenyl)sulfonyl)ethanol **256** (1.20 mg, 5.19 mmol), Et_3N (1.08 mL, 7.79 mmol), benzenesulfonyl chloride (1.00 mL, 7.79 mmol) and pyrrolidine (2.16 mL, 25.97 mmol). The crude product was purified by MPC on silica (petrol: EtOAc 1: 1) to give the product **257** as a yellow crystalline solid (990 mg, 3.49 mmol, 67 %).

R_f 0.33 (petrol: EtOAc 3: 2); Mp = 126-127 °C; UV λ_{max} (EtOH) 249 nm; IR (cm^{-1}) 2930, 2806, 1530, 1344, 1286, 1149; ^{1}H NMR (500 MHz, DMSO-d_6) (ppm) δ 1.44-1.47 (4H, m, H-pyr), 2.25-2.27 (4H, m, H-pyr), 2.72 (2H, t, *J* = 6.8 Hz, H-6'), 3.65 (2H, td, *J* = 5.2 and 5.9 Hz, H-5'), 8.19 (2H, d, *J* = 8.9 Hz, H-3'), 8.43 (2H, d, *J* = 8.9 Hz, H-2'); ^{13}C NMR (125 MHz, DMSO-d_6) (ppm) δ 22.9 (2 x C-pyr), 48.4 (C-6'), 52.7 (2 x C-pyr), 53.4 (C-

5'), 124.4 (C-2'), 129.4 (C-3'), 145.5 (C-4'), 150.3 (C-1'); HRMS calcd for $C_{12}H_{17}N_2O_4S$ $[M+H]^+$ 285.0904, found 285.0899.

***tert*-Butyl 2-((4-nitrophenyl)thio)acetate (260)**

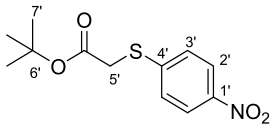

The title compound was synthesised following **general procedure J** using *tert*-butyl chloroacetone (1.01 mL, 7.10 mmol), 4-nitrothiophenol **173** (1.00 g, 6.46 mmol) and Et_3N (1.00 mL, 7.10 mmol). The crude product was purified by MPC on silica (petrol: EtOAc 9: 1) to give the product **260** as a yellow solid (1.56 g, 5.80 mmol, 90%).

R_f 0.77 (petrol: EtOAc 4: 1); Mp = 53-54 °C (lit.,[265] Mp = 47-49 °C); UV λ_{max} (EtOH) 330 nm; IR (cm^{-1}) 2988, 1720, 1504, 1338, 1301, 1153; ^{1}H NMR (500 MHz, DMSO-d_6) (ppm) δ 1.39 (9H, s, H-7'), 4.04 (2H, s, H-5'), 7.53 (2H, d, *J* = 9.0 Hz, H-3'), 8.17 (2H, d, *J* = 9.0 Hz, H-2'); ^{13}C NMR (125 MHz, DMSO-d_6) (ppm) δ 27.5 (C-7'), 34.3 (C-5'), 81.7 (C-6'), 123.8 (C-2'), 126.5 (C-3'), 144.7 (C-4'), 146.2 (C-1'), 167.6 (CO); HRMS calcd for $C_{12}H_{14}NO_4S$ $[M-H]^-$ 268.0649, found 268.0648.

***tert*-Butyl 2-((4-nitrophenyl)sulfonyl)acetate (261)**

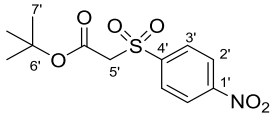

The title compound was synthesised following **general procedure M** using *tert*-butyl 2-((4-nitrophenyl)thio)acetate **260** (1.55 g, 5.76 mmol) and *m*-CPBA (2.81 g, 12.1 mmol). The crude product was purified by MPC on silica (petrol: EtOAc 7: 3) to give the product **261** as a white solid (1.64 g, 5.45 mmol, 95%).

R_f 0.73 (petrol: EtOAc 1: 1); Mp = 85-86 °C; UV λ_{max} (EtOH) 250 nm; IR (cm^{-1}) 2964, 2885, 1738, 1540, 1305, 1262, 1142; ^{1}H NMR (500 MHz, DMSO-d_6) (ppm) δ 1.27 (9H, s, H-7'), 4.74 (2H, s, H-5'), 8.24 (2H, d, *J* = 8.9 Hz, H-3'), 8.50 (2H, d, *J* = 8.9 Hz, H-2'); ^{13}C NMR (125 MHz, DMSO-d_6) (ppm) δ 27.2 (C-7'), 60.3 (C-5'), 82.6 (C-6'), 124.2 (C-2'), 129.9 (C-3'), 144.4 (C-4'), 150.6 (C-1'), 161.4 (CO); HRMS calcd for $C_{12}H_{14}NO_6S$ $[M-H]^-$ 300.0547, found 300.0549.

***tert*-Butyl 2-chloro-2-((4-nitrophenyl)sulfonyl)acetate (262)[220]**

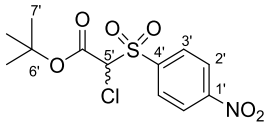

NaH (198 mg, 4.95 mmol) was added to a stirred solution of *tert*-butyl 2-((4-nitrophenyl)sulfonyl)acetate **261** (1.49 g, 4.95 mmol) in dry THF (90 mL) under N_2. The resulting mixture was stirred at r.t. for 30 min. *N*-Chlorosuccinimide (658 mg, 4.95 mmol) was then added and the solution was stirred at r.t. for 18 h. Brine (100 mL) was added and the reaction was extracted with EtOAc (3 x 50 mL). The organic layer was dried over $MgSO_4$ and the solvent was removed *in vacuo*. The crude product was purified by MPC on silica (petrol: EtOAc 9: 1) to give the product **262** as a pale yellow solid (1.29 g, 3.85 mmol, 78%).

R_f 0.47 (petrol: EtOAc 9: 1); Mp = 93-95 °C; UV λ_{max} (EtOH) 251 nm; IR (cm^{-1}) 2974, 1720, 1531, 1347, 1297, 1146; ^{1}H NMR (500 MHz, DMSO-d_6) (ppm) δ 1.37 (9H, s, H-7'), 6.71 (1H, s, H-5'), 8.25 (2H, d, *J* = 8.8 Hz, H-3'), 8.54 (2H, d, *J* = 8.8 Hz, H-2'); ^{13}C NMR (125 MHz, DMSO-d_6) (ppm) δ 27.1 (C-7'), 71.6 (C-5'), 85.5 (C-6'), 124.6 (C-2'), 131.4 (C-3'), 140.7 (C-4'), 151.3 (C-1'), 159.9 (CO); HRMS calcd for $C_{12}H_{13}ClNO_6S$ $[M-H]^-$ 334.0158, found 334.0150.

1-((Chloromethyl)sulfonyl)-4-nitrobenzene (264)

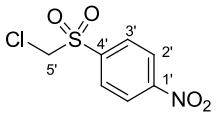

tert-Butyl 2-chloro-2-((4-nitrophenyl)sulfonyl)acetate **262** (100 mg, 0.30 mmol) was solubilised in DCM (3 mL). TFA (0.3 mL, 4.03 mmol) was then added and the resulting solution was stirred at r.t. for 18 h. The precipitate formed was filtered to afford **264** as a white solid (68 mg, 0.29 mmol, 96%).

OR

The title compound was synthesised following **general procedure K** using ethyl 2-chloro-2-((4-nitrophenyl)sulfonyl)acetate **265** (900 mg, 2.93 mmol) and LiOH (2M in THF, 14.6 mL). The product **264** was obtained without further purification as an orange oil (610 mg, 2.60 mmol, 88%).

R_f 0.53 (petrol: EtOAc 7: 3); Mp = 123-125 °C (lit.,[269] Mp = 129-130 °C); UV λ_{max} (EtOH) 250 nm; IR (cm^{-1}) 2957, 1526, 1349, 1282, 1188; ^{1}H NMR (500 MHz, DMSO-*d*$_6$) (ppm) δ 5.52 (2H, s, H-5'), 8.24 (2H, d, *J* = 8.9 Hz, H-3'), 8.51 (2H, d, *J* = 8.9 Hz, H-2'); ^{13}C NMR (125 MHz, DMSO-*d*$_6$) (ppm) δ 57.1 (C-5'), 124.6 (C-2'), 130.7 (C-3'), 141.1 (C-4'), 151.0 (C-1'$_q$); HRMS calcd for $C_7H_5ClNO_4S$ $[M-H]^-$ 233.9633, found 233.9632.

Ethyl 2-chloro-2-((4-nitrophenyl)sulfonyl)acetate (265)

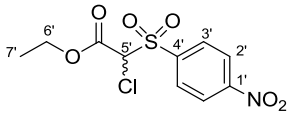

NaH (417 mg, 10.44 mmol) was added to a stirred solution of ethyl 2-((4-nitrophenyl)sulfonyl)acetate **237** (2.84 g, 10.4 mmol) in dry THF (100 mL) under N_2. The resulting mixture was stirred at r.t. for 30 min. *N*-Chlorosuccinimide (1.38 g, 10.4 mmol) was then added and the solution was stirred at r.t. for 18 h. Brine (100 mL) was added and the reaction was extracted with EtOAc (3 x 50 mL). The organic layer was dried over $MgSO_4$ and the solvent was removed *in vacuo*. The crude product was purified by MPC on silica (petrol: EtOAc 4: 1) to give the product **265** as a yellow oil (2.10 g, 6.84 mmol, 66%).

R_f 0.47 (petrol: EtOAc 4: 1); UV λ_{max} (EtOH) 249 nm; IR (cm^{-1}) 2966, 1738, 1532, 1346, 1300, 1134; ^{1}H NMR (500 MHz, DMSO-*d*$_6$) (ppm) δ 1.15 (3H, t, *J* = 7.1 Hz, H-7'), 4.22 (2H, q, *J* = 7.1 Hz, H-6'), 6.84 (1H, s, H-5'), 8.23 (2H, d, *J* = 9.0 Hz, H-3'), 8.52 (2H, d, *J* = 9.0 Hz, H-2'); ^{13}C NMR (125 MHz, DMSO-*d*$_6$) (ppm) δ 13.6 (C-7'), 63.8 (C-6'), 70.5 (C-5'), 124.5 (C-2'), 131.6 (C-3'), 140.2 (C-4'), 151.4 (C-1'), 161.2 (CO); HRMS calcd for $C_{10}H_9ClNO_6S$ $[M-H]^-$ 305.9845, found 305.9843.

2-Chloro-2-((4-nitrophenyl)sulfonyl)ethanol (266)

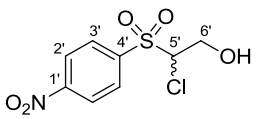

The title compound was synthesised following **general procedure O** using ethyl 2-chloro-2-((4-nitrophenyl)sulfonyl)acetate **265** (2.1 g, 6.84 mmol) and DIBAL (1M in hexanes, 20.5 mL, 20.5 mmol). The crude product was purified by MPC on silica (petrol: EtOAc 3: 2) to give the product **266** as a yellow solid (1.20 g, 4.53 mmol, 66%).

R_f 0.43 (petrol: EtOAc 3: 2); Mp = 95-98 °C; UV λ_{max} (EtOH) 249 nm; IR (cm^{-1}) 3488, 2943, 2877, 1530, 1304, 1136; ^{1}H NMR (500 MHz, DMSO-d_6) (ppm) δ 3.39 (1H, m, H-6'), 4.04 (1H, m, H-6'), 5.67 (1H, br s, OH), 5.76 (1H, dd, *J* = 4.2 and 6.1 Hz, H-5'), 8.23 (2H, d, *J* = 9.0 Hz, H-3'), 8.48 (2H, d, *J* = 8.9 Hz, H-2'); ^{13}C NMR (125 MHz, DMSO-d_6) (ppm) δ 60.4 (C-6'), 74.3 (C-5'), 124.4 (C-2'), 131.3 (C-3'), 141.6 (C-4614'), 151.0 (C-1'); HRMS calcd for $C_8H_7ClNO_5S$ $[M-H]^-$ 263.9739, found 263.9738.

2-((4-Aminophenyl)sulfonyl)-2-chloroethanol (267)

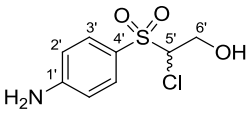

The title compound was synthesised following **general procedure H** using 2-chloro-2-((4-nitrophenyl)sulfonyl)ethanol **266** (500 mg, 1.89 mmol) and zinc powder (1.23 g, 18.9 mmol). The crude product was purified by MPC on silica (DCM: MeOH 9: 1) to give the product **267** as a pale orange oil (374 mg, 1.59 mmol, 84 %).

R_f 0.57 (DCM: MeOH 9: 1); UV λ_{max} (EtOH) 276 nm; IR (cm^{-1}) 3335, 3215, 2928, 1592, 1132; ^{1}H NMR (500 MHz, DMSO-d_6) (ppm) δ 3.55-3.63 (1H, m, H-6'), 4.01-4.05 (1H, m, H-6'), 5.15 (1H, dd, *J* = 3.4 and 8.0 Hz, H-5'), 5.45 (1H, dd, *J* = 6.2 and 6.2 Hz, OH), 6.34 (2H, br s, NH_2), 6.66 (2H, d, *J* = 8.8 Hz, H-3'), 7.50 (2H, d, *J* = 8.8 Hz, H-2'); ^{13}C NMR (125 MHz, DMSO-d_6) (ppm) δ 61.2 (C-6'), 75.4 (C-5'), 112.4 (C-3'), 129.3 (C-4'), 131.5 (C-2'), 139.1 (C-1'); HRMS calcd for $C_8H_{11}ClNO_3S$ $[M+H]^+$ 236.0143, found 236.0143.

2-Chloro-2-((4-((6-(cyclohexylmethoxy)-9*H*-purin-2-yl)amino)phenyl) sulfonyl)ethanol (268)

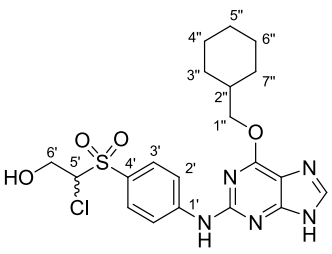

The title compound was synthesised following **general procedure I** using 6-(cyclohexylmethoxy)-2-iodo-9-(4-methoxybenzyl)-9*H*-purine **171** (176 mg, 0.37 mmol), 2-((4-aminophenyl)sulfonyl)-2-chloroethanol **267** (130 mg, 0.55 mmol), K_2CO_3 (102 mg, 0.74 mmol), $Pd(dba)_2$ (7 mg, 0.01 mmol) and XPhos (4 mg, 0.01 mmol). The crude

mixture was then filtered through Celite and the solvent was removed *in vacuo*. The crude mixture was then solubilised in TFA (15 mL). The resulting solution was heated at 70 °C for 2 h. Then the solvent was removed *in vacuo* and the product was purified by MPC (EtOAc 100) to give the product **268** as a yellow oil (56 mg, 0.12 mmol, 33%).

R_f 0.30 (EtOAc 100); UV λ_{max} (EtOH) 316 nm; IR (cm^{-1}) 3259, 3106, 2924, 2850, 1592, 1311; ^{1}H NMR (500 MHz, DMSO-d_6) (ppm) δ 1.08-1.15 (2H, m, H-cyclo), 1.22-1.32 (3H, m, H-cyclo), 1.66-1.69 (1H, m, H-cyclo), 1.73-1.76 (2H, m, H-cyclo), 1.85-1.90 (3H, m, H-cyclo and H-2''), 3.66-3.70 (1H, m, H-6'), 4.06-4.08 (1H, m, H-6'), 4.38 (2H, d, *J* = 6.3 Hz, H-1''), 5.37 (1H, dd, *J* = 3.5 and 7.5 Hz, H-5'), 5.54 (1H, br s, OH), 7.80 (2H, d, *J* = 8.8 Hz, H-3'), 8.09 (2H, d, *J* = 8.8 Hz, H-2'), 8.17 (1H, s, H-8), 10.04 (1H, br s, NH), 13.05 (1H, br s, N^9H); ^{13}C NMR (125 MHz, DMSO-d_6) (ppm) δ 25.2 (2 x C-cyclo), 26.0 (C-cyclo), 29.2 (2 x C-cyclo), 36.8 (C-2''), 60.8 (C-6'), 71.4 (C-1''), 75.1 (C-5'), 117.1 (C-2'), 130.6 (C-3'), 146.9 (C_q), 154.3 (C_q), 160.3 (C_q); HRMS calcd for $C_{20}H_{23}ClN_5O_4S$ $[M-H]^-$ 464.1165, found 464.1164.

Note: Four quaternary carbons were not visible on the ^{13}C NMR spectrum.

Ethyl 2-fluoro-2-((4-nitrophenyl)sulfonyl)acetate (269)

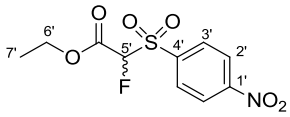

NaH (81 mg, 10.44 mmol) was added to a stirred solution of ethyl 2-((4-nitrophenyl)sulfonyl)acetate **237** (500 mg, 1.84 mmol) in dry THF (20 mL) under N_2. The resulting mixture was stirred at r.t. for 30 min. Then Selectfluor (1.30 g, 3.68 mmol) was added and the solution was stirred at r.t. for 2 h. Brine (20 mL) was added and the reaction was extracted with EtOAc (3 x 50 mL). The organic layer was dried over $MgSO_4$ and the solvent was removed *in vacuo.* The crude product was purified by MPC on silica (petrol: EtOAc 4: 1) to give the product **269** as a white solid (333 mg, 1.15 mmol, 62%).

R_f 0.64 (petrol: EtOAc 7: 3); Mp = 97-98.5 ^{o}C; UV λ_{max} (EtOH) 247 nm; IR (cm^{-1}) 2966, 1748, 1529, 1348, 1304, 1159; ^{1}H NMR (500 MHz, DMSO-d_6) (ppm) δ 1.20 (3H, t, *J* = 7.1 Hz, H-7'), 4.27 (2H, qd, *J* = 2.8 and 7.1 Hz, H-6'), 6.80 (1H, d, *J* = 45.1 Hz, H-5'), 8.22 (2H, d, *J* = 8.9 Hz, H-3'), 8.53 (2H, d, *J* = 8.9 Hz, H-2'); ^{13}C NMR (125 MHz, DMSO-d_6) (ppm) δ 13.7 (C-7'), 63.3 (C-6'), 96.0 (d, *J* = 226.8 Hz, C-5'), 124.9 (C-2'), 131.3 (C-3'), 139.7 (C-4'), 151.6 (C-1'), 160.5 (d, *J* = 23.3 Hz, CO); ^{19}F NMR (470 MHz,

DMSO-d_6) (ppm) δ -183.2; HRMS calcd for $C_{10}H_9FNO_6S$ $[M-H]^-$ 290.0129, found 290.0131.

2-Fluoro-2-((4-nitrophenyl)sulfonyl)ethanol (270)

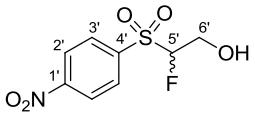

The title compound was synthesised following **general procedure O** using ethyl 2-fluoro-2-((4-nitrophenyl)sulfonyl)acetate **269** (300 mg, 1.03 mmol) and Dibal (1M in hexanes, 3.10 mL, 3.10 mmol). The crude product was purified by MPC on silica (petrol: EtOAc 7: 3) to give the product **270** as a white crystalline solid (175 mg, 0.70 mmol, 68%).

R_f 0.62 (petrol: EtOAc 7: 3); Mp = 95-97 °C; UV λ_{max} (EtOH) 248 nm; IR (cm^{-1}) 3097, 2976, 2926, 1520, 1343, 1081, 1053; ^{1}H NMR (500 MHz, DMSO-d_6) (ppm) δ 3.81-3.90 (1H, m, H-6'), 4.02 (1H, dddd, *J* = 2.8, 6.0, 13.4 and 27.6 Hz, H-6'), 5.59 (1H, t, *J* = 6.0 Hz, OH), 5.95 (1H, ddd, *J* = 2.8, 6.0 and 46.7 Hz, H-5'), 8.21 (2H, d, *J* = 8.9 Hz, H-3'), 8.48 (2H, d, *J* = 9.0 Hz, H-2'); ^{13}C NMR (125 MHz, DMSO-d_6) (ppm) δ 57.7 (d, *J* = 20.0 Hz, C-6'), 102.0 (d, *J* = 218.7 Hz, C-5'), 124.6 (C-2'), 131.0 (C-3'), 141.3 (C-4'), 151.2 (C-1'); ^{19}F NMR (470 MHz, DMSO-d_6) (ppm) δ -186.5 (ddd, *J* = 24.2, 27.6 and 46.7 Hz); HRMS calcd for $C_8H_9FNO_5S$ $[M+H]^+$ 250.0180, found 250.0178.

2-((4-Aminophenyl)sulfonyl)-2-fluoroethanol (271)

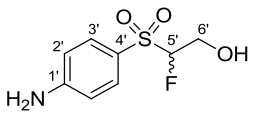

The title compound was synthesised following **general procedure H** using 2-fluoro-2-((4-nitrophenyl)sulfonyl)ethanol **270** (500 mg, 2.01 mmol) and zinc powder (1.30 g, 20.1 mmol). The crude product was purified by MPC on silica (petrol: EtOAc 1: 4) to give the product **271** as an orange oil (270 mg, 1.23 mmol, 62 %).

R_f 0.55 (DCM: MeOH 9: 1); UV λ_{max} (EtOH) 277 nm; IR (cm^{-1}) 3467, 3367, 1588, 1292, 1071; ^{1}H NMR (500 MHz, MeOD) (ppm) δ 3.68 (1H, ddd, *J* = 7.5, 13.2 and 19.0 Hz, H-6'), 3.97 (1H, ddd, *J* = 2.6, 13.2 and 31.3 Hz, H-6'), 5.10 (1H, ddd, *J* = 2.6, 7.5 and 49.0 Hz, H-5'), 6.63 (2H, d, *J* = 8.8 Hz, H-3'), 7.45 (2H, d, *J* = 8.8 Hz, H-2'); ^{13}C NMR (125 MHz, MeOD) (ppm) δ 60.2 (d, *J* = 20.8 Hz, C-6'), 103.9 (d, *J* = 218.1 Hz, C-5'), 114.3

(C-3'), 121.4 (C-4'), 132.5 (C-2'), 156.4 (C-1'); ^{19}F NMR (470 MHz, MeOD) (ppm) δ -186.9 (ddd, *J* = 19.0, 31.3 and 49.0 Hz); HRMS calcd for $C_8H_9FNO_3S$ $[M-H]^-$ 218.0293, found 218.0284.

2-((4-((6-(Cyclohexylmethoxy)-9*H*-purin-2-yl)amino)phenyl)sulfonyl)-2-fluoro ethanol (272)

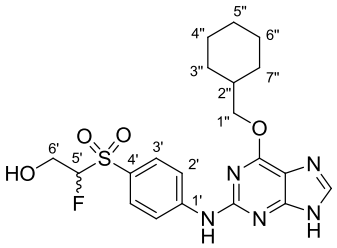

The title compound was synthesised following **general procedure I** using 6-(cyclohexylmethoxy)-2-iodo-9-(4-methoxybenzyl)-9*H*-purine **171** (350 mg, 0.73 mmol), 2-((4-aminophenyl)sulfonyl)-2-fluoroethanol **271** (240 mg, 1.10 mmol), K_2CO_3 (202 mg, 1.46 mmol), $Pd(dba)_2$ (13 mg, 0.01 mmol) and XPhos (7 mg, 0.01 mmol). The crude mixture was then filtered through Celite and the solvent was removed *in vacuo*. The crude mixture was then solubilised in TFA (15 mL). The resulting solution was heated at 70 °C for 2 h. Then the solvent was removed *in vacuo*. The product was purified by MPC (EtOAc 100) to give the product **272** as a yellow oil (112 mg, 0.24 mmol, 33%).

R_f 0.30 (EtOAc 100); UV λ_{max} (EtOH) 316 nm; IR (cm^{-1}) 3300, 3104, 2923, 2849, 1578, 1386, 1137; ^{1}H NMR (500 MHz, DMSO-d_6) (ppm) δ 1.08-1.14 (2H, m, H-cyclo), 1.17-1.21 (1H, m, H-cyclo), 1.24-1.32 (2H, m, H-cyclo), 1.67-1.69 (1H, m, H-cyclo), 1.73-1.76 (2H, m, H-cyclo), 1.85-1.91 (3H, m, H-cyclo and H-2''), 3.66-3.74 (1H, m, H-6'), 3.94-4.06 (1H, m, H-6'), 4.38 (2H, d, *J* = 6.3 Hz, H-1''), 5.49 (1H, dd, *J* = 6.1 and 6.1 Hz, OH), 5.54-5.65 (1H, m, H-5'), 7.79 (2H, d, *J* = 8.9 Hz, H-3'), 8.09-8.14 (3H, m, H-2' and H-8), 10.06 (1H, s, NH), 13.01 (1H, s, N^9H); ^{13}C NMR (125 MHz, DMSO-d_6) (ppm) δ 25.2 (2 x C-cyclo), 26.0 (C-cyclo), 29.2 (2 x C-cyclo), 36.8 (C-2''), 58.2 (d, *J* = 20.1 Hz, C-6'), 71.4 (C-1''), 102.0 (d, *J* = 217.1, C-5'), 115.6 (C_q), 117.4 (C-2'), 125.4 (C_q), 130.2 (C-3'), 139.8 (C-8), 147.0 (C_q), 153.8 (C_q), 154.3 (C_q), 160.2 (C_q); ^{19}F NMR (470 MHz, MeOD) (ppm) δ -185.60 (ddd, *J* = 20.2, 32.7 and 47.7 Hz); HRMS calcd for $C_{20}H_{23}FN_5O_4S$ $[M-H]^-$ 448.1460, found 448.1446.

***tert*-Butyl(2-chloro-2-((4-nitrophenyl)sulfonyl)ethoxy)dimethylsilane (276)**

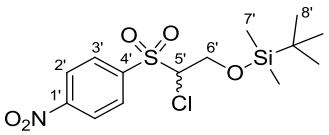

Imidazole (77 mg, 1.13 mmol) and tert-butyldimethylsilylchloride (63 mg, 0.42 mmol) were added at 0 ^{o}C to a solution of 2-chloro-2-((4-nitrophenyl) sulfonyl)ethanol **266** (100 mg, 0.38 mmol) in dry DCM (75 mL) under N_2. The reaction was stirred at 0 ^{o}C for 5 h. Then water (50 mL) was added to quench the reaction and the organic phase was extracted with DCM (3 x 50 mL) and dried over $MgSO_4$. The solvent was removed *in vacuo*. The crude product was purified by MPC on silica (petrol: EtOAc 4: 1) to give the product **276** as a white soil (1.38 g, 3.64 mmol, 85%).

R_f 0.77 (petrol: EtOAc 4: 1); Mp = 83-85 °C; UV λ_{max} (EtOH) 251 nm; IR (cm^{-1}) 2929, 2857, 1529, 1345, 1254, 1131; ^{1}H NMR (500 MHz, DMSO-d_6) (ppm) δ 0.00 (3H, s, H-7'), 0.03 (3H, s, H-7'), 0.80 (9H, s, H-8'), 4.15 (1H, dd, *J* = 4.5 and 12.2 Hz, H-6'), 4.22 (1H, dd, *J* = 4.5 and 12.2 Hz, H-6'), 5.94 (1H, dd, *J* = 4.5 and 4.5 Hz, H-5'), 8.25 (2H, d, *J* = 9.0 Hz, H-3'), 8.51 (2H, d, *J* = 8.9 Hz, H-2'); ^{13}C NMR (125 MHz, DMSO-d_6) (ppm) δ -5.7 (C-7'), 17.9 (C_q), 25.5 (C-8'), 62.1 (C-6'), 73.7 (C-5'), 124.4 (C-2'), 131.3 (C-3'), 141.9 (C-4'), 151.0 (C-1'); HRMS calcd for $C_{14}H_{23}ClNO_5SSi$ $[M+H]^+$ 380.0749, found 380.0751.

2-((4-Nitrophenyl)sulfonyl)oxirane (278)

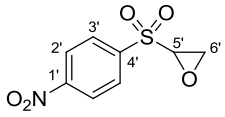

Cs_2CO_3 (92 mg, 0.28 mmol) was added to a stirred solution of 2-chloro-2-((4-nitrophenyl)sulfonyl)ethanol **266** (50 mg, 0.19 mmol) in dry MeCN (1 mL) under N_2. The reaction was stirred at r.t. for 2 h. The reaction mixture was filtered through Celite and the solvent was removed *in vacuo.* The crude product was purified by MPC on silica (DCM: MeOH 1: 1) to give the product **278** as a colourless oil (11 mg, 0.05 mmol, 25%).

R_f 0.25 (DCM: MeOH 9: 1); UV λ_{max} (EtOH) 306 nm; IR (cm^{-1}) 1590, 1495, 1338, 1252, 1110; ^{1}H NMR (500 MHz, DMSO-d_6) (ppm) δ 3.85 (1H, dd, *J* = 2.5 and 8.7 Hz, H-5'), 4.25 (1H, dd, *J* = 8.7 and 11.5 Hz, H-6'), 4.73 (1H, dd, *J* = 2.5 and 11.5 Hz, H-6'), 7.18

(2H, d, *J* = 9.3 Hz, H-3'), 8.21 (2H, d, *J* = 9.3 Hz, H-2'); ^{13}C NMR (125 MHz, DMSO-d_6) (ppm) δ 69.5 (C-6'), 77.2 (C-5'), 115.2 (C-3'), 125.9 (C-2'), 140.9 (C-4'), 163.7 (C-1').

Note: LRMS and HRMS were not available because the compound did not ionise.

1-((2-(Benzyloxy)ethyl)sulfonyl)-4-nitrobenzene (282)

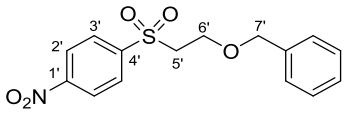

To a stirred suspension of NaH (23 mg, 0.56 mmol) in dry DMF (2 mL), under N_2, was added a solution of 2-((4-nitrophenyl)sulfonyl)ethanol **256** (100 mg, 0.43 mmol) in dry DMF (2 mL) at 0 ^{o}C. The resulting mixture was stirred at r.t. for 1 h. Benzyl bromide (88 uL, 0.74 mmol) was slowly added to the solution. The reaction was stirred at r.t. fo a further 2 h. The reaction was quenched with a saturated aqueous solution of NH_4Cl (5 mL), diluted with EtOAc (10 mL) and washed with brine. The organic layer was dried over $MgSO_4$ and the solvent was removed *in vacuo.* The crude product was purified by MPC on silica (petrol: EtOAc 1: 1) to give the product **282** as a yellow solid (82 mg, 0.26 mmol, 59%).

R_f 0.31 (petrol: EtOAc 7: 3); Mp = 155-156.5 ^{o}C; UV λ_{max} (EtOH) 305 nm; IR (cm^{-1}) 2924, 1588, 1510, 1342, 1289, 1250, 1112, 1017; ^{1}H NMR (500 MHz, DMSO-d_6) (ppm) δ 3.63 (2H, t, *J* = 5.6 Hz, H-6'), 4.54 (2H, t, *J* = 5.6 Hz, H-5'), 4.60 (2H, s, H-7'), 7.25 (2H, d, *J* = 9.2 Hz, H-3'), 7.42-7.44 (5H, m, H-ar), 8.25 (2H, d, *J* = 9.2 Hz, H-2'); ^{13}C NMR (125 MHz, DMSO-d_6) (ppm) δ 50.7 (C-6'), 59.5 (C-7'), 62.5 (C-5'), 115.2 (C-3'), 126.0 (C-2'), 128.2 (C_q), 128.4 (C-ar), 128.5 (2 x C-ar), 131.2 (2 x C-ar), 141.3 (C_q), 162.3 (C_q); HRMS calcd for $C_{15}H_{14}NO_5S$ $[M-H]^-$ 320.0598, found 320.0585.

3-Hydroxy-3-methoxy-2-((4-nitrophenyl)sulfonyl)acrylonitrile (284)

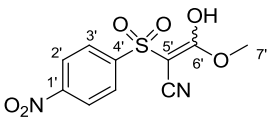

Methyl cyanoacetate **285** (0.79 mL, 9.00 mmol) and Cs_2CO_3 (2.94 g, 9.00 mmol) were stirred in dry MeCN (20 mL), under N_2, with molecular seaves at 0 °C for 1 h. Then 4-nitrobenzenesulfonyl chloride **242** (1.0 g, 4.50 mmol) was added and the reaction was stirred for 1 h at 0 °C. The solvent was removed *in vacuo*. The product was purified by

MPC on silica (DCM: MeOH 9:1) to give the product **284** as an orange oil (650 mg, 2.29 mmol, 51%).

R_f 0.17 (DCM: MeOH 9:1); UV λ_{max} (EtOH) 248 nm; IR (cm^{-1}) 3404, 2192, 1642, 1439, 1347, 1192, 1090; ^{1}H NMR (500 MHz, DMSO-d_6) (ppm) δ 3.36 (3H, s, H-7'), 8.00 (2H, d, *J* = 8.9 Hz, H-3'), 8.32 (2H, d, *J* = 8.9 Hz, H-2'), 8.84 (1H, br s, OH); ^{13}C NMR (125 MHz, DMSO-d_6) (ppm) δ 49.5 (C-7'), 64.2 (C-5'), 119.9 (CN), 123.9 (C-2'), 127.3 (C-3'), 148.5 (C-4'), 151.6 (C-1), 165.3 (C-6); HRMS calcd for $C_{10}H_7N_2O_6S$ $[M-H]^-$ 283.0030, found 283.0024.

2-((4-Nitrophenyl)sulfonyl)acetonitrile (288)

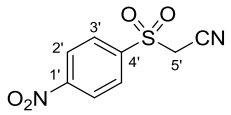

The title compound was synthesised following **general procedure M** using 2-((4-nitrophenyl)thio)acetonitrile **290** (1.00 g, 5.15 mmol) and *m*-CPBA (2.30 g, 10.3 mmol). The crude product was purified by MPC on silica (petrol: EtOAc 1: 1) to give the product **288** as a white powder (386 mg, 1.71 mmol, 33%).

R_f 0.78 (petrol: EtOAc 3: 2); Mp = 151.5-153 ^{o}C; UV λ_{max} (EtOH) 325 nm; IR (cm^{-1}) 2977, 2254, 1519, 1341, 1053; ^{1}H NMR (500 MHz, DMSO-d_6) (ppm) δ 4.48 (1H, d, *J* = 16.7 Hz, H-5'), 4.85 (1H, d, *J* = 16.7 Hz, H-5'), 8.04 (2H, d, *J* = 8.8 Hz, H-3'), 8.49 (2H, d, *J* = 8.8 Hz, H-2'); ^{13}C NMR (125 MHz, DMSO-d_6) (ppm) δ 43.3 (C-5'), 112.7 (CN), 124.3 (C-2'), 126.1 (C-3'), 149.4 (C-4'), 149.6 (C-1'); HRMS calcd for $C_8H_5N_2O_4S$ $[M-H]^-$ 224.9976, found 224.9965.

2-((4-Nitrophenyl)thio)acetonitrile (290)[270]

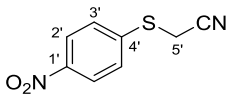

The title compound was synthesised following **general procedure J** using iodoacetonitrile (0.51 mL, 7.10 mmol), 4-nitrothiophenol **173** (1.00 g, 6.45 mmol) and Et_3N (1.08 mL, 7.75 mmol). The crude product was purified by MPC on silica (petrol: EtOAc 4: 1) to give the product **290** as a yellow solid (1.09 g, 5.62 mmol, 87%).

R_f 0.78 (petrol: EtOAc 3: 2); Mp = 85-86 ^{o}C; UV λ_{max} (EtOH) 314 nm; IR (cm^{-1}) 2963, 2254, 1574, 1506, 1337; ^{1}H NMR (500 MHz, DMSO-d_6) (ppm) δ 4.50 (2H, s, H-5'), 7.68

(2H, d, *J* = 9.0 Hz, H-3'), 8.25 (2H, d, *J* = 9.0 Hz, H-2'); ^{13}C NMR (125 MHz, DMSO-d_6) (ppm) δ 16.8 (C-5'), 117.3 (CN), 124.2 (C-2'), 127.3 (C-3'), 143.2 (C-4'), 145.6 (C-1'); HRMS calcd for $C_8H_5N_2O_2S$ $[M-H]^-$ 193.0077, found 193.0069.

3,3,3-Trifluoropropane-1,2-diol (296)[226]

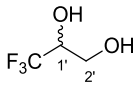

Ethyl pyruvate **295** (0.95 mL, 5.88 mmol) was added dropwise to $LiAlH_4$ (1M in THF, 5.90 mL) at 0 °C, under N_2. The mixture was then refluxed for 2 h. After completion, 2M HCl solution was added until obtaining a clear solution. Et_2O was added (50 mL) and the organic layer was extracted. The organic phase was dried over $MgSO_4$. The solvent was removed *in vacuo* at r.t.. The crude product was purified by distillation under vacuum using a Kügelrohr apparatus (60 °C, 4 mmbar) to give the product **296** as a colourless liquid (625 mg, 4.81 mmol, 82%).

R_f 0.34 (petrol: EtOAc 4: 1); UV λ_{max} (EtOH) 277 nm; IR (cm^{-1}) 3343, 1271, 1112, 1029; ^{1}H NMR (500 MHz, DMSO-d_6) (ppm) δ 3.46 (1H, dd, *J* = 6.7 and 11.4 Hz, H-2'), 3.58 (1H, dd, *J* = 4.2 and 11.4 Hz, H-2'), 3.87-3.95 (1H, m, H-1'), 4.99 (1H, br s, OH), 6.20 (1H, d, *J* = 6.3 Hz, OH); ^{13}C NMR (125 MHz, DMSO-d_6) (ppm) δ 60.2 (q, *J* = 2.0 Hz, C-2'), 70.0 (q, *J* = 27.9 Hz, C-1'), 125.0 (q, *J* = 283 Hz, CF_3); ^{19}F NMR (470 MHz, DMSO-d_6) (ppm) δ -76.07.

3-((*tert*-Butyldiphenylsilyl)oxy)-1,1,1-trifluoropropan-2-ol (297)

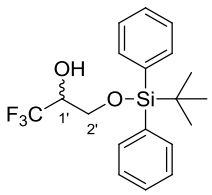

Imidazole (157 mg, 2.31 mmol) and *tert*-butyldiphenylsilyl chloride (0.2 mL, 0.77 mmol) were added to a solution of 3,3,3-trifluoropropane-1,2-diol **296** (100 mg, 0.77 mmol) in dry DCM (5 mL) at 0 °C. The reaction was stirred for 1 h and water (10 mL) was added. The organic phase was extracted with DCM (3 x 10 mL) and dried over $MgSO_4$. Then the solvent was removed *in vacuo*. The product was purified by MPC on silica (petrol: EtOAc 9:1) to give the product **297** as a colourless oil (211 mg, 0.57 mmol, 75%).

R_f 0.48 (petrol: EtOAc 9: 1); UV λ_{max} (EtOH) 265 nm; IR (cm^{-1}) 3512, 2933, 2859, 1143, 1109; ^{1}H NMR (500 MHz, DMSO-*d*$_6$) (ppm) δ 1.00 (9H, s, ^{t}Bu), 3.72 (1H, dd, *J* = 5.5 and 10.9 Hz, H-2'), 3.77 (1H, dd, *J* = 5.3 and 10.9 Hz, H-2'), 4.09-4.12 (1H, m, H-1'), 6.40 (1H, d, *J* = 6.2 Hz, OH), 7.43-7.49 (6H, m, H-ar), 7.63-7.65 (4H, m, H-ar); ^{13}C NMR (125 MHz, DMSO-*d*$_6$) (ppm) δ 26.4 (^{t}Bu), 62.7 (C-2'), 69.4 (q, *J* = 28.6 Hz, C-1'), 124.5 (q, *J* = 283.8 Hz, CF_3), 127.9 (C-ar), 130.0 (C-ar), 132.5 (C-ar), 135.1 (C-ar); ^{19}F NMR (470 MHz, DMSO-*d*$_6$) (ppm) δ -75.6; HRMS calcd for $C_{19}H_{22}F_3O_2Si$ $[M-H]^-$ 367.1347, found 367.1339.

3-(Benzyloxy)-1,1,1-trifluoropropan-2-ol (304)[271]

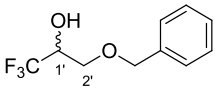

3,3,3-Trifluoro-1,2-propenoxide **306** (1.50 mL, 17.9 mmol) was added to a stirred solution of benzyl acohol **305** (1.85 mL, 17.9 mmol) and boron trifluoride diethyletherate (44.00 μL, 0.36 mmol), under N_2. The reaction mixture was then heated at 40 ^{o}C for 18 h. The reaction was diluted with DCM (50 mL) and washed with brine (2 x 50 mL). The organic phase was dried over $MgSO_4$ and the solvent was removed *in vacuo*. The product was purified by MPC on silica (petrol: EtOAc 9: 1) to give the product **304** as a yellow liquid (3.11 g, 13.95 mmol, 85%).

R_f 0.60 (petrol: EtOAc 4: 1); UV λ_{max} (EtOH) 258 nm; IR (cm^{-1}) 3425, 1453, 1270, 1121; ^{1}H NMR (500 MHz, DMSO-*d*$_6$) (ppm) δ 3.55 (1H, dd, *J* = 6.5 and 10.5 Hz, H-2'), 3.65 (1H, dd, *J* = 4.4 and 10.5 Hz, H-2'), 4.17-4.25 (1H, m, H-1'), 4.56 (2H, s, CH_2), 6.43 (1H, d, *J* = 6.6 Hz, OH), 7.29-7.33 (1H, m, H-ar), 7.34-7.38 (4H, m, H-ar); ^{13}C NMR (125 MHz, DMSO-*d*$_6$) (ppm) δ 68.00 (q, *J* = 29.0 Hz, C-1'), 68.5 (q, *J* = 1.8 Hz, C-2'), 72.4 (CH_2), 125.00 (q, *J* = 283.4 Hz, CF_3), 127.5 (C-ar), 127.6 (2 x C-ar), 128.2 (2 x C-ar), 137.9 (C_q); ^{19}F NMR (470 MHz, DMSO-*d*$_6$) (ppm) δ -72.2; HRMS calcd for $C_{10}H_{10}F_3O_2$ $[M-H]^-$ 219.0627, found 219.1758.

3-(Benzyloxy)-1,1,1-trifluoropropan-2-yl 4-methylbenzenesulfonate (308)

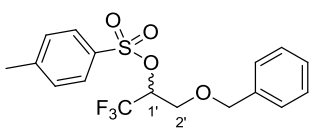

Tosyl chloride (278 mg, 1.46 mmol) was added to a stirred solution of 3-(benzyloxy)-1,1,1-trifluoropropan-2-ol **304** (200 mg, 0.97 mmol) and Et_3N (0.20 mL, 1.46 mmol) in

dry DCM (5 mL) under N_2. The resulting solution was stirred at r.t. for 1 h. The solvent was removed *in vacuo*. The product was purified by MPC on silica (petrol: EtOAc 9: 1) to give the product **308** as a colourless oil (219 mg, 0.59 mmol, 60%).

R_f 0.69 (petrol: EtOAc 4: 1); UV λ_{max} (EtOH) 263 nm; IR (cm^{-1}) 2923, 1597 , 1453, 1274, 1176, 1059; ^{1}H NMR (500 MHz, DMSO-d_6) (ppm) δ 2.40 (3H, s, CH_3), 3.68 (2H, s, CH_2), 4.41 (1H, dd, *J* = 12.0 and 12.0 Hz, H-2'), 4.45 (1H, dd, *J* = 12.0 and 12.0 Hz, H-2'), 5.50-5.56 (1H, m, H-1'), 7.20 (2H, d, *J* = 6.9 Hz, H-ar), 7.30-7.36 (3H, m, H-ar), 7.44 (2H, d, *J* = 8.9 Hz, H-tosyl), 7.85 (2H, d, *J* = 8.9 Hz, H-tosyl); ^{13}C NMR (125 MHz, DMSO-d_6) (ppm) δ 21.1 (CH_3), 65.6 (C-2'), 72.3 (CH_2), 75.1 (q, *J* = 31.6 Hz, C-1'), 122.00 (q, *J* = 281.9 Hz, CF_3), 127.5 (2 x C-ar), 127.6 (C-ar), 127.8 (2 x C-tosyl), 128.2 (2 x C-ar), 130.1 (2 x C-tosyl), 132.4 (C_q), 137.2 (C_q), 137.9 (C_q); ^{19}F NMR (470 MHz, DMSO-d_6) (ppm) δ -73.2; HRMS calcd for $C_{17}H_{16}F_3O_4S$ $[M-H]^-$ 373.0716, found 373.0717.

1-Nitro-4-((2,2,2-trifluoroethyl)sulfonyl)benzene (313)

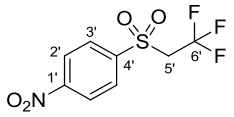

The title compound was synthesised following **general procedure M** using (4-nitrophenyl)(2,2,2-trifluoroethyl)sulfane **314** (1.10 g, 4.67 mmol) and *m*-CPBA (2.07 g, 9.28 mmol). The crude product was purified by MPC on silica (petrol: EtOAc 17: 3) to give the product **313** as a pale yellow solid (0.79 g, 2.94 mmol, 63%).

R_f 0.65 (petrol: EtOAc 17: 3); UV λ_{max} (EtOH) 247 nm; Mp = 96-97 ^{o}C; IR (cm^{-1}) 2995, 1536, 1344, 1259; ^{1}H NMR (500 MHz, DMSO-d_6) (ppm) δ 5.20 (2H, q, *J* = 10.1 Hz, H-5'), 8.26 (2H, d, *J* = 8.9 Hz, H-3'), 8.52 (2H, d, *J* = 8.9 Hz, H-2'); ^{13}C NMR (125 MHz, DMSO-d_6) (ppm) δ 55.7 (q, *J* = 29.9 Hz, C-5'), 124.5 (C-2'), 129.6 (C-3'), 131.0 (q, *J* = 256.2 Hz, CF_3), 143.8 (C-4'), 150.8 (C-1'); ^{19}F NMR (470 MHz, DMSO-d_6) (ppm) δ -59.7 (t, *J* = 10.1 Hz); HRMS calcd for $C_8H_7F_3NO_4S$ $[M+H]^+$ 270.0042, found 270.0037.

(4-Nitrophenyl)(2,2,2-trifluoroethyl)sulfane (314)

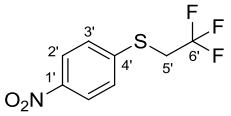

1,1,1-Trifluoro-2-iodoethane (0.95 mL, 9.68 mmol) was added to a stirred solution of 4-nitrothiophenol **173** (1.00 g, 6.45 mmol), K_2CO_3 (2.67 g, 19.4 mmol) and Rongalit (0.90 g, 5.81 mmol) in anhydrous DMF (7 mL) under N_2. The resulting solution was stirred at r.t. for 18 h. After completion, brine (20 mL) was added and the organic phase was extracted with EtOAc (3 x 20 mL). The organic layers were combined and dried over $MgSO_4$. The solvent was removed *in vacuo* and the crude product was purified by MPC on silica (petrol: EtOAc 19: 1) to give the product **314** as a yellow oil (0.95 g, 4.01 mmol, 62%).

R_f 0.68 (petrol: EtOAc 9: 1); UV λ_{max} (EtOH) 317 nm; IR (cm^{-1}) 1512, 1338, 1070; ^1H NMR (500 MHz, DMSO-d_6) (ppm) δ 4.30 (2H, q, J = 10.3 Hz, H-5'), 7.73 (2H, d, J = 9.0 Hz, H-3'), 8.19 (2H, d, J = 9.0 Hz, H-2'); ^{13}C NMR (125 MHz, DMSO-d_6) (ppm) δ 32.5 (q, J = 32.2 Hz, C-5'), 124.0 (C-2'), 125.0 (q, J = 276.8 Hz, CF_3), 127.6 (C-3'), 143.6 (C-4'), 145.5 (C-1'); ^{19}F NMR (470 MHz, DMSO-d_6) (ppm) δ -64.7 (t, J = 10.3 Hz); HRMS calcd for $C_8H_7F_3NO_2S$ $[M+H]^+$ 238.0144, found 238.0142.

1-((4-Nitrophenyl)thio)propan-2-one (318)[272]

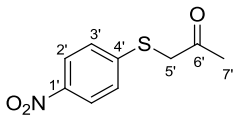

The title compound was synthesised following **general procedure J** using chloroacetate **317** (0.20 mL, 2.93 mmol), 4-nitrothiophenol **173** (500 mg, 3.23 mmol) and Et_3N (0.50 mL, 3.55 mmol). The crude product was purified by MPC on silica (DCM: MeOH 19: 1) to give the product **318** as a yellow solid (615 mg, 2.91 mmol, 98%).

R_f 0.52 (EtOAc: petrol 2: 3); Mp = 65-67 ^oC (lit., [263] Mp = 68-69 °C); UV λ_{max} (EtOH) 334 nm; IR (cm^{-1}) 2910, 2860, 1709, 1576, 1498, 1328; ^1H NMR (500 MHz, DMSO-d_6) (ppm) δ 2.27 (3H, s, H-7'), 4.30 (2H, s, H-5'), 7.46 (2H, d, J = 9.0 Hz, H-3'), 8.13 (2H, d, J = 9.0 Hz, H-2'); ^{13}C NMR (125 MHz, DMSO-d_6) (ppm) δ 28.6 (H-7'), 41.9 (H-5'), 123.8 (C-2'), 126.3 (C-3'), 144.5 (C-4'), 146.6 (C-1'), 202.1 (CO); HRMS calcd for $C_9H_8NO_3S$ $[M-H]^-$ 210.0230, found 210.0227.

1-(1-((4-Nitrophenyl)thio)propan-2-yl)pyrrolidine (319)

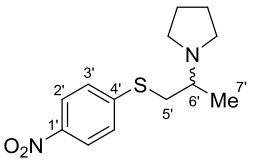

1-((4-Nitrophenyl)thio)propan-2-one **318** (615 mg, 2.91 mmol) was dissolved in anhydrous toluene (15 mL) under N_2. Acetic acid (0.83 mL, 14.6 mmol) and $MgSO_4$ (1,04 g, 8.73 mmol) were added to the reaction, then pyrrolidine (0.87 mL, 10.5 mmol) and the reaction was stirred at r.t. for 2 h. Sodium triacetoxyborohydride (250 mg, 6.41 mmol) was added and the reaction was stirred at r.t. overnight. The reaction mixture was quenched with aqueous $NaHCO_3$ until reaching pH 7. The solution was then extracted with EtOAc (3 x 30 mL). The organic layer was dried over $MgSO_4$ and the solvent was removed *in vacuo*. The crude product was purified by MPC on silica (DCM: MeOH 9: 1) to give the product **319** as an orange oil (443 mg, 1.67 mmol, 57%).

R_f 0.38 (DCM: MeOH 9: 1); UV λ_{max} (EtOH) 333 nm; IR (cm^{-1}) 2966, 2792, 1576, 1508, 1334; ^{1}H NMR (500 MHz, DMSO-d_6) (ppm) δ 1.16 (3H, d, *J* = 6.4 Hz, H-7'), 1.67-1.70 (4H, m, H-pyr), 2.53-2.58 (4H, m, H-pyr), 2.71-2.77 (1H, m, H-6'), 3.18 (1H, dd, *J* = 11.9 and 4.3 Hz, H-5'), 3.30 (1H, dd, *J* = 11.9 and 5.7 Hz, H-5'), 7.50 (2H, d, *J* = 9.0 Hz, H-3'), 8.12 (2H, d, *J* = 9.0 Hz, H-2'); ^{13}C NMR (125 MHz, DMSO-d_6) (ppm) δ 17.1 (C-7'), 23.2 (2 x C-pyr), 37.3 (C-5'), 50.0 (2 x C-pyr), 56.2 (C-6'), 123.8 (C-2'), 126.2 (C-3'), 144.1 (C-4'), 148.8 (C-1'); HRMS calcd for $C_{13}H_{19}N_2O_2S$ $[M+H]^+$ 267.1162, found 267.1166.

4-((2-(Pyrrolidin-1-yl)propyl)thio)aniline (320)

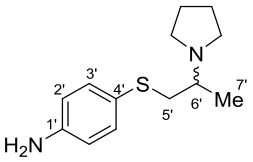

The title compound was synthesised following **general procedure H** using 1-(1-((4-nitrophenyl)thio)propan-2-yl)pyrrolidine **319** (440 mg, 1.66 mmol) and zinc powder (1.08 g, 16.6 mmol). The crude product was purified by MPC on silica (DCM: MeOH 9: 1) to give the product **320** as a yellow oil (250 mg, 1.06 mmol, 64%).

R_f 0.26 (DCM: MeOH 9: 1); UV λ_{max} (EtOH) 254 nm; IR (cm^{-1}) 3146, 2948, 1509, 1389, 1248; ^{1}H NMR (500 MHz, DMSO-d_6) (ppm) δ 1.12 (3H, d, *J* = 6.4 Hz, H-7'), 1.62-1.65

(4H, m, H-pyr), 2.44-2.49 (4H, m, H-pyr), 2.48-2.51 (1H, m, H-6'), 2.64 (1H, dd, *J* = 12.7 and 8.2 Hz, H-5'), 2.98 (1H, dd, *J* = 12.7 and 3.4 Hz, H-5'), 5.20 (2H, br s, NH_2), 6.51 (2H, d, *J* = 8.6 Hz, H-2'), 7.09 (2H, d, *J* = 8.6 Hz, H-3'); ^{13}C NMR (125 MHz, DMSO-d_6) (ppm) δ 17.0 (C-7'), 23.1 (2 x C-pyr), 41.6 (C-5'), 50.0 (2 x C-pyr), 57.4 (C-6'), 114.4 (C-2'), 119.8 (C-4'), 133.2 (C-3'), 148.1 (C-1'); HRMS calcd for $C_{13}H_{21}N_2S$ $[M+H]^+$ 237.1420, found 237.1422.

6-(Cyclohexylmethoxy)-*N*-(4-((2-(pyrrolidin-1-yl)propyl)thio)phenyl)-9*H*-purin-2-amine (321)

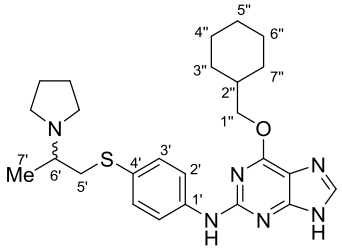

The title compound was synthesised following **general procedure I** using 6-(cyclohexylmethoxy)-2-iodo-9-(4-methoxybenzyl)-9*H*-purine **171** (518 mg, 1.08 mmol), 4-((2-(pyrrolidin-1-yl)propan-2-yl)thio)aniline **320** (280 mg, 1.19 mmol), K_2CO_3 (311 mg, 2.17 mmol), $Pd(dba)_2$ (20 mg, 0.02 mmol) and XPhos (10 mg, 0.02 mmol). The crude mixture was then filtered through Celite and the solvent was removed *in vacuo*. The crude mixture was then solubilised in TFA (15 mL). The resulting solution was heated at 70 °C for 5 h. Then the solvent was removed *in vacuo*. The product was purified by MPC (DCM: MeOH 9: 1) to give the product **321** as an orange oil (255 mg, 0.55 mmol, 50%).

R_f 0.33 (DCM: MeOH 9: 1); UV λ_{max} (EtOH) 268 nm; IR (cm^{-1}) 3152, 2926, 2853, 1668, 1494, 1424, 1176, 1125; ^{1}H NMR (500 MHz, DMSO-d_6) (ppm) δ 1.06-1.13 (2H, m, H-cyclo), 1.17-1.21 (1H, m, H-cyclo), 1.24-1.29 (2H, m, H-cyclo), 1.36 (3H, d, *J* = 6.7 Hz, H-7'), 1.66-1.69 (1H, m, H-cyclo), 1.73-1.75 (2H, m, H-cyclo), 1.84-1.86 (5H, m, H-cyclo, H-pyr and H-2''), 1.95-2.00 (2H, m, H-pyr), 2.96-3.05 (2H, m, H-pyr and H-5'), 3.10-3.14 (1H, m, H-pyr), 3.36-3.40 (1H, m, H-6'), 3.42-3.48 (2H, m, H-pyr and H-5'), 3.54-3.58 (1H, m, H-pyr), 4.34 (2H, d, *J* = 6.3 Hz, H-1''), 7.41 (2H, d, *J* = 8.8 Hz, H-2'), 7.87 (2H, d, *J* = 8.8 Hz, H-3'), 8.14 (1H, s, H-8), 9.50 (1H, br s, NH), 9.82 (1H, br s, N^9H); ^{13}C NMR (125 MHz, DMSO-d_6) (ppm) δ 14.8 (C-7'), 22.7 (C-pyr), 22.8 (C-pyr), 25.2 (2 x C-cyclo), 26.0 (C-cyclo), 29.2 (2 x C-cyclo), 36.5 (C-5'), 36.8 (C-2''), 50.5 (C-pyr), 51.1 (C-pyr), 59.0 (C-6'), 71.2 (C-1''), 118.9 (C-3'), 123.9 (C_q), 125.6 (C_q), 128.5

(C_q), 129.0 (C_q), 131.6 (C-2'), 140.8 (C-8), 142.8 (C_q), 155.2 (C_q); HRMS calcd for $C_{25}H_{35}N_6OS$ $[M+H]^+$ 467.2588, found 467.2582.

6-(Cyclohexylmethoxy)-*N*-(4-((2-(pyrrolidin-1-yl)propyl)sulfonyl)phenyl)-9*H*-purin-2-amine (322)

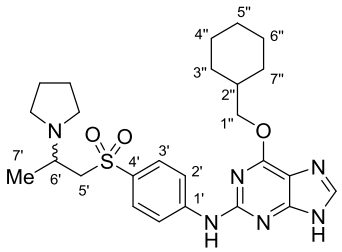

6-(Cyclohexylmethoxy)-*N*-(4-((2-(pyrrolidin-1-yl)propyl)thio)phenyl)-9*H*-purin-2-amine **321** (390 mg, 0.84 mmol) was solubilised in MeOH (10 mL). Oxone (642 mg, 2.09 mmol) in H_2O (5 mL) was added at 0°C and the resulting solution was stirred at r.t. for 18 h. Brine (10 mL) was added and the reaction was extracted with DCM (3 x 20 mL). The organic layer was dried over $MgSO_4$ and the solvent was removed *in vacuo*. The crude product was purified by MPC on silica (DCM: MeOH 9: 1) to give the product **322** as an orange oil (90 mg, 0.18 mmol, 38%).

R_f 0.28 (DCM: MeOH 9: 1); UV λ_{max} (EtOH) 314 nm; IR (cm^{-1}) 3324, 2930, 1631, 1588, 1404, 1143, 1088; ^{1}H NMR (500 MHz, MeOD) (ppm) δ 1.16-1.21 (2H, m, H-cyclo), 1.27-1.30 (1H, m, H-cyclo), 1.32-1.40 (2H, m, H-cyclo), 1.58 (3H, d, *J* = 6.7 Hz, H-7'), 1.73-1.76 (1H, m, H-cyclo), 1.80-1.83 (2H, m, H-cyclo), 1.94-1.96 (3H, m, H-cyclo, H-2''), 2.07-2.09 (2H, m, H-pyr), 3.17-3.23 (2H, m, H-pyr), 3.57-3.60 (2H, m, H-pyr), 3.62-3.67 (1H, m, H-5'), 3.83 (1H, dd, *J* = 14.6 Hz, *J* = 2.2 Hz, H-5'), 3.92-3.97 (1H, m, H-6'), 4.40 (2H, d, *J* = 6.1 Hz, H-1''), 7.88 (2H, d, *J* = 8.8 Hz, H-3'), 8.13 (2H, d, *J* = 8.8 Hz, H-2'), 8.16 (1H, s, H-8); ^{13}C NMR (125 MHz, MeOD) (ppm) δ 17.5 (C-7'), 24.2 (2 x C-pyr), 26.9 (2 x C-cyclo), 27.5 (C-cyclo), 30.9 (2 x C-cyclo), 38.7 (C-2''), 52.7 (2 x C-pyr), 56.8 (C-6'), 58.3 (C-5'), 73.4 (C-1''), 114.5 (C_q), 118.9 (C-2'), 130.4 (C-3'), 130.6 (C_q), 131.4 (C_q), 141.5 (C_q), 148.4 (C-8), 156.7 (C_q), 161.2 (C_q); HRMS calcd for $C_{25}H_{35}N_6O_3S$ $[M+H]^+$ 499.2485, found 499.2486.

(*E*)-6-(Cyclohexylmethoxy)-*N*-(4-(prop-1-en-1-ylsulfonyl)phenyl)-9*H*-purin-2-amine (323)

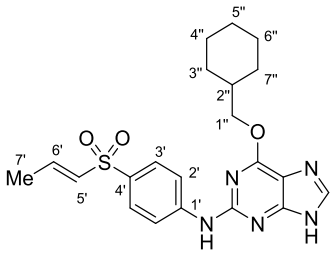

The title compound was synthesised following **general procedure N** using 6-(cyclohexylmethoxy)-*N*-(4-((2-(pyrrolidin-1-yl)propyl)sulfonyl)phenyl)-9*H*-purin-2-amine **322** (80 mg, 0.16 mmol), *m*-CPBA (37 mg, 0.39 mmol) and Cs_2CO_3 (130 mg, 0.40 mmol). The crude product was purified by MPC (DCM: MeOH 19: 1) to give the product **323** as an orange oil (10 mg, 0.02 mmol, 15%).

R_f 0.21 (DCM: MeOH 9: 1); UV λ_{max} (EtOH) 314 nm; IR (cm^{-1}) 3231, 2925, 2852, 1594, 1451, 1387, 1136; ^{1}H NMR (500 MHz, MeOD) (ppm) δ 1.01-1.09 (2H, m, H-cyclo), 1.16-1.18 (1H, m, H-cyclo), 1.19-1.28 (2H, m, H-cyclo), 1.60-1.63 (1H, m, H-cyclo), 1.68-1.70 (2H, m, H-cyclo), 1.81 (3H, d, *J* = 6.9 Hz, *J* = 1.7 Hz, H-7'), 1.82-1.84 (3H, m, H-cyclo, H-2''), 4.27 (2H, d, *J* = 6.1 Hz, H-1''), 6.44 (1H, dd, *J* = 14.9 Hz, *J* = 1.7 Hz, H-5'), 6.77-6.84 (1H, m, H-6'), 7.63 (2H, d, *J* = 9.0 Hz, H-2'), 7.92 (1H, s, H-8), 7.93 (2H, d, *J* = 9.0 Hz, H-3'); ^{13}C NMR (125 MHz, MeOD) (ppm) δ ppm 17.2 (C-7'), 26.9 (2 x C-cyclo), 27.6 (C-cyclo), 30.8 (2 x C-cyclo), 38.7 (C-2''), 73.2 (C-1''), 119.0 (C-3'), 129.3 (C_q), 129.6 (C-2'), 132.6 (C_q), 132.9 (C_q), 133.6 (C-5'), 140.4 (C_q), 142.7 (C-6'), 147.4 (C-8), 156.8 (C_q), 162.1 (C_q); HRMS calcd for $C_{21}H_{26}N_5O_3S$ $[M+H]^+$ 428.1751, found 428.1757.

1-((4-Nitrophenyl)sulfonyl)propan-2-one (324)

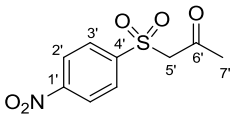

The title compound was synthesised following **general procedure M** using 1-((4-nitrophenyl)thio)propan-2-one **318** (1.47 g, 6.97 mmol) and *m*-CPBA (3.24 g, 13.93 mmol). The crude product was purified by MPC on silica (petrol: EtOAc 3: 2) to give the product **324** as a white solid (1.24 g, 5.10 mmol, 73%).

R_f 0.42 (petrol: EtOAc 3: 2); Mp = 114-116 °C (lit.,[265] Mp = 118 °C); UV λ_{max} (EtOH) 248 nm; IR (cm^{-1}) 2965, 2919, 1717, 1521, 1346, 1295, 1144; ^{1}H NMR (500 MHz, DMSO-d_6) (ppm) δ 2.22 (3H, s, H-7'), 4.97 (2H, s, H-5'), 8.20 (2H, d, *J* = 8.9 Hz, H-3'), 8.47 (2H, d, *J* = 8.9 Hz, H-2'); ^{13}C NMR (125 MHz, DMSO-d_6) (ppm) δ 31.0 (C-7'), 65.1 (C-5'), 124.5 (C-2'), 129.9 (C-3'), 144.4 (C-4'), 150.6 (C-1'), 197.4 (CO); HRMS calcd for $C_9H_8NO_5S$ $[M-H]^-$ 242.0129, found 242.0127.

1-((4-Nitrophenyl)sulfonyl)propan-2-ol (325)

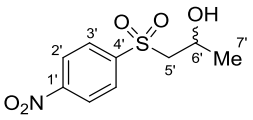

The title compound was synthesised following **general procedure O** using 1-((4-nitrophenyl)sulfonyl)propan-2-one **326** (1.24 g, 5.10 mmol) and Dibal (1M in hexanes, 7.7 mL). The crude product was purified by MPC on silica (petrol: EtOAc 3: 2) to give the product **325** as a pale yellow oil (1.15 g, 4.69 mmol, 92%).

R_f 0.48 (petrol: EtOAc 1: 1); UV λ_{max} (EtOH) 251 nm; IR (cm^{-1}) 3390, 2977, 2928, 1529, 1346, 1292, 1140, 1081; ^{1}H NMR (500 MHz, DMSO-d_6) (ppm) δ 1.14 (3H, d, *J* = 6.3 Hz, H-7'), 3.51 (1H, dd, *J* = 4.4 and 14.6 Hz, H-5'), 3.56 (1H, dd, *J* = 7.5 and 14.6 Hz, H-5'), 4.06-4.10 (1H, m, H-6'), 4.81 (1H, br s, OH), 8.18 (2H, d, *J* = 9.0 Hz, H-3'), 8.44 (2H, d, *J* = 9.0 Hz, H-2'); ^{13}C NMR (125 MHz, DMSO-d_6) (ppm) δ 23.3 (C-7'), 61.8 (C-6'), 62.4 (C-5'), 124.2 (C-2'), 129.5 (C-3'), 146.1 (C-4'), 150.2 (C-1'); HRMS calcd for $C_9H_{10}NO_5S$ $[M-H]^-$ 244.0285, found 244.0285.

1-((4-Aminophenyl)sulfonyl)propan-2-ol (326)

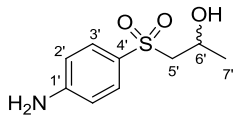

The title compound was synthesised following **general procedure H** using 1-((4-nitrophenyl)sulfonyl)propan-2-ol **325** (1.15 g, 4.69 mmol) and zinc powder (3.05 g, 46.9 mmol). The crude product was purified by MPC on amine silica (DCM: MeOH 19: 1) to give the product **326** as a pale orange solid (845 mg, 3.93 mmol, 84%).

R_f 0.67 (DCM: MeOH 9: 1); Mp = 110-112 ^{o}C; UV λ_{max} (EtOH) 271 nm; IR (cm^{-1}) 3481, 3376, 2967, 2924, 1627, 1594, 1274, 1121; ^{1}H NMR (500 MHz, DMSO-d_6) (ppm) δ 1.12 (3H, d, *J* = 6.3 Hz, H-7'), 3.13 (1H, dd, *J* = 6.1 and 14.1 Hz, H-5'), 3.19 (1H, dd, *J* = 5.7

and 14.1 Hz, H-5'), 3.89-3.96 (1H, m, H-6'), 4.82 (1H, br s, OH), 6.11 (2H, br s, NH_2), 6.64 (2H, d, *J* = 8.8 Hz, H-3'), 7.48 (2H, d, *J* = 8.8 Hz, H-2'); ^{13}C NMR (125 MHz, DMSO-d_6) (ppm) δ 23.4 (C-7'), 61.7 (C-6'), 63.8 (C-5'), 112.6 (C-2'), 124.7 (C-4'), 129.5 (C-3'), 153.5 (C-1'); HRMS calcd for $C_9H_{14}NO_3S$ $[M+H]^+$ 216.0689, found 216.0688.

1-((4-((6-(Cyclohexylmethoxy)-9*H*-purin-2-yl)amino)phenyl)sulfonyl)propan-2-ol (327)

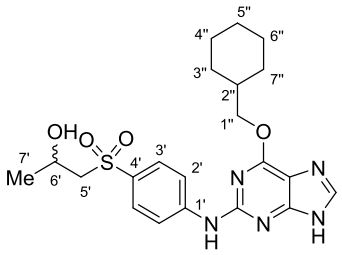

The title compound was synthesised following **general procedure I** using 6-(cyclohexylmethoxy)-2-iodo-9-(4-methoxybenzyl)-9*H*-purine **171** (300 mg, 0.63 mmol), 1-((4-aminophenyl)sulfonyl)propan-2-ol **326** (202 mg, 0.94 mmol), K_2CO_3 (173 mg, 1.26 mmol), $Pd(dba)_2$ (12 mg, 0.01 mmol) and XPhos (6 mg, 0.01 mmol). The crude mixture was then filtered through Celite and the solvent was removed *in vacuo*. The crude mixture was then solubilised in TFA (15 mL). The resulting solution was heated at 70 °C for 2 h. Then the solvent was removed *in vacuo*. The product was purified by MPC on silica (EtOAc 100) to give the product **327** as a pale yellow oil (86 mg, 0.19 mmol, 31%).

R_f 0.37 (EtOAc 100); UV λ_{max} (EtOH) 313 nm; IR (cm^{-1}) 3280, 3112, 2925, 2851, 1594, 1391, 1292, 1130; ^{1}H NMR (500 MHz, DMSO-d_6) (ppm) δ 1.07-1.12 (2H, m, H-cyclo), 1.14 (3H, d, *J* = 6.3 Hz, H-7'), 1.19-1.21 (1H, m, H-cyclo), 1.24-1.32 (2H, m, H-cyclo), 1.66-1.69 (1H, m, H-cyclo), 1.73-1.76 (2H, m, H-cyclo), 1.84-1.90 (3H, m, H-cyclo and H-2''), 3.27 (1H, dd, *J* = 5.6 and 14.3 Hz, H-5'), 3.31 (1H, dd, *J* = 8.3 and 14.3 Hz, H-5'), 3.97-4.02 (1H, m, H-6'), 4.37 (2H, d, *J* = 6.3 Hz, H-1''), 4.88 (1H, d, *J* = 5.3 Hz, OH), 7.77 (2H, d, *J* = 8.8 Hz, H-3'), 8.05 (2H, d, *J* = 8.8 Hz, H-2'), 8.07 (1H, br s, H-8), 9.93 (1H, br s, NH), 12.98 (1H, br s, N^9H); ^{13}C NMR (125 MHz, DMSO-d_6) (ppm) δ 23.4 (C-7'), 25.2 (2 x C-cyclo), 26.0 (C-cyclo), 29.2 (2 x C-cyclo), 36.8 (C-2''), 61.7 (C-6'), 63.4 (C-5'), 71.3 (C-1''), 115.5 (C_q), 117.3 (C-2'), 128.7 (C-3'), 130.8 (C_q), 139.7 (C_q), 145.8 (C_q), 153.9 (C_q), 154.5 (C_q), 160.2 (C_q); HRMS calcd for $C_{21}H_{28}N_5O_4S$ $[M+H]^+$ 446.1857, found 446.1854.

3-((4-Nitrophenyl)thio)butan-2-one (328)

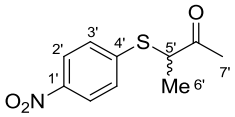

The title compound was synthesised following **general procedure J** using 3-chloro-2-butanone (2.14 mL, 21.3 mmol), 4-nitrothiophenol **173** (3.00 g, 19.4 mmol) and Et_3N (2.96 mL, 21.3 mmol). The crude product was purified by MPC on silica (petrol: EtOAc 9: 1) to give the product **328** as a yellow oil (3.86 g, 17.23 mmol, 89%).

R_f 0.48 (petrol: EtOAc 9: 1); UV λ_{max} (EtOH) 330 nm; IR (cm^{-1}) 2979, 2925, 1710, 1576, 1509, 1334; ^{1}H NMR (500 MHz, DMSO-d_6) (ppm) δ 1.43 (3H, d, *J* = 7.1 Hz, H-6'), 2.26 (3H, s, H-7'), 4.46 (1H, q, *J* = 7.1 Hz, H-5'), 7.55 (2H, d, *J* = 8.6 Hz, H-3'), 8.15 (2H, d, *J* = 8.6 Hz, H-2'); ^{13}C NMR (125 MHz, DMSO-d_6) (ppm) δ 16.0 (C-6'), 26.6 (C-7'), 49.7 (C-5'), 124.0 (C-2'), 128.5 (C-3'), 144.5 (C-4'), 145.4 (C-1'), 204.9 (CO); HRMS calcd for $C_{10}H_{10}NO_3S$ $[M-H]^-$ 224.0387, found 224.0388.

3-((4-Nitrophenyl)sulfonyl)butan-2-one (329)

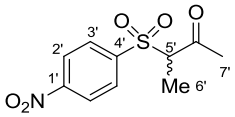

The title compound was synthesised following **general procedure M** using 3-((4-nitrophenyl)thio)butan-2-one **328** (3.86 g, 17.3 mmol) and *m*-CPBA (8.00 g, 34.5 mmol). The crude product was purified by MPC on silica (petrol: EtOAc 7: 3) to give the product **329** as a pale yellow solid (4.07 g, 15.9 mmol, 92%).

R_f 0.36 (petrol: EtOAc 7: 3); Mp = 144-145 °C (lit.,[265] Mp = 47-49 °C); UV λ_{max} (EtOH) 248 nm; IR (cm^{-1}) 2932, 1715, 1527, 1532, 1304, 1232, 1167; ^{1}H NMR (500 MHz, $CDCl_3$) (ppm) δ 1.45 (3H, d, *J* = 7.1 Hz, H-6'), 2.47 (3H, s, H-7'), 4.24 (1H, q, *J* = 7.1 Hz, H-5'), 8.00 (2H, d, *J* = 8.9 Hz, H-3'), 8.40 (2H, d, *J* = 8.9 Hz, H-2'); ^{13}C NMR (125 MHz, $CDCl_3$) (ppm) δ 11.9 (C-6'), 31.0 (C-7'), 70.6 (C-5'), 124.2 (C-2'), 131.0 (C-3'), 141.5 (C-4'), 151.2 (C-1'), 199.8 (CO); HRMS calcd for $C_{10}H_{10}NO_5S$ $[M-H]^-$ 256.0285, found 256.0284.

3-((4-Nitrophenyl)sulfonyl)butan-2-ol (330)

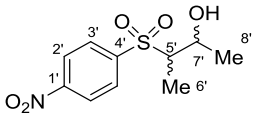

The title compound was synthesised following **general procedure O** using 3-((4-nitrophenyl)sulfonyl)butan-2-one **329** (2.00 g, 7.81 mmol) and DIBAL (1M in hexanes, 11.72 mL). The crude product was purified by MPC on silica (petrol: EtOAc 7: 3) to give the product **330** as a pale yellow oil (2.02 g, 7.80 mmol, 99%).

R_f 0.23 (petrol: EtOAc 7: 3); UV λ_{max} (EtOH) 252 nm; IR (cm^{-1}) 3510, 2981, 2939, 1527, 1349, 1293, 1143; ^{1}H NMR (500 MHz, DMSO-d_6) (ppm) δ 1.10 (0.75H, d, *J* = 6.5 Hz, H-8'), 1.13 (2.25H, d, *J* = 6.5 Hz, H-8'), 1.18 (0.75H, d, *J* = 7.1 Hz, H-6'), 1.20 (2.25H, d, *J* = 7.1 Hz, H-6'), 3.39 (0.25H, qd, *J* = 2.3 and 7.1 Hz, H-5'), 3.50 (0.75H, qd, *J* = 5.4 and 7.1 Hz, H-5'), 4.02 (0.75H, m, H-7'), 4.33 (0.25H, m, H-7'), 4.96 (1H, br s, OH), 8.14 (2H, d, *J* = 8.9 Hz, H-3'), 8.43 (2H, d, *J* = 8.9 Hz, H-2'); ^{13}C NMR (125 MHz, DMSO-d_6) (ppm) δ 7.3 (C-8'), 7.9 (C-8'), 19.3 (C-6'), 21.6 (C-6'), 63.0 (C-7'), 64.3 (C-7'), 64.5 (C-5'), 65.1 (C-5'), 124.0 (C-2'), 124.3 (C-2'), 129.9 (C-3'), 130.7 (C-3'), 144.0 (C-4'), 145.2 (C-4'), 150.3 (C-1'), 150.4 (C-1'); HRMS calcd for $C_{10}H_{12}NO_5S$ $[M-H]^-$ 258.0431, found 258.0443.

Note: A mixture of diastereoisomers was obtained with a ratio of 3:1.

3-((4-Aminophenyl)sulfonyl)butan-2-ol (331)

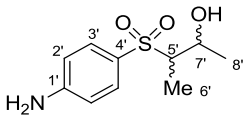

The title compound was synthesised following **general procedure H** using 3-((4-nitrophenyl)sulfonyl)butan-2-ol **330** (2.02 g, 7.72 mmol) and zinc powder (5.01 g, 77.2 mmol). The crude product was purified by MPC on silica (DCM: MeOH 19: 1) to give the product **331** as an orange solid (1.39 g, 6.07 mmol, 78%).

R_f 0.75 (DCM: MeOH 9: 1); UV λ_{max} (EtOH) 270 nm; IR (cm^{-1}) 3446, 3336, 2979, 1590, 1269, 1116; ^{1}H NMR (500 MHz, DMSO-d_6) (ppm) δ 1.05 (3H, d, *J* = 6.4 Hz, H-8'), 1.09 (3H, d, *J* = 7.1 Hz, H-6'), 2.94 (0.2H, qd, *J* = 2.9 and 7.1 Hz, H-5'), 3.11 (0.8H, qd, *J* = 3.4 and 7.1 Hz, H-5'), 4.03-4.08 (0.8H, m, H-7'), 4.13-4.18 (0.2H, m, H-7'), 4.54 (0.8H, d, *J* = 5.6 Hz, OH), 4.86 (0.2H, q, *J* = 4.7 Hz, OH), 6.08 (0.4H, s, NH_2), 6.14 (1.6H, s,

NH_2), 6.62 (0.4H, d, *J* = 8.8 Hz, H-3'), 6.65 (1.6H, d, *J* = 8.8 Hz, H-3'), 7.42 (2H, d, *J* = 8.8 Hz, H-2'); ^{13}C NMR (125 MHz, DMSO-d_6) (ppm) δ 7.1 (C-8'), 7.8 (C-8'), 17.8 (C-6'), 22.2 (C-6'), 63.1 (C-7'), 63.3 (C-7'), 64.4 (C-5'), 65.0 (C-5'), 112.5 (C-3'), 112.7 (C-3'), 122.6 (C-4'), 122.7 (C-4'), 130.1 (C-2'), 130.5 (C-2'), 153.4 (C-1'), 153.6 (C-1'); HRMS calcd for $C_{10}H_{16}NO_3S$ $[M+H]^+$ 230.0845, found 230.0843.

Note: A mixture of diastereoisomers was obtained with a ratio of 4:1.

3-((4-((6-(Cyclohexylmethoxy)-9*H*-purin-2-yl)amino)phenyl)sulfonyl)butan-2-ol (332)

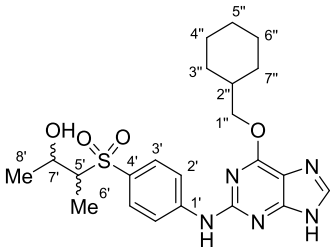

The title compound was synthesised following **general procedure I** using 6-(cyclohexylmethoxy)-2-iodo-9-(4-methoxybenzyl)-9*H*-purine **171** (500 mg, 1.05 mmol), 3-((4-aminophenyl)sulfonyl)butan-2-ol **331** (360 mg, 1.57 mmol), K_2CO_3 (289 mg, 2.09 mmol), $Pd(dba)_2$ (19 mg, 0.02 mmol) and XPhos (10 mg, 0.02 mmol). The crude mixture was then filtered through Celite and the solvent was removed *in vacuo*. The crude mixture was then solubilised in TFA (15 mL). The resulting solution was heated at 70 °C for 2 h and the solvent was removed *in vacuo*. The product was purified by MPC on silica (EtOAc 100) to give the product **332** as a yellow oil (442 mg, 0.96 mmol, 46%).

R_f 0.40 (DCM: MeOH 9: 1); UV λ_{max} (EtOH) 313 nm; IR (cm^{-1}) 3264, 3101, 2923, 1594, 1449, 1276, 1131; ^{1}H NMR (500 MHz, DMSO-d_6) (ppm) δ 1.09 (3H, d, *J* = 6.4 Hz, H-8'), 1.14 (3H, d, *J* = 7.1 Hz, H-6'), 1.10-1.12 (2H, m, H-cyclo), 1.18-1.20 (1H, m, H-cyclo), 1.23-1.31 (2H, m, H-cyclo), 1.65-1.67 (1H, m, H-cyclo), 1.72-1.74 (2H, m, H-cyclo), 1.83-1.88 (3H, m, H-cyclo and H-2''), 3.09 (0.1H, qd, *J* = 2.7 and 7.1 Hz, H-5'), 3.26 (0.9H, qd, *J* = 3.6 and 7.1 Hz, H-5'), 4.06-4.09 (0.9H, m, H-7'), 4.21-4.25 (0.1H, m, H-7'), 4.36 (2H, d, *J* = 6.3 Hz, H-1''), 4.66 (0.1H, d, *J* = 5.7 Hz, OH), 4.93 (0.9H, d, *J* = 4.9 Hz, OH), 7.72 (1.8H, d, *J* = 8.9 Hz, H-3'), 8.02 (0.2H, d, *J* = 8.9 Hz, H-3'), 8.04 (2.7H, m, H-2' and H-8), 8.10 (0.2H, d, *J* = 8.9 Hz, H-2'), 8.31 (0.1H, s, H-8), 9.91 (0.1H, s, NH), 9.95 (0.9H, s, NH), 12.97 (0.9H, br s, N^9H), 13.20 (0.1H, br s, N^9H); ^{13}C NMR (125 MHz, DMSO-d_6) (ppm) δ 7.2 (C-8'), 7.6 (C-8'), 18.0 (C-6'), 22.1 (C-6'), 25.2 (2 x C-cyclo), 26.0 (C-cyclo), 29.2 (2 x C-cyclo), 36.8 (C-2''), 63.1 (C-7'), 63.4 (C-7'), 64.3 (C-5'), 65.0 (C-5'), 71.4 (C-1''), 115.5 (C-2'), 117.2 (C-2'), 128.8 (C_q), 129.3 (C-3'), 129.7 (C-

3'), 139.7 (C-8), 146.0 (C_q), 153.9 (C_q), 154.4 (C_q), 160.2 (C_q); HRMS calcd for $C_{22}H_{30}N_5O_4S$ $[M+H]^+$ 460.2013, found 460.2004.

Note: A mixture of diastereoisomers was obtained with a ratio of 1:9. 1 quaternary carbon was not visible on the ^{13}C NMR spectrum.

_N_-(4-(But-2-en-2-ylsulfonyl)phenyl)-6-(cyclohexylmethoxy)-9_H_-purin-2-amine (333)

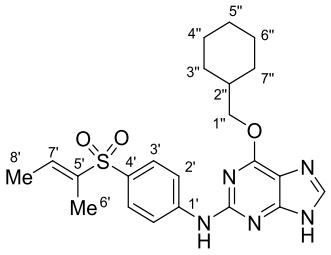

The title compound was synthesised following **general procedure P** using 3-((4-((6-(cyclohexylmethoxy)-9*H*-purin-2-yl)amino)phenyl)sulfonyl)butan-2-ol **332** (126 mg, 0.27 mmol), Et_3N (42.00 µL, 0.30 mmol) and MsCl (24.00 µL, 0.30 mmol). The crude product was purified by reverse phase (MeCN + 0.1% HCOOH: water + 0.1% HCOOH 60: 40) to give the product **333** as a colourless oil (20 mg, 0.05 mmol, 17%).

R_f 0.20 (MeCN + 0.1% HCOOH: water + 0.1% HCOOH 60: 40); UV λ_{max} (EtOH) 316 nm; IR (cm^{-1}) 3258, 2923, 1579, 1385, 1286, 1124; ^1H NMR (500 MHz, MeOD) (ppm) δ 1.13-1.20 (2H, m, H-cyclo), 1.26-1.28 (1H, m, H-cyclo), 1.31-1.38 (2H, m, H-cyclo), 1.72-1.74 (1H, m, H-cyclo), 1.79-1.82 (2H, m, H-cyclo), 1.83-1.84 (2H, m, H-6'), 1.85-1.86 (2H, m, H-8'), 1.93-1.94 (2H, m, H-cyclo), 1.95-1.96 (2H, m, H-2'' and H-6'), 2.12 (1H, qd, *J* = 2.9 and 7.5 Hz, H-8'), 4.39 (2H, d, *J* = 6.2 Hz, H-1''), 6.20 (0.33H, m, H-7'), 6.88-6.92 (0.66H, m, H-7'), 7.71 (1.33H, d, *J* = 8.9 Hz, H-3'), 7.77 (0.66H, d, *J* = 8.9 Hz, H-3'), 8.03-8.06 (3H, m, H-2', H-2', H-8 and H-8); ^{13}C NMR (125 MHz, MeOD) (ppm) δ 11.20 (C-6'), 14.0 (C-, 14.9 (C-8'), 20.2 (C-6'), 26.9 (2 x C-cyclo), 27.6 (C-cyclo), 30.9 (2 x C-cyclo), 38.8 (C-2''), 73.3 (C-1''), 119.0 (C-2'), 129.4 (C-3'), 130.1 (C-3'), 130.8 (C_q), 130.9 (C-2'), 132.8 (C_q), 133.5 (C_q), 135.5 (C_q), 136.5 (C_q), 138.1 (C_q), 139.5 (C_q), 147.4 (C_q), 156.8 (C_q); HRMS calcd for $C_{22}H_{28}N_5O_3S$ $[M+H]^+$ 442.1907, found 442.1902.

Note: A mixture of isomers was obtained with a ratio of 1:2 for *Z*: *E*.

1-Chloro-1-((4-nitrophenyl)sulfonyl)propan-2-ol (336)

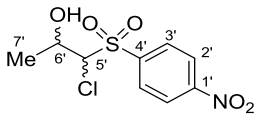

LHMDS (1M in THF, 4.55 mL, 4.55 mmol) was added dropwise to a stirred solution of 1-((chloromethyl)sulfonyl)-4-nitrobenzene **264** (712 mg, 3.03 mmol) and EtOAc (0.74 mL, 7.58 mmol) in dry THF (14 mL) at -78 ^{o}C under N_2. The reaction was stirred at -78 ^{o}C for 1 h and HCl (2M in H_2O, 10 mL) was added. The reaction was warmed up to r.t. and extracted with EtOAc (3 x 15 mL). The organic phases were combined and dried over $MgSO_4$. The solvent was removed *in vacuo* to give **334** without further purification.

Under N_2, $ZnCl_2$ (1.0 g, 5.5 mol) was solubilised in dry Et_2O (10 mL) and the solution was reflux for 1.5 h. The solution was allowed to cool to r.t. The supernatant was added to a stirred suspension of $NaBH_4$ (400 mg, 10.5 mol) in dry Et_2O (30 mL). The resulting suspension was stirred at r.t. for 2 days. The supernatant was collected to afford a solution of $Zn(BH_4)_2$ in Et_2O at 0.18M.

$Zn(BH_4)_2$ in Et_2O (0.18M, 9.2 mL, 1.66 mmol) was added to a stirred solution of 1-chloro-1-((4-nitrophenyl)sulfonyl)propan-2-one **334** (383 mg, 1.38 mmol) in dry THF (6 mL) under N_2. The resulting solution was stirred at r.t. for 2 h. MeOH (3 mL) was added to quench the residual reductive agent. The solvent was removed *in vacuo* and the product was purified by MPC (petrol: EtOAc 3: 2) to give the product **336** as a yellow oil (280 mg, 1.00 mmol, 73%).

R_f 0.27 (petrol: EtOAc 4: 1); UV λ_{max} (EtOH) 251 nm; IR (cm^{-1}) 3511, 3503, 3101, 2871, 1525, 1305, 1152; ^{1}H NMR (500 MHz, DMSO-d_6) (ppm) δ 1.19 (2H, d, *J* = 6.3 Hz, H-7'), 1.29 (1H, d, *J* = 6.3 Hz, H-7'), 4.35-4.36 (0.33 H, m, H-6'), 4.58-4.61 (0.66 H, m, H-6'), 5.36 (0.66 H, d, *J* = 6.1 Hz, OH), 5.62 (0.33 H, d, *J* = 6.1 Hz, OH), 5.68-5.70 (1H, m, H-5' and H-5'), 8.20 (1.33 H, d, *J* = 8.8 Hz, H-3'), 8.24 (0.66 H, d, *J* = 8.8 Hz, H-3'), 8.46 (1.33 H, d, *J* = 8.8 Hz, H-2'), 8.46 (0.66 H, d, *J* = 8.8 Hz, H-2'); ^{13}C NMR (125 MHz, DMSO-d_6) (ppm) δ 19.8 (C-7'), 21.3 (C-7'), 64.3 (C-6'), 65.5 (C-6'), 78.2 (C-5'), 79.7 (C-5'), 124.4 (C-2'), 124.9 (C-2'), 131.4 (C-3'), 132.2 (C-3'), 142.8 (C-4'), 143.1 (C-4'), 151.0 (C-1'), 151.3 (C-1'); HRMS calcd for $C_9H_9ClNO_5S$ [M^{35}Cl-H]$^{-}$ 277.9895, found 277.9883, [M^{37}Cl-H]$^{-}$ 279.9864, found 279.9852.

Note: A mixture of diastereoisomers was obtained with a ratio of 2: 1.

1-((4-Aminophenyl)sulfonyl)-1-chloropropan-2-ol (337)

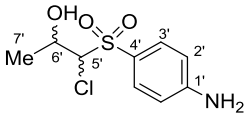

The title compound was synthesised following **general procedure H** using 1-chloro-1-((4-nitrophenyl)sulfonyl)propan-2-ol **336** (280 mg, 1.00 mmol) and zinc powder (8.03 mmol). The crude product was purified by MPC on amine silica (petrol: EtOAC 1: 1) to give the product **337** as an orange oil (178 mg, 0.71 mmol, 71%).

R_f 0.47 (petrol: EtOAc 1: 1); UV λ_{max} (EtOH) 275 nm; IR (cm^{-1}) 3465, 3369, 2979, 2937, 1591, 1298, 1127; ^{1}H NMR (500 MHz, DMSO-d_6) (ppm) δ 1.17 (2H, d, *J* = 6.4 Hz, H-7'), 1.19 (1H, d, *J* = 6.2 Hz, H-7'), 4.34 (0.33 H, qd, *J* = 2.7 and 6.2 Hz, H-6'), 4.41 (0.66 H, qd, *J* = 2.1 and 6.4 Hz, H-6'), 5.09 (0.33 H, d, *J* = 2.7 Hz, H-5'), 5.13 (0.66 H, d, *J* = 2.1 Hz, H-5'), 5.15 (1H, br s, OH and OH), 6.12 (2H, br s, NH_2 and NH_2), 6.63 (1.33 H, d, *J* = 8.8 Hz, H-3'), 6.66 (0.66 H, d, *J* = 8.8 Hz, H-3'), 7.49 (1.33 H, d, *J* = 8.8 Hz, H-2'), 7.51 (0.66 H, d, *J* = 8.8 Hz, H-2'); ^{13}C NMR (125 MHz, DMSO-d_6) (ppm) δ 18.4 (C-7'), 21.6 (C-7'), 64.5 (C-6'), 64.6 (C-6'), 80.1 (C-5'), 80.2 (C-5'), 112.8 (C-3'), 113.1 (C-3'), 120.5 (C-4'), 121.1 (C-4'), 131.7 (C-2'), 132.2 (C-2'), 154.7 (C-1'), 155.0 (C-1'); HRMS calcd for $C_9H_{13}ClNO_3S$ $[M^{35}Cl+H]^+$ 250.0299, found 250.0298, $[M^{37}Cl+H]^+$ 252.0268, found 252.0266.

Note: A mixture of diastereoisomers was obtained with a ratio of 2: 1.

1-Chloro-1-((4-((6-(cyclohexylmethoxy)-9*H*-purin-2-yl)amino)phenyl) sulfonyl) propan-2-ol (338)

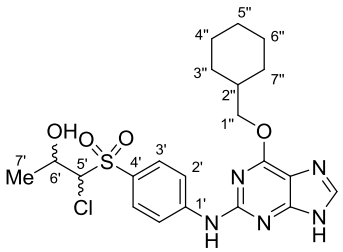

The title compound was synthesised following **general procedure I** using 6-(cyclohexylmethoxy)-2-iodo-9-(4-methoxybenzyl)-9*H*-purine **171** (220 mg, 0.48 mmol), 1-((4-aminophenyl)sulfonyl)-1-chloropropan-2-ol **337** (178 mg, 0.71 mmol), K_2CO_3 (133 mg, 0.96 mmol), $Pd(dba)_2$ (28 mg, 0.05 mmol) and XPhos (23 mg, 0.05 mmol). The crude mixture was then filtered through Celite and the solvent was removed *in vacuo*.

The crude mixture was then solubilised in TFA (15 mL). The resulting solution was heated at 70 °C for 2 h. Then the solvent was removed *in vacuo*. The product was purified by MPC (petrol: EtOAc 1: 4) to give the product **338** as a colourless oil (38 mg, 0.08 mmol, 17%).

R_f 0.40 (petrol: EtOAc 1: 4); UV λ_{max} (EtOH) 315 nm; IR (cm^{-1}) 3259, 3106, 1592, 1131; ^{1}H NMR (500 MHz, MeOD) (ppm) δ 1.17-1.24 (2H, m, H-cyclo), 1.32-1.42 (3H, m, H-cyclo), 1.37 (2H, d, *J* = 6.4 Hz, H-7'), 1.42 (1H, d, *J* = 6.4 Hz, H-7'), 1.75-1.78 (1H, m, H-cyclo), 1.83-1.86 (2H, m, H-cyclo), 1.97-1.99 (3H, m, H-cyclo and H-2''), 4.44 (2H, d, *J* = 6.2 Hz, H-1''), 4.57 (0.33 H, qd, *J* = 3.5 and 6.4 Hz, H-6'), 4.74 (0.66 H, qd, *J* = 2.0 and 6.4 Hz, H-6'), 5.07 (0.66 H, d, *J* = 2.0 Hz, H-5'), 5.08 (0.33 H, d, *J* = 3.5 Hz, H-5'), 7.87 (0.66 H, d, *J* = 8.9 Hz, H-3'), 7.89 (1.33 H, d, *J* = 8.9 Hz, H-3'), 8.10 (1.33 H, d, *J* = 8.9 Hz, H-2'), 8.13 (0.66 H, d, *J* = 8.9 Hz, H-2'), 8.14 (1H, s, H-8); ^{13}C NMR (125 MHz, MeOD) (ppm) δ 17.4 (C-7'), 19.8 (C-7'), 25.5 (2 x C-cyclo), 26.2 (C-cyclo), 29.2 (2 x C-cyclo), 37.2 (C-2''), 64.6 (C-6'), 65.3 (C-6'), 71.9 (C-1''), 79.0 (C-5'), 79.2 (C-5'), 117.0 (C-2'), 117.3 (C-2'), 126.9 (C_q), 127.0 (C_q), 130.4 (C-3'), 130.8 (C-3'), 139.9 (C-8), 146.8 (C_q), 147.0 (C_q), 155.0 (C_q), 153.3 (C_q), 155.4 (C_q), 159.9 (C_q); HRMS calcd for $C_{21}H_{27}ClN_5O_4S$ $[M^{35}Cl+H]^+$ 480.1467, found 480.1454, $[M^{37}Cl+H]^+$ 482.1437, found 482.1423.

Note: A mixture of diastereoisomers was obtained with a ratio of 2: 1.

_N_-(4-((1-Chloroprop-1-en-1-yl)sulfonyl)phenyl)-6-(cyclohexylmethoxy)-9_H_-purin-2-amine (339)

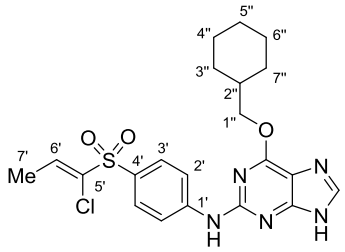

The title compound was synthesised following **general procedure P** using 1-chloro-1-((4-((6-(cyclohexylmethoxy)-9*H*-purin-2-yl)amino)phenyl)sulfonyl) propan-2-ol **338** (33 mg, 0.07 mmol), Et_3N (20.0 µL, 0.14 mmol) and MsCl (10.0 µL, 0.14 mmol). After 1 h, DBU (0.10 mL, 0.69 mmol) was added and the reaction was stirred at r.t. for 1 h. The solvent was removed *in vacuo*. The product was purified by MPC (petrol: EtOAc 1: 4) to give the product **339** as a yellow oil (16 mg, 0.03 mmol, 50%).

R_f 0.10 (petrol: EtOAc 1: 1); UV λ_{max} (EtOH) 320 nm; IR (cm^{-1}) 3262, 2923, 2851, 1580, 1386, 1313, 1147; ^1H NMR (500 MHz, $CDCl_3$) (ppm) δ 1.04-1.12 (2H, m, H-cyclo), 1.18-1.23 (1H, m, H-cyclo), 1.26-1.31 (2H, m, H-cyclo), 1.68-1.71 (1H, m, H-cyclo), 1.74-1.76 (2H, m, H-cyclo), 1.86-1.89 (3H, m, H-cyclo and H-2''), 1.97 (3H, d, *J* = 7.1 Hz, H-7'), 4.35 (2H, d, *J* = 6.2 Hz, H-1''), 7.26 (1 H, q, *J* = 7.1 Hz, H-6'), 7.85 (2 H, d, *J* = 9.3 Hz, H-3'), 7.89 (2 H, d, *J* = 9.3 Hz, H-2'), 8.06 (1H, s, H-8); ^{13}C NMR (125 MHz, $CDCl_3$) (ppm) δ 14.5 (C-7'), 25.7 (2 x C-cyclo), 26.3 (C-cyclo), 29.8 (2 x C-cyclo), 37.2 (C-2''), 72.8 (C-1''), 117.6 (C-2'), 117.8 (C_q), 128.7 (C_q), 130.4 (C-3'), 134.2 (C_q), 134.8 (C-6'), 138.4 (C-8), 145.2 (C_q), 145.3 (C_q), 154.7 (C_q), 160.7 (C_q); HRMS calcd for $C_{21}H_{25}ClN_5O_3S$ $[M^{35}Cl+H]^+$ 462.1361, found 462.1353, $[M^{37}Cl+H]^+$ 464.1331, found 464.1321.

2-((4-Nitrophenyl)thio)cyclohexanol (racemic, 341)[273]

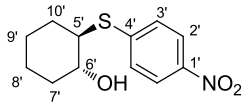

4-Nitrothiophenol **173** (1.00 g, 6.45 mmol) was added to a solution of cyclohexene oxide **340** (0.65 mL, 6.45 mmol) and DIPEA (2.24 mL, 12.9 mmol) in dry DCM (15 mL) under N_2. The resulting solution was stirred at r.t. for 16 h. Water (15 mL) was added and the organic phase was extracted with DCM (3 x 15 mL). The organic layers were combined, dried over $MgSO_4$ and the solvent was removed *in vacuo*. The product was purified by MPC (petrol: EtOAc 4: 1) to give the product **341** as a yellow solid (980 mg, 3.87 mmol, 60%).

R_f 0.40 (petrol: EtOAc 4: 1); Mp = 91-92 °C; UV λ_{max} (EtOH) 346 nm; IR (cm^{-1}) 3357, 2924, 2856, 1578, 1507, 1338; ^1H NMR (500 MHz, DMSO-d_6) ppm 1.28-1.42 (4H, m H-cyclo') 1.58-1.60 (1H, m, H-cyclo'), 1.67-1.69 (1H, m, H-cyclo'), 1.92-1.95 (1H, m, H-cyclo'), 2.07-2.09 (1H, m, H-cyclo'), 3.34-3.43 (2H, m, H-5' and H-6'), 5.12 (1H, d, *J* = 5.0 Hz, OH), 7.57 (2H, d, *J* = 8.9 Hz, H-3'), 8.12 (2H, d, *J* = 8.9 Hz, H-2'); ^{13}C NMR (125 MHz, DMSO-d_6) ppm 23.7 (C-cyclo'), 24.7 (C-cyclo'), 31.1 (C-cyclo'), 34.7 (C-cyclo'), 51.4 (C-5'), 71.4 (C-6'), 123.7 (C-2'), 127.5 (C-3'), 144.3 (C-4'), 147.9 (C-1'); LRMS calcd for $C_{12}H_{16}NO_3S$ $[M+H]^+$ 254.1, found 254.3.

2-((4-Nitrophenyl)sulfonyl)cyclohexanol (racemic, 342)

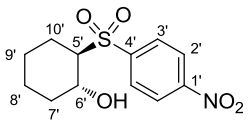

The title compound was synthesised following **general procedure M** using 2-((4-nitrophenyl)thio)cyclohexanol **341** (1.21 g, 4.77 mmol) and *m*-CPBA (2.44 g, 2.20 mmol). The crude product was purified by MPC on silica (petrol: EtOAc 3: 2) to give the product **342** as a pale orange solid (1.25 g, 4.39 mmol, 92%).

R_f 0.33 (petrol: EtOAc 7: 3); Mp = 125-126 °C; UV λ_{max} (EtOH) 235 nm; IR (cm^{-1}) 3423, 2930, 2860, 1523, 1348, 1296; ^{1}H NMR (500 MHz, DMSO-d_6) (ppm) δ 1.18-1.24 (3H, m H-cyclo') 1.34-1.42 (1H, m, H-cyclo'), 1.62-1.64 (1H, m, H-cyclo'), 1.76-1.82 (2H, m, H-cyclo'), 2.17-2.19 (1H, m, H-cyclo'), 3.34-3.39 (1H, m, H-5'), 3.59-3.65 (1H, m, H-6'), 4.87 (1H, d, *J* = 5.7 Hz, OH), 8.17 (2H, d, *J* = 8.9 Hz, H-3'), 8.40 (2H, d, *J* = 8.9 Hz, H-2'); ^{13}C NMR (125 MHz, DMSO-d_6) (ppm) δ 23.3 (C-cyclo'), 23.4 (C-cyclo'), 24.0 (C-cyclo'), 34.9 (C-cyclo'), 67.8 (C-5'), 68.5 (C-6'), 123.8 (C-2'), 129.8 (C-3'), 147.3 (C-4'), 149.9 (C-1'); HRMS calcd for $C_{12}H_{16}NO_5S$ $[M+H]^+$ 286.0744, found 286.0747.

2-((4-Aminophenyl)sulfonyl)cyclohexanol (racemic, 346)

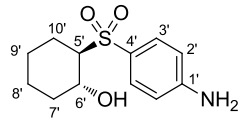

The title compound was synthesised following **general procedure H** using 2-((4-nitrophenyl)sulfonyl)cyclohexanol **342** (720 mg, 2.53 mmol) and zinc powder (1.60 g, 25.3 mmol). The crude product was purified by MPC on silica (DCM: MeOH 9: 1) to give the product **346** as a colourless solid (590 mg, 2.31 mmol, 92 %).

R_f 0.51 (DCM: MeOH 9: 1); Mp = 158-160 °C; UV λ_{max} (EtOH) 270 nm; IR (cm^{-1}) 3449, 3348, 2930, 2861, 1593, 1267, 1126; ^{1}H NMR (500 MHz, DMSO-d_6) (ppm) δ 1.12-1.20 (2H, m H-cyclo'), 1.22-1.29 (2H, m H-cyclo'), 1.57-1.59 (1H, m, H-cyclo'), 1.64-1.65 (1H, m, H-cyclo'), 1.82-1.85 (1H, m, H-cyclo'), 1.90-1.92 (1H, m, H-cyclo'), 2.88-2.93 (1H, m, H-5'), 3.52-3.58 (1H, m, H-6'), 4.68 (1H, d, *J* = 4.8 Hz, OH), 6.10 (2H, s, NH_2), 6.63 (2H, d, *J* = 8.7 Hz, H-3'), 7.45 (2H, d, *J* = 8.7 Hz, H-2'); ^{13}C NMR (125 MHz, DMSO-d_6) (ppm) δ 23.0 (C-cyclo'), 23.7 (C-cyclo'), 24.7 (C-cyclo'), 34.2 (C-cyclo'),

67.7 (C-5'), 67.9 (C-6'), 112.4 (C-3'), 123.7 (C-4'), 130.5 (C-2'), 153.5 (C-5'); HRMS calcd for $C_{12}H_{18}NO_3S$ $[M+H]^+$ 256.1002, found 256.1004.

2-((4-((6-(Cyclohexylmethoxy)-9*H*-purin-2-yl)amino)phenyl)sulfonyl) cyclohexanol (racemic, 347)

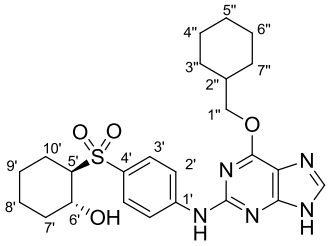

The title compound was synthesised following **general procedure I** using 6-(cyclohexylmethoxy)-2-iodo-9-(4-methoxybenzyl)-9*H*-purine **171** (500 mg, 1.05 mmol), 2-((4-aminophenyl)sulfonyl)cyclohexanol **346** (400 mg, 1.57 mmol), K_2CO_3 (290 mg, 2.09 mmol), $Pd(dba)_2$ (20 mg, 0.02 mmol) and XPhos (10 mg, 0.02 mmol). The crude mixture was then filtered through Celite and the solvent was removed *in vacuo*. The crude mixture was then solubilised in TFA (15 mL). The resulting solution was heated at 70 °C for 3 h. Then the solvent was removed *in vacuo*. The product was purified by MPC (EtOAc: MeOH 9: 1) to give the product **347** as a colourless oil (290 mg, 0.60 mmol, 57%).

R_f 0.45 (EtOAc: MeOH 9: 1); UV λ_{max} (EtOH) 312 nm; IR (cm^{-1}) 3498, 3111, 2927, 2855, 1595, 1392, 1277, 1131; ^{1}H NMR (500 MHz, DMSO-d_6) (ppm) δ 1.07-1.15 (2H, m H-cyclo) 1.17-1.21 (4H, m, 3 x H-cyclo' and H-cyclo), 1.23-1.32 (3H, m, H-cyclo' and 2 x H-cyclo), 1.58-1.61 (1H, m, H-cyclo'), 1.67-1.69 (2H, m, H-cyclo and H-cyclo'), 1.73-1.76 (2H, m, H-cyclo), 1.83-1.87 (4H, m, 2 x H-cyclo, H-cyclo' and H-2''), 2.00-2.02 (1H, m, H-cyclo'), 3.03-3.08 (1H, m, H-cyclo'), 3.60 (1H, td, *J* = 9.3 and 4.4 Hz, H-cyclo'), 4.37 (2H, d, *J* = 6.3 Hz, H-1''), 4.77 (1H, br s, OH), 7.73 (2H, d, *J* = 8.9 Hz, H-3'), 8.02 (2H, d, *J* = 8.9 Hz, H-2'), 8.14 (1H, s, H-8), 9.89 (1H, s, NH) , 13.00 (1H, br s, N^9H); ^{13}C NMR (125 MHz, DMSO-d_6) (ppm) δ 23.3 (C-cyclo'), 23.8 (C-cyclo'), 24.5 (C-cyclo'), 25.2 (2 x C-cyclo), 26.0 (C-cyclo), 29.2 (2 x C-cyclo), 34.6 (C-cyclo'), 36.8 (C-2''), 67.9 (C-cyclo'), 68.0 (C-cyclo'), 71.4 (C-1''), 117.0 (C-2'), 129.5 (C-3'), 130.2 (C_q), 140.6 (C_q), 145.6 (C_q), 147.0 (C_q), 154.5 (C_q); HRMS calcd for $C_{24}H_{32}N_5O_4S$ $[M+H]^+$ 486.2170, found 486.2160.

Note: Two quaternary carbons were not visible on the ^{13}C NMR spectrum.

***N*-(4-(Cyclohex-1-en-1-ylsulfonyl)phenyl)-6-(cyclohexylmethoxy)-9*H*-purin-2-amine (349)**

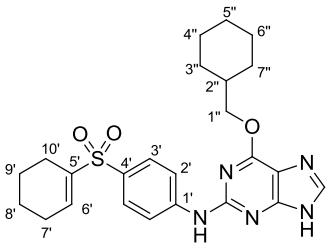

The title compound was synthesised following **general procedure P** using 2-((4-((6-(cyclohexylmethoxy)-9H-purin-2-yl)amino)phenyl)sulfonyl)cyclohexanol **347** (290 mg, 0.60 mmol), Et_3N (0.13 mL, 0.90 mmol) and MsCl (0.07 mL, 0.90 mmol). After 1 h, DBU (0.45 mL, 2.99 mmol) was added and the solution was stirred at r.t. for 3 h. Brine (5 mL) was added and the organic phase was extracted with DCM (3 x 5 mL). The organic phases were combined, dried over $MgSO_4$ and the solvent was removed *in vacuo*. The product was purified by MPC (DCM: MeOH 9: 1) to give the product **349** as a colourless oil (65 mg, 0.14 mmol, 23%).

R_f 0.75 (DCM: MeOH 9: 1); UV λ_{max} (EtOH) 317 nm; IR (cm^{-1}) 3105, 2926, 2853, 1582, 1534, 1450, 1286, 1138; ^{1}H NMR (500 MHz, DMSO-d_6) (ppm) δ 1.09-1.13 (2H, m H-cyclo) 1.18-1.21 (1H, m, H-cyclo), 1.24-1.29 (2H, m, H-cyclo), 1.48-1.51 (2H, m, H-cyclo'), 1.55-1.58 (2H, m, H-cyclo'), 1.63-1.66 (1H, m, H-cyclo), 1.73-1.75 (2H, m, H-cyclo), 1.84-1.87 (3H, m, H-cyclo and H-2''), 2.08-2.09 (2H, m, H-cyclo'), 2.21-2.24 (2H, m, H-cyclo'), 4.37 (2H, d, *J* = 6.3 Hz, H-1''), 6.88-6.91 (1H, m, H-6'), 7.68 (2H, d, *J* = 8.8 Hz, H-2'), 8.04 (2H, d, *J* = 8.9 Hz, H-3'), 8.07 (1H, s, H-8), 9.93 (1H, s, NH) , 12.96 (1H, br s, N^9H); ^{13}C NMR (125 MHz, DMSO-d_6) (ppm) δ 20.4 (C-cyclo'), 21.4 (C-cyclo'), 22.4 (C-cyclo'), 24.8 (C-cyclo'), 25.2 (2 x C-cyclo), 26.0 (C-cyclo), 29.2 (2 x C-cyclo), 36.8 (C-2''), 71.4 (C-1''), 117.6 (C-3'), 128.6 (C-2'), 129.3 (C_q), 137.0 (C-6'), 139.7 (C_q), 139.8 (C-8), 145.8 (C_q), 153.9 (C_q), 154.5 (C_q), 160.2 (C_q), 174.6 (C_q); HRMS calcd for $C_{24}H_{30}N_5O_3S$ $[M+H]^+$ 468.2064, found 468.2054.

4-((6-(Cyclohexylmethoxy)-9-(4-methoxybenzyl)-9*H*-purin-2-yl)amino) benzenesulfonamide (351)

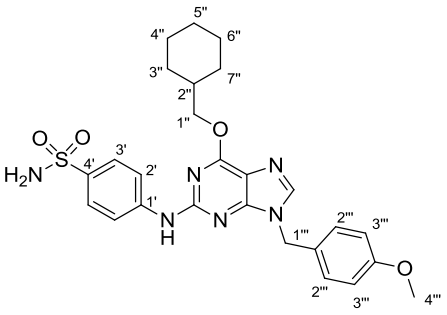

The title compound was synthesised following **general procedure I** using 6-(cyclohexylmethoxy)-2-iodo-9-(4-methoxybenzyl)-9*H*-purine **171** (400 mg, 0.84 mmol), sulfanilamide **350** (173 mg, 1.00 mmol), K_2CO_3 (231 mg, 1.67 mmol), $Pd(dba)_2$ (15 mg, 0.02 mmol) and XPhos (8 mg, 0.02 mmol). The crude product was purified by MPC (DCM: MeOH 19: 1) to give the product **351** as an orange oil (98 mg, 0.18 mmol, 21%).

R_f 0.54 (DCM: MeOH 9: 1); UV λ_{max} (EtOH) 270 nm; IR (cm^{-1}) 3425, 2935, 2847, 1525, 1474, 1398, 1286; ^{1}H NMR (500 MHz, DMSO-d_6) (ppm) δ 0.97-1.04 (2H, m, H-cyclo), 1.18-1.28 (3H, m, H-cyclo), 1.60-1.66 (1H, m, H-cyclo), 1.69-1.73 (2H, m, H-cyclo), 1.76-1.82 (3H, m, H-2'', H-cyclo), 3.73 (3H, s, H-4'''), 4.18 (2H, d, *J* = 6.4 Hz, H-1''), 5.20 (2H, s, H-1'''), 6.02 (2H, s, NH_2), 6.56 (2H, d, *J* = 8.8 Hz, H-3'''), 6.88 (2H, d, *J* = 8.7 Hz, H-2'), 7.29 (2H, d, *J* = 8.7 Hz, H-3'), 7.63 (2H, d, *J* = 8.8 Hz, H-2'''), 8.20 (1H, s, H-8), 11.10 (1H, s, NH); ^{13}C NMR (125 MHz, DMSO-d_6) (ppm) δ 25.1 (2 x C-cyclo), 25.9 (C-cyclo), 29.0 (2 x C-cyclo), 36.6 (C-2''), 45.9 (C-1'''), 55.1 (C-4'''), 71.5 (C-1''), 112.2 (C-3'''), 112.4 (C_q), 114.0 (C-3'), 125.5 (C_q), 127.4 (C_q), 128.7 (C_q), 129.1 (C_q), 129.3 (C-2'), 129.4 (C-2'''), 152.0 (C_q), 152.9 (C_q), 158.9 (C_q), 160.2 (C_q); HRMS calcd for $C_{26}H_{31}N_6O_4S$ $[M+H]^+$ 523.2122, found 523.2115.

***N*-Acryloyl-*N*-((4-((6-(cyclohexylmethoxy)-9-(4-methoxybenzyl)-9*H*-purin-2-yl) amino)phenyl)sulfonyl)acrylamide (352)**

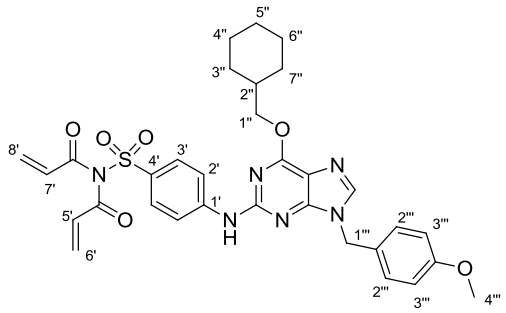

4-((6-(Cyclohexylmethoxy)-9-(4-methoxybenzyl)-9*H*-purin-2-yl)amino)benzene sulfonamide **351** (92 mg, 0.18 mmol) was solubilised in dry DCM (5 mL) under N_2. DIPEA (0.07 mL, 0.36 mmol) and acryloyl chloride (0.03 mL, 0.36 mmol) were added to the solution. The reaction was stirred at r.t. for 1 h. The solution was washed with brine (3 x 5 mL) and the organic layer was dried with $MgSO_4$. Then the solvent was removed *in vacuo*. The product was purified by MPC (petrol: EtOAc 4: 1) to give the product **352** as a pale orange oil (33 mg, 0.05 mmol, 29%).

R_f 0.49 (petrol: EtOAc 4: 1); UV λ_{max} (EtOH) 282 nm; IR (cm^{-1}) 3348, 2927, 2852, 1697, 1590, 1514, 1405, 1358, 1241, 1163; ^{1}H NMR (500 MHz, $CDCl_3$) (ppm) δ 1.08-1.16 (2H, m, H-cyclo), 1.21-1.32 (3H, m, H-cyclo), 1.65-1.71 (1H, m, H-cyclo), 1.76-1.79 (2H, m, H-cyclo), 1.90-1.96 (3H, m, H-2'', H-cyclo), 3.81 (3H, s, H-4'''), 4.41 (2H, d, *J* = 6.4 Hz, H-1''), 5.36 (2H, s, H-1'''), 5.63 (1H, dd, *J* = 10.4 and 1.4 Hz, H-6'), 5.78 (1H, dd, *J* = 16.6 and 10.4 Hz, H-5'), 5.86 (1H, dd, *J* = 10.3 and 1.0 Hz, H-8'), 6.31 (1H, dd, *J* = 16.8 and 10.3 Hz, H-7'), 6.42 (1H, dd, *J* = 16.6 and 1.4 Hz, H-6'), 6.50 (1H, dd, *J* = 16.8 and 1.0 Hz, H-8'), 6.91 (2H, d, *J* = 8.7 Hz, H-3'''), 7.31 (2H, d, *J* = 8.7 Hz, H-2'''), 7.82 (2H, d, *J* = 8.9 Hz, H-2'), 7.93 (1H, s, NH), 8.00 (1H, s, H-8), 8.21 (2H, d, *J* = 8.9 Hz, H-3'); ^{13}C NMR (125 MHz, $CDCl_3$) (ppm) δ 25.7 (2 x C-cyclo), 26.3 (C-cyclo), 29.7 (2 x C-cyclo), 37.2 (C-2''), 47.6 (C-1'''), 55.4 (C-4'''), 73.4 (C-1''), 114.6 (C-3'''), 119.0 (C-3'), 121.2 (C_q), 126.7 (C_q), 127.8 (C-5'), 129.2 (C-8'), 129.7 (C-2'''), 130.7 (C-7'), 130.8 (C-2'), 131.8 (C-6'), 143.1 (C_q), 143.5 (C-8), 149.3 (C_q), 153.0 (C_q), 159.9 (C_q), 161.9 (C_q), 163.8 (CO), 163.9 (CO); HRMS calcd for $C_{32}H_{35}N_6O_6S$ $[M+H]^+$ 631.2333, found 631.2338.

***N*-((4-((6-(Cyclohexylmethoxy)-9*H*-purin-2-yl)amino)phenyl)sulfonyl) acrylamide (353)**

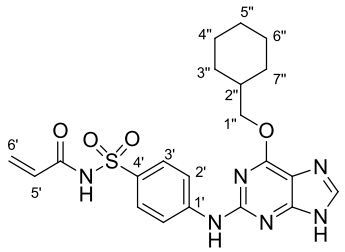

N-Acryloyl-*N*-((4-((6-(cyclohexylmethoxy)-9-(4-methoxybenzyl)-9*H*-purin-2-yl) amino) phenyl)sulfonyl)acrylamide **352** (33 mg, 0.05 mmol) was solubilised in TFA (2 mL). The resulting solution was heated at 70 °C for 3 h. Then the solvent was removed *in vacuo*. The product was purified by MPC (DCM: MeOH 9: 1) to give the product **353** as a colourless oil (12 mg, 0.03 mmol, 53%).

R_f: 0.46 (DCM: MeOH 9: 1); UV λ_{max} (EtOH) 273 nm; IR (cm^{-1}) 3316, 2927, 2852, 1627, 1593, 1438, 1333, 1276, 1146, 1090; ^{1}H NMR (500 MHz, MeOD) (ppm) δ 1.03-1.10 (2H, m, H-cyclo), 1.23-1.26 (1H, m, H-cyclo), 1.27-1.32 (2H, m, H-cyclo), 1.69-1.72 (1H, m, H-cyclo), 1.75-1.78 (2H, m, H-cyclo), 1.82-1.85 (3H, m, H-2'', H-cyclo), 4.17 (2H, d, *J* = 6.2 Hz, H-1''), 5.83 (1H, dd, *J* = 9.0 and 3.0 Hz, H-6'), 6.42-6.44 (2H, m, H-5' and H-6'), 7.86 (2H, d, *J* = 8.4 Hz, H-2'), 8.04 (2H, d, *J* = 8.4 Hz, H-3'), 8.16 (1H, s, H-8); ^{13}C NMR (125 MHz, MeOD) (ppm) δ 26.8 (2 x C-cyclo), 27.5 (C-cyclo), 30.7 (2 x C-cyclo), 38.6 (C-2''), 73.6 (C-1''), 120.4 (C-3'), 128.1 (C_q), 128.8 (C-6'), 129.2 (C_q), 130.1 (C-2'), 132.1 (C-5'), 135.7 (C_q), 136.8 (C_q), 144.3 (C-8), 148.3 (C_q), 153.7 (C_q), 166.3 (CO); HRMS calcd for $C_{21}H_{25}N_6O_4S$ $[M+H]^+$ 457.1653, found 457.1657.

***tert*-Butyl-(4-aminophenyl)carbamate (357)[274]**

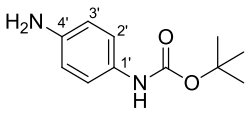

Boc_2O (2.02 g, 9.26 mmol) was added to a solution of *p*-phenylenediamine **356** (1.00 g, 9.26 mmol) and Et_3N (1.29 mL, 9.26 mmol) in dry DMF (5 mL) under N_2. The reaction was stirred at r.t. for 3 h. The solution was then diluted with EtOAc (20 mL) and washed with brine (2 x 30 mL) and water (1 x 30 mL) and the organic layer was dried with $MgSO_4$. The product was purified by MPC (petrol: EtOAc 1: 1) to give the product **357** as a pale orange oil (1.62 g, 7.79 mmol, 84%).

R_f 0.36 (petrol: EtOAc 1: 1); UV λ_{max} (EtOH) 250 nm; IR (cm^{-1}) 3665, 2985, 1693, 1515, 1428, 1234, 1158; ^{1}H NMR (500 MHz, DMSO-d_6) (ppm) δ 1.45 (9H, s, $(CH_3)_3$), 4.73 (2H, s, NH_2), 6.45 (2H, d, *J* = 8.7 Hz, H-3'), 7.07 (2H, d, *J* = 8.7 Hz, H-2'), 8.78 (1H, s, NH); ^{13}C NMR (125 MHz, DMSO-d_6) (ppm) δ 28.3 (3 x CH_3), 78.0 (C), 113.8 (C-3'), 120.2 (C-2'), 143.3 (C-1'), 153.0 (C-4'), 170.5 (CO); HRMS calcd for $C_{11}H_{17}N_2O_2$ $[M+H]^+$ 209.1285, found 209.1284.

***tert*-Butyl (4-(vinylsulfonamido)phenyl)carbamate (358)**

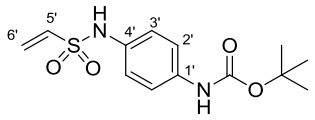

tert-Butyl (4-aminophenyl)carbamate **357** (624 mg, 3.00 mmol) was solubilised in dry DCM (2 mL) under N_2. DIPEA (1.05 mL, 6.00 mmol) and 2-chloroethanesulfonyl chloride (0.32 mL, 3.00 mL) were added. The reaction was stirred at r.t. for 2 h. The solvent was removed *in vacuo*. The product was purified by MPC (petrol: EtOAc 2: 3) to give the product **358** as a colourless oil (320 mg, 1.07 mmol, 36%).

R_f 0.48 (petrol: EtOAc 1: 1); UV λ_{max} (EtOH) 248 nm; IR (cm^{-1}) 3375, 3265, 2982, 1704, 1519, 1325, 1142; ^{1}H NMR (500 MHz, DMSO-d_6) (ppm) δ 1.47 (9H, s, $(CH_3)_3$), 5.98 (1H, d, *J* = 10.1 Hz, H-6'), 6.02 (1H, d, *J* = 16.5 Hz, H-6'), 6.71 (1H, dd, *J* = 10.1 and 16.5 Hz, H-5'), 7.04 (2H, d, *J* = 8.8 Hz, H-3'), 7.37 (2H, d, *J* = 8.8 Hz, H-2'), 9.29 (1H, s, NH), 9.69 (1H, s, NH); ^{13}C NMR (125 MHz, DMSO-d_6) (ppm) δ 28.1 (3 x CH_3), 78.8 (C), 118.9 (C-2'), 121.6 (C-3'), 127.2 (C-6'), 131.5 (C-1'), 136.3 (C-5'), 152.7 (C-4'), 168.9 (CO); HRMS calcd for $C_{13}H_{17}N_2O_4S$ $[M-H]^-$ 297.0915, found 297.0904.

***tert*-Butyl-(4-(2-(pyrrolidin-1-yl)ethylsulfonamido)phenyl)carbamate (359)**

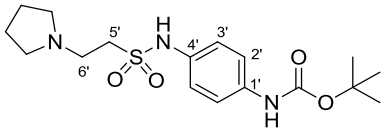

Pyrrolidine (0.36 mL, 4.30 mmol) was added to a stirred solution of *tert*-butyl (4-(vinylsulfonamido)phenyl)carbamate **358** (320 mg, 1.07 mmol) in dry DCM (10 mL) under N_2. The reaction for stirred for 30 min at r.t. The solution was then diluted with DCM (20 mL) and washed with brine (2 x 30 mL) and water (1 x 30 mL) and the organic layer was dried with $MgSO_4$. The product was purified by MPC (EtOAc: MeOH 9: 1) to give the product **359** as a colourless solid (237 mg, 0.64 mmol, 60%).

R_f 0.17 (EtOAc 100); Mp = 75-77 °C; UV λ_{max} (EtOH) 249 nm; IR (cm^{-1}) 2973, 2807, 1704, 1515, 1313, 1146; ^{1}H NMR (500 MHz, DMSO-*d*$_6$) (ppm) δ 1.47 (9H, s, $(CH_3)_3$), 1.60-1.65 (4H, m, H-pyr), 2.35-2.38 (4H, m, H-pyr), 2.75 (2H, t, *J* = 7.6 Hz, H-6'), 3.16 (2H, t, *J* = 7.6 Hz, H-5'), 7.21 (2H, d, *J* = 8.8 Hz, H-3'), 7.39 (2H, d, *J* = 8.8 Hz, H-2'), 9.31 (1H, s, NH), 9.52 (1H, s, NH); ^{13}C NMR (125 MHz, DMSO-*d*$_6$) (ppm) δ 22.9 (2 x C-pyr), 28.1 (3 x CH_3), 49.2 (C-5' and C-6'), 53.3 (2 x C-pyr), 78.3 (C), 118.9 (C-2'), 121.3 (C-3'), 132.3 (C-1'), 136.1 (C-4'), 170.2 (CO); HRMS calcd for $C_{17}H_{28}N_3O_4S$ $[M+H]^+$ 370.1795, found 370.1795.

_N_-(4-((6-(Cyclohexylmethoxy)-9_H_-purin-2-yl)amino)phenyl)-2-(pyrrolidin-1-yl)ethanesulfonamide (361)

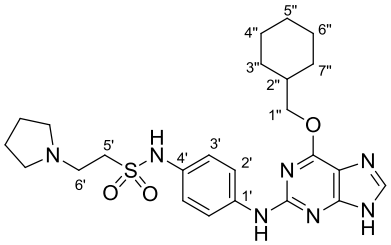

6-(Cyclohexylmethoxy)-2-iodo-9-(4-methoxybenzyl)-9*H*-purine **171** (350 mg, 0.73 mmol), *tert*-butyl (4-(2-(pyrrolidin-1-yl)ethylsulfonamido)phenyl)carbamate **359** (540 mg, 1.46 mmol), Cs_2CO_3 (476 mg, 1.46 mmol) and 2-thiophenecarboxylic acid (28 mg, 0.22 mmol) were solubilised in dry DMSO (2 mL) under N_2. The solution was degased with N_2 for 15 min then Cu(I)I (14 mg, 0.07 mmol) was added. The resulting solution was stirred at 60 °C for 18 h. EtOAc was added (10 mL) and the organic phase was washed with brine (3 x 10 mL). The organic layer was dried with $MgSO_4$ and the solvent was removed *in vacuo*. The crude product was solubilised in TFA (10 mL) and the resulting solution was heated under MW at 110 °C for 45 min. The solvent was removed *in vacuo* and the crude mixture was resuspensed in DCM (10 mL). The oganic phase was washed with brine (2 x 30 mL) and water (1 x 30 mL) and the organic layer was dried with $MgSO_4$. The crude compound was then solubilised in MeOH. $NaBH_4$ (200 mg, 5.40 mmol) was added and the solution was stirred at r.t. for 1 h. Then the solvent was removed *in vacuo*. The product was purified by MPC (DCM: MeOH 9: 1) to give the product **361** as a yellow oil (125 mg, 0.25 mmol, 34%).

R_f 0.36 (DCM: MeOH 9: 1); UV λ_{max} (EtOH) 255 nm; IR (cm^{-1}) 3368, 3218, 2926, 2851, 1590, 1513, 1360, 1270; ^{1}H NMR (500 MHz, MeOD) (ppm) δ 0.96-1.02 (2H, m H-cyclo) 1.18-1.29 (3H, m, H-cyclo), 1.66-1.68 (1H, m, H-cyclo), 1.71-1.75 (5H, m, 4 x H-cyclo

and H-2’’), 1.79-1.81 (4H, m, H-pyr), 2.60-2.62 (4H, m, H-pyr), 3.03-3.06 (2H, m, H-6’), 4.15-4.17 (2H, m, H-5’), 4.19 (2H, d, *J* = 6.7 Hz, H-1’’), 6.72 (2H, d, *J* = 8.6 Hz, H-3’), 7.06 (2H, d, *J* = 8.6 Hz, H-2’), 8.12 (1H, s, H-8); ^{13}C NMR (125 MHz, MeOD) (ppm) δ 24.4 (2 x C-pyr), 26.8 (2 x C-cyclo), 27.5 (C-cyclo), 30.6 (2 x C-cyclo), 38.4 (C-2’’), 50.7 (C-6’), 53.9 (C-5’), 55.0 (2 x C-pyr), 73.7 (C-1’’), 116.1 (C-3’), 122.4 (C_q), 129.3 (C_q), 132.3 (C-2’), 132.6 (C_q), 143.0 (C-8), 149.7 (C_q), 156.5 (C_q), 160.8 (C_q); HRMS calcd for $C_{24}H_{34}N_7O_3S$ $[M+H]^+$ 500.2438, found 500.2431.

_N_-(4-((6-(cyclohexylmethoxy)-9_H_-purin-2-yl)amino)phenyl)ethene sulfonamide (362)

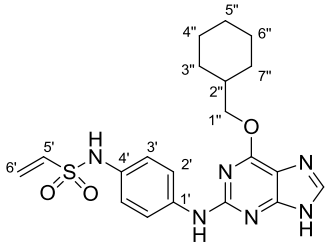

N^1-(6-(Cyclohexylmethoxy)-9*H*-purin-2-yl)benzene-1,4-diamine **364** (330 mg, 0.98 mmol) was solubilised in dry DCM (5 mL) under N_2. DIPEA (0.34 mL, 1.95 mmol) and 2-chloroethanesulfonyl chloride (0.10 mL, 0.98 mL) were added. The reaction was stirred at r.t. for 2 h. The solvent was removed *in vacuo*. The product was purified by MPC on neutral alumina (DCM: MeOH 9: 1) and by semi-prep HPLC (0.1% Formic Acid in H_2O: MeCN 2: 3) to give the product **362** as a colourless oil (13 mg, 0.03 mmol, 3%).

R_f 0.37 (DCM: MeOH 19: 1); UV λ_{max} (EtOH) 299 nm; IR (cm^{-1}) 3261, 2923, 2849, 1586, 1507, 1449, 1212, 1146; ^{1}H NMR (500 MHz, DMSO-d_6) (ppm) δ 1.06-1.12 (2H, m, H-cyclo), 1.15-1.20 (1H, m, H-cyclo), 1.23-1.31 (2H, m, H-cyclo), 1.66-1.68 (1H, m, H-cyclo), 1.72-1.75 (2H, m, H-cyclo), 1.82-1.88 (3H, m, H-cyclo, H-2’’), 4.32 (2H, d, *J* = 5.8 Hz, H-1’’), 6.00 (2H, dd, *J* = 9.8 and 16.3 Hz, H-6’), 6.74 (2H, dd, *J* = 9.8 and 16.3 Hz, H-6’), 7.07 (2H, d, *J* = 8.4 Hz, H-3’), 7.72 (2H, d, *J* = 8.4 Hz, H-2’), 8.25 (1H, br s, H-8), 9.27 (1H, br s, NH), 9.63 (1H, br s, N^9H); ^{13}C NMR (125 MHz, DMSO-d_6) (ppm) δ 25.2 (2 x C-cyclo), 26.0 (C-cyclo), 29.2 (2 x C-cyclo), 36.8 (C-2’’), 71.0 (C-1’’), 119.1 (C-2’), 121.9 (C-3’), 127.2 (C-6’), 133.6 (C-5’); HRMS calcd for $C_{20}H_{25}N_6O_3S$ $[M+H]^+$ 429.1703, found 429.1702.

Note: Seven quaternary carbons were not visible on the ^{13}C NMR spectrum.

_N_-(4-((6-(Cyclohexylmethoxy)-9_H_-purin-2-yl)amino)phenyl)-2-(pyrrolidin-1-yl)ethanesulfonamide (363)

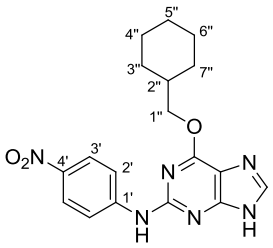

The title compound was synthesised following **general procedure I** using 6-(cyclohexylmethoxy)-2-iodo-9-(4-methoxybenzyl)-9*H*-purine **171** (500 mg, 1.05 mmol), 4-nitroaniline **3524** (217 mg, 1.57 mmol), K_2CO_3 (290 mg, 2.09 mmol), $Pd(dba)_2$ (20 mg, 0.02 mmol) and XPhos (10 mg, 0.02 mmol). The crude mixture was then filtered through Celite and the solvent was removed *in vacuo*. The crude mixture was then solubilised in TFA (15 mL). The resulting solution was heated at 70 °C for 3 h. Then the solvent was removed *in vacuo*. The product was purified by MPC (petrol: EtOAc 1: 1) to give the product **363** as a yellow solid (160 mg, 0.43 mmol, 42%).

R_f 0.48 (petrol: EtOAc 1: 1); Mp = 190-191 °C; UV λ_{max} (EtOH) 370 nm; IR (cm^{-1}) 2926, 2853, 1595, 1497, 1318, 1300, 1110; ^{1}H NMR (500 MHz, DMSO-d_6) (ppm) δ 1.08-1.15 (2H, m H-cyclo) 1.18-1.22 (1H, m, H-cyclo), 1.24-1.32 (2H, m, H-cyclo), 1.67-1.69 (1H, m, H-cyclo), 1.73-1.76 (2H, m, H-cyclo), 1.85-1.88 (3H, m, H-cyclo and H-2’’), 4.38 (2H, d, *J* = 6.3 Hz, H-1’’), 8.07 (2H, d, *J* = 9.4 Hz, H-2’), 8.18 (1H, s, H-8), 8.20 (2H, d, *J* = 9.4 Hz, H-3’), 10.21 (1H, s, NH) , 13.10 (1H, s, N^9H); ^{13}C NMR (125 MHz, DMSO-d_6) (ppm) δ 25.2 (2 x C-cyclo), 26.0 (C-cyclo), 29.2 (2 x C-cyclo), 36.8 (C-2’’), 71.5 (C-1’’), 117.0 (C-2’), 125.0 (C-3’), 135.8 (C_q), 139.8 (C_q), 140.8 (C_q), 147.7 (C_q), 149.6 (C_q), 149.8 (C_q), 154.1 (C_q); HRMS calcd for $C_{18}H_{20}N_6O_3$ $[M+H]^+$ 369.1670, found 369.1671.

_N_-(6-(Cyclohexylmethoxy)-9_H_-purin-2-yl)benzene-1,4-diamine (364)

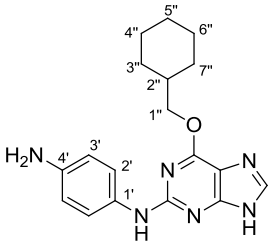

N-(4-((6-(Cyclohexylmethoxy)-9*H*-purin-2-yl)amino)phenyl)-2-(pyrrolidin-1-yl) ethane sulfonamide **363** (290 mg, 0.79 mmol) in MeOH (16 mL) was subjected to palladium

catalysed hydrogenation using an H-Cube® reactor and a 10% Pd/C CatCart. The reaction was conducted at 40 °C for 2 h. The solvent was removed *in vacuo* to give **364** as a brown oil (260 mg, 0.77 mmol, 97%).

R_f 0.77 (DCM: MeOH 9: 1); UV λ_{max} (EtOH) 276 nm; IR (cm^{-1}) 3435, 2925, 2853, 1617, 1584, 1451, 1407, 1142; ^{1}H NMR (500 MHz, DMSO-*d*$_6$) (ppm) δ 1.03-1.10 (2H, m H-cyclo) 1.18-1.20 (1H, m, H-cyclo), 1.23-1.28 (2H, m, H-cyclo), 1.65-1.68 (1H, m, H-cyclo), 1.72-1.74 (2H, m, H-cyclo), 1.82-1.85 (3H, m, H-cyclo and H-2''), 4.28 (2H, d, *J* = 6.3 Hz, H-1''), 5.14 (2H, br s, NH_2), 6.55 (2H, d, *J* = 8.6 Hz, H-3'), 7.40 (2H, d, *J* = 8.6 Hz, H-2'), 7.91 (1H, s, H-8), 8.77 (1H, s, NH), 12.61 (1H, br s, NH); ^{13}C NMR (125 MHz, DMSO-*d*$_6$) (ppm) δ 25.2 (2 x C-cyclo), 26.0 (C-cyclo), 29.2 (2 x C-cyclo), 36.8 (C-2''), 70.7 (C-1''), 113.6 (C_q), 114.4 (C-3'), 120.8 (C-2'), 128.6 (C_q), 131.0 (C_q), 138.4 (C_q), 142.1 (C-8), 156.2 (C_q), 159.7 (C_q); HRMS calcd for $C_{18}H_{22}N_6O$ $[M+H]^+$ 339.1928, found 339.1928.

1-((4-Aminophenyl)sulfonyl)propan-2-one (365)

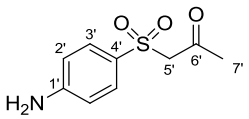

The title compound was synthesised following **general procedure H** using 1-((4-aminophenyl)sulfonyl)propan-2-one **324** (550 mg, 2.26 mmol) and zinc powder (1.47 mg, 22.6 mmol). The crude product was purified by MPC on silica (DCM: MeOH 49: 1) to give the product **365** as an orange oil (370 mg, 1.74 mmol, 77 %).

R_f 0.58 (DCM: MeOH 19: 1); Mp = 114-116 ^{o}C; UV λ_{max} (EtOH) 274 nm; IR (cm^{-1}) 3370, 2919, 1719, 1594, 1284, 1131; ^{1}H NMR (500 MHz, DMSO-*d*$_6$) (ppm) δ 2.19 (3H, s, H-7'), 4.40 (2H, s, H-5'), 6.24 (2H, br s, NH_2), 6.63 (2H, d, *J* = 8.7 Hz, H-3'), 7.47 (2H, d, *J* = 8.7 Hz, H-2'); ^{13}C NMR (125 MHz, DMSO-*d*$_6$) (ppm) δ 31.1 (C-7'), 67.4 (C-5'), 112.6 (C-3'), 129.8 (C-2'), 140.2 (C-4'), 154.0 (C-1'), 190.9 (CO); HRMS calcd for $C_9H_{10}NO_3S$ $[M-H]^-$ 212.0387, found 212.0391.

1-((4-((6-(Cyclohexylmethoxy)-9*H*-purin-2-yl)amino)phenyl)sulfonyl)propan-2-one (366)

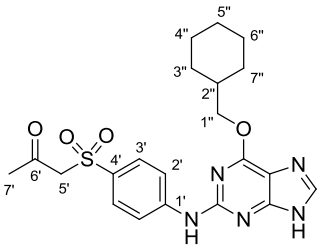

The title compound was synthesised following **general procedure I** using 6-(cyclohexylmethoxy)-2-iodo-9-(4-methoxybenzyl)-9*H*-purine **171** (300 mg, 0.63 mmol), 1-((4-aminophenyl)sulfonyl)propan-2-one **365** (200 mg, 0.94 mmol), K_2CO_3 (173 mg, 1.26 mmol), $Pd(dba)_2$ (12 mg, 0.01 mmol) and XPhos (6 mg, 0.01 mmol). The crude mixture was then filtered through Celite and the solvent was removed *in vacuo*. The crude mixture was then solubilised in TFA (15 mL). The resulting solution was heated at 70 °C for 2 h. Then the solvent was removed *in vacuo*. The product was purified by MPC (petrol: EtOAc 1: 4) to give the product **366** as a pale yellow oil (125 mg, 0.28 mmol, 45%).

R_f 0.28 (petrol: EtOAc 1: 4); UV λ_{max} (EtOH) 313 nm; IR (cm^{-1}) 3199, 2919, 2844, 1710, 1576, 1302, 1136; ^{1}H NMR (500 MHz, DMSO-d_6) (ppm) δ 1.08-1.14 (2H, m, H-cyclo), 1.20-1.22 (1H, m, H-cyclo), 1.25-1.33 (2H, m, H-cyclo), 1.67-1.69 (1H, m, H-cyclo), 1.73-1.76 (2H, m, H-cyclo), 1.85-1.92 (3H, m, H-cyclo and H-2’’), 2.23 (3H, s, H-7’), 4.38 (2H, d, *J* = 6.3 Hz, H-1’’), 4.58 (2H, s, H-5’), 7.77 (2H, d, *J* = 8.8 Hz, H-3’), 8.06 (2H, d, *J* = 8.8 Hz, H-2’), 8.08 (1H, s, H-8), 9.98 (1H, br s, NH), 12.99 (1H, br s, N^9H); ^{13}C NMR (125 MHz, DMSO-d_6) (ppm) δ 25.2 (2 x C-cyclo), 26.0 (C-cyclo), 29.2 (2 x C-cyclo), 31.2 (C-7’), 36.8 (C-2’’), 66.8 (C-5’), 71.4 (C-1’’), 115.5 (C_q), 117.3 (C-2’), 128.9 (C-3’), 129.7 (C_q), 138.7 (C-8), 146.2 (C_q), 153.8 (C_q), 154.4 (C_q), 160.2 (C_q), 197.3 (CO); HRMS calcd for $C_{21}H_{24}N_5O_4S$ $[M-H]^-$ 442.1554, found 442.1553.

4-((Chloromethyl)sulfonyl)aniline (367)

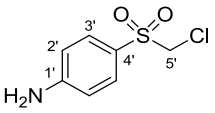

The title compound was synthesised following **general procedure H** using 1-((chloromethyl)sulfonyl)-4-nitrobenzene **264** (300 mg, 1.28 mmol) and zinc powder (664

mg, 10.2 mmol). The crude product was purified by MPC on silica (petrol: EtOAc 3: 2) to give the product **367** as an orange oil (184 mg, 0.90 mmol, 70%).

R_f 0.47 (petrol: EtOAc 1: 1); UV λ_{max} (EtOH) 274 nm; IR (cm^{-1}) 3490, 3388, 3014, 2946, 1592, 1298; ^{1}H NMR (500 MHz, DMSO-*d*$_6$) (ppm) δ 5.02 (2H, s, H-5'), 6.32 (2H, br s, NH_2), 6.66 (2H, d, *J* = 8.8 Hz, H-3'), 7.51 (2H, d, *J* = 8.8 Hz, H-2'); ^{13}C NMR (125 MHz, DMSO-*d*$_6$) (ppm) δ 58.8 (C-5'), 113.3 (C-3'), 120.2 (C-4'), 131.4 (C-2'), 154.9 (C-1'); HRMS calcd for $C_7H_7ClNO_2S$ $[M-H]^-$ 203.9892, found 203.9883.

_N_-(4-((Chloromethyl)sulfonyl)phenyl)-6-(cyclohexylmethoxy)-9_H_-purin-2-amine (368)

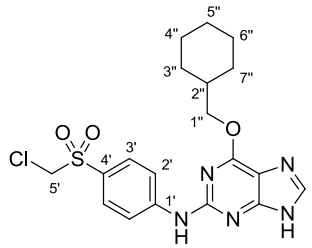

The title compound was synthesised following **general procedure I** using 6-(cyclohexylmethoxy)-2-iodo-9-(4-methoxybenzyl)-9*H*-purine **171** (200 mg, 0.42 mmol), 4-((chloromethyl)sulfonyl)aniline **367** (127 mg, 0.63 mmol), K_2CO_3 (115 mg, 0.84 mmol), $Pd(dba)_2$ (19 mg, 0.02 mmol) and XPhos (10 mg, 0.02 mmol). The crude mixture was then filtered through Celite and the solvent was removed *in vacuo*. The crude mixture was then solubilised in TFA (10 mL). The resulting solution was heated at 70 °C for 2 h. Then the solvent was removed *in vacuo*. The product was purified by MPC (petrol: EtOAc 1: 4) to give the product **368** as a yellow oil (77 mg, 0.18 mmol, 47%).

R_f 0.35 (petrol: EtOAc 1: 4); UV λ_{max} (EtOH) 315 nm; IR (cm^{-1}) 3256, 2924, 2851, 1593, 1310, 1145; ^{1}H NMR (500 MHz, DMSO-*d*$_6$) (ppm) δ 1.07-1.14 (2H, m, H-cyclo), 1.16-1.21 (1H, m, H-cyclo), 1.24-1.32 (2H, m, H-cyclo), 1.66-1.68 (1H, m, H-cyclo), 1.73-1.75 (2H, m, H-cyclo), 1.85-1.87 (3H, m, H-cyclo and H-2''), 4.38 (2H, d, *J* = 6.3 Hz, H-1''), 5.20 (2H, s, H-5'), 7.81 (2H, d, *J* = 8.9 Hz, H-3'), 8.10 (2H, d, *J* = 8.9 Hz, H-2'), 8.19 (1H, s, H-8), 10.05 (1H, br s, NH), 13.07 (1H, br s, N^9H); ^{13}C NMR (125 MHz, DMSO-*d*$_6$) (ppm) δ 25.7 (2 x C-cyclo), 26.5 (C-cyclo), 29.7 (2 x C-cyclo), 37.3 (C-2''), 58.4 (C-5'), 71.9 (C-1''), 117.8 (C-2'), 126.4 (C_q), 130.4 (C-3'), 147.3 (C_q), 154.9 (C_q); HRMS calcd for $C_{19}H_{23}ClN_5O_3S$ $[M^{35}Cl-H]^-$ 436.1205, found 436.1204, $[M^{37}Cl-H]^-$ 438.1174, found 438.1173.

Note: Four quaternary carbons were not visible on the ^{13}C NMR spectrum. The reaction was heated under microwaves at 100 ^{o}C for 30 min.

1-((Fluoromethyl)sulfonyl)-4-nitrobenzene (370)

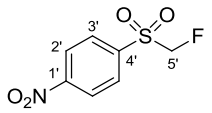

The title compound was synthesised following **general procedure K** using ethyl 2-fluoro-2-((4-nitrophenyl)sulfonyl)acetate **269** (566 mg, 1.95 mmol) and LiOH (2M in THF, 9.8 mL). After work-up, the residue obtained was solubilised in dry MeCN (5 mL) and the resulting solution was heated under MW at 180 ^{o}C, 8 bars for 1 h. The solvent was removed *in vacuo* and the product **370** was obtained without further purification as an orange oil (336 mg, 3.61 mmol, 79%).

R_f 0.55 (petrol: EtOAc 7: 3); UV λ_{max} (EtOH) 246 nm; IR (cm^{-1}) 2938, 2868, 1525, 1337, 1154; ^{1}H NMR (500 MHz, DMSO-d_6) (ppm) δ 5.80 (2H, d, *J* = 45.6 Hz, H-5'), 8.23 (2H, d, *J* = 8.8 Hz, H-3'), 8.52 (2H, d, *J* = 8.8 Hz, H-2'); ^{13}C NMR (125 MHz, DMSO-d_6) (ppm) δ 92.0 (d, *J* = 212.2 Hz, C-5'), 125.3 (C-2'), 131.0 (C-3'), 141.7 (C-4'), 151.7 (C-1'); ^{19}F NMR (470 MHz, DMSO- d_6) (ppm) δ -214.04 (t, *J* = 45.6 Hz); HRMS calcd for $C_7H_5FNO_4S$ $[M-H]^-$ 217.9929, found 217.9919.

4-((Fluoromethyl)sulfonyl)aniline (371)

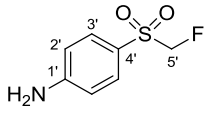

The title compound was synthesised following **general procedure H** using 1-((fluoromethyl)sulfonyl)-4-nitrobenzene **370** (366 mg, 1.67 mmol) and zinc powder (870 mg, 13.37 mmol). The crude product was purified by MPC on silica (petrol: EtOAc 3: 2) to give the product **371** as an orange oil (245 mg, 1.30 mmol, 78%).

R_f 0.45 (petrol: EtOAc 1: 1); UV λ_{max} (EtOH) 273 nm; IR (cm^{-1}) 3477, 3370, 2939, 1633, 1588, 1290, 1130; ^{1}H NMR (500 MHz, DMSO-d_6) (ppm) δ 5.45 (2H, d, *J* = 46.3 Hz, H-5'), 6.35 (2H, br s, NH_2), 6.68 (2H, d, *J* = 8.8 Hz, H-3'), 7.50 (2H, d, *J* = 8.8 Hz, H-2'); ^{13}C NMR (125 MHz, DMSO-d_6) (ppm) δ 92.0 (d, *J* = 210.3 Hz, C-5'), 113.3 (C-3'), 120.0 (C-4'), 131.2 (C-2'), 155.1 (C-1'); ^{19}F NMR (470 MHz, DMSO- d_6) (ppm) δ -212.30 (t, *J* = 46.3 Hz); HRMS calcd for $C_7H_7FNO_2S$ $[M-H]^-$ 188.0187, found 188.0189.

6-(Cyclohexylmethoxy)-*N*-(4-((fluoromethyl)sulfonyl)phenyl)-9*H*-purin-2-amine (372)

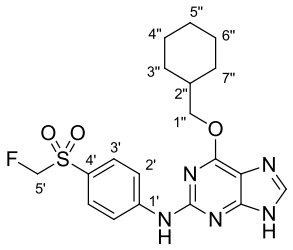

The title compound was synthesised following **general procedure I** using 6-(cyclohexylmethoxy)-2-iodo-9-(4-methoxybenzyl)-9*H*-purine **171** (200 mg, 0.42 mmol), 4-((fluoromethyl)sulfonyl)aniline **371** (119 mg, 0.63 mmol), K_2CO_3 (115 mg, 0.84 mmol), $Pd(dba)_2$ (19 mg, 0.02 mmol) and XPhos (10 mg, 0.02 mmol). The crude mixture was then filtered through Celite and the solvent was removed *in vacuo*. The crude mixture was then solubilised in TFA (10 mL). The resulting solution was heated at 70 °C for 2 h. Then the solvent was removed *in vacuo*. The product was purified by MPC (petrol: EtOAc 1: 9) to give the product **372** as a colourless oil (40 mg, 0.10 mmol, 23%).

R_f 0.30 (petrol: EtOAc 1: 4); UV λ_{max} (EtOH) 315 nm; IR (cm^{-1}) 3254, 2923, 2849, 1592, 1307, 1140; ^{1}H NMR (500 MHz, DMSO-d_6) (ppm) δ 1.07-1.14 (2H, m, H-cyclo), 1.16-1.21 (1H, m, H-cyclo), 1.23-1.32 (2H, m, H-cyclo), 1.66-1.68 (1H, m, H-cyclo), 1.73-1.75 (2H, m, H-cyclo), 1.85-1.87 (3H, m, H-cyclo and H-2’’), 4.38 (2H, d, *J* = 6.3 Hz, H-1’’), 5.60 (2H, d, *J* = 46.0 Hz, H-5’), 7.81 (2H, d, *J* = 8.9 Hz, H-3’), 8.12 (2H, d, *J* = 8.9 Hz, H-2’), 8.18 (1H, s, H-8), 10.07 (1H, br s, NH), 12.95 (1H, br s, N^9H); ^{13}C NMR (125 MHz, DMSO-d_6) (ppm) δ 25.7 (2 x C-cyclo), 26.5 (C-cyclo), 29.6 (2 x C-cyclo), 37.3 (C-2’’), 71.9 (C-1’’), 92.0 (d, J = 210.9 Hz, C-5’), 118.0 (C-2’), 126.3 (C_q), 130.3 (C-3’), 141.1 (C-8), 147.5 (C_q), 154.8 (C_q), 160.0 (C_q); HRMS calcd for $C_{19}H_{23}FN_5O_3S$ $[M+H]^+$ 420.1500, found 420.1499.

Note: Two quaternary carbons were not visible on the ^{13}C NMR spectrum. The reaction was heated under microwaves at 100 ^{o}C for 30 min.

4-((2,2,2-Trifluoroethyl)thio)aniline (373)

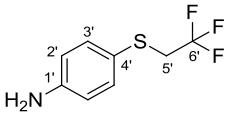

The title compound was synthesised following **general procedure H** using (4-nitrophenyl)(2,2,2-trifluoroethyl)sulfane **314** (820 mg, 3.46 mmol) and zinc powder (1.80 g, 27.7 mmol). The crude product was purified by MPC on silica (petrol: EtOAc 3: 2) to give the product **373** as an orange oil (610 mg, 2.95 mmol, 85 %).

R_f 0.48 (petrol: EtOAc 7: 3); UV λ_{max} (EtOH) 262 nm; IR (cm^{-1}) 3375, 1613, 1595, 1495, 1235; ^{1}H NMR (500 MHz, DMSO-d_6) (ppm) δ 3.59 (2H, q, J = 10.7 Hz, H-5'), 6.53 (2H, d, J = 8.8 Hz, H-3'), 7.20 (2H, d, J = 8.8 Hz, H-2'); ^{13}C NMR (125 MHz, DMSO-d_6) (ppm) δ 38.5 (q, J = 30.0 Hz, C-5'), 114.8 (C-3'), 116.8 (C-4'), 126.0 (q, J = 276.5 Hz, CF_3), 135.2 (C-2'), 150.0 (C-1'); ^{19}F NMR (470 MHz, DMSO-d_6) (ppm) δ -64.7 (t, J = 10.7 Hz); HRMS calcd for $C_8H_9F_3NS$ $[M+H]^+$ 208.0402, found 208.0397.

6-(Cyclohexylmethoxy)-*N*-(4-((2,2,2-trifluoroethyl)thio)phenyl)-9*H*-purin-2-amine (374)

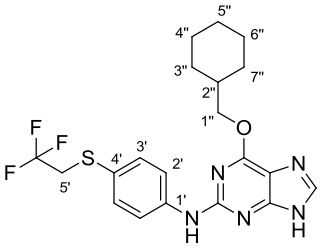

The title compound was synthesised following **general procedure I** using 6-(cyclohexylmethoxy)-2-iodo-9-(4-methoxybenzyl)-9*H*-purine **171** (400 mg, 0.84 mmol), 4-((2,2,2-trifluoroethyl)thio)aniline **373** (260 mg, 1.26 mmol), K_2CO_3 (231 mg, 1.67 mmol), $Pd(dba)_2$ (38 mg, 0.04 mmol) and XPhos (20 mg, 0.04 mmol). The crude mixture was then filtered through Celite and the solvent was removed *in vacuo*. The crude mixture was then solubilised in TFA (15 mL). The resulting solution was heated at 70 °C for 2 h. Then the solvent was removed *in vacuo*. The product was purified by MPC (petrol: EtOAc 2: 3) to give the product **374** as a brown oil (157 mg, 0.36 mmol, 43%).

R_f 0.29 (petrol: EtOAc 1: 1); UV λ_{max} (EtOH) 308 nm; IR (cm^{-1}) 3286, 2927, 2853, 1630, 1193, 1123; ^{1}H NMR (500 MHz, DMSO-d_6) (ppm) δ 1.05-1.12 (2H, m, H-cyclo), 1.16-1.21 (1H, m, H-cyclo), 1.24-1.32 (2H, m, H-cyclo), 1.66-1.68 (1H, m, H-cyclo), 1.72-

1.75 (2H, m, H-cyclo), 1.83-1.86 (3H, m, H-cyclo and H-2''), 3.84 (2H, q, *J* = 10.4 Hz, H-5'), 4.34 (2H, d, *J* = 6.3 Hz, H-1''), 7.45 (2H, d, *J* = 8.7 Hz, H-3'), 7.83 (2H, d, *J* = 8.7 Hz, H-2'), 8.12 (1H, s, H-8), 9.52 (1H, br s, NH), 13.05 (1H, br s, N^9H); ^{13}C NMR (125 MHz, DMSO-d_6) (ppm) δ 25.7 (2 x C-cyclo), 26.5 (C-cyclo), 29.7 (2 x C-cyclo), 37.0 (q, *J* = 31.2 Hz, C-5'), 37.3 (C-2''), 71.7 (C-1''), 119.3 (C-2'), 123.8 (C_q), 126.0 (q, *J* = 276.5 Hz, CF_3), 131.7 (C_q), 132.8 (C-3'), 140.3 (C-8), 141.6 (C_q), 152.0 (C_q), 155.6 (C_q); ^{19}F NMR (470 MHz, DMSO-d_6) (ppm) δ -64.7 (t, *J* = 10.4 Hz); HRMS calcd for $C_{20}H_{21}F_3N_5OS$ $[M-H]^-$ 436.1424, found 436.1421.

Note: The reaction was heated under microwaves at 100 ^{o}C for 30 min.

6-(Cyclohexylmethoxy)-*N*-(4-((2,2,2-trifluoroethyl)sulfonyl)phenyl)-9*H*-purin-2-amine (375)

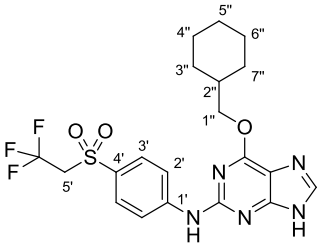

The title compound was synthesised following **general procedure M** using 6-(cyclohexylmethoxy)-*N*-(4-((2,2,2-trifluoroethyl)thio)phenyl)-9*H*-purin-2-amine **374** (150 mg, 0.38 mmol) and *m*-CPBA (180 mg, 0.76 mmol). The crude product was purified by MPC on silica (petrol: EtOAc 3: 7) to give the product **375** as a yellow oil (72 mg, 0.15 mmol, 40%).

R_f 0.25 (petrol: EtOAc 1: 4); UV λ_{max} (EtOH) 315 nm; IR (cm^{-1}) 3260, 2925, 2851, 1594, 1310, 1242, 1145; ^{1}H NMR (500 MHz, DMSO-d_6) (ppm) δ 1.07-1.14 (2H, m, H-cyclo), 1.16-1.21 (1H, m, H-cyclo), 1.23-1.32 (2H, m, H-cyclo), 1.66-1.69 (1H, m, H-cyclo), 1.73-1.75 (2H, m, H-cyclo), 1.85-1.87 (3H, m, H-cyclo and H-2''), 4.37 (2H, d, *J* = 6.3 Hz, H-1''), 4.82 (2H, q, *J* = 9.9 Hz, H-5'), 7.82 (2H, d, *J* = 9.0 Hz, H-3'), 8.08-8.10 (3H, m, H-2' and H-8), 10.05 (1H, br s, NH), 13.01 (1H, br s, N^9H); ^{13}C NMR (125 MHz, DMSO-d_6) (ppm) δ 25.7 (2 x C-cyclo), 26.5 (C-cyclo), 29.7 (2 x C-cyclo), 37.3 (C-2''), 56.7 (q, *J* = 29.1 Hz, C-5'), 71.9 (C-1''), 117.7 (C-2'), 122.0 (q, *J* = 277.5 Hz, CF_3), 129.6 (C-3'), 129.7 (C_q), 140.2 (C-8), 147.2 (C_q), 154.8 (C_q), 160.7 (C_q); ^{19}F NMR (470 MHz, DMSO-d_6) (ppm) δ -60.0. (t, *J* = 9.9 Hz); HRMS calcd for $C_{20}H_{23}F_3N_5O_3S$ $[M-H]^-$ 470.1468, found 470.1463.

Note: Two quaternary carbons were not visible on the ^{13}C NMR spectrum.

Methyl 3-hydroxy-3-(4-nitrophenyl)propanoate (377)

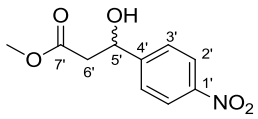

$NaBH_4$ (481 mg, 12.7 mmol) was added dropwise to a stirred solution of ethyl 4-nitrobenzoylacetate **376** (1.00 g, 4.22 mmol) in MeOH (10.5 mL). The reaction was stirred at r.t. for 1 h. The reaction mixture was partitioned with brine (20 mL) and EtOAc (30 mL) and the organic phase was extracted with EtOAc (3 x 30 mL). The organic layer was dried over $MgSO_4$ and the solvent was removed *in vacuo*. The crude product was purified by MPC on silica (petrol: EtOAc 7: 3) to give the product **377** as a yellow oil (603 mg, 2.68 mmol, 64%).

R_f 0.43 (petrol: EtOAc 7: 3); UV λ_{max} (EtOH) 270 nm; IR (cm^{-1}) 3420, 2957, 2852, 1709, 1510, 1347, 1173; ^1H NMR (500 MHz, DMSO-d_6) (ppm) δ 2.62 (1H, dd, *J* = 8.9, 15.1 Hz, H-6'), 2.74 (1H, dd, *J* = 4.6, 15.1 Hz, H-6'), 3.60 (3H, s, OCH_3), 5.11 (1H, ddd, *J* = 4.6, 4.9, 8.9 Hz, H-5'), 5.86 (1H, d, *J* = 4.9 Hz, OH), 7.67 (2H, d, *J* = 8.8 Hz, H-3'), 8.20 (2H, d, *J* = 8.8 Hz, H-2'); ^{13}C NMR (125 MHz, DMSO-d_6) (ppm) δ 44.1 (C-6'), 51.9 (O*C*H_3), 69.1 (C-5'), 123.8 (C-2'), 127.6 (C-3'), 147.1 (C-4'), 152.9 (C-1'), 171.2 (CO); HRMS calcd for $C_{10}H_{10}NO_5$ $[M-H]^-$ 224.0564, found 224.0555.

1-(4-Nitrophenyl)propane-1,3-diol (378)

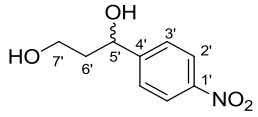

The title compound was synthesised following **general procedure O** using methyl 3-hydroxy-3-(4-nitrophenyl)propanoate **377** (603 mg, 2.68 mmol) and DIBAL (1M in hexanes, 8.00 mL). The crude product was purified by MPC on silica (petrol: EtOAc 1: 1) to give the product **378** as a yellow oil (410 mg, 2.08 mmol, 78%).

R_f 0.18 (petrol: EtOAc 1: 1); UV λ_{max} (EtOH) 274 nm; IR (cm^{-1}) 3317, 2943, 2885, 1512, 1341, 1045; ^1H NMR (500 MHz, DMSO-d_6) (ppm) δ 1.70-1.80 (2H, m, H-7'), 3.41-3.47 (1H, m, H-6'), 3.52-3.58 (1H, m, H-6'), 4.50 (1H, t, *J* = 5.1 Hz, OH), 4.80-4.84 (1H, m, H-5'), 5.48 (1H, d, *J* = 4.7 Hz, OH), 7.60 (2H, d, *J* = 8.7 Hz, H-3'), 8.20 (2H, d, *J* = 8.7 Hz, H-2'); ^{13}C NMR (125 MHz, DMSO-d_6) (ppm) δ 42.7 (C-7'), 58.0 (C-6'), 69.3 (C-5'),

123.8 (C-2'), 127.3 (C-3'), 146.8 (C-4'), 155.0 (C-1'); HRMS calcd for $C_9H_{15}N_2O_4$ $[M+NH_4]^+$ 215.1026, found 215.1025.

3-((*tert*-Butyldiphenylsilyl)oxy)-1-(4-nitrophenyl)propan-1-ol (379)

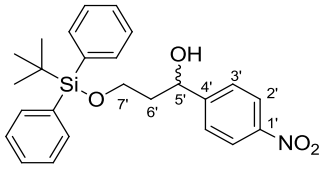

Imidazole (722 mg, 10.6 mmol) and TBDPSCl (0.92 mL, 3.54 mmol) were added to a stirred solution of 1-(4-nitrophenyl)propane-1,3-diol **378** (630 mg, 3.54 mmol) in dry DCM (25 mL) at 0 ^oC, under N_2. The reaction was stirred at 0 ^oC for 1 h. Water (30 mL) was added and the organic phase was extracted with DCM (3 x 30 mL). The organic layer was dried over $MgSO_4$ and the solvent was removed *in vacuo*. The crude product was purified by MPC on silica (petrol: EtOAc 9: 1) to give the product **379** as a yellow oil (672 mg, 1.54 mmol, 44%).

R_f 0.24 (petrol: EtOAc 9: 1); ^1H NMR (500 MHz, DMSO-d_6) (ppm) δ 0.99 (9H, s, ^{t}Bu), 1.88 (2H, dd, *J* = 6.4, 6.4 Hz, H-7'), 3.64-3.69 (1H, m, H-6'), 3.81-3.86 (1H, m, H-6'), 4.88-4.91 (1H, m, H-5'), 5.56 (1H, d, *J* = 4.7 Hz, OH), 7.41-7.47 (6H, m, H-ar), 7.56 (2H, d, *J* = 8.7 Hz, H-3'), 7.59-7.61 (4H, m, H-ar), 8.18 (2H, d, *J* = 8.7 Hz, H-2'); ^{13}C NMR (125 MHz, DMSO-d_6) (ppm) δ 19.2 (^{t}Bu), 27.1 (^{t}Bu), 42.2 (C-7'), 60.8 (C-6'), 69.0 (C-5'), 123.8 (C-2'), 127.3 (C-3'), 128.3 (C-ar), 130.3 (C-ar), 133.7 (Cq), 135.5 (C-ar), 146.8 (C-4'), 154.6 (C-1').

3-((*tert*-Butyldiphenylsilyl)oxy)-1-(4-nitrophenyl)propan-1-one (380)

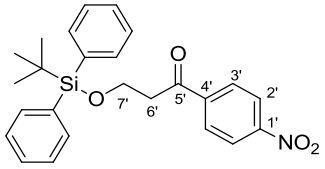

Dess-martin periodinane (0.3 M in DCM, 5.66 mL) was added dropwise to a stirred solution of 3-((*tert*-butyldiphenylsilyl)oxy)-1-(4-nitrophenyl)propan-1-ol **379** (672 mg, 1.54 mmol) in dry DCM (17 mL) under N_2. The resulting solution was stirred at r.t. for 2 h. A saturated aqueous solution of $Na_2S_2O_3$ (15 mL) was added dropwise at 0 ^oC and the organic phase was extracted with DM (3 x 15 mL). The organic layer was dried over $MgSO_4$ and the solvent was removed *in vacuo*. The crude product was purified by MPC

on silica (petrol: EtOAc 19: 1) to give the product **380** as a yellow oil (570 mg, 1.32 mmol, 85%).

R_f 0.48 (petrol: EtOAc 9: 1); UV λ_{max} (EtOH) 264 nm; IR (cm^{-1}) 2972, 2882, 1658, 1534; ^{1}H NMR (500 MHz, DMSO-d_6) (ppm) δ 0.93 (9H, s, ^{t}Bu), 3.39 (2H, t, *J* = 6.1 Hz, H-7'), 4.03 (2H, t, *J* = 6.1 Hz, H-6'), 7.40-7.48 (4H, m, H-ar), 7.46-7.48 (2H, m, H-ar), 7.57-7.59 (4H, m, H-ar), 8.20 (2H, d, *J* = 8.8 Hz, H-3'), 8.35 (2H, d, *J* = 8.8 Hz, H-2'); ^{13}C NMR (125 MHz, DMSO-d_6) (ppm) δ 19.2 (^{t}Bu), 27.0 (^{t}Bu), 42.0 (C-7'), 60.3 (C-6'), 124.3 (C-2'), 128.3 (C-ar), 130.0 (C-3'), 130.3 (C-ar), 133.3 (Cq), 135.5 (C-ar), 141.9 (C-4'), 150.4 (C-1'), 198.7 (CO); HRMS calcd for $C_{25}H_{28}NO_4Si$ $[M+H]^+$ 434.1782, found 434.1786.

1-(4-Nitrophenyl)prop-2-en-1-one (383)

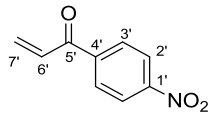

Tributyl(vinyl)tin was added to a solution of 4-nitrobenzoyl chloride **382** (300 mg, 1.61 mmol) and $Pd(PPh_3)_4$ (1 mg, 0.005 mmol) in dry THF (1.5 mL) under N_2. The reaction was degased with N_2 and heated at 65 ^{o}C for 1 h. The reaction was cooled to r.t. and EtOAc (5 mL) was added. The organic phase was washed with a saturated aqueous solution of KF (3 x 5 mL). The organic layer was dried over $MgSO_4$ and the solvent was removed *in vacuo*. The crude product was purified by MPC on silica (petrol: EtOAc 9: 1) to give the product **383** as a pale yellow solid (99 mg, 0.56 mmol, 35%).

R_f 0.62 (petrol: EtOAc 7: 3); Mp = 87-89 ^{o}C; UV λ_{max} (EtOH) 259 nm; IR (cm^{-1}) 2923, 2856, 1665, 1596, 1519, 1341; ^{1}H NMR (500 MHz, DMSO-d_6) (ppm) δ 6.12 (1H, d, *J* = 10.5 Hz, H-7'), 6.40 (1H, d, *J* = 17.0 Hz, H-7'), 7.40 (1H, dd, *J* = 10.5, 17.0 Hz, H-6'), 8.21 (2H, d, *J* = 8.8 Hz, H-3'), 8.37 (2H, d, *J* = 8.8 Hz, H-2'); ^{13}C NMR (125 MHz, DMSO-d_6) (ppm) δ 124.4 (C-2'), 130.4 (C-3'), 132.5 (C-7'), 132.8 (C-6'), 142.0 (C-4'), 150.4 (C-1'), 189.9 (CO); HRMS calcd for $C_9H_6NO_3$ $[M-H]^-$ 176.0342, found 176.0362.

1-(4-Nitrophenyl)-3-(pyrrolidin-1-yl)propan-1-one (384)

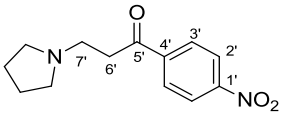

Pyrrolidine (0.37 mL, 4.46 mmol) was added to a stirred solution of 1-(4-nitrophenyl)prop-2-en-1-one **383** (79 mg, 0.45 mmol) in dry DCM (3 mL) under N_2. The resulting solution was stirred at r.t. for 2 h. Brine (5 mL) was added and the organic phase was extracted with DCM (3 x 5 mL). The organic layer was dried over $MgSO_4$ and the solvent was removed *in vacuo.* The crude product was purified by MPC on silica (DCM: MeOH 9: 1) to give the product **384** as a yellow oil (56 mg, 0.23 mmol, 51%).

R_f 0.28 (DCM: MeOH 19: 1); UV λ_{max} (EtOH) 263 nm; IR (cm^{-1}) 2967, 2876, 1520, 1342; ^{1}H NMR (500 MHz, DMSO-d_6) (ppm) δ 1.65-1.68 (4H, m, H-pyr), 2.44-2.47 (4H, m, H-pyr), 2.78 (2H, t, *J* = 7.1 Hz, H-7'), 3.28 (2H, t, *J* = 7.1 Hz, H-6'), 8.20 (2H, d, *J* = 8.9 Hz, H-3'), 8.34 (2H, d, *J* = 8.9 Hz, H-2'); ^{13}C NMR (125 MHz, DMSO-d_6) (ppm) δ 23.6 (C-pyr), 38.8 (C-7'), 50.8 (C-6'), 54.0 (C-pyr), 124.3 (C-2'), 129.8 (C-3'), 141.8 (C-4'), 150.3 (C-1'), 199.0 (CO); HRMS calcd for $C_{13}H_{17}N_2O_3$ $[M+H]^+$ 249.1234, found 249.1237.

Methyl 4-((6-(cyclohexylmethoxy)-9*H*-purin-2-yl)amino)benzoate (387)

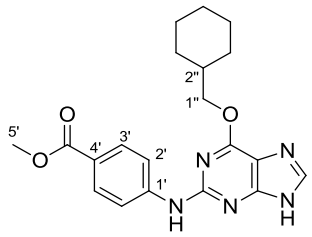

The title compound was synthesised following **general procedure I** using 6-(cyclohexylmethoxy)-2-iodo-9-(4-methoxybenzyl)-9*H*-purine **171** (500 mg, 1.05 mmol), methyl 4-aminobenzoate **386** (237 mg, 1.57 mmol), K_2CO_3 (289 mg, 2.09 mmol), $Pd(dba)_2$ (60 mg, 0.10 mmol) and XPhos (50 mg, 0.10 mmol). The crude mixture was then filtered through Celite and the solvent was removed *in vacuo*. The crude mixture was then solubilised in TFA (20 mL). The resulting solution was heated at 70 °C for 2 h. Then the solvent was removed *in vacuo*. The product was purified by MPC (petrol: EtOAc 1: 4) to give the product **387** as a pale yellow solid (222 mg, 0.58 mmol, 55%).

R_f 0.46 (petrol: EtOAc 1: 4); Mp = 224-226 ^{o}C; UV λ_{max} (EtOH) 321 nm; IR (cm^{-1}) 3280, 2924, 2851, 1704, 1596, 1395, 1266, 1171; ^{1}H NMR (500 MHz, DMSO-d_6) (ppm) δ

1.07-1.14 (2H, m, H-cyclo), 1.18-1.21 (1H, m, H-cyclo), 1.25-1.32 (2H, m, H-cyclo), 1.66-1.69 (1H, m, H-cyclo), 1.73-1.75 (2H, m, H-cyclo), 1.85-1.87 (3H, m, H-cyclo and H-2''), 3.82 (3H, s, H-5'), 4.37 (2H, d, *J* = 6.3 Hz, H-1''), 7.88 (2H, d, *J* = 8.8 Hz, H-2'), 7.97 (2H, d, *J* = 8.8 Hz, H-3'), 8.19 (1H, s, H-8), 9.84 (1H, br s, NH), 12.81 (1H, br s, N^9H); ^{13}C NMR (125 MHz, DMSO-d_6) (ppm) δ 25.7 (2 x C-cyclo), 26.5 (C-cyclo), 29.7 (2 x C-cyclo), 37.3 (C-2''), 52.1 (C-5'), 71.9 (C-1''), 117.9 (C-3'), 121.6 (C_q), 130.6 (C-2'), 146.2 (C_q), 155.3 (C_q), 166.5 (CO); HRMS calcd for $C_{20}H_{24}N_5O_3$ [M+H] 382.1874, found 382.1876.

Note: Four quaternary carbons were not visible on the ^{13}C NMR spectrum. The reaction was heated under microwaves at 100 ^{o}C for 30 min.

4-((6-(Cyclohexylmethoxy)-9*H*-purin-2-yl)amino)-*N*-methoxy-*N*-methyl benzamide (388)

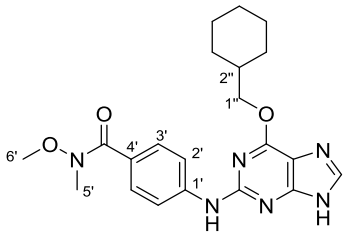

Isopropylmagnesium chloride (2M in THF, 1.08 mL) was added to a stirred solution of methyl 4-((6-(cyclohexylmethoxy)-9*H*-purin-2-yl)amino)benzoate **387** (164 mg, 0.43 mmol) and *N*,*O*-dimethyl hydroxylamine (125 mg, 1.29 mmol) in dry THF (3.5 mL) at 0 ^{o}C, under N_2. The resulting solution was stirred at 0 ^{o}C for 1.5 h. Isopropylmagnesium chloride (2 M in THF, 0.54 mL) was added to the reaction and the solution was stirred for 0.5 h at 0 ^{o}C. A saturated aqueous solution of NH_4Cl (10 mL) was added and the organic phase was extracted with EtOAc (3 x 10 mL). The organic layer was dried over $MgSO_4$ and the solvent was removed *in vacuo*. The crude product was purified by MPC on silica (petrol: EtOAc 1: 9) to give the product **388** as a colourless oil (171 mg, 0.42 mmol, 97%).

R_f 0.48 (EtOAc 100); UV λ_{max} (EtOH) 315 nm; IR (cm^{-1}) 3263, 2923, 2849, 1734, 1596, 1351, 1117; ^{1}H NMR (500 MHz, DMSO-d_6) (ppm) δ 1.06-1.13 (2H, m, H-cyclo), 1.17-1.20 (1H, m, H-cyclo), 1.23-1.32 (2H, m, H-cyclo), 1.66-1.68 (1H, m, H-cyclo), 1.73-1.76 (2H, m, H-cyclo), 1.84-1.91 (3H, m, H-cyclo and H-2''), 3.25 (3H, s, H-5'), 3.58 (3H, s, H-6'), 4.36 (2H, d, *J* = 6.4 Hz, H-1''), 7.60 (2H, d, *J* = 8.8 Hz, H-2'), 7.90 (2H, d, *J* = 8.8 Hz, H-3'), 8.04 (1H, s, H-8), 9.62 (1H, br s, NH), 12.90 (1H, br s, N^9H); ^{13}C NMR

(125 MHz, DMSO-d_6) (ppm) δ 25.7 (2 x C-cyclo), 26.5 (C-cyclo), 29.7 (2 x C-cyclo), 34.0 (C-5'), 37.3 (C-2''), 61.0 (C-6'), 71.7 (C-1''), 117.4 (C-3'), 126.0 (C_q), 129.5 (C-2'), 140.0 (C_q), 144.0 (C_q), 155.4 (C_q), 169.4 (CO); HRMS calcd for $C_{21}H_{25}N_6O_3$ $[M-H]^-$ 409.1994, found 409.2000.

Note: Four quaternary carbons were not visible on the ^{13}C NMR spectrum.

1-(4-((6-(Cyclohexylmethoxy)-9*H*-purin-2-yl)amino)phenyl)prop-2-en-1-one (389)

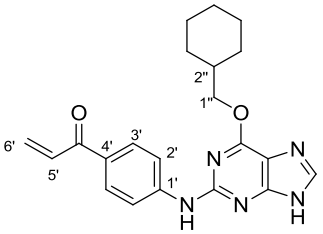

A solution of vinylmagnesium chloride (1.6M in THF, 0.36 mL) was added to a stirred solution of 4-((6-(cyclohexylmethoxy)-9*H*-purin-2-yl)amino)-*N*-methoxy-*N*-methyl benzamide **388** (53 mg, 0.13 mmol) in dry THF (1.2 mL) at 0 ^oC, under N_2. The reaction was stirred for 1 h at 0 ^oC and vinylmagnesium chloride (1.6M in THF, 0.10 mL) was added. The reaction was stirred for a further 1 h and a saturated aqueous solution of NH_4Cl (3 mL) was added. The organic phase was extracted with EtOAc (3 x 5 mL). The organic layer was dried over $MgSO_4$ and the solvent was removed *in vacuo*. The crude product was purified by MPC on silica (petrol: EtOAc 3: 7) to give the product **389** as a yellow oil (18 mg, 0.05 mmol, 36%).

R_f 0.42 (EtOAc 100); UV λ_{max} (EtOH) 335 nm; IR (cm^{-1}) 3263, 2923, 2850, 1662, 1594, 1529, 1392, 1177; ^1H NMR (500 MHz, DMSO-d_6) (ppm) δ 1.07-1.12 (2H, m, H-cyclo), 1.16-1.22 (1H, m, H-cyclo), 1.24-1.33 (2H, m, H-cyclo), 1.67-1.69 (1H, m, H-cyclo), 1.73-1.77 (2H, m, H-cyclo), 1.85-1.89 (3H, m, H-cyclo and H-2''), 4.38 (2H, d, *J* = 6.4 Hz, H-1''), 5.91 (1H, dd, *J* = 2.1 and 10.4 Hz, H-6'), 6.32 (1H, dd, *J* = 2.1 and 16.9 Hz, H-6'), 7.46 (1H, dd, *J* = 10.4 and 16.9 Hz, H-5'), 7.99 (2H, d, *J* = 9.0 Hz, H-2'), 8.01 (2H, d, *J* = 9.0 Hz, H-3'), 8.09 (1H, s, H-8), 9.87 (1H, br s, NH), 13.00 (1H, br s, N^9H); ^{13}C NMR (125 MHz, DMSO-d_6) (ppm) δ 25.7 (2 x C-cyclo), 26.5 (C-cyclo), 29.7 (2 x C-cyclo), 37.3 (C-2''), 71.8 (C-1''), 117.7 (C-3'), 129.2 (C-6'), 130.4 (C-2'), 132.7 (C-5'), 143.2 (C_q), 146.6 (C_q), 155.0 (C_q), 188.0 (CO); HRMS calcd for $C_{21}H_{24}N_5O_2$ $[M+H]^+$ 378.1925, found 378.1928.

Note: Four quaternary carbons were not visible on the ^{13}C NMR spectrum.

1-(4-((6-(Cyclohexylmethoxy)-9*H*-purin-2-yl)amino)phenyl)prop-2-yn-1-one (390)

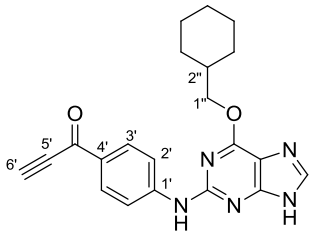

A solution of ethynylmagnesium bromide (0.5M in THF, 1.30 mL) was added to a stirred solution of 4-((6-(cyclohexylmethoxy)-9*H*-purin-2-yl)amino)-*N*-methoxy-*N*-methyl benzamide **388** (89 mg, 0.22 mmol) in dry THF (2.0 mL) at 0 ^{o}C, under N_2. The reaction was stirred for 1 h at 0 ^{o}C and for 18 h at r.t.. A saturated aqueous solution of NH_4Cl (5 mL) was added and the organic phase was extracted with EtOAc (3 x 5 mL). The organic layer was dried over $MgSO_4$ and the solvent was removed *in vacuo.* The crude product was purified by MPC on silica (petrol: EtOAc 3: 7) to give the product **390** as an orange oil (21 mg, 0.06 mmol, 25%).

R_f 0.43 (EtOAc 100); UV λ_{max} (EtOH) 367 nm; IR (cm^{-1}) 3251, 2922, 2850, 1664, 1591, 1528, 1382, 1168; ^{1}H NMR (500 MHz, DMSO-d_6) (ppm) δ 1.07-1.14 (2H, m, H-cyclo), 1.17-1.21 (1H, m, H-cyclo), 1.24-1.30 (2H, m, H-cyclo), 1.66-1.69 (1H, m, H-cyclo), 1.73-1.76 (2H, m, H-cyclo), 1.85-1.90 (3H, m, H-cyclo and H-2''), 4.38 (2H, d, *J* = 6.4 Hz, H-1''), 4.93 (1H, s, H-6'), 8.01 (2H, d, *J* = 9.0 Hz, H-2'), 8.04 (2H, d, *J* = 9.0 Hz, H-3'), 8.12 (1H, s, H-8), 10.04 (1H, br s, NH), 12.99 (1H, br s, N^9H); ^{13}C NMR (125 MHz, DMSO-d_6) (ppm) δ 25.7 (2 x C-cyclo), 26.5 (C-cyclo), 29.7 (2 x C-cyclo), 37.3 (C-2''), 71.9 (C-1''), 81.1 (C-5'), 84.5 (C-6'), 117.6 (C-3'), 118.9 (C_q), 128.8 (C_q), 131.2 (C-2'), 147.9 (C_q), 154.8 (C_q), 175.6 (CO); HRMS calcd for $C_{21}H_{22}N_5O_2$ $[M+H]^+$ 376.1768, found 376.1772.

Note: Three quaternary carbons were not visible on the ^{13}C NMR spectrum.

4-(2,6-Dichlorobenzamido)-*N*-(1-(vinylsulfonyl)piperidin-4-yl)-1*H*-pyrazole-3-carboxamide (395)

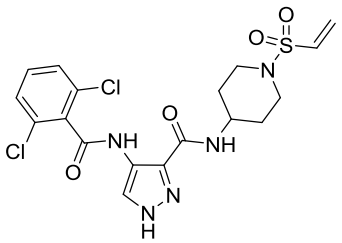

2-Chloroethanesulfonyl chloride (0.03 mL, 0.26 mmol) and DIPEA (0.09 mL, 0.52 mmol) were added to a stirred suspension of 4-(2,6-dichlorobenzamido)-*N*-(piperidin-4-yl)-1*H*-pyrazole-3-carboxamide **401** (100 mg, 0.26 mmol) in dry DCM (2.5 mL) under N_2. The resulting solution was stirred at r.t. for 1 h. Water (5 mL) was added and the organic phase was extracted with DCM (3 x 5 mL) and dried over $MgSO_4$. The solvent was removed *in vacuo* and the crude product was purified by MPC on silica (petrol: EtOAc 2: 3) to give the product **395** as a colourless oil (42 mg, 0.09 mmol, 34%).

R_f 0.76 (petrol: EtOAc 1: 4); UV λ_{max} (EtOH) 266 nm; IR (cm^{-1}) 3206, 2930, 1676, 1635, 1545, 1426; ^{1}H NMR (500 MHz, DMSO-d_6) (ppm) δ 1.66-1.73 (2H, m, H-pip), 1.80-1.83 (2H, m, H-pip), 2.66-2.71 (2H, m, H-pip), 3.52-3.54 (2H, m, H-pip), 3.82-3.88 (1H, m, H-pip), 6.14 (1H, dd, *J* = 0.9 and 16.5 Hz, H-vinyl), 6.16 (1H, dd, *J* = 0.9 and 10.0 Hz, H-vinyl), 6.80 (1H, dd, *J* = 10.0 and 16.5 Hz, H-vinyl), 7.53 (1H, dd, *J* = 6.9 and 9.2 Hz, H-ar), 7.58 (1H, d, *J* = 9.2 Hz, H-ar), 7.60 (1H, d, *J* = 6.9 Hz, H-ar), 8.36 (1H, s, H-5), 8.46 (1H, d, *J* = 8.6 Hz, NH), 10.15 (1H, s, NH), 13.43 (1H, br s, NH); ^{13}C NMR (125 MHz, DMSO-d_6) (ppm) δ 30.9 (2 x C-pip), 45.2 (2 x C-pip), 45.6 (C-pip), 121.2 (C-5), 122.0 (C_q), 128.9 (2 x C-ar), 129.3 (C-vinyl), 131.7 (C-ar), 132.4 (C_q), 133.6 (C-vinyl), 135.9 (C_q), 160.8 (CO), 163.2 (CO); HRMS calcd for $C_{18}H_{18}Cl_2N_5O_4S$ $[M^{35}Cl\text{-}H]^-$ 470.0462, found 470.0469, $[M^{37}Cl\text{-}H]^-$ 472.0432, found 472.0434, $[M^{39}Cl\text{-}H]^-$ 474.0402, found 474.0398.

***N*-(1-Acryloylpiperidin-4-yl)-4-(2,6-dichlorobenzamido)-1*H*-pyrazole-3-carboxamide (396)**

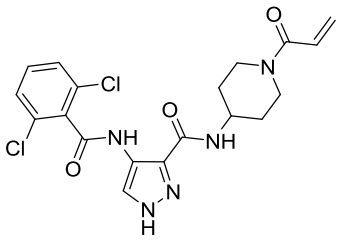

Acryloyl chloride (0.02 mL, 0.26 mmol) was added to a stirred suspension of 4-(2,6-dichlorobenzamido)-*N*-(piperidin-4-yl)-1*H*-pyrazole-3-carboxamide **401** (100 mg, 0.26 mmol) and DIPEA (0.05 mL, 0.29 mmol) in dry THF (2.5 mL) at 0 ^{o}C, under N_2. The resulting solution was stirred at 0 ^{o}C for 1 h. Water (5 mL) was added and the organic phase was extracted with DCM (3 x 5 mL), dried over $MgSO_4$. The solvent was removed *in vacuo* and the crude product was purified by MPC on silica (petrol: EtOAc 1: 9) to give the product **396** as a white solid (61 mg, 0.14 mmol, 53%).

R_f 0.21 (petrol: EtOAc 2: 3); Mp = 152-154 ^{o}C; UV λ_{max} (EtOH) 265 nm; IR (cm^{-1}) 3283, 2952, 1646, 1550, 1454; ^{1}H NMR (500 MHz, DMSO-d_6) (ppm) δ 1.49-1.54 (2H, m, H-pip), 1.75-1.79 (2H, m, H-pip), 2.66-2.71 (1H, m, H-pip), 3.07-3.12 (1H, m, H-pip), 3.98-4.08 (2H, m, H-pip), 4.40-4.43 (1H, m, H-pip), 5.67 (1H, dd, *J* = 2.4 and 10.4 Hz, H-vinyl), 6.10 (1H, dd, *J* = 2.4 and 16.7 Hz, H-ar), 6.82 (1H, dd, *J* = 10.4 and 16.7 Hz, H-vinyl), 7.53 (1H, dd, *J* = 6.9 and 9.1 Hz, H-ar), 7.59 (1H, d, *J* = 9.1 Hz, H-ar), 7.60 (1H, d, *J* = 6.9 Hz, H-ar), 8.36 (1H, s, H-5), 8.42 (1H, d, *J* = 8.0 Hz, NH), 10.17 (1H, s, NH), 13.41 (1H, s, NH); ^{13}C NMR (125 MHz, DMSO-d_6) (ppm) δ 31.4 (C-pip), 32.4 (C-pip), 41.2 (C-pip), 44.7 (C-pip), 46.4 (C-pip), 121.2 (C-5), 122.0 (C_q), 127.6 (C-vinyl), 128.9 (2 x C-ar), 129.0 (C-vinyl), 131.7 (2 x C_q), 132.4 (C-ar), 133.4 (C_q), 135.9 (C_q), 160.8 (CO), 163.1 (CO), 164.6 (CO); HRMS calcd for $C_{19}H_{18}Cl_2N_5O_3$ $[M^{35}Cl\text{-}H]^-$ 343.0797, found 434.0799, $[M^{37}Cl\text{-}H]^-$ 436.0763, found 436.0765, $[M^{39}Cl\text{-}H]^-$ 438.0734, found 438.0732.

***tert*-Butyl 4-(4-amino-1*H*-pyrazole-3-carboxamido)piperidine-1-carboxylate (399)**[84]

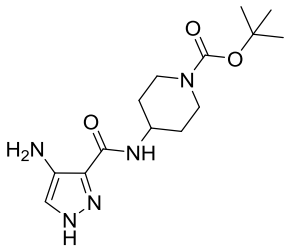

4-Aminopiperidine *N*1-boc **397** (4.20 g, 21.0 mmol), EDCI.HCl (4.40 g, 23.0 mmol) and HOAt (3.10 g, 23.0 mmol) were added to a stirred solution of 4-nitro-1*H*-pyrazole-3-carboxylic acid (3.00 g, 19.1 mmol) in dry DMF (40 mL) under N_2. The reaction was stirred at r.t. for 16 h. The solvent was removed *in vacuo*. The residue was triturated with water to form a beige solid which was collected by filtration. The crude material was solubilised in EtOH (250 mL) and DMF (40 mL) and was subjected to palladium catalyzed hydrogenation using an H-Cube® reactor and a 10% Pd/C CatCart. The reaction was conducted at 40 °C for 16 h. The solvent was removed *in vacuo* and the residue was resuspended in DCM (50 mL). The organic phase was washed with brine (3 x 50 mL), dried over $MgSO_4$ and the solvent was removed *in vacuo*. The crude product was purified by MPC on silica (EtOAc: MeOH 19: 1) to give the product **399** as a brown foam (2.10 g, 6.80 mmol, 36%).

R_f 0.47 (EtOAc 100); UV λ_{max} (EtOH) 287 nm; IR (cm^{-1}) 3323, 3270, 2957, 1669, 1648, 1526, 1428, 1146; ^{1}H NMR (500 MHz, DMSO-d_6) (ppm) δ 1.41 (9H, s, ^{t}Bu), 1.45-1.49 (2H, m, H-pip), 1.70-1.72 (2H, m, H-pip), 2.74-2.89 (2H, m, H-pip), 3.88-3.94 (3H, m, H-pip), 4.58 (2H, br s, NH_2), 7.10 (1H, s, H-5), 7.68 (1H, d, J = 8.3 Hz, NH), 12.50 (1H, s, NH); ^{13}C NMR (125 MHz, DMSO-d_6) (ppm) δ 28.6 (3 x CH_3), 31.9 (2 x C-pip), 40.6 (C-pip), 45.7 (2 x C-pip), 79.1 (C_q), 115.4 (C-5), 132.2 (C_q), 133.4 (C_q), 154.6 (CO), 162.8 (CO); HRMS calcd for $C_{14}H_{22}N_5O_3$ $[M-H]^-$ 308.1728, found 308.1735.

***tert*-Butyl-4-(4-(2,6-dichlorobenzamido)-1*H*-pyrazole-3-carboxamido) piperidine-1-carboxylate (400)**[84]

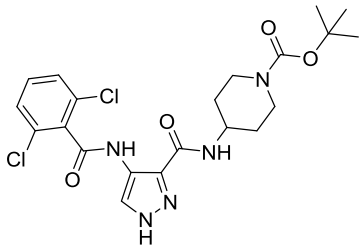

2,6-Dichlorobenzoic acid (1.34 g, 6.99 mmol) was added to a stirred solution of *tert*-butyl 4-(4-amino-1*H*-pyrazole-3-carboxamido)piperidine-1-carboxylate **399** (1.96 g, 6.36 mmol), EDCI.HCl (1.46 g, 7.63 mmol) and HOAt (1.03 g, 7.63 mmol) in dry DMF (100 mL). The resulting solution was stirred at r.t. for 72 h. The solvent was removed *in vacuo* and the residue was resuspended in DCM (50 mL). The organic phase was washed with brine (3 x 50 mL), dried over $MgSO_4$ and the solvent was removed *in vacuo*. The crude product was purified by MPC on silica (petrol: EtOAc 2: 3) to give the product **400** as an off-white solid (1.90 g, 3.94 mmol, 62%).

R_f 0.46 (petrol: EtOAc 1: 1); Mp = 197-199 ^oC; UV λ_{max} (EtOH) 263 nm; IR (cm^{-1}) 3364, 3200, 2995, 2868, 1672, 1649, 1574, 1542, 1430, 1143; ^1H NMR (500 MHz, DMSO-d_6) (ppm) δ 1.40 (9H, s, ^{t}Bu), 1.46-1.54 (2H, m, H-pip), 1.68-1.71 (2H, m, H-pip), 2.70-2.80 (2H, m, H-pip), 3.88-3.94 (3H, m, H-pip), 7.53 (1H, dd, *J* = 6.9 and 9.2 Hz, H-ar), 7.58 (1H, d, *J* = 9.2 Hz, H-ar), 7.60 (1H, d, *J* = 6.9 Hz, H-ar), 8.36 (1H, d, *J* = 1.3 Hz, H-5), 8.40 (1H, d, *J* = 8.4 Hz, NH), 10.17 (1H, s, NH), 13.43 (1H, s, NH); ^{13}C NMR (125 MHz, DMSO-d_6) (ppm) δ 28.6 (3 x CH_3), 31.5 (2 x C-pip), 40.6 (C-pip), 46.3 (2 x C-pip), 79.1 (C_q), 121.2 (C_q), 122.0 (C-5), 128.9 (C-ar), 129.1 (C-ar), 131.7 (C_q), 132.4 (C-ar), 133.4 (C_q), 134.4 (C_q), 135.8 (C_q), 154.4 (CO), 160.7 (CO), 163.1 (CO); HRMS calcd for $C_{21}H_{24}Cl_2N_5O_4$ $[M^{35}Cl\text{-}H]^-$ 480.1211, found 480.1216, $[M^{37}Cl\text{-}H]^-$ 482.1182, found 482.1183, $[M^{39}Cl\text{-}H]^-$ 484.1153, found 484.1150.

4-(2,6-Dichlorobenzamido)-*N*-(piperidin-4-yl)-1*H*-pyrazole-3-carboxamide (401)[84]

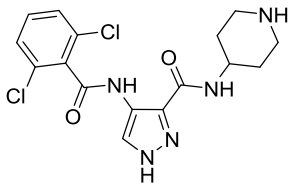

tert-Butyl 4-(4-(2,6-dichlorobenzamido)-1*H*-pyrazole-3-carboxamido)piperidine-1-carboxylate **400** (1.90 g, 3.94 mmol) was solubilised in TFE (40 mL) and the reaction mixture was sealed. The reaction was heated under MW at 160 ^{o}C, 12 bars, for 4 h. The solvent was removed *in vacuo* and the crude product was purified by MPC on amine silica (DCM: MeOH 49: 1) to give the product **401** as a beige solid (918 mg, 2.41 mmol, 61%).

R_f 0.37 (DCM: MeOH 9: 1); Mp = 270-273 ^{o}C; UV λ_{max} (EtOH) 266 nm; IR (cm^{-1}) 3409, 3312, 2942, 2828, 1654, 1574, 1537, 1423; ^{1}H NMR (500 MHz, DMSO-d_6) (ppm) δ 1.42-1.50 (2H, m, H-pip), 1.64-1.66 (2H, m, H-pip), 2.41-2.47 (2H, m, H-pip), 2.91-2.93 (2H, m, H-pip), 3.30 (1H, br s, NH), 3.73-3.79 (1H, m, H-pip), 7.53 (1H, dd, *J* = 6.9 and 9.1 Hz, H-ar), 7.58 (1H, d, *J* = 9.1 Hz, H-ar), 7.60 (1H, d, *J* = 6.9 Hz, H-ar), 8.25 (1H, d, *J* = 7.9 Hz, NH), 8.33 (1H, s, H-5), 10.19 (1H, br s, NH), 13.44 (1H, s, NH); ^{13}C NMR (125 MHz, DMSO-d_6) (ppm) δ 29.5 (C-pip), 33.2 (C-pip), 41.4 (C-pip), 45.8 (C-pip), 47.2 (C-pip), 121.9 (C-5), 128.9(2 x C-ar), 131.7 (2 x C_q), 132.3 (C-ar), 133.3 (C_q), 135.9 (C_q), 146.0 (C_q), 160.8 (CO), 162.7 (CO); HRMS calcd for $C_{16}H_{16}Cl_2N_5O_2$ [M^{35}Cl-H]$^-$ 380.0687, found 380.0691, [M^{37}Cl-H]$^-$ 382.0657, found 382.0657, [M^{39}Cl-H]$^-$ 384.0628, found 384.0624.

Methyl 2-mercaptobenzoate (405)[275]

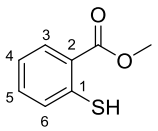

Concentrated H_2SO_4 (0.25 mL) was added slowly to a stirred solution of 2-mercaptobenzoic acid **404** (2.00 g, 13.0 mmol) in MeOH (10 mL). The reaction was refluxed for 48 h. The reaction was then cooled to 0 ^{o}C and a saturated aqueous solution of $NaHCO_3$ (15 mL) was added. The organic phase was extracted with EtOAc (3 x 20 mL), the phases were combined, dried over $MgSO_4$ and the solvent was removed *in vacuo* to give the product **405** as a yellow oil (1.94 g, 11.6 mmol, 89%).

R_f 0.80 (petrol: EtOAc 7: 3); UV λ_{max} (EtOH) 331 nm; IR (cm^{-1}) 2949, 1701, 1588, 1432, 1250, 1062; ^1H NMR (500 MHz, DMSO-d_6) (ppm) δ 3.85 (3H, s, OCH_3), 5.33 (1H, s, SH), 7.23 (1H, dd, *J* = 1.0 and 7.9 Hz, H-4), 7.43 (1H, dd, *J* = 1.5 and 7.9 Hz, H-5), 7.57 (1H, d, *J* = 7.9 Hz, H-6), 7.92 (1H, d, *J* = 7.9 Hz, H-3); ^{13}C NMR (125 MHz, DMSO-d_6) (ppm) δ 52.6 (CH_3), 125.2 (C-4), 126.1 (C-1), 131.5 (C-6), 131.6 (C-3), 133.2 (C-5), 138.6 (C-2), 166.6 (CO); HRMS calcd for $C_8H_7O_2S$ $[M-H]^-$ 167.0172, found 167.0173.

Methyl 2-((2-carbamoylphenyl)thio)acetate (407)

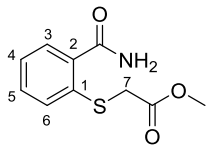

Formamide (0.36 mL, 8.93 mmol) was added to a stirred solution of methyl 2-mercaptobenzoate **405** (500 mg, 2.98 mmol) in dry DMF (21 mL) under N_2. The solution was heated at 70 ^oC for 5 min and NaOMe (25% wt/wt solution in MeOH, 1.57 mL, 6.85 mmol) was added. The mixture was then heated at 120 ^oC for 2 h. The reaction was cooled to r.t. and the solvent was removed *in vacuo*. The crude product was suspended in dry MeCN (12 mL) under N_2, and K_2CO_3 (451 mg, 3.27 mmol) and ethyl chloroacetate (0.35 mL, 3.27 mmol) were added. The reaction was stirred at r.t. for 1 h and then MeOH (10 mL) was added and the suspension was filtered through Celite. The solvent was removed *in vacuo* and the crude product was purified by MPC on silica (petrol: EtOAc 3: 7) to give the product **407** as a white solid (86 mg, 0.38 mmol, 13%).

R_f 0.15 (petrol: EtOAc 7: 3); Mp = 96-98 ^oC; UV λ_{max} (EtOH) 270 nm; IR (cm^{-1}) 3356, 3175, 2955, 1729, 1614, 1548, 1398, 1277; ^1H NMR (500 MHz, DMSO-d_6) (ppm) δ 3.64 (3H, s, OCH_3), 3.87 (2H, s, H-7), 7.21-7.24 (1H, m, H-4), 7.37-7.39 (1H, m, H-5), 7.39-7.42 (1H, m, H-6), 7.43 (1H, br s, NH_2), 7.50 (1H, dd, *J* = 1.2 and 7.6 Hz, H-3), 7.84 (1H, br s, NH_2); ^{13}C NMR (125 MHz, DMSO-d_6) (ppm) δ 35.0 (C-7), 52.7 (CH_3), 125.5 (C-4), 127.8 (C-5), 128.3 (C-3), 129.8 (C-1), 130.7 (C-6), 131.6 (C-2), 161.9 (CO), 170.5 (CO); HRMS calcd for $C_{10}H_{12}NO_3S$ $[M+H]^+$ 226.0532, found 226.0534.

Methyl 2-((2-carbamoylphenyl)sulfonyl)acetate (408)

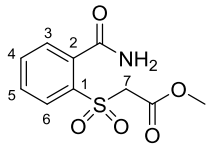

The title compound was synthesised following **general procedure M** using methyl 2-((2-carbamoylphenyl)thio)acetate **407** (85 mg, 0.38 mmol) and *m*-CPBA (136 mg, 0.79 mmol). The crude product was purified by MPC on silica (EtOAc 100) to give the product **408** as a colourless oil (72 mg, 0.28 mmol, 73%).

R_f 0.30 (EtOAc 100); UV λ_{max} (EtOH) 256 nm; IR (cm^{-1}) 3424, 3346, 2954, 1738, 1665, 1611, 1317, 1279; ^{1}H NMR (500 MHz, DMSO-d_6) (ppm) δ 3.61 (3H, s, OCH_3), 4.90 (2H, s, H-7), 7.62 (1H, dd, *J* = 1.2 and 7.5 Hz, H-3), 7.70 (1H, ddd, *J* = 1.2, 7.5 and 7.5 Hz, H-5), 7.74 (1H, br s, NH_2), 7.81 (1H, ddd, *J* = 1.2, 7.5 and 7.5 Hz, H-4), 7.94 (1H, dd, *J* = 1.2 and 7.5 Hz, H-6), 8.17 (1H, br s, NH_2); ^{13}C NMR (125 MHz, DMSO-d_6) (ppm) δ 53.0 (CH_3), 61.4 (C-7), 129.3 (C-3), 130.1 (C-5), 131.1 (C-6), 134.7 (C-4), 136.7 (C-2), 138.4 (C-1), 163.7 (CO), 170.0 (CO); HRMS calcd for $C_{10}H_{12}NO_5S$ $[M+H]^+$ 258.0431, found 258.0431.

4-Ethyl-1*H*-pyrazol-3-amine (412)[276]

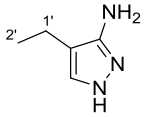

LiHMDS (1M in THF, 12.5 mL, 12.5 mmol) was added dropwise to a stirred solution of butyronitrile **410** (1.09 mL, 12.5 mmol) in dry THF (25 mL), under N_2, at -78 ^{o}C and the resulting solution was stirred at -78 ^{o}C for 1 h. A solution of ethylformate (0.50 mL, 6.25 mmol) in dry THF (0.8 mL) was added dropwise to the solution. The mixture was stirred at -78 ^{o}C for 30 min. A solution of saturated NH_4Cl (10 mL) was added at -78 oC to quench the reaction and stirred until reaching r.t. The organic phase was then extracted with EtOAc (3 x 15 mL). The organic phases were combine, dried over $MgSO_4$ and the solvent was removed *in vacuo* to give a yellow oil. The crude product was dissolved in EtOH (8.5 mL) and hydrazine (0.61 mL, 12.5 mmol) followed by AcOH (0.14 mL, 2.5 mmol) were added. The reaction was carried out in a MW vial so the reaction was sealed and heated at 80 ^{o}C for 40 h. The reaction was then cooled to r.t. and brine (30 mL) was added. The organic phase was extracted with EtOAc (8 x 40 mL). The organic phases were combined, dried over $MgSO_4$ and the solvent was removed *in vacuo*. The crude

product was purified by MPC on silica (EtOAc: MeOH 19: 5) to give the product **412** as a pale yellow solid (372 mg, 3.35 mmol, 54%).

R_f 0.27 (EtOAc 100); Mp = 49-50 ^oC; UV λ_{max} (EtOH) 256 nm; IR (cm^{-1}) 3318, 3167, 2960, 1492; ^1H NMR (500 MHz, DMSO-d_6) (ppm) 1.07 (3H, t, J = 7.6 Hz, H-2'), 2.24 (2H, q, J = 7.6 Hz, H-1'), 4.26 (1H, br s, NH_2), 7.11 (1H, s, H-5), 11.14 (1H, br s, NH); ^{13}C NMR (125 MHz, DMSO-d_6) (ppm) δ 15.0 (C-2'), 16.1 (C-1'), 126.4 (C-5); HRMS calcd for $C_5H_{10}N_3$ $[M+H]^+$ 112.0869, found 112.0867.

Note: Two quaternary carbons were not visible on the ^{13}C NMR spectrum.

3-Ethyl-7-hydroxypyrazolo[1,5-a]pyrimidin-5(4*H*)-one (413)[276]

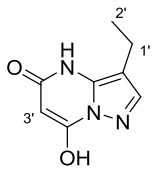

Dimethylmalonate (0.60 mL, 5.30 mmol) and NaOMe (25% wt/wt in MeOH, 3.00 mL, 14.4 mmol) were added to a stirred solution of 4-ethyl-1*H*-pyrazol-3-amine **412** (327 mg, 2.95 mmol) in dry MeOH (5 mL), under N_2. The resulting mixture was heated at reflux for 16 h. After completion, the reaction was cooled to r.t. and Celite (0.35 g) and water (3.6 mL) were added. The mixture was stirred for 10 min and filtered to remove the solid. The filtrate was adjusted to pH ~ 3 with aqueous HCl to effect precipitation. The precipitate was filtered and washed with water. The solid was dried to give the product **413** as a pale beige solid (393 mg, 2.20 mmol, 74%).

R_f 0.17 (EtOAc 100); Mp = degradation; UV λ_{max} (EtOH) 254 nm; IR (cm^{-1}) 3443, 3208, 1659, 1621, 1584; ^1H NMR (500 MHz, DMSO-d_6) (ppm) 1.40 (3H, t, J = 7.5 Hz, H-2'), 2.46 (2H, q, J = 7.5 Hz, H-1'), 3.14 (1H, br s, H-3'), 3.80 (1H, br s, OH), 7.65 (1H, s, H-5), 11.14 (1H, br s, NH); LRMS calcd for $C_8H_8N_3O_2$ $[M-H]^-$ 178.1, found 178.0.

Note: The ^1H NMR was recorded at 100 ^oC because of the keto-enol tautomerism. For the same reason, the ^{13}C NMR was not recorded.

Appendices

- **Kinetic Studies**

2-(3-((6-Ethynyl-9*H*-purin-2-yl)amino)phenyl)acetamide (42)

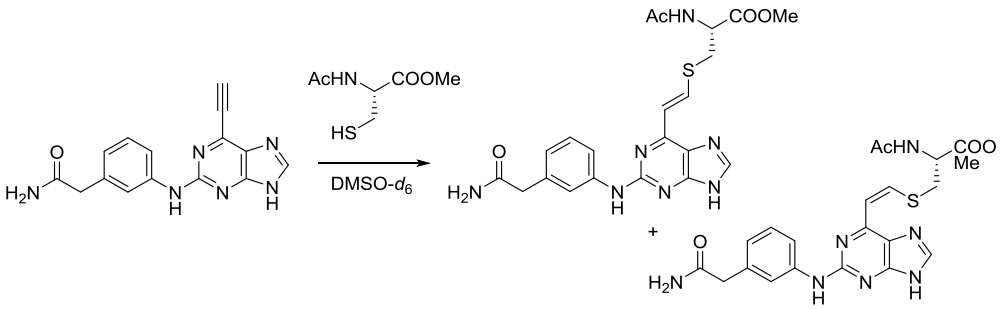

2-(3-((6-Ethynyl-9*H*-purin-2-yl)amino)phenyl)acetamide (**42**) (690 µL from stock solution DMSO-d_6, 1.23 mg, 4.2 µmol) was treated according to general procedure **R**. Disappearance of the singlet at 4.71-4.91 ppm was monitored as a function of time using the ^{1}H qNMR method outlined. Each spectrum was recorded every 10 min using 8 scans per experiment.

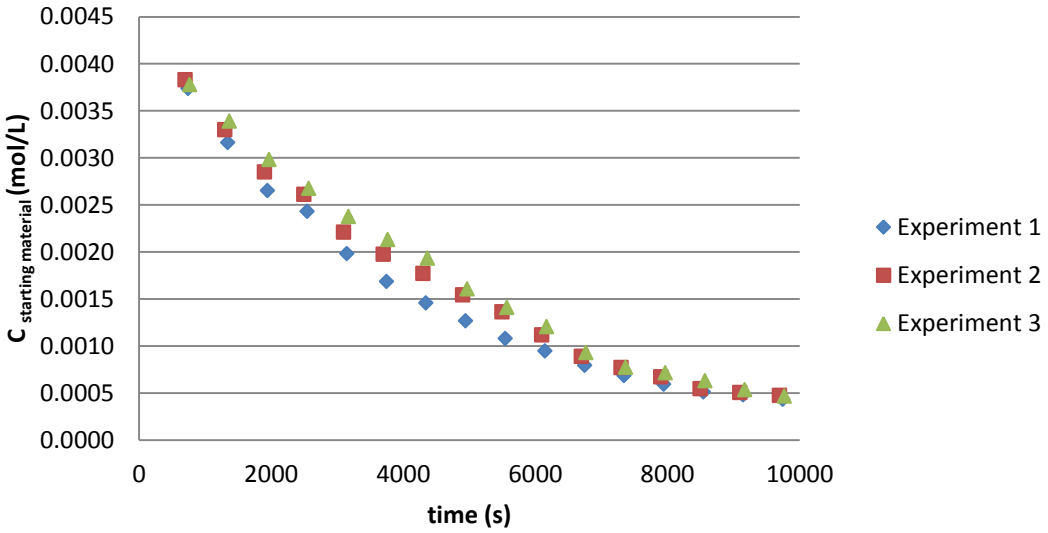

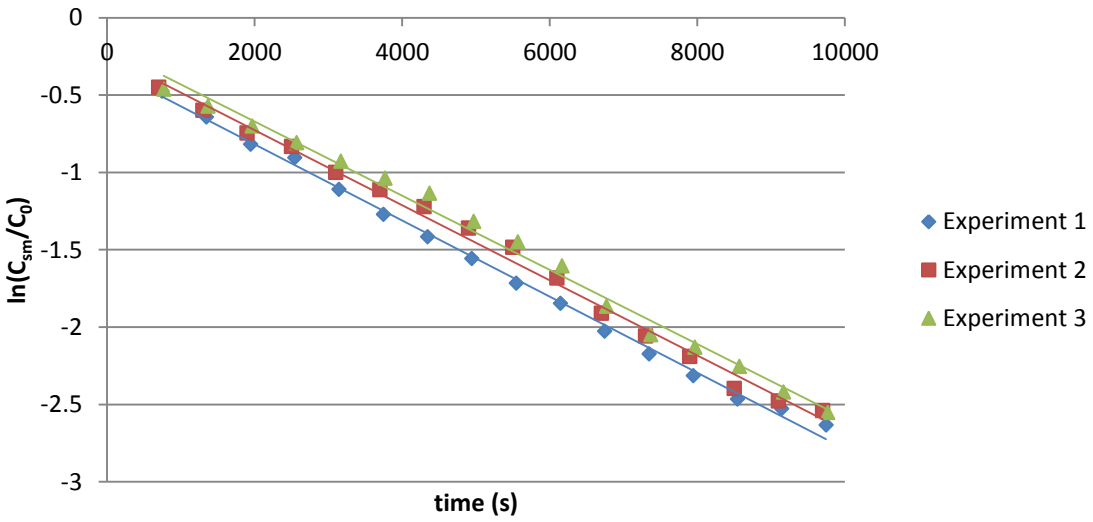

Experiment 1 (R^2 = 1.00; k_{app} = 2.50 × 10^{-4} s^{-1}; $t_{1/2}$ = 2773 s)

Time (s)	Baseline corrected integral	Concentration (mM)	Ln(C_{sm}/C_0)
0	1.00	6.00	0.00
744	0.62	3.74	-0.47
1344	0.53	3.16	-0.64
1944	0.44	2.65	-0.82
2544	0.41	2.43	-0.90
3144	0.33	1.98	-1.11
3744	0.28	1.69	-1.27
4344	0.24	1.46	-1.41
4944	0.21	1.27	-1.56
5544	0.18	1.08	-1.71
6144	0.16	0.95	-1.85
6744	0.13	0.79	-2.02
7344	0.11	0.68	-2.17
7944	0.10	0.59	-2.31
8544	0.09	0.51	-2.47
9144	0.08	0.48	-2.52
9744	0.07	0.43	-2.63

Experiment 2 (R^2 = 0.99; k_{app} = 2.43 × 10^{-4} s^{-1}; $t_{1/2}$ = 2852 s)

Time (s)	Baseline corrected integral	Concentration (mM)	Ln(C_{sm}/C_0)
0	1.00	6.00	0.00
698	0.64	3.83	-0.45
1298	0.55	3.30	-0.60
1898	0.48	2.85	-0.74
2498	0.44	2.61	-0.83
3098	0.37	2.21	-1.00
3698	0.33	1.97	-1.11
4298	0.30	1.77	-1.22

4898	0.26	1.54	-1.36
5498	0.23	1.36	-1.48
6098	0.19	1.12	-1.68
6698	0.15	0.89	-1.91
7298	0.13	0.77	-2.06
7898	0.11	0.67	-2.19
8498	0.09	0.55	-2.40
9098	0.08	0.50	-2.48
9698	0.08	0.47	-2.54

Experiment 3 ($R^2 = 0.99$; $k_{app} = 2.40 \times 10^{-4}$ s^{-1}; $t_{1/2} = 2888$ s)

Time (s)	Baseline corrected integral	Concentration (mM)	$Ln(C_{sm}/C_0)$
0	1.00	6.00	0.00
768	0.63	3.78	-0.46
1368	0.57	3.39	-0.57
1968	0.50	2.98	-0.70
2568	0.45	2.68	-0.81
3168	0.40	2.38	-0.93
3768	0.36	2.13	-1.04
4368	0.32	1.93	-1.13
4968	0.27	1.61	-1.32
5568	0.24	1.41	-1.45
6168	0.20	1.21	-1.60
6768	0.16	0.93	-1.86
7368	0.13	0.77	-2.05
7968	0.12	0.71	-2.13
8568	0.11	0.63	-2.25
9168	0.09	0.53	-2.42
9768	0.08	0.47	-2.55

6-Ethynyl-9-methyl-*N*-phenyl-9*H*-purin-2-amine (61)

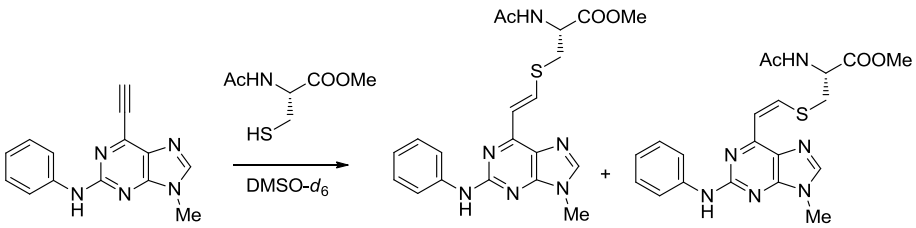

6-Ethynyl-9-methyl-*N*-phenyl-9*H*-purin-2-amine (**61**) (690 µL from stock solution DMSO-d_6, 1.05 mg, 4.2 µmol) was treated according to general procedure **R**. Disappearance of the singlet at 4.75-4.95 ppm was monitored as a function of time using the ^{1}H qNMR method outlined. Each spectrum was recorded every 10 min using 8 scans per experiment.

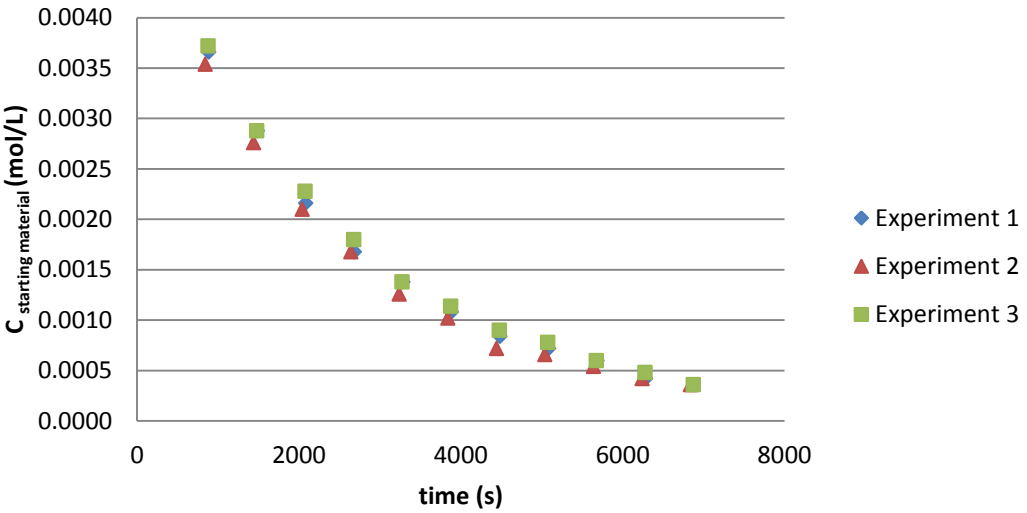

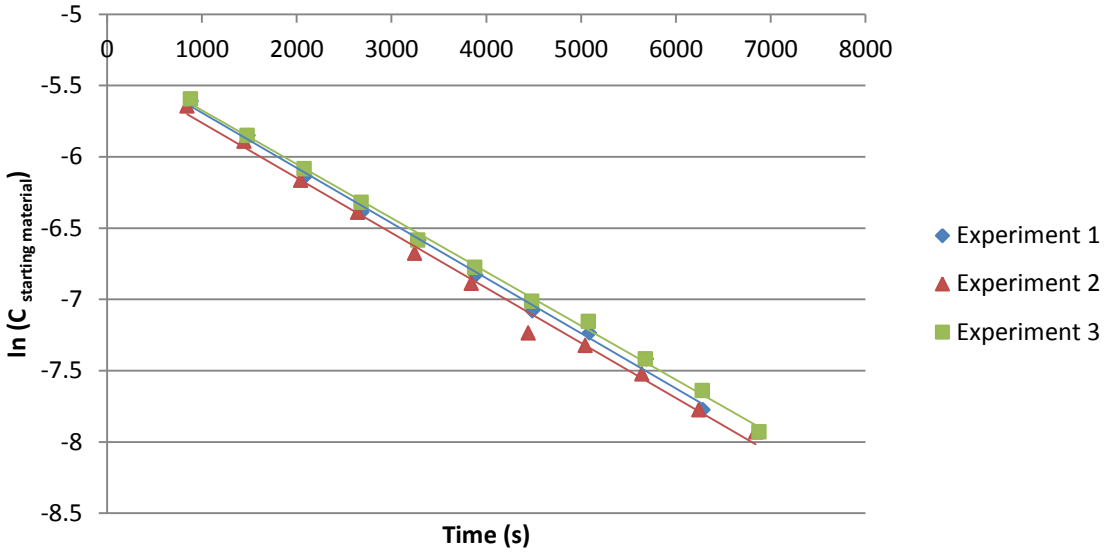

Experiment 1 (R^2 = 1.00, k_{app} = 3.87.10^{-4} s^{-1}; $t_{1/2}$ = 1829 s)

Time (s)	Baseline corrected integral	Concentration (mM)	Ln(C_{sm}/C_0)
0	1	6	-5.12
887	0.61	3.66	-5.61
1487	0.48	2.88	-5.85
2087	0.36	2.16	-6.14
2687	0.28	1.68	-6.39
3287	0.23	1.38	-6.59
3887	0.18	1.08	-6.83
4487	0.14	0.84	-7.08
5087	0.12	0.72	-7.24
5687	0.10	0.60	-7.42
6287	0.07	0.42	-7.78
6887	0.06	0.36	-7.93
7487	0.05	0.30	-8.11

Experiment 2 (R^2 = 0.99, k_{app} = 3.86.10^{-4} s^{-1}; $t_{1/2}$ = 1773 s)

Time (s)	Baseline corrected integral	Concentration (mM)	Ln(C_{sm}/C_0)
0	1	6	-5.12
842	0.59	3.54	-5.64
1442	0.46	2.76	-5.89
2042	0.35	2.10	-6.17
2642	0.28	1.68	-6.39
3242	0.21	1.26	-6.68
3842	0.17	1.02	-6.89
4442	0.12	0.72	-7.24
5042	0.11	0.66	-7.32
5642	0.09	0.54	-7.52
6242	0.07	0.42	-7.78
6842	0.06	0.36	-7.93
7442	0.04	0.24	-8.33

Experiment 3 (R^2 = 0.99, k_{app} = 3.01.10^{-4} s^{-1}; $t_{1/2}$ = 2303 s)

Time (s)	Baseline corrected integral	Concentration (mM)	Ln(C_{sm}/C_0)
0	1	6	-5.12
878	0.62	3.72	-5.59
1478	0.48	2.88	-5.85
2078	0.38	2.28	-6.08
2678	0.30	1.80	-6.32
3278	0.23	1.38	-6.59
3878	0.19	1.14	-6.78
4478	0.15	0.90	-7.01
5078	0.13	0.78	-7.16
5678	0.10	0.60	-7.42
6278	0.08	0.48	-7.64
6878	0.06	0.36	-7.93

6-Ethynyl-7-methyl-*N*-phenyl-7*H*-purin-2-amine (62)

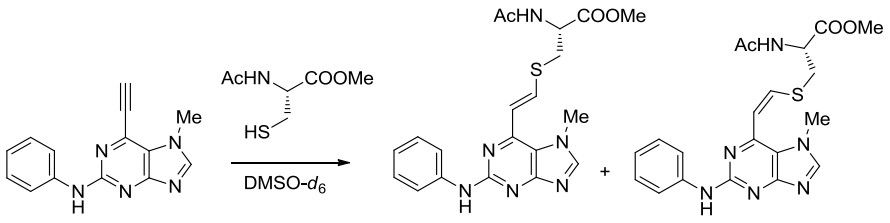

6-Ethynyl-7-methyl-*N*-phenyl-7*H*-purin-2-amine (**62**) (690 µL from stock solution DMSO-d_6, 1.05 mg, 4.2 µmol) was treated according to general procedure **R**. Disappearance of the singlet at 4.90-5.10 ppm was monitored as a function of time using

the ^{1}H qNMR method outlined. Each spectrum was recorded every 10 min using 8 scans per experiment.

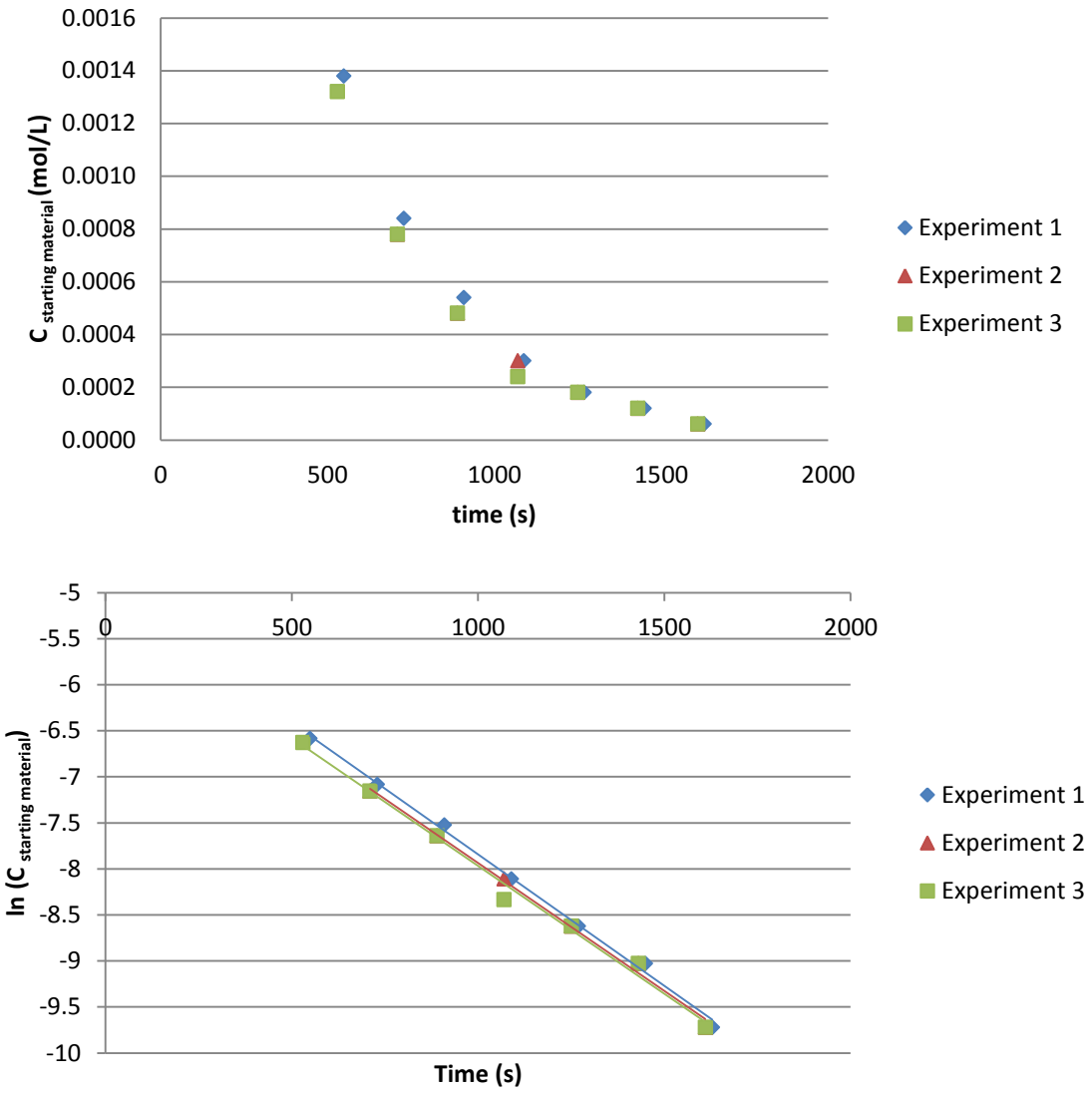

Experiment 1 (R^2 = 1.00, k_{app} = 28.57.10^{-4} s^{-1}; $t_{1/2}$ = 243 s)

Time (s)	Baseline corrected integral	Concentration (mM)	Ln(C_{sm}/C_0)
0	1	6	-5.12
549	0.23	1.38	-6.59
729	0.14	0.84	-7.08
909	0.09	0.54	-7.52
1089	0.05	0.30	-8.11
1269	0.03	0.18	-8.62
1449	0.02	0.12	-9.03
1626	0.01	0.06	-9.72

Experiment 2 (R^2 = 0.99, k_{app} = 27.77.10^{-4} s^{-1}; $t_{1/2}$ = 250 s)

Time (s)	Baseline corrected integral	Concentration (mM)	Ln(C_{sm}/C_0)
0	1	6	-5.12
710	0.13	0.78	-7.16
890	0.08	0.48	-7.64
1070	0.05	0.30	-8.11
1250	0.03	0.18	-8.62
1430	0.02	0.12	-9.03
1610	0.01	0.06	-9.72

Experiment 3 (R^2 = 0.99, k_{app} = 27.77.10^{-4} s^{-1}; $t_{1/2}$ = 250 s)

Time (s)	Baseline corrected integral	Concentration (mM)	Ln(C_{sm}/C_0)
0	1	6	-5.12
530	0.22	1.32	-6.63
710	0.13	0.78	-7.16
890	0.08	0.48	-7.64
1070	0.04	0.24	-8.33
1250	0.03	0.18	-8.62
1430	0.02	0.12	-9.03
1610	0.01	0.06	-9.72

2-(3-((6-Ethynyl-9-methyl-9*H*-purin-2-yl)amino)phenyl)acetamide (63)

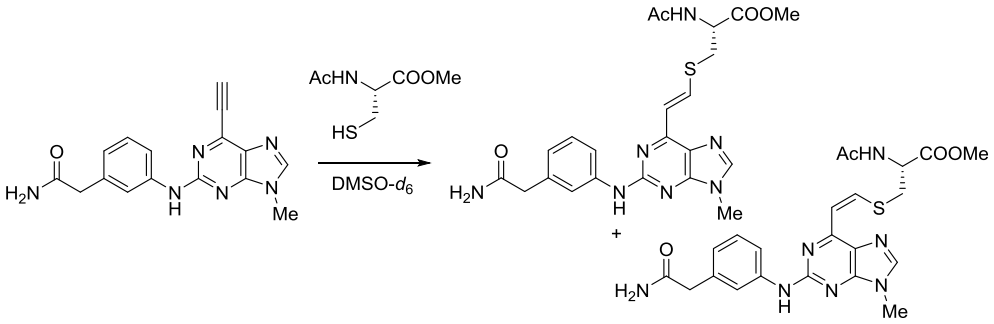

2-(3-((6-Ethynyl-9-methyl-9*H*-purin-2-yl)amino)phenyl)acetamide (**63**) (690 µL from stock solution DMSO-d_6, 1.29 mg, 4.2 µmol) was treated according to general procedure **R**. Disappearance of the singlet at 4.74-4.94 ppm was monitored as a function of time using the ^{1}H qNMR method outlined. Each spectrum was recorded every 10 min using 8 scans per experiment.

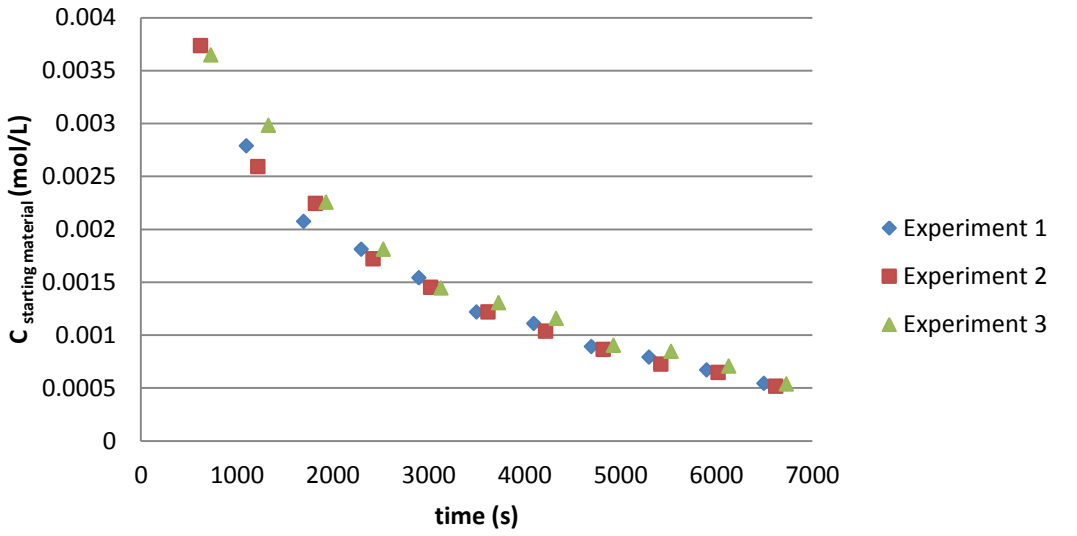

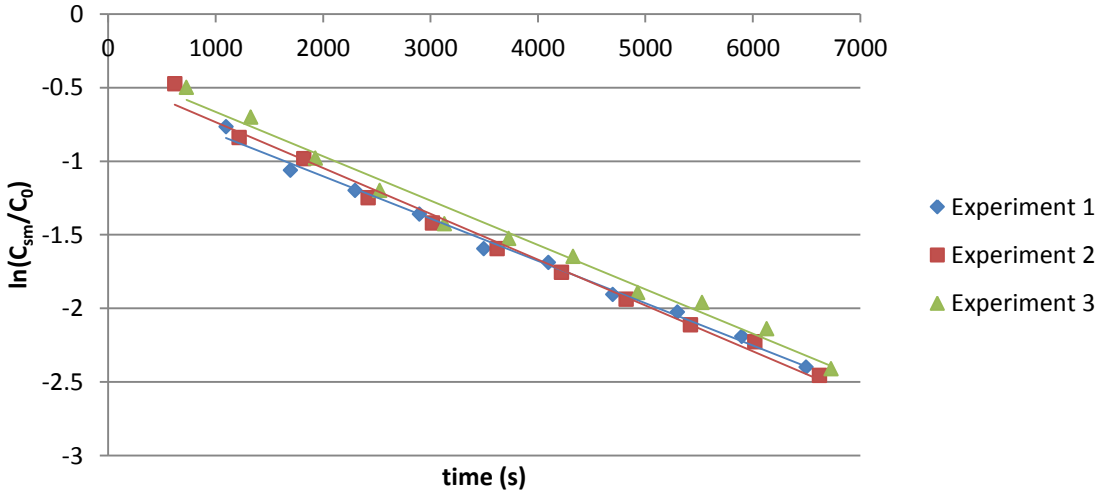

Experiment 1 (R^2 = 0.99, $k_{app} = 2.87.10^{-4}$ s^{-1}; $t_{1/2}$ = 2415 s)

Time (s)	Baseline corrected integral	Concentration (mM)	$Ln(C_{sm}/C_0)$
0	1.00	6.00	0.00
1097	0.47	2.79	-0.77
1697	0.35	2.08	-1.06
2297	0.30	1.81	-1.20
2897	0.26	1.54	-1.36
3497	0.20	1.22	-1.59
4097	0.19	1.11	-1.69
4697	0.15	0.89	-1.90
5297	0.13	0.79	-2.02
5897	0.11	0.67	-2.19
6497	0.09	0.55	-2.40

Experiment 2 (R^2 = 0.99, k_{app} = 3.11.10^{-4} s^{-1}; $t_{1/2}$ = 2229 s)

Time (s)	Baseline corrected integral	Concentration (mM)	Ln(C_{sm}/C_0)
0	1.00	6.00	0.00
620	0.62	3.74	-0.47
1220	0.43	2.59	-0.84
1820	0.37	2.24	-0.98
2420	0.29	1.72	-1.25
3020	0.24	1.45	-1.42
3620	0.20	1.22	-1.59
4220	0.17	1.04	-1.75
4820	0.14	0.86	-1.94
5420	0.12	0.73	-2.11
6020	0.11	0.65	-2.23
6620	0.09	0.52	-2.45

Experiment 3 (R^2 = 0.99, k_{app} = 3.01.10^{-4} s^{-1}; $t_{1/2}$ = 2303 s)

Time (s)	Baseline corrected integral	Concentration (mM)	Ln(C_{sm}/C_0)
0	1.00	6.00	0.00
728	0.61	3.65	-0.50
1328	0.50	2.98	-0.70
1928	0.38	2.26	-0.98
2528	0.30	1.81	-1.20
3128	0.24	1.45	-1.42
3728	0.22	1.31	-1.52
4328	0.19	1.16	-1.65
4928	0.15	0.91	-1.89
5528	0.14	0.85	-1.96
6128	0.12	0.71	-2.14
6728	0.09	0.54	-2.41

2-(3-((6-Ethynyl-7-methyl-7*H*-purin-2-yl)amino)phenyl)acetamide (64)

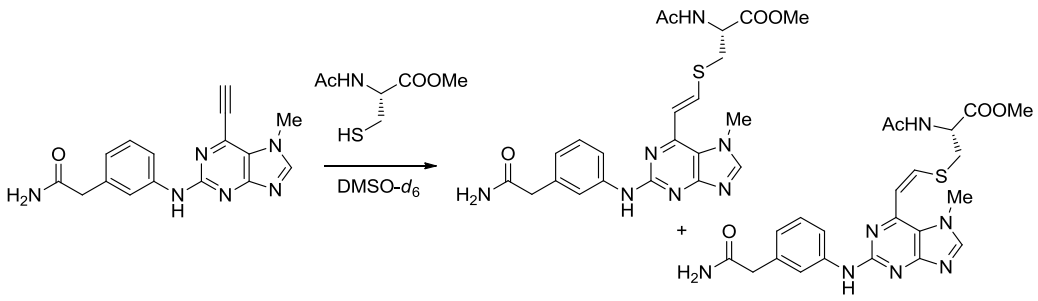

2-(3-((6-Ethynyl-7-methyl-7*H*-purin-2-yl)amino)phenyl)acetamide (**64**) (690 µL from stock solution DMSO-d_6, 1.29 mg, 4.2 µmol) was treated according to general procedure **R**. Disappearance of the singlet at 4.90-5.10 ppm was monitored as a function of time

using the ^{1}H qNMR method outlined. Each spectrum was recorded every 3 min using 4 scans per experiment.

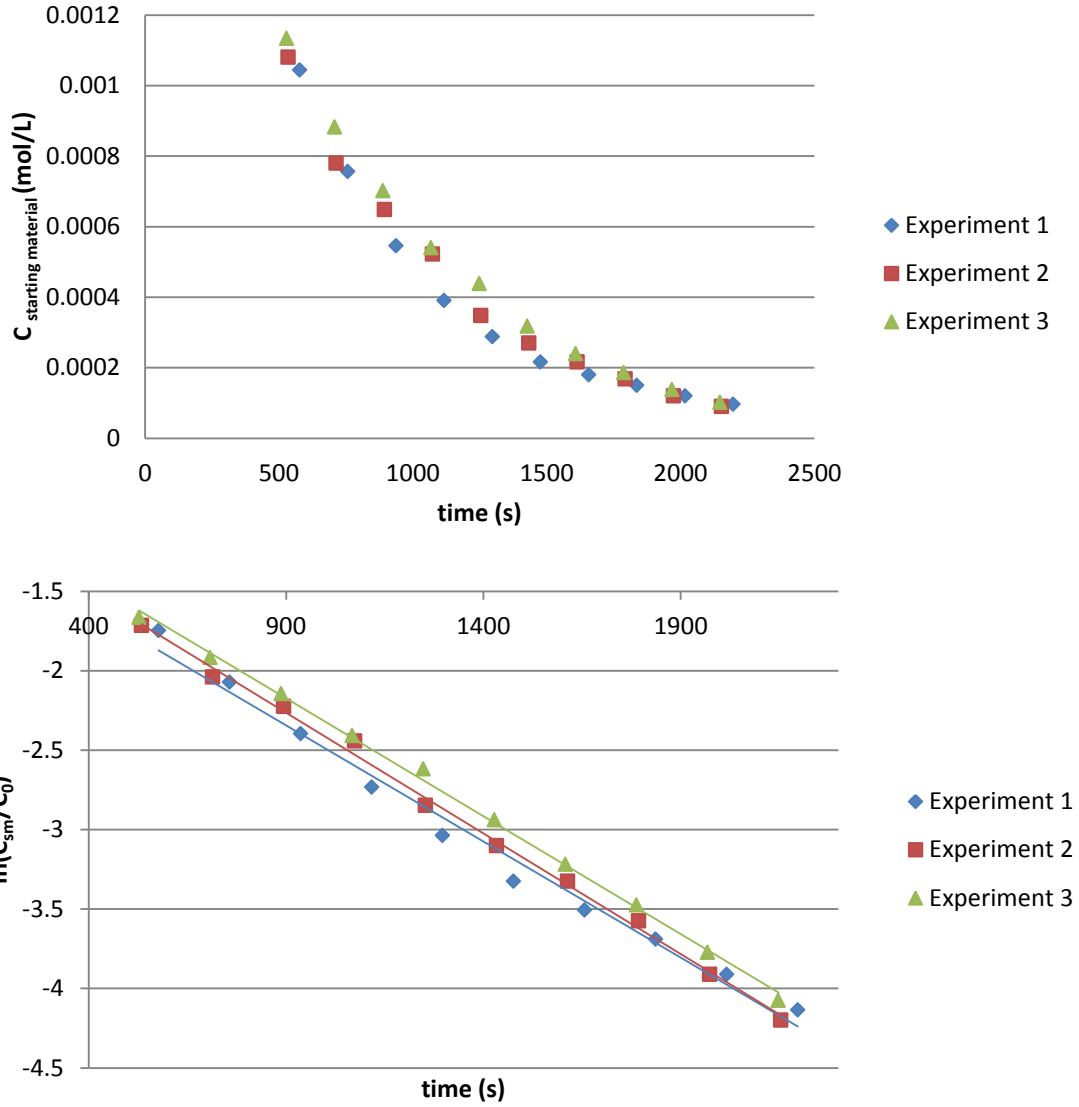

Experiment 1 (R^2 = 0.99, k_{app} = 14.62.10^{-4} s^{-1}; $t_{1/2}$ = 474 s)

Time (s)	Baseline corrected integral	Concentration (mM)	Ln(C_{sm}/C_0)
0	1.00	6.00	0.00
577	0.17	1.04	-1.75
757	0.13	0.76	-2.07
937	0.09	0.55	-2.40
1117	0.07	0.39	-2.73
1297	0.05	0.29	-3.04
1477	0.04	0.22	-3.32
1657	0.03	0.18	-3.51
1837	0.03	0.15	-3.69
2017	0.02	0.12	-3.91
2197	0.02	0.10	-4.14

Experiment 2 (R^2 = 1.00, $k_{app} = 15.19.10^{-4}$ s^{-1}; $t_{1/2}$ = 468 s)

Time (s)	Baseline corrected integral	Concentration (mM)	$Ln(C_{sm}/C_0)$
0	1.00	6.00	0.00
534	0.18	1.08	-1.71
714	0.13	0.78	-2.04
894	0.11	0.65	-2.23
1074	0.09	0.52	-2.44
1254	0.06	0.35	-2.85
1434	0.05	0.27	-3.10
1614	0.04	0.22	-3.32
1794	0.03	0.17	-3.58
1974	0.02	0.12	-3.91
2154	0.02	0.09	-4.20

Experiment 3 (R^2 = 1.00, $k_{app} = 14.83.10^{-4}$ s^{-1}; $t_{1/2}$ = 467 s)

Time (s)	Baseline corrected integral	Concentration (mM)	$Ln(C_{sm}/C_0)$
0	1.00	6.00	0.00
528	0.19	1.13	-1.67
708	0.15	0.88	-1.92
888	0.12	0.70	-2.15
1068	0.09	0.54	-2.41
1248	0.07	0.44	-2.62
1428	0.05	0.32	-2.94
1608	0.04	0.24	-3.22
1788	0.03	0.19	-3.47
1968	0.02	0.14	-3.78
2148	0.02	0.10	-4.07

- **Small molecule *X*-ray Crystallography Data**

2-Iodopurine **101**

Table 24 - Crystal data and structure refinement for **101**

Identification code	rjg12	
Chemical formula (moiety)	$C_{13}H_{17}IN_4O$	
Chemical formula (total)	$C_{13}H_{17}IN_4O$	
Formula weight	372.21	
Temperature	150(2) K	
Radiation, wavelength	MoKα, 0.71073 Å	
Crystal system, space group	monoclinic, $P12_1/c1$	
Unit cell parameters	a = 20.6041(14) Å	α = 90°
	b = 10.2213(6) Å	β = 90.370(7)°
	c = 6.8832(5) Å	γ = 90°
Cell volume	1449.58(17) $Å^3$	

Z	4
Calculated density	1.705 g/cm^3
Absorption coefficient μ	2.208 mm^{-1}
F(000)	736
Crystal colour and size	colourless, 0.30 × 0.10 × 0.02 mm^3
Reflections for cell refinement	2746 (θ range 2.8 to 28.5°)
Data collection method	Xcalibur, Atlas, Gemini ultra thick-slice ω scans
θ range for data collection	2.8 to 26.0°
Index ranges	h –25 to 25, k –12 to 12, l –7 to 8
Completeness to θ = 26.0°	97.4 %
Reflections collected	2784
Independent reflections	2784 (R_{int} = 0.0000)
Reflections with $F^2>2\sigma$	2450
Absorption correction	semi-empirical from equivalents
Min. and max. transmission	0.5572 and 0.9572
Structure solution	direct methods
Refinement method	Full-matrix least-squares on F^2
Weighting parameters a, b	0.0458, 7.7247
Data / restraints / parameters	2784 / 0 / 173
Final R indices [$F^2>2\sigma$]	R1 = 0.0428, wR2 = 0.1064
R indices (all data)	R1 = 0.0500, wR2 = 0.1115
Goodness-of-fit on F^2	1.064
Largest and mean shift/su	0.000 and 0.000
Largest diff. peak and hole	1.66 and –0.67 e Å^{-3}

Table 25 - Atomic coordinates and equivalent isotropic displacement parameters (Å^2) for **101**. U_{eq} is defined as one third of the trace of the orthogonalised U^{ij} tensor.

	x	**y**	**z**	**U_{eq}**
I	0.21039(2)	0.12326(3)	0.36754(7)	0.03328(16)
O	0.22906(16)	–0.3834(3)	0.4345(6)	0.0180(8)
N(1)	0.08634(19)	–0.4141(4)	0.3291(6)	0.0147(9)
N(2)	0.0243(2)	–0.2366(5)	0.2696(6)	0.0204(10)
N(3)	0.1075(2)	–0.0724(4)	0.3211(6)	0.0179(9)
N(4)	0.21187(19)	–0.1611(4)	0.4056(6)	0.0141(8)
C(1)	0.1043(2)	–0.5508(5)	0.3523(9)	0.0206(11)
C(2)	0.0272(3)	–0.3658(6)	0.2795(8)	0.0229(12)
C(3)	0.0857(2)	–0.1983(5)	0.3170(7)	0.0170(10)
C(4)	0.1687(2)	–0.0659(5)	0.3635(7)	0.0153(10)
C(5)	0.1902(2)	–0.2830(5)	0.3982(7)	0.0119(10)
C(6)	0.1249(2)	–0.3055(5)	0.3533(7)	0.0135(10)
C(7)	0.2968(2)	–0.3587(5)	0.4761(9)	0.0220(12)
C(8)	0.3386(2)	–0.4332(5)	0.3344(8)	0.0144(10)
C(9)	0.4094(2)	–0.3923(6)	0.3628(11)	0.0316(14)
C(10)	0.4542(3)	–0.4665(7)	0.2284(11)	0.0393(17)
C(11)	0.4466(3)	–0.6126(6)	0.2540(11)	0.0344(15)
C(12)	0.3765(3)	–0.6557(7)	0.2254(10)	0.0349(15)
C(13)	0.3314(2)	–0.5791(5)	0.3557(9)	0.0209(11)

Table 26 - Bond lengths [Å] and angles [°] for **101**

I–C(4)	2.116(5)	O–C(5)	1.324(6)
O–C(7)	1.445(6)	N(1)–C(1)	1.453(7)
N(1)–C(2)	1.357(7)	N(1)–C(6)	1.375(6)
N(2)–C(2)	1.323(8)	N(2)–C(3)	1.362(7)
N(3)–C(3)	1.364(7)	N(3)–C(4)	1.295(7)
N(4)–C(4)	1.348(6)	N(4)–C(5)	1.325(6)
C(1)–H(1A)	0.980	C(1)–H(1B)	0.980
C(1)–H(1C)	0.980	C(2)–H(2A)	0.950
C(3)–C(6)	1.382(7)	C(5)–C(6)	1.397(6)
C(7)–H(7A)	0.990	C(7)–H(7B)	0.990
C(7)–C(8)	1.511(7)	C(8)–H(8A)	1.000
C(8)–C(9)	1.529(6)	C(8)–C(13)	1.506(7)
C(9)–H(9A)	0.990	C(9)–H(9B)	0.990
C(9)–C(10)	1.515(9)	C(10)–H(10A)	0.990
C(10)–H(10B)	0.990	C(10)–C(11)	1.512(9)
C(11)–H(11A)	0.990	C(11)–H(11B)	0.990
C(11)–C(12)	1.522(9)	C(12)–H(12A)	0.990
C(12)–H(12B)	0.990	C(12)–C(13)	1.513(8)
C(13)–H(13A)	0.990	C(13)–H(13B)	0.990
C(5)–O–C(7)	119.0(4)	C(1)–N(1)–C(2)	127.2(4)
C(1)–N(1)–C(6)	128.1(4)	C(2)–N(1)–C(6)	104.7(4)
C(2)–N(2)–C(3)	103.5(4)	C(3)–N(3)–C(4)	111.9(4)
C(4)–N(4)–C(5)	116.7(4)	N(1)–C(1)–H(1A)	109.5
N(1)–C(1)–H(1B)	109.5	N(1)–C(1)–H(1C)	109.5
H(1A)–C(1)–H(1B)	109.5	H(1A)–C(1)–H(1C)	109.5
H(1B)–C(1)–H(1C)	109.5	N(1)–C(2)–N(2)	114.6(5)
N(1)–C(2)–H(2A)	122.7	N(2)–C(2)–H(2A)	122.7
N(2)–C(3)–N(3)	125.5(5)	N(2)–C(3)–C(6)	110.8(5)
N(3)–C(3)–C(6)	123.6(4)	I–C(4)–N(3)	116.4(4)
I–C(4)–N(4)	113.0(3)	N(3)–C(4)–N(4)	130.7(5)
O–C(5)–N(4)	121.2(4)	O–C(5)–C(6)	119.7(4)
N(4)–C(5)–C(6)	119.1(4)	N(1)–C(6)–C(3)	106.4(4)
N(1)–C(6)–C(5)	135.6(5)	C(3)–C(6)–C(5)	118.0(4)
O–C(7)–H(7A)	109.7	O–C(7)–H(7B)	109.7
O–C(7)–C(8)	109.8(4)	H(7A)–C(7)–H(7B)	108.2
H(7A)–C(7)–C(8)	109.7	H(7B)–C(7)–C(8)	109.7
C(7)–C(8)–H(8A)	108.2	C(7)–C(8)–C(9)	109.1(4)
C(7)–C(8)–C(13)	112.3(4)	H(8A)–C(8)–C(9)	108.2
H(8A)–C(8)–C(13)	108.2	C(9)–C(8)–C(13)	110.6(4)
C(8)–C(9)–H(9A)	109.3	C(8)–C(9)–H(9B)	109.3
C(8)–C(9)–C(10)	111.7(5)	H(9A)–C(9)–H(9B)	107.9
H(9A)–C(9)–C(10)	109.3	H(9B)–C(9)–C(10)	109.3
C(9)–C(10)–H(10A)	109.4	C(9)–C(10)–H(10B)	109.4
C(9)–C(10)–C(11)	111.1(5)	H(10A)–C(10)–H(10B)	108.0
H(10A)–C(10)–C(11)	109.4	H(10B)–C(10)–C(11)	109.4
C(10)–C(11)–H(11A)	109.3	C(10)–C(11)–H(11B)	109.3
C(10)–C(11)–C(12)	111.7(5)	H(11A)–C(11)–H(11B)	107.9
H(11A)–C(11)–C(12)	109.3	H(11B)–C(11)–C(12)	109.3
C(11)–C(12)–H(12A)	109.4	C(11)–C(12)–H(12B)	109.4
C(11)–C(12)–C(13)	111.1(5)	H(12A)–C(12)–H(12B)	108.0
H(12A)–C(12)–C(13)	109.4	H(12B)–C(12)–C(13)	109.4

C(8)–C(13)–C(12)	113.2(5)	C(8)–C(13)–H(13A)	108.9
C(8)–C(13)–H(13B)	108.9	C(12)–C(13)–H(13A)	108.9
C(12)–C(13)–H(13B)	108.9	H(13A)–C(13)–H(13B)	107.8

Table 27 - Anisotropic displacement parameters ($Å^2$) for **101**. The anisotropic displacement factor exponent takes the form: $-2\pi^2[h^2a^{*2}U^{11} + ...+ 2hka^*b^*U^{12}]$

	U^{11}	U^{22}	U^{33}	U^{23}	U^{13}	U^{12}
I	0.0448(3)	0.0198(2)	0.0353(2)	0.00089(17)	–0.00130(19)	–0.00403(17)
O	0.0092(16)	0.0121(17)	0.033(2)	–0.0038(16)	–0.0034(15)	0.0010(13)
N(1)	0.0085(18)	0.020(2)	0.016(2)	–0.0026(18)	–0.0008(16)	–0.0017(16)
N(2)	0.0107(19)	0.033(3)	0.018(2)	0.002(2)	–0.0017(17)	0.0053(19)
N(3)	0.022(2)	0.018(2)	0.014(2)	–0.0005(18)	0.0008(18)	0.0061(18)
N(4)	0.0110(18)	0.017(2)	0.015(2)	0.0013(17)	0.0013(17)	0.0001(17)
C(1)	0.016(2)	0.018(3)	0.027(3)	–0.003(2)	0.000(2)	–0.004(2)
C(2)	0.011(2)	0.038(3)	0.019(3)	–0.002(3)	–0.005(2)	0.000(2)
C(3)	0.018(2)	0.022(3)	0.011(2)	0.001(2)	0.0010(19)	0.004(2)
C(4)	0.022(2)	0.012(2)	0.012(2)	0.001(2)	0.003(2)	0.000(2)
C(5)	0.009(2)	0.014(2)	0.012(2)	–0.001(2)	0.0011(18)	0.0025(18)
C(6)	0.014(2)	0.016(2)	0.010(2)	0.002(2)	0.0025(19)	–0.0001(19)
C(7)	0.008(2)	0.023(3)	0.035(3)	–0.010(2)	–0.008(2)	0.000(2)
C(8)	0.006(2)	0.017(2)	0.021(3)	0.004(2)	0.0003(19)	0.0001(18)
C(9)	0.010(2)	0.024(3)	0.060(4)	–0.008(3)	0.005(3)	–0.006(2)
C(10)	0.017(3)	0.045(4)	0.056(4)	–0.003(4)	0.012(3)	0.001(3)
C(11)	0.022(3)	0.036(4)	0.045(4)	–0.011(3)	0.008(3)	0.008(3)
C(12)	0.032(3)	0.032(3)	0.041(4)	–0.018(3)	–0.003(3)	0.009(3)
C(13)	0.016(2)	0.012(2)	0.034(3)	–0.001(2)	0.001(2)	–0.003(2)

Table 28 - Hydrogen coordinates and isotropic displacement parameters ($Å^2$) for **101**.

	x	y	z	U
H(1A)	0.0665	–0.6062	0.3245	0.031
H(1B)	0.1191	–0.5660	0.4860	0.031
H(1C)	0.1393	–0.5723	0.2621	0.031
H(2A)	–0.0092	–0.4202	0.2539	0.028
H(7A)	0.3071	–0.3867	0.6105	0.026
H(7B)	0.3058	–0.2639	0.4654	0.026
H(8A)	0.3249	–0.4085	0.1997	0.017
H(9A)	0.4136	–0.2973	0.3376	0.038
H(9B)	0.4226	–0.4087	0.4992	0.038
H(10A)	0.4443	–0.4427	0.0920	0.047
H(10B)	0.4998	–0.4414	0.2561	0.047
H(11A)	0.4614	–0.6376	0.3860	0.041
H(11B)	0.4744	–0.6585	0.1590	0.041
H(12A)	0.3636	–0.6423	0.0881	0.042
H(12B)	0.3727	–0.7501	0.2550	0.042
H(13A)	0.2860	–0.6037	0.3251	0.025
H(13B)	0.3402	–0.6035	0.4926	0.025

Table 29 - Torsion angles [°] for **101**.

C(3)–N(2)–C(2)–N(1)	–0.3(6)	C(1)–N(1)–C(2)–N(2)	179.7(5)
C(6)–N(1)–C(2)–N(2)	0.0(6)	C(2)–N(2)–C(3)–N(3)	177.9(5)
C(2)–N(2)–C(3)–C(6)	0.5(6)	C(4)–N(3)–C(3)–N(2)	–177.3(5)
C(4)–N(3)–C(3)–C(6)	–0.3(7)	C(3)–N(3)–C(4)–I	178.3(3)
C(3)–N(3)–C(4)–N(4)	–1.2(8)	C(5)–N(4)–C(4)–I	–177.3(3)
C(5)–N(4)–C(4)–N(3)	2.3(8)	C(7)–O–C(5)–N(4)	–2.2(7)
C(7)–O–C(5)–C(6)	178.5(5)	C(4)–N(4)–C(5)–O	179.0(4)
C(4)–N(4)–C(5)–C(6)	–1.7(7)	C(1)–N(1)–C(6)–C(3)	–179.4(5)
C(1)–N(1)–C(6)–C(5)	2.5(9)	C(2)–N(1)–C(6)–C(3)	0.3(5)
C(2)–N(1)–C(6)–C(5)	–177.9(6)	N(2)–C(3)–C(6)–N(1)	–0.5(5)
N(2)–C(3)–C(6)–C(5)	178.0(4)	N(3)–C(3)–C(6)–N(1)	–177.9(4)
N(3)–C(3)–C(6)–C(5)	0.6(7)	O–C(5)–C(6)–N(1)	–2.3(9)
O–C(5)–C(6)–C(3)	179.8(4)	N(4)–C(5)–C(6)–N(1)	178.4(5)
N(4)–C(5)–C(6)–C(3)	0.4(7)	C(5)–O–C(7)–C(8)	–123.3(5)
O–C(7)–C(8)–C(9)	172.6(5)	O–C(7)–C(8)–C(13)	–64.4(6)
C(7)–C(8)–C(9)–C(10)	178.4(5)	C(13)–C(8)–C(9)–C(10)	54.4(7)
C(8)–C(9)–C(10)–C(11)	–55.8(8)	C(9)–C(10)–C(11)–C(12)	55.5(8)
C(10)–C(11)–C(12)–C(13)	–53.9(8)	C(7)–C(8)–C(13)–C(12)	–175.8(5)
C(9)–C(8)–C(13)–C(12)	–53.6(7)	C(11)–C(12)–C(13)–C(8)	53.6(7)

N^7-methylpurine **64**

Table 30 - Crystal data and structure refinement for **64**.

Identification code	rjg12
Chemical formula (moiety)	$C_{16}H_{14}N_6O \cdot 0.5CH_4O$
Chemical formula (total)	$C_{16.50}H_{16}N_6O_{1.50}$
Formula weight	322.35
Temperature	150(2) K
Radiation, wavelength	MoKα, 0.71073 Å
Crystal system, space group	monoclinic, $P12_1/n1$
Unit cell parameters	a = 15.3730(7) Å α = 90° b = 14.1912(4) Å β = 117.831(6)° c = 16.2612(7) Å γ = 90°
Cell volume	3137.2(2) $Å^3$
Z	8
Calculated density	1.365 g/cm^3
Absorption coefficient μ	0.093 mm^{-1}
F(000)	1352
Crystal colour and size	yellow, 0.30 × 0.30 × 0.20 mm^3
Reflections for cell refinement	10793 (θ range 2.9 to 28.6°)
Data collection method	Xcalibur, Atlas, Gemini ultra thick-slice ω scans
θ range for data collection	2.9 to 28.6°
Index ranges	h –20 to 20, k –19 to 16, l –20 to 21

Completeness to θ = 25.0°	99.9 %
Reflections collected	22860
Independent reflections	6971 (R_{int} = 0.0256)
Reflections with $F^2>2\sigma$	5642
Absorption correction	semi-empirical from equivalents
Min. and max. transmission	0.9725 and 0.9816
Structure solution	direct methods
Refinement method	Full-matrix least-squares on F^2
Weighting parameters a, b	0.0480, 1.5888
Data / restraints / parameters	6971 / 0 / 473
Final R indices [$F^2>2\sigma$]	R1 = 0.0436, wR2 = 0.1046
R indices (all data)	R1 = 0.0569, wR2 = 0.1134
Goodness-of-fit on F^2	1.026
Extinction coefficient	0.0017(4)
Largest and mean shift/su	0.001 and 0.000
Largest diff. peak and hole	0.33 and –0.24 e $Å^{-3}$

Table 31 - Atomic coordinates and equivalent isotropic displacement parameters ($Å^2$) for **64**. U_{eq} is defined as one third of the trace of the orthogonalised U^{ij} tensor.

	x	**y**	**z**	**U_{eq}**
O(2)	0.13596(7)	0.25524(7)	0.70862(7)	0.0240(2)
O(3)	0.71384(9)	–0.17655(10)	0.98258(8)	0.0363(3)
N(7)	–0.01532(10)	0.24940(10)	0.58691(9)	0.0236(3)
N(8)	0.27744(9)	0.59808(9)	0.85838(8)	0.0220(3)
N(9)	0.29180(9)	0.50266(9)	0.98140(8)	0.0212(3)
N(10)	0.33164(9)	0.41005(9)	1.11897(8)	0.0238(3)
N(11)	0.48848(9)	0.45793(9)	1.20213(8)	0.0218(3)
N(12)	0.42367(9)	0.60228(8)	0.99107(8)	0.0202(3)
C(17)	0.04899(10)	0.28165(10)	0.66964(9)	0.0188(3)
C(18)	0.01292(11)	0.35635(10)	0.71346(10)	0.0218(3)
C(19)	0.05864(10)	0.45025(10)	0.71062(10)	0.0205(3)
C(20)	0.02102(11)	0.50168(11)	0.62872(10)	0.0264(3)
C(21)	0.06845(12)	0.58365(12)	0.62517(11)	0.0301(4)
C(22)	0.15238(12)	0.61362(11)	0.70174(10)	0.0261(3)
C(23)	0.18995(10)	0.56326(10)	0.78503(9)	0.0203(3)
C(24)	0.14184(10)	0.48172(10)	0.78908(10)	0.0204(3)
C(25)	0.33163(10)	0.56447(10)	0.94696(9)	0.0193(3)
C(26)	0.35389(10)	0.47345(10)	1.06740(10)	0.0202(3)
C(27)	0.41451(11)	0.40366(11)	1.19796(10)	0.0238(3)
C(28)	0.45079(10)	0.50463(10)	1.11784(9)	0.0196(3)
C(29)	0.48389(10)	0.57240(10)	1.07751(9)	0.0189(3)
C(30)	0.58090(11)	0.61239(10)	1.12422(10)	0.0216(3)
C(31)	0.66149(12)	0.64286(11)	1.16572(11)	0.0264(3)
C(32)	0.58664(12)	0.46424(12)	1.28115(10)	0.0292(3)
C(33)	0.78699(13)	–0.23375(13)	1.05222(12)	0.0361(4)
O(1)	0.98227(9)	–0.51798(10)	0.88206(9)	0.0411(3)
N(1)	0.87278(12)	–0.47099(12)	0.92939(11)	0.0372(4)
N(2)	0.82862(12)	–0.12140(10)	0.88083(10)	0.0325(3)
N(3)	0.90670(10)	0.02332(9)	0.89151(9)	0.0257(3)
N(4)	0.96400(11)	0.18354(10)	0.90586(10)	0.0346(3)
N(5)	0.88375(12)	0.24145(10)	0.98052(11)	0.0385(4)

N(6)	0.79939(10)	–0.00537(9)	0.96008(9)	0.0260(3)
C(1)	0.90370(12)	–0.48062(12)	0.86584(12)	0.0305(4)
C(2)	0.83883(13)	–0.43812(12)	0.77196(12)	0.0337(4)
C(3)	0.86585(13)	–0.33539(12)	0.77555(11)	0.0321(4)
C(4)	0.93098(18)	–0.30517(14)	0.74402(15)	0.0497(5)
C(5)	0.9621(2)	–0.21241(14)	0.75707(18)	0.0620(7)
C(6)	0.93045(18)	–0.14785(13)	0.80162(16)	0.0503(6)
C(7)	0.86499(13)	–0.17786(12)	0.83303(11)	0.0311 (4)
C(8)	0.83304(13)	–0.27071(12)	0.81896(11)	0.0305(4)
C(9)	0.84830(11)	–0.03044(11)	0.91181(10)	0.0252(3)
C(10)	0. 91210(11)	0.11254(11)	0.92037(10)	0.0262(3)
C(11)	0.94415(15)	0.25809(13)	0.94264(14)	0.0417(4)
C(12)	0.86169(12)	0.14690(11)	0.96682(11)	0.0279(3)
C(13)	0.80502(11)	0.08454(11)	0.98726(10)	0.0260(3)
C(14)	0.75129(12)	0.10995(12)	1.03626(11)	0.0312(4)
C(15)	0.70815(15)	0.13116(16)	1.07719(14)	0.0442(5)
C(16)	0.8461(2)	0.31088(15)	1.0224(2)	0.0633(7)

Table 32 - Bond lengths [Å] and angles [°] for **64**.

O(2)–C(17)	1.2404(17)	O(3)–C(33)	1.420(2)
O(3)–H(3)	0.94(3)	N(7)–C(17)	1.3247(19)
N(7)–H(7A)	0.880(19)	N(7)–H(7B)	0.835(19)
N(8)–C(23)	1.4064(18)	N(8)–C(25)	1.3697(18)
N(8)–H(8)	0.831(19)	N(9)–C(25)	1.3335(18)
N(9)–C(26)	1.3388(18)	N(10)–C(26)	1.3776(19)
N(10)–C(27)	1.324(2)	N(11)–C(27)	1.349(2)
N(11)–C(28)	1.3828(18)	N(11)–C(32)	1.4580(19)
N(12)–C(25)	1.3626(18)	N(12)–C(29)	1.3408(18)
C(17)–C(18)	1.519(2)	C(18)–H(18A)	0.990
C(18)–H(18B)	0.990	C(18)–C(19)	1.517(2)
C(19)–C(20)	1.386(2)	C(19)–C(24)	1.393(2)
C(20)–H(20A)	0.950	C(20)–C(21)	1.388(2)
C(21)–H(21A)	0.950	C(21)–C(22)	1.377(2)
C(22)–H(22A)	0.950	C(22)–C(23)	1.396(2)
C(23)–C(24)	1.391(2)	C(24)–H(24A)	0.950
C(26)–C(28)	1.395(2)	C(27)–H(27A)	0.950
C(28)–C(29)	1.388(2)	C(29)–C(30)	1.437(2)
C(30)–C(31)	1.182(2)	C(31)–H(31)	0.92(2)
C(32)–H(32A)	0.980	C(32)–H(32B)	0.980
C(32)–H(32C)	0.980	C(33)–H(33A)	0.980
C(33)–H(33B)	0.980	C(33)–H(33C)	0.980
O(1)–C(1)	1.230(2)	N(1)–C(1)	1.331(2)
N(1)–H(1A)	1.00(3)	N(1)–H(1B)	0.97(2)
N(2)–C(7)	1.402(2)	N(2)–C(9)	1.367(2)
N(2)–H(2)	0.90(2)	N(3)–C(9)	1.332(2)
N(3)–C(10)	1.339(2)	N(4)–C(10)	1.372(2)
N(4)–C(11)	1.319(2)	N(5)–C(11)	1.353(2)
N(5)–C(12)	1.376(2)	N(5)–C(16)	1.462(2)
N(6)–C(9)	1.3637(19)	N(6)–C(13)	1.340(2)
C(1)–C(2)	1.506(2)	C(2)–H(2A)	0.990
C(2)–H(2B)	0.990	C(2)–C(3)	1.509(2)

C(3)–C(4)	1.389(3)	C(3)–C(8)	1.388(2)
C(4)–H(4A)	0.950	C(4)–C(5)	1.383(3)
C(5)–H(5A)	0.950	C(5)–C(6)	1.389(3)
C(6)–H(6A)	0.950	C(6)–C(7)	1.391(2)
C(7)–C(8)	1.387(2)	C(8)–H(8A)	0.950
C(10)–C(12)	1.398(2)	C(11)–H(11A)	0.950
C(12)–C(13)	1.387(2)	C(13)–C(14)	1.436(2)
C(14)–C(15)	1.177(2)	C(15)–H(15)	0.92(2)
C(16)–H(16A)	0.980	C(16)–H(16B)	0.980
C(16)–H(16C)	0.980		
C(33)–O(3)–H(3)	109.2(18)	C(17)–N(7)–H(7A)	117.9(12)
C(17)–N(7)–H(7B)	118.1(12)	H(7A)–N(7)–H(7B)	123.9(17)
C(23)–N(8)–C(25)	129.86(13)	C(23)–N(8)–H(8)	114.8(12)
C(25)–N(8)–H(8)	114.9(12)	C(25)–N(9)–C(26)	113.52(12)
C(26)–N(10)–C(27)	103.61(12)	C(27)–N(11)–C(28)	105.70(12)
C(27)–N(11)–C(32)	125.51(13)	C(28)–N(11)–C(32)	128.79(13)
C(25)–N(12)–C(29)	117.80(12)	O(2)–C(17)–N(7)	122.00(13)
O(2)–C(17)–C(18)	120.90(12)	N(7)–C(17)–C(18)	117.04(13)
C(17)–C(18)–H(18A)	109.9	C(17)–C(18)–H(18B)	109.9
C(17)–C(18)–C(19)	108.84(11)	H(18A)–C(18)–H(18B)	108.3
H(18A)–C(18)–C(19)	109.9	H(18B)–C(18)–C(19)	109.9
C(18)–C(19)–C(20)	120.01(13)	C(18)–C(19)–C(24)	119.61(13)
C(20)–C(19)–C(24)	120.27(14)	C(19)–C(20)–H(20A)	120.3
C(19)–C(20)–C(21)	119.30(14)	H(20A)–C(20)–C(21)	120.3
C(20)–C(21)–H(21A)	119.7	C(20)–C(21)–C(22)	120.65(14)
H(21A)–C(21)–C(22)	119.7	C(21)–C(22)–H(22A)	119.7
C(21)–C(22)–C(23)	120.52(14)	H(22A)–C(22)–C(23)	119.7
N(8)–C(23)–C(22)	116.21(13)	N(8)–C(23)–C(24)	124.83(13)
C(22)–C(23)–C(24)	118.91(13)	C(19)–C(24)–C(23)	120.30(13)
C(19)–C(24)–H(24A)	119.9	C(23)–C(24)–H(24A)	119.9
N(8)–C(25)–N(9)	119.84(13)	N(8)–C(25)–N(12)	112.88(12)
N(9)–C(25)–N(12)	127.27(13)	N(9)–C(26)–N(10)	125.42(13)
N(9)–C(26)–C(28)	124.11(13)	N(10)–C(26)–C(28)	110.47(12)
N(10)–C(27)–N(11)	114.61(13)	N(10)–C(27)–H(27A)	122.7
N(11)–C(27)–H(27A)	122.7	N(11)–C(28)–C(26)	105.61(12)
N(11)–C(28)–C(29)	136.40(14)	C(26)–C(28)–C(29)	117.93(13)
N(12)–C(29)–C(28)	119.24(13)	N(12)–C(29)–C(30)	117.87(13)
C(28)–C(29)–C(30)	122.89(13)	C(29)–C(30)–C(31)	177.23(16)
C(30)–C(31)–H(31)	179.7(13)	N(11)–C(32)–H(32A)	109.5
N(11)–C(32)–H(32B)	109.5	N(11)–C(32)–H(32C)	109.5
H(32A)–C(32)–H(32B)	109.5	H(32A)–C(32)–H(32C)	109.5
H(32B)–C(32)–H(32C)	109.5	O(3)–C(33)–H(33A)	109.5
O(3)–C(33)–H(33B)	109.5	O(3)–C(33)–H(33C)	109.5
H(33A)–C(33)–H(33B)	109.5	H(33A)–C(33)–H(33C)	109.5
H(33B)–C(33)–H(33C)	109.5	C(1)–N(1)–H(1A)	118.0(14)
C(1)–N(1)–H(1B)	120.7(13)	H(1A)–N(1)–H(1B)	119.5(19)
C(7)–N(2)–C(9)	131.84(15)	C(7)–N(2)–H(2)	114.0(14)
C(9)–N(2)–H(2)	114.1(14)	C(9)–N(3)–C(10)	113.17(13)
C(10)–N(4)–C(11)	103.58(14)	C(11)–N(5)–C(12)	105.43(14)
C(11)–N(5)–C(16)	126.81(16)	C(12)–N(5)–C(16)	127.69(15)
C(9)–N(6)–C(13)	118.06(13)	O(1)–C(1)–N(1)	123.29(17)
O(1)–C(1)–C(2)	120.63(15)	N(1)–C(1)–C(2)	116.01(15)

C(1)–C(2)–H(2A)	110.1	C(1)–C(2)–H(2B)	110.1
C(1)–C(2)–C(3)	107.91(14)	H(2A)–C(2)–H(2B)	108.4
H(2A)–C(2)–C(3)	110.1	H(2B)–C(2)–C(3)	110.1
C(2)–C(3)–C(4)	121.12(15)	C(2)–C(3)–C(8)	119.97(15)
C(4)–C(3)–C(8)	118.63(16)	C(3)–C(4)–H(4A)	120.2
C(3)–C(4)–C(5)	119.64(17)	H(4A)–C(4)–C(5)	120.2
C(4)–C(5)–H(5A)	119.1	C(4)–C(5)–C(6)	121.87(18)
H(5A)–C(5)–C(6)	119.1	C(5)–C(6)–H(6A)	120.7
C(5)–C(6)–C(7)	118.61(18)	H(6A)–C(6)–C(7)	120.7
N(2)–C(7)–C(6)	124.95(16)	N(2)–C(7)–C(8)	115.61(15)
C(6)–C(7)–C(8)	119.43(15)	C(3)–C(8)–C(7)	121.81(16)
C(3)–C(8)–H(8A)	119.1	C(7)–C(8)–H(8A)	119.1
N(2)–C(9)–N(3)	120.56(14)	N(2)–C(9)–N(6)	111.82(14)
N(3)–C(9)–N(6)	127.58(14)	N(3)–C(10)–N(4)	125.44(14)
N(3)–C(10)–C(12)	124.02(14)	N(4)–C(10)–C(12)	110.50(14)
N(4)–C(11)–N(5)	114.80(16)	N(4)–C(11)–H(11A)	122.6
N(5)–C(11)–H(11A)	122.6	N(5)–C(12)–C(10)	105.69(14)
N(5)–C(12)–C(13)	135.90(15)	C(10)–C(12)–C(13)	118.40(15)
N(6)–C(13)–C(12)	118.66(14)	N(6)–C(13)–C(14)	117.19(14)
C(12)–C(13)–C(14)	124.15(15)	C(13)–C(14)–C(15)	179.3(2)
C(14)–C(15)–H(15)	179.9(17)	N(5)–C(16)–H(16A)	109.5
N(5)–C(16)–H(16B)	109.5	N(5)–C(16)–H(16C)	109.5
H(16A)–C(16)–H(16B)	109.5	H(16A)–C(16)–H(16C)	109.5
H(16B)–C(16)–H(16C)	109.5		

Table 33 - Anisotropic displacement parameters (Å^2) for **64**. The anisotropic displacement factor exponent takes the form: $-2\pi^2[h^2a^{*2}U^{11} + 2hka^*b^*U^{12}]$

	U^{11}	U^{22}	U^{33}	U^{23}	U^{13}	U^{12}
O(2)	0.0172(5)	0.0277(6)	0.0236(5)	–0.0010(4)	0.0067(4)	0.0004(4)
O(3)	0.0273(6)	0.0376(7)	0.0374(6)	0.0044(5)	0.0096(5)	–0.0070(5)
N(7)	0.0176(7)	0.0268(7)	0.0232(6)	–0.0037(5)	0.0069(5)	0.0021(5)
N(8)	0.0209(6)	0.0214(6)	0.0206(6)	0.0015(5)	0.0071(5)	–0.0045(5)
N(9)	0.0206(6)	0.0236(6)	0.0198(6)	–0.0018(5)	0.0099(5)	–0.0028(5)
N(10)	0.0267(7)	0.0247(7)	0.0229(6)	0.0002(5)	0.0141(5)	–0.0018(5)
N(11)	0.0240(6)	0.0219(6)	0.0191(6)	–0.0001(5)	0.0098(5)	0.0014(5)
N(12)	0.0198(6)	0.0195(6)	0.0211(6)	–0.0023(5)	0.0096(5)	–0.0011(5)
C(17)	0.0192(7)	0.0182(7)	0. 0196(6)	0.0022(5)	0.0096(6)	–0.0033(6)
C(18)	0.0187(7)	0.0257(8)	0.0218(7)	–0.0039(6)	0.0101(6)	–0.0030(6)
C(19)	0.0192(7)	0.0220(7)	0.0216(7)	–0.0034(6)	0.0106(6)	0.0016(6)
C(20)	0.0236(8)	0.0283(8)	0.0193(7)	–0.0033(6)	0.0033(6)	–0.0002(6)
C(21)	0.0348(9)	0.0277(8)	0.0207(7)	0.0044(6)	0.0070(7)	0.0022(7)
C(22)	0. 0294(8)	0.0215(8)	0.0252(7)	0.0015(6)	0.0108(6)	–0.0026(6)
C(23)	0.0196(7)	0.0210(7)	0.0196(7)	–0.0023(5)	0.0087(6)	0.0016(6)
C(24)	0.0202(7)	0.0216(7)	0.0187(6)	0.0003(6)	0.0086(6)	0.0012(6)
C(25)	0.0197(7)	0.0184(7)	0.0198(7)	–0.0032(5)	0.0091(6)	0.0000(6)
C(26)	0.0221(7)	0.0197(7)	0.0207(7)	–0.0032(6)	0.0117(6)	–0.0009(6)
C(27)	0.0294(8)	0.0230(8)	0.0216(7)	–0.0006(6)	0.0143(6)	0.0004(6)
C(28)	0.0213(7)	0.0195(7)	0.0179(6)	–0.0022(5)	0.0091(6)	0.0016(6)
C(29)	0.0188(7)	0.0186(7)	0.0197(6)	–0.0042(5)	0.0093(6)	0.0002(6)
C(30)	0.0235(8)	0.0207(7)	0.0217(7)	0.0003(6)	0.0115(6)	0.0017(6)

C(31)	0.0221(8)	0.0240(8)	0.0307(8)	–0.0012(6)	0.0103(7)	–0.0013(7)
C(32)	0.0265(8)	0.0329(9)	0.0216(7)	0.0020(6)	0.0057(6)	0.0022(7)
C(33)	0.0345(9)	0.0388(10)	0.0292(8)	0.0023(7)	0.0102(7)	–0.0067(8)
O(1)	0.0376(7)	0.0469(8)	0.0419(7)	0.0045(6)	0.0211(6)	0.0092(6)
N(1)	0.0320(8)	0.0425(9)	0.0415(9)	0.0083(7)	0.0209(7)	0.0045(7)
N(2)	0.0482(9)	0.0239(7)	0.0393(8)	–0.0002(6)	0.0322(7)	–0.0011(6)
N(3)	0.0287(7)	0.0262(7)	0.0242(6)	0.0015(5)	0.0139(6)	0.0020(6)
N(4)	0.0390(8)	0.0309(8)	0.0408(8)	–0.0066(6)	0.0245(7)	–0.0079(6)
N(5)	0.0501(9)	0.0279(8)	0.0497(9)	–0.0077(7)	0.0336(8)	–0.0047(7)
N(6)	0.0308(7)	0.0261(7)	0.0245(6)	0.0020(5)	0.0159(6)	0.0027(6)
C(1)	0.0300(9)	0.0237(8)	0.0382(9)	–0.0018(7)	0.0164(7)	–0.0026(7)
C(2)	0.0337(9)	0.0320(9)	0.0320(8)	–0.0075(7)	0.0124(7)	–0.0007(7)
C(3)	0.0422(10)	0.0288(9)	0.0261(8)	0.0006(7)	0.0167(7)	0.0048(7)
C(4)	0.0860(16)	0.0314(10)	0.0600(12)	0.0035(9)	0.0577(13)	0.0097(10)
C(5)	0.108(2)	0.0327(10)	0.0955(18)	0.0081(11)	0.0900(17)	0.0055(12)
C(6)	0.0876(16)	0.0241(9)	0.0726(14)	0.0054(9)	0.0655(13)	0.0022(10)
C(7)	0.0451(10)	0.0256(8)	0.0316(8)	0.0034(7)	0.0254(8)	0.0054(7)
C(8)	0.0367(9)	0.0298(9)	0.0288(8)	0.0004(7)	0.0185(7)	0.0012(7)
C(9)	0.0296(8)	0.0248(8)	0.0222(7)	0.0044(6)	0.0130(6)	0.0058(6)
C(10)	0.0259(8)	0.0288(8)	0.0237(7)	–0.0003(6)	0.0115(6)	0.0001(6)
C(11)	0.0507(11)	0.0327(10)	0.0529(11)	–0.0087(8)	0.0336(10)	–0.0113(8)
C(12)	0.0314(8)	0.0254(8)	0.0288(8)	–0.0016(6)	0.0156(7)	0.0009(7)
C(13)	0.0265(8)	0.0288(8)	0.0226(7)	0.0017(6)	0.0113(6)	0.0042(7)
C(14)	0.0334(9)	0.0319(9)	0.0295(8)	–0.0010(7)	0.0157(7)	0.0019(7)
C(15)	0.0428(11)	0.0574(13)	0.0424(10)	–0.0069(9)	0.0283(9)	0.0040(9)
C(16)	0.0969(19)	0.0305(11)	0.1005(19)	–0.0185(11)	0.0779(17)	–0.0084(11)

Table 34 - Hydrogen coordinates and isotropic displacement parameters ($Å^2$) for **64**.

	x	**y**	**z**	**U**
H(18A)	–0.0597	0.3609	0.6789	0.026
H(18B)	0.0318	0.3391	0.7786	0.026
H(20A)	–0.0366	0.4811	0.5756	0.032
H(21A)	0.0428	0.6194	0.5694	0.036
H(22A)	0.1850	0.6690	0.6979	0.031
H(24A)	0.1659	0.4474	0.8456	0.024
H(27A)	0.4213	0.3640	1.2477	0.029
H(32A)	0.5874	0.4322	1.3349	0.044
H(32B)	0.6043	0.5306	1.2965	0.044
H(32C)	0.6342	0.4341	1.2652	0.044
H(33A)	0.8507	–0.2215	1.0543	0.054
H(33B)	0.7697	–0.3003	1.0376	0.054
H(33C)	0.7910	–0.2189	1.1128	0.054
H(2A)	0.7688	–0.4444	0.7569	0.040
H(2B)	0.8489	–0.4710	0.7234	0.040
H(4A)	0.9540	–0.3480	0.7137	0.060
H(5A)	1.0063	–0.1923	0.7349	0.074
H(6A)	0.9531	–0.0845	0.8105	0.060
H(8A)	0.7875	–0.2906	0.8396	0.037
H(11A)	0.9702	0.3188	0.9426	0.050
H(16A)	0.8832	0.3697	1.0331	0.095

H(16B)	0.8536	0.2867	1.0818	0.095
H(16C)	0.7764	0.3228	0.9804	0.095
H(8)	0.3036(13)	0.6418(13)	0.8439(12)	0.025(4)
H(7A)	0.0048(13)	0.2063(13)	0.5606(12)	0.029(5)
H(7B)	–0.0733(14)	0.2686(13)	0.5644(12)	0.027(5)
H(1A)	0.9218(18)	–0.4795(17)	0.9960(18)	0.064(7)
H(2)	0.7873(16)	–0.1519(16)	0.8972(15)	0.049(6)
H(1B)	0.8101(17)	–0.4415(16)	0.9136(15)	0.056(6)
H(3)	0.735(2)	–0.113(2)	0.992(2)	0.086(9)
H(31)	0.7242(15)	0.6663(14)	1.1980(14)	0.041(5)
H(15)	0.6743(17)	0.1477(18)	1.1093(17)	0.065(7)

Table 35 - Torsion angles [°] for **64**.

O(2)–C(17)–C(18)–C(19)	69.15(16)	N(7)–C(17)–C(18)–C(19)	–108.14(14)
C(17)–C(18)–C(19)–C(20)	78.40(16)	C(17)–C(18)–C(19)–C(24)	–97.94(15)
C(18)–C(19)–C(20)–C(21)	–174.85(14)	C(24)–C(19)–C(20)–C(21)	1.5(2)
C(19)–C(20)–C(21)–C(22)	0.4(2)	C(20)–C(21)–C(22)–C(23)	–1.5(2)
C(21)–C(22)–C(23)–N(8)	178.28(14)	C(21)–C(22)–C(23)–C(24)	0.7(2)
C(25)–N(8)–C(23)–C(22)	–179.67(14)	C(25)–N(8)–C(23)–C(24)	–2.3(2)
N(8)–C(23)–C(24)–C(19)	–176.17(13)	C(22)–C(23)–C(24)–C(19)	1.2(2)
C(18)–C(19)–C(24)–C(23)	174.06(13)	C(20)–C(19)–C(24)–C(23)	–2.3(2)
C(26)–N(9)–C(25)–N(8)	177.92(12)	C(26)–N(9)–C(25)–N(12)	–3.5(2)
C(29)–N(12)–C(25)–N(8)	–178.36(12)	C(29)–N(12)–C(25)–N(9)	2.9(2)
C(23)–N(8)–C(25)–N(9)	–16.4(2)	C(23)–N(8)–C(25)–N(12)	164.80(13)
C(25)–N(9)–C(26)–N(10)	179.89(13)	C(25)–N(9)–C(26)–C(28)	0.8(2)
C(27)–N(10)–C(26)–N(9)	–179.76(14)	C(27)–N(10)–C(26)–C(28)	–0.53(16)
C(26)–N(10)–C(27)–N(11)	0.30(17)	C(28)–N(11)–C(27)–N(10)	0.03(17)
C(32)–N(11)–C(27)–N(10)	179.63(14)	C(27)–N(11)–C(28)–C(26)	–0.36(15)
C(27)–N(11)–C(28)–C(29)	176.62(16)	C(32)–N(11)–C(28)–C(26)	–179.93(14)
C(32)–N(11)–C(28)–C(29)	–3.0(3)	N(9)–C(26)–C(28)–N(11)	179.81(13)
N(9)–C(26)–C(28)–C(29)	2.2(2)	N(10)–C(26)–C(28)–N(11)	0.56(16)
N(10)–C(26)–C(28)–C(29)	–177.08(12)	C(25)–N(12)–C(29)–C(28)	0.44(19)
C(25)–N(12)–C(29)–C(30)	–179.83(12)	N(11)–C(28)–C(29)–N(12)	–179.42(15)
N(11)–C(28)–C(29)–C(30)	0.9(3)	C(26)–C(28)–C(29)–N(12)	–2.7(2)
C(26)–C(28)–C(29)–C(30)	177.56(13)	N(12)–C(29)–C(30)–C(31)	–178(100)
C(28)–C(29)–C(30)–C(31)	2(3)	O(1)–C(1)–C(2)–C(3)	–91.86(19)
N(1)–C(1)–C(2)–C(3)	85.14(19)	C(1)–C(2)–C(3)–C(4)	96.3(2)
C(1)–C(2)–C(3)–C(8)	–77.5(2)	C(2)–C(3)–C(4)–C(5)	–173.3(2)
C(8)–C(3)–C(4)–C(5)	0.5(3)	C(3)–C(4)–C(5)–C(6)	0.4(4)
C(4)–C(5)–C(6)–C(7)	–0.6(4)	C(5)–C(6)–C(7)–N(2)	178.5(2)
C(5)–C(6)–C(7)–C(8)	–0.1(3)	C(9)–N(2)–C(7)–C(6)	–3.4(3)
C(9)–N(2)–C(7)–C(8)	175.29(17)	N(2)–C(7)–C(8)–C(3)	–177.69(16)
C(6)–C(7)–C(8)–C(3)	1.1(3)	C(2)–C(3)–C(8)–C(7)	172.66(16)
C(4)–C(3)–C(8)–C(7)	–1.2(3)	C(10)–N(3)–C(9)–N(2)	174.84(14)
C(10)–N(3)–C(9)–N(6)	–2.9(2)	C(13)–N(6)–C(9)–N(2)	–174.11(14)
C(13)–N(6)–C(9)–N(3)	3.8(2)	C(7)–N(2)–C(9)–N(3)	5.4(3)
C(7)–N(2)–C(9)–N(6)	–176.58(16)	C(9)–N(3)–C(10)–N(4)	–177.61(15)
C(9)–N(3)–C(10)–C(12)	–0.2(2)	C(11)–N(4)–C(10)–N(3)	177.41(17)
C(11)–N(4)–C(10)–C(12)	–0.26(19)	C(10)–N(4)–C(11)–N(5)	0.3(2)

C(12)–N(5)–C(11)–N(4)	–0.2(2)	C(16)–N(5)–C(11)–N(4)	–177.3(2)
C(11)–N(5)–C(12)–C(10)	0.07(19)	C(11)–N(5)–C(12)–C(13)	–179.7(2)
C(16)–N(5)–C(12)–C(10)	177.1(2)	C(16)–N(5)–C(12)–C(13)	–2.7(4)
N(3)–C(10)–C(12)–N(5)	–177.59(15)	N(3)–C(10)–C(12)–C(13)	2.2(2)
N(4)–C(10)–C(12)–N(5)	0.12(19)	N(4)–C(10)–C(12)–C(13)	179.93(14)
C(9)–N(6)–C(13)–C(12)	–1.3(2)	C(9)–N(6)–C(13)–C(14)	178.70(14)
N(5)–C(12)–C(13)–N(6)	178.43(18)	N(5)–C(12)–C(13)–C(14)	–1.6(3)
C(10)–C(12)–C(13)–N(6)	–1.3(2)	C(10)–C(12)–C(13)–C(14)	178.64(15)
N(6)–C(13)–C(14)–C(15)	126(18)	C(12)–C(13)–C(14)–C(15)	–54(18)

Table 36 - Hydrogen bonds for **64** [Å and °].

D–H...A	d(D–H)	d(H...A)	d(D...A)	<(DHA)
N(8)–H(8)...O(2A)	0.831(19)	2.220(19)	3.0476(17)	175(2)
N(7)–H(7A)...N(12B)	0.880(19)	2.23(2)	3.1018(18)	172(2)
N(7)–H(7B)...O(3A)	0.835(19)	2.08(2)	2.9112(18)	175(2)
N(1)–H(1A)...O(1C)	1.00(3)	1.84(3)	2.830(2)	174(2)
N(2)–H(2)...O(3)	0.90(2)	2.19(2)	3.0314(19)	155(2)
N(1)–H(1B)...N(10D)	0.97(2)	2.04(2)	2.989(2)	167(2)
O(3)–H(3)...N(6)	0.94(3)	2.03(3)	2.8660(18)	148(2)

Symmetry operations for equivalent atoms: A –x+1/2,y+1/2,–z+3/2; B –x+1/2, y–1/2, –z+3/2; C –x+2, –y–1, –z+2; D –x+1, –y, –z+2.

N^9-methylpurine **63**

Table 37 - Crystal data and structure refinement for **63**.

Identification code	rjg120010
Chemical formula (moiety)	$C_{16}H_{14}N_6O$
Chemical formula (total)	$C_{16}H_{14}N_6O$
Formula weight	306.33
Temperature	150(2) K
Radiation, wavelength	synchroton, 0.68890 Å
Crystal system, space group	monoclinic, $P2_1/c$
Unit cell parameters	a = 20.880(7) Å α = 90°
	b = 4.7912(15) Å β = 105.544(3)°
	c = 14.900(5) Å γ = 90°
Cell volume	1436.1(8) $Å^3$
Z	4
Calculated density	1.417 g/cm^3
Absorption coefficient μ	0.095 mm^{-1}
F(000)	640
Crystal colour and size	yellow, 0.10 × 0.10 × 0.00 mm^3
Reflections for cell refinement	8029 (θ range 2.7 to 27.3°)
Data collection method	Crystal Logic diffractometer and Rigaku Saturn 724+ CCD thick-slice ω scans
θ range for data collection	1.0 to 27.4°
Index ranges	h –27 to 27, k –6 to 3, l –19 to 19
Completeness to θ = 27.4°	94.9 %

Reflections collected	13223
Independent reflections	3389 (R_{int} = 0.0380)
Reflections with $F^2>2\sigma$	2884
Absorption correction	semi-empirical from equivalents
Min. and max. transmission	0.9905 and 0.9999
Structure solution	direct methods
Refinement method	Full-matrix least-squares on F^2
Weighting parameters a, b	0.0529, 0.5159
Data / restraints / parameters	3389 / 0 / 226
Final R indices [$F^2>2\sigma$]	R1 = 0.0441, wR2 = 0.1174
R indices (all data)	R1 = 0.0512, wR2 = 0.1215
Goodness-of-fit on F^2	1.118
Extinction coefficient	0.044(16)
Largest and mean shift/su	0.000 and 0.000
Largest diff. peak and hole	0.28 and –0.22 e $Å^{-3}$

Table 38 - Atomic coordinates and equivalent isotropic displacement parameters ($Å^2$) for **63**. U_{eq} is defined as one third of the trace of the orthogonalised U^{ij} tensor.

	x	**y**	**z**	**U_{eq}**
O	0.16661(6)	0.5043(2)	0.70303(7)	0.0336(3)
N(1)	0.21534(7)	0.0828(3)	0.72648(9)	0.0337(3)
N(2)	0.20548(5)	0.8195(3)	0.39794(7)	0.0260(3)
N(3)	0.28640(5)	0.7663(2)	0.53946(7)	0.0241(3)
N(4)	0.29791(5)	1.0968(2)	0.42101(7)	0.0233(3)
N(5)	0.38238(5)	0.7561(3)	0.67265(7)	0.0245(3)
N(6)	0.44645(5)	1.0803(3)	0.62783(7)	0.0261(3)
C(1)	0.16895(7)	0.2581(3)	0.67855(9)	0.0266(3)
C(2)	0.11864(7)	0.1431(3)	0.59360(10)	0.0320(3)
C(3)	0.11001(6)	0.3208(3)	0.50677(9)	0.0267(3)
C(4)	0.04911(7)	0.3281(4)	0.43937(11)	0.0354(4)
C(5)	0.04231(7)	0.4864(4)	0.35916(11)	0.0400(4)
C(6)	0.09471(7)	0.6430(4)	0.34632(10)	0.0327(3)
C(7)	0.15574(6)	0.6430(3)	0.41455(8)	0.0242(3)
C(8)	0.16319(6)	0.4749(3)	0.49320(9)	0.0252(3)
C(9)	0.26525(6)	0.8939(3)	0.45605(8)	0.0226(3)
C(10)	0.34625(6)	0.8528(3)	0.58740(8)	0.0224(3)
C(11)	0.38579(6)	1.0527(3)	0.56028(8)	0.0226(3)
C(12)	0.35826(6)	1.1760(3)	0.47317(8)	0.0229(3)
C(13)	0.44149(6)	0.9000(3)	0.69226(9)	0.0265(3)
C(14)	0.36037(7)	0.5481(3)	0.72919(9)	0.0287(3)
C(15)	0.39490(6)	1.3870(3)	0.43913(9)	0.0257(3)
C(16)	0.43154(7)	1.5552(4)	0.42143(10)	0.0313(3)

Table 39 - Bond lengths [Å] and angles [°] for **63**.

O–C(1)	1.2394(18)	N(1)–H(1A)	0.92(2)
N(1)–H(1B)	0.90(2)	N(1)–C(1)	1.335(2)
N(2)–H(2)	0.91(2)	N(2)–C(7)	1.4114(17)
N(2)–C(9)	1.3620(16)	N(3)–C(9)	1.3488(16)
N(3)–C(10)	1.3287(16)	N(4)–C(9)	1.3686(17)
N(4)–C(12)	1.3456(16)	N(5)–C(10)	1.3725(16)

N(5)–C(13)	1.3752(17)	N(5)–C(14)	1.4566(18)
N(6)–C(11)	1.3970(16)	N(6)–C(13)	1.3159(18)
C(1)–C(2)	1.5155(19)	C(2)–H(2A)	0.990
C(2)–H(2B)	0.990	C(2)–C(3)	1.519(2)
C(3)–C(4)	1.3935(19)	C(3)–C(8)	1.3925(19)
C(4)–H(4A)	0.950	C(4)–C(5)	1.390(2)
C(5)–H(5A)	0.950	C(5)–C(6)	1.382(2)
C(6)–H(6A)	0.950	C(6)–C(7)	1.4012(17)
C(7)–C(8)	1.3961(19)	C(8)–H(8A)	0.950
C(10)–C(11)	1.3930(18)	C(11)–C(12)	1. 4015(18)
C(12)–C(15)	1.4398(19)	C(13)–H(13A)	0.950
C(14)–H(14A)	0.980	C(14)–H(14B)	0.980
C(14)–H(14C)	0.980	C(15)–C(16)	1.188(2)
C(16)–H(1)	0.93(2)		
H(1A)–N(1)–H(1B)	120.2(18)	H(1A)–N(1)–C(1)	116.8(13)
H(1B)–N(1)–C(1)	119.1(13)	H(2)–N(2)–C(7)	114.9(12)
H(2)–N(2)–C(9)	115.1(12)	C(7)–N(2)–C(9)	129.58(11)
C(9)–N(3)–C(10)	112.50(11)	C(9)–N(4)–C(12)	117.72(11)
C(10)–N(5)–C(13)	105.46(11)	C(10)–N(5)–C(14)	125.87(11)
C(13)–N(5)–C(14)	128.66(11)	C(11)–N(6)–C(13)	103.30(11)
O–C(1)–N(1)	121.42(13)	O–C(1)–C(2)	121.25(13)
N(1)–C(1)–C(2)	117.32(14)	C(1)–C(2)–H(2A)	108.8
C(1)–C(2)–H(2B)	108.8	C(1)–C(2)–C(3)	113.90(12)
H(2A)–C(2)–H(2B)	107.7	H(2A)–C(2)–C(3)	108.8
H(2B)–C(2)–C(3)	108.8	C(2)–C(3)–C(4)	120.34(13)
C(2)–C(3)–C(8)	120.24(12)	C(4)–C(3)–C(8)	119.41(13)
C(3)–C(4)–H(4A)	120.1	C(3)–C(4)–C(5)	119.78(13)
H(4A)–C(4)–C(5)	120.1	C(4)–C(5)–H(5A)	119.6
C(4)–C(5)–C(6)	120.86(13)	H(5A)–C(5)–C(6)	119.6
C(5)–C(6)–H(6A)	120.0	C(5)–C(6)–C(7)	119.98(14)
H(6A)–C(6)–C(7)	120.0	N(2)–C(7)–C(6)	116.21(12)
N(2)–C(7)–C(8)	124.84(11)	C(6)–C(7)–C(8)	118.95(12)
C(3)–C(8)–C(7)	120.93(12)	C(3)–C(8)–H(8A)	119.5
C(7)–C(8)–H(8A)	119.5	N(2)–C(9)–N(3)	119.02(12)
N(2)–C(9)–N(4)	114.13(11)	N(3)–C(9)–N(4)	126.85(11)
N(3)–C(10)–N(5)	126.63(12)	N(3)–C(10)–C(11)	127.12(12)
N(5)–C(10)–C(11)	106.21(11)	N(6)–C(11)–C(10)	110.45(11)
N(6)–C(11)–C(12)	134.03(12)	C(10)–C(11)–C(12)	115.50(11)
N(4)–C(12)–C(11)	120.28(12)	N(4)–C(12)–C(15)	119.89(11)
C(11)–C(12)–C(15)	119.83(11)	N(5)–C(13)–N(6)	114.57(11)
N(5)–C(13)–H(13A)	122.7	N(6)–C(13)–H(13A)	122.7
N(5)–C(14)–H(14A)	109.5	N(5)–C(14)–H(14B)	109.5
N(5)–C(14)–H(14C)	109.5	H(14A)–C(14)–H(14B)	109.5
H(14A)–C(14)–H(14C)	109.5	H(14B)–C(14)–H(14C)	109.5
C(12)–C(15)–C(16)	171.43(14)	C(15)–C(16)–H(1)	178.3(13)

Table 40 - Anisotropic displacement parameters ($Å^2$) for **63**. The anisotropic displacement factor exponent takes the form: $-2\pi^2[h^2a^{*2}U^{11} + 2hka^*b^*U^{12}]$.

	U^{11}	U^{22}	U^{33}	U^{23}	U^{13}	U^{12}
O	0.0479(6)	0.0248(6)	0.0251(5)	–0.0024(4)	0.0048(4)	–0.0011(4)
N(1)	0.0395(7)	0.0265(8)	0.0331(6)	–0.0007(5)	0.0061(5)	–0.0007(5)
N(2)	0.0242(5)	0.0319(7)	0.0185(5)	0.0031(4)	0.0001(4)	–0.0055(5)
N(3)	0.0227(5)	0.0287(7)	0.0191(5)	0.0008(4)	0.0024(4)	–0.0041(4)
N(4)	0.0240(5)	0.0260(7)	0.0194(5)	0.0004(4)	0.0045(4)	–0.0020(4)
N(5)	0.0231(5)	0.0281(7)	0.0198(5)	0.0032(4)	0.0015(4)	–0.0026(4)
N(6)	0.0225(5)	0.0308(7)	0.0223(5)	0.0009(4)	0.0016(4)	–0.0036(4)
C(1)	0.0331(7)	0.0259(8)	0.0225(6)	–0.0008(5)	0.0102(5)	–0.0055(5)
C(2)	0.0373(7)	0.0293(8)	0.0285(7)	–0.0028(6)	0.0072(6)	–0.0123(6)
C(3)	0.0291(6)	0.0263(8)	0.0243(6)	–0.0052(5)	0.0066(5)	–0.0053(5)
C(4)	0.0264(7)	0.0414(10)	0.0362(7)	–0.0011(7)	0.0046(6)	–0.0118(6)
C(5)	0.0255(7)	0.0502(11)	0.0368(8)	0.0025(7)	–0.0046(6)	–0.0091(7)
C(6)	0.0277(7)	0.0390(9)	0.0266(6)	0.0038(6)	–0.0013(5)	–0.0038(6)
C(7)	0.0229(6)	0.0269(8)	0.0216(6)	–0.0039(5)	0.0037(5)	–0.0030(5)
C(8)	0.0238(6)	0.0281(8)	0.0215(6)	–0.0027(5)	0.0025(5)	–0.0037(5)
C(9)	0.0221(6)	0.0263(8)	0.0186(5)	–0.0006(5)	0.0041(4)	–0.0012(5)
C(10)	0.0228(6)	0.0250(7)	0.0182(5)	–0.0003(5)	0.0034(4)	–0.0010(5)
C(11)	0.0220(6)	0.0240(7)	0.0205(6)	–0.0011(5)	0.0036(4)	–0.0028(5)
C(12)	0.0238(6)	0.0250(7)	0.0201(5)	–0.0014(5)	0.0062(4)	–0.0007(5)
C(13)	0.0222(6)	0.0317(8)	0.0229(6)	0.0014(5)	0.0014(5)	–0.0026(5)
C(14)	0.0301(6)	0.0316(8)	0.0224(6)	0.0058(5)	0.0034(5)	–0.0037(6)
C(15)	0.0250(6)	0.0296(8)	0.0208(6)	0.0008(5)	0.0030(5)	–0.0007(5)
C(16)	0.0297(7)	0.0365(9)	0.0265(6)	0.0052(6)	0.0055(5)	–0.0053(6)

Table 41 - Hydrogen coordinates and isotropic displacement parameters ($Å^2$) for **63**.

	x	y	z	U
H(1A)	0.2410(9)	0.144(4)	0.7833(14)	0.045(5)
H(1B)	0.2109(9)	–0.101(5)	0.7142(14)	0.049(6)
H(2)	0.1937(9)	0.913(4)	0.3427(14)	0.046(5)
H(2A)	0.0751	0.1261	0.6078	0.038
H(2B)	0.1327	–0.0466	0.5806	0.038
H(4A)	0.0124	0.2253	0.4482	0.043
H(5A)	0.0011	0.4869	0.3126	0.048
H(6A)	0.0894	0.7506	0.2912	0.039
H(8A)	0.2051	0.4654	0.5381	0.030
H(13A)	0.4760	0.8716	0.7478	0.032
H(14A)	0.3337	0.4059	0.6885	0.043
H(14B)	0.3334	0.6386	0.7655	0.043
H(14C)	0.3992	0.4598	0.7716	0.043
H(1)	0.4610(9)	1.684(4)	0.4091(14)	0.049(5)

Table 42 - Torsion angles [°] for **63**.

O–C(1)–C(2)–C(3)	50.41(18)	N(1)–C(1)–C(2)–C(3)	–130.34(14)
C(1)–C(2)–C(3)–C(4)	–149.87(14)	C(1)–C(2)–C(3)–C(8)	31.0(2)
C(2)–C(3)–C(4)–C(5)	–178.47(15)	C(8)–C(3)–C(4)–C(5)	0.6(2)
C(3)–C(4)–C(5)–C(6)	–1.7(3)	C(4)–C(5)–C(6)–C(7)	0.1(3)
C(5)–C(6)–C(7)–N(2)	–176.93(14)	C(5)–C(6)–C(7)–C(8)	2.5(2)
C(9)–N(2)–C(7)–C(6)	169.61(14)	C(9)–N(2)–C(7)–C(8)	–9.7(2)
C(2)–C(3)–C(8)–C(7)	–178.88(13)	C(4)–C(3)–C(8)–C(7)	2.0(2)
N(2)–C(7)–C(8)–C(3)	175.77(13)	C(6)–C(7)–C(8)–C(3)	–3.6(2)
C(10)–N(3)–C(9)–N(2)	177.95(12)	C(10)–N(3)–C(9)–N(4)	–1.8(2)
C(7)–N(2)–C(9)–N(3)	7.9(2)	C(7)–N(2)–C(9)–N(4)	–172.31(13)
C(12)–N(4)–C(9)–N(2)	–178.09(11)	C(12)–N(4)–C(9)–N(3)	1.7(2)
C(9)–N(3)–C(10)–N(5)	–177.30(13)	C(9)–N(3)–C(10)–C(11)	0.5(2)
C(13)–N(5)–C(10)–N(3)	177.86(13)	C(13)–N(5)–C(10)–C(11)	–0.30(15)
C(14)–N(5)–C(10)–N(3)	–3.2(2)	C(14)–N(5)–C(10)–C(11)	178.59(12)
N(3)–C(10)–C(11)–N(6)	–177.89(13)	N(3)–C(10)–C(11)–C(12)	0.8(2)
N(5)–C(10)–C(11)–N(6)	0.26(15)	N(5)–C(10)–C(11)–C(12)	178.96(12)
C(13)–N(6)–C(11)–C(10)	–0.10(15)	C(13)–N(6)–C(11)–C(12)	–178.47(15)
C(9)–N(4)–C(12)–C(11)	–0.11(19)	C(9)–N(4)–C(12)–C(15)	179.50(12)
N(6)–C(11)–C(12)–N(4)	177.33(14)	N(6)–C(11)–C(12)–C(15)	–2.3(2)
C(10)–C(11)–C(12)–N(4)	–0.98(19)	C(10)–C(11)–C(12)–C(15)	179.41(12)
C(11)–N(6)–C(13)–N(5)	–0.10(16)	C(10)–N(5)–C(13)–N(6)	0.26(16)
C(14)–N(5)–C(13)–N(6)	–178.59(13)	N(4)–C(12)–C(15)–C(16)	–177.5(10)
C(11)–C(12)–C(15)–C(16)	2.1(11)		

Table 43 - Hydrogen bonds for **63** [Å and °].

D–H...A	d(D–H)	d(H...A)	d(D...A)	<(DHA)
N(1)–H(1A)...N(4A)	0.92(2)	2.42(2)	3.3246(19)	167(2)
N(1)–H(1B)...OB	0.90(2)	2.09(2)	2.941(2)	157(2)
N(2)–H(2)...OC	0.91(2)	2.04(2)	2.9227(17)	162(2)

Symmetry operations for equivalent atoms: A x, –y+3/2, z+1/2; B x, y–1, z; C x, –y+3/2, z–1/2.

- **Results of Dundee Screen**

Table 44 – Results of the Dundee screen of compounds **61**-**64** tested at 1.0 μM

Compound	**61**		**62**		**63**		**64**	
	IC_{50} (μM)[1]	SD[2]	IC_{50} (μM)	SD	IC_{50} (μM)	SD	IC_{50} (μM)	SD
MKK1	93	5	91	10	77	11	83	9
MKK2	94	10	89	5	97	1	101	12
MKK6	93	4	78	3	100	6	91	15
ERK1	83	1	80	12	94	3	96	12
ERK2	93	11	86	14	105	10	99	5
JNK1	81	6	81	14	86	10	88	14
JNK2	82	5	91	13	90	6	85	9
JNK3	95	12	89	3	101	3	93	2
p38a MAPK	93	4	77	3	84	4	89	0
p38b MAPK	95	10	95	2	103	11	103	12
p38g MAPK	104	8	98	4	98	7	108	8
p38d MAPK	112	21	91	12	99	1	125	18
ERK8	84	4	88	1	94	9	107	9
RSK1	81	3	77	19	90	7	94	7
RSK2	93	11	72	3	95	10	82	16
PDK1	101	0	92	7	93	4	103	12
PKBa	90	8	84	4	84	13	103	7
PKBb	87	2	63	9	80	14	67	5
SGK1	109	7	104	11	97	13	106	2
S6K1	84	4	91	6	98	3	92	1
PKA	103	12	100	0	103	3	99	2
ROCK 2	95	2	91	10	93	10	90	5
PRK2	82	1	70	2	81	8	85	12
PKCa	102	7	109	2	99	0	96	1
PKCγ	90	3	85	18	102	7	93	2
PKCz	110	14	99	2	113	2	107	17
PKD1	87	2	74	11	93	1	93	1
STK33	91	7	78	7	82	11	92	1
MSK1	89	1	85	1	92	5	97	1
MNK1	99	9	90	10	106	28	110	19
MNK2	99	14	87	12	98	2	102	6
MAPKAP-K2	109	1	90	5	99	4	103	13

MAPKAP-K3	76	11	75	5	80	12	84	3
PRAK	86	1	82	7	104	6	102	10
CAMKKb	103	7	99	11	96	3	103	1
CAMK1	95	7	82	9	106	9	92	8
SmMLCK	91	2	69	0	90	9	77	1
PHK	94	6	108	4	97	14	114	3
DAPK1	92	6	80	3	100	6	78	7
CHK1	96	2	95	12	93	11	113	5
CHK2	77	4	74	6	87	18	89	8
GSK3b	84	6	79	3	76	3	104	6
CDK2-cyclin A	90	5	92	5	89	1	94	3
CDK9-cyclin T1	100	9	82	3	107	6	86	1
PLK1	100	27	90	2	95	11	105	4
Aurora A	99	1	106	8	96	11	122	9
Aurora B	49	5	48	2	49	7	63	13
TLK1	108	10	118	10	100	5	111	4
LKB1	83	7	97	5	82	1	90	1
AMPK	91	12	90	3	92	6	98	13
MARK1	89	2	88	7	86	5	95	3
MARK2	85	11	90	3	91	1	107	14
MARK3	81	7	78	3	81	4	83	6
MARK4	92	3	79	16	88	3	87	16
BRSK1	97	2	96	11	108	5	103	10
BRSK2	97	10	88	6	95	15	101	3
MELK	99	5	97	14	90	19	110	11
NUAK1	88	11	79	7	86	8	85	16
SIK2	96	10	95	0	90	7	108	9
SIK3	92	12	78	1	80	6	80	7
TSSK1	98	4	87	21	101	0	99	1
CK1γ2	92	5	87	0	84	5	102	5
CK1δ	88	5	83	5	94	8	96	3
CK2	99	6	100	1	99	2	119	14
TTBK1	89	6	84	2	92	8	95	10
DYRK1A	93	4	81	1	92	12	96	5
DYRK2	95	3	82	7	87	2	87	10
DYRK3	91	1	93	2	97	2	112	5
NEK2a	85	1	85	13	79	7	94	16

NEK6	111	4	89	6	107	6	94	3
IKKb	81	6	79	10	89	3	97	14
IKKe	85	9	84	0	75	4	91	3
TBK1	105	9	90	12	98	8	89	3
PIM1	89	2	85	0	96	0	93	1
PIM2	97	1	100	6	100	3	108	7
PIM3	85	4	95	11	101	0	100	9
SRPK1	90	4	72	0	80	1	84	10
EF2K	90	2	75	4	101	2	104	2
EIF2AK3	97	4	88	1	102	5	97	11
HIPK1	97	9	99	1	112	2	109	2
HIPK2	95	4	88	5	100	8	105	10
HIPK3	124	17	114	24	122	5	97	4
CLK2	94	10	90	5	80	5	95	4
PAK2	82	4	85	4	90	8	98	12
PAK4	86	13	74	14	80	2	91	23
PAK5	85	1	88	4	93	5	88	1
PAK6	100	4	90	2	102	3	92	16
MST2	89	2	79	3	81	9	85	1
MST3	76	9	80	17	109	32	92	16
MST4	96	13	82	1	79	7	96	6
GCK	91	1	91	5	86	3	95	18
MINK1	70	0	68	3	74	6	73	2
MEKK1	99	2	81	4	87	10	88	1
MLK1	90	1	77	4	85	2	82	0
MLK3	80	5	67	1	75	3	89	8
TESK1	110	6	76	4	91	8	88	1
TAO1	102	8	94	3	97	3	98	5
ASK1	115	0	99	8	92	11	117	11
TAK1	89	4	79	10	88	2	94	2
IRAK1	107	4	110	13	101	1	113	7
IRAK4	84	17	86	18	86	4	97	9
RIPK2	82	0	77	5	98	4	89	6
OSR1	99	16	101	6	118	9	100	0
TTK	106	20	97	25	100	24	113	25
MPSK1	98	1	98	9	101	2	97	6
WNK1	96	2	100	0	108	3	96	2

Src	81	2	70	1	88	6	83	0
Lck	102	4	85	7	101	3	103	11
CSK	66	6	62	4	85	11	81	8
YES1	109	8	104	12	113	5	111	6
ABL	101	3	92	3	104	0	95	2
BTK	71	2	54	0	119	48	71	4
JAK2	92	8	93	14	99	5	86	3
SYK	98	4	107	6	104	17	101	3
ZAP70	107	19	92	1	89	5	104	33
TIE2	81	6	79	5	109	3	96	2
BRK	94	25	109	1	100	9	132	6
EPH-A2	107	3	82	2	79	4	109	1
EPH-A4	107	8	90	2	127	3	100	4
EPH-B1	94	6	96	9	91	5	94	1
EPH-B2	128	3	143	49	110	4	161	26
EPH-B3	107	7	102	10	119	9	122	1
EPH-B4	95	2	90	4	95	12	132	3
FGF-R1	89	7	78	13	82	3	91	12
HER4	100	1	85	12	109	2	81	11
IGF-1R	102	16	104	7	84	5	116	20
IR	71	10	61	4	67	8	75	1
IRR	89	3	88	7	92	3	97	8
TrkA	101	4	107	10	102	6	101	9
DDR2	105	3	95	15	102	26	109	12
VEG-FR	70	11	75	4	82	13	87	1

[1] Compounds screened in duplicate – average value of n =2 given. [2] Standard deviation.

References

1. W. L. Donegan, *Breast Cancer, 2nd Edition. Chapter 1. History of Breast Cancer*, BC Becker, New York, **2006**.
2. L. P. Bignold, Alkylating Agents and DNA Polymerases, *Anticancer Res.*, **2006**, *26*, 1327-1336.
3. R. Airley, *Cancer Chemotherapy - Basic science to the clinic*, Wiley-Blackwell, **2009**.
4. J. D. Watson and F. H. C. Crick, Molecular Structure of Nucleic Acids: A Structure for Deoxyribose Nucleic Acid, *Nature*, **1953**, *171*, 737-738.
5. P. Irigaray, J. A. Newby, R. Clapp, L. Hardell, V. Howard, L. Montagnier, S. Epstein and D. Belpomme, Lifestyle-related factors and environmental agents causing cancer: An overview, *Biomed. Pharmacother.*, **2007**, *61*, 640-658.
6. D. Belpomme, The contribution of the physico-chemical environment to the genesis of cancer: what extent and how to measure it?, *Bull. Mem. Acad. R. Med. Belg.*, **2005**, *160*, 163-180.
7. I. Berenblum, The Cocarcinogenic Action of Croton Resin *Cancer Res.*, **1941**, *1*, 44-47.
8. G. Szabo, Consequences of alcohol consumption on host defence, *Alcohol Alcohol.*, **1999**, *34*, 830-841.
9. R. Singh, J. Sandhu, B. Kaur, T. Juren, W. P. Steward, D. Segerbäck and P. B. Farmer, Evaluation of the DNA Damaging Potential of Cannabis Cigarette Smoke by the Determination of Acetaldehyde Derived N^2-Ethyl-2′-deoxyguanosine Adducts, *Chem. Res. Toxicol.*, **2009**, *22*, 1181-1188.
10. G. Block, B. Patterson and A. Subar, Fruit, vegetables, and cancer prevention: A review of the epidemiological evidence, *Nutr. Cancer*, **1992**, *18*, 1-29.
11. H. Bartsch and J. Nair, Oxidative stress and lipid peroxidation-derived DNA-lesions in inflammation driven carcinogenesis, *Cancer Detect. Prev.*, **2004**, *28*, 385-391.
12. P. Irigaray, V. Ogier, S. Jacquenet, V. Notet, P. Sibille, L. Méjean, B. E. Bihain and F. T. Yen, Benzo[a]pyrene impairs β-adrenergic stimulation of adipose tissue lipolysis and causes weight gain in mice, *FEBS J.*, **2006**, *273*, 1362-1372.
13. S. J. Talbot and D. H. Crawford, Viruses and tumours - an update, *Eur. J. Cancer*, **2004**, *40*, 1998-2005.

14. B. S. Blumberg, B. Larouzé, W. T. London, B. Werner, J. E. Hesser, I. Millman, G. Saimot and M. Payet, The relation of infection with the hepatitis B agent to primary hepatic carcinoma, *Am. J. Pathol.*, **1975**, *81*, 669-682.
15. R. Wakeford, The cancer epidemiology of radiation, *Oncogene*, **2004**, *23*, 6404-6428.
16. P. D. Darbre, Underarm cosmetics are a cause of breast cancer, *Eur. J. Cancer Prev.*, **2001**, *10*, 389-394.
17. R. R. Lassiter and T. G. Hallam, Survival of the fattest: Implications for acute effects of lipophilic chemicals on aquatic populations, *Environ, Toxicol. Chem.*, **1990**, *9*, 585-595.
18. D. Hanahan and R. A. Weinberg, Hallmarks of Cancer: The Next Generation, *Cell*, **2011**, *144*, 646-674.
19. M. Collado and M. Serrano, Senescence in tumours: evidence from mice and humans, *Nat. Rev. Cancer*, **2010**, *10*, 51-57.
20. D. L. Burkhart and J. Sage, Cellular mechanisms of tumour suppression by the retinoblastoma gene, *Nat. Rev. Cancer*, **2008**, *8*, 671-682.
21. J. M. Adams and S. Cory, The Bcl-2 apoptotic switch in cancer development and therapy, *Oncogene*, **2007**, *26*, 1324-1337.
22. M. R. Junttila and G. I. Evan, p53 - a Jack of all trades but master of none, *Nat. Rev. Cancer*, **2009**, *9*, 821-829.
23. L. Galluzzi and G. Kroemer, Necroptosis: A Specialized Pathway of Programmed Necrosis, *Cell*, **2008**, *135*, 1161-1163.
24. M. A. Blasco, Telomeres and human disease: ageing, cancer and beyond, *Nat Rev Genet*, **2005**, *6*, 611-622.
25. D. Hanahan and J. Folkman, Patterns and Emerging Mechanisms of the Angiogenic Switch during Tumorigenesis, *Cell*, **1996**, *86*, 353-364.
26. N. Ferrara, Vascular Endothelial Growth Factor, *Arterioscl. Throm. Vas.*, **2009**, *29*, 789-791.
27. V. Baeriswyl and G. Christofori, The angiogenic switch in carcinogenesis, *Semin. Cancer Biol.*, **2009**, *19*, 329-337.
28. B.-Z. Qian and J. W. Pollard, Macrophage Diversity Enhances Tumor Progression and Metastasis, *Cell*, **2010**, *141*, 39-51.
29. J. E. Talmadge and I. J. Fidler, AACR Centennial Series: The Biology of Cancer Metastasis: Historical Perspective, *Cancer Res.*, **2010**, *70*, 5649-5669.

30. K. Kessenbrock, V. Plaks and Z. Werb, Matrix Metalloproteinases: Regulators of the Tumor Microenvironment, *Cell*, **2010**, *141*, 52-67.
31. R. Demicheli, M. W. Retsky, W. J. M. Hrushesky, M. Baum and I. D. Gukas, The effects of surgery on tumor growth: a century of investigations, *Ann. Oncol.*, **2008**, *19*, 1821-1828.
32. S. Weinhouse, O. Warburg, D. Burk and A. L. Schade, On Respiratory Impairment in Cancer Cells, *Science*, **1956**, *124*, 267-272.
33. S. P. Jackson and J. Bartek, The DNA-damage response in human biology and disease, *Nature*, **2009**, *461*, 1071-1078.
34. D. C. Strauss and J. M. Thomas, Transmission of donor melanoma by organ transplantation, *Lancet Oncol.*, **2010**, *11*, 790-796.
35. S. I. Grivennikov, F. R. Greten and M. Karin, Immunity, Inflammation, and Cancer, *Cell*, **2010**, *140*, 883-899.
36. E. A. Nigg, Mitotic kinases as regulators of cell division and its checkpoints, *Nat. Rev. Mol. Cell Biol.*, **2001**, *2*, 21-32.
37. A. R. Barr and F. Gergely, Aurora-A: the maker and breaker of spindle poles, *J. Cell Sci.*, **2007**, *120*, 2987-2996.
38. M. Malumbres, E. Harlow, T. Hunt, T. Hunter, J. M. Lahti, G. Manning, D. O. Morgan, L.-H. Tsai and D. J. Wolgemuth, Cyclin-dependent kinases: a family portrait, *Nat. Cell Biol.*, **2009**, *11*, 1275-1276.
39. M. Malumbres and M. Barbacid, Mammalian cyclin-dependent kinases, *Trends Biochem. Sci.*, **2005**, *30*, 630-641.
40. S. Lapenna and A. Giordano, Cell cycle kinases as therapeutic targets for cancer, *Nat. Rev. Drug Discovery*, **2009**, *8*, 547-566.
41. J. W. Harper and P. D. Adams, Cyclin-Dependent Kinases, *Chem. Rev.*, **2001**, *101*, 2511-2526.
42. A. Ray, M. K. James, S. Larochelle, R. P. Fisher and S. W. Blain, p27Kip1 Inhibits Cyclin D-Cyclin-Dependent Kinase 4 by Two Independent Modes, *Mol. Cell Biol.*, **2009**, *29*, 986-999.
43. M. D. Larrea, J. Liang, T. Da Silva, F. Hong, S. H. Shao, K. Han, D. Dumont and J. M. Slingerland, Phosphorylation of p27Kip1 Regulates Assembly and Activation of Cyclin D1-Cdk4, *Mol. Cell Biol.*, **2008**, *28*, 6462-6472.
44. G. K. Schwartz and M. A. Shah, Targeting the Cell Cycle: A New Approach to Cancer Therapy, *J. Clin. Oncol.*, **2005**, *23*, 9408-9421.

45. J.-M. Egly and F. Coin, A history of TFIIH: Two decades of molecular biology on a pivotal transcription/repair factor, *DNA Repair*, **2011**, *10*, 714-721.
46. K. A. Merrick and R. P. Fisher, Putting one step before the other: Distinct activation pathways for Cdk1 and Cdk2 bring order to the mammalian cell cycle, *Cell Cycle*, **2010**, *9*, 706-714.
47. N. P. Pavletich, Mechanisms of cyclin-dependent kinase regulation: structures of cdks, their cyclin activators, and cip and INK4 inhibitors, *J. Mol. Biol.*, **1999**, *287*, 821-828.
48. D. O. Morgan, Principles of CDK regulation, *Nature*, **1995**, *374*, 131-134.
49. M. E. M. Noble, J. A. Endicott, N. R. Brown and L. N. Johnson, The cyclin box fold: protein recognition in cell-cycle and transcription control, *Trends Biochem. Sci.*, **1997**, *22*, 482-487.
50. J. Wade Harper and S. J. Elledge, Cdk inhibitors in development and cancer, *Curr. Opin. Genet. Dev.*, **1996**, *6*, 56-64.
51. C. J. Sherr and J. M. Roberts, Inhibitors of mammalian G1 cyclin-dependent kinases, *Genes Dev.*, **1995**, *9*, 1149-1163.
52. L. O'Regan, J. Blot and A. M. Fry, Mitotic regulation by NIMA-related kinases, *Cell Div.*, **2007**, *2*.
53. M. N. Ronald, Mitotic mutants of Apergillus nidulans, *Genet. Res.*, **1976**, *26*, 237-254.
54. B. R. Oakley and R. Morris, A mutation in aspergillus nidulans that blocks the transition from interphase to prophase, *J. Cell Biol.*, **1983**, *96*, 1155-1158.
55. A. M. Fry, The Nek2 protein kinase: a novel regulator of centrosome structure, *Oncogene*, **2002**, *21*, 6184-6194.
56. S. J. Schultz and E. A. Nigg, Identification of 21 novel human protein kinases, including 3 members of a family related to the cell cycle regulator nimA of Aspergillus nidulans, *Cell Growth Differ*, **1993**, *4*, 821-830.
57. A. R. R. Forrest, D. Taylor, R. G. Group, G. S. L. Members and S. Grimmond, Exploration of the Cell-Cycle Genes Found Within the RIKEN FANTOM2 Data Set, *Genome Res.*, **2003**, *13*, 1366-1375.
58. K. P. Lu and T. Hunter, Evidence for a NIMA-like mitotic pathway in vertebrate cells, *Cell*, **1995**, *81*, 413-424.
59. M. J. O'Connell, M. J. E. Krien and T. Hunter, Never say never. The NIMA-related protein kinases in mitotic control, *Trends Cell Biol.*, **2003**, *13*, 221-228.

60. R. S. Hames and A. M. Fry, Alternative splice variants of the human centrosome kinase Nek2 exhibit distinct patterns of expression in mitosis, *Biochem. J.*, **2002**, *361*, 77-85.
61. K. Uto, N. Nakajo and N. Sagata, Two Structural Variants of Nek2 Kinase, Termed Nek2A and Nek2B, Are Differentially Expressed in Xenopus Tissues and Development, *Dev. Biol.*, **1999**, *208*, 456-464.
62. A. M. Fry, T. Mayor, P. Meraldi, Y.-D. Stierhof, K. Tanaka and E. A. Nigg, C-Nap1, a Novel Centrosomal Coiled-Coil Protein and Candidate Substrate of the Cell Cycle–regulated Protein Kinase Nek2, *J. Cell Biol.*, **1998**, *141*, 1563-1574.
63. S. Bahe, Y.-D. Stierhof, C. J. Wilkinson, F. Leiss and E. A. Nigg, Rootletin forms centriole-associated filaments and functions in centrosome cohesion, *J. Cell Biol.*, **2005**, *171*, 27-33.
64. N. R. Helps, X. Luo, H. M. Barker and P. T. Cohen, NIMA-related kinase 2 (Nek2), a cell-cycle-regulated protein kinase localized to centrosomes, is complexed to protein phosphatase 1, *Biochem. J.*, **2000**, *349*, 509-518.
65. M. Eto, E. Elliott, T. D. Prickett and D. L. Brautigan, Inhibitor-2 Regulates Protein Phosphatase-1 Complexed with NimA-related Kinase to Induce Centrosome Separation, *J. Biol. Chem.*, **2002**, *277*, 44013-44020.
66. M. Casenghi, P. Meraldi, U. Weinhart, P. I. Duncan, R. Körner and E. A. Nigg, Polo-like Kinase 1 Regulates Nlp, a Centrosome Protein Involved in Microtubule Nucleation, *Dev. Cell*, **2003**, *5*, 113-125.
67. Q. Liu, Y. Hirohashi, X. Du, M. I. Greene and Q. Wang, Nek2 targets the mitotic checkpoint proteins Mad2 and Cdc20: A mechanism for aneuploidy in cancer, *Exp. Mol. Pathol.*, **2010**, *88*, 225-233.
68. S. Kim, K. Lee and K. Rhee, NEK7 is a centrosomal kinase critical for microtubule nucleation, *Biochem. Biophys. Res. Commun.*, **2007**, *360*, 56-62.
69. C. Belham, J. Roig, J. A. Caldwell, Y. Aoyama, B. E. Kemp, M. Comb and J. Avruch, A Mitotic Cascade of NIMA Family Kinases: Nercc1/Nek9 activates the Nek6 and Nek7 kinases, *J. Biol. Chem.*, **2003**, *278*, 34897-34909.
70. J. Roig, A. Mikhailov, C. Belham and J. Avruch, Nercc1, a mammalian NIMA-family kinase, binds the Ran GTPase and regulates mitotic progression, *Genes Dev.*, **2002**, *16*, 1640-1658.
71. S. Llamazares, A. Moreira, A. Tavares, C. Girdham, B. A. Spruce, C. Gonzalez, R. E. Karess, D. M. Glover and C. E. Sunkel, polo encodes a protein kinase homolog required for mitosis in Drosophila, *Genes Dev.*, **1991**, *5*, 2153-2165.

72. F. A. Barr, H. H. W. Sillje and E. A. Nigg, Polo-like kinases and the orchestration of cell division, *Nat. Rev. Mol. Cell Biol.*, **2004**, *5*, 429-440.
73. D. M. Glover, M. H. Leibowitz, D. A. McLean and H. Parry, Mutations in aurora prevent centrosome separation leading to the formation of monopolar spindles, *Cell*, **1995**, *81*, 95-105.
74. R. R. Adams, M. Carmena and W. C. Earnshaw, Chromosomal passengers and the (aurora) ABCs of mitosis, *Trends Cell Biol.*, **2001**, *11*, 49-54.
75. M. Carmena and W. C. Earnshaw, The cellular geography of aurora kinases, *Nat. Rev. Mol. Cell Biol.*, **2003**, *4*, 842-854.
76. R. A. Engh and D. Bossemeyer, Structural aspects of protein kinase control—role of conformational flexibility, *Pharmacol. Ther.*, **2002**, *93*, 99-111.
77. G. Manning, D. B. Whyte, R. Martinez, T. Hunter and S. Sudarsanam, The Protein Kinase Complement of the Human Genome, *Science*, **2002**, *298*, 1912-1934.
78. M. E. M. Noble, J. A. Endicott and L. N. Johnson, Protein Kinase Inhibitors: Insights into Drug Design from Structure, *Science*, **2004**, *303*, 1800-1805.
79. J. Zhang, P. L. Yang and N. S. Gray, Targeting cancer with small molecule kinase inhibitors, *Nat. Rev. Cancer*, **2009**, *9*, 28-39.
80. P. Cohen, Protein kinases - the major drug targets of the twenty-first century?, *Nat. Rev. Drug Discov.*, **2002**, *1*, 309-315.
81. Q. Liu, Y. Sabnis, Z. Zhao, T. Zhang, Sara J. Buhrlage, Lyn H. Jones and Nathanael S. Gray, Developing Irreversible Inhibitors of the Protein Kinase Cysteinome, *Chem. Biol.*, **2013**, *20*, 146-159.
82. I. Shchemelinin, L. Sefc and E. Necas, *Protein kinases, their function and implication in cancer and other diseases*, **2006**.
83. M. D'Abramo, N. Besker, G. Chillemi and A. Grottesi, Modelling conformational transitions in kinases by molecular dynamics simulations: achievements, difficulties and open challenges, *Front. Genet.*, **2014**, *5*.
84. P. G. Wyatt, A. J. Woodhead, V. Berdini, J. A. Boulstridge, M. G. Carr, D. M. Cross, D. J. Davis, L. A. Devine, T. R. Early, R. E. Feltell, E. J. Lewis, R. L. McMenamin, E. F. Navarro, M. A. O'Brien, M. O'Reilly, M. Reule, G. Saxty, L. C. A. Seavers, D.-M. Smith, M. S. Squires, G. Trewartha, M. T. Walker and A. J. A. Woolford, Identification of N-(4-Piperidinyl)-4-(2,6-dichlorobenzoylamino)-1H-pyrazole-3-carboxamide (AT7519), a Novel Cyclin Dependent Kinase

Inhibitor Using Fragment-Based X-Ray Crystallography and Structure Based Drug Design, *J. Med. Chem.*, **2008**, *51*, 4986-4999.

85. H. L. De Bondt, J. Rosenblatt, J. Jancarik, H. D. Jones, D. O. Morgant and S.-H. Kim, Crystal structure of cyclin-dependent kinase 2, *Nature*, **1993**, *363*, 595-602.
86. F. Sicheri, I. Moarefi and J. Kuriyan, Crystal structure of the Src family tyrosine kinase Hck, *Nature*, **1997**, *385*, 602-609.
87. N. M. Levinson, O. Kuchment, K. Shen, M. A. Young, M. Koldobskiy, M. Karplus, P. A. Cole and J. Kuriyan, A Src-Like Inactive Conformation in the Abl Tyrosine Kinase Domain, *PLoS Biol.*, **2006**, *4*, e144.
88. X. Min, B.-H. Lee, M. H. Cobb and E. J. Goldsmith, Crystal Structure of the Kinase Domain of WNK1, a Kinase that Causes a Hereditary Form of Hypertension, *Structure*, **2004**, *12*, 1303-1311.
89. P. Rellos, F. J. Ivins, J. E. Baxter, A. Pike, T. J. Nott, D.-M. Parkinson, S. Das, S. Howell, O. Fedorov, Q. Y. Shen, A. M. Fry, S. Knapp and S. J. Smerdon, Structure and Regulation of the Human Nek2 Centrosomal Kinase, *J. Biol. Chem.*, **2007**, *282*, 6833-6842.
90. D. Bossemeyer, R. A. Engh, V. Kinzel, H. Ponstingl and R. Huber, Phosphotransferase and substrate binding mechanism of the cAMP-dependent protein kinase catalytic subunit from porcine heart as deduced from the 2.0 A structure of the complex with Mn2+ adenylyl imidodiphosphate and inhibitor peptide PKI(5-24), *EMBO J.*, **1993**, *12*, 849-859.
91. S. R. Hubbard, Crystal structure of the activated insulin receptor tyrosine kinase in complex with peptide substrate and ATP analog, *EMBO J.*, **1997**, *16*, 5572-5581.
92. N. Jura, X. Zhang, Nicholas F. Endres, Markus A. Seeliger, T. Schindler and J. Kuriyan, Catalytic Control in the EGF Receptor and Its Connection to General Kinase Regulatory Mechanisms, *Mol. Cell*, **2011**, *42*, 9-22.
93. M. J. Robinson, P. C. Harkins, J. Zhang, R. Baer, J. W. Haycock, M. H. Cobb and E. J. Goldsmith, Mutation of Position 52 in ERK2 Creates a Nonproductive Binding Mode for Adenosine 5‘-Triphosphate, *Biochemistry*, **1996**, *35*, 5641-5646.
94. A. P. Kornev, N. M. Haste, S. S. Taylor and L. F. Ten Eyck, Surface comparison of active and inactive protein kinases identifies a conserved activation mechanism, *Proc. Natl. Acad. Sci.*, **2006**, *103*, 17783-17788.

95. A. P. Kornev, S. S. Taylor and L. F. Ten Eyck, A helix scaffold for the assembly of active protein kinases, *Proc. Natl. Acad. Sci.*, **2008**, *105*, 14377-14382.

96. M. N. Deininger, Basic science going clinical: molecularly targeted therapy of chronic myelogenous leukemia, *J. Cancer Res. Clin.*, **2004**, *130*, 59-72.

97. T. Barf and A. Kaptein, Irreversible Protein Kinase Inhibitors: Balancing the Benefits and Risks, *J. Med. Chem.*, **2012**, *55*, 6243-6262.

98. R. Morphy, Selectively Nonselective Kinase Inhibition: Striking the Right Balance, *J. Med. Chem.*, **2009**, *53*, 1413-1437.

99. G. Hatzivassiliou, K. Song, I. Yen, B. J. Brandhuber, D. J. Anderson, R. Alvarado, M. J. C. Ludlam, D. Stokoe, S. L. Gloor, G. Vigers, T. Morales, I. Aliagas, B. Liu, S. Sideris, K. P. Hoeflich, B. S. Jaiswal, S. Seshagiri, H. Koeppen, M. Belvin, L. S. Friedman and S. Malek, RAF inhibitors prime wild-type RAF to activate the MAPK pathway and enhance growth, *Nature*, **2010**, *464*, 431-435.

100. A. Morabito, M. C. Piccirillo, F. Falasconi, G. De Feo, A. Del Giudice, J. Bryce, M. Di Maio, E. De Maio, N. Normanno and F. Perrone, Vandetanib (ZD6474), a Dual Inhibitor of Vascular Endothelial Growth Factor Receptor (VEGFR) and Epidermal Growth Factor Receptor (EGFR) Tyrosine Kinases: Current Status and Future Directions, *Oncologist*, **2009**, *14*, 378-390.

101. J. Singh, R. C. Petter, T. A. Baillie and A. Whitty, The resurgence of covalent drugs, *Nat. Rev. Drug Discov.*, **2011**, *10*, 307-317.

102. M. H. Potashman and M. E. Duggan, Covalent Modifiers: An Orthogonal Approach to Drug Design, *J. Med. Chem.*, **2009**, *52*, 1231-1246.

103. T. D. Warner and J. A. Mitchell, Cyclooxygenase-3 (COX-3): Filling in the gaps toward a COX continuum?, *Proc. Natl. Acad. Sci.*, **2002**, *99*, 13371-13373.

104. L. Olbe, E. Carlsson and P. Lindberg, A proton-pump inhibitor expedition: the case histories of omeprazole and esomeprazole, *Nat. Rev. Drug Discov.*, **2003**, *2*, 132-139.

105. H. Xu, C. Faber, T. Uchiki, J. Racca and C. Dealwis, Structures of eukaryotic ribonucleotide reductase I define gemcitabine diphosphate binding and subunit assembly, *Proc. Natl. Acad. Sci. USA*, **2006**, *103*, 4028-4033.

106. H. J. Burstein, Y. Sun, L. Y. Dirix, Z. Jiang, R. Paridaens, A. R. Tan, A. Awada, A. Ranade, S. Jiao, G. Schwartz, R. Abbas, C. Powell, K. Turnbull, J. Vermette, C. Zacharchuk and R. Badwe, Neratinib, an Irreversible ErbB Receptor Tyrosine Kinase Inhibitor, in Patients With Advanced ErbB2-Positive Breast Cancer, *J. Clin. Oncol.*, **2010**, *28*, 1301-1307.

107. M. R. V. Finlay, M. Anderton, S. Ashton, P. G. Ballard, R. H. Bradbury, S. Butterworth, N. Colclough, D. A. E. Cross, H. L. McFarland, M. J. Mellor, R. A. Ward and M. J. Waring, Abstract B94: Discovery of and first disclosure of the clinical candidate AZD9291, a potent and selective third-generation EGFR inhibitor of both activating and T790M resistant mutations that spares the wild type form of the receptor, *Mol. Cancer Ther.*, **2013**, *12*, B94.

108. J. A. Burger and J. J. Buggy, Bruton tyrosine kinase inhibitor ibrutinib (PCI-32765), *Leuk. Lymphoma*, **2013**, *54*, 2385-2391.

109. Z. Pan, H. Scheerens, S.-J. Li, B. E. Schultz, P. A. Sprengeler, L. C. Burrill, R. V. Mendonca, M. D. Sweeney, K. C. K. Scott, P. G. Grothaus, D. A. Jeffery, J. M. Spoerke, L. A. Honigberg, P. R. Young, S. A. Dalrymple and J. T. Palmer, Discovery of Selective Irreversible Inhibitors for Bruton's Tyrosine Kinase, *ChemMedChem*, **2007**, *2*, 58-61.

110. C. Lammert, S. Einarsson, C. Saha, A. Niklasson, E. Bjornsson and N. Chalasani, Relationship between daily dose of oral medications and idiosyncratic drug-induced liver injury: Search for signals, *Hepatology*, **2008**, *47*, 2003-2009.

111. R. Mah, J. R. Thomas and C. M. Shafer, Drug discovery considerations in the development of covalent inhibitors, *Bioorg. Med. Chem. Lett.*, **2014**, *24*, 33-39.

112. P. A. Schwartz, P. Kuzmic, J. Solowiej, S. Bergqvist, B. Bolanos, C. Almaden, A. Nagata, K. Ryan, J. Feng, D. Dalvie, J. C. Kath, M. Xu, R. Wani and B. W. Murray, Covalent EGFR inhibitor analysis reveals importance of reversible interactions to potency and mechanisms of drug resistance, *Proc. Natl. Acad. Sci.*, **2014**, *111*, 173-178.

113. A. J. T. Smith, X. Zhang, A. G. Leach and K. N. Houk, Beyond Picomolar Affinities: Quantitative Aspects of Noncovalent and Covalent Binding of Drugs to Proteins, *J. Med. Chem.*, **2008**, *52*, 225-233.

114. E. L. Kwak, R. Sordella, D. W. Bell, N. Godin-Heymann, R. A. Okimoto, B. W. Brannigan, P. L. Harris, D. R. Driscoll, P. Fidias, T. J. Lynch, S. K. Rabindran, J. P. McGinnis, A. Wissner, S. V. Sharma, K. J. Isselbacher, J. Settleman and D. A. Haber, Irreversible inhibitors of the EGF receptor may circumvent acquired resistance to gefitinib, *Proc. Natl. Acad. Sci. USA*, **2005**, *102*, 7665-7670.

115. W. Zhou, W. Hur, U. McDermott, A. Dutt, W. Xian, S. B. Ficarro, J. Zhang, S. V. Sharma, J. Brugge, M. Meyerson, J. Settleman and N. S. Gray, A Structure-Guided Approach to Creating Covalent FGFR Inhibitors, *Chem. Biol.*, **2010**, *17*, 285-295.

116. M. S. Cohen, C. Zhang, K. M. Shokat and J. Taunton, Structural Bioinformatics-Based Design of Selective, Irreversible Kinase Inhibitors, *Science*, **2005**, *308*, 1318-1321.

117. D. W. Fry, A. J. Bridges, W. A. Denny, A. Doherty, K. D. Greis, J. L. Hicks, K. E. Hook, P. R. Keller, W. R. Leopold, J. A. Loo, D. J. McNamara, J. M. Nelson, V. Sherwood, J. B. Smaill, S. Trumpp-Kallmeyer and E. M. Dobrusin, Specific, irreversible inactivation of the epidermal growth factor receptor and erbB2, by a new class of tyrosine kinase inhibitor, *Proc. Natl. Acad. Sci.*, **1998**, *95*, 12022-12027.

118. J. B. Smaill, G. W. Rewcastle, J. A. Loo, K. D. Greis, O. H. Chan, E. L. Reyner, E. Lipka, H. D. H. Showalter, P. W. Vincent, W. L. Elliott and W. A. Denny, Tyrosine Kinase Inhibitors. 17. Irreversible Inhibitors of the Epidermal Growth Factor Receptor: 4-(Phenylamino)quinazoline- and 4-(Phenylamino)pyrido[3,2-d]pyrimidine-6-acrylamides Bearing Additional Solubilizing Functions, *J. Med. Chem.*, **2000**, *43*, 1380-1397.

119. A. Wissner, M. B. Floyd, B. D. Johnson, H. Fraser, C. Ingalls, T. Nittoli, R. G. Dushin, C. Discafani, R. Nilakantan, J. Marini, M. Ravi, K. Cheung, X. Tan, S. Musto, T. Annable, M. M. Siegel and F. Loganzo, 2-(Quinazolin-4-ylamino)-[1,4]benzoquinones as Covalent-Binding, Irreversible Inhibitors of the Kinase Domain of Vascular Endothelial Growth Factor Receptor-2, *J. Med. Chem.*, **2005**, *48*, 7560-7581.

120. L. Toral-Barza, W.-G. Zhang, X. Huang, L. A. McDonald, E. J. Salaski, L. R. Barbieri, W.-D. Ding, G. Krishnamurthy, Y. B. Hu, J. Lucas, V. S. Bernan, P. Cai, J. I. Levin, T. S. Mansour, J. J. Gibbons, R. T. Abraham and K. Yu, Discovery of lactoquinomycin and related pyranonaphthoquinones as potent and allosteric inhibitors of AKT/PKB: mechanistic involvement of AKT catalytic activation loop cysteines, *Mol. Cancer Ther.*, **2007**, *6*, 3028-3038.

121. N. Kwiatkowski, T. Zhang, P. B. Rahl, B. J. Abraham, J. Reddy, S. B. Ficarro, A. Dastur, A. Amzallag, S. Ramaswamy, B. Tesar, C. E. Jenkins, N. M. Hannett, D. McMillin, T. Sanda, T. Sim, N. D. Kim, T. Look, C. S. Mitsiades, A. P. Weng, J. R. Brown, C. H. Benes, J. A. Marto, R. A. Young and N. S. Gray, Targeting transcription regulation in cancer with a covalent CDK7 inhibitor, *Nature*, **2014**, *511*, 616-620.

122. M. Legraverend and D. S. Grierson, The purines: Potent and versatile small molecule inhibitors and modulators of key biological targets, *Bioorg. Med. Chem.*, **2006**, *14*, 3987-4006.
123. N. Tsunoda, T. Kokuryo, K. Oda, T. Senga, Y. Yokoyama, M. Nagino, Y. Nimura and M. Hamaguchi, Nek2 as a novel molecular target for the treatment of breast carcinoma, *Cancer Sci.*, **2009**, *100*, 111-116.
124. D. G. Hayward and A. M. Fry, Nek2 kinase in chromosome instability and cancer, *Cancer Lett.*, **2006**, *237*, 155-166.
125. K. Suzuki, T. Kokuryo, T. Senga, Y. Yokoyama, M. Nagino and M. Hamaguchi, Novel combination treatment for colorectal cancer using Nek2 siRNA and cisplatin, *Cancer Sci.*, **2010**, *101*, 1163-1169.
126. T. Kokuryo, T. Senga, Y. Yokoyama, M. Nagino, Y. Nimura and N. Hamaguchi, Nek2 as an effective target for inhibition of tumorigenic growth and peritoneal dissemination of cholangiocarcinoma, *Cancer Res.*, **2007**, *67*, 9637-9642.
127. L. Fletcher, G. J. Cerniglia, E. A. Nigg, T. J. Yen and R. J. Muschel, Inhibition of Centrosome Separation after DNA Damage: A Role for Nek2, *Radiat. Res.*, **2004**, *162*, 128-135.
128. S. Sonn, I. Khang, K. Kim and K. Rhee, Suppression of Nek2A in mouse early embryos confirms its requirement for chromosome segregation, *J. Cell Sci.*, **2004**, *117*, 5557-5566.
129. Y. Lou, J. Yao, A. Zereshki, Z. Dou, K. Ahmed, H. Wang, J. Hu, Y. Wang and X. Yao, NEK2A Interacts with MAD1 and Possibly Functions as a Novel Integrator of the Spindle Checkpoint Signaling, *J. Biol. Chem.*, **2004**, *279*, 20049-20057.
130. B. Frett, R. V. Brown, M. Ma, W. Hu, H. Han and H.-y. Li, Therapeutic Melting Pot of Never in Mitosis Gene A Related Kinase 2 (Nek2): A Perspective on Nek2 as an Oncology Target and Recent Advancements in Nek2 Small Molecule Inhibition, *J. Med. Chem.*, **2014**, *57*, 5835-5844.
131. W. Zhou, Y. Yang, J. Xia, H. Wang, Mohamed E. Salama, W. Xiong, H. Xu, S. Shetty, T. Chen, Z. Zeng, L. Shi, M. Zangari, R. Miles, D. Bearss, G. Tricot and F. Zhan, NEK2 Induces Drug Resistance Mainly through Activation of Efflux Drug Pumps and Is Associated with Poor Prognosis in Myeloma and Other Cancers, *Cancer Cell*, **2013**, *23*, 48-62.
132. S. Solanki, P. Innocenti, C. Mas-Droux, K. Boxall, C. Barillari, R. L. M. van Montfort, G. W. Aherne, R. Bayliss and S. Hoelder, Benzimidazole Inhibitors Induce a DFG-Out Conformation of Never in Mitosis Gene A-Related Kinase 2

(Nek2) without Binding to the Back Pocket and Reveal a Nonlinear Structure-Activity Relationship, *J. Med. Chem.*, **2011**, *54*, 1626-1639.

133. J. C. Henise and J. Taunton, Irreversible Nek2 Kinase Inhibitors with Cellular Activity, *J. Med. Chem.*, **2011**, *54*, 4133-4146.
134. J. Flory, R. Brog, L. Y. Meng, L. Call, H. Vankayalapati, G. Tricot, F. Zhan and D. J. Bearss, Overexpression of Nek2 promotes bortezomib resistance in multiple myeloma cells, *Cancer Res.*, **2013**, *73*.
135. D. G. Hayward, Y. Newbatt, L. Pickard, E. Byrne, G. Mao, S. Burns, N. K. Sahota, P. Workman, I. Collins, W. Aherne and A. M. Fry, Identification by High-Throughput Screening of Viridin Analogs as Biochemical and Cell-Based Inhibitors of the Cell Cycle–Regulated Nek2 Kinase, *J. Biomol. Screen.*, **2010**, *15*, 918-927.
136. C. J. Matheson, Newcastle University, **2012**.
137. D. M. Turner, Newcastle University, **2013**.
138. S. Akli, C. S. Van Pelt, T. Bui, L. Meijer and K. Keyomarsi, Cdk2 is Required for Breast Cancer Mediated by the Low-Molecular-Weight Isoform of Cyclin E, *Cancer Res.*, **2011**, *71*, 3377-3386.
139. D. Etemadmoghadam, G. Au-Yeung, M. Wall, C. Mitchell, M. Kansara, E. Loehrer, C. Batzios, J. George, S. Ftouni, B. A. Weir, S. Carter, I. Gresshoff, L. Mileshkin, D. Rischin, W. C. Hahn, P. M. Waring, G. Getz, C. Cullinane, L. J. Campbell and D. D. Bowtell, Resistance to CDK2 Inhibitors Is Associated with Selection of Polyploid Cells in CCNE1-Amplified Ovarian Cancer, *Clin. Cancer Res.*, **2013**, *19*, 5960-5971.
140. N. Johnson, J. Bentley, L. Z. Wang, D. R. Newell, C. N. Robson, G. I. Shapiro and N. J. Curtin, Pre-clinical evaluation of cyclin-dependent kinase 2 and 1 inhibition in anti-estrogen-sensitive and resistant breast cancer cells, *Brit. J. Cancer*, **2009**, *102*, 342-350.
141. J. H. Kim, M. J. Kang, C. U. Park, H. J. Kwak, Y. Hwang and G. Y. Koh, Amplified CDK2 and cdc2 activities in primary colorectal carcinoma, *Cancer*, **1999**, *85*, 546-553.
142. O. Tetsu and F. McCormick, Proliferation of cancer cells despite CDK2 inhibition, *Cancer Cell*, **2003**, *3*, 233-245.
143. D. Horiuchi, N. E. Huskey, L. Kusdra, L. Wohlbold, K. A. Merrick, C. Zhang, K. J. Creasman, K. M. Shokat, R. P. Fisher and A. Goga, Chemical-genetic analysis of cyclin dependent kinase 2 function reveals an important role in cellular

transformation by multiple oncogenic pathways, *Proc. Natl. Acad. Sci.*, **2012**, *109*, E1019–E1027.

144. C. Berthet, E. Aleem, V. Coppola, L. Tessarollo and P. Kaldis, Cdk2 Knockout Mice Are Viable, *Curr. Biol.*, **2003**, *13*, 1775-1785.
145. C. Barrière, D. Santamaría, A. Cerqueira, J. Galán, A. Martín, S. Ortega, M. Malumbres, P. Dubus and M. Barbacid, Mice thrive without Cdk4 and Cdk2, *Mol. Oncol.*, **2007**, *1*, 72-83.
146. D. Santamaria, C. Barriere, A. Cerqueira, S. Hunt, C. Tardy, K. Newton, J. F. Caceres, P. Dubus, M. Malumbres and M. Barbacid, Cdk1 is sufficient to drive the mammalian cell cycle, *Nature*, **2007**, *448*, 811-815.
147. J. J. Molenaar, M. E. Ebus, D. Geerts, J. Koster, F. Lamers, L. J. Valentijn, E. M. Westerhout, R. Versteeg and H. N. Caron, Inactivation of CDK2 is synthetically lethal to MYCN over-expressing cancer cells, *Proc. Natl. Acad. Sci.*, **2009**, *106*, 12968-12973.
148. C. K. Cheng, W. C. Gustafson, E. Charron, B. T. Houseman, E. Zunder, A. Goga, N. S. Gray, B. Pollok, S. A. Oakes, C. D. James, K. M. Shokat, W. A. Weiss and Q.-W. Fan, Dual blockade of lipid and cyclin-dependent kinases induces synthetic lethality in malignant glioma, *Proc. Natl. Acad. Sci.*, **2012**, *109*, 12722-12727.
149. A. Huwe, R. Mazitschek and A. Giannis, Small Molecules as Inhibitors of Cyclin-Dependent Kinases, *Angew. Chem. Int. Ed.*, **2003**, *42*, 2122-2138.
150. J. Cicenas and M. Valius, The CDK inhibitors in cancer research and therapy, *J. Cancer Res. Clin.*, **2011**, *137*, 1409-1418.
151. I. Shchemelinin, L. Sefc and E. Necas, Protein Kinase Inhibitors, *Folia Biol.*, **2006**, *52*, 137-148.
152. N. Villerbu, A.-M. Gaben, G. Redeuilh and J. Mester, Cellular effects of purvalanol A: A specific inhibitor of cyclin-dependent kinase activities, *Int. J. Cancer*, **2002**, *97*, 761-769.
153. C. E. Arris, F. T. Boyle, A. H. Calvert, N. J. Curtin, J. A. Endicott, E. F. Garman, A. E. Gibson, B. T. Golding, S. Grant, R. J. Griffin, P. Jewsbury, L. N. Johnson, A. M. Lawrie, D. R. Newell, M. E. M. Noble, E. A. Sausville, R. Schultz and W. Yu, Identification of Novel Purine and Pyrimidine Cyclin-Dependent Kinase Inhibitors with Distinct Molecular Interactions and Tumor Cell Growth Inhibition Profiles, *J. Med. Chem.*, **2000**, *43*, 2797-2804.
154. M. Canavese, L. Santo and N. Raje, Cyclin dependent kinases in cancer: Potential for therapeutic intervention, *Cancer Biol. Ther.*, **2012**, *13*, 451-456.

155. S.-H. Chao and D. H. Price, Flavopiridol Inactivates P-TEFb and Blocks Most RNA Polymerase II Transcription in Vivo, *J. Biol. Chem.*, **2001**, *276*, 31793-31799.

156. M. Aklilu, H. L. Kindler, R. C. Donehower, S. Mani and E. E. Vokes, Phase II study of flavopiridol in patients with advanced colorectal cancer, *Ann. Oncol.*, **2003**, *14*, 1270-1273.

157. S. Burdette-Radoux, R. Tozer, R. Lohmann, I. Quirt, D. S. Ernst, W. Walsh, N. Wainman, A. D. Colevas and E. Eisenhauer, Phase II trial of flavopiridol, a cyclin dependent kinase inhibitor, in untreated metastatic malignant melanoma, *Invest New Drugs*, **2004**, *22*, 315-322.

158. G. Liu, D. R. Gandara, P. N. Lara, D. Raghavan, J. H. Doroshow, P. Twardowski, P. Kantoff, W. Oh, K. Kim and G. Wilding, A Phase II Trial of Flavopiridol (NSC #649890) in Patients with Previously Untreated Metastatic Androgen-Independent Prostate Cancer, *Clin. Cancer Res.*, **2004**, *10*, 924-928.

159. K. F. Byth, C. Geh, C. L. Forder, S. E. Oakes and A. P. Thomas, The cellular phenotype of AZ703, a novel selective imidazo[1,2-a]pyridine cyclin-dependent kinase inhibitor, *Mol. Cancer Ther.*, **2006**, *5*, 655-664.

160. H. N. Bramson, J. Corona, S. T. Davis, S. H. Dickerson, M. Edelstein, S. V. Frye, R. T. Gampe, P. A. Harris, A. Hassell, W. D. Holmes, R. N. Hunter, K. E. Lackey, B. Lovejoy, M. J. Luzzio, V. Montana, W. J. Rocque, D. Rusnak, L. Shewchuk, J. M. Veal, D. H. Walker and L. F. Kuyper, Oxindole-Based Inhibitors of Cyclin-Dependent Kinase 2 (CDK2): Design, Synthesis, Enzymatic Activities, and X-ray Crystallographic Analysis, *J. Med. Chem.*, **2001**, *44*, 4339-4358.

161. D. Parry, T. Guzi, F. Shanahan, N. Davis, D. Prabhavalkar, D. Wiswell, W. Seghezzi, K. Paruch, M. P. Dwyer, R. Doll, A. Nomeir, W. Windsor, T. Fischmann, Y. Wang, M. Oft, T. Chen, P. Kirschmeier and E. M. Lees, Dinaciclib (SCH 727965), a Novel and Potent Cyclin-Dependent Kinase Inhibitor, *Mol. Cancer Ther.*, **2010**, *9*, 2344-2353.

162. M. P. Martin, S. H. Olesen, G. I. Georg and E. Schönbrunn, Cyclin-Dependent Kinase Inhibitor Dinaciclib Interacts with the Acetyl-Lysine Recognition Site of Bromodomains, *ACS Chem. Biol.*, **2013**, *8*, 2360-2365.

163. M. Malumbres, P. Pevarello, M. Barbacid and J. R. Bischoff, CDK inhibitors in cancer therapy: what is next?, *Trends Pharmacol. Sci*, **2008**, *29*, 16-21.

164. T. G. Davies, J. Bentley, C. E. Arris, F. T. Boyle, N. J. Curtin, J. A. Endicott, A. E. Gibson, B. T. Golding, R. J. Griffin, I. R. Hardcastle, P. Jewsbury, L. N. Johnson,

V. Mesguiche, D. R. Newell, M. E. M. Noble, J. A. Tucker, L. Wang and H. J. Whitfield, Structure-based design of a potent purine-based cyclin-dependent kinase inhibitor, *Nat. Struct. Biol.*, **2002**, *9*, 745-749.

165. A. J. Henderson, Newcastle University, **2005**.

166. R. J. Griffin, A. Henderson, N. J. Curtin, A. Echalier, J. A. Endicott, I. R. Hardcastle, D. R. Newell, M. E. M. Noble, L.-Z. Wang and B. T. Golding, Searching for Cyclin-Dependent Kinase Inhibitors Using a New Variant of the Cope Elimination, *J. Am. Chem. Soc.*, **2006**, *128*, 6012-6013.

167. E. Meschini, Newcastle University, **2011**.

168. J. W. Beach, H. O. Kim, L. S. Jeong, S. Nampalli, Q. Islam, S. K. Ahn, J. R. Babu and C. K. Chu, A highly stereoselective synthesis of anti-HIV 2',3'-dideoxy- and 2',3'-didehydro-2',3'-dideoxynucleosides, *J. Org. Chem.*, **1992**, *57*, 3887-3894.

169. R. Chinchilla and C. Nájera, The Sonogashira Reaction: A Booming Methodology in Synthetic Organic Chemistry, *Chem. Rev.*, **2007**, *107*, 874-922.

170. R. Marek and V. Sklenář, in *Annual Reports on NMR Spectroscopy*, Academic Press, 2004, vol. Volume 54, pp. 201-242.

171. B. Carbain, C. R. Coxon, H. Lebraud, K. J. Elliott, C. J. Matheson, E. Meschini, A. R. Roberts, D. M. Turner, C. Wong, C. Cano, R. J. Griffin, I. R. Hardcastle and B. T. Golding, Trifluoroacetic Acid in 2,2,2-Trifluoroethanol Facilitates SNAr Reactions of Heterocycles with Arylamines, *Chem. Eur. J.*, **2014**, *20*, 2311-2317.

172. J. J. Parlow, M. L. Vazquez and D. L. Flynn, A mixed resin bed for the quenching and purification of tetrabutylammonium fluoride mediated desilylating reactions, *Bioorg. Med. Chem. Lett.*, **1998**, *8*, 2391-2394.

173. D. E. Butler, S. M. Alexander, J. W. McLean and L. B. Strand, Synthesis of 1-methyl-1-(substituted benzyl)hydrazines, *J. Med. Chem.*, **1971**, *14*, 1052-1054.

174. H. Harada, O. Asano, Y. Hoshino, S. Yoshikawa, M. Matsukura, Y. Kabasawa, J. Niijima, Y. Kotake, N. Watanabe, T. Kawata, T. Inoue, T. Horizoe, N. Yasuda, H. Minami, K. Nagata, M. Murakami, J. Nagaoka, S. Kobayashi, I. Tanaka and S. Abe, 2-Alkynyl-8-aryl-9-methyladenines as Novel Adenosine Receptor Antagonists: Their Synthesis and Structure−Activity Relationships toward Hepatic Glucose Production Induced via Agonism of the A2B Receptor, *J. Med. Chem.*, **2000**, *44*, 170-179.

175. D. S. Surry and S. L. Buchwald, Dialkylbiaryl phosphines in Pd-catalyzed amination: a user's guide, *Chem. Sci.*, **2011**, *2*, 27-50.

176. A. R. Katritzky, F. Saczewski and C. M. Marson, .alpha.-Lithiation of N-alkylcarbazoles: preparation of N-(E)-styrylcarbazole, *J. Org. Chem.*, **1985**, *50*, 1351-1355.

177. H. Lebraud, C. Cano, B. Carbain, I. R. Hardcastle, R. W. Harrington, R. J. Griffin and B. T. Golding, Trifluoroethanol solvent facilitates selective N-7 methylation of purines, *Org. Biomol. Chem.*, **2013**, *11*, 1874-1878.

178. T. C. Norman, N. S. Gray, J. T. Koh and P. G. Schultz, A structure-based library approach to kinase inhibitors, *J. Am. Chem. Soc.*, **1996**, *118*, 7430-7431.

179. J. H. Lister, Purine studies. 12. Occurrence of N-methylation and C-methylation on diazomethane treatment of 2-methhylthiopurine, *Aust. J. Chem.*, **1979**, *32*, 2771-2776.

180. V. Kotek, N. Chudikova, T. Tobrman and D. Dvorak, Selective Synthesis of 7-Substituted Purines via 7,8-Dihydropurines, *Org. Lett.*, **2010**, *12*, 5724-5727.

181. K. Kohda, K. Baba and Y. Kawazoe, Chemical reactivity of alkylguanines. I. Methylation of O6-methylguanine derivatives, *Tetrahedron Lett.*, **1987**, *28*, 6285-6288.

182. C. Dalby, C. Bleasdale, W. Clegg, M. R. J. Elsegood, B. T. Golding and R. J. Griffin, Regiospecific alkylation of 6-chloropurine and 2,6-dichloropurine at N7 by transient protection of N3/N9 by methylcobaloxime, *Angew. Chem. Int. Ed.*, **1993**, *32*, 1696-1697.

183. S. Lee, B. R. Bowman, Y. Ueno, S. Wang and G. L. Verdine, Synthesis and Structure of Duplex DNA Containing the Genotoxic Nucleobase Lesion N7-Methylguanine, *J. Am. Chem. Soc.*, **2008**, *130*, 11570-11571.

184. L. R. Barrows and P. N. Magee, Nonenzymatic methylation of DNA by S-adenosylmethionine in vitro, *Carcinogenesis*, **1982**, *3*, 349-351.

185. G. Boysen, B. F. Pachkowski, J. Nakamura and J. A. Swenberg, The formation and biological significance of N7-guanine adducts, *Mutat. Res. Genet. Tox. En.*, **2009**, *678*, 76-94.

186. S. S. Hecht, DNA adduct formation from tobacco-specific N-nitrosamines, *Mutat. Res. Fund. Mol. M.*, **1999**, *424*, 127-142.

187. E. H. Rubinson, A. S. P. Gowda, T. E. Spratt, B. Gold and B. F. Eichman, An unprecedented nucleic acid capture mechanism for excision of DNA damage, *Nature*, **2010**, *468*, 406-411.

188. K. S. Gates, T. Nooner and S. Dutta, Biologically Relevant Chemical Reactions of N7-Alkylguanine Residues in DNA, *Chem. Res. Toxicol.*, **2004**, *17*, 839-856.

189. A. M. Maxam and W. Gilbert, A new method for sequencing DNA, *Proc. Natl. Acad. Sci.*, **1977**, *74*, 560-564.

190. J.-P. Bégué, D. Bonnet-Delpon and B. Crousse, Fluorinated Alcohols: A New Medium for Selective and Clean Reaction, *Synlett*, **2004**, *1*, 18-29.

191. P. Ballinger and F. A. Long, Acid Ionization Constants of Alcohols. I. Trifluoroethanol in the Solvents H2O and D2O1, *J. Am. Chem. Soc.*, **1959**, *81*, 1050-1053.

192. M. Colombo, S. Bossolo and A. Aramini, Phosphorus Trichloride-Mediated and Microwave-Assisted Synthesis of a Small Collection of Amides Bearing Strong Electron-Withdrawing Group Substituted Anilines, *J. Comb. Chem.*, **2009**, *11*, 335-337.

193. B. Carbain, R. Bayliss, K. Boxall, C. Coxon, H. Lebraud, C. Matheson, D. Turner, L. Zhen-Wang and R. J. Griffin, 2-Arylamino-6-ethynylpurines as Potent Irreversible Inhibitors of the Mitotic Kinase Nek2, *Eur. J. Cancer*, **2012**, *48*, 37, supplement 36, poster 118.

194. C. R. Coxon, Newcastle University, **2010**.

195. M. R. Becker, W. R. Ewing, R. S. Davis, H. W. Pauls, C. Ly, A. Li, H. J. Mason, Y. M. Choi-Sledeski, A. P. Spada, V. Chu, K. D. Brown, D. J. Colussi, R. J. Leadley, R. Bentley, J. Bostwick, C. Kasiewski and S. Morgan, Synthesis, SAR and in vivo activity of novel thienopyridine sulfonamide pyrrolidinones as factor Xa inhibitors, *Bioorg. Med. Chem. Lett.*, **1999**, *9*, 2753-2758.

196. I. Cikotiene, E. Pudziuvelyte, A. Brukstus and S. Tumkevicius, Study on the reactions of 4-amino-5-nitro-6-phenylethynylpyrimidines with amines and thiols, *Tetrahedron*, **2007**, *63*, 8145-8150.

197. S. Nishikawa, M. Sato, H. Kojima, C.-e. Suzuki, N. Yamada, M. Inagaki, N. Kashimura and H. Mizuno, Convenient Synthesis and Cytokinin Activity of β-Substituted 4-Styrylpyridines, the Simplest Cytokinin Analogs with a Moderate Cell Division-Promoting Activity, *J. Agric. Food Chem.*, **1996**, *44*, 1337-1342.

198. R. M. LoPachin, T. Gavin, A. DeCaprio and D. S. Barber, Application of the Hard and Soft, Acids and Bases (HSAB) Theory to Toxicant-Target Interactions, *Chem. Res. Toxicol.*, **2012**, *25*, 239-251.

199. S. K. Bharti and R. Roy, Quantitative 1H NMR spectroscopy, *TrAC Trend. Anal. Chem.*, **2012**, *35*, 5-26.

200. J. L. Jungnickel and J. W. Forbes, Quantitative Measurement of Hydrogen Types by Intergrated Nuclear Magnetic Resonance Intensities, *Anal. Chem.*, **1963**, *35*, 938-942.

201. U. Holzgrabe, R. Deubner, C. Schollmayer and B. Waibel, Quantitative NMR spectroscopy - Applications in drug analysis, *J. Pharm. Biomed. Anal.*, **2005**, *38*, 806-812.

202. G. F. Pauli, B. U. Jaki and D. C. Lankin, A Routine Experimental Protocol for qHNMR Illustrated with Taxol, *J. Nat. Prod.*, **2007**, *70*, 589-595.

203. J. C. Lindon and J. K. Nicholson, Analytical technologies for metabonomics and metabolomics, and multi-omic information recovery, *TrAC Trend. Anal. Chem.*, **2008**, *27*, 194-204.

204. M. Maiwald, T. Grützner, E. Ströfer and H. Hasse, Quantitative NMR spectroscopy of complex technical mixtures using a virtual reference: chemical equilibria and reaction kinetics of formaldehyde - water - 1,3,5-trioxane, *Anal. Bioanal. Chem.*, **2006**, *385*, 910-917.

205. U. Holzgrabe, Quantitative NMR spectroscopy in pharmaceutical applications, *Prog. Nucl. Mag. Res. Sp.*, **2010**, *57*, 229-240.

206. S. Bharti, N. Sinha, B. Joshi, S. Mandal, R. Roy and C. Khetrapal, Improved quantification from 1H-NMR spectra using reduced repetition times, *Metabolomics*, **2008**, *4*, 367-376.

207. T. D. W. Claridge, *High-Resolution NMR Techniques in Organic Chemistry*, Elsevier, **2008**.

208. C. K. Larive, D. Jayawickrama and L. Orfi, Quantitative Analysis of Peptides with NMR Spectroscopy, *Appl. Spectrosc.*, **1997**, *51*, 1531-1536.

209. B. M. Trost and I. Fleming, *Comprehensive Organic Synthesis - Selectivity, Strategy and Efficiency in Modern Organic Chemistry*, Elsevier, Oxford, **1991**.

210. A. Böhme, D. Thaens, A. Paschke and G. Schüürmann, Kinetic Glutathione Chemoassay To Quantify Thiol Reactivity of Organic Electrophiles - Application to α,β-Unsaturated Ketones, Acrylates, and Propiolates, *Chem. Res. Toxicol.*, **2009**, *22*, 742-750.

211. H. B. Burgi, J. D. Dunitz and E. Shefter, Geometrical reaction coordinates. II. Nucleophilic addition to a carbonyl group, *J. Am. Chem. Soc.*, **1973**, *95*, 5065-5067.

212. J. H. Espenson, *Chemical kinetics and reaction mechanisms*, McGraw-Hill, Inc, **1995**.

213. M. S. Newman, *Steric Effects in Organic Chemistry*, J. Wiley, **1956**.
214. S. L. Chien and R. Adams, Stereochemistry of Diphenyls. XXXV.1 The Effect of 3' Substituents on the Rate of Racemization of 2-Nitro-6-carboxy-2'-methoxydiphenyl, *J. Am. Chem. Soc.*, **1934**, *56*, 1787-1792.
215. H. C. Brown, *Boranes in Organic Chemistry*, Cornell University Press, Ithaca, New York, **1972**.
216. K. E. Pfitzner and J. G. Moffatt, A New and Selective Oxidation of Alcohols, *J. Am. Chem. Soc.*, **1963**, *85*, 3027-3028.
217. R. W. Thies and L. E. Schick, Thermal .pi.-route rearrangement of 4-cycloheptene-1-methyl acetate, *J. Am. Chem. Soc.*, **1974**, *96*, 456-460.
218. T. P. Inc., WO2006/99379 A2, **2006**.
219. C.-U. Lee and T. N. Grossmann, Reversible Covalent Inhibition of a Protein Target, *Angew. Chem. Int. Ed.*, **2012**, *51*, 8699-8700.
220. J. D. Weaver and J. A. Tunge, Decarboxylative Allylation using Sulfones as Surrogates of Alkanes, *Org. Lett.*, **2008**, *10*, 4657-4660.
221. M. Kamlar, P. Putaj and J. Vesely, Organocatalytic alkynylation of densely functionalized monofluorinated derivatives: C(sp3)-C(sp) coupling, *Tetrahedron Lett.*, **2013**, *54*, 2097-2100.
222. N. Asao, T. Kasahara and Y. Yamamoto, σ-π Chelation-controlled chemoselective ring openings of epoxides, *Tetrahedron Lett.*, **2001**, *42*, 7903-7905.
223. A. R. Katritzky, R. Akue-Gedu and A. V. Vakulenko, C-Cyanation with 1-Cyanobenzotriazole, *Arkivoc*, **2007**, 5-12.
224. D. Kahne and D. B. Collum, Kinetic cyanations of ketone enolates, *Tetrahedron Lett.*, **1981**, *22*, 5011-5014.
225. http://www.chem.wisc.edu/areas/reich/pkatable/.
226. X. J. Wang, H. S. Lee, H. Li, X. Q. Yang and X. J. Huang, The effects of substituting groups in cyclic carbonates for stable SEI formation on graphite anode of lithium batteries, *Electrochem. Commun.*, **2010**, *12*, 386-389.
227. C. Wong, R. J. Griffin, I. R. Hardcastle, J. S. Northen, L.-Z. Wang and B. T. Golding, Synthesis of sulfonamide-based kinase inhibitors from sulfonates by exploiting the abrogated SN2 reactivity of 2,2,2-trifluoroethoxysulfonates, *Org. Biomol. Chem.*, **2010**, *8*, 2457-2464.

228. N. Shibata, A. Matsnev and D. Cahard, Shelf-stable electrophilic trifluoromethylating reagents: A brief historical perspective, *Beilstein J. Org. Chem.*, **2010**, *6*, 65.
229. B. M. Trost and D. P. Curran, Chemoselective oxidation of sulfides to sulfones with potassium hydrogen persulfate, *Tetrahedron Lett.*, **1981**, *22*, 1287-1290.
230. N. Suryakiran, P. Prabhakar, T. Srikanth Reddy, K. Chinni Mahesh, K. Rajesh and Y. Venkateswarlu, Chemoselective mono halogenation of β-keto-sulfones using potassium halide and hydrogen peroxide; synthesis of halomethyl sulfones and dihalomethyl sulfones, *Tetrahedron Lett.*, **2007**, *48*, 877-881.
231. W. J. Gensler, F. Johnson and A. D. B. Sloan, Compounds Related to Podophyllotoxin. XII. Podophyllotoxone, Picropodophyllone and Dehydropodophyllotoxin1, *J. Am. Chem. Soc.*, **1960**, *82*, 6074-6081.
232. P. B. Hopkins and P. L. Fuchs, Chlorosulfenylation-dehydrochlorination reactions. New and improved methodology for the synthesis of unsaturated aryl sulfides and aryl sulfones, *J. Org. Chem.*, **1978**, *43*, 1208-1217.
233. H. Jhoti, Structural biology, *Nat. Rev. Drug Discov.*, **2008**, *7*, 783-783.
234. A. Carvalho, J. Trincão and M. Romão, in *Ligand-Macromolecular Interactions in Drug Discovery*, ed. A. C. A. Roque, Humana Press, 2010, vol. 572, ch. 3, pp. 31-56.
235. D. C. Rees, M. Congreve, C. W. Murray and R. Carr, Fragment-based lead discovery, *Nat. Rev. Drug Discov.*, **2004**, *3*, 660-672.
236. www.gelifesciences.co.jp/catalog/pdf/28962284.pdf.
237. richsingiser.com/4402/Novagen%20pET%20system%20manual.pdf.
238. A. J. McCoy, *Protein Crystallography with Coffee*, University of Cambridge, **2009**.
239. http://xds.mpimf-heidelberg.mpg.de/.
240. http://www.mrc-lmb.cam.ac.uk/harry/pre/aimless.html.
241. http://www.ysbl.york.ac.uk/~alexei/molrep.html.
242. G. N. Murshudov, P. Skubak, A. A. Lebedev, N. S. Pannu, R. A. Steiner, R. A. Nicholls, M. D. Winn, F. Long and A. A. Vagin, REFMAC5 for the refinement of macromolecular crystal structures, *Acta Cryst.*, **2011**, *67*, 355-367.
243. http://www2.mrc-lmb.cam.ac.uk/personal/pemsley/coot/.
244. David C. Chatfield, A. Augsten, C. D'Cunha, E. Lewandowska and Stanislaw F. Wnuk, Theoretical and Experimental Study of the Regioselectivity of Michael Additions, *Eur. J. Org. Chem.*, **2004**, *2004*, 313-322.

245. M. Page and A. Williams, *Organic & Bio-organic Mechanisms*, Addison Wesley Longman, Edinburgh, **1997**.
246. J. C. Slater, Atomic Radii in Crystals, *J. Chem. Phys.*, **1964**, *41*, 3199-3204.
247. D. O'Hagan, Understanding organofluorine chemistry. An introduction to the C-F bond, *Chem. Soc. Rev.*, **2008**, *37*, 308-319.
248. R. C. West, M. J. Astle and W. H. Beyer, *Handbook of Chemistry and Physics, 65th Edition*, CRC Press, Boca Raton, FL, **1984**.
249. D. A. Nicoll-Griffith, Use of cysteine-reactive small molecules in drug discovery for trypanosomal disease, *Expert Opin. Drug Discov.*, **2012**, *7*, 353-366.
250. C. Bryant, I. D. Kerr, M. Debnath, K. K. H. Ang, J. Ratnam, R. S. Ferreira, P. Jaishankar, D. Zhao, M. R. Arkin, J. H. McKerrow, L. S. Brinen and A. R. Renslo, Novel non-peptidic vinylsulfones targeting the S2 and S3 subsites of parasite cysteine proteases, *Bioorg. Med. Chem. Lett.*, **2009**, *19*, 6218-6221.
251. R. Ettari, E. Nizi, M. E. Di Francesco, M.-A. Dude, G. Pradel, R. Vicík, T. Schirmeister, N. Micale, S. Grasso and M. Zappalà, Development of Peptidomimetics with a Vinyl Sulfone Warhead as Irreversible Falcipain-2 Inhibitors, *J. Med. Chem.*, **2008**, *51*, 988-996.
252. J. B. Smaill, H. D. H. Showalter, H. Zhou, A. J. Bridges, D. J. McNamara, D. W. Fry, J. M. Nelson, V. Sherwood, P. W. Vincent, B. J. Roberts, W. L. Elliott and W. A. Denny, Tyrosine Kinase Inhibitors. 18. 6-Substituted 4-Anilinoquinazolines and 4-Anilinopyrido[3,4-d]pyrimidines as Soluble, Irreversible Inhibitors of the Epidermal Growth Factor Receptor, *J. Med. Chem.*, **2000**, *44*, 429-440.
253. H. Galons, N. Oumata, O. Gloulou and L. Meijer, Cyclin-dependent kinase inhibitors closer to market launch?, *Expert Opin. Ther. Pat.*, **2013**, *23*, 945-963.
254. http://accelrys.com/products/datasheets/discovery-studio-visualizer.pdf.
255. A. Ramirez, B. Mudryk, L. Rossano and S. Tummala, A Mechanistic Study on the Amidation of Esters Mediated by Sodium Formamide, *J. Org. Chem.*, **2011**, *77*, 775-779.
256. http://web.expasy.org/docs/expasy_tools05.pdf.
257. N. S. Gray, S. Kwon and P. G. Schultz, Combinatorial synthesis of 2,9-substituted purines, *Tetrahedron Lett.*, **1997**, *38*, 1161-1164.
258. E. Moreau, S. Fortin, J. Lacroix, A. Patenaude, J. L. C. Rousseau and R. C-Gaudreault, *N*-Phenyl-*N'*-(2-chloroethyl)ureas (CEUs) as potential antineoplastic

agents. Part 3: Role of carbonyl groups in the covalent binding to the colchicine-binding site, *Bioorg. Med. Chem.*, **2008**, *16*, 1206-1217.

259. M. Brændvang and L.-L. Gundersen, Synthesis, biological activity, and SAR of antimycobacterial 2- and 8-substituted 6-(2-furyl)-9-(p-methoxybenzyl)purines, *Bioorg. Med. Chem.*, **2007**, *15*, 7144-7165.
260. M. Legraverend, O. Ludwig, E. Bisagni, S. Leclerc, L. Meijer, N. Giocanti, R. Sadri and V. Favaudon, Synthesis and in vitro evaluation of novel 2,6,9-trisubstituted purines acting as cyclin-dependent kinase inhibitors, *Bioorg. Med. Chem.*, **1999**, *7*, 1281-1293.
261. R. El-Haggar, K. Kamikawa, K. Machi, Z. Ye, Y. Ishino, T. Tsumuraya and I. Fujii, Molecular design of small organic molecules based on structural information for a conformationally constrained peptide that binds to G-CSF receptor, *Bioorg. Med. Chem. Lett.*, **2010**, *20*, 1169-1172.
262. A. Latorre, I. Lopez, V. Ramirez, S. Rodriguez, J. Izquierdo, F. V. Gonzalez and C. Vicent, Radical Mechanism in the Elimination of 2-Arylsulfinyl Esters, *J. Org. Chem.*, **2012**, *77*, 5191-5197.
263. A. M. Cheh and R. E. Carlson, Determination of potentially mutagenic and carcinogenic electrophiles in environmental samples, *Anal. Chem.*, **1981**, *53*, 1001-1006.
264. Y. Nagao, S. Miyamoto, M. Miyamoto, H. Takeshige, K. Hayashi, S. Sano, M. Shiro, K. Yamaguchi and Y. Sei, Highly Stereoselective Asymmetric Pummerer Reactions That Incorporate Intermolecular and Intramolecular Nonbonded S···O Interactions, *J. Am. Chem. Soc.*, **2006**, *128*, 9722-9729.
265. S. Colonna, S. Banfi, R. Annunziata and L. Casella, Enantio and diastereoselectivity in the periodate oxidation of sulfides catalyzed by bovine serum albumin. 2, *J. Org. Chem.*, **1986**, *51*, 891-895.
266. D. Mirk, J.-M. Grassot and J. Zhu, Synthesis of 4-Nitrophenyl Sulfones and Application in the Modified Julia Olefination, *Synlett*, **2006**, *2006*, 1255-1259.
267. M. Mag, J. Muth, K. Jahn, A. Peyman, G. Kretzschmar, J. W. Engels and E. Uhlmann, Synthesis and binding properties of oligodeoxynucleotides containing phenylphosphon(othio)ate linkages, *Bioorg. Med. Chem.*, **1997**, *5*, 2213-2220.
268. C. G. J. Verhart and G. I. Tesser, New base-labile amino-protective groups for peptide synthesis, *Rec. Trav. Chim. Pays-Bas*, **1988**, *107*, 621-626.

269. D. Hodson, G. Holt and D. K. Wall, α-Diazosulphones and related compounds from the base-induced cleavage of α-diazo-β-ketosulphones, *J. Chem. Soc. C*, **1968**, 2201-2205.
270. R. Hohlweg and P. H. Olesen, Indole derivatives for treatment of obesity, **2005**.
271. Y. Xiao, W.-C. Chang, H.-W. Liu and P. Liu, Study of IspH, a Key Enzyme in the Methylerythritol Phosphate Pathway Using Fluoro-Substituted Substrate Analogues, *Org. Lett.*, **2011**, *13*, 5912-5915.
272. B. W. K. Lee, H. G. Sun, T. Zang, B. J. Kim, J. F. Alfaro and Z. S. Zhou, Enzyme-Catalyzed Transfer of a Ketone Group from an S-Adenosylmethionine Analogue: A Tool for the Functional Analysis of Methyltransferases, *J. Am. Chem. Soc.*, **2010**, *132*, 3642-3643.
273. R. B. Diebold, T. Gero, P. Grover, S. Huang, S. Ioannidis, C. A. Ogoe, J. C. Saeh and J. G. Varnes, N-acylsulfonamide apoptosis promoters, **2012**.
274. K. Keiji, T. Mamoru, H. Eiji H, T. Takahiko, F. Yoshiyuki, K. Masaki and N. Masaharu, Triazole derivative and use thereof, PCT/JP2006/307797, **2009**.
275. O. Kinzel, C. Gege, C. Steeneck, G. Kleymann and T. Hoffmann, Seven-Membered Sulfonamides as Modulators of Rar-related Orphan Receptor-gamma (RORgamma, NR1F3) WO 2013/ 064231 A1, **2013**.
276. J. Kong, T. Meng, P. E. McNamara, X. Liang and J. K. Wong, Synthesis of 3-amino-4-substituted pyrazole derivatives, US 2006/ 281756 A1, **2006**.